

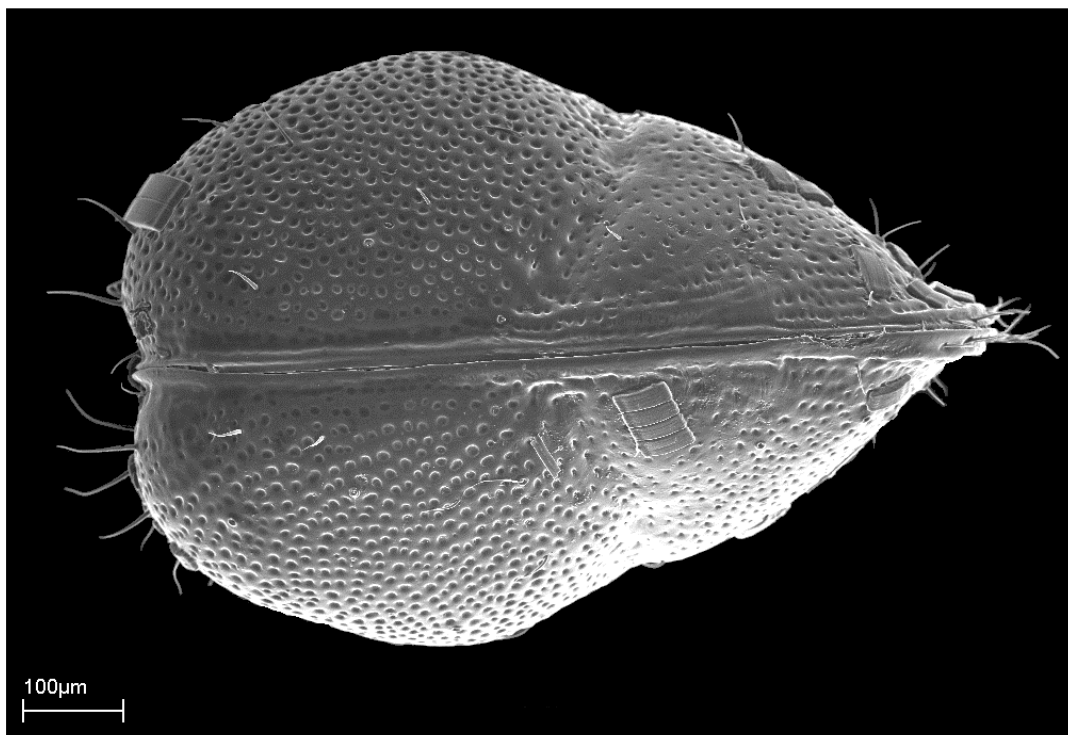


IODP/ICDP

Kolloquium 2017

IGeo, Technische Universität Braunschweig

14. - 16. März 2017





Stadtplan Braunschweig
Open Geodata 2016, Lizenz: dl-de/by-2-0

Cover picture: Scanning electron microscope image of the ostracode *Cytheridella ilosvayi* from Lake Petén Itzá, Guatemala (Length: 837 microns , Width: 590 microns). Ostracodes are used to quantitatively infer changes in past lake levels, and are therefore great indicators of droughts or wet conditions. Souce: L. Pérez Alvarado, UNAM, México.

Dienstag, 14. März 2017		
10:00	13:00	Registrierung
13:00	13:30	Eröffnung
Neues aus den Programmen		
13:30	13:50	Sebastian Krastel - ICDP Rückblick auf 2016 - Wie geht es weiter?
13:50	14:10	André Bornemann/Jochen Erbacher - IODP Rückblick auf 2016 - Wie geht es weiter?
IODP Fahrtberichte		
14:10	14:25	Jan Behrmann - IODP Expedition 357: Atlantis Massif Serpentinization and Life
14:25	14:40	Andreas Koutsodendris - IODP Expedition 361: Southern African Climates and Agulhas LGM Density Profile
14:40	14:55	André Hüpers - IODP Expedition 362: Drilling the inputs to the Sumatra subduction zone
14:55	15:10	Ann Holbourn - IODP Expedition 363: Western Pacific Warm Pool
15:10	16:40	Posterpräsentation Kaffeepause
16:40	16:55	Michael Poelchau - IODP-ICDP Expedition 364: Drilling the Peak Ring of the Chicxulub Impact Crater
16:55	17:10	Achim Kopf - Shallow observatory installations unravel earthquake processes in the Nankai accretionary complex (IODP Expedition 365)
17:10	17:25	Verena Heuer - Preliminary results from IODP Expedition 370 (Temperature Limit of the Deep Biosphere off Muroto, T-LIMIT)
IODP & ICDP Themen		
17:25	17:45	Thomas Wilke - Integration of geological and biological histories: Unraveling drivers of diversification in ancient Lake Ohrid
17:45	18:05	Torsten Dahm - Drilling the Eger Rift: Magmatic fluids driving the earthquakes swarms and the deep biosphere
Im Anschluss	Icebreaker und Posterpräsentation	

Mittwoch, 15. März 2017		
08:30	08:50	Volkhard Spieß - Development of an IODP Drilling Proposal at Campi Flegrei linking to active ICDP Drilling Initiatives
08:50	09:10	Sherilyn Fritz - Trans-Amazon Drilling Project
09:10	09:30	Sebastian Steinig - Early Cretaceous climate and arctic variability in the Kiel Climate Model
09:30	09:50	David De Vleeschouwer - Quantifying K, U and Th contents of marine sediments using shipboard natural gamma radiation spectra measured on DV JOIDES Resolution
09:50	10:10	Marieke Ahlborn - Late Holocene changes in torrential rainstorm frequency inferred from a Dead Sea sediment core
10:10	10:30	Frank Schäbitz - Chew Bahir, the HSPDP drill site: half a million years of environmental history from southern Ethiopia
10:30	13:00	Posterpräsentation / Kaffeepause / Mittagspause
<i>Parallel stattfindend:</i>		
10:30	12:30	Geo-Show „Unterirdisch“ (Millennium-Halle, Madamenweg 77)
13:00	13:20	Christoph Heubeck - Early Archean Surface Processes and Environments - Drilling the Moodies Group, Barberton Greenstone Belt, South Africa
13:20	13:40	Ascelina Hasberg - The ICDP drilling project on Lake Towuti, Indonesia: recent developments and contributions of the DFG “Towuti Bundle”
13:40	14:00	André Friese - First biogeochemical characterization of sediments from ferruginous and ultraoligotrophic Lake Towuti
14:00	14:20	Aurèle Vuillemin - Isotopic record of diagenetic siderites from Lake Towuti's ferruginous sequence, Indonesia
14:20	14:40	Anna Joy Drury - Mind the Gap: integrating Atlantic and Pacific deep-sea benthic isotope records into a global late Miocene (5.33 to 8.10 Ma) reference stack
14:40	15:00	Kim Jakob - Sea-level and deep-sea temperature evolution during the Plio-Pleistocene intensification of northern hemisphere glaciation: new insights from the eastern equatorial Pacific and the North Atlantic
15:00	16:30	Posterpräsentation / Kaffeepause
16:30	16:50	Thomas Westerhold - Astronomical Calibration of the Ypresian Geomagnetic Polarity Time Scale: Implications for Seafloor Spreading Rates and the Chaotic Behaviour of the Solar System?
16:50	17:10	Barbara Huber - Orogenic erosion centres in the crossfire of climate and tectonics: Insights from a single grain provenance analysis of Surveyor Fan sediments, Gulf of Alaska, IODP Expedition 341
17:10	17:30	Frank Lamy - IODP proposal DYNAPACC: Plio-Pleistocene Dynamics of the Pacific Antarctic Circumpolar Current
17:30	17:50	Thomas Burschil - Advanced seismic imaging of overdeepened alpine valleys preparatory to DOVE
17:50	18:10	Jürgen Koepke - Report from the ICDP Oman Drilling Project: Phase 1 is in progress
19:30		Gemeinsames Abendessen in der Maschinenhalle des Steigenberger-Parkhotel (Nimes-Straße 2).

Donnerstag, 16. März 2017		
09:00	09:20	Philipp Brandl - The arc arises: the links between volcanic output, arc evolution and melt composition
09:20	09:40	Ulrich Riller - Mechanisms of deformation during peak-ring formation of large impact structures inferred from Expedition 364 drill core
09:40	10:00	André Hüpers - Clay mineralogy and composition of sediments sampled at Integrated Ocean Drilling Program Site C0002: Implications for the lithification of prism sediments in the Nankai Trough subduction zone
10:00	10:20	Qi Liu - Microbial processes in the deep biosphere of the active CO₂-dominated fault zone in NW Bohemia
10:20	11:30	Posterpräsentation Kaffeepause
11:30	11:50	Lars Wörmer - Massive contribution of bacterial endospores to the marine deep biosphere - a global view
11:50	12:10	Rishi Ram Adhikari - Subseafloor life and carbon cycling in the Bengal Fan (IODP Expedition 354)
12:10	13:00	Posterprämierung und Schlussworte
13:00		Tagungsende

Donnerstag, 16. März 2017	
Im <u>Anschluss</u> an das IODP/ICDP Kolloquium	
13:30	GESEP School 2017: "The link between Geo- and Bioscience utilizing soft sediment cores"
Key Topics:	
<ol style="list-style-type: none"> 1. Scientific drilling and soft sediment coring 2. Initial core handling and description 3. Bioindicators in sediments 4. Microbiology and microbiological sampling 5. Molecular biology and modeling 	
<u>ENDE:</u> Freitag, 17. März 2017, ca. 17:00 Uhr	

Teilnehmerliste

Name	Vorname	Institution und Ort
Adhikari	Rishi Ram	MARUM - Zentrum für Marine Umweltwissenschaften, Universität Bremen
Adler	Karsten	GFZ, Helmholtz-Zentrum Potsdam, Deutsches GeoForschungsZentrum, Potsdam
Ahlborn	Marieke	GFZ, Helmholtz-Zentrum Potsdam, Deutsches GeoForschungsZentrum, Potsdam
Alawi	Mashal	GFZ, Helmholtz-Zentrum Potsdam, Deutsches GeoForschungsZentrum, Potsdam
Alexandrakis	Catherine	Institut für Geophysik und Geoinformatik, TU Bergakademie Freiberg
Almeev	Renat	Institut für Mineralogie, Universität Hannover
Bahlburg	Heinrich	Institut für Geologie und Paläontologie, Universität Münster
Bahr	André	Institut für Geowissenschaften, Universität Heidelberg
Bauersachs	Thorsten	Institut für Geowissenschaften, Universität Kiel
Behrens	Harald	Institut für Mineralogie, Universität Hannover
Behrman	Jan	GEOMAR, Helmholtz-Zentrum für Ozeanforschung, Kiel
Bender	Vera Barbara	MARUM - Zentrum für Marine Umweltwissenschaften, Universität Bremen
Bergmann	Fenna	Fachbereich Geowissenschaften, Universität Bremen
Blaser	Patrick	Institut für Umweltphysik, Universität Heidelberg
Böhm	Florian	GEOMAR, Helmholtz-Zentrum für Ozeanforschung, Kiel
Bornemann	André	IODP, BGR, Bundesanstalt für Geowissenschaften und Rohstoffe, Hannover
Brachert	Thomas	Institut für Geophysik und Geologie, Universität Leipzig
Brandl	Philipp	GEOMAR, Helmholtz-Zentrum für Ozeanforschung, Kiel
Bräuer	Karin	Helmholtz-Zentrum für Umweltforschung UFZ, Halle
Brauer	Achim	GFZ, Helmholtz-Zentrum Potsdam, Deutsches GeoForschungsZentrum, Potsdam
Bretschneider	Lisa	GEOMAR, Helmholtz-Zentrum für Ozeanforschung, Kiel
Brzelinski	Swaantje	Institut für Geowissenschaften, Universität Heidelberg
Burmeister	Christian	Institut für Geographie und Geologie, Universität Greifswald
Burschil	Thomas	LIAG, Leibnitz-Institut für Angewandte Geophysik, Hannover
Buske	Stefan	Institut für Geophysik und Geoinformatik, TU Bergakademie Freiberg
Caceres	Francisco	Institut für Geo- und Umweltwissenschaften, Universität München
Catunda	Maria Carolina A.	Institut für Geowissenschaften, Universität Heidelberg
Chiang	Oscar	ICBM, Institut für Chemie und Biologie des Meeres, Universität Oldenburg
Christensen	Beth	Adelphi University, New York, USA
Ciażela	Jakub	Institut für Mineralogie, Universität Hannover
Cohuo	Sergio	Institut für Geosysteme und Bioindikation, TU Braunschweig
Dahm	Torsten	GFZ, Helmholtz-Zentrum Potsdam, Deutsches GeoForschungsZentrum, Potsdam
Deik	Hanaa	Geologisches Institut, RWTH Aachen
Dersch-Hansmann	Michaela	Hessische Staatskanzlei, Abteilung Europa und Internationale Angelegenheiten, Wiesbaden
Deutsch	Alex	Institut für Planetologie, Universität Münster
De Vleeschouwer	David	MARUM - Zentrum für Marine Umweltwissenschaften, Universität Bremen
Drath	Gabriela	IODP, BGR, Bundesanstalt für Geowissenschaften und Rohstoffe, Hannover
Drury	Anna Joy	MARUM, Zentrum für Marine Umweltwissenschaften, Universität Bremen
Dultz	Stefan	Institut für Bodenkunde, Universität Hannover
Dummann	Wolf	Institut für Geologie und Mineralogie, Universität Köln
Dupont	Lydie	MARUM - Zentrum für Marine Umweltwissenschaften, Universität Bremen
Eder	Wolfgang	GeoCentre, Universität Göttingen
Egger	Lisa	Institut für Geowissenschaften, Universität Heidelberg
Engelen	Bert	ICBM, Institut für Chemie und Biologie des Meeres, Universität Oldenburg
Engelhardt	Tim	ICBM, Institut für Chemie und Biologie des Meeres, Universität Oldenburg
Erbacher	Jochen	IODP, BGR, Bundesanstalt für Geowissenschaften und Rohstoffe, Hannover
Erzinger	Jörg	GFZ, Helmholtz-Zentrum Potsdam, Deutsches GeoForschungsZentrum, Potsdam
Felis	Thomas	MARUM - Zentrum für Marine Umweltwissenschaften, Universität Bremen
Flögel	Sascha	GEOMAR, Helmholtz-Zentrum für Ozeanforschung, Kiel
Förster	Verena	Institut für Erd- und Umweltwissenschaften, Universität Potsdam
Francke	Alexander	Institut für Geologie und Mineralogie, Universität Köln
Frank	Martin	GEOMAR, Helmholtz-Zentrum für Ozeanforschung, Kiel
Friedrich	Oliver	Institut für Geowissenschaften, Universität Heidelberg
Friese	André	GFZ, Helmholtz-Zentrum Potsdam, Deutsches GeoForschungsZentrum, Potsdam
Fritz	Sherilyn	Department of Earth and Atmospheric Sciences, University of Nebraska - Lincoln, USA
Gabriel	Gerald	LIAG, Leibniz-Institut für Angewandte Geophysik, Hannover

Garbe-Schönberg	Dieter	Institut für Geowissenschaften, Universität Kiel
Giese	Rüdiger	GFZ, Helmholtz-Zentrum Potsdam, Deutsches GeoForschungsZentrum, Potsdam
Gischler	Eberhard	Institut für Geowissenschaften, Universität Frankfurt
Groeneveld	Jeroen	MARUM - Zentrum für Marine Umweltwissenschaften, Universität Bremen
Grunert	Patrick	Institut für Erdwissenschaften, Universität Graz, Österreich
Grützner	Jens	AWI, Helmholtz-Zentrum für Polar- und Meeresforschung, Alfred-Wegener-Institut, Bremerhaven
Gussone	Nikolaus	Institut für Mineralogie, Universität Münster
Gutjahr	Marcus	GEOMAR, Helmholtz-Zentrum für Ozeanforschung, Kiel
Haberzettl	Torsten	Institut für Geographie, Universität Jena
Hallenberger	Maximilian	Energy & Mineral Resources Group, RWTH Aachen
Harms	Ulrich	Scientific Drilling ICDP, GFZ, Helmholtz-Zentrum Potsdam, Deutsches GeoForschungsZentrum, Potsdam
Hasberg	Ascelina	Institut für Geologie und Mineralogie, Universität Köln
Hathorne	Edmund	GEOMAR, Helmholtz-Zentrum für Ozeanforschung, Kiel
Hauße	Torsten	Department of Animal Ecology & Systematics, Universität Giessen
Henkel	Susann	AWI, Helmholtz-Zentrum für Polar- und Meeresforschung, Alfred-Wegener-Institut, Bremerhaven
Hess	Kai-Uwe	Department für Geo- und Umweltwissenschaften, Universität München
Heubeck	Christoph	Institut für Geowissenschaften, Universität Jena
Heuer	Verena	MARUM - Zentrum für Marine Umweltwissenschaften, Universität Bremen
Hierold	Johannes	GFZ, Helmholtz-Zentrum Potsdam, Deutsches GeoForschungsZentrum, Potsdam
Hochmuth	Katharina	AWI, Helmholtz-Zentrum für Polar- und Meeresforschung, Alfred-Wegener-Institut, Bremerhaven
Hoffmann	Julia	Institut für Geowissenschaften, Universität Heidelberg
Hofmann	Peter	Institut für Geologie und Mineralogie, Universität Köln
Holbourn	Ann	Institut für Geowissenschaften, Universität Kiel
Holtz	François	Institut für Mineralogie, Universität Hannover
Hoerst	Andreas	Institut für Geophysik und extraterrestrische Physik, TU Braunschweig
Huang	Huang	GEOMAR, Helmholtz-Zentrum für Ozeanforschung, Kiel
Huber	Barbara	Institut für Geologie und Paläontologie, Universität Münster
Hüpers	André	MARUM - Zentrum für Marine Umweltwissenschaften, Universität Bremen
Iovine	Raffaella	Geowissenschaftliches Zentrum, Universität Göttingen
Jakob	Kim	Institut für Geowissenschaften, Universität Heidelberg
Janssen	Christoph	GFZ, Helmholtz-Zentrum Potsdam, Deutsches GeoForschungsZentrum, Potsdam
Jonas	Ann-Sophie	Institut für Geowissenschaften, Universität Kiel
Jovanovska	Elena	Department of Animal Ecology & Systematics, Universität Giessen
Just	Janna	Institut für Geologie und Mineralogie, Universität Köln
Kallmeyer	Jens	GFZ, Helmholtz-Zentrum Potsdam, Deutsches GeoForschungsZentrum, Potsdam
Kämpf	Horst	GFZ, Helmholtz-Zentrum Potsdam, Deutsches GeoForschungsZentrum, Potsdam
Kinkel	Hanno	ESSAC Science Coordinator, GEOMAR, Helmholtz-Zentrum für Ozeanforschung, Kiel
Kochhann	Karlos G.D.	Institut für Geowissenschaften, Universität Kiel
Koepke	Jürgen	Institut für Mineralogie, Universität Hannover
Kollaske	Tina	BGR, Bundesanstalt für Geowissenschaften und Rohstoffe, Hannover
Kopf	Achim	MARUM - Zentrum für Marine Umweltwissenschaften, Universität Bremen
Kotthoff	Ulrich	Institut für Geologie, Universität Hamburg
Kotov	Sergey	MARUM - Zentrum für Marine Umweltwissenschaften, Universität Bremen
Kousis	Ilias	Institut für Geowissenschaften, Universität Heidelberg
Koutsodendris	Andreas	Institut für Geowissenschaften, Universität Heidelberg
Krastel	Sebastian	ICDP-Deutschland, Institut für Geowissenschaften, Universität Kiel
Krauß	Felix	GFZ, Helmholtz-Zentrum Potsdam, Deutsches GeoForschungsZentrum, Potsdam
Krauze	Patryk	GFZ, Helmholtz-Zentrum Potsdam, Deutsches GeoForschungsZentrum, Potsdam
Kriegerowski	Marius	GFZ, Helmholtz-Zentrum Potsdam, Deutsches GeoForschungsZentrum, Potsdam
Kudraß	Hermann-Rudolph	MARUM - Zentrum für Marine Umweltwissenschaften, Universität Bremen
Kuhn	Gerhard	AWI, Helmholtz-Zentrum für Polar- und Meeresforschung, Alfred-Wegener-Institut, Bremerhaven
Kuhnt	Wolfgang	Institut für Geowissenschaften, Universität Kiel
Kukowski	Nina	Institut für Geowissenschaften, Universität Jena
Kutterolf	Steffen	GEOMAR, Helmholtz-Zentrum für Ozeanforschung, Kiel
Lamy	Frank	AWI, Helmholtz-Zentrum für Polar- und Meeresforschung, Alfred-Wegener-Institut, Bremerhaven
Lebas	Elodie	Institut für Geowissenschaften, Universität Kiel
Lehnert	Oliver	Geozentrum Nordbayern, Universität Erlangen-Nürnberg

Leicher	Niklas	Institut für Geologie und Mineralogie, Universität Köln
Leupold	Maike	Institute of Geology & Palaeontology, RWTH Aachen
Lindhorst	Katja	Institut für Geowissenschaften, Universität Kiel
Link	Jasmin M.	Institut für Umweltphysik, Universität Heidelberg
Linsler	Stefan	Institut für Mineralogie, Universität Hannover
Liu	Qi	GFZ, Helmholtz-Zentrum Potsdam, Deutsches GeoForschungsZentrum, Potsdam
Lorbeer	Nina	Institut für Geowissenschaften, Universität Kiel
Lückge	Andreas	BGR, Bundesanstalt für Geowissenschaften und Rohstoffe, Hannover
Lüniger	Guido	DFG Deutsche Forschungsgemeinschaft, Bonn
Macario	Laura	Institut für Geosysteme und Bioindikation, TU Braunschweig
Mangelsdorf	Kai	GFZ, Helmholtz-Zentrum Potsdam, Deutsches GeoForschungsZentrum, Potsdam
McCormack	Jeremy	Institut für Geologie, Mineralogie und Geophysik, Universität Bochum
Meschede	Martin	Institut für Geographie und Geologie, Universität Greifswald
Mock	Dominik	Institut für Mineralogie, Universität Hannover
Müller	Juliane	AWI, Helmholtz-Zentrum für Polar- und Meeresforschung, Alfred-Wegener-Institut, Bremerhaven
Müller	Samuel	Institut für Geowissenschaften, Universität Kiel
Muñoz	Gerard	GFZ, Helmholtz-Zentrum Potsdam, Deutsches GeoForschungsZentrum, Potsdam
Neugebauer	Ina	GFZ, Helmholtz-Zentrum Potsdam, Deutsches GeoForschungsZentrum, Potsdam
Neuhaus	Martin	Institut für Geophysik Und Extraterrestrische Physik, TU Braunschweig
Nickschick	Tobias	Institut für Geophysik und Geologie, Universität Leipzig
Nürnberg	Dirk	GEOMAR, Helmholtz-Zentrum für Ozeanforschung, Kiel
Oberhänsli	Hedwig	Museum für Naturkunde, Leibniz-Institut für Evolutions- und Biodiversitätsforschung, Berlin
Oberhänsli	Roland	ICDP-Deutschland, Institut für Erd- und Umweltwissenschaften, Universität Potsdam
Osborne	Anne	GEOMAR, Helmholtz-Zentrum für Ozeanforschung, Kiel
Panagiotopoulos	Kostas	Institut für Geologie und Mineralogie, Universität Köln
Petrick	Benjamin	Max-Planck-Institut für Chemie, Mainz
Piller	Werner	Institut für Erdwissenschaften, Universität Graz, Österreich
Poelchau	Michael	Institut für Geo- und Umweltnaturwissenschaften, Universität Freiburg
Pöppelmeier	Frerk	Institut für Umweltphysik, Universität Heidelberg
Pross	Jörg	Institut für Geowissenschaften, Universität Heidelberg
Raddatz	Jacek	Institut für Geowissenschaften, Universität Frankfurt
Reiche	Sönke	Institute for Applied Geophysics and Geothermal Energy, RWTH Aachen
Reichenbacher	Bettina	Department für Geo- und Umweltwissenschaften, Paläontologie & Geobiologie, Universität München
Renaudie	Johan	Museum für Naturkunde, Leibniz-Institut für Evolutions- und Biodiversitätsforschung, Berlin
Reolid	Jesús	Institut für Geologie, Universität Hamburg
Reuning	Lars	Energy & Mineral Resources Group, RWTH Aachen
Ridolfi	Filippo	Institut für Mineralogie, Universität Hannover
Riller	Ulrich	Institut für Geologie, Universität Hamburg
Röhl	Ulla	MARUM - Zentrum für Marine Umweltwissenschaften, Universität Bremen
Rösner	Alexander	MARUM - Zentrum für Marine Umweltwissenschaften, Universität Bremen
Sarnthein	Michael	Institut für Geowissenschaften, Universität Kiel
Schäbitz	Frank	Institut für Geographiedidaktik, Universität Köln
Schindlbeck	Julie C.	GEOMAR, Helmholtz-Zentrum für Ozeanforschung, Kiel
Schippers	Axel	BGR, Bundesanstalt für Geowissenschaften und Rohstoffe, Hannover
Schmincke	Hans-Ulrich	GEOMAR, Helmholtz-Zentrum für Ozeanforschung, Kiel
Schubert	Florian	Institut für Erd- und Umweltwissenschaften, Universität Potsdam
Schuck	Bernhard	GFZ, Helmholtz-Zentrum Potsdam, Deutsches GeoForschungsZentrum, Potsdam
Schulte	Felix	Institut für Geologie, Universität Hamburg
Schulze	Nora	Fachbereich Geowissenschaften, Universität Bremen
Schwab	Markus	GFZ, Helmholtz-Zentrum Potsdam, Deutsches GeoForschungsZentrum, Potsdam
Schwalb	Antje	Institut für Geosysteme und Bioindikation, TU Braunschweig
Schwenk	Tilman	Fachbereich Geowissenschaften, Universität Bremen
Simon	Helge	Institut für Geophysik und Geoinformatik, TU Bergakademie Freiberg
Spieß	Volkhard	Fachbereich Geowissenschaften, Universität Bremen
Stein	Rüdiger	AWI, Helmholtz-Zentrum für Polar- und Meeresforschung, Alfred-Wegener-Institut, Bremerhaven
Steinig	Sebastian	GEOMAR, Helmholtz-Zentrum für Ozeanforschung, Kiel
Steinmann	Lena	Fachbereich Geowissenschaften, Universität Bremen
Strack	Dieter	International Oil & Gas Consultant, Ratingen
Stranghöner	Marius	Institut für Mineralogie, Universität Hannover
Stuch	Beatrix	DFG Deutsche Forschungsgemeinschaft, Bonn

Süfke	Finn	GEOMAR, Helmholtz-Zentrum für Ozeanforschung, Kiel
Sumita	Mari	GEOMAR, Helmholtz-Zentrum für Ozeanforschung, Kiel
Tanganan	Deborah N.	MARUM - Zentrum für Marine Umweltwissenschaften, Universität Bremen
Thiede	Jörn	GEOMAR, Helmholtz-Zentrum für Ozeanforschung, Kiel
Thomas	Ariel	Institute for Applied Geophysics and Geothermal Energy, RWTH Aachen
Tiedemann	Ralph	Institut für Biochemie und Biologie, Universität Potsdam
Timmerman	Martin	ICDP-Deutschland, Institut für Erd- Und Umweltwissenschaften, Universität Potsdam
Turner	Andreas	Fachbereich Geowissenschaften, Universität Bremen
Turner	Stephanie	BGR, Bundesanstalt für Geowissenschaften und Rohstoffe, Hannover
Umlauf	Josefine	Institut für Geophysik und Geologie, Universität Leipzig
Uenzelmann-Neben	Gabriele	AWI, Helmholtz-Zentrum für Polar- und Meeresforschung, Alfred-Wegener-Institut, Bremerhaven
Vandijken	Verona	ICBM, Institut für Chemie und Biologie des Meeres, Universität Oldenburg
Viehberg	Finn	Institut für Geologie und Mineralogie, Universität Köln
Villinger	Heinrich	Fachbereich Geowissenschaften, Universität Bremen
Virgil	Christopher	Institut für Geophysik und extraterrestrische Physik, Technische Universität Braunschweig
Voigt	Janett	MARUM - Zentrum für Marine Umweltwissenschaften, Universität Bremen
Voigt	Silke	Institut für Geowissenschaften, Universität Frankfurt
Vuillemin	Aurèle	GFZ, Helmholtz-Zentrum Potsdam, Deutsches GeoForschungsZentrum, Potsdam
Wagner	Bernd	Institut für Geologie und Mineralogie, Universität Köln
Wagner	Dirk	GFZ, Helmholtz-Zentrum Potsdam, Deutsches GeoForschungsZentrum, Potsdam
Wallrabe-Adams	Hans-Joachim	MARUM - Zentrum für Marine Umweltwissenschaften, Universität Bremen
Wang	Meng	Institut für Mineralogie, Universität Hannover
Weber	Michael	Institut für Geologie, Mineralogie und Paläontologie, Universität Bonn
Weber	Tobias	GFZ, Helmholtz-Zentrum Potsdam, Deutsches GeoForschungsZentrum, Potsdam
Wefer	Gerold	MARUM - Zentrum für Marine Umweltwissenschaften, Universität Bremen
Westerhold	Thomas	MARUM - Zentrum für Marine Umweltwissenschaften, Universität Bremen
Wiersberg	Thomas	Scientific Drilling ICDP, GFZ, Helmholtz-Zentrum Potsdam, Deutsches GeoForschungsZentrum, Potsdam
Wilke	Thomas	Institut für Tierökologie & Spezielle Zoologie, Universität Gießen
Wilkens	Roy H.	Hawaii Institute of Geophysics and Planetology, Honolulu, USA
Wittke	Andreas	Institut für Mineralogie, Universität Münster
Wodtke	Tanja	BGR, Bundesanstalt für Geowissenschaften und Rohstoffe, Hannover
Wojewódka	Marta	Polish Academy of Sciences, Warschau, Polen
Wörmer	Lars	MARUM - Zentrum für Marine Umweltwissenschaften, Universität Bremen
Wrozyna	Claudia	Institut für Erdwissenschaften, Universität Graz, Österreich
Yilmaz	Tim	Department für Geo- und Umweltwissenschaften, Universität München
Zhang	Chao	Institut für Mineralogie, Universität Hannover
Zhao	Xueru	GFZ, Helmholtz-Zentrum Potsdam, Deutsches GeoForschungsZentrum, Potsdam
Zheng	Xufeng	AWI, Helmholtz-Zentrum für Polar- und Meeresforschung, Alfred-Wegener-Institut, Bremerhaven

Autor	Titel	SPP	Seite
FAHRTBERICHTE:			
Behrmann, J.H., Fröh-Green, G.L., Orcutt, B.N., Green, S., Cotterill, C. and the Expedition 357 Scientists	Short Expedition Report: IODP Exp. 357, Atlantis Massif Serpentinization and Life	IODP	16
Grützner, J., Just, J., Koutsodendris, A., Tangunan, D., Hall, I., Hemming, S., Levay, L. and Expedition 361 Scientists	IODP Expedition 361 – Southern African Climates and Agulhas LGM Density Profile	IODP	17
Hüpers, A., Kutterolf, S., McNeill, L.M., Dugan, B., Petronotis, K., and the Expedition 362 Shipboard Scientists	Report on IODP Expedition 362: Drilling the inputs to the Sumatra subduction zone	IODP	18
Holbourn, A., Rosenthal, Y., Kulhanek, D., Drury, A.J. and the Expedition 363 Shipboard Scientific Party	IODP Expedition 363 “Western Pacific Warm Pool”	IODP	19
Poelchau, M.H., Riller, U., Gebhardt, C., Morgan, J., Gulick, S. and Expedition 364 Scientists	IODP-ICDP Expedition 364: Drilling the Peak Ring of the Chicxulub Impact Crater	IODP	21
Kopf, A., Saffer, D.M., Toczko, S. and Expedition Scientists 365.	Shallow observatory installations unravel earthquake processes in the Nankai accretionary complex (IODP Expedition 365)	IODP	22
Heuer, V.B., Inagaki, F., Morono, Y., Kubo, Y., Henkel, S., Schubotz, F., Viehweger, B. and the IODP Expedition 370 Scientists	Preliminary results from IODP Expedition 370 (Temperature Limit of the Deep Biosphere off Muroto, T-LIMIT)	IODP	23
ABSTRACTS:			
Adhikari, R.R., Heuer, V.B., Hoshino, T., Inagaki, F., Jabinski, S., Kallmeyer, J., Kitte, A., Wörmer, L., Hinrichs, K.-U.	Subseafloor life and carbon cycling in the Bengal Fan (IODP Exp. 354)	IODP	26
Adler, K., Alawi, M., Liu, Q., Bussert, R., Vylita, T., Schulz, H.-M., Kämpf, H., Plessen, B., Wagner, D., Mangelsdorf, K.	Impact of geogenic CO ₂ on the depth distribution of and feedstock provision for deep microbial ecosystems in the Hartoušov mofette system in NW Bohemia	ICDP	26
Ahlborn, M., Armon, M., Ben Dor, Y., Neugebauer, I., Schwab, M.J., Tjallingii, R., Shoqeir, J.H., Morin, E., Enzel, Y., Brauer, A.	Late Holocene changes in torrential rainstorm frequency inferred from a Dead Sea sediment core	ICDP	28
Ahlborn, M., Tjallingii, R., Ben Dor, Y., Enzel, Y., Neugebauer, I., Schwab, M.J., Brauer, A.,	Flash floods in the Dead Sea basin during the Pleistocene/Holocene transition inferred from ICDP core 5017-1	ICDP	29
Alawi, M., Liu, Q., Bussert, R., Kämpf, H., Nickschick, T., Vylita, T., Wagner, D.	Deep drilling into an active, CO ₂ -dominated fault zone in NW Bohemia - preliminary results	ICDP	30
Alexandrakis, C., Kieslich, A., Löberich, E., Calo, M., Vavrycuk, V.	Swarm-dependent velocity models in the West Bohemia Seismic Zone	ICDP	30
Almeev, R., Portnyagin, M., Garbe-Schönberg, D.	Chalcophile elements in Shatsky Rise basalts as potential indicators of the mantle plume origin?	IODP	32
Almeev, R.R., Portnyagin, M.V., Botcharnikov, R.E., Linsler, S.A., Schuth, S., Oeser, M., Garbe-Schönberg, D., Holtz, F.	Subduction initiation: geochemical and experimental study of boninites from the Izu-Bonin-Mariana island arc	IODP	33
Bach, W., Kahl, W.-A. Törke, A.	Rates and processes of tephra alteration in Surtsey volcano: a combined observational and experimental approach	ICDP	34
Bahr, A., Kaboth, S., Hodell, D.	Enhanced Subtropical Gyre circulation feeding ice sheet growth during the Mid-Pleistocene Transition (500 – 1400 ka, Site U1385)	IODP	35

Bergmann, F., Lantzsch, H., Spiess, V., Schwenk, T., France-Lanord, C., IODP Expedition 354 Scientific Party	The active channel-levee system of the Bengal Fan at 8°N – a high-resolution evolutionary study based on seismo-acoustic data and IODP Expedition 354 drill Site U1454	IODP	35
Blaser, P., Lippold, J., Gutjahr, M., Pöppelmeier, F., Frank, N., Link, J.M.	The evolution of deep water circulation in the subpolar North Atlantic during the last glacial termination	IODP	38
Böhm, F., Rocholl, A., Wiedenbeck, M., Liebetrau, V., Eisenhauer, A.	Macroscale and Microscale Calcium Isotope Variations in Calcites from Ocean Crust Basalts	IODP	40
Bohnhoff, M., Dresen, G., Ceken, U., Kadirioğlu, F.T., Kartal, R.F., Kilic, T., Nurlu, M., Yanik, K., Acarel, D., Bulut, F., Ito, H., Johnson, W., Malin, P.E., Mencin, D.	GONAF – A borehole Geophysical Observatory around the North Anatolian Fault in the Eastern Sea of Marmara	ICDP	41
Brandl, P.A., Hamada, M., Arculus, R.J., Johnson, K., Marsaglia, K.M., Savov, I.P., Ishizuka O., Li, H.	The arc arises: the links between volcanic output, arc evolution and melt composition	IODP	41
Brust, P.C., Wienholz, D.J., Kotthoff, U.	Agricultural activity in the Baltic region and coeval terrestrial and marine ecosystem changes – palynological pilot studies (IODP Exp. 347 Sites M0059, M0063)	IODP	42
Brzelinski, S., Friedrich, O., Bornemann, A.	Mechanisms of glacial/interglacial changes during the „middle“ Oligocene	IODP	42
Burschil, T., Bunes, H., Tanner, D., Gabriel, G., Krawczyk, C.M.	Advanced seismic imaging of overdeepened alpine valleys preparatory to DOVE	ICDP	43
Catunda, M.C.A., Bahr, A., Friedrich, O.	Evolution of the oceanic circulation in the subtropical Atlantic across the Mid-Pleistocene Transition	IODP	44
Chiang, O.E., Engelhardt, T., Engelen, B., Vandieken, V.	Detection of filamentous viruses of <i>Vibrio diazotrophicus</i> strains isolated from sub-surface sediments of the Baltic Sea	IODP	45
Ciążela, J., Koepke, J., Strauss, H., Pieterek, B., Bender, M., Dick, H.J.B., Kuhn, T., Muszyński, A.	Sulfide-rich interval in gabbros of the IODP drill core from site U1473 (Atlantis Bank, Southwest Indian Ridge, SWIR)	IODP	47
Cohuo, S., Macario-González, L., Pérez, L., Sylvestre, F., Pailles, C., Curtis, J., Kutterolf, S., Wojewódka, M., Szeroczyńska, K., Zawisza, E., Schwalb, A.	Ultrastructure and aquatic community response to Heinrich Stadials (HS5a-HS1) in the continental northern Neotropics	ICDP	47
Conze, R., Hierold, J., Harms, U.	GESEP-Portal – Die Weiterentwicklung zu einem katalogbasiertem Datenportal	ICDP	48
Dahm, T., Fischer, T., Anesio, A.M., Alexandrakis, C., Bräuer, K., Buske, S., Dolejs, D., Horalek, J., Korn, M., Krüger, F., Malek, J., Shelly, D., Wagner, D.	Drilling the Eger Rift: Magmatic fluids driving the earthquakes swarms and the deep biosphere	ICDP	49
Deik, H., Reuning, L., Benjamin, P., Expedition 356 Scientists	Aragonite sedimentation and dissolution on a subtropical carbonate ramp, Carnarvon Ramp, SW Shelf of Australia	IODP	49
De Vleeschouwer, D., Dunlea, A.G., Auer, G., Anderson, C.H., Brumsack, H., De Loach, A., Gurnis, M.C., Huh, Y., Ishiwa, T., Jang, K., Kominz, M.A., März, C., Schnetger, B., Murray, R.W., Pälike, H., Expedition 356 Shipboard Scientists	Quantifying K, U and Th contents of marine sediments using shipboard natural gamma radiation spectra measured on DV <i>JOIDES Resolution</i>	IODP	50
Drury, A.J., Westerhold, T., Frederichs, T., Wilkens, R., Channell, J., Evans, H., Hodell, D., John, C.M., Lyle, M., Röhl, U., Tian, J.	Mind the Gap: integrating Atlantic and Pacific deep-sea benthic isotope records into a global late Miocene (5.33 to 8.10 Ma) reference stack	IODP	51
Dummann, W., Hofmann, P., Osborne, A., Wagner, T., Herrle, J.O., Lenz, M., Frank, M., Flögel, S., Steinig, S., Kusch, S., Rethemeyer, J.	Evolving carbon sinks in the young South Atlantic: New constraints from Nd-Isotopes on the opening of the Falkland Plateau gateway	IODP	52
Egger, L.M., Friedrich, O., Norris, R.D., Wilson, P.A., Pross, J.	The Oligocene/Miocene transition in the western North Atlantic (IODP Expedition 342): Surface-water changes reconstructed from dinoflagellate cysts	IODP	54

Engelhardt, T., Engelen, B., Cypionka, H.	Viral infection history and virus-host interaction in sulfate-reducing bacteria from subsurface sediments of Juan de Fuca ridge, IODP Exp. 301	IODP	55
Felis, T., Deschamps, P., Hathorne, E.C., Asami, R.	Tropical Pacific climate during Meltwater Pulse-1A from IODP Expedition 310 corals	IODP	56
Foerster, V., Asrat, A., Chapot, M., Cohen, A.S., Dean, J.R., Deino, A., Günter, C., Junginger, A., Lamb, H.F., Leng, M., Roberts, H., Schaebitz, F., Trauth, M.H., HSPDP Science Team	Deciphering climate information from the long Chew Bahir sediment cores: Towards a continuous half-million year climate record from the Southern Ethiopian Rift	ICDP	56
Francke, A., Wagner, B., Tauber, P., Just, J., Leicher, N.	Progress and prospects of the ICDP SCOPSCO project at Lake Ohrid (Macedonia, Albania)	ICDP	57
Francke, A., Dosseto, A., Rothacker, L., Menozzi, D.	Unraveling natural and human-accelerated erosional and weathering processes at Lake Ohrid (Macedonia, Albania) using Uranium series analyses	ICDP	58
Friese, A., Glombitza, C., Simister, R., Vuillemin, A., Nomosatryo, S., Bauer, K., Ordonez, L., Henny, C., Ariztegui, D., Crowe, S., Wagner, D., Kallmeyer, J.	First biogeochemical characterization of sediments from ferruginous and ultraoligotrophic Lake Towuti	ICDP	59
Fritz, S.C., Baker, P.A.	Trans-Amazon Drilling Project	ICDP	60
Garbe-Schönberg, D., Koepke, J., Müller, S., Müller, T., Strauss, H.	Trace element systematics in gabbros from the Wadi Gideah transect (Wadi Tayin Massif, Oman ophiolite) – constraints on accretion processes in fast-spread oceanic crust	ICDP	61
Gischler, E., Anselmetti, F.S.	Geomorphology of the Belize Barrier Reef margin: a survey for IODP drilling	IODP	62
Grimmer, F., Dupont, L.M.	Early Pliocene vegetation and hydrology changes in western equatorial South America	IODP	62
Groeneveld, J., Henderiks, J., Renema, W., Mchugh, C.M., De Vleeschouwer, D., Christensen, B.A., Exp. 356 Scientists	Shifts in Miocene Southern Hemisphere Westerlies and varying southward heat transport by the Leeuwin Current	IODP	63
Grunert, P., García-Gallardo, A., Balestra, B., Richter, C., Auer, G., Van Der Schee, M., Flores, J.A., Sierro, F.J., Jiménez-Espejo, F., Alvarez Zarikian, C., Röhl, U., Piller, W.E.	Pliocene history of Mediterranean-Atlantic exchange	IODP	64
Gruetzner, J., Uenzelmann-Neben, Expedition 361 Scientists	The Indian-Atlantic Ocean gateway during the Pliocene: current dynamics and changing sediment provenance	IODP	64
Gussone, N., Inoue, M., Yokoyama, Y., Suzuki, A., Kawahata, H.,	Fluctuation of Ca isotope ratios in corals from the Great Barrier Reef during the last deglaciation	IODP	65
Hasberg, A.K.M., Melles, M., Held, P., Just, J., Wennrich, V., Morlock, M., Vogel, H., Russell, J.M., Bijaksana, S., Opitz, S., Friese, A., Kallmeyer, J., Vuillemin, A., Herder, F., v. Rintelen, T., Hesse, K., T. Wonik, T., ICDP-TDP Scientific Party	The ICDP drilling project on Lake Towuti, Indonesia: recent developments and contributions of the DFG 'Towuti Bundle'	ICDP	67
Hathorne, E.C., Gebregiorgis, D., Giosan, L., Kerr, K., Anand, P., Nürnberg, D., Frank, N.	Two million years of Andaman Sea sediment elemental composition: Pleistocene sealevel and South Asian monsoon controls	IODP	70
Henkel, S.	How stable iron isotope geochemistry can help to find the temperature limit of the deep biosphere (IODP Exp. 370)	IODP	70
Heubeck, C.	Early Archean Surface Processes and Environments – Drilling the Moodies Group, Barberton Greenstone Belt, South Africa	ICDP	71
Hierold, J., Harms, U., Schwalb, A., Wittig, V.	Hipercorig – A Direct Push Coring Tool for extended reach in unconsolidated on- and offshore formations and its availability	ICDP	72
Hochmuth, K., Gohl, K.	Paleobathymetry of the Southern Ocean and its role in paleoclimate variations	IODP	73
Hoffmann, J., Bahr, A., Schönfeld, J., Friedrich, O., Pross, J.	Reconstructing hydrological changes in (sub)tropical South America during Dansgaard-Oeschger cycles: insights into the low-latitude expressions of high-latitude climate forcing	DFG	74

Huang, H., Gutjahr, M., Kuhn, G., Eisenhauer, A.	Southern Ocean and Weddell Sea bottom water Pb isotope compositions trace ice sheet dynamics and regional circulation patterns today and during the past 140 ka	IODP	75
Huber, B., Bahlburg, H.	Orogenic erosion centres in the crossfire of climate and tectonics: Insights from a single grain provenance analysis of Surveyor Fan sediments, Gulf of Alaska, IODP Expedition 341	IODP	76
Hüpers, A., L. Warr, Grathoff, G., Wemmer, K., Kopf, A.	Clay mineralogy and composition of sediments sampled at Integrated Ocean Drilling Program Site C0002: Implications for the lithification of prism sediments in the Nankai Trough subduction zone	IODP	76
Iovine, R.S., Wörner, G., Fedele, L., Mazzeo, F.C., Arienzo, I., Civetta, L., Orsi, G., D'Antonio, M.	Ba-zonation modelling on sanidine phenocrysts from the Agnano-Monte Spina Eruption (4.7ka), Campi Flegrei caldera (Napoli, southern Italy)	ICDP	77
Jakob, K.A., Wilson, P.A., Pross, J., Fiebig, J., Friedrich, O.	Sea-level and deep-sea temperature evolution during the Plio-Pleistocene intensification of Northern Hemisphere Glaciation: new insights from the Eastern Equatorial Pacific and the North Atlantic	IODP	78
Jonas, A.-S., Schwark, L., Bauersachs, T.	Variation in the flow path of the Kuroshio Current and its impact on NW Pacific paleoclimate evolution	IODP	80
Just, J., Expedition 361 Scientists	Plio/Pleistocene SW Indian Ocean paleoceanography and stratigraphy using magnetic data (PLIOmag)	IODP	82
Kallmeyer, J., Schubert, F., Treude, T., IODP Exp. 370 Scientific Party	Exploring microbial sulphate reduction under high temperature and pressure – Results of a pilot study on samples from IODP Exp. 370	IODP	84
Karas, C., Nürnberg, D., Bahr, A., Groeneveld, J., Herrle, J.O., Tiedemann, R., Demenocal, P.B.	Pliocene oceanic seaways and global climate	IODP	84
Kochhann, K.G.D., Kuhnt, W., Holbourn, A., Andersen, N., Scheible, S.	Deep water circulation and productivity in the equatorial Indian Ocean (IODP Site U1443) through the Miocene Climatic Optimum	IODP	86
Koepke, J., Garbe-Schönberg, D., Müller, S., Mock, D., Oman Drilling Project Science Team	Report from the ICDP Oman Drilling Project: Phase 1 is in progress	ICDP	86
Kotov, S., Paelike, H.,	MyDTW – Dynamic Time Warping program for stratigraphical time series	IODP	87
Kousis, I., Koutsodendris, A., Knipping, M., Pross, J., SCOPSCO Science Party	Unraveling the trigger mechanisms for climate change in SE Europe during MIS 12-11 based on a new high-resolution pollen record from Lake Ohrid	ICDP	87
Krastel, S., Kutterolf, S., Lebas, E., Hagemann, K., Strauch, W.	Seismic reconnaissance survey for the ICDP proposal 'Paleoclimate, Paleoenvironment, and Paleoecology of Neogene Central America: Bridging Continents and Oceans (NICA-BRIDGE)'	ICDP	88
Krauß, F., Hedin, P., Almqvist, B., Simon, H., Pierdominici, S., Giese, R., Buske, S., Juhlin, C., Lorenz, H.	Integration of downhole logging and borehole seismic data to characterise mid-crustal deformation patterns in the Scandinavian Caledonides	ICDP	89
Krauze, P., Kämpf, H., Horn F., Wagner, D., Alawi, M.	Microbiological survey of mofette and mineral waters of the Cheb Basin, Czech Republic	ICDP	89
Kriegerowski, M., Cesca, S., Dahm, T., Krüger, F.	Q Inversion employing double difference amplitude spectral ratio method: A case study of North West Bohemia	ICDP	90
Kuhnt, W., Holbourn, A., Jöhnck, J., Andersen, N.	Indian monsoon variability in a warmer world: Exploring the Miocene-Pliocene sediment archives of IODP Expedition 353 Sites U1447 and U1448 (Andaman Sea)	IODP	91
Kutterolf, S., Schindlbeck, J.C.	Traces of explosive eruptions in Cretaceous to Quaternary Indian Ocean sediments	IODP	92
Lamy, F., Anderson, R., Arz, H.W., Cortese, G., Esper, O., Gohl, K., Hall, I., Hillenbrand, C.D., Hübscher, C., Lange, C., Lembke-Jene, L., Martinez-Garcia, A., Ninnemann, U., Nürnberg, D., Pahnke, K., Polonia, A., Stoner, J., Tiedemann, R., Uenzelmann-Neben, G., Winckler, G.	IODP proposal DYNAPACC: Plio-Pleistocene <u>D</u> ynamics of the <u>P</u> acific <u>A</u> ntarctic <u>C</u> ircumpolar <u>C</u> urrent	IODP	93

Lay, V., Buske, S., Townend, J., Kellett, R., Savage, M., Eccles, J., Schmitt, D., Constantinou, A., Bertram, M., Hall, K., Lawton, D., Gorman, A., DFDP Whataroa 2016 Science Team	Imaging the Alpine Fault: preliminary results from a detailed 3D-VSP experiment at the DFDP-2 drill site in Whataroa, New Zealand	ICDP	94
Lebas, E., Krastel, S., Wagner, B., Gromig, R., Fedorov, F., Melles, M.	Preliminary results of a seismic pre-site survey at Levinson-Lessing Lake, Northern Siberia	ICDP	96
Leicher, N., Francke, A., Wagner, B., Just, J., Zanchetta, G., Sulpizio, R., Giaccio, B., Nomade, S.	Tephrostratigraphy of the DEEP site sediment record, Lake Ohrid (Albania, FYROM)	ICDP	97
Leupold, M., Pfeiffer, M., Garbe-Schönberg, D.	Calibration of the coral Sr/Ca thermometer with in situ and satellite SST of open ocean and lagoonal settings in the tropical Indian Ocean – implications for fossil corals	DFG	99
Lindhorst, K., Krastel, S., Schramm, B., Wagner, B.	Preliminary results of Multichannel Seismic Pre-site Surveys on Lake Prespa suggest a long sedimentary history	ICDP	99
Link, J.M., Blaser, P., Lippold, J., Gutjahr, M., Pöppelmeier, F., Osborne, A.H., Böhm, E., Frank, M., Friedrich, O., Frank, N.	The Atlantic Deep Circulation During the Past One Million Years	IODP	100
Linsler, S.A., Almeev, R.R., Holtz, F., Botcharnikov, R.E., Portnyagin, M.V.	Subduction initiation: petrological and experimental study of fore-arc basalts from the Izu-Bonin-Mariana island arc	IODP	101
Liu, Q., Kämpf, H., Nickschick, T., Kyslik, P., Baldrian, P., Bussert, R., Plessen, B., Wagner, D., Alawi, M.	Microbial processes in the deep biosphere of the active CO ₂ -dominated fault zone in NW Bohemia	ICDP	103
Lorbeer, N., Schwark, L., Bauersachs, T-	Climate change promotes the formation of cyanobacterial blooms in the Baltic Sea	IODP	104
Macario, L., Cohuo, S., Anselmetti, F., Schmid, D., Pérez, L., Kutterolf, S., Curtis, J., Schwalb, A.	Environmental history of the last 400,000 years in the northern Neotropical region based on Lake Petén Itzá sediments	ICDP	106
McCormack, J., Immenhauser, A., Kwiecień, O.	A closer look at Lake Van's carbonates: Implications for lacustrine stable isotope analysis	ICDP	107
Methe, P., A. Goepel, A., Kukowski, N.	Lithology estimations from cluster analysis on borehole logging data, evaluated and extrapolated from core data	ICDP	108
Mock, D., Ildefonse, B., Koepke, J., Müller, T., Garbe-Schönberg, D.	ICDP Oman Drilling Project: crystallographic preferred orientations in the lower crust - The Wadi Gideah transect	ICDP	108
Müller, J., Romero, O., Cowan, E., Forwick, M., McClymont, E., Asahi, H., März, C., Moy, C., Suto, I., Mix A., Stoner, J.	Mid Pleistocene productivity events in the NE Pacific: multiple fertilization from aeolian dust, icebergs, and volcanic ash	IODP	109
Mueller, S., Koepke, J., Garbe-Schönberg, D., Tramm, F., Hoernle, K.	Hydrous lower oceanic crust: continuous activity of seawater-derived fluids at very high to medium temperatures – records from the Oman ophiolite (Wadi Gideah, Wadi Tayin Massif)	ICDP	110
Muñoz, G., Weckmann, U., Pek, J., Meqbel, N., Kováčiková, S., Klanica, R.	Earthquake swarms, Moffettes and mid Pleistocene volcanism – Electromagnetic imaging of the Eger Rift (W Bohemia)	ICDP	111
Neugebauer, I., Schwab, M.J., Wulf, S., Serb, J., Plessen, B., Tjallingii, R., Appelt, O., Stein, M., Brauer, A.	First cryptotephra finding in sediment cores from the Dead Sea – Potential for further constraining the chronology of the ICDP Dead Sea palaeoclimate record	ICDP	111
Osborne, A., Frank, M., Kroon, D., Wright, J.D., Groeneveld, J., Gutjahr, M., Reuning, L., Tiedemann, R.	Gulf Stream hydrography during the Late Pliocene/early Pleistocene: low versus high latitude forcing of the Atlantic Meridional Overturning Circulation	IODP	112
Panagiotopoulos, K., Holtvoeth, J., Pancost, R.D., Wagner, B., Melles, M.	First results from a Mediterranean biodiversity hotspot from palynological and biomarker analyses of Lake Ohrid sediments from the Early Pleistocene (> 1.2 Ma)	ICDP	114
Petrick, B.F., Auer, G., De Vleeschouwer, D., Christensen, B.A., Stolfi, C., Reuning, L., Martinez-Garcia, A., Haug, G., Buckley, T., Gallagher, S.J., Fulthorpe, C.S., Bogus, K., IODP 356 Shipboard Science Party	Indian Ocean circulation changes over the middle Pleistocene transition	IODP	115

Pöppelmeier, F., Blaser, P., Schulz, H., Gutjahr, M., Lippold, J., Frank, N.	The interaction of authigenic and detrital Nd in North Atlantic sediments	IODP	116
Reichenbacher, B., Grunert, P., Harzhauser, M., Hinderer, M., Holcová, K., Kempf, O., Kováč, M., Krijgsman, W., Mandic, O., Matys Grygar, T., Nehyba, S., W. Orsi, Piller, W., Sachsenhofer, R.F., Schlunegger, F., Sharman, G.R., Stockli, D.	A proposal for a new ICDP task in Europe: The 'MICLIME' project	ICDP	117
Renaudie, J., Fontorbe, G., Drews, E.-L., Böhne, S., Lazarus, D.	Constraining the history of the Cenozoic marine silicon cycle with siliceous microplankton	IODP	118
Reolid, J., Betzler, C., Eberli, G.P., Lüdmann, T., Alvarez-Zarikian, C., IODP Exp. 359 Ship-Board Scientists	Sequence stratigraphy and palaeoenvironment of Miocene platform slope deposits from the Maldives	IODP	120
Reuning, L., Back, S., Gallagher, S.J., Fulthorpe, C.S., Rastegar Lari, A., Himmler, T., Iwatani, H., Auer, G., Bogus, K., Expedition 356 Scientists	The rapid switch from inorganic tropical carbonates to bioclastic sedimentation across a drowning unconformity (North West Shelf of Australia)	IODP	120
Riedel, M., Reiche, S., Asshoff, K., Buske, S.	Sequence boundaries from time to depth: A seismic depth imaging workflow for groundwater modeling offshore New Jersey	IODP	121
Riller, U., Poelchau, M., Rae, A.S.P., Kring, D., Grieve, R.A.F., Lofi, J., Morgan, J., Gulick, S., IODP Expedition 364 Science Party	Mechanisms of deformation during peak-ring formation of large impact structures inferred from Expedition 364 drill core	IODP	121
Rösner, A., Kopf, A., Saffer, D., Toczko, S., Expedition 365 Scientists	Formation fluid pressure and temperature transients along the Nankai Trough Kumano Transect - SE Japan	IODP	122
Schäbitz, F., HSPDP- and CRC806-Team	Chew Bahir, the HSPDP drill site: half a million years of environmental history from southern Ethiopia	ICDP	122
Scheu, B., Caceres, F., Wadsworth, F., Hess, K.-U., Dingwell, D.B.	Decompression of Krafla magma: From immobile magma to explosive foaming?	ICDP	122
Schindlbeck, J.C., Kutterolf, S.	Tephrostratigraphy, provenance and cyclicities – Findings from Expeditions 350 and 352	IODP	123
Schuck, B., Janssen, C., Schleicher, A.M., Toy, V.G., Dresen, G.	Fault core deformation mechanisms deduced from microstructures, mineralogy and geochemistry of the Alpine Fault, New Zealand	ICDP	125
Schulte, F.M., Riller, U., Grieve, R.A.F., Kring, D.A., Claeys, Ph., IODP Expedition 364 Science Party	Structural characteristics of the impact melt rock and suevite of the Chicxulub Peak Ring – Initial results from IODP-ICDP Expedition 364	IODP	126
Schulze, N., Spiess, V., Daut, G., Haberzettl, T., Wang, J., Zhu, L.	ICDP seismic pre-site survey on Lake Nam Co (Tibetan Plateau)	ICDP	127
Schwab, M.J., Ahlborn, M., Tjallingii, R., Plessen, B., Neugebauer, I., Enzel, Y., Hasan, J., Brauer, A., Palex Scientific Team	The PALEX project –PALEohydrology and EXtreme Floods from the Dead Sea ICDP Core - First Years of Trilateral Dead Sea Research	ICDP	129
Schwenk, T., Spiess, V., Bergmann, F.	How did Pleistocene and Holocene sediments reach the sites of IODP Expedition 354 – an analysis of the surface channel pattern on the Bengal Fan	IODP	130
Simon, H., Buske, S., Flechsig, C., Günther, T., Nickschick, T.	Joint high-resolution seismic and large-scale geoelectrical surveys for characterization of the planned PIER-ICDP fluid monitoring site in the Eger Rift zone of NW-Bohemia	ICDP	130
Simon, H., Krauß, F., Buske, S., Giese, R., Hedin, P., Juhlin, C.	Seismic imaging in anisotropic crystalline environment at the COSC-1 borehole, central Sweden	ICDP	131
Spieß, V., Bergmann, F., Schwenk, T., Lantzsch, H., France-Lanord, C., IODP Expedition 354 Scientific Party	Structure and buildup of the Middle Bengal Fan at 8°N from multichannel seismic surveys and the IODP Expedition 354 drilling transect	IODP	133
Spieß, V., Reusch, A., Oberhänsli, H., Gebhardt, C., Abdrakmatov, K.	Long term tectonic and paleoclimatic history of Lake Issyk-Kul, Kyrgyzstan - preliminary results from an ICDP-related deep seismic pre-site survey campaign	ICDP	133

Spieß, V., Sacchi, M., De Natale, D., Steinmann, L.	Report about a Magellan+ Workshop in February 2017: <i>Structure and Evolution of Magmatic and Hydrothermal Volcanic Systems in offshore collapse/resurgent calderas - Development of an IODP Drilling Proposal at Campi Flegrei linking to active ICDP Drilling Initiatives</i>	ICDP & IODP	134
Steinig, S., Flögel, S., Park, W., Latif, M., Dummann, W., Hofmann, P., Wagner, T., Herrle, J.O.	Early Cretaceous climate and arctic variability in the Kiel Climate Model	IODP	135
Steinmann, L., Spiess, V.	Shallow structures of the marine Campi Flegrei Caldera and the volcanoclastic and sedimentary deposits in the Bay of Naples	ICDP	137
Stranghöner, M., Behrens, H., Dultz, S., Schippers, A.	Interface driven Fe transfer from volcanic rocks of ICDP site Hawaii to ocean surface waters	ICDP	138
Süfke, F., Gutjahr, M., Gilli, A., Anselmetti, F., Glur, L., Eisenhauer, A.	Isotopic chemical weathering behaviour of Pb derived from a high-Alpine Holocene lake-sediment record	ICDP	138
Thomas, A., Reiche, S., Riedel, M., Buske, S.	Seismic interpretation of Miocene sequences and facies distribution model, New Jersey shelf	IODP	139
Tiedemann, R., Krüger, J., Havenstein, K., Trauth, M.H., Henneberger, K., Hartmann, S., Hofreiter, M.	DNA-Metabarcoding of phyto- and zooplankton in East African lake sediments as proxies for past environmental perturbation	ICDP	140
Turner, S., Schippers, A.	Microbial nitrogen cycling potential in deep sediments of the Baltic Sea	IODP	140
Umlauf J., Flores Estrella, H., Korn, M.	Imaging fluid channels within the NW Bohemia/Vogtland region using ambient seismic noise and MFP Analysis	ICDP	140
Uenzelmann-Neben, G.	Prydz Bay sediment drifts: Archives of modifications in East Antarctic climatic and oceanographic conditions	IODP	141
Voigt, J., Hathorne, E.C., Fietzke, J., Pälike, H.	Dissolution and recrystallisation in planktonic foraminifera	IODP	142
Vuillemin, A., Kallmeyer, J., Kemnitz, H., Wirth, R., Luecke, A., Mayr, C., Schuessler, J.A., Henny, C., Crowe, S.A., Russell, J.M., Bijaksana, S., Vogel, H., ICDP Towuti Drilling Project Science Team	Isotopic record of diagenetic siderites from Lake Towuti's ferruginous sequence, Indonesia.	ICDP	143
Wang, M., Namur, O., Almeev, R., Charlier, B., Neave, D A., Holtz, F.	Petrogenesis of Snake River Plain basalts from the Kimama core and an experimental study on the link with associated rhyolites	ICDP	144
Weber, M.E., Dekens, P.S., Reilly, B.T., Lantzsch, H., Selkin, P.A., Das, S.K., Williams, T., Martos Martin, Y., Adhikari, R.R., Gyawali, B.R., Jia, G., Fox, L.R., Ge, J., Manoj, M.C., Savian, J.F., Meynadier, L., Adhikari, R.R., Spiess, V., France-Lanord, C., IODP Expedition 354 Scientists	Chronology of the Lower Bengal Fan (IODP Expedition 354) for the Late Quaternary – paleoclimate implications	IODP	146
Weber, T., Saynisch, J., Uenzelmann-Neben, G., Thomas, M.	Transport, Removal and Accumulation of sediments Numerically Simulated for Paleo-Oceans and Reconstructed from cores of The Eirik Drift (TRANSPORTED)	IODP	147
Westerhold, T., Röhl, U., Frederichs, T., Agnini, C., Raffi, I., Wilkens, R.H., Zachos, J.C.	Astronomical Calibration of the Ypresian Geomagnetic Polarity Time Scale: Implications for Seafloor Spreading Rates and the Chaotic Behaviour of the Solar System?	IODP	148
Wilke, T., Wagner, B., Albrecht, C., Francke, A., Hauffe, T., Jovanovska, E., Stelbrink, B., SCOPSCO Science Team	Integration of geological and biological histories: Unraveling drivers of diversification in ancient Lake Ohrid	ICDP	149
Wilkens, R.H., Westerhold, T., Drury, A.J., Lyle, M., Gorgas, T., Tian, J.	Code for Ocean Drilling Data (CODD) - A New Tool for Integrating Complex Data Streams and Advancing Astronomical Tuning	IODP	151
Wittke, A., Gussone, N., März, C., Teichert, B.M.A.	Effect of sampling techniques on Ca concentrations and isotope ratios of marine porewaters	IODP	152

Wojewódka, M., Zawisza, E., Szeroczyńska, K., Cohuo, S., Macario-Gonzalez, L., Perez, L., Kutterolf, S., Schwalb, A.	Subfossil Cladocera assemblages in Lake Petén Itzá (Guatemala) sediments	ICDP	153
Wojewódka, M., Zawisza, E., Szeroczyńska, K., Cohuo, S., Macario-Gonzalez, L., Perez, L., Schwalb, A.	The Cladocera community of Central America - ecology and distribution	ICDP	154
Wörmer, L., Hoshino, T., Viehweger, B., Morono, Y., Inagaki, F., Hinrichs, K.-U.	Massive contribution of bacterial endospores to the marine deep biosphere – a global view (Project SPP 527/35 HI 616/17-1)	IODP	154
Yilmaz, T.I., Gilg, H.A., Janots, E., Mayer, K., Hess, K.-U., Nakada, S., Dingwell, D.B.	Chemistry, mineralogy and hydrothermal alteration of the Mt Unzen conduit (Shimabara/Japan)	ICDP	156
Zhang, C., Koepke, J., R. Meyer, R., Namur, O., Feig, S.	Origin of the primitive layered gabbros from Hess Deep (EPR; IODP Expedition 345): Insights from mineral trace elements and MORB-peridotite interaction experiments	IODP	156

Fahrtberichte

Short Expedition Report: IODP Exp. 357, Atlantis Massif Serpentinization and Life

J.H. BEHRMANN¹, G.L. FRÜH-GREEN², B.N. ORCUTT³, S. GREEN⁴
C. COTTERILL⁴ AND THE EXPEDITION 357 SCIENTISTS

¹ GEOMAR Helmholtz Centre for Ocean Research Kiel, Wischhofstr. 1-3, 24148 Kiel, Germany

² Institute of Geochemistry and Petrology, ETH Zürich, Clausiusstrasse 25, NW E 76.2, CH-8092 Zürich, Switzerland

³ Bigelow Laboratory for Ocean Sciences 60 Bigelow Drive, PO Box 380, East Boothbay ME 04544, USA

⁴ ECORD Science Operator, British Geological Survey, The Lyell Centre, Research Avenue South, Edinburgh EH14 4AP, United Kingdom

During the offshore part of the scientific activities (26 October to 11 December 2015) International Ocean Discovery Program (IODP) Expedition 357 successfully cored an east–west transect across the southern wall of Atlantis Massif. The onshore part of the expedition, comprising the description and sampling of the cores took place at MARUM, University of Bremen, Germany, from 20 January to 5 February, 2016. Atlantis Massif is an oceanic core complex below a major detachment zone on the western flank of the Mid-Atlantic Ridge. It is mainly composed of mafic igneous rocks and variably serpentinized ultramafics. Principal objective was to study links between serpentinization processes and microbial activity in the shallow subsurface of highly altered ultramafic and mafic sequences. The expedition examined the role of serpentinization in driving hydrothermal systems, sustaining microbial communities, and sequestering carbon, characterized the tectonomagmatic processes causing lithospheric heterogeneity and low-angle faulting, and studied the abiotic and biotic processes associated with the different in rock types and their progressive exposure at the seafloor.

Seventeen holes were drilled at nine sites across Atlantis Massif, essentially along an east-west traverse near the southern wall. Two sites are located on the eastern end (Sites M0068 and M0075), three in the central section near the Lost City hydrothermal field (Sites M0069, M0072, and M0076), and two sites at the western end (Sites M0071 and M0073). Two additional ones were drilled north of the southern wall in the direction of the central dome of Atlantis Massif (Sites M0070 and M0074), geographically connected to IODP Site U1309. The use of seabed rock drills resulted in more than 57 m of core, with borehole penetration ranging from 1.3 to 16.44 meters below seafloor, and core recoveries as high as 75% of total penetration. This was achieved despite technically challenging rock types such as serpentinites, talc schists, shear zone rocks and breccias. Such a high level of recovery of shallow mantle rock sequences is unprecedented in the history of ocean drilling. Lithology in the cores recovered along the southern wall of Atlantis Massif is highly heterogeneous, with respect to protolith, types of alteration, and degrees of deformation. The ultramafic rocks are mostly harzburgites with intercalated

dunite, and cut by minor pyroxenite veins. Gabbroic rocks occur as melt impregnations and veins. These provide valuable insight into early magmatic processes and the magmatic evolution of the southern part of Atlantis Massif. Dolerite dikes and basaltic rocks are late-stage manifestations of magmatic activity.

Overall, the ultramafic rocks recovered during Expedition 357 showed strong of serpentinization, as well as metasomatic alteration to talc-amphibole-chlorite schists, and local formation of rodingite. Metasomatism postdates an earlier phase of serpentinization, but predates the intrusion and alteration of dolerite dikes, and the extrusion of basalt. The intensity of alteration is generally lower in the gabbroic and doleritic rocks than in the ultramafics. Important observations from Site M0075 are chilled margins in dolerite intruded into talc-amphibole-chlorite. Natural deformation in the cores is widespread, but variable, and dominated by brecciation and formation of localized shear zones. The amount of carbonate veins found was lower than anticipated. All variably altered and deformed ultramafic and mafic rocks occur as components in sedimentary breccias and as fault scarp rubble. Where found the overlying sedimentary rocks include basaltic breccias with a carbonate sand matrix and/or fossiliferous carbonate. Fresh glass on basaltic components was documented in some of the breccias. A more detailed descriptive account of shipboard and early shorebased work results can be found in Früh-Green et al. (2016).

A range of technologies new to IODP was successfully applied during Expedition 357. Firstly there was extensive use of an *in situ* sensor package and water sampling system. This was mounted to the seabed drills to analyze in real-time dissolved oxygen and methane, pH, oxidation-reduction potential, temperature, and conductivity. Secondly a borehole plug system was deployed to seal boreholes at four sites, to allow access for future sampling. Thirdly it was proved that tracers may be delivered into drilling fluids when using seabed drills. The sensor packages and water sampling enabled detection of elevated dissolved methane and hydrogen concentrations during and/or after drilling, with significant hydrogen observed over Sites M0068–M0072 and methane over Sites M0070–M0072. Shipboard determination of contamination confirmed appropriate sample handling procedures for microbiological and geochemical analyses. This will aid all microbiological investigations, and verifies this new tracer delivery technology for seabed drill rigs. Shipboard investigation of biomass density in select samples showed relatively low and variable cell densities. Shipboard enrichment experiments revealed growth. Thus, it is anticipated to achieve many of the objectives of the expedition related to deep biosphere questions.

Although not an objective of the expedition, a high-resolution (20 m) multibeam bathymetry map across the entire Atlantis Massif, the fracture zone to the south, and the off-axis eastern conjugate side of the spreading ridge segment, was generated during the expedition. This was to take advantage of weather and operational downtime, and led to a high quality base map to support post-expedition research and scientific interpretation of Atlantis Massif.

Reference:

Früh-Green, G.L., Orcutt, B.N., Green, S., Cotterill, C., and the Expedition 357 Scientists, 2016. *Expedition 357 Preliminary Report: Atlantis Massif Serpentinization and Life*. International Ocean Discovery Program. <http://dx.doi.org/10.14379/iodp.pr.357.2016>

IODP Expedition 361 – Southern African Climates and Agulhas LGM Density Profile

J. GRÜTZNER¹, J. JUST², A. KOUTSODENDRIS³, D. TANGUNAN⁴, I. HALL⁵, S. HEMMING⁶, L. LEVAY⁷ AND EXPEDITION 361 SCIENTISTS

¹ Alfred-Wegener Institute for Polar and Marine Research, Bremerhaven, Germany

² Institute of Geology and Mineralogy, University of Cologne, Cologne, Germany

³ Institute of Earth Science, Heidelberg University, Heidelberg, Germany

⁴ Department of Geosciences, University of Bremen, Bremen, Germany

⁵ School of Earth and Ocean Sciences, Cardiff University, Cardiff, UK

⁶ Department of Earth and Environmental Sciences, Lamont-Doherty Earth Observatory of Columbia University, Palisades NY, USA

⁷ International Ocean Discovery Program, Texas A&M University, College Station, USA

IODP Expedition 361 drilled six sites (U1474 – U1479) on the southeast African margin and the Indian-Atlantic ocean gateway from 30 January to 31 March 2016. The sites, situated in the Mozambique Channel, Natal Valley, Agulhas Plateau, and Cape Basin, were targeted to reconstruct the history of the Greater Agulhas Current System over the past ~5 Ma (Fig. 1). More specifically, the main objectives of Expedition 361 were: (i) to establish the sensitivity of the Agulhas Current to climate change during the Plio-Pleistocene in association with transient to long-term changes of high-latitude climates, tropical heat budgets, and the monsoon system; (ii) to determine the dynamics of the Indian-Atlantic gateway circulation in association with changing wind fields and migrating ocean fronts; (iii) to examine the connection of the Agulhas leakage and the Atlantic Meridional Overturning Circulation; (iv) to address the influence of the Agulhas Current on African terrestrial climates, notably rainfall patterns and river runoff, and potential links to hominid evolution. Additionally, the expedition set out to fulfill the needs of the Ancillary Project Letter, consisting of high-resolution interstitial water samples aiming at constraining the temperature and salinity profiles of the ocean during the Last Glacial Maximum.

In total, 5175 m of core was recovered (average recovery 102 %) from a region poorly represented in the database of drill sites for scientific purposes. Physical property records derived from core-logging of the recovered sequences allowed complete spliced stratigraphic sections to be generated that span the interval of 0 to between ~0.13 and 7 Ma (Fig. 2). A high-resolution program of interstitial water samples was carried out at Sites U1474, U1475, U1476, and U1478. The expedition made major strides toward fulfilling the scientific objectives despite of ~11 days of lost operational time due to weather conditions, a medical evacuation, and delays in attaining the necessary permissions to operate in Mozambique exclusive economic zone waters.

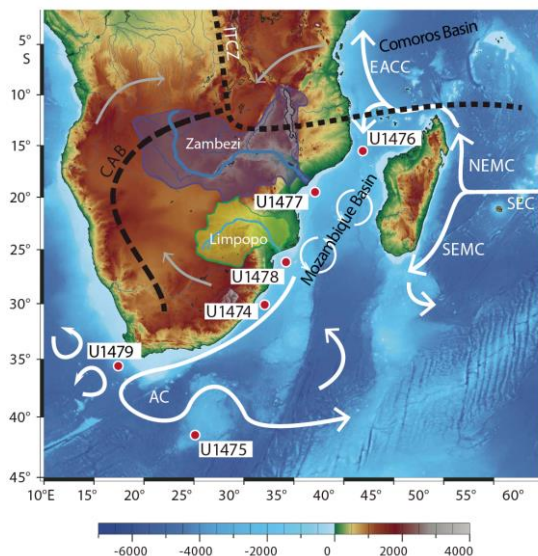


Figure 1: Expedition 361 site locations. Yellow and orange arrows: main surface ocean currents; gray arrows: main pathways of moisture supply to the African continent from the northwest Atlantic (via Congo) and the northwest and southwest Indian Ocean; dashed lines: approximate position of the Intertropical Convergence Zone (ITCZ) and Congo Air Boundary (CAB); purple shaded area: Zambezi Catchment; green shaded area: Limpopo Catchment. AC: Agulhas Current; SEC: South Equatorial Current; SEMC: South East Madagascar Current; NEMC: North East Madagascar Current; EACC: East Africa Coastal Current (modified from Hall et al., 2016).

Site U1474 (3034 meters below sea level [mbsl]; Fig. 1), located in the northernmost Natal Valley, consists of eight holes ranging in penetration depth from 3.1 to 254.1 m drilling depth below seafloor (dsf). A total of 910.8 m of sediment was recovered, predominantly consisting of foraminifer-bearing clay with nanofossils. Based on the shipboard bio- and magnetostratigraphic datums, the sedimentary sequence extends back to the late Miocene (~6.2 Ma; Fig. 2). This record represents the only site situated beneath the main flow of the fully constituted Agulhas Current and therefore provides the opportunity for high-resolution climate reconstructions of Agulhas Current warm-water transports and upstream variability that may allow the identification of connections between Agulhas leakage and its headwater variability. It also holds significant potential to investigate the connections between southern African terrestrial climates and southeast Indian Ocean heat budgets and the links to the cultural evolution of early modern humans.

Site U1475 (2669 mbsl; Fig. 1), located on the southwestern flank of the Agulhas Plateau, consists of six holes ranging in penetration depth from 1.5 to 277.0 m dsf. A total of 1015.9 m of sediment was recovered, predominantly consisting of nanofossil ooze. Shipboard bio- and magnetostratigraphic data suggest that the sedimentary sequence extends back to the late Miocene (~7 Ma; Fig. 2). This record provides the opportunity for high-resolution climate reconstructions of the Agulhas Return Current and connections with the Subtropical Front, productivity, and deep-water circulation.

Site U1476 (2165 mbsl; Fig. 1), located at the northern entrance of the Mozambique Channel, consists of five holes ranging in penetration depth from 5.7 to 234.8 m dsf.

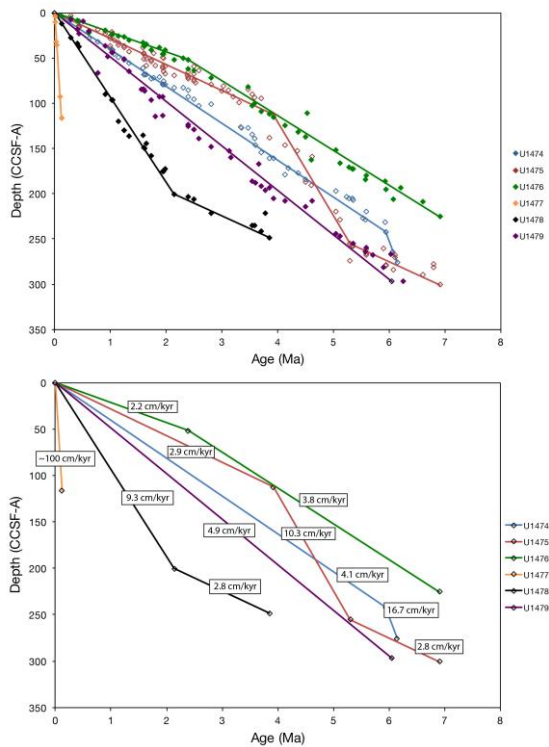


Figure 2: Age-depth relationships, IODP Sites U1474–U1479. A. Time estimates based on a mixture of major planktonic foraminifer, calcareous nannoplankton, diatom, and paleomagnetic datums. B. Implied sedimentation rates (adapted from Hall et al., 2016).

A total of 873.8 m of sediment was recovered, predominantly consisting of foraminifer-rich nannofossil ooze. The sedimentary sequence extends back to the late Miocene (~6.9 Ma; Fig. 2), as inferred from the shipboard bio- and magnetostratigraphic data. The site boasts excellent biostratigraphy and notably cyclic physical properties. It therefore provides the opportunity for high-resolution reconstructions of tropical faunal assemblages, which will allow identification of connections between Agulhas leakage and its headwater variability. It also holds significant potential to investigate the connections between southern African terrestrial climates and southeast Indian Ocean heat budgets and thermocline and deep-water variability with likely links to the development of the Indonesian Throughflow as well as aridification of east Africa. Because of the excellent preservation of foraminifers, this is an ideal site for a long record of surface-ocean pH from boron isotopes.

Site U1477 (429 mbsl; Fig. 1), located in the western Mozambique Channel east of the Zambezi River delta, consists of three holes ranging in penetration depth from 119.4 to 181.2 m dsf. A total of 490.0 m of sediment was recovered, predominantly consisting of sandy clay with foraminifers and nannofossils. Based on correlations to a nearby ^{14}C dated cores and two biostratigraphic markers, the sedimentary sequence extends back to the Late Pleistocene (~0.13 Ma; Fig. 2). The extreme accumulation rate (~1 m/ky) at this site provides the opportunity for exceptionally high resolution reconstructions of terrestrial climate and thermocline characteristics during the last glacial cycle.

Site U1478 (488 mbsl; Fig. 1), located in the western Mozambique Channel east of the Limpopo River delta, consists of four holes ranging in penetration depth from

216.0 to 248.4 m dsf. A total of 922.1 m of sediment was recovered, predominantly consisting of sand or clayey/sandy silt with foraminifers and nannofossils. The shipboard age-model suggests that the sedimentary sequence extends back to the Pliocene (~4 Ma; Fig. 2). This record provides the opportunity for high-resolution climate reconstructions of faunal, biogeochemical, and terrigenous tracers that are characteristic of the upper reaches of the Agulhas Current warm-water transports that will allow connections between Agulhas leakage and its headwater variability. The site also holds significant potential to investigate the connections between southern African terrestrial climates and southeast Indian Ocean heat budgets, and examine the relationship between such climate variability and early human evolution.

Site U1479 (2615 mbsl; Fig. 1), located in Cape Basin, consists of nine holes ranging in penetration depth from 1.0 to 300.7 m dsf. A total of 963.1 m of sediment was recovered, predominantly consisting of nannofossil ooze with or without foraminifers. According to the shipboard bio- and magnetostratigraphy-based age model, the sedimentary sequence extends back to the late Miocene (~7 Ma; Fig. 2). This record represents the only site situated in the immediate Agulhas leakage pathway. It will therefore provide the opportunity for high-resolution climate reconstructions of the leakage and temporal comparisons with deep-water circulation.

Reference:

Hall, I.R., Hemming, S.R., LeVay, L.J., and the Expedition 361 Scientists, 2016. Expedition 361 Preliminary Report: South African Climates (Agulhas LGM Density Profile). International Ocean Discovery Program. <http://dx.doi.org/10.14379/iodp.pr.361.2016>

Report on IODP Expedition 362: Drilling the inputs to the Sumatra subduction zone

A. HÜPERS¹, S. KUTTEROLF², L. M. MCNEILL³, B. DUGAN⁴, K. PETRONOTIS⁵ AND THE EXPEDITION 362 SHIPBOARD SCIENTISTS

¹ MARUM-Center for Marine Environmental Sciences, University of Bremen, Bremen, Germany, ahuepers@uni-bremen.de

² GEOMAR, Helmholtz Center for Ocean Research, Kiel, Germany

³ Ocean and Earth Science, National Oceanography Centre Southampton, University of Southampton, Southampton, United Kingdom

⁴ Department of Geophysics, Colorado School of Mines, Golden, USA

⁵ International Ocean Discovery Program, Texas A&M University, College Station, USA

From August 6 to October 6 2016 International Ocean Discovery Program (IODP) Expedition 362 logged and sampled the Indian oceanic plate lithostratigraphy incoming to the North Sumatra subduction zone where the devastating Mw ~9.2 earthquake and tsunami took place in December 2004. Two sites (Sites U1480 and U1481) were drilled down to a maximum depth of 1500 meters below seafloor (mbsf) approximately 250 km seaward of the deformation front to groundtruth the material properties causing the unexpectedly shallow seismogenic slip and a distinctive forearc prism structure of the North Sumatra subduction zone.

Preliminary assessment of the identified primary lithologies, mineralogy, depositional environments and sediment accumulation rates shows that the oceanic

basement is covered by Late Cretaceous to Miocene abyssal-plain environment facies consisting of mixed tuffaceous and pelagic sediments and a series of intercalated pelagic and igneous materials. Subsequently a thick sequence of siliciclastic sediments (mostly siliciclastic mud, siliciclastic sand and calcareous mud) is emplaced associated with the Nicobar fan. Shipboard physical property measurements provided insights into the consolidation state, strength, and deformation of the input sediments showing that two zones of anomalous porosity exist at Site U1480, one indicating undercompaction and one indicating overcompaction. In addition to mechanical compaction, some isolated intervals with calcite cementation were observed; primarily as calcite-cemented sandstones. Geochemical profiles of the dissolved constituents in the pore fluids reflect the combined effects of organic matter diagenesis, alteration of volcanogenic sediments, calcite-cementation and reactions in oceanic basement. In the deeper pre-Nicobar Fan sequence pore fluid freshening was observed, indicated by a very sharp chloride change. A preliminary interpretation is that this reflects the first in a series of dehydration reactions that could affect the development of fluid pressures and sediment strength as the sediment approaches the subduction zone.

In summary, the cores recovered in combination with successful wireline logging provide an excellent foundation for further postcruise experimental and modeling studies to shed light on the evolving properties of the sediment incoming to the North Sumatra subduction zone and the potential effect of these properties on seismogenesis, tsunamigenesis, and forearc development.

IODP Expedition 363 “Western Pacific Warm Pool”

A. HOLBOURN, Y. ROSENTHAL, D. KULHANEK³, A.J. DRURY⁴ AND THE EXPEDITION 363 SHIPBOARD SCIENTIFIC PARTY

¹ Institute of Geosciences, Christian-Albrechts-Universität zu Kiel, 24118 Kiel, Germany

² Institute of Marine and Coastal Sciences Rutgers, The State University of New Jersey, New Brunswick NJ 08901-8521, USA

³ International Ocean Discovery Program Texas A&M University College Station TX 77845, USA

⁴ MARUM, University of Bremen, 28359 Bremen, Germany

International Ocean Discovery Program (IODP) Expedition 363 (October 6th to December 8th 2016) sought to document the regional expression (e.g., temperature, precipitation, and productivity) and driving mechanisms of Neogene climate variability in the Western Pacific Warm Pool (WPWP), as they relate to the evolution of Earth’s climate on millennial, orbital and geological timescales. To achieve these objectives, sites were chosen to provide broad spatial coverage in order to capture the most salient features of the WPWP (Figure 1). Nine sites were cored with R/V “JOIDES Resolution” recovering a record total of 6956 m of sediment cores in 875–3421 m water depth with an average recovery of 101.3% during 39.6 days of on-site operations (Rosenthal, Holbourn, Kulhanek et al., in press). Most of the sites were cored primarily using the Advanced Piston Coring (APC) system until refusal, generally between 250 and 350 meters below sea floor (mbsf) (Figure 2). Below this depth the Half-Length APC (HLAPC) and Extended Core Barrel (XCB) systems were used. Downhole logging was conducted in one hole (U1482C), which was cored to 534 mbsf, on the

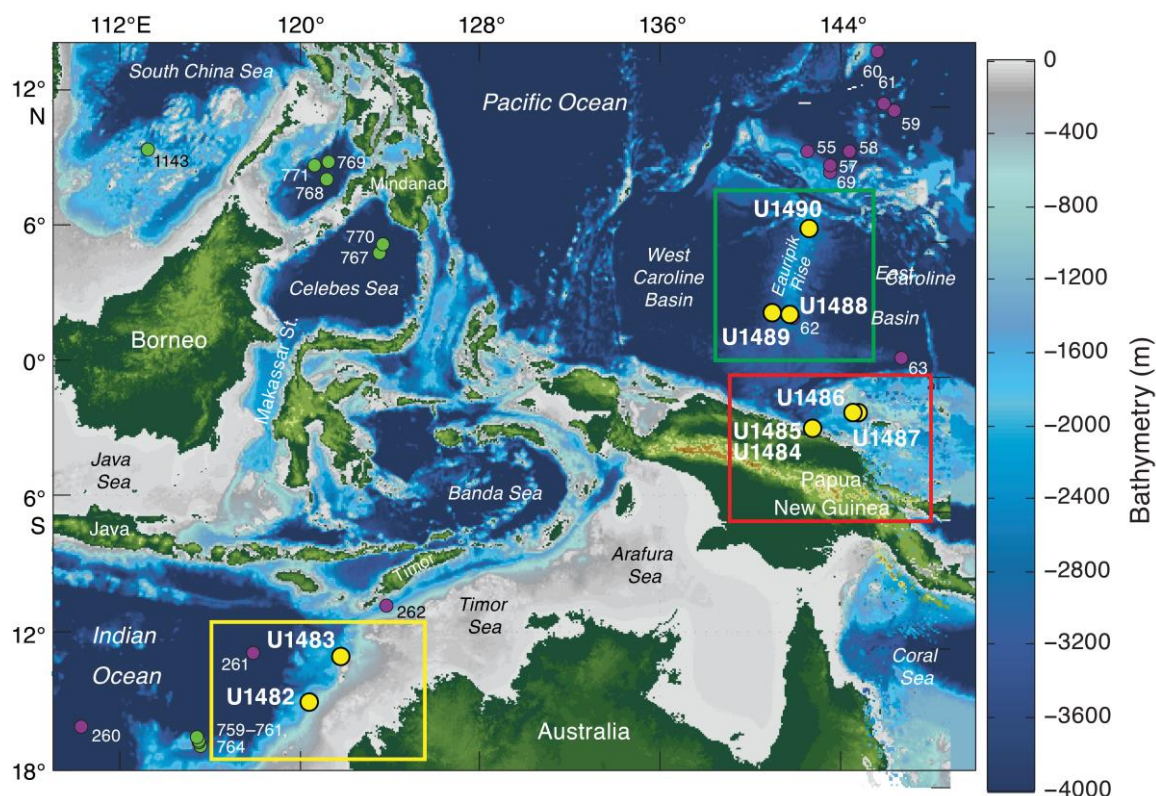


Figure 1: Bathymetric map showing locations of the three main areas cored during IODP Expedition 363: northwestern Australian shelf, Papua New Guinea/Manus Basin, and Eauripik Rise, from Rosenthal, Holbourn, Kulhanek et al., in press. Yellow circles = Expedition 363 sites, purple and green circles = previously cored DSDP and ODP sites.

northwestern Australian margin. Overall, clement weather and smooth seas allowed for speedy transits to drilling locations, and there was no significant loss of operational time due to mechanical breakdown or equipment damage.

Combining sites with rapidly accumulating sediment at marginal locations and more typical open-ocean sites with relatively low accumulation rates offers the opportunity to retrace the evolution of the WPWP through the Neogene at different temporal resolutions. Furthermore, spanning a large range of water depth (Figure 2), the sites allow reconstruction of the thermocline and intermediate water contributions from the Northern and Southern Hemispheres to the low-latitude inter-ocean exchange through the Indonesian Throughflow (ITF), as well as monitoring of water mass changes in response to tectonic- and/or climate-related processes. Two of the sites are located off northwestern Australia at the southwestern edge of the WPWP, spanning the late Miocene to present. Seven sites are situated in the core area of the WPWP including two on the northern margin of Papua New Guinea (PNG) with very high sedimentation rates spanning the last ~450 ky. Two sites were drilled in the Manus Basin north of PNG with moderate sedimentation rates recovering upper Pliocene to present sequences, and three low-sedimentation rate sites are located on the southern and northern parts of the Eauripik Rise spanning the early Miocene to present.

Previous studies of long-term climate variability in the WPWP relied primarily on the low sedimentation-rate (~2–3 cm/ky over the Pleistocene and most of the Miocene) Ocean Drilling Program (ODP) Site 806 on the Ontong Java Plateau (Kroenke, Berger, Janecek, et al., 1991), which serves as a warm end-member to monitor broad-scale zonal and meridional gradients through the Neogene (e.g., LaRiviere et al., 2012; Zhang et al., 2014). However, the lack of higher resolution WPWP records has prevented resolution of orbital and suborbital variability, inhibiting detailed comparisons across basins and precise correlation with high-latitude climatic events. Thus, variations in the interhemispheric thermal gradient under different climate

background states and changes in water mass structure within the WPWP, which is a crossroad for thermocline and intermediate waters originating from the high latitudes of both hemispheres, remain largely enigmatic over most of the Neogene. Furthermore, considerable uncertainty exists regarding the response of the tropical Pacific climate to rising greenhouse gas concentrations due to our limited understanding of the WPWP past variability and conflicting results from data and model simulations

With excellent recovery, IODP Expedition 363 sites are ideal for detailed paleoceanographic reconstructions at orbital and suborbital resolution from the middle Miocene to Pleistocene (Rosenthal, Holbourn, Kulhanek et al., in press). High-resolution interstitial water sampling at selected sites will be used to reconstruct density profiles of the western equatorial Pacific deep water during the Last Glacial Maximum. Recovery of expanded upper Pleistocene sequences will provide the opportunity to reconstruct climate variations with exceptional resolution comparable to that of ice cores, North Atlantic sediment drifts and Southeast Asian speleothem records. Extended Neogene climate archives will be used to monitor the long-term behavior of the WPWP under different mean-state background conditions and to refine the astronomical tuning, magneto-, isotope, and biostratigraphy of hitherto poorly constrained intervals of the Geological Timescale, specifically within the late Miocene. The late Miocene to early Pliocene interval is of primary interest and a main research target for the two German participants on IODP Expedition 363 (Anna Joy Drury and Ann Holbourn), as it offers an unmatched opportunity to explore climate-carbon cycle dynamics in a warmer-than-today Earth, to investigate the impact of WPWP variations on the Australian Monsoon, the ITF and zonal equatorial Pacific processes (e.g. past El-Niño), and, thus, help guide models and constrain predictions of climate change and sensitivity.

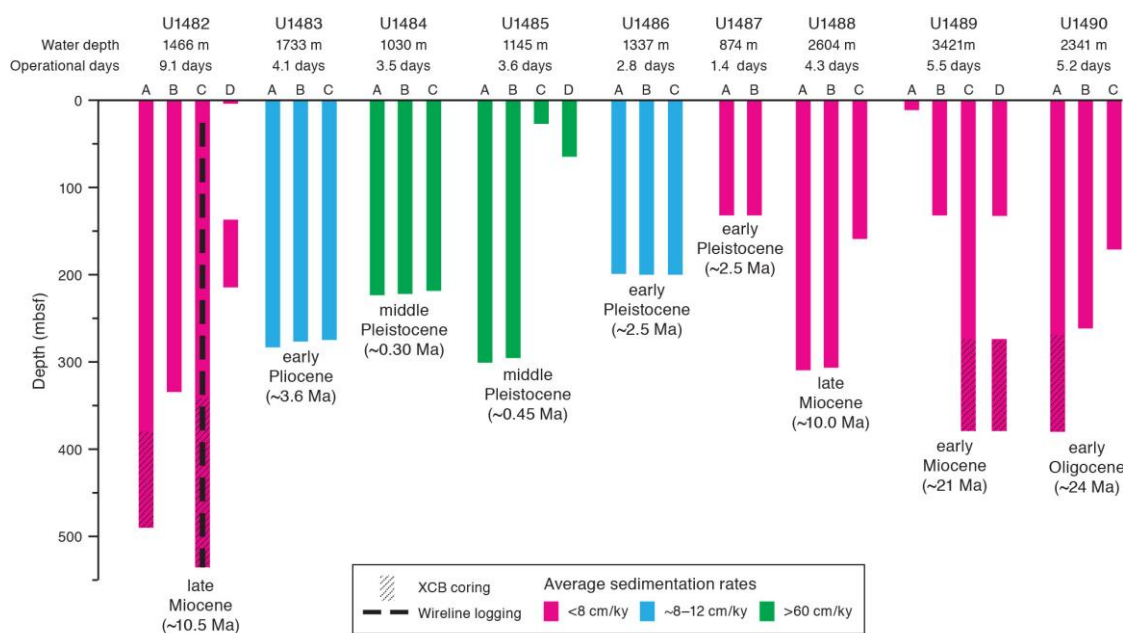


Figure 2: Summary of core recovery and temporal resolution of IODP Expedition 363 drill sites from Rosenthal, Holbourn, Kulhanek et al., in press.

References:

- Kroenke, L.W., Berger, W.H., Janecek, T.R., et al 1991. *Proceedings of the Ocean Drilling Program, Initial Reports* 130, College Station, TX, Ocean Drilling Program. <http://dx.doi.org/10.2973/odp.proc.ir.130.1991>
- LaRiviere, J.P., Ravelo, A.C., Crimmins, A., Dekens, P.S., Ford, H.L., Lyle, M., and Wara, M.W., 2012. Late Miocene decoupling of oceanic warmth and atmospheric carbon dioxide forcing. *Nature* 486 (7401), 97–100. <http://dx.doi.org/10.1038/nature11200>
- Rosenthal, Y., Holbourn, A., Kulhanek, D.K., and the Expedition 363 Scientists, in press. *Expedition 363 Preliminary Report: Western Pacific Warm Pool*. International Ocean Discovery Program. <http://dx.doi.org/10.14379/iodp.pr.363.2017>
- Zhang, Y.G., Pagani, M., and Liu, Z., 2014. A 12-million-year temperature history of the tropical Pacific Ocean. *Science*, 344 (6179), 84–87. <http://dx.doi.org/10.1126/science.1246172>

IODP-ICDP Expedition 364: Drilling the Peak Ring of the Chicxulub Impact Crater

M. H. POELCHAU¹, U. RILLER², C. GEBHARDT³, J. MORGAN⁴, S. GULICK⁵, AND EXPEDITION 364 SCIENTISTS

¹ University of Freiburg, Geology, Freiburg, Germany

² Institut für Geologie, Universität Hamburg, Hamburg, Germany

³ Alfred Wegener Institute, Bremerhaven, Germany

⁴ Department of Earth Science and Engineering, Imperial College London, UK

⁵ Institute for Geophysics, University of Texas, Austin, TX, USA

During April and May 2016, IODP and ICDP jointly drilled the peak ring of the Chicxulub impact crater in Mexico. The ~200 km wide Chicxulub crater was formed at the end of the Cretaceous by an asteroid impact into the Yucatán Peninsula and is now buried under hundreds of meters of platform sediments. Seismic surveys and other geophysical methods have imaged the crater's internal structure, and show a well-preserved peak ring within the crater. Peak rings are mountainous, sometimes discontinuous rings that rise above the crater floor and are internal to the crater rim, and while commonly observed in large impact craters on other planetary bodies, are only rarely found on Earth in such a pristine state as in the Chicxulub crater.

The prime objectives of Expedition 364 are to investigate: (1) the nature and formational mechanism of peak rings and test between two contrasting formation models, (2) how rocks are weakened during large impacts, (3) the nature and extent of postimpact hydrothermal circulation, (4) the deep biosphere and habitability of the peak ring, and (5) the recovery of life in a potentially sterile zone.

A single hole, M0077A, was drilled at ~21° 27' W, 89° 57' N using a jack-up platform, the L/B Myrtle, contracted from Montco Offshore. An Atlas Copco mining rig was cantilevered from the bow of the platform, and drilling services were provided by DOSECC. 829 m core were recovered using a PQ3-sized bit. The core diameter is ~83 mm and core recovery was close to 100%. Open hole drilling was performed from the sea floor at ~17 m below sea level for the first ~500 m. Coring of the peak ring began at 505.7 mbsf (meters below sea floor). The 829 m of core were halved and subject to standard IODP measurements at the MARUM /Universität Bremen from 21 September to 15 October, 2016.

The top ~110 m of core consists of post-impact Eocene and Paleocene sedimentary rocks (Fig. 1). These consist mainly of laminated marlstone, claystone, wackestone and packstone that transition to calcareous siltstone near the

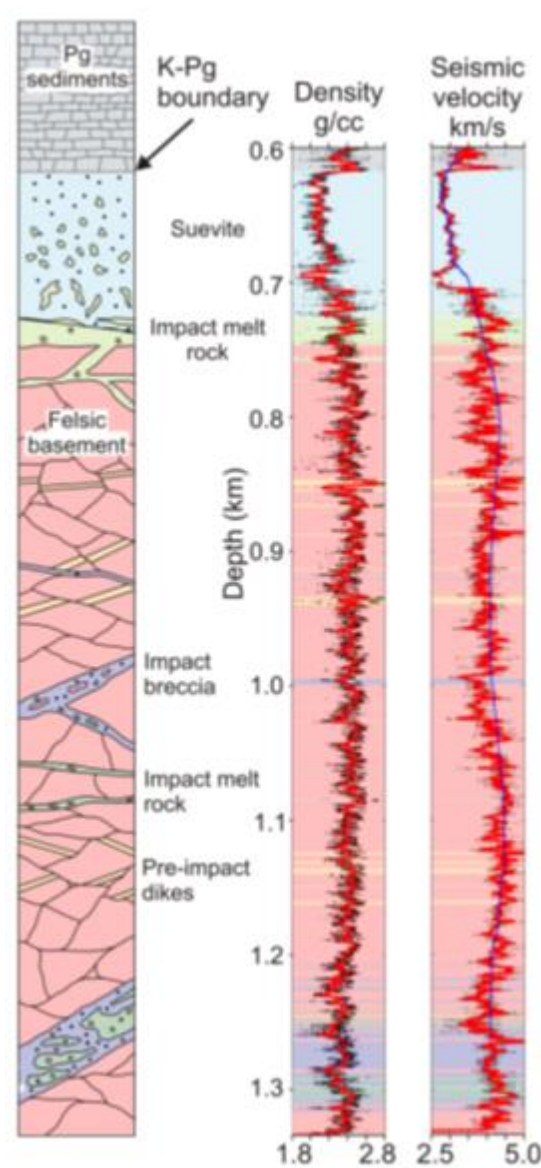


Figure 1

K-Pg boundary. The uppermost rocks of the peak ring of the impact crater were encountered at 617.34 mbsf and are a ~130 m thick succession of suevite and impact melt rock. The upper suevite shows signs of reworking and can be subdivided based on fining and coarsening upwards sequences. Both suevite and impact melt rock contain a lithologically diverse range of basement and sedimentary rock fragments.

A suite of granitoid rocks interspersed with minor pre-impact magmatic intrusions occurs below 747.1 mbsf down to the final coring depth of 1334.7 mbsf (Fig. 1). The granitoid rocks are pervasively affected by shock metamorphism and are remarkably brittle. These rocks contain several meter-sized bodies of impact melt rock and suevite. A ~58 m thick suevite and impact melt rock body is present near the bottom of the core. It is noteworthy that fragments in this body are purely basement rocks; sedimentary clasts are lacking. This result may suggest different sources for the top and basal suevites and impact melt rocks.

One of the main interests of the German participants of IODP-ICDP Expedition 364 lies in gaining a deeper

understanding of the deformation mechanisms that enable the formation of peak rings and large impact basins, and in particular unraveling the deformation history of the recovered peak ring rocks. Structural indicators for successive phases of deformation were observed during offshore and onshore coring and logging. Deformation in the granitoid rocks shows a large range of respective structures, including hairline fractures, sub-mm-thick brittle shear faults, mm- to cm-thick (ultra)cataclasites, striated shear planes that occasionally show multiple shear orientations, and dm-thick zones of foliated and crenulated mineral fabrics. Fractures and faults are observed throughout the granitoid cores. Spacing of prominent shear faults is typically on the order of one to several dm, but isolated portions of macroscopically undeformed granitic rock may reach 1-2 m. Some fractures and faults show multiple deformation episodes, and are potential indicators for the process of acoustic fluidization, which is a weakening mechanism theorized to be active during crater formation.

Preliminary orientation analysis of pre-impact magmatic dikes points to a lack of large differential rotations, in spite of the documented evidence for polyphase impact-induced structural evolution of the respective host rock. Thus, a large portion of the ~500 m succession of granitoid rocks may have behaved mechanically largely as a coherent block during crater excavation and modification. Large-scale thrusting of the drilled target rocks during peak-ring formation appears to have occurred without inducing internal rotation.

Finally, geophysical models published before the drilling show that the Chicxulub peak ring is formed from rocks with a relatively low seismic velocity and density. This finding appeared to contradict a numerical model for peak-ring formation that postulated that uplifted basement rocks form the peak ring, as crystalline basement typically has higher velocities and densities than those measured. Drilling confirmed that the Chicxulub peak ring is formed from felsic basement rocks that have a low velocity (3.9-4.5 km/s) and density (2.2-2.45 g/cm³; Fig. 1). The peak ring rocks must have been uplifted several kilometers because the felsic basement is covered by >3 km of Mesozoic sedimentary rock outside of the crater. Basement rocks that form the peak ring are highly fractured and shocked, and their position on top of downthrown Mesozoic sediments is consistent with the dynamic collapse model of peak-ring formation.

Expedition 364 Scientists: Elise Chenot, Gail Christeson, Philippe Claeys, Charles Cockell, Marco J. L. Coolen, Ludovic Ferrière, Catalina Gebhardt, Kazuhisa Goto, Sean Gulick, Heather Jones, David A. Kring, Johanna Lofi, Christopher Lowery, Claire Mellett, Joanna Morgan, Rubén Ocampo-Torres, Ligia Perez-Cruz, Annemarie Pickersgill, Michael Poelchau, Auriol Rae, Cornelia Rasmussen, Mario Rebolledo-Vieyra, Ulrich Riller, Honami Sato, Jan Smit, Sonia Tikoo, Naotaka Tomioka, Jaime Urrutia-Fucugauchi, Michael Whalen, Axel Wittmann, Long Xiao, Kosei Yamaguchi, William Zylberman.

Reference:

Morgan J. V. et al. (2016) *Science*, 354, 878-882.

Shallow observatory installations unravel earthquake processes in the Nankai accretionary complex (IODP Expedition 365)

KOPF A.¹, SAFFER D.M.², TOCZKO S.³, AND EXPEDITION SCIENTISTS 365.

¹. MARUM, Center for Marine Environmental Sciences, University of Bremen, Bremen, Germany

². Department of Geosciences, The Pennsylvania State University, USA

³. CDEX (Center for Deep Earth Exploration, Japan Agency for Marine-Earth Science and Technology), Yokohama Japan

NanTroSEIZE is a multi-expedition IODP project to investigate fault mechanics and seismogenesis along the Nankai Trough subduction zone through direct sampling, in situ measurements, and long-term monitoring. Recent Expedition 365 had three primary objectives at a major splay thrust fault (termed the “megasplay”) in the forearc: (1) retrieval of a temporary observatory (termed a GeniusPlug) that has been monitoring temperature and pore pressure within the fault zone at 400 meters below seafloor for since 2010; (2) deployment of a complex long-term borehole monitoring system (LTBMS) across the same fault; and (3) coring of key sections of the hanging wall, deformation zone and footwall of the shallow megasplay.

Expedition 365 achieved its primary monitoring objectives, including recovery of the GeniusPlug with a >5-year record of pressure and temperature conditions, geochemical samples, and its in situ microbial colonization experiment; and installation of the LTBMS. The pressure records from the GeniusPlug include high-quality records of formation and seafloor responses to multiple fault slip events, including the 2011 M9 Tohoku and the 1 April Mie-ken Nanto-oki M6 earthquakes. The geochemical sampling coils yielded in situ pore fluids from the fault zone, and microbes were successfully cultivated from the colonization unit. The LTBMS incorporates multi-level pore pressure sensing, a volumetric strainmeter, tiltmeter, geophone, broadband seismometer, accelerometer, and thermistor string. This multi-level hole completion is one of the most ambitious and sophisticated observatory installations in scientific ocean drilling (similar to that in Hole C0002G, deployed in 2010). Overall, the installation went smoothly, efficiently, and was connected to a real-time DONET seafloor cabled network for tsunami early warning and earthquake monitoring a few weeks after the expedition.

Coring the shallow megasplay site in the Nankai forearc presented challenging hole conditions. A total of four holes were required to recover ca. 100m of material across the fault zone, with >50% recovery for both zones. In the hangingwall of the megasplay fault, we recovered indurated silty clay with occasional ash layers and sedimentary breccias. The mudstones show different degrees of deformation spanning from occasional fractures to intensely fractured scaly claystones of up to >10 cm thickness. Sparse faulting with low displacement (usually <2 cm) is seen in both normal and, rarely, reverse sense of slip. When present, the ash was entrained along fractures and faults. The footwall sediments are horizontally to gently dipping and mainly comprise siltstones that are less indurated than the hangingwall mudstones. The material is less intensely deformed than the mudstones and represents

a wedge of slope apron deposits overridden by the megasplay. Post-cruise rock deformation experiments will relate physical properties to the earthquake response monitored by the observatory array.

Preliminary results from IODP Expedition 370 (Temperature Limit of the Deep Biosphere off Muroto, T-LIMIT)

V.B. HEUER¹, F. INAGAKI^{2,3}, Y. MORONO³, Y. KUBO⁴, S. HENKEL^{1,5}, F. SCHUBOTZ¹, B. VIEHWEGER¹, AND THE IODP EXPEDITION 370 SCIENTISTS

¹ MARUM – Center for Marine Environmental Sciences, University of Bremen, 28334 Bremen, Germany

² Research and Development Center for Ocean Drilling Science, Japan Agency for Marine-Earth Science and Technology (JAMSTEC), 3173-25 Showa-machi, Kanazawa-ku, Yokohama, Kanagawa 236-0001, Japan

³ Kochi Institute for Core Sample Research, JAMSTEC, Monobe B200, Nankoku, Kochi 783-8502, Japan

⁴ Center for Deep Earth Exploration, JAMSTEC, 3173-25 Showa-machi, Kanazawa-ku, Yokohama, Kanagawa 236-0001, Japan

⁵ Alfred Wegener Institute, Helmholtz Center for Polar and Marine Research, Am Handelshafen 12, 27570 Bremerhaven, Germany

IODP Expedition 370 (September 10 – November 23, 2016) aimed to explore the limits of life in the deep seafloor biosphere at a location where temperature increases with depth at an intermediate rate and exceeds the known temperature maximum of microbial life (~120°C) at the sediment/basement interface. Such conditions are met in the prot thrust zone of the Nankai Trough off Cape Muroto, Japan, where Expedition 370 established Site C0023 in the vicinity of ODP Sites 808 and 1174 at a water depth of 4776 m using DV Chikyu. Since Site C0023 is located ~125 km off Kochi Prefecture on Shikoku Island, selected samples could be transferred to the Kochi Core Center (KCC) by helicopter, where further sampling and analysis followed without delay in super-clean environment laboratories. Expedition 370 was the first expedition dedicated to seafloor microbiology that achieved time-critical processing and analyses of deep-sea samples by simultaneous shipboard and shore-based investigations.

In the course of nearly 50 years of scientific ocean drilling, microbial cells have been found everywhere, even in sediments of Cretaceous age (Roussel et al., 2008), in extremely nutrient poor sediments below the ocean gyres (D'Hondt et al., 2009, 2015), in the so far deepest sampled sediments retrieved from ~2500 meters below seafloor (mbsf) (Inagaki et al., 2015), and in basement rocks (Orcutt et al., 2011; Lever et al., 2013). Metabolic activities of deep seafloor microbes are extraordinary low (D'Hondt et al., 2002, 2004), but most deeply buried microbial cells are physiologically active (Morono et al., 2011) or quiescent as dormant phase or spore (Lomstein et al., 2012). The exact size of the seafloor biosphere is still a matter of debate (Parkes et al., 1994, 2000; Whitman et al., 1998; Lipp et al., 2008; Kallmeyer et al., 2012; Hinrichs and Inagaki, 2012). To date, the bottom of the deep seafloor biosphere has not been located, the biosphere-geosphere interactions at this important boundary have not been explored, and it remains to be resolved which factors pose ultimate limits to life in the seafloor environmental

setting. By addressing these scientific challenges, the International Ocean Discovery Program (IODP) aims to shed light on one of the largest continuous ecosystems on Earth (IODP Science Plan, Challenge 6 [<http://www.iodp.org/about-iodp/iodp-science-plan-2013-2023>]).

The primary objective of Expedition 370 was to study the relationship between the deep microbial biosphere and temperature (Hinrichs et al., 2016). Temperature is commonly used as the variable defining the deepest boundary of the deep biosphere in estimates of its size (Whitman et al., 1998; Parkes et al., 2000; Lipp et al., 2008; Heberling et al., 2010; Kallmeyer et al., 2012; Hinrichs and Inagaki, 2012; Parkes et al., 2014). The currently known upper temperature limit of life for microorganisms inhabiting comparatively energy rich hydrothermal vent environments is at around 120°C (Blöchl et al., 1997; Kashefi and Lovley, 2003; Takai et al., 2008). However, studies of petroleum biodegradation in deeply buried basins suggest that sterilization takes place at formation temperatures between 80° and 90°C (Head et al., 2003; Wilhelms et al., 2001), and this finding might be more relevant for the energy-limited deep seafloor biosphere.

Expedition 370 returned to Site 1174, where Ocean Drilling Program (ODP) Leg 190 had revealed the presence of microbial cells down to a depth of ~600 mbsf, which corresponds to an estimated temperature of ~70°C, and reliably identified a single zone of higher cell concentrations just above the décollement at around 800 mbsf, where temperature presumably reached 90°C; no cell counts were reported for other sediment layers in the 70-120°C range, possibly because at that time the detection limit of manual cell counting (~10⁵ cells/cm³) was too high for the low-biomass samples (Moore, Taira, Klaus, et al., 2001). With the establishment of Site C0023, we aimed (a) to detect and investigate the presence or absence of life and biological processes at the biotic-abiotic transition with unprecedented analytical sensitivity and precision; (b) to comprehensively study the factors that control biomass, activity, and diversity of microbial communities; (c) to determine geochemical, geophysical, and hydrogeological characteristics in sediment and the underlying basaltic basement; and (d) to elucidate if the supply of fluids containing thermogenic and/or geogenic nutrients and energy substrates support seafloor microbial communities in the Nankai accretionary complex.

To address these primary scientific objectives, we advanced Hole C0023A across the sediment/basement interface down to a total depth of 1180 mbsf and retrieved 112 cores with an average recovery of 75.9%. From these cores, more than 13,000 samples were collected. All samples for time-, oxygen-, and contamination-sensitive microbiological and biogeochemical investigations were taken in the form of whole-round cores (WRCs) from the most undisturbed parts of freshly retrieved core sections, which were identified by careful visual inspection and X-ray computed tomography (CT) image scan. The outer layer of the WRCs was removed immediately after retrieval to avoid potential intrusion of contaminants from drilling fluid. WRC sampling was completed as soon as possible, usually within a few hours after a core had arrived on deck. Samples for oxygen-sensitive analyses were processed under anaerobic conditions. For microbiological

samples, a super-clean and anaerobic working environment was established by installing a tabletop air filtration unit and ionizer inside an anaerobic chamber, thus preventing potential sample contamination by laboratory air. In order to avoid alteration of samples and loss of information during storage, in-depth investigations were started as soon as possible after core recovery. To this end, 92 boxes with carefully cleaned and anaerobically packed high-priority samples were transferred to KCC by helicopter on an almost daily basis. At KCC, pre-cleaned core samples were carefully treated under super-clean conditions in a timely manner for further removal of potentially contaminated surface at either a dust-free super-clean room that meets International Organization for Standardization (ISO) Class 1 clean room standards, an all air exhaust clean bench, or a tabletop air filtration system–equipped anaerobic chamber with monitoring for airborne particles and microbial cells. Also, all microbiological analyses were conducted in an ISO Class 1 clean environment established in a super-clean room at KCC. During drilling, in situ temperatures were measured between 189 and 408 mbsf, and after completion of coring operations a long-term temperature observatory with 13 thermistor arrays was installed in the borehole down to 863 mbsf. Recovery of the data by ROV is planned for March 2018, using the JAMSTEC research vessel *Kairei* and the ROV *Kaiko*.

A shipboard temperature model based on the already available in situ temperature measurements and laboratory thermal conductivity measurements points to a temperature of $\sim 120^{\circ}\text{C}$ at the sediment/basement interface, thus corroborating the suitability of the environmental setting for addressing research questions as planned (Heuer, Inagaki, Morono, Kubo, Maeda et al., 2017). Preliminary cell count data suggest that cell concentrations are notably lower than those previously reported at Site 1174 but at the same time point to the presence of intact microbial cells in low abundance to at least ~ 600 mbsf (Fig. 1). Therefore, the obtained samples and data provide an excellent basis for extensive microbiological, biogeochemical, geological, and geophysical analyses in postcruise research projects

that will potentially provide new insights into the effects of temperature on biological, geochemical, and geophysical processes in the deep seafloor at Site C0023. The ongoing and future research in the context of Expedition 370 will ultimately shed more light on the extent, habitability and evolutionary nature of the deep seafloor biosphere on Earth.

While most expedition goals could be reached, some remain unfulfilled for now, mainly due to time constraints. Because of the challenging geological formation, unstable borehole conditions were a major concern throughout the expedition, consumed more operational time than expected, and led to the decision to install the temperature observatory only in the upper 858 mbsf that had been stabilized by a casing. However, a further deepening and instrumentation of the observatory could be achieved during a future return to Hole C0023A.

From an operational point of view, Expedition 370 was overall successful. We carried out nearly all planned operations, established a robust temperature model based on downhole measurements, and conducted all sampling and scientific analyses with an unprecedentedly high level of QA/QC. With respect to expedition logistics, in particular the smooth operations for the transfer of cored samples from ship to shore, the successful collaboration of simultaneously working shipboard and shore-based expedition scientists, and the efficient preparation of Expedition 370 with a short lead time of less than 6 months, are worth mentioning.

Acknowledgments – We would like to thank all shipboard and shore-based personnel involved in the operations of DV *Chikyu*, investigations at Kochi Core Center, and helicopter transportation of samples for their dedicated support, professional collaboration, and smooth operations throughout the expedition. VBH, SH, FS, and BV gratefully acknowledge the funding of their participation in Exp. 370 by the Deutsche Forschungsgemeinschaft.

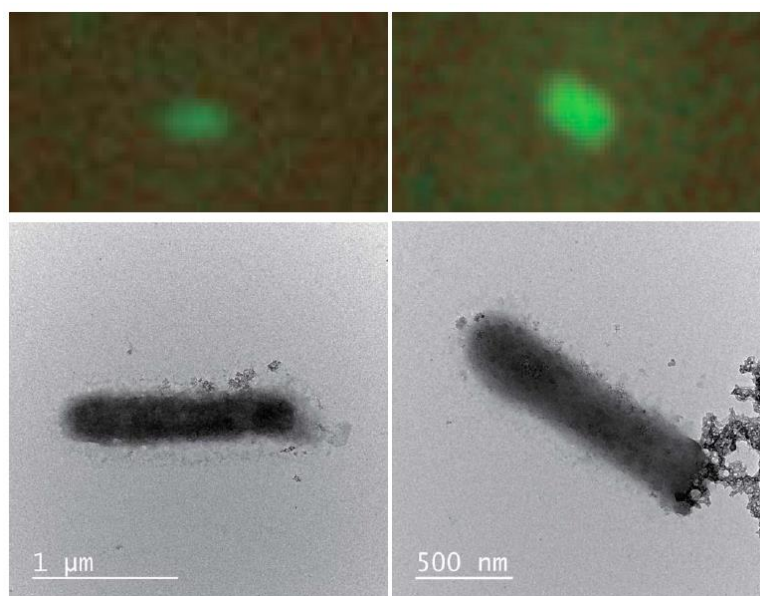


Figure 1: Transmission electron micrographs of microorganisms separated and sorted from sediment in Core 6F (304 mbsf) (Heuer, Inagaki, Morono, Kubo, Maeda et al., 2017).

References:

- Blöchl, E., Rachel, R., Burggraf, S., Hafenbradl, D., Jannasch, H. W., and Stetter, K. O., 1997. *Pyrolobus fumarii*, gen. and sp. nov., represents a novel group of archaea, extending the upper temperature limit for life to 113°C. *Extremophiles* 1:14-21.
- D'Hondt S, Rutherford S, Spivack AJ (2002) Metabolic activity of subsurface life in deep-sea sediments. *Science*, 295:2067-2070.
- D'Hondt S, Jørgensen BB, Miller DJ, Batzke A, Blake R, Cragg BA, Cypionka H, Dickens GR, Ferdelman T, Hinrichs K-U, Holm NG, Mitterer R, Spivack A, Wang G, Bekins B, Engelen B, Ford K, Gettemy G, Rutherford SD, Sass H, Skilbeck CG, Aiello IW, Guerin G, House C, Inagaki F, Meister P, Naehr T, Niituma S, Parkes RJ, Schippers A, Smith DC, Teske A, Wiegel J, Padilla CN, Acosta JLS (2004) Distributions of microbial activities in deep seafloor sediments. *Science*, 306:2116-2121.
- D'Hondt S, Spivack A J, Pockalny R, Ferdelman, T. G., Fisher, J. P., Kallmeyer, J., Abrams, L. J., Smith, D. C., Graham, D., Hasiuk, F., Schrum, H., and Stancin, A. M., 2009. Subseafloor sedimentary life in the South Pacific Gyre. *Proc. Natl. Acad. Sci. USA*, 106:11651-11656.
- D'Hondt, S., Inagaki, F., Zarikian, C. A., Abrams, L. J., Dubois, N., Engelhardt, T., Evans, H., Ferdelman, T., Gribsholt, B., Harris, R. N., Hoppie, B. W., Hyun, J.-H., Kallmeyer, J., Kim, J., Lynch, J. E., McKinley, C. C., Mitsunobu, S., Morono, Y., Murray, R. W., Pockalny, R., Sauvage, J., Shimono, T., Shiraishi, F., Smith, D. C., Smith-Duque, C., Spivack, A. J., Steinsbu, B. O., Suzuki, Y., Szpak, M., Toffin, L., Uramoto, G., Yamaguchi, T. Y., Zhang, G., Zhang, X.-H., and Ziebis, W., 2015. Presence of oxygen and aerobic communities from seafloor to basement in deep-sea sediment. *Nat. Geosci.*, 8(4):299-304.
- Head, I. M., Jones, D. M., and Larter, S. R., 2003. Biological activity in the deep subsurface and the origin of heavy oil. *Nature*, 426:344-352.
- Heberling C., Lowell R.P., Liu L., Fisk M.R. (2010) Extent of the microbial biosphere in the oceanic crust. *Geochemistry Geophysics Geosystems* 11: Q08003, doi:10.1029/2009GC002968.
- Heuer, V.B., Inagaki, F., Morono, Y., Kubo, Y., Maeda, L., and the Expedition 370 Scientists. Expedition 370 Preliminary Report: Temperature Limit of the Deep Biosphere off Muroto. International Ocean Discovery Program. <http://dx.doi.org/10.14379/iodp.pr.370.2017>
- Hinrichs, K.-U., and Inagaki, F., 2012. Downsizing the deep biosphere. *Science*, 338(6104):204-205.
- Hinrichs, K.-U., Inagaki, F., Heuer, V.B., Kinoshita, M., Morono, Y., and Kubo, Y., 2016. Expedition 370 Scientific Prospectus: T-Limit of the Deep Biosphere off Muroto (T-Limit). International Ocean Discovery Program. <http://dx.doi.org/10.14379/iodp.sp.370.2016>
- Inagaki, F., Hinrichs, K.-U., Kubo, Y., Bowles, M. W., Heuer, V. B., Hong, W.-L., Hoshino, T., Ijiri, A., Imachi, H., Ito, M., Kaneko, M., Lever, M. A., Lin, Y.-S., Methé, B. A., Morita, S., Morono, Y., Tanikawa, W., Bihan, M., Bowden, S. A., Elvert, M., Glombitza, C., Gross, D., Harrington, G. J., Hori, T., Li, K., Limmer, D., Liu, C.-H., Murayama, M., Ohkouchi, N., Ono, S., Park, Y.-S., Phillips, S. C., Prieto-Mollar, X., Purkey, M., Riedinger, N., Sanada, Y., Sauvage, J., Snyder, G., Susilawati, R., Takano, Y., Tasumi, E., Terada, T., Tomaru, H., Trembath-Reichert, E., Wang, D. T., and Yamada, Y., 2015. Exploring deep microbial life down to ~2.5 km below the ocean floor. *Science*, 349(6246):420-424.
- Kallmeyer, J., Pockalny, R., Adhikari, R.R., Smith, D. C., and D'Hondt, S., 2012. Global distribution of microbial abundance and biomass in seafloor sediment. *Proc. Natl. Acad. Sci. USA*, 109:16213-16216.
- Kashefi, K., Lovley, D. R., 2003. Extending the upper temperature limit for life. *Science*, 301:934-934.
- Lever, M.A., Rouxel, O., Alt, J.C., Shimizu, N., Ono, S., Coggon, R.M., Shanks, W.C., III, Lapham, L., Elvert, M., Prieto-Mollar, X., Hinrichs, K.-U., Inagaki, F. and Teske, A. (2013) Evidence for Microbial Carbon and Sulfur Cycling in Deeply Buried Ridge Flank Basalt. *Science*, 339, 1305-1308. doi: 10.1126/science.1229240
- Lipp, J. S., Morono, Y., Inagaki, F., and Hinrichs, K.U., 2008. Significant contribution of Archaea to extant biomass in marine subsurface sediments. *Nature*, 454:991-994.
- Lomstein BA, Langerhuus AT, D'Hondt S, Jørgensen BB, Spivack A (2012) Endospore abundance, microbial growth and necromass turnover in deep seafloor sediment. *Nature* 484: 101-104.
- Moore, G. F., Taira, A., Klaus, A., et al., 2001. *Proc. ODP, Init. Repts.*, 190: College Station, TX (Ocean Drilling Program). doi:10.2973/odp.proc.ir.190.2001
- Morono, Y., Terada, T., Nishizawa, M., Hillion, F., Ito, M., Takahata, N., Sano, Y., and Inagaki, F., 2011. Carbon and nitrogen assimilation of deep seafloor microbial cells. *Proc. Natl. Acad. Sci., USA*, 108:18295-18300.
- Orcutt, B.N., Bach, W., Becker, K., Fisher, A.T., Hentscher, M., Toner, B.M., Wheat, C.G. and Edwards, K.J. (2011) Colonization of subsurface microbial observatories deployed in young ocean crust. *Isme Journal* 5, 692-703. doi: 10.1038/ismej.2010.157
- Parkes RJ, Cragg BA, Bale SJ, Getliff JM, Goodman K, Rochelle PA, Fry JC, Weightman AJ, Harvey SM (1994) Deep bacterial biosphere in Pacific Ocean sediments. *Nature*, 371:410-413.
- Parkes, R. J., Cragg, B. A., and Wellsbury, P., 2000. Recent studies on bacterial populations and processes in seafloor sediments: A review. *Hydrogeol. J.*, 8:11-28.
- Parkes, R.J., Cragg, B., Roussel, E., Webster, G., Weightman, A. and Sass, H. (2014) A review of prokaryotic populations and processes in seafloor sediments, including biosphere:geosphere interactions. *Marine Geology*, 352:409-425.
- Roussel EG, Bonavita MA, Querrelou J, Cragg BA, Webster G, Prieur D, Parkes RJ (2008) Extending the seafloor biosphere. *Science*, 320:1046.
- Takai, K., Nakamura, K., Toki, T., Tsunogai, U., Miyazaki, M., Miyazaki, J., & Horikoshi, K., 2008. Cell proliferation at 122°C and isotopically heavy CH₄ production by a hyperthermophilic methanogen under high-pressure cultivation. *Proc. Natl. Acad. Sci. USA*, 105(31):10949-10954.
- Whitman, W.B., Coleman, D.C., Wiebe, W.J., 1998. Prokaryotes: The unseen majority. *PNAS, USA*, 95:6578-6583.
- Wilhelms, A., Larter, S.R., Head, I., Farrimond, P., di-Primio, R., Zwach, C., 2001. Biodegradation of oil in uplifted basins prevented by deep-burial sterilization. *Nature*, 411:1034-1037.

Abstracts

IODP

Subseafloor life and carbon cycling in the Bengal Fan (IODP Exp. 354)

R. R. ADHIKARI¹, V. B. HEUER¹, T. HOSHINO², F. INAGAKI², S. JABINSKI¹, J. KALLMEYER³, A. KITTE³, L. WÖRMER¹, K.-U. HINRICHS¹

¹MARUM - Center for Marine Environmental Sciences, University of Bremen, Leobener Str. 8, 28359 Bremen, Germany

²Geomicrobiology Group, Kochi Institute for Core Sample Research, JAMSTEC, Monobe B200, Nankoku, Kochi 783-8502, Japan

³Geomicrobiology, Helmholtz Centre Potsdam, GFZ German Research Centre for Geosciences, Telegrafenberg, 14473 Potsdam, Germany

The Bengal Fan, one of the largest sediment reservoirs in the world, provides a long geological record for Himalayan orogeny and tectonics-climate interactions (France-Lanord et al., 2016). The Bengal Fan sedimentary environment is also a large subseafloor habitat for microorganisms, which has barely been investigated so far. For a better understanding of the role of Bengal Fan sediments in global biogeochemical cycles, it is thus important to investigate how subseafloor microbial processes impact the preservation and remineralization of sedimentary organic matter. Especially variations in the sedimentation (from few to tens of cm ky⁻¹) and organic carbon accumulation rates over geological time scales may have an impact in energy and carbon supply to the deep biosphere. To investigate such interactions, we recovered samples from seven drill sites (U1449 – U1455) along a 8° North transect during IODP Expedition 354 (February – March 2015, Singapore-Colombo, Sri Lanka).

Our postcruise investigations comprise several microbiological and molecular approaches, such as estimation of prokaryotes, endospores, potential enzymatic activity etc., e.g.; (i) for the determination of prokaryotic cell concentrations we used flow cytometer after detachment of microbes from sediment particles; (ii) based on a unique biomarker dipicolinic acid concentration, we estimated the abundance of endospores; and (iii) using radiotracer based hydrogenase enzyme assay (Adhikari et al., 2016), we quantified potential microbial activity. Hydrogenases are ubiquitous enzymes in subsurface microorganisms and they facilitate hydrogen metabolism, a key metabolite for microbial activity in any environment. We also (iv) investigated microbial community composition using ultra-high-throughput analysis on the Illumina MiSeq platform.

Here we present depth profiles of the different microbiological parameters from all seven drill sites. The deepest sample (1042 mbsf) that we analyzed was collected from Hole U1451B. The preliminary results from Site U1449 show that the prokaryotic cell density decreases exponentially with depth by several orders of magnitude; and the number of endospores varies mainly between 2.6×10^4 and 7.9×10^6 cells g⁻¹ sediment, which is comparable to previous studies (Fichtel et al., 2008; Lomstein et al., 2012). In addition, we observed a relation between endospore concentrations and organic carbon

contents. At all depths and sites, we detected hydrogenase enzyme activity and the potential hydrogen utilization rate ranged from 4 nmol to 4 μmol H₂ g⁻¹ d⁻¹. DNA sequencing shows that both bacteria and archaea are abundant at all depths at Hole U1450B. Among sites, we observed, however no significant spatial variation in the number of prokaryotes, endospores and hydrogenase enzyme activity.

From our initial observations we conclude that the deep biosphere of the Bengal Fan harbors substantial microbial biomass and is enzymatically active. The number of prokaryotes, endospores and enzyme activity indicate that the microbial population is related to the quality and availability of organic matter. Our observations lead us to further investigations in setting up incubation experiments to track carbon flow in Bengal Fan sediments.

References:

- France-Lanord, C., Spiess, V., Klaus, A., Schwenk, T., and the Expedition 354 Scientists 2016. Bengal Fan. Proceedings of the International Ocean Discovery Program, 354: College Station, TX
- Adhikari, R.R., Glombitza, C., Nickel, J.C., Anderson, C.H., Dunlea, A.G., Spivack, A.J., Murray, R.W., D'Hondt, S. and Kallmeyer, J. 2016 Hydrogen Utilization Potential in Subsurface Sediments. *Frontiers in Microbiology* 7:8
- Fichtel, J., Köster, J., Rullkötter, J., & Sass, H. 2008. High variations in endospore numbers within tidal flat sediments revealed by quantification of dipicolinic acid. *Geomicrobiology Journal*, 25(7-8), 371-380
- Lomstein, B.A., Langerhuus, A.T., D'hondt, S., Jorgensen, B.B., and Spivack, A.J. 2012. Endospore abundance, microbial growth and necromass turnover in deep sub-seafloor sediment. *Nature* 484, 101-104

ICDP

Impact of geogenic CO₂ on the depth distribution of and feedstock provision for deep microbial ecosystems in the Hartoušov mofette system in NW Bohemia

K. ADLER¹, M. ALAWI¹, Q. LIU¹, R. BUSSERT², T. VYLITA³, H.-M. SCHULZ¹, H. KÄMPF¹, B. PLESSEN¹, D. WAGNER¹, K. MANGELSDORF¹

¹ GFZ German Research Centre for Geosciences – Helmholtz Centre Potsdam, Germany

² TU Berlin – Technical University Berlin, Germany

³ AGUAS CF, Ltd., Geology and Balneotechnics, Czech Republic

A mofette is a natural cold either dry or wet gas vent releasing CO₂-rich gases into the atmosphere. The Hartoušov mofette system is located in the northern Cheb Basin (NW Bohemia, Eger Rift). The area is characterized by active seismicity in form of periodically occurring swarm earthquakes and lithospheric mantle derived gas emanations (> 99 % CO₂). The exhaling free gas phase of the Bublak mofette, the best investigated degassing site of the area, shows CO₂ with a comparatively heavy δ¹³C signal (ca. -2 ‰) compared to atmospheric CO₂ (ca. -8 ‰) (MANGELSDORF ET AL., 2008) and is characterized by a subcontinental mantle helium isotope signature of 5.9 Ra (BRÄUER ET AL., 2011). Magmatic fluids from lithospheric mantle, entering the whole crust, are the main reason for periodic/episodic earthquake swarm activity in this area (BRÄUER ET AL., 2003).

In early 2016 a borehole was drilled by GFZ in the framework of a DFG-ICDP project (Alawi, AL 1898/1). The drilling was performed in a mofette system near the village of Hartoušov. Below a Holocene sediment cover the 108.5 m deep borehole exposed Quaternary to Pliocene

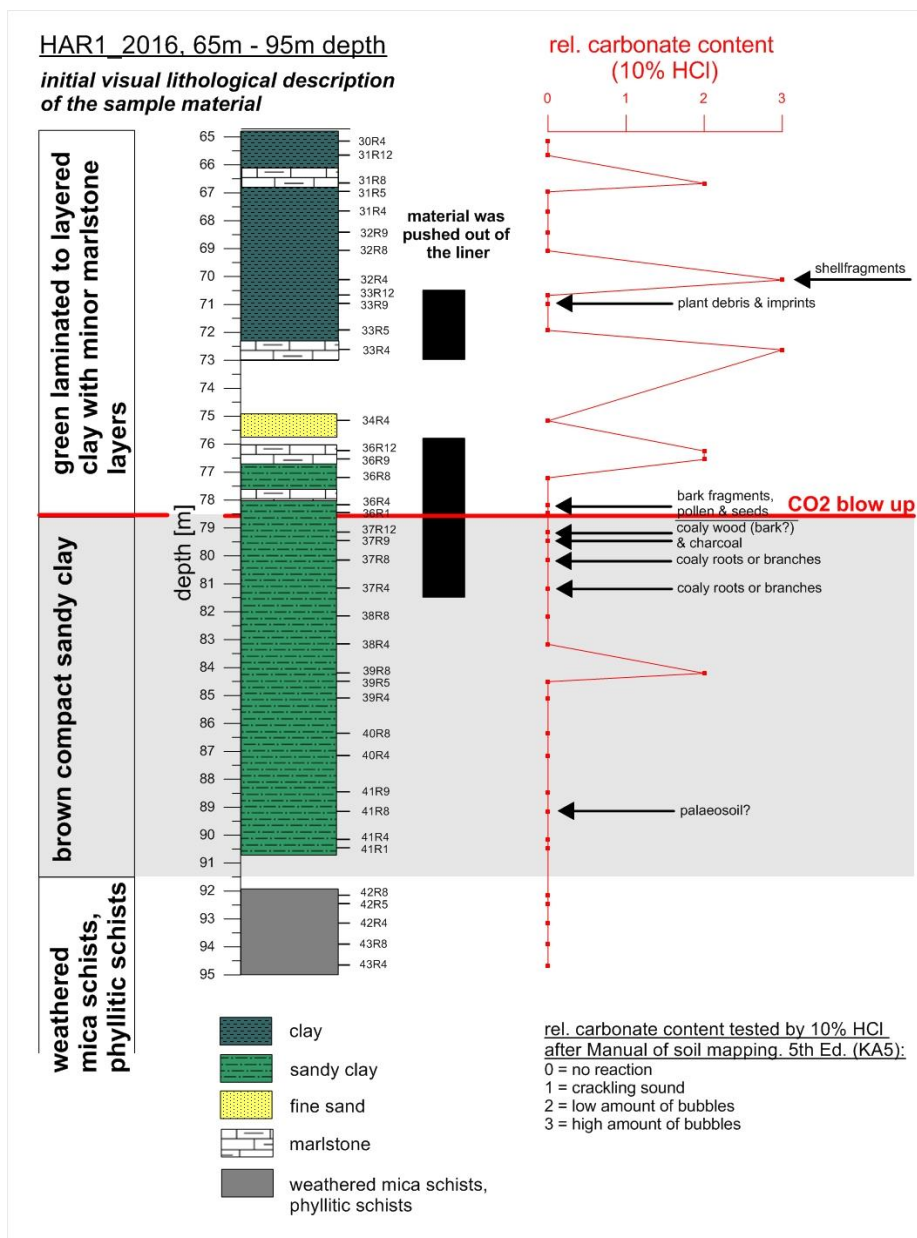


Figure 1: Initial visual lithological description for the depth interval 65 m – 95 m of the HAR1 borehole drilled into the Hartoušov mofette system.

sand and gravel, laminated to bedded lacustrine Miocene claystones, a compact sandy claystone and a weathered Palaeozoic basement. During the drilling campaign CO₂-rich sediments were recovered between 73 m and 76 m depth representing a sandy aquifer bordered by marlstone layers. After penetrating a deeper marlstone layer at 78.5 m a CO₂ blow out occurred indicating a CO₂ reservoir below this layer in the sandy clay (Figure 1). A pumping test between ca. 80 m to 90 m depth revealed the presence of mineral water dominated by Na⁺, Ca²⁺, HCO₃⁻, SO₄²⁻.

The ascending CO₂ is not only affecting the sedimentary matrix as indicated by high mineral contents and dissolved CO₂ in groundwaters, and presumably causes mineral alterations along vein-like structures and possible carbonate precipitations at the boundaries of CO₂-containing aquifers, but can also act as a substrate for deep microbial ecosystems. Thus, the aim of the current study is to investigate both the impact of geogenic CO₂ on deep microbial communities and on their surrounding sedimentary life habitat.

In this context the sedimentary succession from 65 to 95 m depth will be examined for the abundance and distribution of specific microbial biomarkers indicating living (phospholipids, PLs) and past (archaeol and glycerol dialkyl glycerol tetraethers, GDGTs) microbial communities. Compound specific carbon isotope analyses on these microbial markers will be used to unravel links between the geogenic CO₂ and the indigenous microbial communities, since the geogenic CO₂ differs in its isotopic signals from the sedimentary terrestrial or lacustrine organic material.

In addition the life habitats for the deep microbial ecosystems will be assessed for potential substrates others than CO₂ and for electron acceptors probably provided by mineral dissolution and groundwater transport. Furthermore, the impact of CO₂-containing fluids on the sedimentary matrix will be investigated by characterizing the mineralogical rock composition and gas-migration pathways through vein-like structures both with related mineral alterations.

Acknowledgments

We would like to thank the “Deutsche Forschungsgemeinschaft (DFG)” for funding this project (MA 2470/5-1 and AL 1898/1).

References:

- Bräuer K., Kämpf H., Strauch G., Weise S M (2003) Isotopic evidence ($^3\text{He}/^4\text{He}$, $^{13}\text{C}/^{12}\text{C}$) of fluid triggered intraplate seismicity. *J. Geophys. Res.*, 108(B2), 2070. doi:10.1029/2002JB002077.
- Bräuer K., Kämpf H., Koch U., Strauch G (2011) Monthly monitoring of gas and isotope compositions in the free gas phase at degassing locations close to the Nový Kostel focal zone in the western Eger Rift, Czech Republic. *Chem. Geol.*, 290, 163–176.
- Mangelsdorf K., Wohlfart K., Kämpf H., Pfanz H (2008) Investigation of the impact of geogenic CO_2 on the grass *Deschampsia cespitosa* in a mofette area. *Geophys. Res. Abstr.* 10, EGU2008-A-09563.

ICDP

Late Holocene changes in torrential rainstorm frequency inferred from a Dead Sea sediment core

MARIEKE AHLBORN¹, MOSHE ARMON², YOAV BEN DOR², INA NEUGEBAUER³, MARKUS J. SCHWAB¹, RIK TJALLINGH¹, JAWAD HASAN SHOQEIR⁴, EFRAT MORIN², YEHOUDA ENZEL², ACHIM BRAUER¹

- ¹ Section 5.2: Climate Dynamics and Landscape Evolution, GFZ German Research Centre for Geosciences, Germany
- ² The Fredy and Nadine Herrmann Institute of Earth Sciences, The Hebrew University of Jerusalem, Israel
- ³ Department of Earth Sciences, University of Geneva, Switzerland
- ⁴ Department of Earth and environmental sciences, Al-Quds University, Palestine

In the eastern Mediterranean, an increase in torrential rainstorms under increasing aridity in the context of ongoing climate change is a common hypothesis. However, conclusive understanding of the link between rainstorms and the long-term climate trend is still lacking but essential for assessing the impacts of climate change and developing future scenarios. Here, we present evidence of an increased frequency of localized torrential rainstorms during a multi-century late Holocene drought in the eastern Mediterranean, presumably caused by changes in the synoptic atmospheric circulation pattern. By combining sedimentological data with modern observations we infer the synoptic conditions and the threshold of rainstorms, which triggered debris flows in the Dead Sea catchment and link these implications to the long-term climate trend.

The unique location of shallow water Dead Sea sediment core DSEn is exposed to debris flow activities from the western escarpments of the Dead Sea but sheltered from the influence of the nearby ephemeral streams Nahal David, Nahal Arugot, and Nahal Hever (Figure 1). According to modern observations the fine-grained fraction of the debris flows is flushed into the lake or accumulates on the mudflats, while the coarse-grained material settles as debris flow fans when reaching the low gradient slopes at the base of the escarpments (Figure 2). Further modern observations show that debris flows are triggered by localized, exceptionally heavy rainstorms pouring rain directly on the escarpments. For debris flow initiation such rainstorms must exceed a threshold of 30 mm h^{-1} for the duration of one hour and are commonly associated with the Active Red Sea Trough synoptic atmospheric circulation pattern (Ben David-Novak et al., 2004). Results of the microfacies analysis show that the



Figure 1: Satellite image of coring location (circle), the western escarpments (solid line), 1st-2nd order drainage basins (arrows), ephemeral streams Nahal David, Nahal Arugot, and Nahal Hever (dashed line), the Road 90 (thin gray line) roughly traces the late Holocene lake levels.

distal debris flow deposits are recorded as discrete graded layers within laminated sediments in core DSEn. A time series of debris flows and associated rainstorms (3.3-1.8 cal ka BP) revealed changes in debris flow frequency through time. In total, twenty-three debris flows were counted



Figure 2: Debris flow deposits with coring location (arrow) on the mudflat (black line), Road 90 roughly traces the late Holocene lake levels. Please note the person as scale (white bar); Bartov et al., 2006.

occurring during a multi-century drought (3.0-2.4 cal ka BP; Neugebauer et al., 2015). The accumulation of rainstorms during times of a regional drought indicates a shift in the synoptic atmospheric circulation pattern in the investigated time interval. Fewer passages of eastern Mediterranean cyclones likely caused the drought and favored the increased frequency of rainstorm-bearing Active Red Sea Troughs leading to more rainstorms during generally drier conditions. This interpretation is supported by detailed analysis of modern meteorological data from four nearby gauging stations. Particularly, in hyperarid areas the return period for rainstorms exceeding the threshold for debris flows initiation is markedly lower than in moister Mediterranean climate.

Ongoing research focuses on older time intervals in the Dead Sea ICDP core 5017-1, particularly the early Holocene and late Pleistocene. Preliminary results from the Pleistocene/Holocene transition (~15-11 cal ka BP) show that flash floods are preserved as discrete graded or homogeneous detrital layers intercalated within regularly laminated sediments. Reworking of proximal sediments, potentially due to lake level decrease and overturn of the water column, is indicated by lacustrine turbidites with a basal sublayer of primary gypsum. These results will allow investigating the link between rainstorms and the long-term climate trend in the eastern Mediterranean to reveal if rainstorms preferentially occur at specific climate conditions. This study is part of the trilateral research project *PALEX (Paleoclimate in the Eastern Mediterranean Region – Levant: Paleohydrology and Extreme Flood Events)* implemented in the framework of the DFG priority program 1006 ICDP (International Continental Scientific Drilling Program).

References:

- Bartov, Y., Bookman, R., and Enzel, Y., 2006, Current depositional environments at the Dead Sea margins as indicators of past lake levels, in Enzel, Y., Agnon, A., and Stein, M., eds., *New frontiers in Dead Sea paleoenvironmental research*: Boulder, Colorado, Geological Society of America Special Papers 401, p. 127-140, doi: 10.1130/2006.2401(08).
- Ben David-Novak, H., Morin, E., and Enzel, Y., 2004, Modern extreme storms and the rainfall thresholds for initiating debris flows on the hyperarid western escarpment of the Dead Sea, Israel: *Geological Society of America Bulletin*, v. 116, p. 718-728, doi: 10.1130/B25403.2.
- Neugebauer, I., et al., 2015, Evidences for centennial dry periods at ~3300 and ~2800 cal. yr BP from micro-facies analyses of the Dead Sea sediments: *The Holocene*, v. 25, p. 1358-1371, doi: 10.1177/0959683615584208.

ICDP

Flash floods in the Dead Sea basin during the Pleistocene/Holocene transition inferred from ICDP core 5017-1

MARIEKE AHLBORN¹, RIK TJALLINGII¹, YOAV BEN DOR²,
YEHOUDA ENZEL², INA NEUGEBAUER³, MARKUS J.
SCHWAB¹, ACHIM BRAUER¹

¹ Section 5.2, Climate Dynamics and Landscape Evolution, GFZ German Research Centre for Geosciences, Germany

² The Fredy and Nadine Herrmann Institute of Earth Sciences, The Hebrew University of Jerusalem, Israel

³ Department of Earth Sciences, University of Geneva, Switzerland

Flash floods associated with heavy rainstorms occur regularly during the winter rainy season in the Dead Sea basin and adjacent western mountain ranges. Although identifying climates favoring extreme weather is a primary

goal of paleoclimate and paleohydrologic research, the link between heavy rainstorms and the long-term climate trend in the eastern Mediterranean is only little understood. Therefore, present and past flash flood events and associated heavy rainstorms are the main focus of the trilateral project *PALEX (Paleoclimate in the Eastern Mediterranean Region – Levant: Paleohydrology and Extreme Floods from the Dead Sea ICDP core)* implemented in the framework of the DFG priority program 1006 ICDP. An interdisciplinary team of Palestinian, Israeli, and German researchers aim to improve the understanding of long-term variability in flood occurrences under diverse climates in the eastern Mediterranean.

The ICDP Dead Sea Deep Drilling Project (DSDDP) site 5017-1 covers a 455 m long sediment sequence from the northern basin of the Dead Sea (Stein et al., 2011). Previous studies of this core revealed mainly laminated sediments frequently intercalated by mass wasting deposits (Neugebauer et al., 2014). Late Holocene thick and coarse detrital layers have been interpreted as frequent flash floods during a regional multi-century drought (Neugebauer et al., 2015). However, little is known on the frequency of extreme storms and floods during the rapid and high amplitude aridification during the latest Pleistocene (~15-11 cal ka BP). A drastic lake level drop of ~180 m (Torfstein et al., 2013) at the Pleistocene/Holocene transition terminated the Lake Lisan phase, established the Dead Sea in its present form, and resulted in increased gypsum precipitation (Torfstein et al., 2008; Neugebauer et al., 2014). Here, we present initial results of a microfacies analysis of discrete graded or homogeneous layers embedded in mainly laminated sediments of the upper Lisan Formation. Based on their sedimentology, these layers are preliminary interpreted as individual flash flood deposits. Furthermore, lacustrine turbidites with basal sublayers of primary gypsum indicate reworking of littoral sediments and were probably caused by rapid lake level decrease associated with an overturn of the water column. Results of high-resolution microfacies analysis were compared to multivariate statistical clustering of micro X-ray fluorescence (XRF) data to advance a rapid geochemical identification and constrain the origin of the detrital fraction of the laminated sediments.

References:

- Neugebauer, I., et al., 2014, Lithology of the long sediment record recovered by the ICDP Dead Sea Deep Drilling Project (DSDDP): *Quaternary Science Reviews*, v. 102, p. 149-165.
- Neugebauer, I., et al., 2015, Evidences for centennial dry periods at ~3300 and ~2800 cal. yr BP from micro-facies analyses of the Dead Sea sediments: *The Holocene*, v. 25, p. 1358-1371.
- Stein, M., Ben-Avraham, Z., and Goldstein, S.L., 2011, Dead Sea Deep Cores: A Window into Past Climate and Seismicity: *EOS*, v. 92, p. 453-454.
- Torfstein, A., Gavrieli, I., Katz, A., Kolodny, Y., and Stein, M., 2008, Gypsum as a monitor of the paleo-limnological-hydrological conditions in Lake Lisan and the Dead Sea: *Geochimica et Cosmochimica Acta*, v. 72, p. 2491-2509.
- Torfstein, A., Goldstein, S.L., Stein, M., and Enzel, Y., 2013, Impacts of abrupt climate changes in the Levant from Last Glacial Dead Sea levels: *Quaternary Science Reviews*, v. 69, p. 1-7, doi: <http://dx.doi.org/10.1016/j.quascirev.2013.02.015>

ICDP

Deep drilling into an active, CO₂-dominated fault zone in NW Bohemia - preliminary results

M. ALAWI¹, Q. LIU¹, R., BUSSERT³, H. KÄMPF², T. NICKSCHICK², T. VYLITA⁴, D. WAGNER¹,

^{1,2} GFZ German Research Centre for Geosciences, Helmholtz Centre Potsdam, ¹ Sect. 5.3 Geomicrobiology, ² Sect. 3.2 Organic Geochemistry, Telegrafenberg, 14469 Potsdam, mashal.alawi@gfz-potsdam.de

³ TU Berlin – Technical University Berlin, Germany

⁴ AGUAS CF, Ltd., Geology and Balneotechnics, Czech Republic

The Cheb Basin (W Eger Rift, NW Bohemia) is characterised by a network of diffuse degassing structures in CO₂-mofette areas along an seismically active fault zone (Kämpf et al., 2013). Further specific characteristics of this area are periodically occurring earthquake swarms and magmatic activities having strong impact on the changes in the composition and dynamics of the outflowing, mantle CO₂-dominated gases (Bräuer et al., 2005). From a biogeochemical and microbiological point of view these CO₂ seeps form an interesting and unique life habitat for microbial communities. The intense geogenic CO₂ fluxes provide a particular carbon and energy source forming the setting for a specific indigenous microbial community being well adapted to these specific environmental conditions.

We hypothesize that in active fault zones, due to an intensified substrate support, microbial processes are significantly accelerated compared to other continental Deep Biosphere ecosystems. Therefore active fault zones could be seen as „Hot Spots“ of microbial life in the deep subsurface. The main objective of the planned study is therefore to advance our understanding of the specific biogeo interactions between microbial communities and the seismic active environment in the Cheb Basin.

As a pilot study for the ICDP deep drilling campaign (Drilling the Eger Rift: Magmatic fluids driving the earthquake swarms and the deep biosphere) we conducted a first drilling campaign into a CO₂ degassing mofette structure from March to April 2016. The drilling site was chosen due to the unusually high CO₂ gas fluxes occurring at this particular spot (Nickschick et al., 2015). Coring was performed over the entire section which reached a maximum depth of 108.5 m. After drilling through a thin caprock-like structure at 78.5 m a CO₂ blow out occurred indicating a CO₂ reservoir in the sandy clay. A pumping test revealed the presence of mineral water dominated by Na⁺, Ca²⁺, HCO₃⁻, SO₄²⁻ having a temperature of 18.6 °C and a conductivity of 6760 µs cm⁻¹. Drilling was conducted using strict contamination control. Fluorescein was added as a contamination tracer to the drilling fluid (Pellizzari et al. 2013). Core material was also recovered from the transition zone between sediment and crystalline basement. A detailed stratigraphical, microbiological, geochemical and mineralogical analysis of the obtained material is in progress.

References:

Bräuer, K., Kämpf, H., Faber, E., Koch, U., Nitzsche, H.-M., Strauch, G., 2005. Seismically triggered microbial methane production relating to the Vogtland-NW Bohemia earthquake swarm period 2000, Central Europe. *Geochemical Journal* 39, 441-450.

Kämpf, H., Bräuer, K., Schumann, J., Hahne, K., Strauch, G., 2013. CO₂ discharge in an active, non-volcanic continental rift area (Czech Republic): Characterisation (δ¹³C, ³He/⁴He) and quantification of diffuse and vent CO₂ emissions. *Chemical Geology* 339, 71-83.

Nickschick, T., Kämpf, H., Flechsig, C., Mrlina, J., Heinicke, J., 2015. CO₂ degassing in the Hartoušov mofette area, western Eger Rift, imaged by CO₂ mapping and geoelectrical and gravity surveys. *International Journal of Earth Sciences*, 104(8), 2107–2129

Pellizzari, L., et al. 2013. "The use of tracers to assess drill-mud penetration depth into sandstone cores during deep drilling: method development and application." *Environmental Earth Sciences* 70(8): 3727-3738

ICDP

Swarm-dependent velocity models in the West Bohemia Seismic Zone

C. ALEXANDRAKIS¹, A. KIESLICH¹, E. LÖBERICH², M. CALO³, V. VAVRYCUK⁴

¹ TU Bergakademie Freiberg

² Universität Wien

³ Universidad Nacional Autonoma de Mexico

⁴ Czech Academy of Science

The West Bohemia Seismic Zone is a geodynamically active area characterized by frequent earthquake swarms and an abundance of CO₂ degassing sites. Chemical analysis indicates that the fluids originate in the mantle (Bräuer et al., 2011). Decades long monitoring has shown that there are some correlations between the chemical composition at the gas sites and swarm earthquakes, but the relationship is not yet clear considering degassing sites lay in the direct vicinity of the most active swarm areas. This is one of the main questions that will be addressed by the ICDP Eger Rift project.

Within the West Bohemia Seismic Zone, the most active swarm area is located near the Czech village Novy Kostel. This village lies at the junction of the north-south trending Pocatky-Plesna shear zone and the northwest-southeast trending Marianske Lazne fault. The Marianske Lazne fault marks the eastern boundary of the Cheb basin and the western extent of the Eger Rift. The seismicity and gas exhalation sites are predominantly located within the basin. Typically, the Novy Kostel swarms rupture either the northern or southern section of the active fault. This indicates ongoing stress changes at the seismically active depths (~5-15 km). Considering the periodic mass energy release in the form of swarm earthquakes, the correlation between gas chemistry and seismicity, there must be a point of interaction within the crust. However, the offset between gas exhalation sites and seismicity indicates the fluids do not follow the fault plane. The reason behind this deviation could be solved by investigating the subsurface structures in the area near and above the focal zone.

One way to investigate the crustal structures is through 3D velocity analysis. Over the last years, several groups have independently developed velocity models of the Cheb basin, with special emphasis on the Novy Kostel seismic zone. Most studies used either earthquake recordings from a single swarm (Alexandrakis et al., 2014), the back catalog of earthquake observations (Mousavi et al., 2015), or a combination of back catalog and active sources (Ruzek and Horalek, 2013). Tomography studies have typically used local earthquake tomography methods to invert for a 3D velocity model. These methods work best with

scattered sources which can provide a varied ray path coverage. This is a challenge in the West Bohemia Seismic Zone, since the seismicity typically occurs in localized swarms. In order to maximize the ray path coverage, past studies used events from a variety of swarm events. This strategy has proven successful for calculating a time-averaged velocity model for the region. However, the disadvantage of this method is that the mixed data masks small-scale, swarm-dependent velocity changes that occur during the swarms, as observed in studies of the Vp/Vs ratio (Dahm and Fischer, 2014). Until now, no study has made a direct comparison between a 3D tomography velocity model calculated from a single swarm and a model from the time-averaged catalog, in order to make a direct assessment of any temporal changes that might occur.

In this investigation, we use the well-studied 2011 and 2008 swarms, which ruptured the northern and southern fault sections, respectively, to focus on the local changes occurring during the ruptures. As a comparison, the back catalog between 1991 and 2011 is used to produce a swarm-averaged model. Three-dimensional P-velocity and S-velocity models are inverted using double-difference tomography (Zhang and Thurber, 2006). From these models, we directly calculate a P- to S-velocity ratio model (Vp/Vs). Double-difference tomography uses both the absolute travel time and the arrival time difference between two closely spaced earthquakes to invert for the velocity model. By using the time difference, velocity changes near the recording station are removed, emphasizing the velocity heterogeneities near to and within the focal zone.

The data for this analysis was a catalog of 9763 earthquake locations and their P- and S-wave travel time picks provided by the Webnet Group. Due to the small rupture area, this catalog of earthquakes contained many effectively redundant hypocenters, which would result in oversampling and possible bias in the model calculation. To avoid this, the dataset was reduced to include a maximum of 30 events per cubic kilometer, with the larger events preferentially reserved. After this reduction, the remaining 1516 earthquakes maintained a similar data coverage and timeline. This reduced dataset was used to calculate a 1D P-wave velocity model using the program Velest (Kissling et al., 1994). Over 50 starting models and many parameterizations were tested before coming to a P-wave velocity model with minimum errors. This model, together with the regional average Vp/Vs of 1.70 (Malek et al., 2005), was then used as the starting model for the 3D double-difference tomography inversion. We first calculated a velocity model using 1516 events listed in the back catalog dating between 1991 and 2011. This inversion included both absolute and differential times, and P- and S-wave travel times. Using the same starting parameterization and inversion strategy, two swarm-specific models were also calculated. The swarm-specific datasets used all events listed in the Webnet catalog: 1874 events for the 2008 swarm and 498 events for the 2011 swarm. Due to the differences in the earthquake datasets, it was necessary to adjust the damping level was adjusted in order to maintain the same smoothness across all calculated models. Otherwise, the inversion parameters were not modified.

The resulting P- and S-wave velocity models were used to directly calculate the Vp/Vs model. As previously observed, the earthquakes are all located in a zone of high Vp/Vs (Alexandrakis et al., 2014). In the 2008 swarm model and the swarm-independent model, the Vp/Vs above the earthquakes is lower with respect to the average regional value (1.70). The transition from low to high occurs at about 7 km depth. In the 2011 swarm model, the Vp/Vs is generally greater than 1.70 throughout the model, and the low- to high-Vp/Vs is not clearly observed. However, when models are analyzed in a more general sense, by examining the average ratio for each depth layer, the transition from low to high is clear in all cases. The average ratio for each 1-km thick layer was determined using only the inverted velocities (not interpolated) within the inner +/- 10 km. This area covers the full focal zone.

This transition from low- to high-Vp/Vs correlates well with structures found by other methods and data, such as earthquake phase analysis (Hrubcova et al., 2016), a nearby active seismic profile (Mullick et al., 2015), and gravity models of the basin (Hecht et al., 1997). The transition observed in the Vp/Vs model may be imaging the base of the Fichtelgebirge pluton. The granitic rock may have a higher competence and lower permeability than the underlying material, resulting in a fluid trap. The more brittle material in the focal zone preferentially fractures as the pore pressure increases, resulting in the periodic swarms (Alexandrakis et al., 2014). Since this structure is not directly imaged by the 2011 swarm data, but is evident in the averaged model, it may indicate that the Vp/Vs contrast is weakened during that swarm period. Further study of the northern fault plane swarms is needed to understand this phenomenon and its implications to the swarm-fluid connection.

References:

- Alexandrakis, C., Calo, M., Bouchaala, F., & Vavrycuk, V., 2014. Velocity structure and the role of fluids in the West Bohemia seismic Zone, *Solid Earth*, 5, 2, 863-872.
- Bräuer, K., Kämpf, H., Koch, U. & Strauch, G., 2011. Monthly monitoring of gas and isotope compositions in the free gas phase at degassing locations close to the Novy Kostel focal zone in the western Eger Rift, Czech Republic, *Chem. Geol.*, 290, 163-176.
- Dahm, T. & Fischer, T., 2014. Velocity ratio variations in the source region of earthquake swarms in NW Bohemia obtained from arrival time double-differences. *Geophys. J. Int.*, 196, 957-970, doi: 10.1093/gji/ggt410.
- Hecht, L., Vignerresse, J.L. & Morteani, G., 1997. Constraints on the origin of donation of the granite complexes in the Fichtelgebirge (Germany and Czech Republic): evidence from a gravity and geochemical study. *Geol. Rundsch.*, 86, 1, 93-109.
- Hrubcova, P., Vavrycuk, V., Bouskova, A. & Bohnhoff, M., 2016. Shallow crustal discontinuities inferred from waveforms of micro earthquakes: Method and application to KTB Drill Site and West Bohemia Swarm Area. *J. Geophys. Res.: Solid Earth*, 121, doi: 10.1002/2015JB012548.
- Kissling, E., Ellsworth, W., Eberhart-Phillips, D. & Kradolfer, U., 1994. Initial reference models in local earthquake tomography. *J. Geophys. Res.: Solid Earth*, 99, B10, 19635-19646.
- Malek, J., Horalek, J. & Jansky, J., 2005. One-dimensional qP-wave velocity model of the upper crust for the West Bohemia/Vogtland earthquake swarm region, *Stud. Geophys. Geod.* 49, 501-524.
- Mousavi, S., Bauer, K., Korn, M. & Hejrani, B., 2015. Seismic tomography reveals a mid-crustal intrusive body, fluid pathways and their relation to the earthquake swarms in West Bohemia/Vogtland. *Geophys. J. Int.*, 203, 1113-1127.
- Mullick, N., Buske, S., Hrubcova, P., Ruzek, B., Shapiro, S., Wigger, P. & Fischer, T., 2015. Seismic imaging of the geodynamic activity at the western Eger rift in central Europe. *Tectonophysics*, 646-648., 105-111.
- Ruzek, B. & Horalek, J., 2013. Three-dimensional seismic velocity model of the West Bohemia / Vogtland seismoactive region. *Geophys. J. Int.*, 195, 2, 1251-1266.

Zhang, H. & Thurber, C., 2006. Development and applications of double-difference seismic tomography. *Pure App. Geophys.*, 163, 2-3, 373-403.

IODP

Chalcophile elements in Shatsky Rise basalts as potential indicators of the mantle plume origin?

R. ALMEEV¹, M. PORTNYAGIN², D. GARBE-SCHÖNBERG³

¹ Leibniz Universität Hannover, Hannover

² GEOMAR, Kiel

³ Christian-Albrechts University Kiel, Kiel

Igneous oceanic plateaus, such as Shatsky Rise, represent one of the least understood types of basaltic magmatism on Earth. In the case of Shatsky Rise, two main models were proposed to explain their origin: (1) melting of deep-sourced mantle plume head, (2) melting at a mid oceanic ridge (MOR) with unusual characteristics (e.g., anomalously high dynamics or spreading-induced upwelling of eclogite). In 2009, Integrated Ocean Drilling Program Expedition 324 has cored an early Cretaceous Shatsky Rise oceanic plateau to test its plume vs. non-plume origin (Expedition 324 Scientists, 2010). Consequent post-cruise petrological and geochemical studies including isotope determinations of Sr, Nd, Hf and He in the rocks testified that the majority of the Shatsky Rise magmas originated from a slightly enriched MORB-type source and underwent MORB-like crystal fractionation. The data did not, however, provide unequivocal evidence of the Shatsky Rise formation by one of the two main proposed scenarios (plume vs. non-plume origin).

Some hotspot-related magmas were previously recognized to have elevated concentrations of strongly chalcophile elements (Cu, Au) compared to typical MORB, providing potential proxy for a deep mantle plume origin (Figure 1a). For example, Jenner & O'Neill (2012) have shown that submarine-quenched glass samples collected along known hot spot tracks or close to areas associated with plume-related magmatism (e.g. Galapagos Spreading

Centre, Reykjanes Ridge) have higher Cu contents at a given MgO compared to the typical MORB range. Similarly, bulk rock data compiled by Jenner et al. (2012) for Ko'olau and Moloka'i Hawaiian volcanoes, Iceland, Kwaimbaita-Type magmas from the Ontong Java Plateau and the Galápagos Islands have higher Cu at a given MgO than the MORB array, indicating that elevated Cu contents is a common characteristic of magmas associated with mantle plumes (Figure 1a). Exceptions were Krogenke-Type lavas from the Ontong Java Plateau, and particularly, samples from the Samoan islands. Webber et al. (2013) and Momme et al. (2003) have shown that quenched glasses and rocks from the Reykjanes Ridge and from Iceland are 2-5 times enriched in Au (up to 5-7 ppb) compared to typical MORB with Au < 1 ppb. An overall enrichment in Au of ocean island basalts in comparison with MORB has also been noted in a review by Pitcairn (2011).

As discussed by Jenner et al. (2012), the most straightforward explanation for the elevated Cu content in plume-related magmas is sulphide undersaturation of their parental magmas. In this case, Cu, Au and other chalcophile elements behave as incompatible trace elements, and their concentrations increase as magmas evolve to low MgO. In contrast, the behavior of chalcophile elements in MORB is strongly controlled by a sulphide phase present on the liquidus of fractionated magmas that causes concentrations of strongly chalcophile elements such as Cu and Au to decrease. Sulphide undersaturation of plume-related magmas at low crystallization pressure might be related to the increasing sulphur solubility in silicate melts with decreasing pressure and/or oxygen fugacity (e.g. Mavrogenes, 1999).

The present dataset available for Shatsky Rise basalts includes only whole-rock Cu contents (Figure 1b), whose elevated values in some rock types can also be explained by post-magmatic sulfidization. In the course of our new initiated research project we plan to carry out new geochemical investigations of the Shatsky Rise basaltic glasses with the focus on (1) in-situ analysis of strongly chalcophile elements in pristine glasses (Cu, Ag, Au, Se), and (2) determination of the oxidation state of magmas. The data will be used to test plume vs. non-plume origin of the Shatsky Rise oceanic plateau.

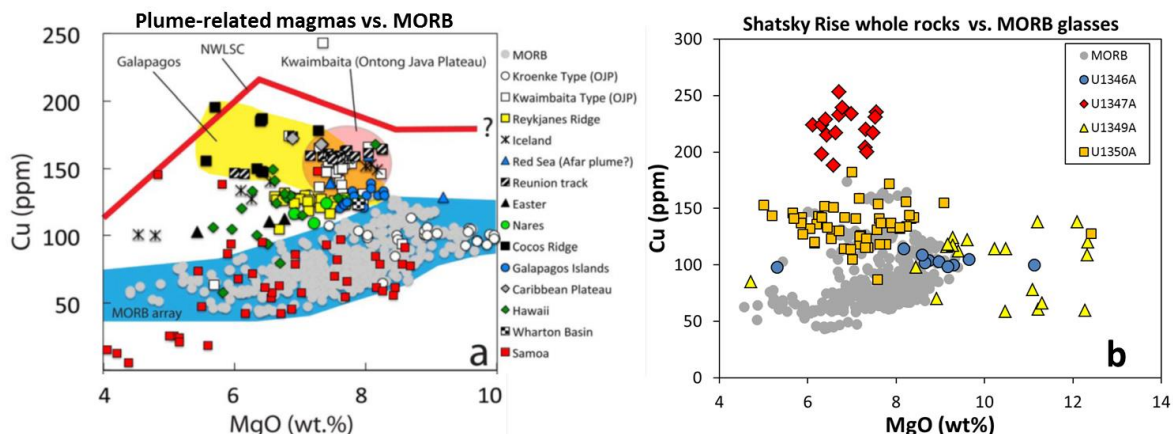


Figure 1: Systematics of MgO and Cu in oceanic magmas: (a) Comparison of MORB and plume-related magmas (Jenner et al. 2012). Most of plume-related magmas are richer in Cu than MORB at given MgO; (b) Comparison of MORB and Shatsky Rise. The rocks from the oldest and largest massif in Shatsky Rise, Tamu massif (U1347A) are strongly enriched in Cu compared to all MORB glasses and most plume-related samples in figure (a). Rocks from the site U1350A on a flank of Ori Massif have lower Cu contents than the Tamu rocks but higher than typical MORB and similar to some MORB glasses from the regions of plume-ridge interaction, e.g. from Galapagos Spreading Center and Reykjanes Ridge (not included in blue-colored MORB array in figure (a)). The rocks from the site 1349A at Ori Massif and 1346A at Shirshov Massif have Cu content within the MORB range. Shatsky Rise whole rock data are from Sano et al. (2012)

References:

- Expedition 324 Scientists (2010). IODP Prel. Rept. 324.
 Jenner, F.E. & O'Neill, H.S.C. (2012). *Geochemistry Geophysics Geosystems* 13, Q02005.
 Mavrogenes, J.A. O'Neill, H.S.C. (1999). *Geochimica et Cosmochimica Acta* 63 (7-8), 1173-1180
 Pitcairn, I.K. (2011). *Applied Earth Science* 120, 31-38.
 Sano, T. et al. (2012). *Geochemistry Geophysics Geosystems* 13, Q08010.
 Webber, A.P. et al. (2013). *Geology* 41 (1), 87-90.

IODP

Subduction initiation: geochemical and experimental study of boninites from the Izu-Bonin-Mariana island arc

R. R. ALMEEV¹, M. V. PORTNYAGIN², R. E. BOTCHARNIKOV¹, S. A. LINSLER¹, S. SCHUTH¹, M. OESER¹, D. GARBE-SCHÖNBERG³, F. HOLTZ¹

¹Institute of Mineralogy, Leibniz Universität Hannover, Callinstr. 3, 30167 Hannover, Germany

²Helmholtz Centre for Ocean research (GEOMAR), Division of the Ocean Floor, Wischhofstr. 1-3, 24148 Kiel, Germany

³Christian-Albrechts University Kiel, Kiel

Understanding of the forearc basalt – boninite lineage is crucial to understand the birth of subduction which is a principal driving force for plate motion and plate tectonics on Earth. Our research project (started in 2016) is aimed at understanding the evolution of petrological and geochemical characteristics of magmatic rocks at the initiation of a subduction process and during early arc development. Using the unique sample collection gained by IODP Expedition 352 at the Izu-Bonin-Mariana (IBM) arc (Expedition 352 Scientists, 2015), we plan to contribute to the interpretation of the geochemical differences between FAB and boninite. Particular attention is given to understand the role of mantle melting conditions (e.g., fO_2 , volatiles, degree of melting) on the behavior of “redox-sensitive” siderophile and chalcophile elements to provide new geochemical tracers of subduction initiation, when melting regime in the mantle changes from decompressional to fluid-driven, and to constrain the conditions of magma storage and differentiation at the transition between FAB and boninite volcanic activity. Here we present preliminary experimental and geochemical data for boninites collected after first year of the running project. Experimental investigations of the fore-arc basalts are presented in a companion abstract (Linsler *et al.*, 2017, this volume).

Boninitic lavas from holes U1439C and U1442A are *Ol*- and *Opx*-phyric rocks with a groundmass of pale glass and acicular pyroxene. In contrast to moderately evolved FABs (Expedition 352 Scientists, 2015; Linsler *et al.*, 2017, this volume), lavas in both of the boninite sites have strongly primitive compositions (8-20 wt% MgO, indicative of possible crystall accumulation) and poorly overlap with boninitic glasses, which have MgO contents ranging from 10 to 2 wt%. To study this link between two clusters of boninitic compositions (via *e.g.* fractional crystallization, crystal accumulation etc.) one can use phase equilibria models (*e.g.* MELTs or COMAGMAT), however application of these models in H₂O-rich boninitic system is now limited by the lack of accurate data for the effect of

H₂O on orthopyroxene crystallization. In addition, whole rock boninites demonstrate variety of compositions – low and high silica boninites, basaltic boninites etc. (Expedition 352 Scientists, 2015) and, thus, the recognition of parental melt composition(s) is questionable.

To solve the problem we conducted a set of partial melting experiments using high-Si (16 wt% MgO, 57 wt% SiO₂), low-Si (16.7 wt% MgO, 53 wt% SiO₂) and some intermediate natural boninites. Experiments were conducted in internally heated pressure vessel at pressures 2 and 5 kbars, temperatures between 1100 and 1250°C in the range of water concentration from 1.6 to 6 wt% H₂O. Our first experimental results show that the trend defined by low-Si boninites (most of whole rocks from Site U1439) are controlled by *Ol* fractionation, whereas high-Si boninites (whole rocks from site U1442) could have been formed by *Ol*+*Opx* fractionation. The lack of recovered high-magnesian boninitic glasses (> than 10 wt% MgO) simply indicate that whole rock boninite compositions are representing lavas with high proportion of accumulated olivine and orthopyroxene phenocrysts in various proportions. In general, the trend(s) defined by boninitic bulk rocks does not represent the liquid line of descent.

Our pilot measurements of the $Fe^{2+}/\Sigma Fe$ using colorimetric wet chemistry method (Schuessler *et al.*, 2008) demonstrate values from 0.85 (in two boninites) to 0.95 (in two FABs), corresponding to FMQ+0.5 and FMQ-2 oxygen buffers respectively (calculated after Sack *et al.*, 1980). This large difference in fO_2 between FABs and boninites is intriguing but should be confirmed with other proxies of the magma oxidation state, which could be independent from possible late-stage magma oxidation. In our project, we proposed to use systematics of redox-sensitive lithophile and chalcophile elements to have independent insights into the oxidation state of FABs and boninites. To achieve the best analytical results the relatively abundant chalcophile elements (Cu, Zn) and redox sensitive elements (V, Sc, Ga) were analyzed by femtosecond LA-ICP-MS (Element XR) in Hannover. Advantage of using low-energy femtosecond laser is a much reduced matrix effect and a lack of inter-element fractionation during sample ablation (this allows accurate determinations of the elements with low condensation temperatures, such as chalcophile elements, Jochum *et al.*, 2014). Very low-abundance elements such as Au and Ag are however difficult to quantify with fs-LA-ICP-MS because of insufficient ion yield. These elements in glasses have been analyzed in the Institute of Geosciences at the Christian-Albrecht University of Kiel. The first results will be shown after data reduction.

References:

- Expedition 352 Scientists. (2015) IODP Prel. Rept. 352.
 Jochum, K.P. *et al.*, (2014) *Geostandards and Geoanalytical Research* 38, 265-292.
 Linsler *et al.*, (2017) *this volume*.
 Sack, R.O. *et al.*, (1980) *Contributions to Mineralogy and Petrology* 75, 369-376.
 Schuessler, J.A. *et al.*, (2008) *American Mineralogist* 93, 1493-1504.

ICDP

Rates and processes of tephra alteration in Surtsey volcano: a combined observational and experimental approach

W. BACH¹, W.-A. KAHL¹, A. TÜRKE¹

¹Fachbereich Geowissenschaften, Universität Bremen, Klagenfurter Str., 28359 Bremen

ICDP supports the SUSTAIN drilling project, which is aimed at investigating the formation and hydrothermal alteration of Surtsey volcano in the Vestmannaeyjar archipelago, Iceland. Rapid and intense alteration of tephra has been key to the post-eruption evolution of Surtsey. We are funded to conduct comprehensive and systematic investigations of the role of temperature and permeability in the processes and rates of tephra alteration. The field program was originally proposed to start in August of 2016 but was postponed by one year due to funding and permitting delays in Iceland. We here report on the goals and plans of SUSTAIN and our individual research project, which is one of 17 within SUSTAIN.

SUSTAIN (A New Drill Core at Surtsey Volcano: A Natural Laboratory for Time-Lapse Characterization of Hydrothermal Seawater and Microbial Interactions with Basaltic Tephra) aims to sample the complete succession of a neo-volcanic island from the surface to the underlying oceanic crust. Understanding the internal structure and facies architecture of the type locality of Surtseyan volcanism is a prime aim of the program. Another unique opportunity within SUSTAIN is time lapse monitoring of Surtsey's active hydrothermal system, its permeability and fluid geochemistry evolutions as well as related microbial activity. In particular, recovered drill core and post-drilling borehole experiments will allow us to examine the coupled changes of porosity and permeability by mineral dissolution and precipitation and the consequences for changes in rock physics properties.

Specific research objectives of SUSTAIN include:

1) assessing the structure of the volcano and heat transfer in the hydrothermal system to understand processes of tephra lithification, which protected Surtsey from incessant marine erosion;

2) using volcanic facies, grain size and vesicularity analysis as a reference for thermal granulation experiments to refine models for explosive magmatic and phreatomagmatic fragmentation and production of airborne ash clouds;

3) quantifying hydrothermal-seawater-rock interactions, including palagonitization and authigenic mineral (zeolites, tobermorite) formation, and as a function of proximity to the dike swarm heat source

4) determining how time, temperature variation, and aqueous environment influence both the material and physical properties of altered tephra and lithified tuff as well as the compositions, crystal chemistry, and cation-exchange properties of Al-tobermorite and zeolite assemblages above and below sea level; and

5) exploring the nature and extent of chemosynthetic life that evolved in the harsh subsurface conditions at Surtsey through coupled microbiological and geochemical sampling and analysis, both during drilling and in the course of the "Surtsey Subsurface Observatory" for

monitoring, sampling and in situ experimental studies of water-microbe-rock interactions.

For reaching these varied aims, an inclined >200-meter deep hole is planned to sample the conduit system of the 1963 eruption. A second vertical hole will be 200 meters deep and sample hydrothermally altered tephra down to the underlying oceanic basement next to the 1979 drill hole. More details about SUSTAIN are provided by Jackson et al. (2015)

As part of **our DFG SPP 1006 grant**, the "Surtsey Subsurface Observatory" will be installed for long-term monitoring and *in situ* experiments. The installment is to be placed in the vertical hole, which will be cased with anodized aluminum to facilitate exploring basement water chemistry and water-rock-microbe interactions over time. The observatory consists of miniature temperature loggers and perforated PEEK-incubators that contain hyaloclastite from Surtsey as well as forsteritic olivine. PEEK (polyetheretherketone) is a machinable, semicrystalline, thermoplastic material. Duplicate incubators will be used for mineralogical (in Bremen) and microbiological studies (at the University of Bergen). The incubation devices will be hung down the hole on a Vectran rope and placed in areas where the casing is perforated to allow for flow of basement fluid. The anticipated incubation depths are 40, 75, 105, and 155 m below the surface, and temperature is expected to be maximal at 105 m depth (120°C). The incubators and autonomous temperature loggers will be left in the hole for two years.

In the meantime, work on ICDP drill core will be conducted: Mini cores of 19-mm diameter will be cut from core from both drill holes to produce μ -CT images of the main lithologies and to examine the distribution of primary versus secondary phases versus pore space. These images and data will be used to retrieve permeability information and will allow us to derive empirical relations between porosity, permeability, the extent of replacement of primary phases, and nature and distribution of secondary phases. Based on these images, thin sections will be cut to sample the critical areas of the rocks for microbeam-analytical work. This work will be coordinated with collaborating researchers within SUSTAIN. The combined results will allow us to relate mineral chemical and textural information in order to gain specific insights into the relations between pore space evolution and mass transfer reactions.

A third work package of the project uses flow-through experiments to investigate the linked progress of hyaloclastite alteration reactions and pore space evolution. The experiments will be performed using a flow-through reaction cell that consists of x-ray transparent PEEK and has been designed to allow for concomitant monitoring of the reaction progress and the porosity-permeability evolution in the course of the ongoing experiment. Solutions will be sampled in the outflow to monitor reaction progress and calculate mineral saturation states.

Reference:

Jackson, M.D. and 21 co-authors, including W.Bach and A.Türke (2015) Time-lapse characterization of hydrothermal seawater and microbial interactions with basaltic tephra at Surtsey Volcano. *Sci. Drill.*, 20, 51–58

IODP

Enhanced Subtropical Gyre circulation feeding ice sheet growth during the Mid-Pleistocene Transition (500 – 1400 ka, Site U1385)

A. BAHR¹, S. KABOTH², D. HODELL³¹ Institute of Earth Sciences, Im Neuenheimer Feld 234, 69120 Heidelberg, Germany² Department of Earth Sciences, Faculty of Geosciences, Utrecht University, Heidelberglaan 2, 3584CS, Utrecht, The Netherlands³ Department of Earth Sciences, University of Cambridge, Downing Street, Cambridge, Cambridgeshire, CB2 3EQ, UK

A fundamental shift in the glacial/interglacial cyclicity from a “41 kyr world” into the present-day “100 kyr world” took place during the mid-Pleistocene Transition (MPT), at around ~900 ka, accompanied by a distinct growth of glacial ice shields¹. The growth of ice volume goes along with more pronounced winter cooling in high latitudes, necessary to sustain large ice sheets². However, high latitude cooling reduces the amount of moisture available to generate snow fall necessary for building up large ice sheets. An important role for circumventing this paradox situation might be played by the North Atlantic Subtropical Gyre, which plays a decisive role for the heat distribution between low and high latitudes. To study whether subtropical gyre dynamics during the mid-Pleistocene we study surface and subsurface properties (temperature, salinity) on IODP Site 1385 (“Shackleton Site”), drilled during IODP Exp. 339 at the Iberian Margin. Focus is the time interval of 500 – 1400 kyr (MIS 14 – 44), which captures the major changes during the MPT. Site 1385 is located at the eastern margin of the North Atlantic Subtropical Gyre, an area characterized by the accumulation of warm and saline subsurface waters. The aim of the project is to assess variations in heat transport towards the Iberian Margin, which strongly depends on the intensity of the Subtropical Gyre Circulation. To constrain upper ocean variability, we reconstructed sea surface and subsurface temperatures (SST and subT) and salinity (SSS and subS), by combined $\delta^{13}\text{C}$, $\delta^{18}\text{O}$ and Mg/Ca records on the shallow dwelling foraminifer *Globigerinoides bulloides* and the deep dweller (i.e. ~200-300 m water depth) *Globorotalia inflata*. The combination of $\delta^{18}\text{O}$ and Mg/Ca-derived surface and subsurface temperatures (SST, and Tsub, respectively) allows for the calculation of the ice-volume corrected $\delta^{18}\text{O}_{\text{seawater}}$ ($\delta^{18}\text{O}_{\text{ice-sw}}$) as an approximation of salinity.

SST and subT generally follows the glacial-interglacial pattern. However, we observe that the long-term trend of subT as well as of $\delta^{18}\text{O}_{\text{ice-sw}}$ are opposed to that of successively more intensified glacials imprinted into the SST records from the North Atlantic. Notably, relatively weak glacials such as MIS 38 and 40 are accompanied by persistent and strong subsurface cooling, interpreted as a much reduced or absent influence of gyre waters. In contrast, glacials MIS 18 and 20 show persistent warm subT. Strong subT cooling subsequently reappears again with MIS 16. The advection of warm subsurface waters to the Iberian Margin during the MPT might be explained by a southward shift and strengthening of the zonal wind belts as a response to enhanced ice sheet growth. Intensified surface winds cause a deepening of the thermocline at the Iberian Margin, which could on subsurface level at least partly compensate for the stronger surface cooling. A strengthening and southward displacement of the mid-

latitude wind fields would have far reaching consequences not only for the oceanic circulation but alter the moisture distribution over the continent. Providing excess moisture during glacial inceptions might further help to grow and sustain the enhanced continental ice shield growth during the MPT.

Notably, subS records are overprinted by orbital precession which is not prominent in the temperature records. The precession signal might be derived from the precession-paced trade wind intensity which drives the cold, southward flowing Portugal Current. However, in this case subT should show precession-related variability as well. Alternatively, the precession-signal might represent a direct or indirect influence of the highly saline Mediterranean Outflow Water (MOW). Notably, phases of maximum subS and subT at Site U1385 coincide with very strong MOW production (Zr/Al records from Site U1387, Gulf of Cadiz). While the intermediate water mass of the MOW resides below the recent habitat of *G. inflata*, its high-salinity waters might shoal considerably for certain periods of strong MOW production, and thus enhance subS at Site U1385. In a more indirect way strong MOW might lead to arming off Iberia as buoyancy-driven sinking of dense MOW fosters the eastward expansion of the warm and saline Azores Current transporting subtropical water towards the Iberian Margin.

References:

- 1 Clark, P. U. et al. The middle Pleistocene transition: characteristics, mechanisms, and implications for long-term changes in atmospheric pCO₂. *Quaternary Science Reviews* 25, 3150-3184 (2006).
- 2 McClymont, E. L., Sosdian, S. M., Rosell-Melé, A. & Rosenthal, Y. Pleistocene sea-surface temperature evolution: Early cooling, delayed glacial intensification, and implications for the mid-Pleistocene climate transition. *Earth-Science Reviews* 123, 173-193 (2013).

IODP

The active channel-levee system of the Bengal Fan at 8°N – a high-resolution evolutionary study based on seismo-acoustic data and IODP Expedition 354 drill Site U1454

F. BERGMANN¹, H. LANTZSCH¹, V. SPIESS¹, T. SCHWENK¹, C. FRANCE-LANORD² AND IODP EXPEDITION 354 SCIENTIFIC PARTY¹ Department of Geosciences, University of Bremen, Klagenfurter Strasse 2-4, D-28359 Bremen, Germany² Centre de Recherches Pétrographiques et Géochimiques, CNRS Université de Lorraine, BP 20, 54501 Vandoeuvre les Nancy, France

The Bengal Fan is the largest submarine fan on Earth covering almost the entire Bay of Bengal. Almost 80% of the eroded material from the Himalayan Mountains is transported towards and stored in the Bengal Fan. The fan provides the most complete sedimentary record of the erosional and tectonic history covering the time from fan initiation in the early Eocene to present (France-Lanord et al., 2016, Curray et al., 2003).

In the modern situation, the sediment is transported from the Himalayan Mountains to the Bengal Shelf via the major rivers Ganges and Brahmaputra. Merging a number of smaller tributary rivers they drain the northern as well as the southern flank of the mountain range. Episodically occurring turbidity currents transport the sediments further to the deep sea. Since the Late Miocene, these turbidity

currents construct channel-levee systems on their way downslope, which are since then the main architectural elements of the Bengal Fan (Schwenk and Spieß, 2009). Frequent channel avulsions on the upper fan result in the abandonment of old channels and the formation of new channel-levee systems or even channel-reoccupation leading to a complex erosional/depositional system with lateral depocenter migration over the entire fan (Curry et al., 2003, Schwenk and Spieß, 2009). In contrast to most other large submarine fans, the Bengal Fan was also active during deglacial sea level rise and Holocene high stand along the transport pathway of the 'active channel' (Weber et al., 1997; 2003).

In February/March 2015 the Bengal Fan was target of IODP Expedition 354 'Neogene and late Paleogene record of Himalayan orogeny and climate: a transect across the Middle Bengal Fan'. The expedition drilled 3 deep (900-1200 mbsf) and 4 shallow (200-300 mbsf) sites along a W-E transect at 8°N in order to address the major research questions of (i) the emergence of the Himalaya and the onset of fan deposition, (ii) the fan evolution in Miocene and Pliocene times and the monsoonal impact on sediment supply and flux throughout this time, (iii) the role of the Himalaya-Bengal Fan source-to-sink system in the global carbon cycle and climate and (iv) the spatial depocenter variability and its control on the fan architecture. Numerous channel-levee systems and inter-channel deposits were drilled, representing fan activity from stacked sequences as well as absence of fan deposition by hemipelagic background sedimentation. The westernmost Site U1454 retrieved sediments from the western levee of the active channel and provides an overview on Quaternary fan history as well as the opportunity to study depositional processes along the active channel in high-resolution.

The evolution of channel-levee systems has been a long-term research subject but is primarily based on indirect observations. Most recent studies use numerical or sandbox modeling, but have limitations compared to natural conditions due to their simplified boundary conditions such as static sinuosity, downsizing or non-erosive channels (e.g. Straub et al., 2008, Huang et al.,

2012). However, it is evident that deposition along a meandering channel is asymmetric, and this asymmetry has to be considered during flux estimations of sediments from a levee.

Drilling results from Site U1454 and a net of (very) high-resolution acoustic profiles in the vicinity of the active channel-levee system opened the opportunity to study the spatial depositional pattern near a recently active sinuous channel-levee system, to investigate the depositional style and facies succession as well as its evolution in space and time. Such investigation is carried out within the framework of the DFG funded project 'The Bengal Fan stratigraphy as a function of tectonic and climate – Correlation of IODP Expedition 354 results and available seismic data from the Bay of Bengal'. Utilizing the cores recovered from the western levee, acoustic data are linked with sediment properties, e.g. grain size, and lithology. To determine sedimentary fluxes based on the IODP Expedition 354 drilling locations, it is important to assess, if changes in deposition are controlled locally by channel geometry or by changes in the source region.

On the poster we will present the correlation of Parasound data and Site U1454 drilling results as well as thickness maps of specific levee units showing their distribution relative to the channel. Parasound Line GeoB97-020 (Figure 1) crosses Site U1454 and the channel almost perpendicular at the apex of a meander bend. The channel is flanked by the western and the eastern wedge-shaped levees, and is here 65 m deep and 4 km wide. The channel was formerly eroded more than 100 meter beneath the levee base but refilled by 62 m of sediments. The levee is 27 m high at Site U1454, but has maximum thicknesses of 30 m and 35 m at the western and eastern side, respectively. The levee base is marked by a distinct reflector representing a rapid upward change from sand-dominated to a clay- and silt-dominated lithology, which marks the onset of overspill deposition onto the channel overbank areas (Figure 1B). Based on acoustic properties and core lithology, the levee has been divided into 5 individual units, Turbidite Units (TU) 1-3 and Calcareous Clay Units (CCU) 1 and 2 (Figure 1B). The three Turbidite

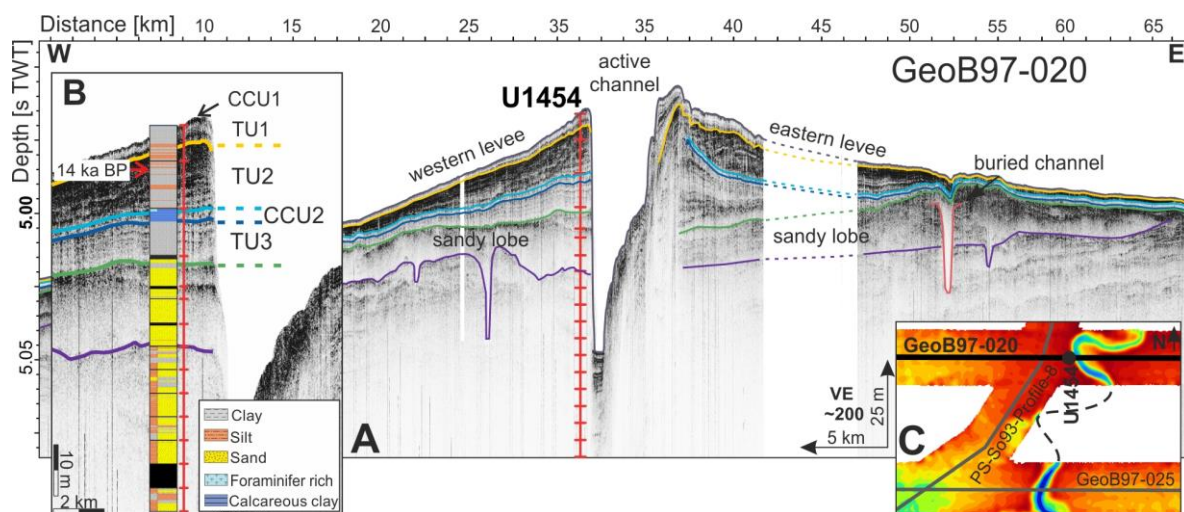


Figure 1: Overview of the active channel-levee system and drill Site U1454 (A) W-E trending Parasound Line GeoB97-020 crosses the active channel-levee system and Site U1454. Individual levee units and the underlying lobe are marked with colored horizons. (B) Close-up of Site U1454 illustrating the five levee units in correlation with the corresponding core lithology (yellow: sand; orange: silt; grey: clay; blue: calcareous clay). (C) Bathymetry along the active channel-levee system indicating the location of Line GeoB97-020 in relation to the channel geometry.

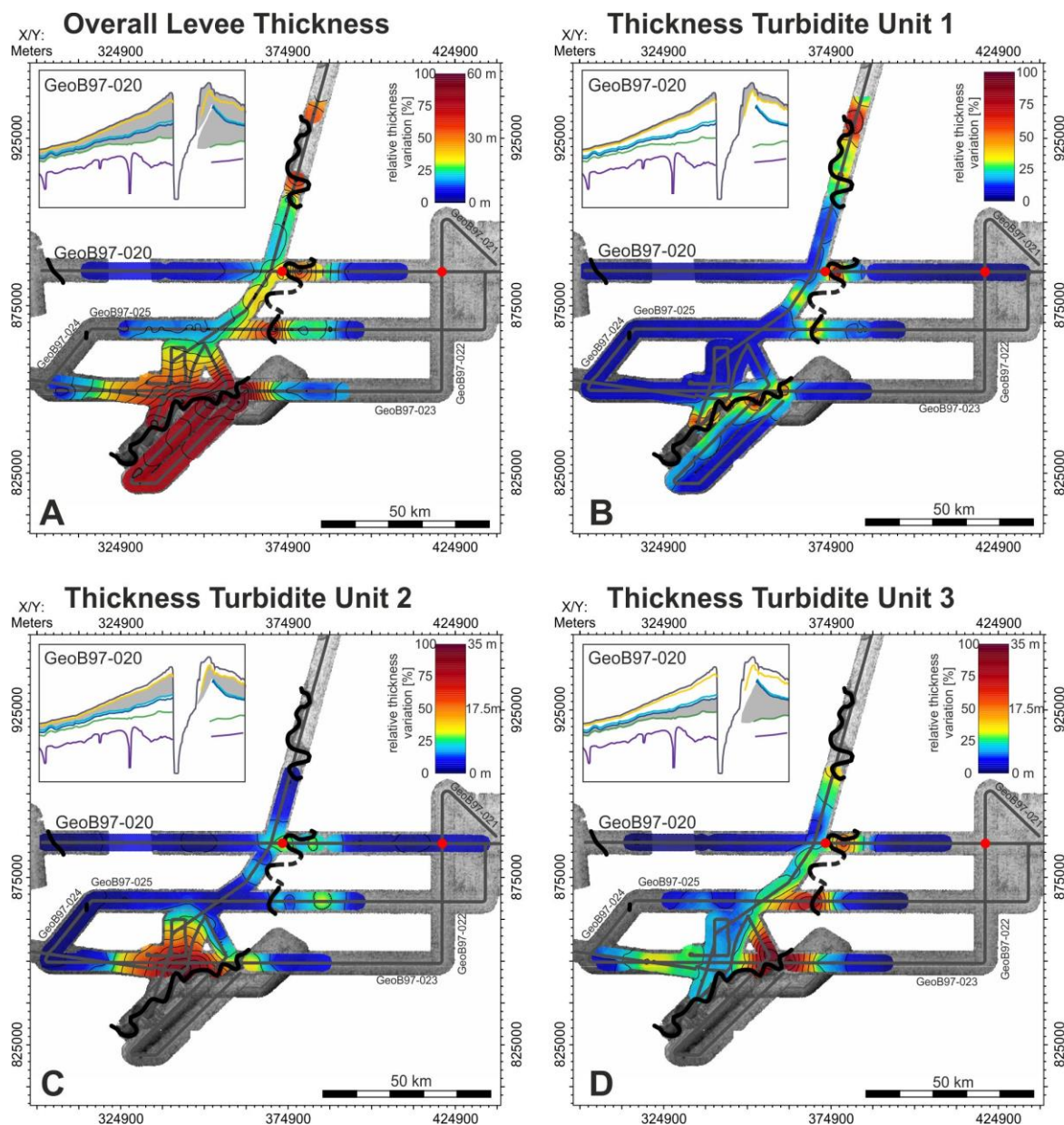


Figure 2: Thickness maps calculated based on the Parasound data in the vicinity of the active channel-levee system and Site U1454 of (A) the entire levee, (B) the uppermost Turbidite Unit TU1, (C) the Turbidite Unit TU2, and (D) the oldest Turbidite Unit TU3. All maps illustrate the spatial variation of levee deposition over time as a function of channel sinuosity.

Units TU1-3 represent overspill deposition on top of the levee by turbidity currents. They all show a divergent reflection pattern and thin out with increasing distance to the channel (Figure 1A). Whereas TU1 and 3 reflections show medium amplitudes, TU2 is characterized by reflections of high amplitude, which show a downward decreasing trend. This corresponds to the lithology of the TUs. Turbidites constructing Units TU1 and TU3 are dominated by clay, turbidites of Unit TU2 show slightly higher silt content (Figure 1B). Based on visual core descriptions, digital color imaging and magnetic susceptibility logs, 190 individual turbiditic events with a median thickness of 9 cm and a maximum thickness of 86 cm could be identified in cores of Site U1454 within the Units TU1-3.

Unit CCU2 is deposited between TU3 and TU2. It is characterized by low amplitudes in the Parasound data and consists of calcareous clay. The lithology reveals two

subunits within CCU2. The lower 1.9 meter of CCU2 represent clay-dominated turbiditic deposition. The upper 46 cm of CCU2 contain nannofossils and foraminifera indicating significantly reduced overspill deposition. A similar overspill reduction is the case for Unit CCU1, which is 22 cm thick, draping the levees and being as well interpreted as hemipelagic background sedimentation. CCU1 cannot be resolved with Parasound data.

Average sedimentation rates for both overspill and non-overspill background sedimentation could be determined based on two time markers, the Toba Ash layer and radiocarbon dating (Christian France-Lanord, personal communication). These markers allowed the establishment of a preliminary stratigraphy for the active channel-levee system at 8°N. The onset of overspill deposition occurred around ~44 ka before present (BP), significantly earlier than previously assumed, at least for the channel at

16°30'N (Weber et al., 1997). At ~39 ka BP, overspilling was interrupted for almost 21 ky, until 18 ka BP. Following this time of quiescence, turbiditic deposition on the levee was reactivated for another 8 ky. At ~10 ka BP, the active phase of overspilling finally stopped and the deposition of a calcareous clay drape started. According to this stratigraphy, levee growth along the active channel-levee system must have stopped earlier at 8°N than at 16°30'N, where turbidite deposition lasted at least until 6 ka BP (Weber et al., 1997). Under the assumption that the levee was constructed by at least 190 individual overspill events, turbidity currents reaching Site U1454 had recurrence rates of 60 to 65 years.

Mapping of the turbidite units was conducted along the net of Parasound profiles in the vicinity of the active channel-levee system. The resulting thickness maps (Figure 2) were used to investigate the link of channel geometry and variations in levee deposition in space and over time. Overall levee thickness increases closer to the channel and towards the south, but deposition appears to be more or less equally spread between the eastern and western side of the channel. Since TU1 is the youngest of the 3 Turbidite Units, a channel geometry similar to the present situation can be assumed for the time span of its deposition. TU1 has its maximum thickness close to the channel axis and thins out with distance. The unit appears to be deposited almost symmetrically on the eastern and western levee but at banded sections of the channel deposits at the outer bend levee (cut bar) tend to be thicker than at the inner bend levee (point bar).

A more distinct levee asymmetry was observed for TU2, which has a clear maximum of deposition in the south of the study area with some depositional highs close to the channel. The difference between the eastern and western levee thickness increases from north to south. At the northernmost Parasound profile the thickness is symmetric across the channel, but a distinct increase in deposition is observed for the western levee on the southernmost Parasound profile. This style of deposition confirms a strong influence of the channel sinuosity, which dynamically changes over time, on the overspilling deposition. Vice versa, the external geometry and thickness of the levee units provide a strong tool to reconstruct former meander-bend positions. The significant cross-channel asymmetry of TU3 implies a channel pathway that must have been opposite to the present channel geometry. These findings illustrate, for the first time with field data, variations in levee deposition in time and space in response to channel meandering. On a short time scale the style of overspill deposition appears to be quite complex. However, on a longer timescale, as seen in the overall levee thickness, deposition becomes more and more symmetric.

These results emphasize the influence of channel sinuosity on the deposition and enable the scientific party to assess and evaluate sedimentary fluxes and budgets measured at the drill sites. It also shows, that a sufficiently long-time average must be used when determining sediment budgets. Where no multiple coverage of a channel-levee system is available, budgets should be averaged over the entire lifetime of one system in order to minimize statistical errors generated by short-term fluctuations.

References:

- Curry, J.R., Emmel, F.J., and Moore, D.G., 2003. The Bengal Fan: morphology, geometry, stratigraphy, history and processes. *Marine and Petroleum Geology*, 19(10):1191–1223.
- France-Lanord, C., Spiess, V., Klaus, A., Schwenk, T., and the Expedition 354 Scientists, 2016. Bengal Fan. Proceedings of the International Ocean Discovery Program, 354: College Station, TX (International Ocean Discovery Program). <http://dx.doi.org/10.14379/iodp.proc.354.2016>
- Huang, H., Imran, J., Pirmez, C., 2012. The depositional characteristics of turbidity currents in submarine sinuous channels. *Marine Geology* 329–331, 93–102.
- Schwenk, T. & Spieß, V., 2009. Architecture and stratigraphy of the Bengal Fan as response to tectonic and climate revealed from high resolution seismic data. In Kneller, B., Martinsen, O.J., and McCaffrey, B., eds., *External Controls on Deep-Water Depositional Systems: SEPM Special Publication 92*, p. 107–131.
- Straub, K.M., Mohrig, D., McElroy, B., Buttles, J., Pirmez, C., 2008. Interactions between turbidity currents and topography in aggrading sinuous submarine channels: A laboratory study. *Geological Society of America Bulletin* 120, 368–385.
- Weber, M.E., Wiedicke, M.H., Kudrass, H.R., Hübscher, C., Erlenkeuser, H., 1997. Active growth of the Bengal Fan during sea-level rise and highstand. *Geology* 25, 315–318.
- Weber, M.E., Wiedicke-Hombach, M., Kudrass, H.R., Erlenkeuser, H., 2003. Bengal Fan sediment transport activity and response to climate forcing inferred from sediment physical properties. *Sedimentary Geology* 155, 361–381.

IODP

The evolution of deep water circulation in the subpolar North Atlantic during the last glacial termination

P. BLASER¹, J. LIPPOLD², M. GUTJAHR³, F. PÖPPELMEIER¹, N. FRANK^{1,2}, J. M. LINK^{1,2}

¹Institute of Environmental Physics, Heidelberg University, Germany

²Institute of Earth Sciences, Heidelberg University, Germany

³GEOMAR Helmholtz Centre for Ocean Research, Kiel, Germany

Authigenic neodymium (Nd) isotopes have become a valuable proxy for the reconstruction of past ocean water mass provenance. For an accurate interpretation of Nd isotope palaeo records, however, a precise knowledge of the Nd isotope signatures of possible water mass end members is imperative. While there is evidence that the Nd isotopic composition of North Atlantic Deep Water and its glacial pendant remained constant during the last glacial cycles [1], there is also data that conflicts with such constancy in deeper waters [2]. The subpolar North Atlantic is both the source region of North Atlantic Deep Waters, as well as an area of very dynamic water mass mixing that reacts sensitively to climatic changes like ice cover and surface temperatures. Furthermore, it is a region with vastly variable input in terms of Nd isotope compositions. For the first time, we reconstruct the deep water Nd isotope composition from several IODP sites across the deep subpolar North Atlantic during the last transition from glacial to warm climate. These reconstructions are complicated by variable inputs of easily weathered material from the continents.

For the reconstruction of past deep water Nd isotope compositions, we apply acid-reductive bulk sediment leaches to the sediment samples. In order to avoid significant leaching of different detrital components, we apply the leaching method proposed by Blaser et al. (2016) [3]. Our results showed that this method reliably extracts a Nd isotope signature that agrees with foraminiferal data and is very close to seawater measurements from a variety of Atlantic sediments. Additionally, we make use of the

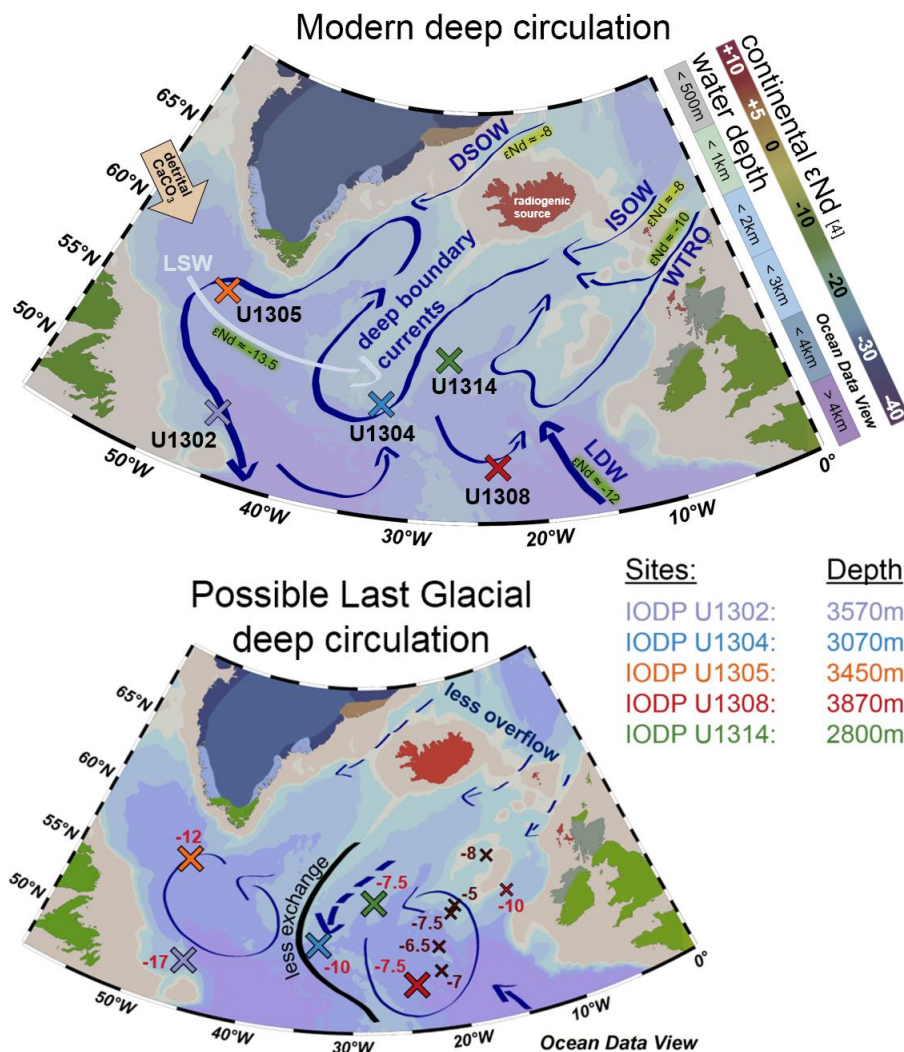


Figure 1: Deep circulation scheme of today’s subpolar North Atlantic, as well as proposed deep circulation during the Last Glacial Maximum based on our neodymium isotope reconstructions. The continents are colour coded according to their approximate Nd isotope composition, based on [4]. Nd isotope compositions are given in ϵ notation (deviation from CHUR standard $\times 10,000$). Water mass abbreviations stand for: LSW: Labrador Sea Water; DSOW: Denmark Strait Overflow Water; ISOW: Iceland-Scotland Overflow Water; WTRO: Wyville-Thompson Ridge Overflow; LDW: Lower Deep Water. Numbers in the lower map are the reconstructed Nd isotope signatures during the Last Glacial Maximum from this study and [5] and [6].

rare earth element patterns, Al/Nd and Sr/Ca ratios to identify leachates in which a detrital input plays a significant role.

We are confident that the remaining leachates record changes in deep ocean circulation, and the reconstructed Nd isotope compositions reflect changes in the input of Nd into the deep waters and mixing of different water masses. Our results show that water exchange between the deep eastern and western basins was limited during the last glacial maximum, probably due to the weakening of overflow waters from the North-East. During the early Holocene, a vigorous exchange between the two basins was established, evident through a homogenised Nd isotope signature across East and West. However, the Nd isotope composition throughout the deep boundary currents further changes towards more radiogenic isotope signatures in both basins during the mid- to late Holocene. This continued change could indicate a strengthening of overflows exporting more radiogenic Nd from Iceland. With such

pronounced variations in the Nd isotope composition of the deep boundary currents, it is hard to imagine a composition of the resulting North Atlantic Deep Water that would retain a constant Nd isotope signature throughout the last deglaciation.

References:

- [1] Foster et al. (2007), *Geology*
- [2] Böhm et al. (2015), *Nature*
- [3] Blaser et al. (2016), *Chemical Geology*
- [4] Jeandel et al. (2007), *Chemical Geology*
- [5] Roberts & Piotrowski (2015), *Earth and Planetary Science Letters*
- [6] Crocker et al. (2016), *Quaternary Science Reviews*

IODP

Macroscale and Microscale Calcium Isotope Variations in Calcites from Ocean Crust Basalts

FLORIAN BÖHM¹, ALEXANDER ROCHOLL², MICHAEL WIEDENBECK², VOLKER LIEBETRAU¹, ANTON EISENHAEUER¹

¹GEOMAR Helmholtz Centre for Ocean Research Kiel, Wischhofstr. 1-3, 24148 Kiel, Germany

²GFZ German Research Centre for Geosciences, Telegrafenberg, 14473 Potsdam, Germany

Calcite cements in ocean crust basalts of the deep sea form from mixtures of cold seawater and warm hydrothermal fluids (about 0-70°C). Such low temperature alteration (LTA) calcites have recently gained new interest as proxy recorders of seawater composition (Coggon et al., 2010; Rausch et al. 2013; Li et al. 2014; Coogan & Dosso, 2015). Reconstructions of the evolution of seawater Sr/Ca and Mg/Ca based on LTA calcites indicate considerably increases of seawater Sr/Ca and Mg/Ca ratios from the Paleogene to Recent times. These reconstructions are based on two basic assumptions. First, $^{87}\text{Sr}/^{86}\text{Sr}$ ratios and $\delta^{18}\text{O}$ are used as proxies for the impact of crustal alteration on the fluid composition recorded in the LTA calcites. This assumes that calcium in the LTA circulation systems is closely coupled to strontium. If, however, at low temperatures calcium more easily mobilised from the ocean crust than strontium, recorded Sr/Ca ratios could appear lower than the original seawater composition. Second, it is generally assumed that the LTA calcites have not been diagenetically altered and preserve their original composition. However, with burial by several hundreds of meters of sediments in close contact to basalt and circulating pore fluids for many millions of years, burial alteration might have changed the recorded signals, especially if the original minerals were metastable aragonites or Mg-rich calcites.

For testing the reliability of the LTA calcite records we use an extended multi-proxy approach: in addition to oxygen isotopes and $^{87}\text{Sr}/^{86}\text{Sr}$ ratios we analysed stable calcium and strontium isotopes ($\delta^{44/40}\text{Ca}$, $\delta^{88/86}\text{Sr}$) as potential indicators of basement influence on the calcite composition. On a macroscopic scale we find low $\delta^{44/40}\text{Ca}$ values for DSDP and ODP sites where the $^{87}\text{Sr}/^{86}\text{Sr}$ ratios of LTA calcites indicate basement influence. On the other hand, for some sites the $^{87}\text{Sr}/^{86}\text{Sr}$ values indicate precipitation from pristine seawater, while low $\delta^{44/40}\text{Ca}$ values indicate basement influence. All of the latter sites are either older than 50 Myr or show calcite precipitation temperatures $>50^\circ\text{C}$. Sites that are younger than 25 Myr and had formation temperatures $<10^\circ\text{C}$ show high $\delta^{44/40}\text{Ca}$ values indicating absence of basement influence, in agreement with the $^{87}\text{Sr}/^{86}\text{Sr}$ ratios.

Stable strontium isotopes show little variability ($\delta^{88/86}\text{Sr}_{\text{SRM987}} = 0.30$ to 0.35‰). Only at temperatures $>50^\circ\text{C}$ significantly higher $\delta^{88/86}\text{Sr}$ values were observed. The $\delta^{88/86}\text{Sr}$ values of the “cold” LTA calcites lie between the mean hydrothermal fluid/basalt value of 0.24‰ and the seawater value of 0.39‰ (Pearce et al. 2015). We found no correlation between $\delta^{88/86}\text{Sr}$ and basement influence (indicated by negative $^{87}\text{Sr}/^{86}\text{Sr}$ offsets from contemporary seawater). This is not surprising, as addition of more than

about 15% of basement strontium is necessary for a resolvable influence on $\delta^{88/86}\text{Sr}$. The measured $^{87}\text{Sr}/^{86}\text{Sr}$ offsets, however, indicate less than 5% addition of mantle strontium ($^{87}\text{Sr}/^{86}\text{Sr} = 0.703$) to the fluid.

The calcium isotope results indicate a resolvable basement influence on LTA calcite composition already at temperatures $>10^\circ\text{C}$. Radiogenic strontium isotopes, in contrast, appear as unequivocal basement influence indicators only at temperatures above 30°C . Below about 20°C $^{87}\text{Sr}/^{86}\text{Sr}$ ratios are no reliable indicators of basement influence. All LTA calcites of sites older than 50 Myr formed at temperatures $>15^\circ\text{C}$ and show low $\delta^{44/40}\text{Ca}$ values indicating that about one third of the calcium was derived from leaching of basement rocks. Recorded Sr/Ca ratios may consequently be 30% lower than seawater values.

In order to get more information on microscale variability of calcium isotopes in the LTA calcites we used the Cameca 1280-HR SIMS at the GFZ Helmholtz Zentrum Potsdam. External reproducibility was $\pm 0.3\text{‰}$ on $\delta^{44/40}\text{Ca}$, comparable to other published SIMS applications (Rollion-Bard et al. 2007). A 10 mm transect through a calcite filled vug in a sample from Core 81-553A (Rockall Plateau, basement age 57 Ma) showed significant, systematic variability. The sample formed at a temperature of about 55°C and shows a significant basement influence in the $^{87}\text{Sr}/^{86}\text{Sr}$ ratio (0.70757) and the low Mg/Ca ratio (0.03 mmol/mol). TIMS measurements showed a bulk $\delta^{44/40}\text{Ca}$ of 1.1 ‰, indicating significant input of basaltic calcium ($\delta^{44/40}\text{Ca} = 0.8\text{‰}$, Amini et al. 2009). The $\delta^{88/86}\text{Sr}$ was 0.34 ‰. SIMS transects show a 1.2‰ $\delta^{44/40}\text{Ca}$ gradient, with high values near the rim and low values at the center of the vug. The vug is completely filled with blocky calcite.

The consistently higher $\delta^{44/40}\text{Ca}$ values near the rim indicate a sequential filling of the void from a fluid that evolved from a seawater like composition to a strongly basement influenced hydrothermal fluid. They are not in line with a post-depositional alteration by fluids infiltrating from the rim, i.e from the basalt surrounding the vug.

We are currently carrying out micromill sampling to verify the SIMS results by double spike TIMS measurements of milled microsamples. Future work will include oxygen isotope measurements, which according to our interpretation are expected to show increasing temperatures ranging from deep-sea conditions to hydrothermal conditions.

References:

- Amini M., Eisenhauer A., Böhm F., Holmden C., Kreissig K., Hauff F., Jochum K. (2009) Calcium Isotopes ($\delta^{44/40}\text{Ca}$) in MPI-DING Reference Glasses, USGS Rock Powders and Various Rocks: Evidence for Ca Isotope Fractionation in Terrestrial Silicates. *Geostandards and Geoanalytical Research* 33, 231-247.
- Coggon, R. M., Teagle, D. A. H., Smith-Duque, C. E., Alt, J. C., & Cooper, M. J. (2010). Reconstructing past seawater Mg/Ca and Sr/Ca from mid-ocean ridge flank calcium carbonate veins. *Science*, 327, 1114-1117.
- Coogan, L. A., & Dosso, S. E. (2015). Alteration of ocean crust provides a strong temperature dependent feedback on the geological carbon cycle and is a primary driver of the Sr-isotopic composition of seawater. *Earth and Planetary Science Letters*, 415, 38-46.
- Li, S., Geldmacher, J., Hauff, F., Garbe-Schönberg, D., Yu, S., Zhao, S., & Rausch, S. (2014). Composition and timing of carbonate vein precipitation within the igneous basement of the Early Cretaceous Shatsky Rise, NW Pacific. *Marine Geology*, 357, 321-333.
- Pearce C., Parkinson I., Gaillardet J., Charlier B., Mokadem F., Burton K. (2015) Reassessing the stable ($\delta^{88/86}\text{Sr}$) and radiogenic ($^{87}\text{Sr}/^{86}\text{Sr}$) strontium isotopic composition of marine inputs. *Geochimica et Cosmochimica Acta* 157, 125-146.

Rausch, S., Böhm, F., Bach, W., Klügel, A., & Eisenhauer, A. (2013). Calcium carbonate veins in ocean crust record a threefold increase of seawater Mg/Ca in the past 30 million years. *Earth and Planetary Science Letters*, 362, 215–224.

Rollion-Bard C., Vigier N., Spezzaferri S. (2007) In situ measurements of calcium isotopes by ion microprobe in carbonates and application to foraminifera. *Chemical Geology* 244, 679-690,

ICDP

GONAF – A borehole Geophysical Observatory around the North Anatolian Fault in the Eastern Sea of Marmara

MARCO BOHNHOFF^{1,2}, GEORG DRESEN¹, ULUBEY CEKEN³, FILIZ TUBA KADIRIOGLU³, RECAI FEYIZ KARTAL³, TUGBAY KILIC³, MURAT NURLU³, KENAN YANIK³, DIGDEM ACAREL¹, FATI H BULUT¹, HISAO ITO⁴, WADE JOHNSON⁵, PETER ERIC MALIN¹, DAVE MENCIN⁵

¹ GFZ German Research Centre for Geosciences, Section 4.2 'Geomechanics and Rheology', Potsdam, 14473, Germany (bohnhoff@gfz-potsdam.de)

² Free University Berlin, Department of Earth Sciences, Berlin, 12249, Germany

³ AFAD Disaster and Emergency Management Presidency, Earthquake Department Ankara, 06510, Turkey

⁴ Japan Agency for Marine-Earth Science and Technology (JAMSTEC), Yokohama, 236-0001, Japan

⁵ UNAVCO, Boulder, Colorado, 80301, USA

The Marmara section of the North Anatolian Fault Zone (NAFZ) runs underwater and is located less than 20 km from the 15-million-person population center of Istanbul at its eastern portion. Based on historical recurrence times, it is overdue for a magnitude M>7 earthquake. The permanent GONAF Geophysical Observatory at the North Anatolian Fault has been installed around this section to help capture the seismic and strain activity preceding, during, and after such an anticipated event.

The GONAF observatory is currently comprised of seven 300 m deep vertical seismic profiling stations and four collocated 100 m deep borehole strainmeters. Five of the stations are located on the land surrounding the Princes Islands segment below the eastern Sea of Marmara, two are on the near-fault Princes Islands south of Istanbul. The 300 m boreholes have 1, 2, and 15 Hz 3-C seismometers near their bottoms. Above this are vertical, 1 Hz, seismometers at ~210, 140, and 70 m depths. The strainmeter boreholes are located within a few meters of the seismometers and contain horizontal strain tensor sensors and 2 Hz 3-C seismometers at their bottoms. This selection of instruments and depths was done so as to ensure high-precision and broad-frequency earthquake monitoring and vertical profiling, all under low-noise conditions.

GONAF is the first ICDP-driven project with a primarily focus on long-term monitoring of fault-zone dynamics. It has already contributed to earthquake hazard studies in the Istanbul area in several ways. Combining GONAF recordings with existing regional seismic stations now allows monitoring of the NAFZ offshore Istanbul down to magnitudes M<0. This has improved resolution of earthquake hypocenters and source parameters, better defining local fault branches, their seismicity, and earthquake potential. Using its vertical distribution of sensors, it has directly measured depth-dependent seismic site-effects for ground shaking studies. As mentioned here, it is starting to address fundamental questions related to

earthquake nucleation, rupture dynamics, temporal changes of material properties and strain.

IODP

The arc arises: The links between volcanic output, arc evolution and melt composition

P.A. BRANDL^{1,2}, M. HAMADA^{3,4}, R.J. ARCULUS², K. JOHNSON⁵, K.M. MARSAGLIA⁵, I.P. SAVOV⁶, O. ISHIZUKA^{4,7}, H. LI⁸

¹ GEOMAR Helmholtz Centre for Ocean Research Kiel, Wischhofstr. 1-3, 24148 Kiel, Germany.

² Research School of Earth Sciences, The Australian National University, 142 Mills Road, Acton ACT 2601, Australia.

³ Department of Solid Earth Geochemistry, Japan Agency for Marine-Earth Science and Technology, 2-15 Natsushima-cho, Yokosuka 237-0061, Japan.

⁴ Research and Development Center for Ocean Drilling Science, Japan Agency for Marine-Earth Science and Technology, 2-15 Natsushima-cho, Yokosuka 237-0061, Japan.

⁵ Department of Geological Sciences, California State University Northridge, 18111 Nordhoff Street, Northridge, CA 91330-8266, USA.

⁶ School of Earth and Environment, The University of Leeds, Institute of Geophysics and Tectonics, Leeds LS2 9JT, United Kingdom.

⁷ Geological Survey of Japan/AIST, Central 7 1-1-1 Higashi, Tsukuba, Ibaraki 305-8567, Japan.

⁸ Guangzhou Institute of Geochemistry, Chinese Academy of Sciences, 511 Kehua Street, Wushan Guangzhou 510640, China.

Subduction initiation is a key process for global plate tectonics. Individual lithologies developed during subduction initiation and arc inception have been identified in the trench wall of the Izu-Bonin-Mariana (IBM) island arc but a continuous record of this process has not previously been described. Here, we present results from International Ocean Discovery Program Expedition 351 that were recently published in *Earth and Planetary Science Letters* (Brandl et al., 2017). IODP Exp. 351 drilled a single site (U1438) west of the Kyushu-Palau Ridge (KPR), a chain of extinct and rifted stratovolcanoes that represents the proto-IBM island arc, active for ~25 Ma following subduction initiation in the early Eocene. Site U1438 recovered 150 m of oceanic igneous basement and ~1450 m of overlying sediments. The lower 1300 m of these sediments comprise volcanoclastic gravity-flow deposits shed from the evolving KPR arc front. We separated fresh magmatic minerals from Site U1438 sediments, and analyzed 339 glass (formerly melt) inclusions, hosted by clinopyroxene and plagioclase.

Compositions of 304 pristine glass inclusions preserve a temporal magmatic record of the juvenile island arc, complementary to the predominant mid-Miocene to recent activity determined from tephra layers recovered by drilling in the IBM forearc. The glass inclusions record the progressive transition of melt compositions dominated by an early 'calc-alkalic', high-Mg andesitic stage (a last 'glimpse' of the boninite stage during island arc inception) to a younger tholeiitic stage over a time period of 11 Ma. High-precision trace element analytical data record a simultaneously increasing influence of a deep subduction component (e.g., increase in Th vs. Nb, light rare earth element enrichment) and a more fertile mantle source (reflected in increased high field strength element abundances). This compositional change is accompanied by increased deposition rates of volcanoclastic sediments reflecting magmatic output and maturity of the arc. We conclude the 'calc-alkalic' stage of arc evolution may

endure as long as mantle wedge sources are not mostly advected away from the zones of arc magma generation, or the rate of wedge replenishment by corner flow does not overwhelm the rate of magma extraction.

Reference:

Brandl, P.A., Hamada, M., Arculus, R.J., Johnson, K., Marsaglia, K.M., Savov, I.P., Ishizuka, O., & Li, H. (2017): The arc arises: The links between volcanic output, arc evolution and melt composition. *Earth and Planetary Science Letters* 461, 73-84 (Open Access). doi:10.1016/j.epsl.2016.12.027

IODP

Agricultural activity in the Baltic region and coeval terrestrial and marine ecosystem changes – palynological pilot studies (IODP Exp. 347 Sites M0059, M0063)

P. C. BRUST¹, D. J. WIENHOLZ¹, U. KOTTHOFF¹

¹ Centrum für Naturkunde und Institut für Geologie, Universität Hamburg, 20146 Hamburg

IODP Expedition 347 to the Baltic Sea, among other goals, aimed at the reconstruction of ecosystem, climate, and sea level dynamics and the underlying forcing in different settings in the Baltic Sea region from the Marine Isotope Chron 5 until today. During Expedition 347, an exceptional set of long sediment cores from eight different sites was recovered from the Baltic Sea, which allow new high-resolution reconstructions (e.g. Andrén et al. 2015a, b).

The Baltic Sea region is of particular interest for the reconstruction of past changes in terrestrial ecosystems, since it is adjacent to different vegetation zones, from cool temperate forest with mixed coniferous and deciduous trees in the South to closed boreal forest with taiga-like conditions in the North. In addition to climate, anthropogenic impact influenced the terrestrial ecosystem development in the Baltic region, particularly during the past 2000 yr. Anthropogenic impact on vegetation can be identified in the framework of palynological studies, e.g. via increasing presence of cultivated taxa in the pollen data, and by indications of anthropogenically-caused deforestations. There already are pollen records for the southern Baltic region which indicate agricultural activity, but they do not allow to assess coeval changes in the marine realm. Considering the dynamic Holocene history of the Baltic Sea with alternating freshwater and brackish water stages and with its complex shoreline development, it would be particularly important to see which changes in marine ecosystems occurred during the interval of increasing agricultural activity. One option to achieve this is the examination of pollen grains in marine records, allowing a direct correlation with marine proxies, e.g. dinoflagellate cysts.

Here, we present reconstructions of the evolution of terrestrial and marine ecosystems in the central (IODP-Exp.-347 Site M0063) and southwestern Baltic region (Site M0059) during the Late Holocene which have been generated in the framework of a BSc- (Wienholz 2016) and a MSc-thesis (Brust 2017), and of an ongoing multi-proxy study (e.g. Kotthoff et al. 2016). Our low-resolution results show that increasing percentages of pollen grains of cultivated Poacea (mainly rye and probably wheat) occur around 1500 yr BP at both sites according to preliminary age models (Andrén 2016 and Obrochta 2016; both pers. communication), coevally with a relative decrease in

broad-leaved tree pollen. At Site M0063, the increase of agricultural activity is coeval with high occurrences of the still enigmatic palynomorph *Radiosperma corbiferum* and decreasing salinity (as indicated by dinocyst process lengths and low dinocyst occurrences). At Site M0059, increased presence of rye pollen is also coeval with a decrease in organic-walled dinocysts, with exception of dinocysts of the Genus *Gymnodinium*, which show a rapid increase. In the framework of a future project, it shall be analyzed if these marine signals are connected to factors such as nutrient input.

References:

Andrén, T., Jørgensen, B.B., Cotterill, C., and the Expedition 347 Scientists (2015a): Baltic Sea Paleoenvironment. Proceedings IODP, 347. College Station, TX (Integrated Ocean Drilling Program), doi:10.2204/iodp.proc.347.101.2015.

Andrén, T., Barker Jørgensen, B., Cotterill, C., Green, S., IODP expedition 347 scientific party (2015b): Baltic Sea basin paleoenvironment and biosphere. *Scientific Drilling* 20, 1-12, doi:10.5194/sd-20-1-2015.

Brust, P.C. (2017): Nachweis landwirtschaftlicher Aktivität im Ostseegebiet – ein palynologischer Ansatz. Masterarbeit im Studiengang Geowissenschaften, Institut für Geologie, Universität Hamburg.

Kotthoff, U (2016): Reconstructing Holocene palaeo-environmental conditions in the Baltic: A multi-proxy comparison from the Little Belt (IODP Expedition 347, Site M0059)

Kotthoff, U., Andrén, E., Andrén, T., Ash, J.L., Bauersachs, T., Fanget, A.-S., Granoszewski, W., Groeneveld, J., Krupinski, N.Q., Peyron, O., Slomp, C.P., Stepanova, A., Warnock, J., van Helmond, N.A.G.M., Expedition 347 Science Party (2016): Reconstructing Holocene palaeo-environmental conditions in the Baltic: A multi-proxy comparison from the Little Belt (IODP Expedition 347, Site M0059). Abstract/Poster Presentation, EGU 2016, Vienna.

Wienholz, D.J. (2016): Klima- und Ökosystementwicklung im zentralen Ostseegebiet – ein palynologischer Ansatz. Bachelorarbeit im Studiengang Geowissenschaften, Institut für Geologie, Universität Hamburg.

IODP

Mechanisms of glacial/interglacial changes during the „middle“ Oligocene

S. BRZELINSKI¹, O. FRIEDRICH¹, A. BORNEMANN²

¹ Sedimentology & Marine Paleoenvironmental Dynamics, Institute of Earth Sciences, Heidelberg University, Heidelberg, Germany

² Bundesanstalt für Geowissenschaften und Rohstoffe, Hannover, Germany

The transition from a world lacking large-scale continental ice sheets and rapid eustatic sea-level changes to one dominated by these factors qualifies the Oligocene to be arguably one of the most interesting episodes of the Cenozoic. The Oligocene climate was characterised by recurrent glaciations as evidenced by a pronounced variability in deep-water $\delta^{18}\text{O}$ [1, 2] and sea level lowstands (e.g. [3]). Thereby, pronounced glaciations of the early to “middle” Oligocene may have reached sea-level drops of up to 65 m [4], thus possibly being similar in magnitude to that at the E/O boundary (e.g., [5]). Nonetheless, the existence of Northern Hemisphere ice sheets and their potential contribution to the global deep-sea $\delta^{18}\text{O}$ signal is still a controversially discussed topic for large parts of the late Paleogene.

The clay-rich Eocene to early Miocene sediments recovered by IODP Expedition 342 in summer 2012 provide the unique opportunity to significantly advance the knowledge of Oligocene climate evolution, paleoceanography and ice-sheet dynamics due to well-preserved microfossils and high deposition rates. The aim of the international consortium is to establish a suborbital

(between magnetochron boundary C8r/C9n to C6AAr.2n/C6AAr.3r; 26.4 to 21.7 Ma) benthic foraminiferal stable-isotope record from IODP Site U1406. Preliminary results of benthic foraminiferal $\delta^{18}\text{O}$ values in the interval

128-123 m CCSF show a glacial/interglacial pattern characterised by continuous, step-wise increases and abrupt, "termination-like" decreases. Comparing the morphology of "middle" Oligocene glacial/interglacials to those of the Late Pleistocene reveals an unexpected similarity of sawtooth-like patterns. It is known that eccentricity-dominated cycles resulted in the saw-tooth morphology of Late Pleistocene glacials (e.g., [6]; [7]). This mechanism is difficult to imagine for the unipolar glaciated Oligocene with continental ice mainly on Antarctica. Furthermore, available $\delta^{18}\text{O}$ data from Site U1406 are much lighter than those of the Late Pleistocene [8] suggesting a smaller global ice volume.

To obtain a mechanistic understanding of the processes that led to the differences in the morphology of glacial/interglacial cycles during the "middle" Oligocene, it is planned to generate high-resolution (~600-800 years) paleoclimate proxy record using benthic and planktic foraminiferal geochemistry (stable isotopes and Mg/Ca) on IODP Site U1406 (off Newfoundland). Generating a high-resolution (~600 years) Mg/Ca and $\delta^{18}\text{O}$ record using the benthic foraminifera *Oridorsalis umbonatus* will give insight to what extent individual $\delta^{18}\text{O}$ shifts represent ice-sheet growth and/or deep-water cooling. Furthermore, the data set will allow quantification of sea-level change during the study interval. Mg/Ca and $\delta^{18}\text{O}$ analyses of the planktic foraminifera *Globigerina praebulloides* will be used to reconstruct SST and surface-water $\delta\omega$ changes. Providing this information will allow detailed insight into the evolution of the deep and surface ocean for a truly critical interval of Cenozoic climate evolution (i.e., the Oligocene rise of the icehouse climate). Moreover, the data will allow a sophisticated comparison of the driving mechanisms behind glacial/interglacial cycles during the unipolar glaciated world of the Oligocene (studied herein) and the bipolar glaciated world of the Pleistocene.

References:

- [1] Pälike, H., et al., 2006. The heartbeat of the Oligocene climate system. *Science* 314, 1894-1898.
- [2] Zachos, J.C., Dickens, G.R., Zeebe, R.E., 2008. An early Cenozoic perspective on greenhouse warming and carbon-cycle dynamics. *Nature* 451, 279-283.
- [3] Miller, K.G., Wright, J.D., Fairbanks, R.G., 1991. Unlocking the ice house: Oligocene-Miocene oxygen isotopes, eustasy, and margin erosion. *J. Geophys. Res.* 96, 6829-6848.
- [4] Wade, B.S., Pälike, H., 2004. Oligocene climate dynamics. *Paleoceanography* 19, doi:10.1029/2004PA001042.
- [5] Miller, K.G., et al., 2009. Climate threshold at the E/O transition: Antarctic ice sheet influence on ocean circulation. *GSA Spec. Pap.* 452, 169-178.
- [6] Shackleton, N.J., 2000. The 100,000-year ice-age cycle identified and found to lag temperature, carbon dioxide, and orbital eccentricity. *Science* 289, 1897-1902.
- [7] Clark, P.U. et al., 2006. The middle Pleistocene transition: characteristics, mechanisms, and implications for long-term changes in atmospheric pCO_2 . *Quart. Sci. Rev.* 25, 3150-3184.
- [8] Lisiecki, L. E., and M. E. Raymo, 2005. A Pliocene-Pleistocene stack of 57 globally distributed benthic $\delta^{18}\text{O}$ records. *Paleoceanography* 20, PA1003, doi:10.1029/2004PA001071.

ICDP

Advanced seismic imaging of overdeepened alpine valleys preparatory to DOVE

T. BURSCHIL¹, H. BUNESS¹, D. TANNER¹, G. GABRIEL¹, C.M. KRAWCZYK^{2,3}

¹ Leibniz Institute for Applied Geophysics, Stillweg 2, 30655 Hannover

² now at Helmholtz Centre Potsdam, GFZ German Research Centre for Geosciences, Telegrafenberg, 14473 Potsdam, Germany,

³ TU Berlin, Ernst-Reuter-Platz 1, 10587 Berlin, Germany

Major valleys and basins in the European Alps are densely populated areas that bear infrastructure of international importance (Preusser et al., 2010). To protect the environment by, e.g., geohazard assessment or groundwater estimation, the understanding of the geological structure of these valleys is essential. The shape and deposits of a valley can clarify its genesis and allows the prediction of behaviour in future glaciations. The term "overdeepened" refers to valleys and basins, in which pressurized melt-water under the glacier eroded the valley below the fluvial level. Most overdeepened valleys or basins were thus refilled during the ice melt or remain in the form of lakes.

The ICDP project Drilling Overdeepened Alpine Valleys (DOVE, Anselmetti et al., 2016) intends to correlate the sedimentary succession from boreholes between valleys in the entire alpine range and capture the climate history. Hereby, seismic exploration is essential in order to predict the most promising well path and drilling site of extensive drill cores. In addition, seismic interpretation spatially extend 1-D information from boreholes in to 2-D or 3-D. Nonetheless, drilling and borehole information are important to verify seismic interpretation, especially with varying facies in overdeepened valleys.

In a first step this DFG-funded project investigates the benefit of multi-component techniques for seismic imaging. At two test sites, the Tannwald Basin (Germany) and the Lienz Basin (Austria), the Leibniz Institute for Applied Geophysics (LIAG) acquired P-wave reflection profiles to gain structural and facies information. Based on the P-wave information, several S-wave reflection profiles were acquired on parts of the P-wave profiles in the pure SH-wave domain as well as 6-C reflection profiles using a horizontal S-wave source in inline and crossline excitation. To evaluate and avoid 3-D effects, inlines and crosslines were recorded sporadically during the P-wave and the S-wave campaigns.

Five P-wave sections reveal the structure of the Tannwald Basin, which is a distal branch basin of the Rhine glacier. Strong reflections mark the base of the basin, which has a maximum depth of 240 metres. Internal structures and facies strongly vary spatially, but allow a facies characterization between lacustrine and glacio-fluvial deposits. SH-wave and 6-C profiles can be correlated to gross structures of the P-wave image and give additional information, though lacking in image quality. Based on the P-wave interpretation, two possible drilling sites are suggested for DOVE, which will also prove the seismic interpretation and explain differences in P-wave and S-wave images. One drilling site would record the sedimentary archive at maximum depth of the basin, and ensure the longest core for DOVE, whereas the other suggested drilling site would better serve geophysical research aspects addressed by DOVE and intersect several

different seismic facies units, well observed in seismic imaging and ensure a varying core for DOVE. The later would also help to asset the methodology of seismic multi-component imaging.

At the other test site, the Lienz Basin, the seismic campagins comprise four parallel P-wave sections perpendicular to the basin axis, which show the asymmetrical shape of the basin. The sedimentary base is well imaged with steep-dipping flanks and has an approximate depth of 0.6 km. Internal reflectors in the valley infill point to diverse fill. Here, S-wave imaging produces less distinct sections and require a more sophisticated processing, which has not yet been carried out.

In summary, P-wave imaging is suitable to map overdeepened structures in the Alps while S-wave imaging can contribute additional information.

References:

- Anselmetti et al. (2016). Drilling overdeepened Alpine Valleys (DOVE). ICDP Full Proposal, 174pp.
 Preusser et al. (2010). Distribution, geometry, age and origin of overdeepened valleys and basins in the Alps and their foreland. *Swiss Journal of Geosciences*, 103(3), 407-426.

IODP

Evolution of the oceanic circulation in the subtropical Atlantic across the Mid-Pleistocene Transition

M. C. A. CATUNDA¹, A. BAHR¹, O. FRIEDRICH¹

¹ Institut für Geowissenschaften, Universität Heidelberg, Heidelberg, Deutschland.

The Mid-Pleistocene Transition (MPT) was characterized by significant changes in the global climate system, the most remarkable being the development of the present-day 100 kyr eccentricity related glacial cyclicity^{1,2}. This switch from a previous 41 kyr obliquity-paced glacial/interglacial rhythm in the absence of changes in the orbital parameters characterizes the matter as a conundrum about which scientists are still actively debating. The MPT took place between ca. 1250 and 600 ka (i.e. Marine Isotope Stages, MIS, 35 – 15) and was followed by increased ice volume in the Northern Hemisphere during stadials^{3,4}. The growth of continental ice sheets seems to have been a key aspect of the Mid-Pleistocene climate evolution as it may have preconditioned the prolongation of glacial conditions¹. While lower temperatures provide background conditions favorable for sustaining large ice sheets, the paradox situation arises that low sea-surface temperatures (SST) reduce the amount of moisture available for snow accumulation and thereby inhibit ice-sheet growth^{1,5}. The mechanisms responsible for the mid-Pleistocene waxing and waning of the heat distribution observed in the North Atlantic are still poorly understood.

A mechanistic understanding of the oceanic heat transport into the high northern latitudes is essential for fully appreciating the dynamics of Quaternary climate evolution. Considering the crucial role of the Gulf Stream for present-day climate conditions in Europe and the recent indications that its heat transport has weakened substantially during the last decades⁸, such knowledge is also important in order to forecast the potential consequences of anthropogenic climate change⁹.

The North Atlantic Subtropical Gyre plays a central role in the transport of heat and moisture into the higher-

latitude North Atlantic. Exploring changes in the heat and salinity budget within the gyre and the strength and spatial configuration of its circulation pattern during MIS 15-35 may provide clues about such high-latitude climate fluctuations. On the search for the mechanism that would have provided a strong, persistent northward heat transport during glacial inception and full glacial conditions we will use multi-proxy data from two marine sediment cores: ODP Site 1058 and IODP Site U1313, located on the Northern Subtropical Gyre western and northern boundaries, respectively.

IODP Site 1058 is situated along the Gulf Stream current pathway and close to its source region. Trace elements and stable isotopes data from shallow dwelling planktic foraminifera from this core will be used to reconstruct SST variations between MIS 15 and 35. This record will then be compared with a counterpart from the Iberian Margin to disentangle which factors may have exerted the main influence for the northward heat transport during the MPT. In addition, deep dweller foraminifera data from IODP Site U1313, located at the northern boundary of the Subtropical Gyre, will be used to scrutinize the circulation strength and spatial extent of the gyre. The combination of both records (ODP Site 1058 and IODP Site U1313) will generate a complete picture of the North Atlantic Subtropical Gyre evolution and thus will be instrumental for resolving the puzzle of amplified ice-sheet growth during the MPT.

References:

- Clark, P. U., Archer, D., Pollard, D., et al., 2006, The middle Pleistocene transition: characteristics, mechanisms, and implications for long-term changes in atmospheric pCO₂: *Quat. Sci. Rev.*, 25, 3150-3184.
- McClymont, E. L., Sosdian, S. M., Rosell-Melé, A., et al., 2013, Pleistocene sea-surface temperature evolution: Early cooling, delayed glacial intensification, and implications for the mid-Pleistocene climate transition: *Earth-Science Rev.*, 123, 173-193.
- Raymo, M. E., Lisiecki, L. E., and Nisancioglu, K. H., 2006, Plio-Pleistocene ice volume, Antarctic climate, and the global $\delta^{18}O$ record: *Science*, 313, 492-495. 4. Sosdian and Rosenthal, 2009
- Ruddiman, W., McIntyre, A., 1979, Warmth of the subpolar North Atlantic Ocean during Northern Hemisphere ice-sheet growth: *Science*, 204, 173-175.
- Lawrence, K., Sosdian, S., White, H., et al., 2010, North Atlantic climate evolution through the PlioPleistocene climate transitions: *EPSL*, 300, 329-342.
- Ruddiman, W. F., Raymo, M. E., Martinson, D. G., et al., 1989, Pleistocene evolution: Northern hemisphere ice sheets and North Atlantic Ocean: *Paleoceanogr.*, 4, 353-412.
- Rahmstorf, S., Box, J. E., Feulner, G., et al., 2015, Exceptional twentieth-century slowdown in Atlantic Ocean overturning circulation: *Nature Clim. Change*, 5, 475-480.
- IPCC, 2014, *Climate Change 2013: The Physical Science Basis: Working Group I Contribution to the Fifth Assessment Report of the Intergovernmental Panel on Climate Change*, Cambridge University Press.

IODP

Detection of filamentous viruses of *Vibrio diazotrophicus* strains isolated from sub-surface sediments of the Baltic Sea

O.E. CHIANG, T. ENGELHARDT, B. ENGELEN, V. VANDIEKEN

Institut für Chemie und Biologie des Meeres, Carl von Ossietzky Universität Oldenburg, Carl-von-Ossietzky Straße 9-11, D-26129 Oldenburg, Germany, www.pmbio.icbm.de

The marine sub-surface sediment (>1 m below the sediment surface) holds a high abundance and diversity of bacteria and archaea (Kallmeyer *et al.* 2012). As the deep sediments are cut off from carbon supply of the water column, the microbial communities slowly become buried in the sediment. Thus, they can only consume the organic material buried in the sediment which becomes more and more recalcitrant (Jørgensen and Marshall, 2016). Additionally to energy limitation, changes of other environmental conditions with depth, such as temperature, pressure and the availability of terminal electron acceptors, challenge the microbial community during the burial.

Often overlooked viruses represent an additional stressor for microbial life in the deep biosphere. Virus numbers exceed the abundance of prokaryotic cells (bacteria + archaea), and viruses have been detected in marine sediments as deep as 320 m (Engelhardt *et al.* 2014). However, their activity and role in the deep biosphere still remains largely unknown. In surface sediments, viruses have been shown to influence the diversity and abundance of microbial communities, with variable impacts that rely on their “life” style (Hobbs *et al.* 2016). Replication of viruses is mainly led by two life cycles: lytic and lysogenic. During the lytic cycle, a virus redirects the host’s metabolism towards the production of viral progeny. Whereas in the lysogenic cycle, the virus genome is integrated into the host genome (so called “prophage”) and replicates along with the host, until the lytic cycle is induced during conditions of stress. For instance, changes in salinity, pH or oxygen concentration could act as viral inducing agents. Both cycles ultimately lead to the death of the prokaryotic host cell, and the viral lysis releases nutrients to stimulate new microbial growth via the viral shunt (Suttle, 2005). While both lytic and lysogenic cycles are the most common viral life styles, the production of new viruses can also take place without lysing the host cells: chronic infection. In this regard, filamentous viruses (*Inoviridae*) can be slowly secreted through the outer cell membrane without killing their host (Rakonjac *et al.* 2011).

The International Ocean Discovery Program (IODP) Expedition 347, “Baltic Sea Paleoenvironment” provided the opportunity to cultivate new bacterial strains and alongside their prophages. Baltic Sea sediments have experienced an increase of the salt concentration by salinity changes of the overlying water column that started at the end of the last glaciation (Andr n *et al.*, 2015). Consequently, seawater ions are still diffusing into deeper sediment layers, slowly increasing salinity during the last 9,000 years, exerting a challenge for the microbial communities. Here we present our studies on new bacterial isolates, where we investigated salinity tolerance and the adaptation to low-energy environments. Furthermore, life strategies of prophages were investigated on selected strains.

Sub-surface sediments samples were taken during IODP Expedition 347 from four sites (M0059, M0060, M0063, M0065). New bacterial strains were isolated into pure cultures from all four sites, belonging to *Gammaproteobacteria*, *Deltaproteobacteria*, *Bacteroidetes* and *Firmicutes*. Physiological tests, such as salt tolerance, were performed on the new isolates. The strains showed considerable differences in their salt tolerance with optimum growth at freshwater, brackish or marine conditions as well as narrow or broad salinity tolerances.

Four novel endospore-forming bacteria of the *Firmicutes* were isolated from the subsurface sediment of the Baltic Sea. Based on the 16S rRNA gene sequences and physiological characterization, one of the strains was proposed as a new genus and new species *Marinisorobacter balticus* gen. nov., sp. nov., while the remaining three were proposed to represent two new species *Desulfosporosinus nitroreducens* sp. nov. and *Desulfosporosinus fructosivorans* sp. nov. (Vandiek *et al.* submitted). *Marinisorobacter balticus* grew as an obligate heterotroph by aerobic respiration and anaerobically by fermentation. In contrast, the two *Desulfosporosinus* strains were strictly anaerobic sulfate reducers. They additionally used thiosulfate, elemental sulfur, sulfite and DMSO as electron acceptors and hydrogen as electron donor. As members of the *Firmicutes* constitute a major fraction of the marine deep biosphere (Biddle *et al.*, 2008), it remains unclear whether spore-forming taxa are active or persist in a resting stage, i.e., as spores (Jørgensen & Marshall, 2014).

Belonging to the phylum *Bacteroidetes*, four new strains were isolated (Vandiek *et al.* in prep.). Based on physiological, chemotaxonomic and genotypic characterization, it is proposed that the four strains represent two new species within a new genus, with the proposed names *Labilibaculum manganireducens* gen. nov., sp. nov. and *Labilibaculum filiformis* sp. nov. The draft genomes of two strains were 5.2 and 5.3 Mb and reflected the major physiological capabilities. The strains were psychrotolerant, neutrophilic and halotolerant growing at NaCl concentrations of 0-6.5%. All of the strains grew by fermentation of mono- and disaccharides as well as pyruvate, lactate and glycerol. In the presence of glucose, electrons (<5%) were transferred to Fe(III) oxides by all strains, while one of the strains also slowly reduced Mn(IV) oxides. Thus, the strains represent the “fermentative metal reducer type”, which transfers only a small part of the electron equivalents to the metal (typically less than 5%), while most of the electron equivalents are recovered in fermentation products (Lovley, 2013). However, even if only a small part of electron equivalents was transferred to iron oxides, it has been shown to improve the fermentative balance resulting in thermodynamically more favorable conditions (Lehours *et al.* 2010; Dong *et al.* 2016). Thus, the available substrates can be used more efficiently by the fermenting bacterium. Overall, both halotolerance and metal reduction might be beneficial for life in deep subsurface sediments of the Baltic Sea.

Viruses of the Baltic Sea sediments were studied in prophage-host systems using the new bacterial isolates. We identified more than ten strains to produce viruses. The morphology of these viruses was observed by electron microscopy, observing different morphologies belonging to the families *Podoviridae* and *Myoviridae*. Six isolates that

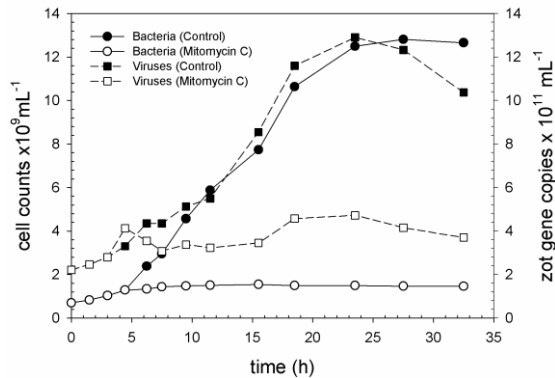


Figure 1: Induction experiment of *Vibrio* strain 60.18M. Cultures were grown aerobically at 15°C. At the beginning of the exponential phase, the culture was split and one was treated with mitomycin C. Bacteria abundance and copy of the *zot* gene were quantified over time.

are affiliated to *Vibrio diazotrophicus* were subjected to whole genome sequencing and were predicted to possess *Myovirus* and *Inovirus* as prophages integrated in their genomes. The first represents a tailed, double-stranded DNA virus, while the latter are filamentous, single-stranded DNA viruses. The *Inovirus* cannot be detected by epifluorescence microscopy because of their small filament and genome sizes. Therefore, we designed and standardized a method for quantification of the filamentous viruses of our strains based on a real-time polymerase chain reaction (qPCR). Here, a viral gene fragment is specifically amplified and fluorescence is continuously measured along the amplification cycles. The signal is proportional to the amount of amplified target gene copies and, thus, leading to a quantification of viral genes. Specific primers were designed to target the *zot* gene inserted in the prophage genome. The *zot* gene product is involved in morphogenesis and assembly (Mai-Prochnow *et al.* 2015) and represents a hallmark gene of *Inovirus*. Initial tests confirmed that filamentous viruses were successfully detected and quantified by both PCR and qPCR in 5 of the 6 *Vibrio* strains confirming the result from the genomic analysis. Induction experiments with mitomycin C were performed in order to estimate the production rate of the filamentous viruses for the five strains (Fig 1). Bacterial abundance was determined by flow cytometry, while the abundance of viruses was measured by qPCR as the number of copies of the *zot* gene. The abundance of filamentous viruses shows significant differences between control and mitomycin C treatment (Fig. 1). In the control, viral abundance increased constantly over time from 2.2×10^{11} to 1.0×10^{12} viruses mL^{-1} following the increase of bacterial cell numbers, whereas mitomycin C-treated cells stopped growing and viruses numbers stayed constant (4.7×10^{11} viruses mL^{-1} ; Fig. 1). The estimated viral production rate was 5×10^{10} viruses $\text{mL}^{-1} \text{ h}^{-1}$, which implies that in average 1.5-2 viruses $\text{cell}^{-1} \text{ min}^{-1}$ are produced during the cultivation. Thus, we concluded that the five *Vibrio* strains are infected by filamentous viruses that cannot be induced by mitomycin C but represent a chronic infection. The morphology of the viruses was confirmed by transmission electron microscope as being filamentous with a width of 6-6.5 nm (Fig. 2).

The development of a detection system for *Inovirus* provides an outstanding opportunity for further research

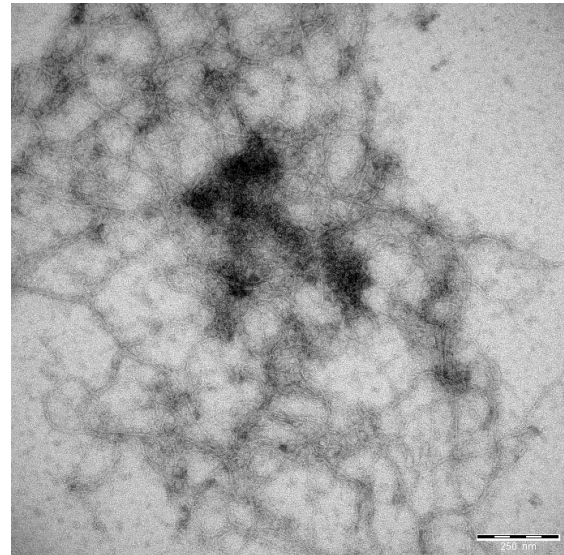


Figure 2: Electron microscopic images of filamentous viruses of *Vibrio* strain 60.18M. Scale bar: 250 nm.

particularly in the deep biosphere. While the existence of filamentous viruses in sub-surface sediments has been overlooked, recent metagenomic evidence suggests they could account for a significant proportion of the viral community in deep sediments (Engelhardt *et al.* 2015). Thus, because the viruses cannot be counted by fluorescence microscopy, our new method will allow the quantification of *Inovirus* and, thus their contribution to the deep virosphere.

In future studies, we are planning to investigate the *Myovirus*, which were additionally detected in the genomes of two *Vibrio* strains, for their induction with mitomycin C, as they are expected to represent the lysogenic life cycle of viruses. Furthermore, of special interest for life in the subsurface of the Baltic Sea, we plan to perform experiments with changing salinities to study the impact on virus life cycles and growth of the host cells.

References:

- Andr n, T., J rgensen, B.B., Cotterill, C., Green, S., and the Expedition 347 Scientists (2015) Proceedings of the Integrated Ocean Drilling Program, Volume 347. College Station, TX: Integrated Ocean Drilling Program.
- Biddle J F, Fitz-Gibbon S, Schuster S C, Brenchley JE. & House CH (2008) Metagenomic 260 signature of the Peru Margin subsurface biosphere show a genetically distinct environment. *Proc Natl Acad Sci* **105**: 10583-10588.
- Dong Y, Sanford RA, Boyanov MI, Kemner KM, Flynn TM, O'Loughlin EJ, Changa YJ, Locke RA, Weberh JR, Egani SM, Mackiea RI, Canna I & Fouke BW (2016) *Orenia metallireducens* sp. nov. strain Z6, a novel metal-reducing member of the phylum *Firmicutes* from the deep subsurface. *Appl Environ Microbiol* **82**: 6440-6453.
- Engelhardt T, Orsi WD & Jorgensen BB (2015) Viral activities and life cycles in deep subsurface sediments. *Environ Microbiol Rep* **7**: 868-873.
- Hobbs Z & Abedon ST (2016) Diversity of phage infection types and associated terminology: the problem with "Lytic and lysogenic". *FEMS Microbiol Lett* **363**: 1-8.
- J rgensen BB & Marshall IPG (2016) Slow microbial life in the seabed. *Ann Rev Mar Sci* **8**: 311-332.
- Kallmeyer J, Pockalny R, Adhikari RR, Smith DC, D'Hondt S.(2012). Global distribution of microbial abundance and biomass in subsurface sediment. *Proc Natl Acad Sci* **109**: 16213-16216.
- Lehours AC, Rabiet M, Morel-Desrosiers N, Morel JP, Jouve L, Arbeille B, Mailhot G & Fonty G (2010) Ferric iron reduction by fermentative strain BS2 isolated from an iron-rich anoxic environment (Lake Pavin, France). *Geomicrobiol J* **27**: 714-722.
- Mai-Prochnow A, Hui JGK, Kjelleberg S, Rakonjac J, McDougald D & Rice SA (2015) 'Big things in small packages: the genetics of

filamentous phage and effects on fitness of their host'. *FEMS*

Microbiol Rev. **39**, 465–487,

Rakonjac J, Bennett NJ, Spagnuolo J, Gagic D & Rakonjac MR (2011)

Filamentous Bacteriophage: Biology, Phage Display and Nanotechnology Applications. *Curr. Issues Mol. Biol.* **13**: 51–76.

Suttle CA (2005) Viruses in the sea. *Nature* **437**: 356–361.

Vandieken V, Niemann H, Engelen B & Cypionka H. *Marinisporobacter*

balticus gen. nov., sp. nov., *Desulfosporosinus nitroreducens* sp. nov.

and *Desulfosporosinus fructosivorans* sp. nov., new spore-forming

bacteria isolated from subsurface sediments of the Baltic Sea.

Submitted to *International Journal of Systematic and Evolutionary*

Microbiology.

Vandieken V, Marshall IPG, Niemann H, Engelen B & Cypionka.

Labilibaculum manganireducens gen. nov., sp. nov. and *Labilibaculum*

filiformis sp. nov., new gliding bacteria isolated from subsurface

sediments of the Baltic Sea. In preparation.

IODP

Sulfide-rich interval in gabbros of the IODP drill core from site U1473 (Atlantis Bank, Southwest Indian Ridge, SWIR)

J. CIAZELA^{1,2}, J. KOEPKE¹, H. STRAUSS³, B. PIETEREK², M. BENDER¹, H.J.B. DICK⁴, T. KUHN⁵, A. MUSZYNSKI²

¹ Institute of Mineralogy, Leibniz University of Hannover, Callinstr. 3, D-30167 Hannover, Germany

² Institute of Geology, Adam Mickiewicz University, ul. Bogumila Krygowskiego 12, 61-680 Poznań, Poland

³ Institute of Geology and Paleontology - Historische und Regionale Geologie, Westfälische Wilhelms-University of Münster, Corrensstr. 24, D-48149 Münster, Germany

⁴ Department of Geology and Geophysics, Woods Hole Oceanographic Institution, MS #8, McLean Laboratory, Woods Hole, MA 02543-1539, USA

⁵ Federal Institute for Geosciences and Natural Resources, Stilleweg 2, D-30655 Hannover, Germany.

IODP expedition 360 drilled the 810-m-deep U1473A hole into the lower crust of the Atlantis Bank ocean core complex at the Southwest Indian Ridge (Dick et al., 2016). We found a long section of sulfide-rich gabbro at a depth of 615 to 730 mbsf. Sulfides with grain sizes up to 7 mm are characteristic for the gabbro from this depth interval. To the best of our knowledge, sulfide grains of this size are unusual in the lower oceanic crust *in situ*. The occurrence of these sulfides is thus intriguing and raises question about their origin.

The sulfides in the investigated interval are concomitant with oxides, and the ratio of sulfides to oxides is about 25%. The sulfides occur in polysulfide grains composed of pyrrhotite (~70 vol.%), chalcopyrite (~28 vol.%), and pentlandite (~2 vol.%). The pentlandite contain from 12 to 17 wt.% Co. The mineral composition of the large sulfides from the sulfide-rich interval is similar to the mineral composition of smaller polysulfide grains from the upper part of the hole. These small sulfides are on average composed of 70 vol.% of pyrrhotite, 25 vol.% of chalcopyrite and 5 vol.% of pentlandite.

The relatively homogenous mineral composition of the polysulfide grains throughout the hole suggests a magmatic origin. The high Co content along with variable Fe/Ni ratio of the pentlandite indicates an equilibrium temperature of >400 °C suggesting that these sulfides exsolved from a monosulfide solid solution (Kaneda et al., 1986). Similar assemblages of magmatic sulfides are found in magmatic sulfide deposits, e.g. in the Bushveld complex (e.g., Kanitpanyacharoen and Boudreau, 2013). In the Atlantis Bank gabbros, however, sulfides are always concomitant with very abundant oxides. To better understand the

formation of sulfides in gabbros from the Atlantis Bank at SWIR, we have begun a study on the trace element and isotope geochemistry of the sulfides.

References:

Dick H. J. B., Macleod C. J., Blum P. and the Expedition 360 Scientists (2016) Expedition 360 Preliminary report: Southwest Indian Ridge lower crust and Moho., International Ocean Discovery Program.

Kaneda H., Takenouchi S. and Shoji T. (1986) Stability of pentlandite in the Fe-Ni-Co-S system. *Miner. Depos.* **21**, 169–180.

Kanitpanyacharoen W. and Boudreau A. E. (2013) Sulfide-associated mineral assemblages in the Bushveld Complex, South Africa: Platinum-group element enrichment by vapor refining by chloride-carbonate fluids. *Miner. Depos.* **48**, 193–210.

ICDP

Ultrastructure and aquatic community response to Heinrich Stadials (HS5a-HS1) in the continental northern Neotropics

SERGIO COHUO¹, LAURA MACARIO-GONZÁLEZ¹, LISETH PÉREZ², FLORENCE SYLVESTRE³, CHRISTINE PAILLES³, JASON CURTIS⁴, STEFFEN KUTTEROLF⁵, MARTA WOJEWÓDKA⁶, KRYSZYNA SZEROCZYŃSKA⁶, EDYTA ZAWISZA⁶, ANTIJE SCHWALB¹

¹ Institut für Geosysteme und Bioindikation, Technische Universität Braunschweig, Braunschweig, Germany.

² Instituto de Geología, Universidad Nacional Autónoma de México, México.

³ Centre Européen de Recherche et d'Enseignement de Géosciences de l'Environnement. IRD-CEREGE, Marseille, France.

⁴ Department of Geological Sciences and Land Use and Environmental Change Institute, University of Florida, Gainesville, FL, USA.

⁵ GEOMAR Helmholtz-Zentrum für Ozeanforschung, Kiel, Germany.

⁶ Institute of Geological Sciences, Polish Academy of Sciences, Research Centre in Warsaw, Warsaw, Poland

Heinrich stadials (HS) are currently recognized as fast-acting “pulses” of worldwide rapid environmental change, affecting climate and causing large scale alterations in species composition and distribution. For tropical regions, the effects of such abrupt alterations remain poorly understood, although these regions are recognized as highly sensitive to climate change and harbor the highest biological diversity on Earth. Our study uses a high resolution multiproxy approach to test qualitatively and quantitatively the magnitude of climatic fluctuations and their effects on temperature and lake water conductivity in the northern Neotropical region during HS5a-HS1. Freshwater ostracodes serve as model group to test the responses of the aquatic communities to such alterations. Sediment cores PI-6 (71m wd) and PI-2 (54m wd) from Lake Petén Itzá, Guatemala, were used in this study.

Calibration data set, transfer functions and fossil assemblage analysis

Modern ostracode assemblages were used to quantitatively estimate lake water conductivity and temperature variations during HSs by means of transfer functions. The calibration training set consisted of 120 aquatic ecosystems. In order to ensure the inclusion of a broad range of measurements of the variables of interest, sampling sites were located across conductivity and elevational gradients. Lake water conductivity values range from 32.2 to 5 960 $\mu\text{S cm}^{-1}$ and water temperature from 12.5 to 35.2°C, respectively, along an elevation gradient from 100 to 3097 m a.s.l. Species richness and relative

abundance of fossil assemblages were quantified independently for each HS using 5g of dry sediment. Alpha diversity was calculated for each HS using the Shannon-Wiener (H'), Simpson (1-D) and alpha-fischer (αF) indices. The evenness (J) index, which measures how equal the communities are with respect to the number of species, was used to compare the results obtained from alpha indices. We additionally estimated the beta diversity to compare the species turnover between different HSs assemblages.

Heinrich stadials climatic ultrastructure

Results from sedimentology and geochemistry show that typical characteristics of HSs are sediments characterized by gypsum layers, low magnetic susceptibility and high CaCO₃ contents. This suggest that HSs were dry, altering the predominantly humid conditions between 53-14 ka BP. The ultrastructure of the HSs, however, shows that climatic conditions were internally highly variable making and greatly contrasting to each other. We identified four different types of climatic conditions associated to HSs; 1) prevailing dry conditions but changing to wet as in HS5 and HS3; 2) predominantly wetter conditions but changing to arid as in HS2; 3) fluctuating humid-dry-humid conditions as shown by HS4 and HS1; and 4) arid conditions with high water mineralization during HS5a. The continuous presence of tropical ostracode species during HSs suggests that water temperatures were not drastically affected. Ostracode-based transfer functions (RMSEP= 0.78°C) indicate that during cold phases, i.e during HS1, water temperatures may have decreased between 1-3°C in comparison to mean modern temperatures. Lake water conductivity and lake levels were, on the other hand, the variables most drastically affected by HSs, because we observed rapid turnovers between planktonic and benthic diatoms, switching of saline tolerant and freshwater ostracode species, lithologies characterized by gypsum layers and highly variable values of geochemical indicators such as TIC and CaCO₃, indicating fluctuating solute concentrations. HS5a and HS1 were the periods during which higher ostracode-derived conductivity values were estimated with values > 800 $\mu S cm^{-1}$, comparable to values characteristic of estuarine environments.

Ostracode species community alteration in response to HSs

Diversity analysis shows that each HS was characterized by a particular combination of species richness and abundance. The ANOVA test demonstrated that they differ significantly among each other, suggesting that climate fluctuations affected independently and in different ways the species composition during each stadial. Furthermore, beta diversity index shows that HS5a, HS4 and HS1 were the stadials with higher species heterogeneity likely caused by the presence of high species richness and turnovers between saline and freshwater species as in case of HS5a. Contrastingly, HS2, HS3, HS5 were the most homogeneous HSs due to low richness and continuous freshwater ostracode composition. Highest diversities coincided with HS5a, HS4 and HS1, which display greater climatic alterations. Strong climatic alteration thus seems to exert a positive effect on the aquatic ecosystem in the northern Neotropics by increasing species diversity. This is especially true for littoral and medium depth organisms for which a fluctuating climate may produce an increase habitat heterogeneity and food supply.

This study investigates for the first time the climatic ultrastructure of HSs and the biological effects in aquatic ecosystems exerted by climatic fluctuations, being therefore relevant as analogue for understanding possible effects of changes in precipitation and temperature regimes in the Neotropical region caused by ongoing global warming.

Acknowledgements

Funding was provided by the Deutsche Forschungsgemeinschaft (DFG, SCHW 671/16-1, KU2685/3-1) and Technische Universität Braunschweig. CONACYT (Mexico) provided fellowships (218604, 218639) to the first two authors.

ICDP

GESEP-Portal – Die Weiterentwicklung zu einem katalogbasiertem Datenportal

RONALD CONZE¹, JOHANNES HIEROLD¹, ULRICH HARMS¹

¹Zentrum für Wissenschaftliches Bohren, Helmholtz-Zentrum Potsdam, Deutsches Geoforschungszentrum

Kontakt: conze@gfz-potsdam.de, hierold@gfz-potsdam.de, ulrich.harms@gfz-potsdam.de

Das deutsche Forschungsbohrkonsortium GESEP e.V. bündelt wissenschaftliche Expertise und Infrastruktur des wissenschaftlichen Bohrens im terrestrischen, marinen und glazialen Bereich. Neben Leistungen im Bereich Fortbildung Beratung, Planung und Management dient GESEP als Informationsplattform. GESEP hat auch die Schaffung eines kombinierten Bohrkernlagers für terrestrische Proben am MARUM in Bremen und an der BGR in Berlin-Spandau initiiert. Zu diesen Kernlagerproben wurde auch ein Datenportal zu Projekten und Probenmaterialien aufgebaut.

Bisher sind zu sieben Projekten digitale Informationen zu Daten und Proben im Datenportal zugänglich. Geplant ist jetzt in einer weiteren Aufbau-Phase die Integration zusätzlicher Projekte und Kerne sowie die digitale Vernetzung mit weiteren Probenlagern mit dem Ziel das GESEP Portal als digitalen Einstieg zu diversen Programmen, Projekten und Proben zu etablieren. Zu diesem Zweck soll das Design des Portals übersichtlicher und benutzerfreundlicher gestaltet werden. Zur Planung dieses Vorhabens wurde von GESEP ein Workshop am 17.11. 2016 in Hannover an der BGR durchgeführt.

Der Hauptzweck dieses Datenportals ist der Nachweis des verfügbaren Probenmaterials an den jeweiligen Standorten der GESEP und anderer teilnehmender Kernlager. Anhand einer vorstrukturierten Suche, die nach und nach mit zusätzlichen Kriterien weiter präzisiert werden kann, erhält der Nutzer die Informationen, welches Material in welchem Umfang und unter welchen Bedingungen an den entsprechenden Standorten verfügbar ist. Ist das Ergebnis der Recherche für den Nutzer interessant, kann direkt aus dem Portal eine entsprechende Probenanforderung an das jeweilige Kuratorenteam abgesetzt werden. Die weitere Abwicklung erfolgt dann nach den jeweiligen Bedingungen des betreffenden Kernlagers. Um die Suche im neuen GESEP Portal möglichst anwendungsgerecht auszurichten, wurde eine

noch laufende Umfrage unter an Bohrprojekten beteiligten Wissenschaftlern in Deutschland gestartet.

Ganz neue Möglichkeiten eröffnet die zunehmende Verwendung der International Geo Sample Number, IGSN. Dieser persistente Identifikator ist der DOI-Kennzeichnung von Veröffentlichungen vergleichbar. Die IGSN wird zum Beispiel bei Forschungsbohrprojekten direkt für jede Probe vergeben und wird bei wissenschaftlicher Untersuchung und Publikation der Probe und den dazu gewonnenen Daten zugeordnet. Mittels der IGSN kann dann nicht nur das Probenlager und die Probe sondern auch die dazu gehörigen Publikationen und Daten gefunden werden (Conze et al., 2017).

Neben dem Nachweis von gesuchtem Probenmaterial, soll das Portal aber auch den beteiligten Standorten die Möglichkeit bieten, ihr gesamtes Angebot in einer attraktiven Form zu präsentieren. Das können neueste Nachrichten sein, z.B. welches Probenmaterial gerade neu eingelagert wurde, besondere Proben und Publikationen, die instrumentelle und räumliche Ausstattung, die Infrastruktur, Angebote zu Lehrgängen und Workshops sowie die Kontaktdaten und Nutzungsbedingungen.

Reference:

Conze, R. et al., (2017). Utilizing the International Geo Sample Number Concept in Continental Scientific Drilling During ICDP Expedition COSC-1. *Data Science Journal*. 16(1), p.2. DOI: <http://doi.org/10.5334/dsj-2017-002>

ICDP

Drilling the Eger Rift: Magmatic fluids driving the earthquakes swarms and the deep biosphere

T. DAHM^{1,2}, T. FISCHER³, A.M. ANESIO, C. ALEXANDRAKIS, K. BRÄUER, S. BUSKE, D. DOLEJS, J. HORALEK, M. KORN, F. KRÜGER, J. MALEK, D. SHELLY, D. WAGNER

¹ GFZ German Research Centre for Geosciences, Potsdam, Germany

² University of Potsdam, Germany

³ Charles University in Prague, Faculty of Science, Czech Republic

The ICDP Eger proposal has recently been accepted by ICDP for supprting five shallow drill holes in NW Bohemia and Germany. In the framework of ICDP Eger we want to develop a modern, comprehensive laboratory at depth for the study of three interconnected areas of primary research: i) flow of mantle-derived CO₂ through the crust and its degassing at the surface, ii) earthquake swarms, iii) the composition and processes of the deep biosphere (Dahm et al., 2013). We aim to study each of these individual topics, and investigate the interconnections between them. Specifically, such a laboratory will comprise a novel concept of 3D seismic arrays with a set of shallow boreholes in order to reach a new level of high-frequency, near source, and multi-parameter observation of ES and related phenomena. One site of three boreholes will be also equipped with modern continuous real-time fluid monitoring at different depth levels, combined with the monitoring and sampling of the deep microbial biosphere.

The presentation summarizes the scientific questions and the methodical and technical approach of the project.

Reference:

Dahm, T., Hrubcová, P., Fischer, T., Horálek, J., Korn, M., Buske, S., and Wagner, D., 2013. Eger Rift ICDP: an observatory for study of non-volcanic, mid-crustal earthquake swarms and accompanying phenomena, *Sci. Drill.*, 16, 93-99, doi:10.5194/sd-16-93-2013

IODP

Aragonite sedimentation and dissolution on a subtropical carbonate ramp, Carnarvon Ramp, SW Shelf of Australia

H. DEIK¹, L. REUNING¹, P. BENJAMIN² AND EXPEDITION 356 SCIENTISTS

¹ EMR-Group, Geological Institute, RWTH Aachen University

² Max Planck Institute for Chemistry, Mainz

The role of aragonite sedimentation and dissolution in subtropical carbonate systems is poorly studied. IODP Site U1460 on the Carnarvon Ramp (SW Shelf of Australia) recovered a nearly continuous Pliocene to Recent record of outer shelf sediments deposited at the transition between cool and warm water environments. The origin and composition of the carbonate sediments were investigated using scanning electron microscopy, X-ray diffraction (XRD) and X-ray fluorescence-scanning (XRF). The sediments are largely composed of skeletal fragments of planktic/benthic foraminifers, ascidians, bivalves, echinoderms, bryozoans, gastropods, sponges and coccoliths. Bioclastic aragonite was produced from the shells of pteropods, ascidians and bryozoans (Cheilostomatida). Maceration, a breakdown of grains into their microscopic structural elements, led to the formation of aragonite needles and granules. Inorganic aragonite, such as reported for the Northern Carnarvon Basin, seems to be absent. X-ray diffraction analyses indicate a systematic decrease in aragonite contents with depth. To achieve a higher resolution, the XRD analyses were calibrated with X-ray fluorescence-scan data, since the aragonite content is positive correlated with Sr/Ca ratios. Variable Sr/Ca ratios over the first 100 mbsf likely are related to sea-level variations, with high aragonite values related to sea-level high stands. Isolated high strontium peaks at greater depth are interpreted as celestite (SrSO₄). Interstitial water data show that the strontium content sharply increases with depth due to aragonite dissolution, before it starts to decrease. Geochemical modelling using phreeqc indicates that aragonite dissolution and an increase of sulfate with depth contributes to celestite supersaturation, while a parallel increase in salinity hampers further celestite precipitation.

IODP

Quantifying K, U and Th contents of marine sediments using shipboard natural gamma radiation spectra measured on DV *JOIDES Resolution*.

DAVID DE VLEESCHOUWER¹, ANN G. DUNLEA^{2,3}, GERALD AUER⁴,
 CHLOE H. ANDERSON², HANS BRUMSACK⁵, AARON DE LOACH⁶,
 MICHAEL C. GURNIS⁷, YOUNGSOOK HUH⁸, TAKESHIGE ISHIWA⁹,
 KWANGCHUL JANG⁸, MICHELLE A. KOMINZ¹⁰, CHRISTIAN MÄRZ¹¹,
 BERNHARD SCHNETGER⁵, RICHARD W. MURRAY², HEIKO PÄLIKE¹,
 AND EXPEDITION 356 SHIPBOARD SCIENTISTS¹²

¹ MARUM - Center for Marine Environmental Science,
 Leobenerstraße, D-28359 Bremen, Germany.

² Department of Earth and Environment, Boston University,
 Boston, Massachusetts 02215, USA.

³ Department of Geology and Geophysics, Woods Hole
 Oceanographic Institution, Woods Hole, Massachusetts
 02543, USA

⁴ Institute of Earth Sciences, University of Graz, Heinrichstrasse
 26, Graz 8010, Austria.

⁵ Institute for Chemistry and Biology of the Marine Environment
 (ICBM), University of Oldenburg, Carl-von-Ossietzky-Str.9-
 11, 26129 Oldenburg, Germany.

⁶ International Ocean Discovery Program, Texas A&M University,

1000 Discovery Drive, College Station, Texas 77845-9547,
 USA.

⁷ Division of Geological and Planetary Sciences, California
 Institute of Technology, 1200 East California Boulevard, MC
 2520-21, Pasadena, California 91125, USA.

⁸ School of Earth and Environmental Sciences, Seoul National
 University, Seoul 151-747, Republic of Korea.

⁹ Atmosphere and Ocean Research Institute, The University of
 Tokyo, 5-1-5 Kashiwanoha, Kashiwa-shi, Chiba 277-8564,
 Japan.

¹⁰ Department of Geosciences, Western Michigan University, 1903
 West Michigan Avenue, 1187 Rood Hall, Kalamazoo MI
 49008, USA.

¹¹ School of Earth and Environment, University of Leeds, LS2 9JT
 Leeds, UK.

¹²

<http://iodp.tamu.edu/scienceops/precruise/indonesianthrufLOW/participants.html>

During International Ocean Discovery Program (IODP) expeditions, shipboard-generated data provide the first insights into the cored sequences. The natural gamma radiation (NGR) of the recovered material, for example, is routinely measured on the ocean drilling research vessel DV *JOIDES Resolution*. At present, only total NGR counts are readily available as shipboard data, although full NGR spectra (counts as a function of gamma-ray energy level) are produced and archived. These spectra contain unexploited information, as one can estimate the

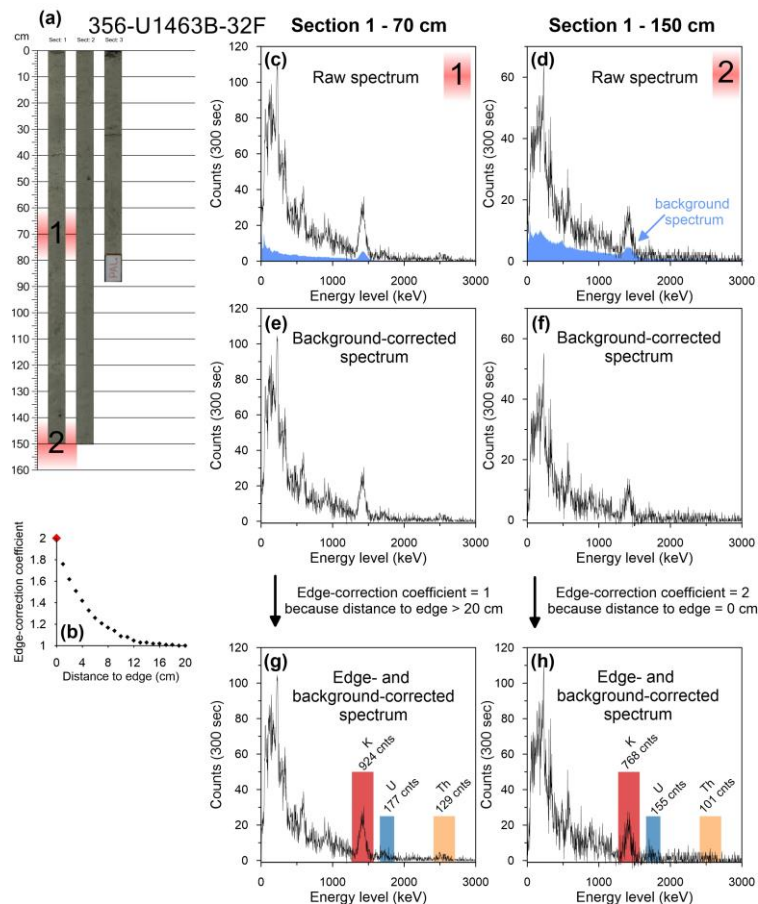


Figure 1: Schematic description of the algorithm. (a) Core Composite image of Core U1463B-31F, consisting of homogenous mudstone. The two depth intervals highlighted in red produced the NGR spectra used in parts c-h of this figure. (b) Edge-correction coefficient as a function of the distance between the detector and the edge of the measured core section. (c-d) Raw NGR spectra (black) with the background spectra (blue) produced by the sediment highlighted in part (a) of this figure. (e-f) The two NGR spectra after subtraction of the measured background spectra. (g-h) Because the NGR spectrum from the second depth interval is taken closer than 20 cm from a section edge, the spectrum counts are multiplied by an edge-correction coefficient. Counts of the spectra from both depth intervals are then integrated over three energy intervals characteristic of K (red), U (blue), and Th (yellow). The integrated counts are subsequently compared to the corresponding peak in the spectra of a known standard (Fig. 1) and adjusted for density to produce K, U, and Th concentrations for both of the depth intervals.

sedimentary contents of potassium (K), thorium (Th), and uranium (U) from the characteristic gamma-ray energies of isotopes in the ^{40}K , ^{232}Th , and ^{238}U radioactive decay series.

Dunlea et al. [2013] quantified K, Th and U contents in sediment from the South Pacific Gyre by integrating counts over specific energy levels of the NGR spectrum. However, the algorithm used in their study is unavailable to the wider scientific community due to commercial proprietary reasons. Here, we present a new MATLAB algorithm for the quantification of NGR spectra that is transparent and accessible to future NGR users. We demonstrate the algorithm's performance by comparing its results to shore-based inductively coupled plasma-mass spectrometry (ICP-MS), inductively coupled plasma-emission spectrometry (ICP-ES), and quantitative wavelength-dispersive X-ray fluorescence (XRF) analyses. Samples for these comparisons come from eleven sites (U1341, U1343, U1366-U1369, U1414, U1428-U1430, U1463) cored in two oceans during five expeditions. In short, our algorithm rapidly produces detailed high-quality information on sediment properties during IODP expeditions at no extra cost.

Reference:

Dunlea, A. G., R. W. Murray, R. N. Harris, M. A. Vasiliev, H. Evans, A. J. Spivack, and S. D'Hondt (2013), Assessment and use of NGR instrumentation on the JOIDES Resolution to quantify U, Th, and K concentrations in marine sediment, *Scientific Drilling*, 15, 57-63.

IODP

Mind the Gap: integrating Atlantic and Pacific deep-sea benthic isotope records into a global late Miocene (5.33 to 8.10 Ma) reference stack

A.J. DRURY¹, T. WESTERHOLD¹, T. FREDERICH², R. WILKENS³,
J. CHANNELL⁴, H. EVANS⁵, D. HODELL⁶, C.M. JOHN⁷, M. LYLE⁸,
U. RÖHL¹, J. TIAN⁹

¹ MARUM - Center for Marine Environmental Sciences, University of Bremen, Leobener Strasse, 28359 Bremen, Germany

² Department of Geosciences, University of Bremen, P.O. Box 330440, D-28334 Bremen, Germany

³ School of Ocean and Earth Science and Technology (SOEST), University of Hawai'i at Manoa, Honolulu, Hawai'i, USA;

⁴ Department of Geological Sciences, University of Florida, Gainesville, FL 32611, USA

⁵ International Ocean Discovery Program, Texas A&M University, 1000 Discovery Drive, College Station Texas 77845-9547, USA

⁶ Department of Earth Sciences, University of Cambridge, Cambridge CB2 3EQ, UK;

⁷ Department of Earth Science and Engineering, Imperial College London, London, SW7 2BP, UK;

⁸ College of Earth, Ocean, and Atmospheric Sciences, Oregon State University, USA;

⁹ State Key Laboratory of Marine Geology, Tongji University, China;

The late Miocene (8-5 Ma) is characterised by intervals of long-term reduced benthic foraminiferal $\delta^{18}\text{O}$ with distinctive short-term $\delta^{18}\text{O}$ cycles superimposed, notably around the Tortonian-Messinian boundary and during the Messinian Salinity Crisis (MSC), when the Mediterranean basin became isolated from the Atlantic between ~5.96 Ma and 5.33 Ma (Krijgsman et al., 1999). The late Miocene carbon isotope shift (LMCIS) marks a permanent -1 ‰

shift in oceanic $\delta^{13}\text{C}_{\text{DIC}}$, which is the largest, long-term marine carbon cycle perturbation since the mid Miocene Monterey excursion. Following the LMCIS, near modern oceanic $\delta^{13}\text{C}$ gradients are established between the major ocean basins (Hodell and Venz-Curtis, 2006). Understanding the origin of late Miocene climate dynamics, such as the $\delta^{18}\text{O}$ cyclicity and the LMCIS, requires integration of high-resolution records with accurate age control from the major oceanic basins. We intend to build a global benthic isotope compilation by integrating deep-sea benthic isotope stratigraphies from the Pacific (Integrated Ocean Drilling Program – IODP – Sites U1337 and U1338) and Atlantic Oceans (Ocean Drilling Program – ODP – Sites 926, 982 and 1264).

A crucial step is to develop a stable isotope and magnetic polarity reference section to underpin the global compilation. We present the first independent high-resolution chemo-, magneto-, and cyclostratigraphy for the interval between 8.3-6.0 Ma, generated at Site U1337. Additionally, to form a stratigraphically robust late Miocene Pacific end member between 8.3-5.33 Ma, the integrated U1337 stratigraphy is combined with a high-resolution benthic isotope stratigraphy from U1338 (Drury et al., 2016) using Milankovitch-related cycles in core images, physical property and X-ray fluorescence core scanning data. Between 7.7-6.9 Ma, the new U1337 benthic $\delta^{18}\text{O}$ and $\delta^{13}\text{C}$ data show distinctive obliquity-driven saw-tooth patterns indicating that high-latitude forcing dominated late Miocene climate dynamics. Additionally, the LMCIS is astronomically calibrated and anchored to the GPTS for the first time, between Chrons C4n.1n and C3An.2n, which will facilitate comparison with terrestrial records of the C3/C4 vegetation shift.

To achieve comparable high-resolution benthic foraminiferal stratigraphies between 5 and 8 Ma for the North, equatorial and South Atlantic Ocean, we used high-resolution physical property data and, where available, high-resolution XRF core scanning data to verify the splices of Atlantic ODP Sites 926 (equatorial), 982 (North) and 1264 (South). The shipboard splices of 982 and 1264 required considerable revision: at Site 982 revisions resulted in ~11 m of gaps in the published isotope data (Hodell et al., 2001); at Site 1264 revisions resulted in ~2.75 m of gaps in the unpublished benthic stable isotope stratigraphy. Some gaps observed at Site 982 are ~2-3 meters, equivalent to ~40 - 50 kyr on the original Hodell et al. (2001) age model, which could be the source of reported inconsistencies between Site 982 and other late Miocene records (Bickert et al., 2004; van der Laan et al., 2012). New benthic isotope data was generated at Sites 982 and 1264 to fill the gaps revealed during the splice revisions. At Site 926, only minor revision to the Zeeden et al. (2013) splice was required (Wilkens et al., 2017), and the resolution of the existing stable isotope stratigraphy (Shackleton and Hall, 1997) was increased to ~3 kyr resolution and extended from 7.0 to 8.0 Ma.

Comparison of the benthic isotope stratigraphies from Pacific Site U1337 and Atlantic Site 926 on their independent age models (ODP 926 from Zeeden et al., 2013) shows remarkable agreement between the two records, supporting the robustness of both astrochronologies. Following splice verification, the new high-resolution (2.5 kyr) benthic isotope stratigraphies from Sites 982 and 1264 are ideal for orbital tuning. The

independent astrochronologies will facilitate the integration of the new high-resolution stable isotope stratigraphies from Atlantic Sites 926, 982 and 1264 and Pacific Sites U1337 and U1338 to generate a global compilation of benthic $\delta^{13}\text{C}$ and $\delta^{18}\text{O}$. Constructing a stacked benthic $\delta^{18}\text{O}$ record will provide a stratigraphic reference section for the late Tortonian and Messinian and extend the Quaternary-Pliocene LR04 benthic stack (Lisiecki and Raymo, 2005) from 5.33 to 8.10 Ma. Generating a robust, high-resolution benthic $\delta^{18}\text{O}$ stratigraphy between 5.33 and 6.0 Ma could particularly help constrain the role of glacio-eustatic change in the MSC by determining the exact timing and extent of the large glacial cycles (TG12/14 and TG20/22), which occur in a similar time frame.

References:

- Bickert, T., Haug, G.H., and Tiedemann, R., 2004, Late Neogene benthic stable isotope record of Ocean Drilling Program Site 999: Implications for Caribbean paleoceanography, organic carbon burial, and the Messinian Salinity Crisis: *Paleoceanography*, v. 19, no. 1, doi: 10.1029/2002PA000799.
- Drury, A.J., John, C.M., and Shevenell, A.E., 2016, Evaluating climatic response to external radiative forcing during the late Miocene to early Pliocene: New perspectives from eastern equatorial Pacific (IODP U1338) and North Atlantic (ODP 982) locations: *Paleoceanography*, v. 31, no. 1, p. 167–184, doi: 10.1002/2015PA002881.
- Hodell, D.A., Curtis, J.H., Sierro, F.J., and Raymo, M.E., 2001, Correlation of late Miocene to early Pliocene sequences between the Mediterranean and North Atlantic: *Paleoceanography*, v. 16, no. 2, p. 164–178, doi: 10.1029/1999pa000487.
- Hodell, D.A., and Venz-Curtis, K.A., 2006, Late Neogene history of deepwater ventilation in the Southern Ocean: *Geochemistry Geophysics Geosystems*, v. 7, no. 9, p. (Q09001), doi: 10.1029/2005GC001211.
- Krijgsman, W., Hilgen, F.J., Raffi, I., Sierro, F.J., and Wilson, D.S., 1999, Chronology, causes and progression of the Messinian salinity crisis: *Nature*, v. 400, no. 6745, p. 652–655, doi: 10.1038/23231.
- van der Laan, E., Hilgen, F.J., Lourens, L.J., de Kaenel, E., Gabori, S., and Iaccarino, S., 2012, Astronomical forcing of Northwest African climate and glacial history during the late Messinian (6.5–5.5Ma): *Palaeogeography, Palaeoclimatology, Palaeoecology*, v. 313–314, p. 107–126, doi: 10.1016/j.palaeo.2011.10.013.
- Lisiecki, L.E., and Raymo, M.E., 2005, A Pliocene-Pleistocene stack of 57 globally distributed benthic $\delta^{18}\text{O}$ records: *Paleoceanography*, v. 20, no. 1, p. PA1003, doi: 10.1029/2004PA001071.
- Shackleton, N.J., and Hall, M.A., 1997, The Late Miocene Stable Isotope Record, Site 926, in Shackleton, N.J., Curry, W.B., Richter, C., and Bralower, T.J. eds., *Proceedings of the Ocean Drilling Program, Scientific Results*, College Station, TX (Ocean Drilling Program), p. 367–373.
- Wilkens, R., Westerhold, T., Drury, A.J., Lyle, M., Gorgas, T., and Tian, J., 2017, Revisiting the Ceara Rise, equatorial Atlantic Ocean: isotope stratigraphy of ODP Leg 154: *Climate of the Past Discussions*, p. 1–22, doi: 10.5194/cp-2016-140.
- Zeeden, C., Hilgen, F., Westerhold, T., Lourens, L., Röhl, U., and Bickert, T., 2013, Revised Miocene splice, astronomical tuning and calcareous plankton biochronology of ODP Site 926 between 5 and 14.4 Ma: *Palaeogeography, Palaeoclimatology, Palaeoecology*, v. 369, p. 430–451, doi: 10.1016/j.palaeo.2012.11.009.

IODP

Evolving carbon sinks in the young South Atlantic: New constrains from Nd-Isotopes on the opening of the Falkland Plateau gateway

W. DUMMANN¹, P. HOFMANN¹, A. OSBORNE⁴, T. WAGNER², J.O. HERRLE³, M. LENZ¹, M. FRANK⁴, S. FLÖGEL⁴, S. STEINIG⁴, S. KUSCH¹, J. RETHEMEYER¹

¹Institute of Geology and Mineralogy, University of Cologne, Zùlpicher Str. 49a, D-50674 Cologne, Germany

²Sir Charles Lyell Centre, School of Energy, Geoscience, Infrastructure and Society, Heriot-Watt University, Edinburgh, EH14 4AS, UK

³Institute of Geosciences, Goethe-University Frankfurt, Altenhöferallee 1, D-60438 Frankfurt am Main, Germany

⁴GEOMAR Helmholtz Centre for Ocean Research Kiel, Wischhofstr. 1-3, D-24148 Kiel, Germany

Emerging ocean basins are sites favourable for drawdown and burial of atmospheric carbon due to their distinct bathymetry (i.e., high shelf-to-open ocean ratio) and restricted circulation. These features turn young ocean basins into potential drivers (or at least modulators) of long-term climate trends and probably also of short-term global carbon cycle perturbations. The opening of the South Atlantic and Southern Ocean basins during the Early Cretaceous (i.e., Aptian-Albian) is accompanied by extensive black shale deposition and formation of prolific hydrocarbon provinces along both continental margins. Modelling results suggest that carbon burial in the Early Cretaceous South Atlantic and Southern Ocean (representing 5% of the Cretaceous global ocean by area) accounted for 35% of the atmospheric carbon sequestered by the world's ocean (McAnena et al., 2013).

In this project we test if carbon sequestration in the South Atlantic, at least partly, caused global carbon cycle perturbations during the Aptian-Albian (i.e., “Oceanic Anoxic Event 1a” and “Late Aptian Cold Snap”, see Fig. 1a) and if the dynamics of carbon burial in the South Atlantic were controlled by multiple gateway openings (Georgia Basin/ Falkland Gateway and Walvis Ridge Gateway). To validate these hypotheses we combine multiproxy-based paleoceanographic reconstructions derived from South Atlantic and Southern Ocean DSDP drill cores with a novel general circulation (KCM) and biogeochemical modelling approach to quantify the effect on the global carbon budget.

The first phase of the project focussed on the the opening history of the southern gateways (Falkland Plateau Gateway and Georgia Basin Gateway) and carbon sequestration in the South Atlantic and Southern Ocean represented by DSDP Site 361 (Cape Basin), DSDP Sites 511 and 327 (Falkland Plateau) as well as DSDP Site 249 (Mozambique Ridge) and ODP Site 693 (Weddell Sea), respectively (see Fig. 1c). We present an improved stratigraphic framework for the study sites based on $\delta^{13}\text{C}_{\text{org}}$ / $\delta^{13}\text{C}_{\text{carb}}$ -isotope stratigraphy, the reconstruction of ocean current flow paths derived from Nd-isotope signatures and the history of the Falkland Gateway deduced from TEX₈₆, XRF-derived and rare earth element (REE) proxies.

During the lowermost Aptian (NC6), prior to 124 Ma, delivery of sediments from the Eastern Cape Fold Belt to the Falkland Plateau, and a Nd-isotope water mass

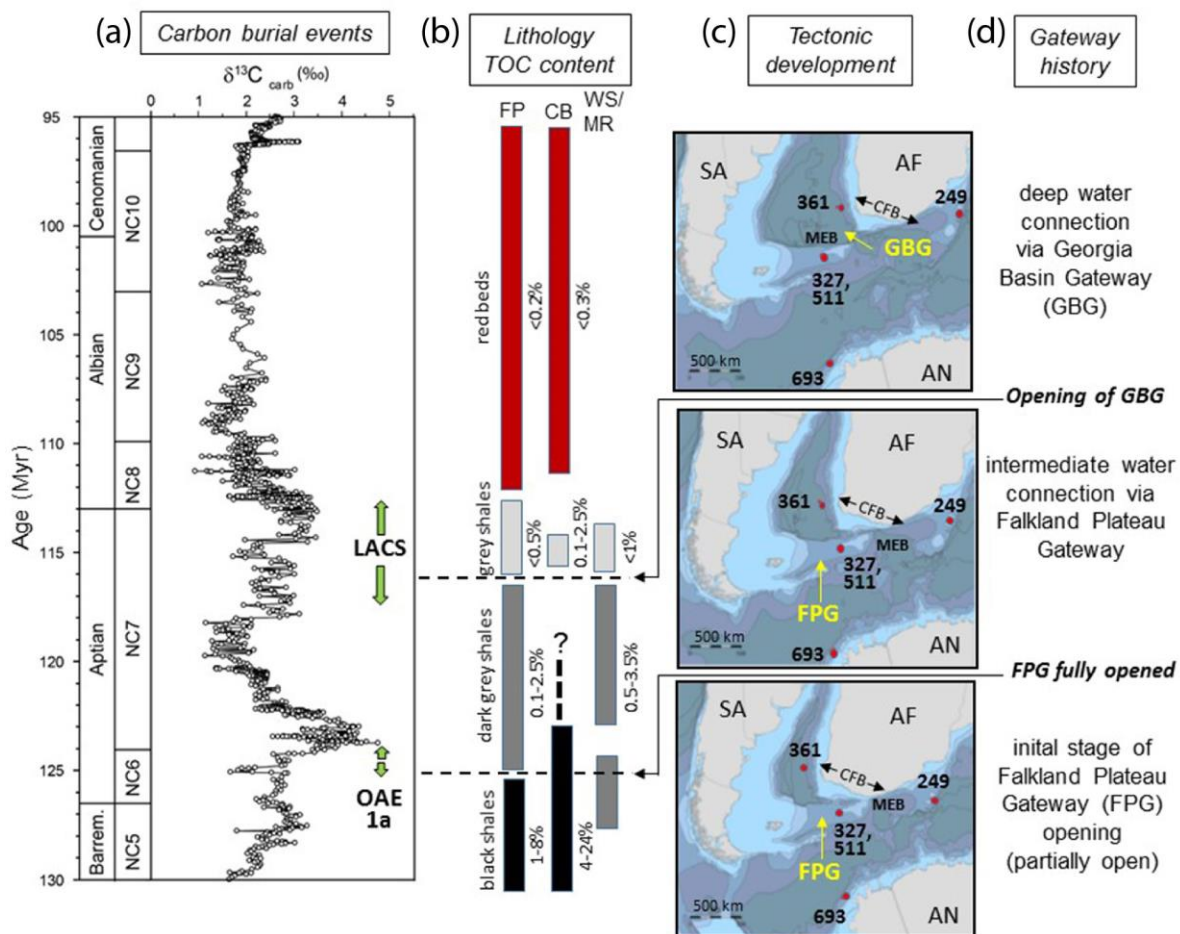


Figure 1: (a) Long-term composite carbon isotope stack (Herrle et al., 2015) indicating carbon cycle perturbations (OAE: Oceanic Anoxic Event, LACS: Late Aptian Cold Snap) in relationship to (b) sediment characteristics and total organic carbon contents of DSDP and ODP cores under investigations (FP: Falkland Plateau, CB: Cape Basin, WS: Weddell Sea, MR: Mozambique Ridge), (c) plate tectonic reconstruction (according to Seton et al., 2012) and (d) successive stages of gateway opening deduced from multi-proxy data. DSDP and ODP Sites are marked by red dots. SA, AF, AN, CFB and MEB refer to South America, Africa, Antarctica, Cape Fold Belt and Maurice Ewing Bank, respectively. Gateways are indicated by yellow arrows: Georgia Basin Gateway (GBG) and Falkland Plateau Gateway (FPG)

signature common of the Southern Ocean and the Falkland Plateau indicates an only partially open Falkland Plateau Gateway (see Fig. 1c and d). Restricted circulation in and between the South Atlantic and Southern Ocean led to conditions favouring enhanced carbon burial in the South Atlantic consistent with reducing conditions and high total organic carbon content at Site 361 (see Fig. 1b). The westward drift and progressive opening of the Falkland Plateau resulted in a shift in redox conditions (euxinic to oxic) and a shift in the primary producer assemblage (increase of silica-fixing organisms) on the Falkland Plateau (Site 511), probably induced by the inflow of cooler nutrient-rich surface water from the Southern Ocean.

Diverging Nd-isotope signatures between the Southern Ocean (Site 249) and the Falkland Plateau (Sites 327 and 511) and the reduction of sediment delivery with African source characteristics to the Falkland Plateau suggest that the Falkland Plateau Gateway was fully opened after ~124 Ma (see Fig. 1c and d). Upon a fully open Falkland Plateau Gateway, Sites 327 and 511 (300 and 800 m paleo-water depth; Holbourn et al. 2001) became progressively inundated by warm, trace metal-enriched and more radiogenic intermediate water masses, most likely originating from the northern South Atlantic (generation of

an outflowing warm and saline intermediate water mass is predicted by the KCM model, as is the area of intermediate water formation on the shallow shelves of the subtropical northern part of the South Atlantic). The intermediate water mass on the Falkland Plateau was isotopically distinct from the South Atlantic deep water represented by Site 361 (paleo-water depth >3000 m, Bolli et al., 1978) indicating a stratified South Atlantic, which functioned as a carbon sink with ideal conditions for organic carbon production and burial.

Convergence of the Nd-isotopic signatures of the deep South Atlantic, Southern Ocean and Falkland Plateau after ~116 Ma heralds the detachment of the Maurice Ewing Bank (easternmost part of the Falkland Plateau) from the African continent and the opening of the Georgia Basin Gateway (see Fig. 1c and d). Red bed sedimentation in all ocean basins indicates mixing of deep water masses resulting in oxic conditions in both ocean basins (see Fig. 1b). This marks the termination of the South Atlantic as a major carbon sink.

References:

Bolli, H. M., Ryan, W. B. F., Foresman, J. B., Hottman, W. E., Kagami, H., Longoria, J. F., McKnight, B. K., Melguen, M., Natland, J., and Proto-

- Decima, F., 1978, Cape Basin continental rise sites 360 and 361: Initial Reports of the Deep Sea Drilling Project, v. 40, p. 29-182.
- Herrle, J. O., Schröder-Adams, C. J., Davis, W., Pugh, A. T., Galloway, J. M., and Fath, J., 2015, Mid-Cretaceous High Arctic stratigraphy, climate, and oceanic anoxic events: *Geology*, v. 43, no. 5, p. 403-406.
- Holbourn, A., Kuhnt, W., and Soeding, E., 2001, Atlantic paleobathymetry, paleoproductivity and paleocirculation in the late Albian: the benthic foraminiferal record: *Palaeogeography, Palaeoclimatology, Palaeoecology*, v. 170, no. 3-4, p. 171-196.
- McAnena, A., Flögel, S., Hofmann, P., Herrle, J. O., Griesand, A., Pross, J., Talbot, H. M., Rethemeyer, J., Wallmann, K., and Wagner, T., 2013, Atlantic cooling associated with a marine biotic crisis during the mid-Cretaceous period: *Nature Geoscience*, v. 6, no. 7, p. 558-561.
- Seton, M., Müller, R. D., Zahirovic, S., Gaina, C., Torsvik, T. H., Shephard, G., Talsma, A., Gurnis, M., Turner, M., Maus, S., and Chandler, M., 2012, Global continental and ocean basin reconstructions since 200 Ma: *Earth-Science Reviews*, v. 113, no. 3-4, p. 212-270.

IODP

The Oligocene/Miocene transition in the western North Atlantic (IODP Expedition 342): Surface-water changes reconstructed from dinoflagellate cysts

L.M. EGGER¹, O. FRIEDRICH¹, R.D. NORRIS², P.A. WILSON³, J. PROSS¹

¹ Institute of Earth Sciences, Heidelberg University, Im Neuenheimer Feld 234, 69120 Heidelberg, Germany

² Scripps Institution of Oceanography, University of California, San Diego, 9500 Gilman Drive, La Jolla, CA 92093-0244, USA

³ National Oceanography Centre, University of Southampton, European Way, Southampton SO14 3ZH, UK

After the Eocene/Oligocene transition, Antarctic ice sheets decreased in size during the late Oligocene, reaching their next culmination in a major glaciation across the Oligocene/Miocene transition (OMT). Ice-sheet expansion started at ~23.4 Ma and ended at ~22.6 Ma (Liebrand et al.,

2011). This intense glacial maximum, which probably represents a change from half to full present-day Antarctic ice-sheet configuration (Liebrand et al., 2011), is generally referred to as Mi-1 isotope event and accompanied by a ~1 ‰ positive shift in benthic foraminiferal $\delta^{18}\text{O}$ (Miller et al., 1991). The Mi-1 isotope event is intrinsically connected to southern hemisphere ice-sheet dynamics, but its effect on surface-water temperatures in the northern hemisphere (and particularly the higher northern latitudes) is yet poorly known. Clearly, more data on sea-surface characteristics (notably temperature) are needed to better understand the effects of the Mi-1 glaciation in the higher northern latitudes.

During IODP Expedition 342 ('Paleogene Newfoundland Sediment drifts'), a continuous succession spanning the OMT has been recovered at Site U1405. In order to reconstruct surface-water changes across the OMT in the western North Atlantic, a high-resolution (~15 ka) dinoflagellate cyst (dinocyst) dataset has been generated from Site U1405; it spans from ~22.5 to ~23.4 Ma.

All samples from the study interval yielded rich and well-preserved dinocyst assemblages and are characterized by a relatively high diversity. Across the OMT, there is an increase in the absolute number of dinocyst specimens paralleled by increasing numbers of taxa usually occurring in more proximal areas of the continental shelf. This observation may reflect increased transport of proximal taxa to Site U1405 as a result of decreasing sea-level due to intensified Antarctic glaciation. The increasing dominance of heterotrophic peridinioid dinocyst taxa (typical for highly productive surface-waters; Fig. 1) co-occurring with peak benthic $\delta^{18}\text{O}$ values (and therefore maximum ice-sheet expansion) might be the result of sea-level variations and additional input of nutrients. Using spectral analysis, an influence of obliquity is seen in the productivity-related index (P/G index; Fig. 1), suggesting that primary

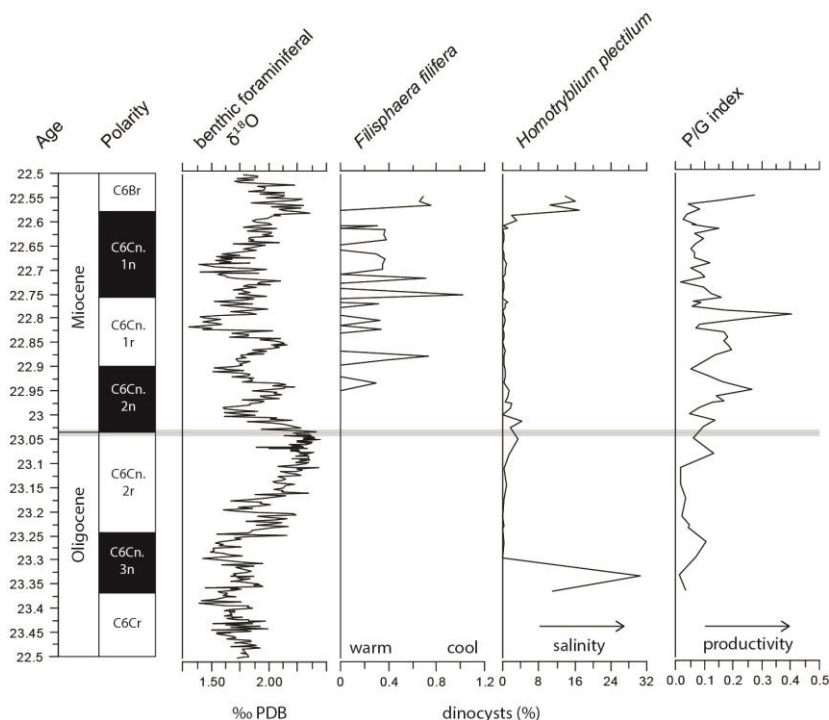


Figure 1: Record of the dinoflagellate cyst species *Filisphaera filifera* and *Homotryblium plectilum*, and the G/P (peridinioid/gonyaulacoid) index of dinocysts across the Oligocene/Miocene boundary at Site U1405. Isotope record from Liebrand et al., 2016; magnetostratigraphic age calibration from Norris et al. (2014).

production was influenced by orbital forcing.

In terms of temperature change, our new data reveal a distinct, long-term decrease of sea-surface temperatures, beginning at about 22.9 Ma and continuing until the end of our record at 22.5 Ma. The cold-water species *Filisphaera filifera* (Fig. 1), which was previously mainly known from the Pliocene onwards, appears periodically within this interval. Surface-water cooling began right after the initial Mi-1 excursion, pointing to permanent changes in the uppermost water column off Newfoundland, probably resulting from the intrusion of cool surface waters from the subarctic North Atlantic.

The salinity-sensitive species *Homotryblum plectilum* (Fig. 1) shows increasing abundances associated with the Mi-1 excursion. The appearance of two additional intervals with high *H. plectilum* abundances, one before Mi-1 at 23.3 Ma and one at the end of our record at 22.6 Ma (Fig. 1), is still unclear.

References:

- Liebrand, D., Beddow, H., Lourens, L.J., Pälike, H., Raffi, I., Bohaty, S.M., Hilgen, F.J., Saes, M.J.M., Wilson, P.A., van Dijk, A.E., Hodell, D.A., Kroon, D., Huck, C.E., Batenburg, S.J., 2016. Cyclostratigraphy and eccentricity tuning of the early Oligocene through early Miocene (30.1–17.1 Ma): *Cinicides mundulus* stable oxygen and carbon isotope records from Walvis Ridge Site 1264. *Earth and Planetary Science Letters* 450, 392–405.
- Liebrand, D., Lourens, L.J., Hodell, D.A., de Boer, B., van de Wal, R.S.W., Pälike, H., 2011. Antarctic ice sheet and oceanographic response to eccentricity forcing during the early Miocene. *Climate of the Past* 7, 869–880.
- Miller, K.G., Wright, J.D., Fairbanks, R.G., 1991. Unlocking the icehouse: Oligocene-Miocene oxygen isotopes, eustasy and margin erosion. *Journal of Geophysical Research* 96, 6829–6848.
- Norris, R.D., Wilson, P.A., Blum, P., Fehr, A., Agnini, C., Bornemann, A., Boulila, S., Bown, P.R., Cournede, C., Friedrich, O., Ghosh, A.K., Hollis, C.J., Hull, P.M., Jo, K., Junium, C.K., Kaneko, M., Liebrand, D., Lippert, P.C., Liu, Z., Matsui, H., Moriya, K., Nishi, H., Opdyke, B.N., Penman, D., Romans, B., Scher, H.D., Sexton, P., Takagi, H., Turner, S.K., Whiteside, J.H., Yamaguchi, T., Yamamoto, Y., 2014. Site U1405. In: Norris, R.D., Wilson, P.A., Blum, P., the Expedition 342 Scientists (Eds.), *Proceedings of the Integrated Ocean Drilling Program 342*. College Station, Texas.

IODP

Viral infection history and virus-host interaction in sulfate-reducing bacteria from subsurface sediments of Juan de Fuca ridge, IODP Exp. 301

TIM ENGELHARDT¹, BERT ENGELEN¹, HERIBERT CYPIONKA¹

¹Carl von Ossietzky University Oldenburg, Institut for Chemistry and Biology of the Marine Environment (ICBM), Oldenburg, Germany

The oceanic crust is a large interconnected aquifer with intense fluid circulation. Diffusive flow of fluids from the crust aquifer transports nutrients and electron acceptors to the overlying sediments. This effect is pronounced near oceanic ridges. At the Juan de Fuca ridge (IODP Exp. 301), a geochemical zonation is established and results in three compartments of an upper and lower sulfate zone and a sulfate-minimum zone that spreads in between. Microbial communities in the upper sediments have access to relatively young sources of organic carbon and sulfate as main terminal electron acceptor. For the lower sulfate zone, the available organic carbon is recalcitrant, however, the

introduction of nutrients from the crust fluid has been shown to support microbial activities (Engelen et al., 2008).

Viruses are active parts of deeply buried microbial communities with diverse virus-host interactions (Engelhardt et al., 2015). Viral genomes can be integrated into the host cell genomes (provirus) and may be induced to eventually lyse the host cell. Viral-mediated cell lysis results in carbon turnover by providing bioavailable organic carbon.

Three strain affiliated to *Desulfovibrio indonesiensis* (strain P34, P12, P23) were isolated from the lower sulfate zone at Juan de Fuca ridge in depths of 239.5, 251.9 and 260 meter below seafloor, respectively, and were shown to be an abundant and viable inhabitants in deeply buried sediments (Fichtel et al., 2012). We performed whole genome sequencing of the three stains to analyze the virus-host interactions and the infection history based on the provirus and on so-called CRISPR systems (clustered regularly interspaced short palindromic repeats). CRISPR systems are involved in the prokaryotic immune response against viral attacks and invasive DNA. By accumulating signals of previous viral attacks in genomic spacer regions, information from CRISPR systems contain a record of the infection history of the host cell.

The genomes of strain P34 and P12 harbored five proviruses each, while strain P23 had 4 integrated proviruses. Each strain encoded two CRISPR systems in its genome and carried an enormous number of spacer sequences, between 69 and 112. The numerous proviruses and spacers give evidence for a high frequency of virus-host interactions.

The analysis of sequence information from CRISPR-spacers showed that all strains shared some part of their early viral infection history. Thus, it became apparent that the three strains had a common ancestor and got separated during long-term burial. The presence of unique proviruses in strain P23 provided additional support for an individual infection history. Furthermore, some proviruses carried “auxiliary genes” which encode for beneficial metabolic functions to support the host cell, e.g. arsenate resistance for strain P23. Accordingly, viral infections and integration of proviruses might be a burden for the host cell, but it might also be a fitness factor that increases survivability.

These first results indicate that *Desulfovibrio indonesiensis* strains were prone to numerous viral attacks and survived the long-term burial process. This was in part probably due to their successful defense against viruses by using CRISPR systems and conceivably by viral encoded fitness factors acquired by horizontal gene transfer. However, the proviruses have been shown to be still functional and to cause a continuous lysis of the host cells. Thus, viruses potentially contribute to the maintenance of a labile organic carbon pool for deeply buried microbial communities.

References:

- Engelen B, Ziegelmeüller K, Wolf L, Köpke B, Gittel A, Treude T, Nakagawa S, Inagaki F, Lever MA, Steinsbu BO, Cypionka H (2008)

Fluids from the oceanic crust support microbial activities within the deep biosphere. *Geomicrobiol J* 25:56-66

Fichtel K, Mathes F, Könneke M, Cypionka H, Engelen B (2012) Isolation of sulfate-reducing bacteria from sediments above the deep-subseafloor aquifer. *Front Microbio* 3:65

Engelhardt T, Orsi WD, Jørgensen BB (2015) Viral activities and life cycles in deep subseafloor sediments. *EMI Rep* 7(6): 868–873.

IODP

Tropical Pacific climate during Meltwater Pulse-1A from IODP Expedition 310 corals

T. FELIS¹, P. DESCHAMPS², E.C. HATHORNE³, R. ASAMI⁴

¹ MARUM – Center for Marine Environmental Sciences, University of Bremen, Bremen, Germany

² CEREGE, Aix-Marseille University, CNRS, IRD, Aix-en-Provence, France

³ GEOMAR Helmholtz Centre for Ocean Research Kiel, Kiel, Germany

⁴ Department of Physics and Earth Sciences, University of the Ryukyus, Senbaru, Okinawa, Japan

IODP Expedition 310 'Tahiti Sea Level' (Camoïn et al., 2007, 2012) has provided important insights into ice-sheet collapse and sea-level rise at the Bølling warming 14,600 years ago, by constraining the amplitude and timing of meltwater pulse (MWP) 1A (Deschamps et al., 2012). Applying U-Th dating to shallow-water corals drilled offshore from Tahiti in the tropical South Pacific Ocean it was shown that MWP-1A started no earlier than 14,650 years ago and ended before 14,310 years ago, making it coeval with the Bølling warming. The results revealed that the increase in sea level at Tahiti was between 12 and 22 metres, with a most probable value between 14 and 18 metres, establishing a significant meltwater contribution from the Southern Hemisphere (Deschamps et al., 2012). Furthermore, geochemical proxies in IODP Expedition 310 corals have provided insights into past changes in seasonality, interannual variability and mean conditions in tropical Pacific sea surface temperature during the North Atlantic cold episodes of the Younger Dryas and Heinrich Stadial 1 (Asami et al., 2009; Hathorne et al., 2011; Felis et al., 2012), revealing Younger Dryas cooling (Asami et al., 2009) and pronounced interannual variability at typical ENSO periodicities during Heinrich Stadial 1 (Felis et al., 2012) at Tahiti. Importantly, U-Th dating indicates that a noticeable number of *Porites* corals partly analysed at monthly resolution for the Sr/Ca and $\delta^{18}\text{O}$ temperature proxies grew during MWP-1A. However, the paleoclimatic and paleoceanographic interpretation of these coral proxy records had been hampered by (1) the relative shortness of most of the records, (2) presumably subtle diagenetic alteration of the skeleton in some corals apparently affecting the performance of the temperature proxies in resolving clearly the annual cycle, and (3) the lack of a sufficient number of modern monthly coral Sr/Ca and $\delta^{18}\text{O}$ records from Tahiti in order to provide a robust present-day benchmark. Here we suggest to provide unique insights into past changes in seasonality, interannual variations and mean conditions of tropical Pacific sea surface temperatures during MWP-1A, by using a new collection of modern Tahiti *Porites* corals from the vicinity of the Expedition 310 drill sites, and Expedition 310 *Porites* corals. The results will provide snapshots of tropical Pacific temperature variability at unprecedented temporal

resolution during a period of dramatic sea-level rise and abrupt climate change of the last deglaciation.

References:

- Asami, R., Felis, T., Deschamps, P., Hanawa, K., Iryu, Y., Bard, E., Durand, N., Murayama, M. Evidence for tropical South Pacific climate change during the Younger Dryas and the Bølling-Allerød from geochemical records of fossil Tahiti corals. *Earth and Planetary Science Letters* **288**, 96-107, doi:10.1016/j.epsl.2009.09.011 (2009).
- Camoïn, G. F., Iryu, Y., McInroy, D. B. & the Expedition 310 Scientists. *Proceedings IODP, Vol. 310* (Integrated Ocean Drilling Program Management International, Inc., Washington, DC), (2007).
- Camoïn, G. F., Seard, C., Deschamps, P., Webster, J. M., Abbey, E., Braga, J. C., Iryu, Y., Durand, N., Bard, E., Hamelin, B., Yokoyama, Y., Thomas, A. L., Henderson, G. M., Dussouillez, P. Reef response to sea-level and environmental changes during the last deglaciation: Integrated Ocean Drilling Program Expedition 310, Tahiti Sea Level. *Geology* **40**, 643-646, doi:10.1130/g32057.1 (2012).
- Deschamps, P., Durand, N., Bard, E., Hamelin, B., Camoïn, G., Thomas, A. L., Henderson, G. M., Okuno, J. i., Yokoyama, Y. Ice-sheet collapse and sea-level rise at the Bølling warming 14,600 years ago. *Nature* **483**, 559-564, doi:10.1038/nature10902 (2012).
- Felis, T., Merkel, U., Asami, R., Deschamps, P., Hathorne, E. C., Kölling, M., Bard, E., Cabioch, G., Durand, N., Prange, M., Schulz, M., Cahyarini, S. Y., Pfeiffer, M. Pronounced interannual variability in tropical South Pacific temperatures during Heinrich Stadial 1. *Nature Communications* **3**, 965, doi:10.1038/ncomms1973 (2012).
- Hathorne, E. C., Felis, T., James, R. H., Thomas, A. Laser ablation ICP-MS screening of corals for diagenetically affected areas applied to Tahiti corals from the last deglaciation. *Geochimica et Cosmochimica Acta* **75**, 1490-1506, doi:10.1016/j.gca.2010.12.011 (2011).

ICDP

Deciphering climate information from the long Chew Bahir sediment cores: Towards a continuous half-million year climate record from the Southern Ethiopian Rift

V. FOERSTER¹, A. ASRAT², M. CHAPOT³, A. S. COHEN⁴, J. R. DEAN⁵, A. DEINO⁶, C. GÜNTER⁷, A. JUNGINGER⁸, H. F. LAMB³, M. LENG⁵, H. ROBERTS³, F. SCHAEBITZ¹, M. H. TRAUTH⁷ & HSPDP SCIENCE TEAM

¹ University of Cologne, Institute of Geography and Didactics, Cologne Germany

² Addis Ababa University, Department of Earth Sciences; Addis Ababa, Ethiopia

³ Aberystwyth University, Institute of Geography and Earth Sciences, Aberystwyth, UK

⁴ University of Arizona, Department of Geosciences, Tucson AZ, USA

⁵ British Geological Survey, Keyworth, Nottingham, UK

⁶ Berkeley Geochronology Center, Berkeley, USA

⁷ University of Potsdam, Institute of Earth and Environmental Science, Potsdam, Germany

⁸ Eberhard Karls Universität Tübingen, Department of Earth Sciences, Tübingen, Germany

As a contribution towards an enhanced understanding of human-climate interactions, the Hominin Sites and Paleolakes Drilling Project (HSPDP) has successfully completed coring five dominantly lacustrine archives of climate change during the last ~3.5 Ma in East Africa (Cohen et al., 2016). All five sites in Ethiopia and Kenya are adjacent to key paleoanthropological research areas encompassing diverse milestones in human evolution, dispersal episodes, and technological innovation. The 280 m-long Chew Bahir sediment records, recovered from a tectonically-bound basin in the southern Ethiopian rift in late 2014, cover the past 550 ka of environmental history, a time period that includes the transition to the Middle Stone Age, and the origin and dispersal of modern *Homo sapiens*.

Deciphering climate information from lake sediments is challenging, due to the complex relationship between climate parameters and sediment composition. We will present the first results in our efforts to develop a reliable climate-proxy tool box for Chew Bahir by deconvolving the relationship between sedimentological and geochemical sediment composition and strongly climate-controlled processes in the basin, such as incongruent weathering, transportation and authigenic mineral alteration. Combining our first results from the long cores with those from a pilot study of short cores taken in 2009/10 along a NW-SE transect of the basin, we have developed a hypothesis linking climate forcing and paleoenvironmental signal-formation processes in the basin (Foerster et al., 2015). X-ray diffraction analysis of the first sample sets from the long Chew Bahir record reveals similar processes that have been recognized for the uppermost ~20 m during the pilot-study of the project: the diagenetic illitization of smectites during episodes of higher alkalinity and salinity in the closed-basin lake induced by a drier climate. The precise time resolution, largely continuous record and (eventually) a detailed understanding of site specific proxy formation, will give us a continuous record of environmental history on decadal to orbital timescales. Our data will allow tests of the various hypotheses about the impact of climate variability -from climate flickers to orbital driven transitions- on the evolution and dispersal of anatomically modern humans.

References:

- Cohen, A. et al., 2016. The Hominin Sites and Paleolakes Drilling Project: Inferring the Environmental Context of Human Evolution from Eastern African Rift Lake Deposits. *Scientific Drilling* 21, 1-16, doi:10.5194/sd-21-1-2016.
- Foerster, V. et al., 2015. Environmental Change and Human Occupation of Southern Ethiopia and Northern Kenya during the last 20,000 years. *Quaternary Science Reviews* 129, 333–340.

ICDP

Progress and prospects of the ICDP SCOPSCO project at Lake Ohrid (Macedonia, Albania)

A. FRANCKE¹, B. WAGNER¹, P. TAUBER¹, J. JUST¹ AND N. LEICHER¹

¹ University of Cologne, Institute of Geology and Mineralogy, Zùlpicher Str. 49a, 50674 Cologne, Germany

Since the deep drilling campaign at Lake Ohrid was carried out under the umbrella of the ICDP SCOPSCO (“Scientific Collaboration on Past Speciation Conditions in Lake Ohrid”) project in spring 2013, core processing at the University of Cologne focused on the so-called DEEP and PESTANI drill sites. At the DEEP site, the main drill site located in the central part of the lake at 250 m water depth, more than 1400 meter of cores from 4 neighboring boreholes have been compiled to a continuous composite profile down to the maximum penetration depth of ~584 m. Core scanning (XRF, MSCL), as well as biogeochemical (TIC, TOC, TN, TS) and sedimentary (grain-size) analyses have been carried out on the composite profile at regular sampling intervals of 0.25 cm, 1 cm, 16 cm, and 64 cm, respectively. In concert with geotectonic, seismic and biological information, the data imply that the Ohrid basin formed by transension during the Miocene, opened during the Pliocene and Pleistocene, and that the lake established in the still relatively narrow valley between 1.9 and 1.3 Ma ago. Gravels and pebbles indicating fluvial conditions in

the lowermost few meters of the DEEP site succession hampered a deeper penetration during the drilling activities. Lithological information indicate that the history of Lake Ohrid can roughly be separated into two parts, with the older section between 584 and 450 m sediment depth being characterized by coarse-grained lacustrine deposits with low organic matter (low TOC) and endogenic calcite (low TIC) concentrations intercalated with coarse silt to sand-sized horizons and lignite layers. The precise age of the onset of the shallow water conditions remains uncertain until today. The second part above 450 m sediment depth, which is characterized by fine-grained lacustrine deposits with variable TIC and TOC concentrations, corresponds to deeper water conditions that persisted in Lake Ohrid over the last 1.3 Ma ago. The biogeochemical proxy data in this part respond to global glacial/interglacial variability, with warm periods being characterized by high TIC and TOC concentrations and cold periods by negligible TIC and low TOC contents, respectively. This consistent pattern enabled the first age estimation for the pelagic DEEP site sediments (Wagner et al., 2014; Francke et al., 2016). Further chronostratigraphic work on the DEEP site sediments including tephrostratigraphic and paleomagnetic analyses will improve the age model in the near future. To date, 56 tephra and crypto-tephra horizons have been found in the upper 450 m of the DEEP site sequence (see Leicher et al., 2016 and this volume for more details about the chronological framework of the DEEP site sequence). The Brunhes/Matuyama boundary (0.781 Ma) is clearly visible at 283 m sediment depth. While the exact depth of the top of the Jaramillo chron (~0.988 Ma) is blurred within an interval between 347-336 m due to an early diagenetic overprint, the base of the Jaramillo (~1.072 Ma) is sharply recorded at 373 m. Ongoing high-resolution analytical work will further constrain the timing of these paleomagnetic boundaries.

Tephrochronology (Leicher et al., 2016) in combination with tuning biogeochemical proxy data to orbital parameters also provided the basis of a detailed age model for the upper 247.8 m of the DEEP site sediments, covering the time window between 637 ka and present days (Francke et al., 2016). The multi-proxy dataset (sedimentary information, pollen and stable isotope data) for this time interval have recently been published in a special issue (*Biogeosciences*) and indicates long-term variability with a change from cooler and wetter to drier and warmer glacial and interglacial periods around 300 ka, respectively (Lacey et al., 2016; Sadori et al., 2016). A reconstruction of past water depths based on hydro-acoustic and sediment core data imply that lake level fluctuation in Lake Ohrid probably responded to this long-term drying trend (Wagner et al., 2016).

Evolutionary studies on the extant fauna indicate that Lake Ohrid was not a refugial area for regional freshwater animals (Föller et al., 2015). This differs from the terrestrial ecosystem in the catchment, where the mountainous setting with relatively high water availability provided a refugial area for temperate and montane trees during the relatively cold and dry glacial periods (Sadori et al., 2016). Although Lake Ohrid experienced significant environmental change over the last 637 kyr, preliminary molecular data from extant microgastropod species do not indicate significant changes in diversification rate during this period. The reasons for this constant rate remain largely unknown, but a possible lack of environmentally induced extinction events in Lake Ohrid and/or the high resilience of the ecosystems may have played a role.

In addition to the long-term environmental variability recorded in the lake sediments, short-term environmental

change also had a considerable impact on Lake Ohrid. For example, tephra deposition led to distinct modifications in the diatom assemblages (Jovanovska et al., 2016), and the climatic impact of millennial-scale Dansgaard-Oeschger and Heinrich events triggered modification in the primary productivity and decomposition processes in the water column (Wagner et al., 2016).

A single borehole down to ~195 m has been retrieved from the PESTANI core site, located at the eastern shoreline at a comparable water depth like at the DEEP site location. The PESTANI cores have been processed and analyzed (XRF at 0.5 cm resolution, MSCL at 1 cm resolution) at the University of Cologne in 2016. Whereas core opening and sub-sampling at 22 cm resolution for (bio-)geochemistry and grain size analyses and at 44 cm for paleomagnetic studies is already finished, analytical work is still ongoing. The aim of this coring location was to obtain more detailed information about the early development of Lake Ohrid. First lithological information implies that shallow water conditions, indicated by coarse material, lignite layer, and the high abundance of shell fragments, persisted between ~195 and ~140 m sediment depth, whereas deep water deposits occur above. In the upper part of the PESTANI sequence, mass movement deposits originating from the steep slopes close by are common. High-resolution XRF and MSCL data in concert with paleomagnetic and tephrostratigraphic information will be used to transfer the age model of the DEEP site sequence to the PESTANI cores. The knowledge about the onset of the deep-water conditions at both coring sites will then provide more detailed insights into the early lake history.

References:

- Föller, K., Stelbrink, B., Hauffe, T., Albrecht, C., and Wilke, T.: Constant diversification rates of endemic gastropods in ancient Lake Ohrid: ecosystem resilience likely buffers environmental fluctuations, *Biogeosciences*, 12, 7209-7222, 10.5194/bg-12-7209-2015, 2015.
- Francke, A., Wagner, B., Just, J., Leicher, N., Gromig, R., Baumgarten, H., Vogel, H., Lacey, J. H., Sadori, L., Wonik, T., Leng, M. J., Zanchetta, G., Sulpizio, R., and Giaccio, B.: Sedimentological processes and environmental variability at Lake Ohrid (Macedonia, Albania) between 637 ka and the present, *Biogeosciences*, 13, 1179-1196, 10.5194/bg-13-1179-2016, 2016.
- Jovanovska, E., Cvetkoska, A., Hauffe, T., Levkov, Z., Wagner, B., Sulpizio, R., Francke, A., Albrecht, C., and Wilke, T.: Differential resilience of ancient sister lakes Ohrid and Prespa to environmental disturbances during the Late Pleistocene, *Biogeosciences*, 13, 1149-1161, 10.5194/bg-13-1149-2016, 2016.
- Lacey, J. H., Leng, M. J., Francke, A., Sloane, H. J., Milodowski, A., Vogel, H., Baumgarten, H., Zanchetta, G., and Wagner, B.: Northern Mediterranean climate since the Middle Pleistocene: a 637 ka stable isotope record from Lake Ohrid (Albania/Macedonia), *Biogeosciences*, 13, 1801-1820, 10.5194/bg-13-1801-2016, 2016.
- Leicher, N., Zanchetta, G., Sulpizio, R., Giaccio, B., Wagner, B., Nomade, S., Francke, A., and Del Carlo, P.: First tephrostratigraphic results of the DEEP site record from Lake Ohrid (Macedonia and Albania), *Biogeosciences*, 13, 2151-2178, 10.5194/bg-13-2151-2016, 2016.
- Sadori, L., Koutsodendris, A., Panagiotopoulos, K., Masi, A., Bertini, A., Combourieu-Nebout, N., Francke, A., Kouli, K., Joannin, S., Mercuri, A. M., Peyron, O., Torri, P., Wagner, B., Zanchetta, G., Sinopoli, G., and Donders, T. H.: Pollen-based paleoenvironmental and paleoclimatic change at Lake Ohrid (south-eastern Europe) during the past 500 ka, *Biogeosciences*, 13, 1423-1437, 10.5194/bg-13-1423-2016, 2016.
- Wagner, B., Wilke, T., Krastel, S., Zanchetta, G., Sulpizio, R., Reichert, K., Leng, M. J., Grahzdani, A., Trajanovski, S., Francke, A., Lindhorst, K., Levkov, Z., Cvetkoska, A., Reed, J. M., Zhang, X., Lacey, J. H., Wonik, T., Baumgarten, H., and Vogel, H.: The SCOPSCO drilling project recovers more than 1.2 million years of history from Lake Ohrid, *Sci. Drill.*, 17, 19-29, 10.5194/sd-17-19-2014, 2014.
- Wagner, B., Wilke, T., Francke, A., Albrecht, C., Baumgarten, H., Bertini, A., Combourieu-Nebout, N., Cvetkoska, A., D'Addabbo, M., Donders, T. H., Föller, K., Giaccio, B., Grahzdani, A., Hauffe, T., Holtvoeth, J., Joannin, S., Jovanovska, E., Just, J., Kouli, K., Koutsodendris, A., Krastel, S., Lacey, J. H., Leicher, N., Leng, M. J., Levkov, Z., Lindhorst, K., Masi, A., Mercuri, A. M., Nomade, S., Nowaczyk, N., Panagiotopoulos, K., Peyron, O., Reed, J. M., Regattieri, E., Sadori, L.,

Sagnotti, L., Stelbrink, B., Sulpizio, R., Toflovska, S., Torri, P., Vogel, H., Wagner, T., Wagner-Cremer, F., Wolff, G. A., Wonik, T., Zanchetta, G., and Zhang, X. S.: The environmental and evolutionary history of Lake Ohrid (FYROM/Albania): Interim results from the SCOPSCO deep drilling project, *Biogeosciences Discuss.*, 2016, 1-51, 10.5194/bg-2016-475, 2016.

ICDP

Unraveling natural and human-accelerated erosional and weathering processes at Lake Ohrid (Macedonia, Albania) using Uranium series analyses

A. FRANCKE^{1,2}, A. DOSSETO², L. ROTHACKER², D. MENOZZI²

¹University of Cologne, Institute of Geology and Mineralogy, Zülpicher Str. 49a, 50674 Cologne, Germany

²University of Wollongong, School of Earth and Environmental Sciences, Wollongong Isotope Geochronology Laboratory, Wollongong, NSW 2522, Australia

Climate change and tectonic uplift are considered to be the major control of erosional processes and landscape evolution. While tectonic uplift affects erosional processes on long time scales (millions of years), the recent global warming due to anthropogenic greenhouse gas emission might trigger a more rapid erosion and landscape evolution (years to centuries). In addition, erosional processes can be accelerated by human induced wood clearance and agricultural land-use (Dosseto and Schaller, 2016). Assessing more information about present days mode of erosional and sediment transport processes will also contribute to our understanding of the formation of depositional (paleoenvironmental-) records (such as in marine or lake basins), elemental cycles controlled by sediment residence time in catchments, and the erosion-driven fixation of atmospheric CO₂ by silicate weathering.

Although it is fundamentally important to understand erosion and landscape evolution, and despite the increasing ability to reconstruct past environmental and climatic conditions during the Quaternary, it has remained challenging to quantify the rates and time scales of sediment formation, transport, and deposition on geological time scales. The so-called "comminution age" approach is an excellent method to address the question about erosion and landscape evolution in the geological history. This approach enables the determination of the time that has elapsed since chemical and physical weathering of the bedrock formed detrital grains <50 µm in diameter by using uranium isotope (U isotope) analyses. The comminution age encompasses the time of sediment storage in the weathering profile (i.e. soils), the sediment transport in rivers or creeks, temporary storage in alluvial plains and/or subaquatic slopes, and the time since the final deposition in a sedimentary basin. By subtracting the depositional age, the comminution age equals in confined catchments the „paleo-regolith time“ (Dosseto and Schaller, 2016). Until today, the comminution age approach has mostly been applied on fluvial and marine deposits. Only one study focuses on a lacustrine, Late Glacial to Holocene record from Lake Dojran (Macedonia, Greece). The data from the Lake Dojran core clearly shows variability of the erosional processes on millennial and centennial time scales, which can be explained by abrupt climate change (8.2 event, 4.2 event), and by human impact, respectively.

In a new upcoming project starting in April 2017, the comminution age approach will now be applied on a long sediment core (DEEP site location) from Lake Ohrid,

which was retrieved from the central part of the lake in spring 2013 under the umbrella of the ICDP SCOPSCO (Scientific Collaboration on Past Speciation Conditions in Lake Ohrid) project. The DEEP site sequence covers the past 1.9 to 1.3 Ma and several studies about sedimentary (grain size, (bio-)geochemistry), rock magnetic, pollen, and stable isotope data, which have recently been published focusing on the past 637 ka years, show evidence for the high sensitivity of Lakes Ohrid sediments to local environmental and global climate change (Francke et al., 2016; Just et al., 2016; Lacey et al., 2016; Sadori et al., 2016). This existing data about past climatic and local environmental change will be linked with the U isotope data in order to

- (a) substantially improve the understanding of past catchment dynamics and clastic sediment formation at Lake Ohrid since the penultimate glacial period,
- (b) to determine the impact of human-induced wood clearance and agricultural land-use in Lake Ohrid's catchment during the Late Holocene.

In order to achieve the first goal (a), U isotope analyses will be carried out at low resolution (~2000 years) on the sediments of the DEEP site succession covering the time since the penultimate glacial period. The data shall be used to determine time periods of fast erosion characterized by for example gully erosion or glacial abrasion, and time periods of slow erosion, such as when hill slope or sheet wash erosion persisted. Thereby, of particular interest are glacial to interglacial transitions, as most severe environmental and climatic variations naturally occur during these time intervals at Lake Ohrid.

High resolution studies (~500 years) will be carried out for the Holocene part of the DEEP site sequence in order to unravel the impact of natural modifications versus human impact on the erosional processes (goal (b)). The results will be compared to the findings about most severe environmental modifications during glacial to interglacial transitions and to the information obtained from the Lake Dojran core in order to examine how the size of the catchment and lake affects the U isotope data.

The information will contribute to the understanding of erosional processes and landscape evolution in changing environmental and climatic conditions as a basis for predictions under recent global warming. Gaining more information about the erosional processes related to modifications in hydrological conditions (isotope data), temperature (TIC data), and vegetation density (pollen data) will also provide detailed insights about the feedback mechanism in the catchment dynamics to modern climate change even beyond Lake Ohrid's catchment.

References:

- Dosseto, A. and Schaller, M.: The erosion response to Quaternary climate change quantified using uranium isotopes and in situ-produced cosmogenic nuclides, *Earth-Science Reviews*, 155, 60-81, 10.1016/j.earscirev.2016.01.015, 2016.
- Francke, A., Wagner, B., Just, J., Leicher, N., Gromig, R., Baumgarten, H., Vogel, H., Lacey, J. H., Sadori, L., Wonik, T., Leng, M. J., Zanchetta, G., Sulpizio, R., and Giaccio, B.: Sedimentological processes and environmental variability at Lake Ohrid (Macedonia, Albania) between 637 ka and the present, *Biogeosciences*, 13, 1179-1196, 10.5194/bg-13-1179-2016, 2016.
- Just, J., Nowaczyk, N. R., Sagnotti, L., Francke, A., Vogel, H., Lacey, J. H., and Wagner, B.: Environmental control on the occurrence of high-coercivity magnetic minerals and formation of iron sulfides in a 640 ka sediment sequence from Lake Ohrid (Balkans), *Biogeosciences*, 13, 2093-2109, 10.5194/bg-13-2093-2016, 2016.
- Lacey, J. H., Leng, M. J., Francke, A., Sloane, H. J., Milodowski, A., Vogel, H., Baumgarten, H., Zanchetta, G., and Wagner, B.: Northern Mediterranean climate since the Middle Pleistocene: a 637 ka stable

isotope record from Lake Ohrid (Albania/Macedonia), *Biogeosciences*, 13, 1801-1820, 10.5194/bg-13-1801-2016, 2016.

- Sadori, L., Koutsodendris, A., Panagiotopoulos, K., Masi, A., Bertini, A., Combourieu-Nebout, N., Francke, A., Kouli, K., Joannin, S., Mercuri, A. M., Peyron, O., Torri, P., Wagner, B., Zanchetta, G., Sinopoli, G., and Donders, T. H.: Pollen-based paleoenvironmental and paleoclimatic change at Lake Ohrid (south-eastern Europe) during the past 500 ka, *Biogeosciences*, 13, 1423-1437, 10.5194/bg-13-1423-2016, 2016.

ICDP

First biogeochemical characterization of sediments from ferruginous and ultraligotrophic Lake Towuti

A. FRIESE¹, C. GLOMBITZA², R. SIMISTER⁴, A. VUILLEMIN¹, S. NOMOSATRYO³, K. BAUER⁴, L. ORDONEZ⁵, C. HENNY³, D. ARIZTEGUI⁵, S. CROWE⁴, D. WAGNER¹ and J. KALLMEYER¹

¹ Helmholtz Centre Potsdam, GFZ German Research Centre for Geosciences, Section 4.5 Geomicrobiology, 14473 Potsdam, Germany

² Department of Biosciences, Center for Geomicrobiology, Aarhus University, Aarhus, Denmark

³ Research Center for Limnology, Indonesian Institute of Sciences (LIPI), Cibinong-Bogor, Indonesia

⁴ Department of Microbiology and Immunology and Department of Earth, Ocean, and Atmospheric Sciences, University of British Columbia, Vancouver, Canada.

⁵ Department of Earth Sciences, University of Geneva, rue des Maraichers 13, 1205 Geneva, Switzerland

Lake Towuti is a tropical 200 m deep tectonic lake. Its catchment is mainly composed of ophiolitic rocks and lateritic soils (Russell et al., 2016). The tropical climate and lateritic weathering of the catchment lead to a high flux of iron(oxy)hydroxides into the lake, scavenging most of the bioavailable phosphorus and thereby driving the lake toward ultra-oligotrophic conditions (Zegeye et al., 2012). The water column is weakly thermally stratified with anoxic bottom waters below 130 m water depth (Costa et al., 2015). Lake Towuti sediment thus provides a unique opportunity to develop a better understanding of the metabolic diversity and activity of microbial communities in metal-rich subsurface sedimentary environments.

A first biogeochemical characterization of short (<35 cm) sediment cores showed that, despite extremely low pore water nitrate and sulfate concentrations (single μM), the sediment is substantially colonized by microbial populations that perform metabolisms related to sulfur, iron and methane cycling (Vuillemin et al., 2016). From May to July 2015 an ICDP drilling campaign took place on Lake Towuti that, for the first time in ICDP history, retrieved a dedicated core for geomicrobiological investigations. We analyzed pore water concentration and quantified total microbial abundance throughout the ca. 115 m long sediment drill core. This dataset represents the first biogeochemical characterization of a non-sulfidic, iron-rich deep biosphere sedimentary system.

Pore water samples were extracted under anoxic conditions and concentrations of cat- and anions as well as volatile fatty acids determined via ion chromatography and photometry. Alkalinity was determined by titration and total microbial abundance quantified via fluorescence microscopy.

Detectable cat- and anions were sodium, potassium, ammonium, magnesium calcium and chloride, phosphate, nitrate, sulfate, respectively. Detectable volatile fatty acids were acetate, formate, lactate, butyrate and propionate. Most ions show major concentration changes in

the upper 20m and remain rather constant below. Sodium and chloride both increase with depth but do not correlate. Chloride concentrations might be affected by lake level changes, revealing elevated concentrations in two sedimentary units, a deeper one reflecting the early stage of formation of Lake Towuti and the depth interval between 3 and 7 m that recorded a lower lake level between ~33 and 16 ka B.P (Russell et al., 2014). Three narrow horizons with elevated cation and sulfate concentrations could be identified at 51 m, 87,5 m and 103,5 m, which potentially point towards tephra layers. Total cell counts are highest at the top of the core (10^8 cells cm^{-3}) and rapidly decrease to below the limit of detection (10^5 cells cm^{-3}) within the first 20m indicating low microbial abundance below that depth. Total microbial abundance seems to be related to the availability of acetate, formate and lactate, as these simple organic molecules are the most important carbon sources for microorganisms.

These data will form the basis of further geochemical and microbiological analyses that will help to unravel the dominant microbial processes as well as the biogeochemical features that control microbial activity and diversity in the metal rich sediment of Lake Towuti.

References:

- Costa, K.M., Russell, J.M., Vogel, H., Bijaksana, S., 2015. Hydrological connectivity and mixing of Lake Towuti, Indonesia in response to paleoclimatic changes over the last 60,000 years. *Palaeogeography, Palaeoclimatology, Palaeoecology* 417, 467-475.
- Russell, J.M., Bijaksana, S., Vogel, H., Melles, M., Kallmeyer, J., Ariztegui, D., Crowe, S., Fajar, S., Hafidz, A., Haffner, D., Hasberg, A., Ivory, S., Kelly, C., King, J., Kirana, K., Morlock, M., Noren, A., O'Grady, R., Ordonez, L., Stevenson, J., von Rintelen, T., Vuillemin, A., Watkinson, I., Wattrus, N., Wicaksono, S., Wonik, T., Bauer, K., Deino, A., Friese, A., Henny, C., Imran, Marwoto, R., Ngoimani, L.O., Nomosatryo, S., Safiuddin, L.O., Simister, R., Tamuntuan, G., 2016. The Towuti Drilling Project: paleoenvironments, biological evolution, and geomicrobiology of a tropical Pacific lake. *Sci. Dril.* 21, 29-40.
- Russell, J.M., Vogel, H., Konecky, B.L., Bijaksana, S., Huang, Y., Melles, M., Wattrus, N., Costa, K., King, J.W., 2014. Glacial forcing of central Indonesian hydroclimate since 60,000 y BP. *Proceedings of the National Academy of Sciences* 111, 5100-5105.
- Vuillemin, A., Friese, A., Alawi, M., Henny, C., Nomosatryo, S., Wagner, D., Crowe, S., Kallmeyer, J., 2016. Geomicrobiological features of ferruginous sediments from Lake Towuti, Indonesia. *Frontiers in Microbiology* 7.
- Zegeye, A., Bonneville, S., Benning, L.G., Sturm, A., Fowle, D.A., Jones, C., Canfield, D.E., Ruby, C., MacLean, L.C., Nomosatryo, S., Crowe, S.A., Poulton, S.W., 2012. Green rust formation controls nutrient

availability in a ferruginous water column. *Geology* 40, 599-602.

ICDP

Trans-Amazon Drilling Project

S.C. FRITZ¹, P.A. BAKER²

¹ Department of Earth and Atmospheric Sciences, University of Nebraska – Lincoln, USA

² Division of Earth and Ocean Sciences, Duke University, USA and Yachay Tech University, Ecuador

The Amazon/Andes of tropical South America is a key region on Earth, and its rainforests host over half of all terrestrial plant species. The forests and their biota have evolved together with the physical landscape, closely linking processes in the Earth's interior with surface climate and landscapes, ecosystems, and biodiversity. The proposed Trans-Amazon Drilling Project will address fundamental questions about the geologic and biotic evolution of the Amazon, focusing on (1) how Cenozoic climate and geologic history, including uplift of the Andes and development of the Amazon fluvial system, influenced the origins of the Amazon rainforest and its incomparable biodiversity; and (2) the origin of the Amazonian "Pentecaua" diabase sills, one of Earth's largest intrusive complexes, and the impacts of this intrusion on the atmospheric gas composition and mass extinction at the Triassic/Jurassic boundary. These goals require long sedimentary records, which, in most of the Amazon region, can only be obtained by drilling. We propose an ICDP project to drill the entire Cenozoic sequence in four different ancient sedimentary basins that are aligned along the modern Amazon River and that transect the entire near-equatorial Amazon region of Brazil, from the Andean foreland to the Atlantic Ocean, coupled with proposed IODP drilling of sites on the Amazon continental margin. The transect of sites is essential for distinguishing basin-wide and continental-scale patterns of climate, landscape, and biotic evolution; evaluating questions about west-to-east gradients and hydrologic connectivity; and correlating the continental strata with a site dated using marine

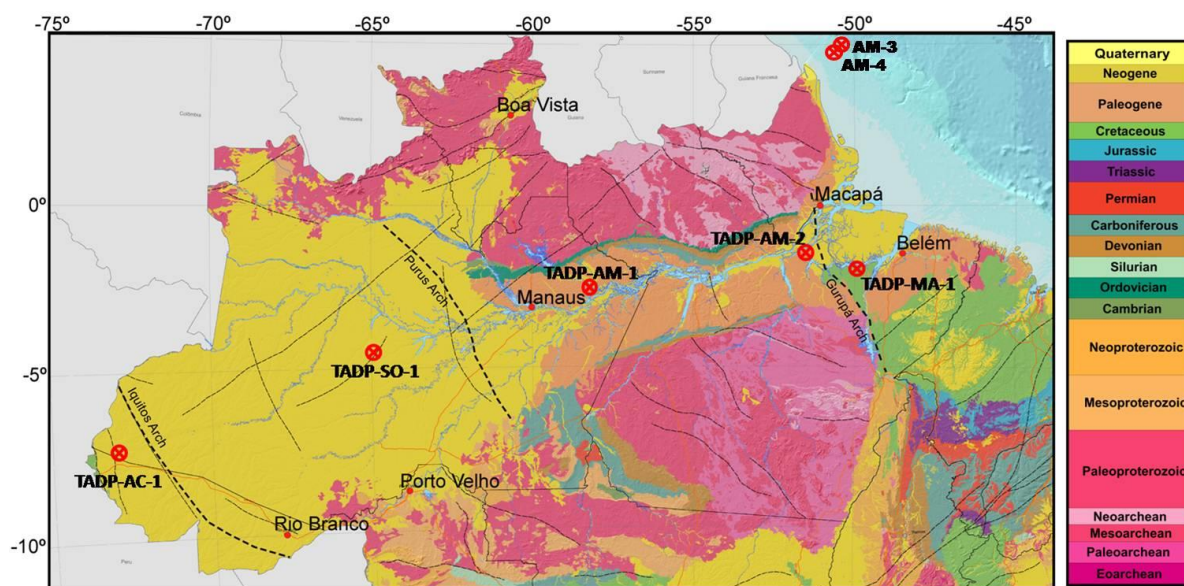


Figure 1

biostratigraphy. In addition, in the Amazonas Basin, we propose to drill both the Cenozoic sedimentary sequence and the entire 1100 m thick underlying diabase sequence along with its interbedded host meta-sediments. This ICDP-IODP transect will span 40°W to 73°W, thus encircling nearly 10% of Earth's equatorial circumference. We believe that this work will provide transformative understanding of Amazonian geological and biotic evolution that addresses important and long-standing questions about the linkages between the geophysical environment and its biotic history.

ICDP

Trace element systematics in gabbros from the Wadi Gideah transect (Wadi Tayin Massif, Oman ophiolite) – constraints on accretion processes in fast-spread oceanic crust

D. GARBE-SCHÖNBERG¹, J. KOEPKE², S. MÜLLER¹, T. MÜLLER², H. STRAUSS³

¹ Christian-Albrechts-Universität zu Kiel, 24098 Kiel, Germany
(dgs@gpi.uni-kiel.de)

² Leibniz-Universität Hannover, Institut für Mineralogie, 30167 Hannover, Germany

³ Westfälische-Wilhelms-Universität Münster, Geologisch-Paläontologisches Institut, 48149 Münster, Germany

The Oman Drilling Project (<http://www.omandrilling.ac.uk/>) started its active phase in December 2016 and completed already the first two drill holes GT-2 and GT-1 (400m each) in upper and lower gabbros of fast-spread oceanic paleo-crust in the Oman ophiolite (Wadi Gideah, Wadi Tayin Massif). Our current ICDP project (see the complementary papers by Müller et al. and Koepke et al., this meeting) focuses on depth logs with respect to (1) petrology, (2) major and trace element geochemistry of rocks and minerals, (3) crystallographic preferred orientations (CPO), (4) the evolution of hydrothermal alteration, and (5) the sulfur cycle. Within a previous project, we performed several field campaigns with systematic and continuous sampling along the Wadi Gideah through the entire plutonic section. More than 300 collected samples represent the first continuous transect covering the entire oceanic crust from the mantle/crust boundary up to the dike/gabbro transition zone. The data set from this transect provides a reference frame for the current individual crustal drillings within the Oman Drilling Project.

Here we present trace element data for both bulk rock and selected minerals displaying systematic compositional trends in the plutonic suite that are correlated with stratigraphic distance from the MOHO transition zone. Most trace element concentrations show minor variation with only weak and more or less monotonous trends in the layered gabbro section. Further upwards, concentrations of incompatible trace elements (e.g., Th, Nb, Ta, REE, Zr, Hf) increase significantly from foliated towards varitextured gabbros. In contrast, the ratios of these incompatible elements Nb/Ta, Nb/La, Zr/Hf, La/Yb etc. show significant variation and fractionation in the layered gabbros but only minor fractionation of HFSE elemental ratios can be

observed in the upper varitextured and isotropic gabbros of the fossil axial melt lens (AML). One possible process leading to strong fractionation of these elements is *in situ* crystallization in a lower solidification zone (Langmuir, 1989) during reactive porous flow (Lissenberg *et al.*, 2012) where reactions lead to a strong enrichment in, and fractionation of, incompatible elements in the interstitial melt. Evolved interstitial melt is documented in compositional zonation of clinopyroxene and plagioclase, and there is evidence from our data that Zr must have reached concentrations in the interstitial liquid allowing for crystallization of zircon. Further up, fractional crystallization processes in a well-mixed magma chamber (AML) control the composition of varitextured and isotropic gabbros with very little fractionation of incompatible elements.

Our data will be used for testing hypotheses on accretion processes during the formation of plutonic, fast-spread oceanic crust that are currently described by two conceptual endmember models: The 'gabbro glacier' model (e.g., (Nicolas *et al.*, 1988)) assumes crystallization of primitive melts within a small melt lens (AML) sandwiched between upper gabbros and sheeted dikes. From here, crystal mush subsides down along the flanks of the ridge axis forming the layered gabbros. In contrast, the 'sheeted sill' model (e.g., (Kelemen *et al.*, 1997)) postulates that the lower crust is accreted *in-situ* by lateral sill intrusions. Our systematic compositional trends seem to be in favor of the latter model and support the view of (Lissenberg *et al.*, 2012) that the lower oceanic crust plays a significant role in modifying the composition of MORB. However, fractional crystallization from the AML might play a major role for the formation of the upper gabbros.

References:

- Kelemen, P. B., Koga, K. & Shimizu, N. (1997). Geochemistry of gabbro sills in the crust-mantle transition zone of the Oman ophiolite: implications for the origin of the oceanic lower crust. *Earth and Planetary Science Letters* 146, 475–488.
- Langmuir, C. H. (1989). Geochemical consequences of *in situ* crystallization. *Nature* (ISSN 0028-0836), 199–205.
- Lissenberg, C. J., Macleod, C. J., Howard, K. A. & Godard, M. (2012). Pervasive reactive melt migration through fast-spreading lower oceanic crust (Hess Deep, equatorial Pacific Ocean). *Earth and Planetary Science Letters*. Elsevier 1–12.
- Nicolas, A., Reuber, I. & Benn, K. (1988). A new magma chamber model based on structural studies in the Oman ophiolite. *Tectonophysics* 151, 87–105.

IODP

Geomorphology of the Belize Barrier Reef margin: a survey for IODP drilling

EBERHARD GISCHLER¹, FLAVIO S. ANSELMETTI²

¹ Institut für Geowissenschaften, Goethe-Universität,
Altenhöferallee 1, D-60438 Frankfurt am Main, Germany

² Institut für Geologie, Universität Bern, Baltzerstrasse 1+3, CH-3012 Bern, Switzerland

As precondition for IODP drilling along the Belize Barrier Reef, the largest reef system in the Atlantic Ocean, a detailed bathymetric study is planned along selected sections of the forereef area between ca. 20-150 m water depth of this major reef margin using multibeam bathymetric and shallow seismic techniques. To date, no detailed and GPS-controlled bathymetry and continuous high-resolution seismic data of this barrier reef margin exists. Based on the data to be acquired, we intend to select suitable sites for IODP drilling. We aim at locating fore-reef sites, which will be suitable to recover postglacial (20-10 kyr BP) and underlying older Pleistocene deposits along a series of core traverses. Furthermore, an international workshop is planned to bring together interested scientists in order to explore the possibilities of developing a drill proposal for the IODP.

The subsequent IODP proposal could have four potential objectives including the reconstruction of postglacial sea-level rise, to analyze and quantify postglacial reef composition and architecture as response to sea-level and climate change, and to obtain environmental data on temperature and carbonate saturation during that time window. In addition, aspects of Pleistocene reef initiation and paleoecology may be investigated, depending on recovery of older Pleistocene successions. In the light of the modelled 21st century increases in sea-level rise, especially postglacial drowned reef sequences along the Belize margin can potentially be used for future sea-level projections.

In contrast to the Indo-Pacific region where several highly resolved and scientifically robust reef-based postglacial sea-level records have been acquired (Huon Peninsula, Tahiti, Great Barrier Reef), there is only one such record in the tropical western Atlantic (Barbados, eastern Caribbean). The Barbados sea-level record remains controversial, however, as the recently acquired sea-level data from Tahiti (IODP leg 310) and the Great Barrier Reef (IODP leg 325) only recorded meltwater pulse (MWP) 1A whereas MWP 1B is missing. Also, abundant postglacial microbialite facies as found in Tahiti and the Great Barrier Reef and many other early Holocene reefs is apparently absent in Barbados for hitherto unknown reasons. This asks for investigations of additional and independent sites, because microbialite facies in postglacial reefs were formed by simple organisms (bacteria) and may provide key proxy data (thickness, volume) that are largely environmentally controlled and presumably easier to interpret as proxy data (growth and calcification rates, $\delta^{18}\text{O}$, Sr/Ca) from enzymatically controlled reef-builders such as corals. It has been debated whether microbialite abundance is linked to the nature of the hinterland, carbonate saturation, and rate of sea-level rise. In summary, a second postglacial reefal archive from Belize would certainly help to answer these open and debated questions and to constrain the nature of postglacial sea-level rise in the western Atlantic / Caribbean realm.

IODP

Early Pliocene vegetation and hydrology changes in western equatorial South America

F. GRIMMER¹ & L.M. DUPONT¹

¹ MARUM – Center for Marine Environmental Sciences,
University of Bremen, Leobener Str., 28359

During the Pliocene, two major tectonic events triggered a profound reorganization of ocean and atmospheric circulation in the Eastern Equatorial Pacific (EEP), the Caribbean Sea, and on adjacent land masses: the progressive closure of the Central American Seaway (CAS) and the uplift of the northern Andes. These events presumably lead to a shift in the mean latitudinal position of the Intertropical Convergence Zone (ITCZ), which would have affected the continental climate. The direction of an ITCZ shift however is still debated, because numerical modelling results and paleoceanographic data indicate shifts in opposite directions. To resolve this contradiction, an independent hydrological record of the region is needed. A study site in the EEP (ODP Site 1239A) was chosen to reconstruct the vegetation and climatic history of western Ecuador with palynological techniques, focusing on two time windows: 4.7-4.2 Ma and 3.6-3.1 Ma. The presented pollen record comprises representatives from five vegetation types: lowland rainforest, lower montane forest, upper montane forest, páramo, and broad range taxa. The main finding is the persistence of a broad tropical rainforest coverage in the whole study area throughout the early Pliocene. From 4.7 to 4.44 Ma and around 4.2 Ma, the record reveals increasing humidity. This is reflected through increasing percentages of lowland rainforest and lower montane forest, a high spore content and high linear sedimentation rates. The development of the different vegetation types reveals stable, permanently humid conditions. This finding would rather be in agreement with paleoceanographic data indicating a southward ITCZ shift in response to CAS closure. However, the very stable conditions suggest that the critical thresholds of surface water restriction of the CAS and of Andean uplift, which presumably triggered changes in atmospheric circulation, might have been reached even earlier.

IODP

Shifts in Miocene Southern Hemisphere Westerlies and varying southward heat transport by the Leeuwin Current

J. GROENEVELD^{1*}, J. HENDERIKS², W. RENEMA³, C.M. MCHUGH⁴,
D. DE VLEESCHOUWER¹, B.A. CHRISTENSEN⁵, AND EXP. 356
SCIENTISTS

¹ MARUM—Center for Marine and Environmental Sciences and Department of Geosciences, University of Bremen, 28359 Bremen, Germany.

² Department of Earth Sciences, Uppsala University, Villavägen 16, Uppsala 75236, Sweden.

³ PO Box 9517, Leiden 2300 Netherlands.

⁴ School of Earth and Environmental Sciences, Queens College (C.U.N.Y.), 65-30 Kissena Blvd. Flushing NY 11367, USA.

⁵ Environmental Studies, Adelphi University, 1 South Ave. SCB 201, Garden City NY 11530, USA.

* Corresponding author. Email: jgroeneveld@uni-bremen.de

International Ocean Discovery Program (IODP) Expedition 356 (August–September 2015) drilled a transect across 10° latitude of seven shelf and upper slope sites (Sites U1458–U1464) off Western Australia from the Perth Basin, through the Northern Carnarvon Basin, to the Roebuck Basin with the RV Joides Resolution. One of the main objectives was documenting the evolution of the Indonesian Throughflow (ITF), a critical component of global thermohaline circulation and a driver of the southward-flowing Leeuwin Current (Gallagher et al., 2014). This in turn has influenced the development of aridity in Australia, the onset of the Australian monsoon, and varying heat transport towards high southern latitudes.

Global climate underwent a major reorganization when the Antarctic ice sheet (AIS) expanded ~14 million years ago (Ma). This event impacted global atmospheric circulation, including the strength and position of the Westerlies and the Intertropical Convergence Zone (ITCZ), and therefore precipitation patterns. We present new shallow-marine

sediment records of relative aridity and moisture based on downhole wireline logs of thorium and potassium from IODP Sites U1459 and U1464 off Western Australia (Groeneveld et al., *subm.*). These records provide the first empirical evidence linking high latitude cooling around Antarctica to climate change in the (sub)tropics during the Miocene (Groeneveld et al., *subm.*). We show that Western Australia was arid during most of the middle Miocene. Southwest Australia became wetter during the late Miocene creating a climate gradient with the arid interior, while northwest Australia remained arid throughout. Precipitation and river runoff in southwest Australia gradually increased from 12 to 8 Ma, which we relate to a northward migration or intensification of the Westerlies possibly due to increased sea ice in the Southern Ocean. Abrupt aridification indicates that the Westerlies shifted back to a position south of Australia after 8 Ma. Our mid-latitude Southern Hemisphere data are consistent with the inference that expansion of sea ice around Antarctica resulted in a northward movement of the Westerlies. This in turn may have pushed tropical atmospheric circulation and the ITCZ northward, shifting the main precipitation belt over large parts of southeast Asia.

In a next step, it is intended to reconstruct paleo sea water temperatures and upwelling episodes along the western shelf of Australia, as well as sea water temperatures in the Tasman Sea as representing the Southern Ocean. This will allow to reconstruct the heat transport from, and therewith intensity of, the Indonesian Throughflow and the Leeuwin Current towards high southern latitudes from the late Miocene into the Pliocene. Temperatures off Western Australia will be reconstructed using ODP Site 763; a Pliocene record already exists (Karas et al., 2011), which will be extended into the late Miocene. Sites U1460 and U1463 (neighbouring sites U1459 and U1464, resp.) will be used for stable isotope reconstructions and planktonic foraminiferal analyses to identify periods during which upwelling occurred and a temperature gradient existed vs. periods with oligotrophic conditions caused by an active Leeuwin Current. As representative for high-latitude sea

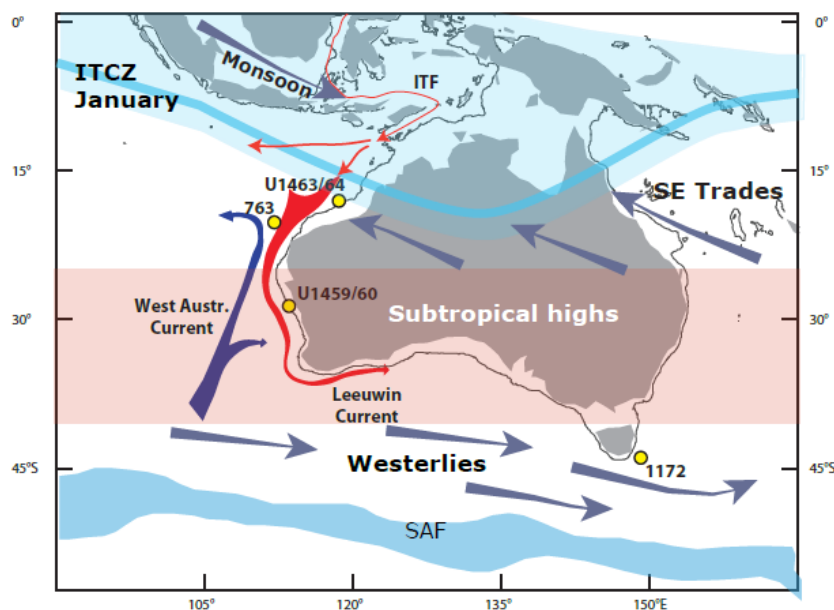


Figure 1: Map with sites to be used in this proposal. Important oceanographic (ITF (Indonesian Throughflow), Leeuwin Current, West Australian Current, Subantarctic Front (SAF) and atmospheric (ITCZ, trade winds, Westerlies) features are indicated and major players in the interpretation of the proposed reconstructions.

water temperatures ODP Site 1172 on the Tasman Plateau is chosen allowing to construct a temperature gradient between the low latitude sites of Western Australia and the Southern Ocean.

References:

- Gallagher, S.J., Fulthorpe, C.S., Bogus, K.A., (2014). Reefs, oceans, and climate: a 5 million year history of the Indonesian Throughflow, Australian monsoon, and subsidence on the northwest shelf of Australia. *International Ocean Discovery Program Scientific Prospectus*, 356. <http://dx.doi.org/10.14379/iodp.sp.356.2014>
- Groeneveld, J., Henderiks, J., Renema, W., McHugh, C.M., De Vleeschouwer, D., Christensen, B.A., Fulthorpe, C.S., Reuning, L., Gallagher, S., Bogus, K., Auer, G., Ishiwa, T., and Exp. 356 Scientists (subm.). Australian shelf sediments reveal shifts in Miocene Southern Hemisphere Westerlies.
- Karas, C., Nürnberg, D., Tiedemann, R., Garbe-Schönberg, D., (2011). Pliocene Indonesian Throughflow and Leeuwin Current dynamics: Implications for Indian Ocean polar heat flux. *Paleoceanography* 26, PA2217, doi:10.1029/2010PA001949.

IODP

Pliocene history of Mediterranean-Atlantic exchange

PATRICK GRUNERT¹, ÁNGELA GARCÍA-GALLARDO¹, BARBARA BALESTRA², CARL RICHTER³, GERALD AUER¹, MARLIES VAN DER SCHEE⁴, JOSÉ-ABEL FLORES⁴, FRANCISCO J. SIERRA⁴, FRANCISCO JIMÉNEZ-ESPEJO⁵, CARLOS ALVAREZ ZARIKIAN⁶, ULLA RÖHL⁷, WERNER E. PILLER¹

¹ Institute of Earth Sciences, University of Graz, NAWI Graz, Heinrichstrasse 26, 8010 Graz, Austria

² Institute of Marine Sciences, University of California Santa Cruz, United States of America

³ School of Geosciences, University of Louisiana at Lafayette, United States of America

⁴ Department of Geology, University of Salamanca, Spain

⁵ Department of Biogeochemistry, Japan Agency for Marine-Earth Science and Technology (JAMSTEC), Yokosuka, Japan

⁶ International Ocean Discovery Program, Texas A&M University, College Station, TX 77845, United States of America

⁷ MARUM – Center for Marine Environmental Sciences, University of Bremen, Germany

Mediterranean Outflow Water (MOW) is a considerable source of heat and salt for today's North Atlantic and is considered to contribute to maintaining the Atlantic meridional overturning circulation (AMOC). There is evidence that MOW intensity varied on glacial/interglacial and stadial/interstadial timescales in the past, and that phases of MOW intensification potentially preconditioned thermohaline circulation for its interglacial mode in the late Pleistocene (Rogerson et al., 2012; Bahr et al, 2014). Until recently, however, efforts towards a better understanding of MOW behavior through time and potential climatic feedback mechanisms between MOW, the African Monsoon, AMOC, and eustatic sea-level fluctuations have been impeded by the limitation of available sample material largely to the uppermost Pleistocene and Holocene. In 2011/12, IODP Expedition 339 drilled several sites in the Gulf of Cadiz and off the western Iberian Margin, recovering a total of 4.5 km of Pliocene to Holocene contouritic deposits of MOW (Hernández-Molina et al., 2014).

In this paper, we present new findings on early MOW history from IODP Sites U1387 and U1389, specifically its onset after the Messinian Salinity Crisis and its behavior at

the transition from the Pliocene warmhouse to Pleistocene icehouse climate. New micropalaeontological and geochemical records suggest that IODP Site U1387 is affected by Mediterranean water shortly after the opening of the Gibraltar Strait and before the onset of contourite drift deposition, representing the first indications of Mediterranean-Atlantic exchange (Van der Schee et al., 2016). At IODP Site U1389, a substantially revised and refined age model for the time interval between 3.6 and 2.5 Myrs allows the evaluation of long- and short-term trends in data from XRF core-scanning, and their comparison to proxy records from the Mediterranean and North Atlantic (Khelifi et al., 2014). Cyclostratigraphic analysis of Zr/Al records in well-recovered intervals suggest that the long-term strengthening of MOW at the onset of Northern Hemisphere Glaciation is underpinned by a strong precessional control on bottom current strength.

This study contributes to project P25831-N29 of the Austrian Science Fund (FWF) and is financially supported by grants of ECORD and the Max Kade Foundation.

References:

- Bahr, A., Jiménez-Espejo, F.J., Kolasinac, N., Grunert, P., Hernández-Molina, F.J., Röhl, U., Voelker, A.H.L., Escutia, C., Stow, D.A.V., Hodell, D., Alvarez-Zarikian, C.A., 2014. Deciphering bottom current velocity and paleoclimate signals from contourite deposits in the Gulf of Cádiz during the last 140 kys: An inorganic geochemical approach. *Geochemistry, Geophysics, Geosystems* 15, doi:10.1002/2014GC005356.
- Hernández-Molina, F.J., Stow, D.A.V., Alvarez Zarikian, C.A., Acton, G., Bahr, A., Balestra, B., Ducassou, E., Flood, R.D., Flores, J.-A., Furota, S., Grunert, P., Hodell, D., Jimenez-Espejo, F., Kim, J.K., Krissek, L., Kuroda, J., Li, B., Llave, E., Lofi, J., Lourens, L., Miller, M., Nanayama, F., Nishida, N., Richter, C., Roque, A.C., Sanchez Goni, M.F., Sierro, F.J., Singh, A.D., Sloss, C., Takashimizu, Y., Tzanova, A., Voelker, A., Williams, T., Xuan, C., 2014. Onset of Mediterranean outflow into the North Atlantic. *Science* 344, 1244–1250.
- Rogerson, M., Rohling, E.J., Bigg, G.R., Ramirez, J., 2012. Paleocyanography of the Atlantic-Mediterranean exchange: overview and first quantitative assessment of climatic forcing. *Reviews of Geophysics* 50, RG2003.
- Van der Schee, M., Sierro, F.J., Jiménez-Espejo, F.J., Hernández-Molina, F.J., Flecker, R., Flores, J.A., Acton, G., Gutjahr, M., Grunert, P., García-Gallardo, A., Andersen, N. (2016). Evidence of early bottom water current flow after the Messinian Salinity Crisis in the Gulf of Cadiz. *Marine Geology*, 380, 315–329.

IODP

The Indian-Atlantic Ocean gateway during the Pliocene: current dynamics and changing sediment provenance

J. GRUETZNER¹, G. UENZELMANN-NEBEL¹, AND THE EXPEDITION 361 SCIENTISTS

¹ Alfred-Wegener-Institut, Helmholtz-Zentrum für Polar- und Meeresforschung, Bremerhaven, Germany
(Jens.Gruetzner@awi.de)

The Pliocene epoch represents a discrete interval which reversed a long-term trend of late Neogene cooling and is also the most recent geological interval in which global temperatures were several degrees warmer than today. It is therefore often considered as the best analogue for a future anthropogenic greenhouse world. However, there is growing evidence that the Pliocene was not a stable period but can rather be subdivided in several distinct climate phases. Our understanding of Pliocene climate variability in the Southern Hemisphere, and especially in the Atlantic-Indian ocean gateway, is limited by scarce marine records

and poor age control on existing terrestrial climate archives. At five from six drilling locations of IODP Exp. 361 (Jan. – March 2016) high resolution complete Pliocene/Pleistocene sections have been recovered (see IODP Expedition 361 – Southern African Climates and Agulhas LGM Density Profile by Gruetzner et al., this Volume).

Our new research proposal focuses on three of these sites forming a latitudinal transect in the Atlantic-Indian Ocean gateway and combines chemical, physical property and seismic methods. Primary site for our investigations is Site U1475 with the focus on the interplay between northern and southern sourced deep water masses at the Agulhas Plateau. This will be augmented by investigations at Sites U1479 (Cape Basin) and U1474 (Natal Valley), both located in the pathway of modern NADW. Our research is driven by three main working hypotheses:

Seismic stratigraphies for the last 6 Ma and sediment drift growth in the Atlantic-Indian gateway are mainly controlled by bottom water flow changes

Using the new sediment archives and physical property records from IODP Exp. 361 (Hall et al., 2016) we aim to construct detailed seismic stratigraphies for the Agulhas Plateau, the Natal valley and the Cape basin for the last 6 Ma. At all Exp. 361 sites *P*-wave velocity and density records are of sufficient quality to enable detailed correlations of drilling results and site survey data through the calculation of synthetic seismograms. Our working hypothesis implies that seismic reflection patterns and sediment accumulation during the Pliocene are closely linked to deep water circulation changes associated with climate Pliocene phases. Furthermore four distinct high latitude Pliocene glaciation events have been identified. We speculate that these phases and events have led to deep water circulation changes in Agulhas region, have altered the sediment physical properties and thus may be recognized as reflectors in the seismic profiles. How did the sediment input of terrigenous vs. biogenic sediment components in the gateway change during these events? Are these changes driven by dilution, dissolution, or productivity? We strive to answer these questions by interpreting the physical and chemical (XRF) core scanning records.

Trajectories and intensities of deep water masses in the Agulhas region during the Pliocene were influenced by Antarctic ice volume rather than by the closure of the Central American Seaway.

The Exp. 361 drill sites offer the possibility to inter-correlate different flow speed proxies and to derive a detailed picture of flow changes during the Pliocene. By comparing core-measurements of sortable silt (S_{1-6}^{2-6}), physical properties and XRF-core scanning data with seismic features we will tie the major flow speed changes to our seismic grid covering the Agulhas Plateau such that changing current intensities and pathways can be mapped together. Here we hypothesize that these changes are mainly driven by climate (Antarctic ice volume). What were the main changes associated with the Pliocene instability of Antarctic ice sheets and was the production of Antarctic Bottom Water (AABW) reduced or enhanced during these intervals? How have the sedimentation patterns changed under the growing influence of North Atlantic Deep Water (NADW)? Was there also a potential

influence of tectonic processes on the flow changes in the Agulhas region? Especially the closure of the Central American Seaway CAS between ~14 and ~2.7 Ma is thought to have had a profound impact on climate.

The Pliocene variability in sediment provenance on millennial timescales is subdued when compared to the Pleistocene.

Understanding the mechanisms and causes of abrupt climate change is one of the major challenges in global climate change research today and there is growing evidence that millennial scale climate variability was enhanced during times when a critical threshold in continental ice volume was surpassed. Dramatic millennial scale climate shifts are well documented for the “glacial world” of the late Pleistocene but are examined to a much lesser extent for earlier time periods. We suggest testing the potential threshold behaviour for the Atlantic-Indian gateway by comparing short term fluctuations in sediment composition and siliciclastic provenance in the Agulhas region before and after the onset of the Northern Hemisphere glaciation (NHG) at ~2.7 Ma. Time series of sediment provenance dated by “orbital tuning” will be analysed in the time and frequency domain to investigate at what times during the interval 2 – 6 Ma millennial scale climate variability was enhanced or subdued.

References:

- Gruetzner, J., J. Just, A. Koutsodendris, D. Tanguan, I. Hall, S. Hemming, and L. LeVay (2017), IODP Expedition 361 – Southern African Climates and Agulhas LGM Density Profile, *Gemeinsames Kolloquium - DFG-Schwerpunktprogramme ICDP (International Continental Scientific Drilling Program) und IODP (Integrated Ocean Drilling Program)*, Braunschweig.
- Hall, I. R., S. R. Hemming, L. J. LeVay, and the Expedition 361 Scientists (2016), Expedition 361 Preliminary Report: South African Climates (Agulhas LGM Density Profile), International Ocean Discovery Program, College Station.

IODP

Fluctuation of Ca isotope ratios in corals from the Great Barrier Reef during the last deglaciation

N. GUSSONE¹, M. INOUE^{1,2}, Y. YOKOYAMA³, A. SUZUKI⁴, H. KAWAHATA³

¹ Institut für Mineralogie, Westfälische-Wilhelms-Universität Münster, Germany

² Graduate School of Natural Science and Technology, Okayama University, 3-1-1 Tsushima-naka, Okayama 700-8530, Japan

³ Atmosphere and Ocean Research Institute, The University of Tokyo, 5-1-5 Kashiwanoha, Kashiwa, Chiba 277-8564, Japan

⁴ Geological Survey of Japan, National Institute of Advanced Industrial Science and Technology (AIST), 1-1-1 Higashi Tsukuba, AIST Tsukuba Central 7, Ibaraki 305-8567, Japan

Corals play important roles within the System Earth and for unraveling past changes in climate dynamics. As one of the major producers of continental shelf carbonates, coral growth is of great interest, because of their social-economic relevance e.g. in coastal protection, due to the stabilisation of shore areas as well as because of their great potential for recording paleoclimatic information. Several geochemical and isotopic proxies, such as Sr/Ca element or oxygen isotope ratios have been developed and successfully applied on coral material. For instance,

paleoclimatic changes during the last glacial termination have been reconstructed using fossil *Porites* corals collected from Tahiti by IODP Exp. 310 (e.g., Felis et al., 2012). However, corals do not only record changes in the climate system, but due to their significant contribution to the oceanic CaCO₃ precipitation, they are directly linked to the global C-cycling and thus environmental changes. One important parameter for the oceanic C chemistry is the Ca concentration of the seawater, as it controls via the CaCO₃ solubility the precipitation of Ca carbonate minerals. During calcium carbonate precipitation, light Ca isotopes are enriched in the solid phase, leading to a depletion of heavy Ca isotopes in the residual fluid. The Ca isotopic composition of past seawater, recorded in marine carbonates is therefore used as tool to reconstruct changes in the oceanic Ca budget through time. Following this approach demands a careful determination of Ca isotope fractionation of marine biogenic carbonates, to determine the isotopic composition of the sedimentary Ca output flux, as well as for the calculation of the Ca isotope composition of past seawater from fossil carbonate shells. Because corals belong to the dominant marine CaCO₃ producers, the determination of their Ca isotope fractionation in response to environmental changes, as well as gaining an understanding of the fractionation mechanisms involved in biomineralisation, is of special importance.

Experiment on multiple colonies of *Porites* corals cultured under temperature, pH and light controlled environments that investigated the relationship between $\delta^{44}\text{Ca}$ in skeleton grown during the cultured period and each environmental parameters, showed that only temperature significantly affects Ca isotope fractionation during coral biomineralisation (Inoue et al 2015), consistent with observations for other coral species (cf. Böhm et al. 2006). The small temperature sensitivity of 0.02‰/°C observed for the temperature range from 21 to 29°C is similar to inorganic aragonite (Gussone et al. (2003), but the degree of isotope fractionation is about +0.4 ‰ offset in corals relative to inorganic aragonite. Due to coral-specific biomineralization processes, the overall mean $\delta^{44}\text{Ca}$ of scleractinian corals including results from previous studies are different from other biogenic aragonites like sponges and pteropods, which resemble inorganic aragonite. Apparently, coral Ca isotope ratios are more similar to those of calcitic coccolithophores, which Ca isotope composition was suggested to be governed by biological fractionation processes. Other factors such as pH (7.4 to 8.0) and photon flux density were shown not to influence the Ca isotopic composition of the coral skeleton (Inoue et al. 2015). To test, if the experimentally determined Ca isotope fractionation characteristic also apply to natural corals from downcore records, we determined Ca isotope ratios of natural *Acropora* (sp.) and *Isopora* (sp.) corals from the Great Barrier Reef collected during IODP expedition 325 (Yokoyama et al., 2011). For isotope measurements, 300-400 ng Ca were loaded on Re-single filaments with a tantalum activator after addition of a ⁴²Ca-⁴³Ca double spike. Calcium isotope ratios were determined on a Finnigan TRITON TI TIMS following the method described in Gussone et al. (2011). The isotope values are expressed relative to NIST SRM 915a as $\delta^{44}\text{Ca} = ((^{44}\text{Ca}/^{40}\text{Ca})_{\text{sample}} / (^{44}\text{Ca}/^{40}\text{Ca})_{\text{SRM915a}} - 1) \times 1000$.

The fossil corals from IODP expedition 325 that we investigated, were drilled from the shelf edge seaward of the modern Great Barrier Reef, covering the time between 24 and 11 ka. Our results show a gradual increasing of $\delta^{44}\text{Ca}$ from the LGM towards the Holocene. Given the small temperature dependence of Ca isotope fractionation in corals, the temperature rise towards the holocene appears to be not large enough to explain the $\delta^{44}\text{Ca}$ rise observed at the Great Barrier Reef in total. Alternative explanations for the increase in $\delta^{44}\text{Ca}$ may include short term fluctuations in the isotopic composition of the seawater or previously unconsidered factors influencing Ca isotope fractionation in coral skeleton.

References:

- Böhm, F., Gussone, N., Eisenhauer, A., Dullo, W.-C., Reynaud, S., Paytan, A. (2006) Calcium Isotope Fractionation in Modern Scleractinian Corals. *Geochimica et Cosmochimica Acta* 70, 4452-4462.
- Felis, T., Merkel, U., Asami, R., et al. (2012) Pronounced interannual variability in tropical South Pacific temperatures during Heinrich Stadial 1. *Nat. Commun.* 3:965, doi: 10.1038/ncomms1973.
- Gussone, N., Eisenhauer, A., Heuser, A., Dietzel, M., Bock, B., Böhm, F., Spero, H. J., Lea, D.W., Bijma, J., and Nägler, Th.F. (2003) Model for Kinetic Effects on Calcium Isotope Fractionation ($\delta^{44}\text{Ca}$) in Inorganic Aragonite and Cultured Planktonic Foraminifera. *Geochimica et Cosmochimica Acta* 67 (7) 1375-1382.
- Gussone, N., Nehrke, G., Teichert, B.M.A. (2011) Calcium isotope fractionation in ikaite and vaterite. *Chem. Geol.* 285, 194–202.
- Inoue, M., Gussone, N. Koga, Y., et al. (2015) Controlling factors of Ca isotope fractionation in scleractinian corals evaluated by temperature, pH and light controlled culture experiments. *Geochim. Cosmochim. Acta*, 167, 80–92.
- Yokoyama, Y., Webster, J. M., Cotterill, C., Braga, J. C., Jovane, L., Mills, H., Morgan, S., Suzuki, A. and the IODP Expedition 325 Scientists (2011) IODP Expedition 325: Great Barrier Reefs Reveals Past Sea-Level, Climate and Environmental Changes Since the Last Ice Age. *Scientific Drilling* 12, 32-45. doi:10.2204/iodp.sd.12.04.2011.

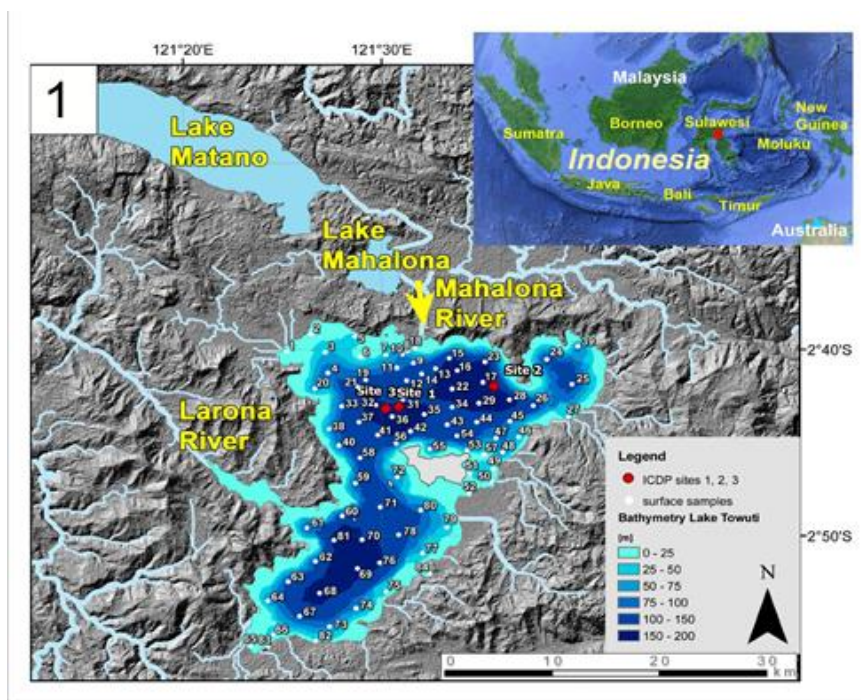


Figure 1: Digital Elevation Model (DEM) of the Lake Towuti area showing the lakes Matano and Mahalona further upstream, the major inlets, the outlet Larona River, the lake bathymetry, and the sampling sites. The inset shows the location of Lake Towuti (red dot) on Sulawesi Island, southeastern Asia.

ICDP

The ICDP drilling project on Lake Towuti, Indonesia: recent developments and contributions of the DFG 'Towuti Bundle'

A. K. M. HASBERG¹, M. MELLES¹, P. HELD¹, J. JUST¹, V. WENNRICH¹, M. MORLOCK², H. VOGEL², J. M. RUSSELL³, S. BIJAKSANA⁴, S. OPITZ⁵, A. FRIESE⁶, J. KALLMEYER⁶, A. VUILLEMIN⁶, F. HERDER⁷, T. V. RINTELEN⁸, K. HESSE⁹, T. WONIK⁹, AND THE ICDP-TDP SCIENTIFIC PARTY

¹ Institute of Geology and Mineralogy, University of Cologne, Zùlpicher Str. 49a, 50674 Cologne, Germany, e-mail: hasberg.ascelina@uni-koeln.de

² Institute of Geological Sciences, & Oeschger Centre for Climate Change Research, University of Bern, Baltzerstrasse 1+3, 3012 Bern, Switzerland

³ Department of Earth, Environmental and Planetary Sciences, Brown University, 324 Brook St. BOX 1846, Providence, RI 02912, USA

⁴ Faculty of Mining and Petroleum Engineering, Institut Teknologi Bandung, Jalan Ganesa 10, Bandung, 40132, Indonesia

⁵ Geographical Institute, University of Cologne, Zùlpicher Str. 45, 50674 Cologne, Germany

⁶ GFZ German Research Center For Geosciences, Section 5.3. Geomicrobiology, 14473 Potsdam, Germany

⁷ Sektion Ichthyologie, Zoologisches Forschungsmuseum Alexander Koenig, Adenauerallee 160, 53113 Bonn, Germany

⁸ Museum für Naturkunde, Leibniz-Institut für Evolutions- und Biodiversitätsforschung, Invalidenstraße 43, 10115 Berlin, Germany

⁹ Leibniz-Institute for Applied Geophysics (LIAG), Stilleweg 2, 30655 Hannover, Germany

Introduction

This presentation summarises ongoing developments in the international ICDP Lake Towuti drilling project, Indonesia, and highlights recent findings made within the scope of four DFG projects that are linked in the so-called 'Towuti Bundle', plus an additional DFG project that was

proposed and granted separately but clearly falls within the scope of the bundle. All projects address the environmental history, evolutionary biology, geomicrobiology, and downhole logging at Lake Towuti.

The Towuti Drilling Project (TDP)

Lake Towuti (2.5°S, 121°E) is a 560 km² large, 200 m deep tectonic lake located on central Sulawesi Island, Indonesia (Fig. 1). The geographic position of the lake is located within the center of the Indo-Pacific Warm Pool (IPWP), which provides an important opportunity to reconstruct long-term terrestrial paleoclimate changes in a climatically very important, yet understudied region in the heart of the El Niño-Southern Oscillation (ENSO). Furthermore, Lake Towuti has high rates of floral and faunal endemism and is surrounded by one of the most diverse tropical forests on Earth, making it a hotspot of Southeast Asian biodiversity. Finally, the ultramafic (ophiolitic) bedrocks and lateritic soils surrounding Lake Towuti provide ferruginous metal substrates that feed a diverse, exotic microbial community in the lake and its sediments, potentially analogous to the microbial ecosystems that operated in the Archean Oceans and on Mars. Hence, the Towuti Drilling Project (TDP) has a high potential to provide valuable new information concerning the climatic, biological, and geomicrobiological evolution of this unique system.

Following an extensive site survey that was conducted between 2007 and 2013 (e.g., Russell et al. 2014, Costa et al. 2015, Vogel et al. 2015), ICDP funding for the TDP was approved in 2014. Subsequently, complementary funding was obtained from the US National Science Foundation (NSF), the German Research Foundation (DFG), and the Swiss National Science Foundation (SNSF), and GFZ-Potsdam as well as the University of Cologne thus allowing for a drilling operation to take place on Lake Towuti from

May to July 2015. Drilling was carried out using the ICDP Deep Lakes Drilling System (DLDS) at three sites in the northern lake basin, in water depths between 156 to 200 m (Russell et al. 2016; Fig. 1). Two of three sites were logged by multiple-sensor borehole logging. We recovered a total of 1018 m of core from 11 holes. Recovery averaged 91.7 % and the maximum drilling depth was 175 m below the lake floor, penetrating the entire sedimentary infill of the basin. In addition, we used some time available during set up the drilling technique to collect 84 lake surface samples that reflect the modern sedimentary processes.

Except for the dedicated geomicrobiology core 1A, which was mainly samples already at the drill site, the sediment cores were opened, described, line-scan imaged, scanned by multi-sensor core logger (MSCL, whole core and archive half), and subsampled at the US National Lacustrine Core (LacCore) Facility of the University of Minnesota, USA, during two sampling parties in November 2015 and January 2016. Afterwards, nearly 5,000 subsamples were distributed to members of the science party in Indonesia, the US, Germany, Switzerland, UK, Canada, and Australia for a wide range of analyses. This includes shipment of the archive core halves from sites 1 and 2 to the Universities of Bern, Switzerland, and Cologne, Germany, respectively, for high-resolution X-Ray Fluorescence (XRF) scanning of the chemical composition.

From 8 to 10 January, 2017, an international Towuti Workshop was held in Bandung, Indonesia, in which c. 35 members of the TDP Science Party presented and discussed first results. The initial data suggest that the cores record the evolution of a highly dynamic tectonic and limnological system, with clear indications of orbital-scale climate variability during the mid- to late Pleistocene. The workshop participants further agreed on priorities and responsibilities of the upcoming analyses, and on the publication strategy for the next 1-2 years.

The DFG ‘Towuti Bundle’

The national collaboration within the TDP is organised in the DFG ‘Towuti Bundle’. The bundle provides the umbrella for the research initiatives by scientists from four institutions, which intend to contribute important aspects to the overarching research questions of the TDP in a coordinated manner:

- (1) Environmental history
- (2) Evolutionary biology
- (3) Geomicrobiology
- (4) Downhole logging

Re (1): The project ‘Decadal- to orbital-scale climate variability in the Indo-Pacific Warm Pool during the past ca. 650,000 years’ by Martin Melles (University of Cologne) was funded based on an application submitted in 2013. The project commenced in January 2015, a few months prior to the drilling campaign, to provide the PhD student Ascelina Hasberg with sufficient time to investigate the samples obtained within the scope of her PhD project. This includes both the surface sediment sample sets and the sediment samples from TDP Site 2.

The 84 lake surface sediment samples were taken using a grab sampler (UWITEC Corp., Austria) and are distributed over the entirety of Lake Towuti. They were investigated for physical, chemical, mineralogical and biological proxies, in order to understand the modern

processes of sedimentation operating in the lake under known environmental conditions. Outcomes will support the interpretation of the depositional history in dependence on past climatic and environmental conditions, as reflected in the sediment composition of the ICDP drill cores. Obtained geochemical and mineralogical data reflects fluvial sediment supply to Lake Towuti from five geologically distinct provenances. Further sediment transport within the lake is driven by mass movement events such as turbidites, winnowing by waves, and other turbulent processes rather than distinct lake currents. Biogenic sedimentation of diatoms and sponge spicules is concentrated in micro-niches, characterized by shallow, relatively nutrient-rich, clear waters.

On the 136 m long core composite from TDP site 2 a total of 672 subsamples were investigated for sedimentological (grain size, smear-slide and thin-sections microscopy), geochemical (total organic carbon, nitrogen, sulphur), and mineralogical properties (X-Ray Diffraction, supplemented by visible to near-infrared spectroscopy at Brown University, USA). Radiocarbon dating provides a reliable age model for the uppermost c. 40 m of the core. The core consists of pelagic sediments, which in concert with those from site 1 provide important information concerning the climate history at Lake Towuti. Event layers from mass movement, which are incised into the pelagic sediments, provide complementary information on the hydrological connectivity in the catchment as well as on lake-level fluctuations.

Re (2): The project ‘The lacustrine species flocks in the ancient lakes of Sulawesi (Indonesia): Linking organismic diversification and key environmental events’ by Thomas von Rintelen (Museum für Naturkunde, Berlin) and Fabian Herder (Universität Bonn) also was approved in 2014. Within the scope of their project they investigated Lake Poso and the five lakes of the Malili system containing a highly diverse and endemic fauna with major species flocks of molluscs, crustaceans and fishes. All flocks have arisen in situ in the process of adaptive radiation, with striking adaptations of the feeding apparatus to alternative food sources. Hybridization is widespread, especially in snails and fishes, where it is suspected to promote adaptive divergence. The conspicuous body colouration common to all taxa, may also accelerate diversification processes. There are no shared species between Lake Poso and the Malili lakes, and even within the Malili system, the vast majority is endemic to one or two lakes only. In addition to ecological factors, past and present connectivity between the lake drainages has likely contributed to diversification by both, isolation and hybridization following secondary contact. A comparative molecular clock approach revealed a wide range of estimated ages for the lacustrine species flocks in the entire Malili lakes (< 1 mya to 9 mya) and even for sub-flocks endemic to single lakes. Reconciling these dates with emerging data on the age of the Malili Lakes/Lake Towuti will be a major but crucial challenge for understanding biological evolution in these lakes – and beyond.

Re (3): The project ‘GeoFeLT: Geomicrobiological investigations of ferruginous Lake Towuti’ by Jens Kallmeyer and Dirk Wagner (Deutsches GeoForschungsZentrum, GFZ, Potsdam) is the third

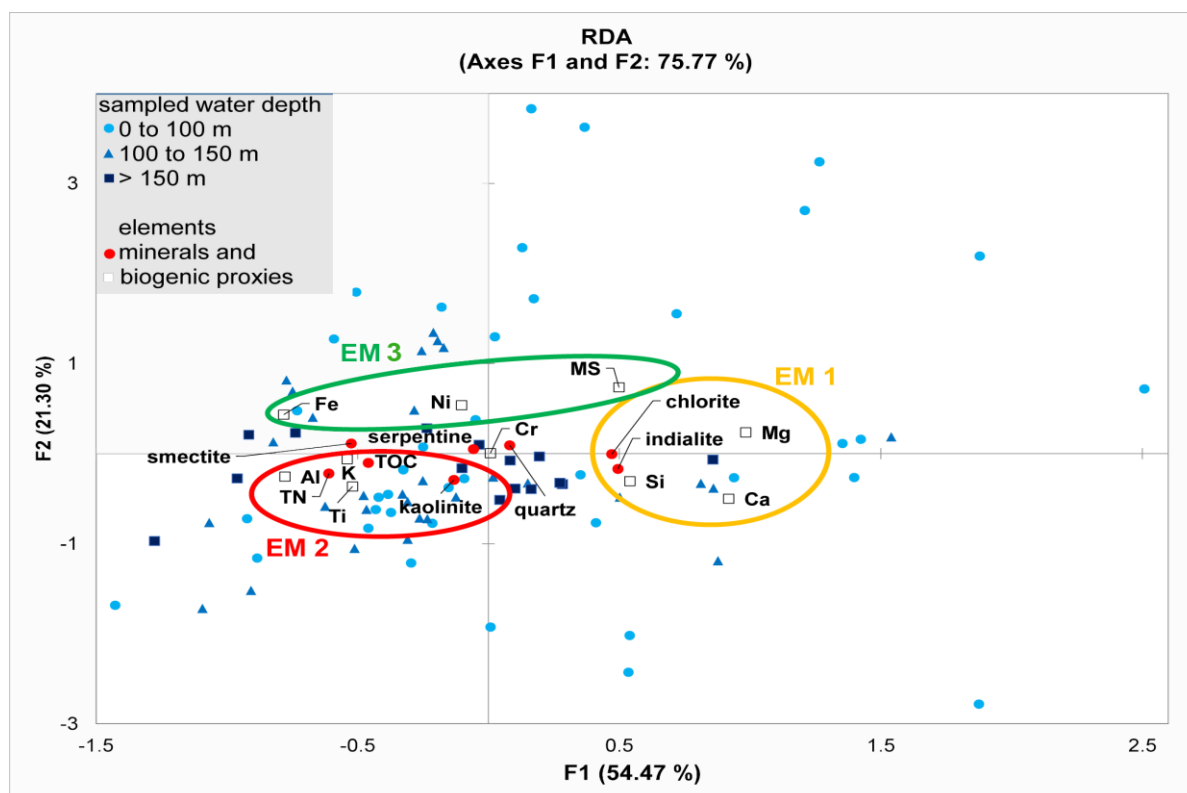


Figure 2: Redundancy analysis (RDA) showing the surface samples in different water depths along with most of the geochemical, physical, and mineralogical data obtained. The endmembers 1 to 3 show individual composition that reflects different sediment

bundle project that was approved in 2014. Also in 2014, Aurèle Vuillemin applied successfully for a separate project (FAMAFed: Formation of authigenic minerals associated with microbial activity in ferruginous sediments) with strong ties to the bundle.

Exploration of subsurface environments relies on drilling, which requires the use of a drilling fluid being an issue for geomicrobiological investigations a sub-project of the GeoFeLT developed a new technique for assessing contamination during drilling operations, and tested it successfully drilling core 1A. To assess infiltration of drilling fluid and therefore non-indigenous materials and microbes from the surface into the drill core, usually a tracer is mixed into the drilling fluid. In past drilling operations a variety of tracers have been used, each has specific strengths and weaknesses. For microspheres the main problem was the high price, which limited their use to spot checks or drilling operations that require only small amounts of drilling fluid. A modified microsphere tracer approach was developed using an aqueous fluorescent pigment dispersion, that costs four orders of magnitude less, allowing for a much more liberal use even in large drilling operations but with the same sensitivity as established techniques. Contamination control of core TDP-1A showed that most (~75%) of the sediment samples from the interior of the core were not contaminated and therefore suitable for geomicrobiological investigations. Drilling fluid infiltration of up to $10\mu\text{l cm}^{-3}$ into the center of the sediment core occurred in the upper 10 meters as well as in some deeper intervals (25 – 35m). These results will be essential for the interpretation of the pore water data and microbiological analyses (Friese in press.).

In addition, the FAMAFED project investigate authigenic minerals, and identified diagenetic siderite,

vivianite, and magnetite, which suggest successive phases of sedimentary microbial iron reduction. Their structures and isotopic compositions are currently being analysed in order to reconstruct past redox fluctuations and sediment diagenesis.

Re (4): The project 'Paleoenvironmental indications and cyclostratigraphic studies of sediments from tropical lake Towuti obtained from downhole logging' by Thomas Wonik (LIAG) most likely got approved in 2016, following rejection of an earlier proposal submitted in 2014. Katja Hesse is working with the downhole logging data collected from the deepest holes of site 1 and 2. A total of three holes including 1B, 1F and 2C were logged with spectral gamma ray, magnetic susceptibility sonic, resistivity, caliper and acoustic imager. The acquired data were treated post logging with respect to processing depth matching. The correlation of logging and core data is being discussed as well as the hole-to-hole correlation. Finally a first approach based on cluster analysis was used to derive the lithology from logging data that reflects the findings from core data.

References:

- Costa KM, Russell JM, Vogel H, Bijaksana S. (2015) Hydrological connectivity and mixing of Lake Towuti, Indonesia in response to paleoclimatic changes over the last 60,000 years. *Palaeogeogr, Palaeoclimatol, Palaeoecol* 417:467-475
- Friese A, Kallmeyer J, Kitte JA, Martinez IM, Bijaksana S, Wagner D, the ICDP Lake Chalco Drilling Science Team, and the ICDP Towuti Drilling Science Team (2017) A simple and inexpensive technique for assessing contamination during drilling operations. *Limnology and Oceanography: Methods* in press. doi: 10.1002/lom3.10159
- Russell JM, Bijaksana S, Vogel H, Melles M, Kallmeyer J, Ariztegui D, Crowe S, Fajar S, Hafidz A, Haffner D, Hasberg A, Ivory S, Kelly C, King J, Kirana K, Morlock M, Noren A, apos, Grady R, Ordenez L, Stevenson J, von Rintelen T, Vuillemin A, Watkinson I, Wattrus N, Wicaksono S, Wonik T, Bauer K, Deino A, Friese A, Henny C, Imran, Marwoto R, Ngkoimani LO, Nomosatryo S, Safiuddin LO, Simister R,

- Tamuntuan G (2016) The Towuti Drilling Project: paleoenvironments, biological evolution, and geomicrobiology of a tropical Pacific lake. *Scientific Drilling* 21:29-40
- Russell JM, Vogel H, Konecky BLK, Bijaksana S, Yongsong H, Melles M, Wattrus N, Costa K, King J (2014) Glacial forcing of central Indonesian hydroclimate since 60,000 y B.P. *PNAS* 111:5100-5105.
- Vogel H, Russell JM, Cahyarini SY, Bijaksana S, Wattrus N, Rethemeyer J, Melles M. (2015) Depositional modes and lake-level variability at Lake Towuti, Indonesia, during the past ~29 kyr BP. *J Paleolimnol* 54:359-377.

IODP

Two million years of Andaman Sea sediment elemental composition: Pleistocene sealevel and South Asian monsoon controls

E.C. HATHORNE¹, D. GEBREGIORGIS¹, L. GIOSAN², K. KERR³, P. ANAND³, D. NÜRNBERG¹, M. FRANK¹

¹ GEOMAR Helmholtz-Zentrum für Ozeanforschung Kiel, Wischhofstr. 1-3, 24148 Kiel, Germany

² Woods Hole Oceanographic Institution, 360 Woods Hole Rd., Woods Hole, MA 02543, USA

³ The Open University, Walton Hall, Milton Keynes, United Kingdom

Although computer models making seasonal forecasting of the monsoon are becoming more complex and increasingly accurate, temporal variations within each season over time scale of few days to weeks are still poorly understood and difficult to model. To help improve models and predictions it is critical to examine monsoon variability beyond the instrumental record. Many records of the East Asian monsoon have been generated from China and the South China Sea while past variability of the South Asian Monsoon is mostly known from records of monsoon wind strength over the Arabian Sea. IODP Expedition 353 "Indian Monsoon Rainfall" obtained high resolution sedimentary records from the core of the South Asian Monsoon precipitation field and here we present a 1 cm (<200 yrs) resolution, continuous record of sediment elemental composition for the last 2 million years.

Sites U1448 and NGHP 17 were drilled at around 1300 m water depth near Little Andaman Island in the Andaman Sea. Previous work on NGHP 17 sediments has demonstrated that the majority of silicate sediments, mostly clays, are derived from the Irrawaddy river basin some 600 km to the north, with no change in source during the last glacial and deglaciation (Ali et al., 2015). Only one hole was cored for NGHP 17 and the Advanced Piston Corer (APC) section was scanned using the XRF core scanner at WHOI. Site U1448 was cored twice through most depths and the spliced composite section was scanned using the XRF core scanner at the University of Kiel. Discrete sample measurements using a hand held XRF device were conducted for parts of the upper most section at The Open University. The discrete sample measurements were calibrated using international standards to quantify elemental concentrations. The age model is mostly based on benthic foraminifera stable oxygen isotope stratigraphy from NGHP 17 and the XRF Ti/Ca ratios in the older parts where large gaps are present between cores at NGHP 17.

The Ti/Ca ratio of both sites is remarkably consistent enabling cross site correlation. The variability and phasing of Ti/Ca is virtually identical to global sea level suggesting

a strong transport control on the amount of terrigenous material delivered to the site. This is most likely the result of a large shallow shelf at the Irrawaddy mouth that was exposed during sea level low stands. Lower Ti during interglacials likely reflects the increased trapping efficiency of sediments in the Gulf of Martaban once the shelf is inundated. Si/Al ratios are much less influenced by sealevel with stronger variability in the obliquity and precession bands. Here we explore using Si/Al ratios as a weathering proxy to reconstruct monsoon strength in the Irrawaddy catchment. We test possible techniques to extract the sealevel influence on the records and investigate the relationship between global climate and monsoon weathering, at an unprecedented resolution for the last 2 million years.

Reference:

- Ali, S., E. C. Hathorne, M. Frank, D. Gebregiorgis, K. Statterger, R. Stumpf, S. Kutterolf, J. E. Johnson, and L. Giosan (2015), South Asian monsoon history over the past 60 kyr recorded by radiogenic isotopes and clay mineral assemblages in the Andaman Sea, *Geochem. Geophys. Geosyst.*, 16, 505–521, doi:10.1002/2014GC005586.

IODP

How stable iron isotope geochemistry can help to find the temperature limit of the deep biosphere (IODP Exp. 370)

S. HENKEL¹

¹ Alfred Wegener Institute Helmholtz Centre for Polar and Marine Sciences, Am Handelshafen 12, 27570 Bremerhaven, Germany

Reduction of Fe(III) is considered one of the most ancient forms of microbial respiration (Vargas et al., 1998). This and the observation that iron reducers can grow under high temperature and pressure conditions (Kashefi & Lovley, 2003) suggests that microbes that use Fe(III) as electron acceptors represent a significant part of the deep biosphere. This presentation will explain how stable iron isotopes can help unravelling drivers of Fe cycling and how this can help reaching the goals of Exp. 370: "T-Limit of the Deep Biosphere off Muroto". Aim of Exp. 370 was to assess how microbial communities at Site C0023 (Nankai Trough), change with depth, by which factors (temperature, nutrients) these changes are controlled, and where microbial life ceases.

Stable iron isotopes ($\delta^{56}\text{Fe}$) are a tool for tracing Fe sources and reaction pathways (e.g. Johnson & Beard, 2007, Wiederhold et al., 2015). Natural iron consists of four stable isotopes: ^{54}Fe (5.85%), ^{56}Fe (91.75%), ^{57}Fe (2.12%), and ^{58}Fe (0.28%). Mass-dependent Fe isotope fractionation in natural systems is small (~5‰), but sufficient to be resolved by Multicollector-ICP-MS analysis (e.g., Weyer & Schwieters, 2003). As microbes preferentially reduce ^{54}Fe , pore water Fe^{2+} is isotopically light. This is also reflected by Fe minerals forming from pore water Fe^{2+} . The residual Fe(III) pool, in contrast, becomes progressively enriched in ^{56}Fe (concept of mass balance). Consequently, Fe minerals in sediments possess different $\delta^{56}\text{Fe}$ signatures due to 1) the different origins of the Fe that is incorporated and 2) the different reactivity of minerals towards microbial reduction and sulfidation (e.g., Raiswell & Canfield, 2012). Pronounced fractionation

($\delta^{56}\text{Fe}_{\text{pore water}} \geq -2.5\text{‰}$) is produced by dissimilatory iron reduction (e.g., Johnson & Beard, 2005). In contrast, reactions of iron with sulfide enrich ^{56}Fe in pore water (e.g., Johnson & Beard, 2005, Severmann et al., 2006) as kinetically controlled FeS precipitation preferentially incorporates ^{54}Fe (Butler et al., 2005). Equilibrium isotope fractionation during sulfide formation shows an opposite trend. However, since in natural systems kinetic processes dominate, a discrimination between microbial reduction and abiotic iron - sulfur interactions based on $\delta^{56}\text{Fe}$ is feasible (Johnson & Beard, 2005).

Recent studies indicate that the classical redox sequence after Froelich et al. (1979) needs to be complemented by Fe reduction in methanic sediments (Beal et al., 2009; Sivan et al., 2011; Egger et al., 2015; Riedinger et al., 2014) and that biogeochemical processes in sediments show a stronger link to mineralogy than to a strict vertical sequence of reactions according to calculated energy yields (Treude et al., 2014). So far, there is only one study in which $\delta^{56}\text{Fe}$ was used to investigate iron reduction in methanic sediments: Based on pore water $\delta^{56}\text{Fe}$, Sivan et al. (2011) suggested the occurrence of Fe(III)-mediated anaerobic oxidation of methane in Lake Kinneret sediments (Israel).

To use $\delta^{56}\text{Fe}$ of solid phases for tracing microbial reduction, Fe fractions that possess different isotopic fingerprints need to be separated. Amorphous Fe(III) oxides are commonly leached with 0.5 M HCl (e.g., Severmann et al. 2006). Unfortunately, this also dissolves carbonates, iron monosulfides, and some silicate minerals (Kostka and Luther, 1994). A recently developed protocol for the removal of extraction solution matrices by repetitive oxidation of samples, thermal destruction of complexes, and Fe precipitation (Henkel et al., 2016) now allows to process leachates of the sequential extraction protocol by Poulton & Canfield (2005) for $\delta^{56}\text{Fe}$ analyses. This new protocol enables phase-specific $\delta^{56}\text{Fe}$ analysis on 1) Fe-carbonates, 2) ferrihydrite and lepidocrocite, 3) goethite and hematite, and 4) magnetite.

A combination of microbiological investigations as performed during and after Exp. 370 with pore water and the solid phase analyses including $\delta^{56}\text{Fe}$ could provide the means for correlation network analyses and for deciphering metabolic pathways, in which Fe oxides potentially play a so far underestimated role.

References:

- Beal, E.J., C.H. House, V.J. Orphan (2009) Manganese- and iron-dependant marine methane oxidation. *Science* 325, 184-187.
- Butler, I.A., C. Archer, D. Vance, A. Oldroyd, D. Rickard (2005) Fe isotope fractionation on FeS formation in ambient aqueous solution. *EPSL* 236, 430-442.
- Egger, M., O. Rasigraf, C.J. Sapart, T. Jilbert, M.S.M. Jetten, T. Röckmann, C. van der Veen, N. Bändä, B. Kartal, K.F. Eitwig, C.P. Slomp (2015) Iron-mediated anaerobic oxidation of methane in brackish coastal sediments. *ES&T* 49, 277-283.
- Froelich, P.N., G.P. Klinkhammer, M.L. Bender, N.A. Luedtke, G.R. Heath, D. Cullen, P. Dauphin, D. Hammond, B. Hartman, V. Maynard (1979) Early oxidation of organic matter in pelagic sediments of the eastern equatorial Atlantic: suboxic diagenesis: *GCA* 43, 1075-1090.
- Henkel, S., S. Kasten, S.W. Poulton, M. Staubwasser (2016) Determination of the stable iron isotopic composition of sequentially leached iron phases in marine sediments. *Chem. Geol.* 421, 93-102.
- Johnson, C.M., B.L. Beard (2005) Biogeochemical cycling of iron isotopes. *Science* 309, 1025-1027.
- Johnson, C.M., B.L. Beard (2007) Fe isotopes: An emerging technique for understanding modern and ancient biogeochemical cycles. *GSA Today* 16(11).
- Kashefi, K., D.R. Lovley (2003) Extending the upper temperature limit for life. *Science* 301, 934-934.
- Kostka, J.E.; G.W. Luther (1994) Partitioning and speciation of solid iron in saltmarsh sediments. *GCA* 58, 1701-1710.
- Poulton, S.W., D.E. Canfield (2005) Development of a sequential extraction procedure for iron: implications for iron partitioning in continentally derived particulates. *Chem. Geol.* 214, 209-221.
- Raiswell, R., D.E. Canfield (2012) The iron biogeochemical cycle past and present. *Geochem. Perspect.* 1(1).
- Riedinger N., M.J. Formolo, T.W. Lyons, S. Henkel, A. Beck, S. Kasten (2014) An inorganic geochemical argument for coupled anaerobic oxidation of methane and iron reduction in marine sediments. *Geobiology* 12, 172-181.
- Severmann, S., C.M. Johnson, B.L. Beard, J. McManus, (2006) The effect of early diagenesis on the Fe isotope compositions of porewaters and authigenic minerals in continental margin sediments. *GCA* 70, 2006-2022.
- Sivan, O., M. Adler, A. Pearson, F. Gelman, I. Bar-Or, S.G. John, W. Eckert (2011) Geochemical evidence for iron-mediated anaerobic oxidation of methane.
- Treude, T., S. Krause, J. Maltby, A.W. Dale, R. Coffin, L.J. Hamdan (2014) Sulfate reduction and methane oxidation activity below the sulfate-methane transition zone in Alaskan Beaufort Sea continental margin sediments: Implications for deep sulfur cycling. *GCA* 144, 217-237.
- Vargas, M., K. Kashefi, E.L. Blunt-Harris, D.R. Lovley (1998) Microbiological evidence for Fe(III) reduction on early Earth. *Nature* 395, 65-67.
- Weyer, S., J.B. Schwieters (2002) High precision Fe isotope measurements with high mass resolution MC-ICPMS. *IJMS* 226, 355-368.
- Wiederhold, J.G. (2015) Metal stable isotope signatures as tracers in environmental geo-chemistry. *ES&T*, 2606-2624.

ICDP

Early Archean Surface Processes and Environments – Drilling the Moodies Group, Barberton Greenstone Belt, South Africa

HEUBECK, C.¹

¹ Institut für Geowissenschaften, Jena University, Burgweg 11, 07749 Jena; christoph.heubeck@uni-jena.de

An international group of scientists coordinated by the author has submitted a workshop proposal for drilling a number of short stratigraphic sections through the oldest well-preserved siliclastic shallow-water strata on Earth, the Moodies Group of the Barberton Greenstone Belt (ca. 3.22 Ga). This unit is probably unique worldwide in allowing the detailed analysis and interpretation of micro-scale and high-resolution Archean analytical data in regional and temporal context. The overall objective of the proposed drilling project is to learn about the nature of Archean surface environments, in particular those related to the origin and evolution of life, and to constrain Archean basin dynamics.

Moodies Group strata reach up to 3.5 km in stratigraphic thickness, are lithologically variable and were probably deposited within a short time frame (ca. 1-14 Ma) in depositional environments ranging from alluvial to prodelta. Their metamorphic grade is lower greenschist facies; ca. 330°C. Widespread early-diagenetic silicification preserved micro- and macrot textures virtually without strain despite tight regional folding. Moodies strata thus represent a very clear window of Archean surface conditions and processes. Their coastal and fluvial-alluvial facies (*sensu lato*) is ideal to investigate and combine information from adjacent terrestrial and marine settings.

Analytical work in Moodies strata, based on detailed field studies, has identified several features related to Archean surface processes and the interactions of the bio-, geo-, atmo- and hydrosphere. These include extensive microbial mats in tidal and fluvial facies, pedogenic concretions and biogenic diagenetic reactions in paleosols, weathering rinds, eolian strata, shallow-water banded-iron formations,

exquisitely preserved microfossils and detailed reconstructions of shoreline processes.

Moodies strata are largely preserved in the cores of large (up to 15 km long, up to 5 km wide) synclines, with steeply dipping, or overturned fold limbs. All proposed drillholes would therefore aim to drill highly inclined (ca. 45°) trajectories in order to penetrate maximum stratigraphic thickness.

The principal objective of the applied-for workshop (October 2017 ?) is to discuss sites where it may be possible to obtain fresh samples of critically important geological units that are unavailable at the surface. Because minerals crystallized and strata were laid down under anoxic and reducing Archean conditions, there are a host of redox-sensitive minerals such as siderite, Fe-rich dolomite, sulfides and carbonaceous matter that are affected by Phanerozoic surface alteration. These are, however, key to making useful estimates of Archean surface processes, including atmospheric and ocean composition, the abundance of oxygen in the atmosphere or in local surface environments (“oxygen oases”), the distribution and nature of early life, preservation pathways, and the response of depositional environments to the surface system. Without knowing the original composition of these Archean sedimentary materials, it becomes almost impossible to estimate which minerals precipitated from seawater, were consumed or produced by microbial mats, settled from suspension, or created by alteration.

South African local, regional, and national bodies are becoming aware of the high scientific value of the Barberton-Makhonjwa Mountains. As of December, 2016, large parts of the Mountainland have been included in a proposal to consider the region as a world heritage site and thus to preserve (and make accessible) its rich geological heritage. The proposal was accepted by the South African government and will be submitted to UNESCO in late January, 2017. A regionally and locally funded pilot project, the Barberton Mountain Geotrail along a scenic paved road, inaugurated in 2013, has become a resounding cultural and economic success and Barberton’s principal tourist attraction. Regional planning documents, including architectural plans for a WHS visitor center (including facilities for scientific research) have been prepared, and the region is conscientiously developing geotourism as a major economic base.

The local WHS organizing committee welcomes the type of scientific research proposed here because the drilling and its results will showcase and enhance the scientific value of the WHS. The drilling operations will be documented and featured by local and regional media, and the results displayed, possibly permanently, in the visitor center or in a stylish display near one of the drill sites. Because the drilling operations in the vicinity and within the proposed WHS will be accessible to the public, well advertised and have major public-outreach branches, the project would probably be perceived as a resoundingly positive international confirmation of a South African conservation effort.

The project is supported by CIMERA, the South African Centre of Excellence for Integrated Mineral and Energy Resource Analysis, which holds experience in scientific drilling, will assist with engineering, permitting operations and outreach, and participate in the science. Research on the core will likely attract sedimentary geologists, stratigraphers, biogeochemists, volcanologists, geochronologists, and paleomagnetists.

ICDP

Hipercorig – A Direct Push Coring Tool for extended reach in unconsolidated on- and offshore formations and its availability

J. HIEROLD¹, ULRICH HARMS¹, ANTJE SCHWALB², VOLKER WITTIG³

¹ Helmholtz-Zentrum Potsdam, Deutsches Geoforschungszentrum

² Technische Universität Braunschweig

³ Internationales Geothermiezentrum, Hochschule Bochum

Kontakt: hierold@gfz-potsdam.de

A new and efficient tool to recover continuous sediment cores from up to 100 m depth in water depths of up to 300 m is currently being tested for use by the scientific community. The device will close the gap between simple, man-powered piston corers that reach sediment depths of merely 30 m and professional heavy-duty drilling rigs reaching depths of 1000 m while requiring professional drill crew and intense logistics.

A crucial issue with piston coring is the loss of power along the drill string due to dampening effects. This can be



Figure 1: (left) Design model of Hipercorig (Graphics: R. Niederreiter); (right) Field test at Mondsee/Austria (Photo: R. Niederreiter)



Figure 2: Drillcore from first coring test in gravel (Photo: R. Niederreiter)

eliminated by deploying a down-the-hole hydraulic hammer directly above the piston. Taking this into account, the novel design of Hipercorig integrates advanced, inexpensive piston coring with a field-proven, hydraulic hammer powered by a high-pressure pump in a modular system. This includes a modular barge, the coring system, service boat and other auxiliary equipment all transportable in three 20-foot standard containers.

Areas of operation include not only lakes, estuaries and shallow marine areas but also land-based utilization in bogs, environmental sites. Barge deployment can be achieved without docks and heavy cranes due to the modular design. Costs of operations depend mainly on mobilization costs, i.e. shipping of the 20-foot containers. A minimum of one or two coring experts plus at least two helpers will be needed to operate the instrument.

The acquisition and test is funded by the German Research Foundation, DFG. The coring system has been verified successfully on Mondsee in November 2016, as displayed in fig. 1. Gravel beds of 50 cm thickness and lake sediments of 10 m have been penetrated very successfully showing the capability of the instrument, see fig. 2. The next milestones include the construction and testing of the platform, the boat and auxiliary parts as well as coring trials with borehole measurements on Lake Constance in spring 2017.

Hipercorig will be available for scientific projects for a maintenance fee that will serve to sustain the tool including repairs and spare parts as well as improvements. The device will be provided to science teams with funded drilling projects. It will also be used for demonstration and training purposes, e.g. GESEP School or other trainings courses.

IODP

Paleobathymetry of the Southern Ocean and its role in paleoclimate variations

K. HOCHMUTH¹, K. GOHL¹

¹ Alfred-Wegener-Institut Helmholtz-Zentrum für Polar- und Meeresforschung, Am Alten Hafen 26, 27568 Bremerhaven

Paleo-ocean circulation models of the Southern Ocean suffer from missing boundary conditions, which accurately describe the geometries of the seafloor surfaces at their geological epoch and their dynamics over time-scales. The accurate parameterisation of these models controls the meaning and implications of regional and global paleoclimate models. Existing paleobathymetric models consider only the top of the oceanic basement based on paleo-age models from magnetic seafloor spreading anomalies or simplify the sedimentary cover by outdated isopach maps. Therefore, the available multichannel seismic reflection (MCS) data need to be re-evaluated and linked to DSDP, ODP or IODP drill sites to be able to calculate paleobathymetric grids for the Cenozoic. This project aims to unify the seismic stratigraphy of the Southern Ocean as a community effort. During the past 10 months, we created a network of cooperation partners, which provide additional data and interpreted horizon data. The ultimate goal of this project is to enable the reconstruction the paleobathymetric grids in approx. 2 m.y. steps throughout the Cenozoic in order to match the time periods used by ice sheet and paleoceanographic modelers. The calculated grids for time-slices such as i.e. the Eocene-Oligocene transition or the Mid-Miocene Climate Optimum will be made available by publications linked with data repository entries such as in PANGAEA.

For reconstructing the geometry of the sedimentary units, we compiled multichannel seismic reflection (MCS) data, acquired by numerous other research institutes as well as our own data. These spatial data are linked to DSDP/ODP/IODP drill sites within the Southern Ocean. The integration between geophysical line data and the sedimentary parameters measured in the cores, such as P-wave velocity, porosity or density, allows the interpolation of these parameters as well as chronological information across the Southern Ocean.

We updated the sediment thickness grid of the Southern Ocean by adding new data and combining published regional grids after a careful revision. The re-evaluation of the MCS data revealed that regional sedimentary thickness was overestimated partly by 200%, but up to 900% within some sedimentary basins of the Southern Ocean (e.g. Weddell Sea). The sedimentary cover of basement highs and ridges was, on the other hand, overestimated. Therefore, our new updated version of the sedimentary thickness of the Southern Ocean draws a more complete and detailed picture of the sediment deposition within the Southern Ocean. The integration of borehole data into MCS sections allows the dating of known unconformities within the seismic sections but also an improved age dating of additional horizons, which are relevant for target time-slices of the primary paleobathymetric grids. A first calculation of the tectonic subsidence via backstripping algorithms shows that the conjugate margins of Antarctica and Australia developed symmetrically since the break-up of Gondwana, whereas the presence of a grounded ice sheet on the Antarctic continental shelves leads to an increase in tectonic subsidence, linked to the massive increase of sediment input by advancing grounded ice.

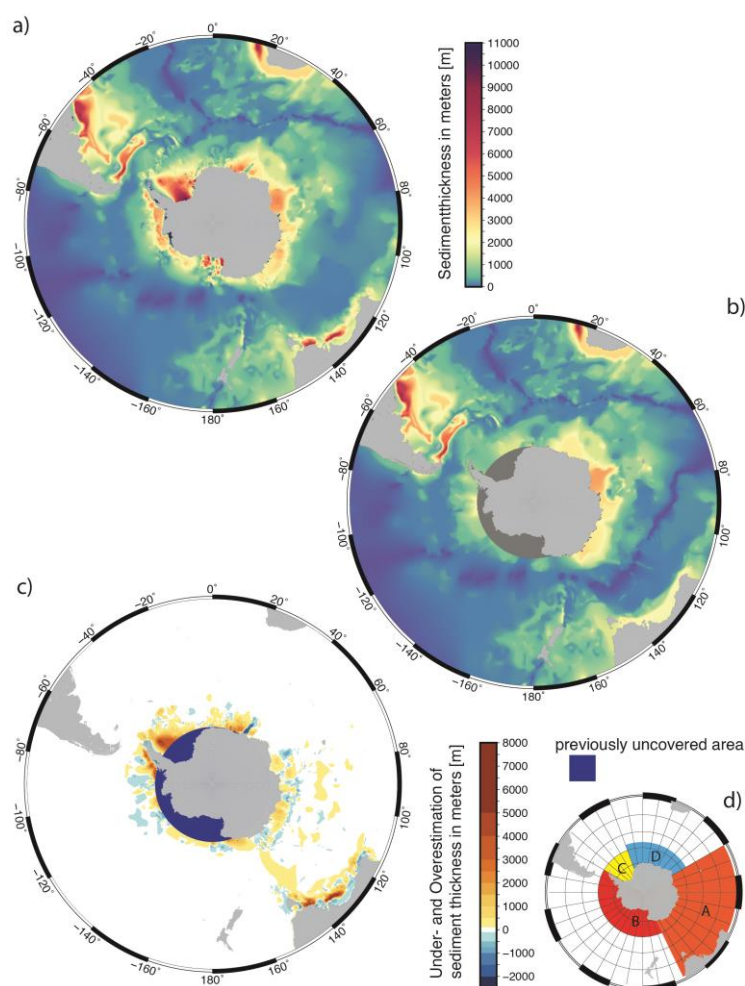


Figure 1: a) updated sediment thickness grid of the Southern Ocean, b) outdated sediment thickness grid by Divins [2003] c) difference between updated grid and Divins [2003] d) overview on combined gridfiles Whittaker et al. 2013 (A), Wobbe et al. 2014 (B), Huang et al. 2014 (C), additional data (D)

DFG

Reconstructing hydrological changes in (sub)tropical South America during Dansgaard-Oeschger cycles: Insights into the low-latitude expressions of high-latitude climate forcing

JULIA HOFFMANN¹, ANDRÉ BAHR¹, JOACHIM SCHÖNFELD²,
OLIVER FRIEDRICH¹, JÖRG PROSS¹

¹ Institute of Earth Sciences, Heidelberg University, Im
Neuenheimer Feld 234–236, 69120 Heidelberg, Germany

² GEOMAR-Helmholtz-Center for Ocean Research, Wischhofstr.
1-3, 24148 Kiel, Germany

The hydrological cycle in tropical South America depends strongly on the intensity of the South American Summer Monsoon (SASM) and the latitudinal migration of the Intertropical Convergence Zone (ITCZ). Particularly in eastern Brazil, precipitation is extremely seasonal, with an eight-months-long dry season between March and October and a relatively rainy season between November and February. The exceptionally long dry season makes this region highly sensitive to changes in the amount of rainfall received. This does not only entail a very high vulnerability

of the region's terrestrial ecosystems to prolonged draughts, but has also severe societal consequences, as for example effects on agriculture. As NE Brazil currently experiences historic droughts, it is essential to constrain the natural climatic variability in that region, thereby assessing the potential impacts of future climate change on continental moisture availability. Considering that the expected rate of global warming is paralleled by only few periods of Earth's history, the presented study aims to assess the hydrological variability in South America by studying analogue periods of extremely rapid climatic shifts during the last glacial (i.e., Dansgaard-Oeschger cycles).

To achieve this goal, we aim to disentangle the impact of insolation and abrupt oceanic forcing on continental moisture availability via reconstructing river run-off in climatically highly sensitive regions of tropical South America during the Dansgaard-Oeschger cycles. Therefore, we rely on marine cores from strategically located positions within the Amazon (ODP Site 942) and Orinoco (M78/1-235-1) outflow areas. Both cores capture the outflow of the respective rivers, reflecting the climate variability of the area due to insolation-driven shifts of the ITCZ. Reconstructions are based on multi-proxy data comprising foraminiferal Ba/Ca, Mg/Ca, $\delta^{18}\text{O}$, XRF- and color-scanning. Focus will be on a critical time interval

with high rates of climate change, more precisely Marine Isotope Stage 3 with Dansgaard-Oeschger cycles 5-7. As both sites are strongly influenced by abrupt climate shifts, novel insights will be gained about the sensitivity of the continental hydrological cycle during climatically highly dynamic periods.

During the LGM, a southward position of the ITCZ affects the Amazon catchment, while the Orinoco catchment remains unaffected. This relationship, however, might be significantly different during phases with high summer insolation, when the ITCZ was situated far in the north. Ba/Ca and Mg/Ca values were measured in high-resolution (1 cm) for Core M78/1-235-1 and in lower resolution (4 cm) for Site 942 for the interval 36-28 kyr, which corresponds to maximum boreal summer insolation. The results indicate a high Ba/Ca variability, partly in excess of the amplitudes observed for the deglaciation previously measured (Hoffmann et al., 2014), indicating that the particular background conditions of high insolation caused a highly variable Orinoco and Amazon discharge. Therefore, the study obtains novel information on insolation-paced monsoonal dynamics and the influence of high-latitude climate forcing mechanisms on low-latitude climate during Marine Isotope Stage 3.

Reference:

Hoffmann, J., Bahr, A., Voigt, S., Schönfeld, J., Nürnberg, D., Rethemeyer, J. (2014), Disentangling abrupt deglacial hydrological changes in northern South America: Insolation versus oceanic forcing, *Geology*, v 42, p. 579-582, doi:10.1130/G35562.1

IODP

Southern Ocean and Weddell Sea bottom water Pb isotope compositions trace ice sheet dynamics and regional circulation patterns today and during the past 140 ka

H.HUANG¹, M. GUTJAH¹, G. KUHN², A. EISENHAEUER¹

¹ GEOMAR Helmholtz Centre for Ocean Research Kiel, Wischhofstrasse 1-3, 24148 Kiel, Germany

² Alfred Wegener Institute, Helmholtz Centre for Polar and Marine Research, Am Alten Hafen 26, 27568 Bremerhaven, Germany

Dissolved lead (Pb) is mainly supplied to the oceans by physical and chemical weathering on the continents. The short residence time of Pb in seawater on the order of only a few decades makes its isotopic compositions an excellent tracer for local continental inputs. Lead was found to be incongruently released during early chemical weathering on the continents (Erel et al., 1994), often generating a more radiogenic runoff signal compared to the bulk rock compositions (Gutjahr et al., 2009; Kurzweil et al., 2010; Crocket et al., 2012; Crocket et al., 2013). In addition, the presence of abundant ice-rafted detrital material (IRD) may also release a highly radiogenic signature in high latitude settings (Kurzweil et al., 2010; Crocket et al., 2012). In the (sub-)Antarctic marine environment, authigenic Pb isotope records from core top sediments offer the possibility of assessing spatial seawater Pb isotopic variability of subglacial Antarctic runoff. Furthermore, palaeo-seawater Pb isotope records extracted from authigenic Fe-Mn oxyhydroxides will likely record periods of enhanced

iceberg calving, freshwater input, and/or associated circulation changes.

Since the leaching method for extracting authigenic Pb from Antarctic proximal bulk sediments has not been studied to date, we firstly evaluated and refined existing reductive leaching methods (Gutjahr et al., 2007; Blaser et al., 2016;) for efficient and reliable chemical extraction of bottom seawater Pb isotope signals from Weddell Sea and Southern Ocean core top sediment samples. We investigated the effects of (i) the MgCl₂ pre-treatment, (ii) the effectiveness of chelates as well as (iii) exposure time of sediments to reducing reagents on the Pb isotopic signals. Chelate EDTA shows stronger complexation ability to Pb than DTPA and can significantly prevent Pb from readsorption back onto sediment surfaces during leaching as described in previous studies (Gutjahr et al., 2007). We also found that leaching without extended (>20 min) shaking, hence only agitating sediments for less than a minute on a vortex mixer to help sediment disperse into leaching solution, can extract quantities of Pb as extracted with via leaching for 20 minutes in a shaker. Using this short-term “vortexing” method, reproducible and in most cases accurate isotopic ratios identical or close to seawater signals can be obtained. Therefore we suggest using the vortexing method with EDTA and without MgCl₂ pre-treatment to recover authigenic Pb from Antarctic ice shelf-proximal bulk sediments.

Employing this new method, we present Pb isotope records from 90 core top sediment samples from the Weddell Sea and the Atlantic sector of Southern Ocean covering ~4000 km of the Weddell Sea Antarctic continental margin. Furthermore, first results are presented from IODP Site 1094 delineating the authigenic Pb isotopic evolution over the past 140 ka tracing Antarctic ice sheet dynamics and Southern Ocean circulation.

References:

- Blaser, P., Lippold, J., Gutjahr, M., Frank, N., Link, J.M., Frank, M., 2016. Extracting foraminiferal seawater Nd isotope signatures from bulk deep sea sediment by chemical leaching. *Chemical Geology* 439, 189-204.
- Crocket, K.C., Foster, G.L., Vance, D., Richards, D.A., Tranter, M., 2013. A Pb isotope tracer of ocean-ice sheet interaction: the record from the NE Atlantic during the Last Glacial/Interglacial cycle. *Quaternary Science Reviews* 82, 133-144.
- Crocket, K.C., Vance, D., Foster, G.L., Richards, D.A., Tranter, M., 2012. Continental weathering fluxes during the last glacial/interglacial cycle: insights from the marine sedimentary Pb isotope record at Orphan Knoll, NW Atlantic. *Quaternary Science Reviews* 38, 89-99.
- Erel, Y., Harlavan, Y., Blum, J.D., 1994. Lead isotope systematics of granitoid weathering. *Geochimica et Cosmochimica Acta* 58, 5299-5306.
- Gutjahr, M., Frank, M., Halliday, A.N., Keigwin, L.D., 2009. Retreat of the Laurentide ice sheet tracked by the isotopic composition of Pb in western North Atlantic seawater during termination 1. *Earth and Planetary Science Letters* 286, 546-555.
- Gutjahr, M., Frank, M., Stirling, C.H., Klemm, V., Flierdt, T., Halliday, A.N., 2007. Reliable extraction of a deepwater trace metal isotope signal from Fe-Mn oxyhydroxide coatings of marine sediments. *Chemical Geology* 242, 351-370.
- Kurzweil, F., Gutjahr, M., Vance, D., Keigwin, L., 2010. Authigenic Pb isotopes from the Laurentian Fan: Changes in chemical weathering and patterns of North American freshwater runoff during the last deglaciation. *Earth and Planetary Science Letters* 299, 458-465.

IODP

Orogenic erosion centres in the crossfire of climate and tectonics: Insights from a single grain provenance analysis of Surveyor Fan sediments, Gulf of Alaska, IODP Expedition 341

B. HUBER, H. BAHLBURG

Institut für Geologie und Paläontologie, Westfälische Wilhelms-Universität Münster, Germany; barbara.huber@uni-muenster.de

The Cenozoic St. Elias orogen at the southern margin of Alaska is an example of pronounced tectonic and climatic interaction in mountain building. Orogeny coincides with major climatic events considered to exert a strong influence on mountain building processes. Absence of onshore sediment traps allows fast transport of the orogenic sediments to the ocean and into the Miocene to Holocene Surveyor Fan depositional system, Gulf of Alaska, making the Surveyor Fan sediments a promising archive for analysing onshore denudation processes. We present results of a single grain geochemical provenance study of amphibole and garnet geochemistry and U-Pb geochronology of zircons together with REE and trace element fingerprinting of samples from two IODP 341 expedition sites on the distal and proximal Surveyor Fan (site U1417 and U1418, respectively). Deciphering the provenance of these sediments allows reconstructing centres of erosion and exhumation in the context of tectonic-climatic interactions.

U/Pb age spectra of zircons from Miocene to Pleistocene sediments show a prominent peak between ca. 50 and 60 Ma. This is typical for the Chugach Metamorphic Complex (CMC). Zircon REE patterns also match published zircon patterns from the CMC. Geochemical compositions of amphibole and garnet point to mostly amphibolite facies metamorphic source rocks together with some igneous and greenschist facies metamorphic lithologies, all contained in the Chugach-Prince William and Yakutat terranes.

A change in sediment composition in the Miocene expressed by a reduction of the mica and detrital coal content and the appearance of amphibole and garnet predates the onset of glaciation and points to a tectonically induced change in erosion centres. This is probably connected to the rise of the Chugach Mountains and the resulting start of alpine glaciation. Garnet and amphibole data suggest the amphibolite facies metamorphic and felsic igneous rocks of the CMC to be the main sediment source. From Miocene to Pliocene, the amphibole signal changes to dominant (felsic) igneous sources and higher input from greenschist facies metamorphic rocks while garnet data imply input from a metabasite belt in the Chugach terrane. This change in provenance, favouring low grade metamorphic areas at the western and southern flanks of the orogen, coincides with the advance of glaciers to the tidewater line, and reflects a relocation of erosion centres through climatic factors.

In the Pleistocene, the dominance of detritus derived from amphibolite facies metamorphic and (felsic) igneous source rocks indicates erosion centres focussed again in the area of the CMC where exhumation is considered to be very high as a result of tectonic factors (e.g. Enkelmann et al., 2010). After the middle Pleistocene transition, increased glaciation did not cause significant changes in the composition of amphiboles and garnets.

This suggests a persistence of the main erosion centres and the Bering and Malaspina glacial systems through time. We conclude that tectonic uplift prevailed over climatically induced glacial erosion and exhumation in the relative balance of the climate-tectonic interactions controlling mountain building in the evolving St. Elias orogen.

Reference:

Enkelmann, E., Zeitler, P.K., Garver, J.I., Pavlis, T.L. and Hooks, B.P., 2010. The thermochronological record of tectonic and surface process interaction at the Yakutat-North American collision zone in southeast Alaska: *American Journal of Science*, v. 310, no. 4, p. 231-260, doi: 10.2475/04.2010.01.

IODP

Clay mineralogy and composition of sediments sampled at Integrated Ocean Drilling Program Site C0002: Implications for the lithification of prism sediments in the Nankai Trough subduction zone

A. HÜPERS¹, L. WARR², G. GRATHOFF², K. WEMMER³ AND A. KOPF¹

¹ MARUM – Center for Marine Environmental Sciences, University of Bremen, Germany

² Institute for Geography and Geology, Ernst-Moritz-Arndt University Greifswald, Germany

³ Geoscience Centre, University of Göttingen, Germany

In subduction zone forearcs elastic strain energy accumulation and subsequent release during an earthquake necessitates the lithification of accreted and subducted sediment. The spatio-temporal characterization of diagenetic processes in accretionary prism sediments may therefore provide important constraints on sediment mechanical behavior. Here, we present data from the active Nankai Trough subduction zone, where accretion of a trench wedge and a clay-rich hemipelagic facies led to a wide accretionary prism. During Integrated Ocean Drilling Program (IODP) Expeditions 338 and 348 the inner accretionary prism was sampled down to 3058 m below seafloor (mbsf) at Site C0002, which is located at the seaward limit of co-seismic slip inferred for the 1944 Tonankai earthquake. We examined the mineralogical and geochemical composition of the clay sized fraction of cuttings and core material recovered from 1000 to 3048 mbsf by X-ray diffraction analysis (XRD), transmission electron microscopy in combination with energy dispersive X-ray spectrometry (TEM-EDX), scanning electron microscopy (SEM) and K-Ar dating to identify clay diagenetic processes.

Qualitative XRD and TEM-EDX analysis show that the overall clay mineralogical composition is very similar downhole consisting of montmorillonite, illite, chlorite and kaolinite. From TEM-EDX analysis we infer that the montmorillonite is characterized by interlayer charges of <0.4. In addition, we identified two subgroups of illite with different morphology and geochemical composition. The first subgroup appears as lath-shaped crystals with cleavage cracks parallel to the long axis and frayed ends, which we interpret as detrital originated. The interlayer charges are between 0.33 and 0.45 suggesting that these particles have undergone chemical leaching. The second illite subgroup comprises idiomorphic lath-shaped crystals of variable size

with interlayer charges between 0.47 and 0.74. The idiomorphic form suggests an authigenic origin, possibly in a K depleted environment. In SEM images we find evidence for neof ormation by the presence of fibrous illite and grain-to-grain bridges. Depth estimates of 2000 to 2600 mbsf for the 60°C isotherm at Site C0002 from published thermal models suggest that authigenic illite could be derived from the temperature-driven smectite-to-illite transition. To test this hypothesis we set up a numerical model in which the smectite-to-illite reaction kinetics are tracked along the sediments' travel path through the accretionary prism. We find that the reaction kinetics are sluggish when the sediment enters Site C0002 with little increase of illite in illite/smectite pointing to another, possibly low temperature origin of the authigenic illite. K-Ar dating revealed ages between ~60 and 9 Ma, which represent the age of the detrital components and the depositional age, respectively, and suggest that the neof ormation could have been formed syndepositional. Further analysis are underway to test this hypothesis.

ICDP

Ba-zonation modelling on sanidine phenocrysts from the Agnano-Monte Spina Eruption (4.7 ka), Campi Flegrei caldera (Napoli, southern Italy)

RAFFAELLA SILVIA IOVINE¹, GERHARD WÖRNER¹, LORENZO FEDELE², FABIO CARMINE MAZZEO², ILENIA ARIENZO³, LUCIA CIVETTA^{4,2}, GIOVANNI ORSI², MASSIMO D'ANTONIO²

¹ Geowissenschaftliches Zentrum, Georg-August-Universität, Göttingen, Germany

² Department of Earth, Environmental and Resources Science, University Federico II of Naples, Italy

³ Istituto Nazionale di Geofisica e Vulcanologia - sezione di Napoli Osservatorio Vesuviano, Naples, Italy

⁴ Istituto Nazionale di Geofisica e Vulcanologia - sezione di Palermo, Italy

We applied Ba diffusion chronometry to sanidine phenocrysts from the trachytic Agnano-Monte Spina eruption (A-MS ~4.7 ka) in order to constrain the time between reactivation and eruption of magma batches in the Campi Flegrei caldera (CFc, Napoli, southern Italy), one of the most hazardous volcanic areas on Earth. The A-MS products display variable ⁸⁷Sr/⁸⁶Sr and trace elements features that suggest magma mixing between two magma end-members. Resulting zonation patterns in phenocryst minerals are an ideal case to study timescales of magma mobilization at the CFc.

Ba zonation profiles of 50 sanidine phenocrysts (Fig. 1) have been determined through combined energy-dispersive and wavelength-dispersive electron microprobe analyses

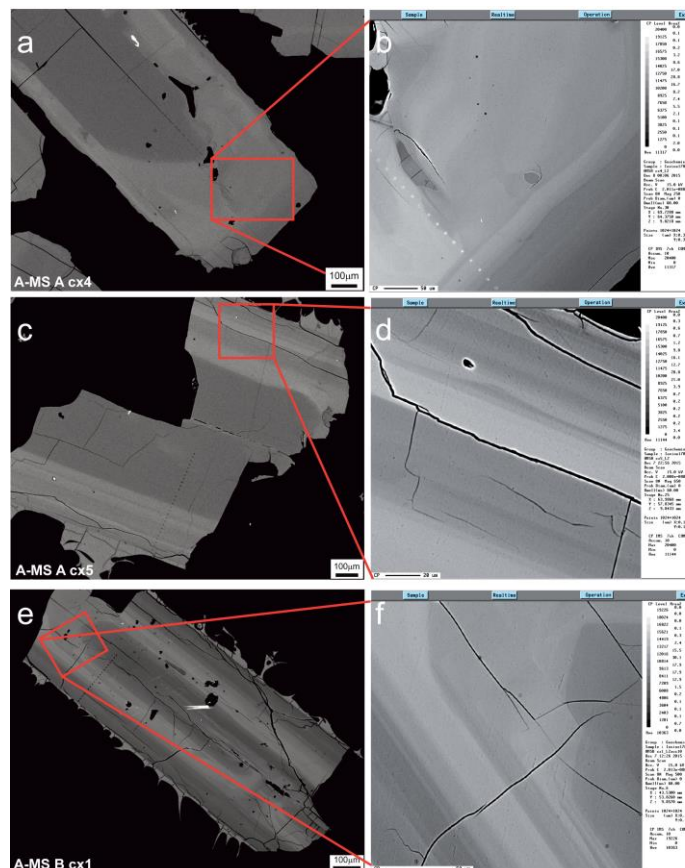


Figure 1: Selected BSE (left) and accumulated detailed (right) images of sanidine phenocrysts from A-MS eruption.

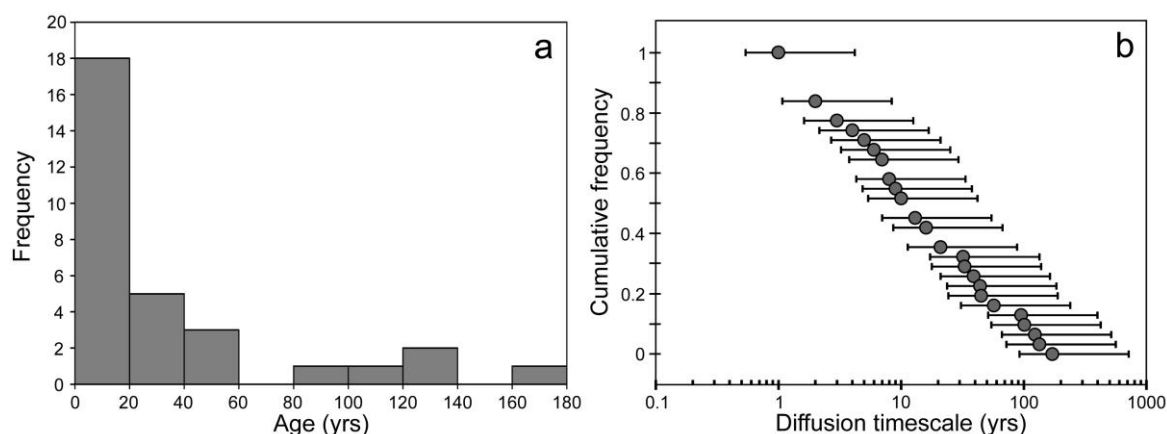


Figure 2: Frequency histogram (a) and cumulative frequency diagram (b) for diffusion times estimated from 24 gray-scale swath profiles at 930 °C.

(EDS-WDS-EMPA). We focused on compositional breaks near the rim of the crystals that represent the last mixing event prior to eruption. Profiles were measured by approaches: (1) quantitative BaO point-measurements at 10 μm spatial resolution, (2) gray-scale swath profiles from accumulated BSE images and (3) Ba X-ray scans. Since Ba dominates the backscattered electron intensities in sanidines, grayscale gradients extracted from the images using ImageJ® are a diffusive tracer proxy. Each profile from the different approaches was interpolated through a non-linear Boltzmann fit curve with Mathematica® software. We always choose the steepest gradients close to the crystal rims. However, any effects from cutting angles or crystal orientation always give longer apparent diffusion times. Our diffusion time estimates are thus minimum values.

Gray-scale swath profiles and X-ray scans modelled for 930°C give short diffusion times of <60 years, only few profiles gave diffusion times up to 180 years (Fig. 2). BaO point analysis profiles, by contrast, give residence times up to thousands of years. The higher spatial resolution of gray-scale and X-ray profiles results in steeper gradients, providing lower values of diffusion time by almost an order of magnitude compared to profiles based on quantitative point measurements. Thus, shorter diffusion times derived from gray-value swath profiles are more reliable.

Based on volcanological and geochronological data a centuries to decades timescale is in agreement with the timing of eruption-triggerung processes preceding the A-MS eruption. In particular we argue that the timescales estimated by diffusion chronology are similar to the inferred time intervals occurred between eruption, and thus may represent the reactivation time of a magma that was residing in a shallow reservoir, after the influx of a new magma batch that triggered the eruption. Such short timescales thus represent the final reactivation/remobilization of a magma from shallow depth in the A-MS plumbing system, after longer residence as testified by the complex core-rim interior zoning of sanidine phenocrysts and our previously obtained U-Th isotope dating on phenocryst minerals (Arienzo et al., 2011).

Reference:

Arienzo I, Heumann A, Wörner G, Civetta L, Orsi G (2011) Time scales of magma crystallization and storage prior to the Campanian Ignimbrite eruption (Campi Flegrei, Italy). *Earth Planet Sci Lett* 306:217-228

IODP

Sea-level and deep-sea temperature evolution during the Plio-Pleistocene intensification of Northern Hemisphere Glaciation: New insights from the Eastern Equatorial Pacific and the North Atlantic

KIM. A. JAKOB¹, PAUL A. WILSON², JÖRG PROSS¹, JENS FIEBIG³,
OLIVER FRIEDRICH¹

¹ Institute of Earth Sciences, Heidelberg University, Im Neuenheimer Feld 234–236, 69120 Heidelberg, Germany

² National Oceanography Centre Southampton, University of Southampton, European Way, Southampton SO14 3ZH, UK

³ Institute of Geosciences, Goethe-University Frankfurt, Altenhöferallee 1, 60438 Frankfurt, Germany

In lights of the increasing manifestation of anthropogenic forcing on Earth's climate it becomes essentially important to increase our knowledge about the potential response of ice volume/sea level to global warming. In this context, paleoclimatic research is a powerful tool for understanding processes and mechanisms on various timescales that allows to model and predict future climate change. While several sea-level records on high resolution exist for the past 500 kyr [e.g., *Siddall et al.*, 2003; *Rohling et al.*, 2009], our knowledge on high-resolution sea-level and deep-sea temperature fluctuations during older periods is limited. Continuous, highly resolved records of sea-level variation under warmer-than-modern climatic background conditions are, however, essential to understand past climate evolution and to reliably predict future climate change. For the late Pliocene/early Pleistocene intensification of Northern Hemisphere Glaciation (iNHG) – a critical time interval encompassing the transition from a warmer Pliocene climate without large ice sheets on the Northern Hemisphere to a progressively cooler Pleistocene climate dominated by a stronger response of the climate-cryosphere system to orbital forcing [*Lisiecki and Raymo*, 2005] – sea-level proxy records are on low resolution and cover a wide range. Highest sea-level lowstand estimates (in m below present) of -110 m to -80 m for prominent iNHG glacials Marine Isotope Stages (MIS) 100–96 derive from continental margin sequence stratigraphy [*Naish*, 1997]. Sea-level lowstand estimates calculated from combined benthic Mg/Ca and $\delta^{18}\text{O}$ [*Dwyer et al.*, 1995; *Sosdian and Rosenthal*, 2009] produce values of -55 m to -75 m for MIS

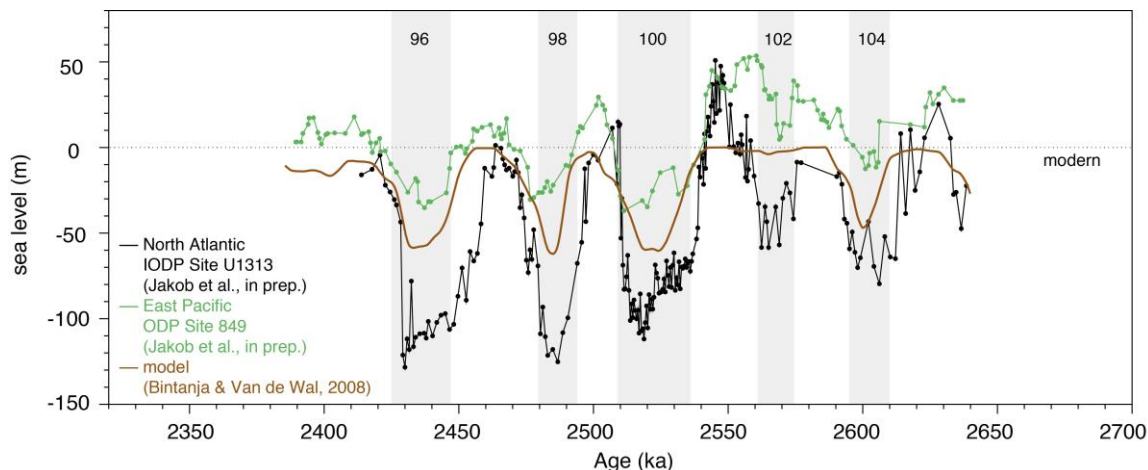


Figure 1: Comparison between sea-level records from east Pacific ODP Site 849 (green; this study), North Atlantic IODP Site U1313 (black; this study) and model simulations (brown) [Bintanja and Van de Wal, 2008].

100, -65 m to -70 m for MIS 98, and -60 m to -90 m for MIS 96. Model simulations estimate lowstands in the range of -65 m to -75 m for glacials MIS 100–96 [Bintanja and Van de Wal, 2008]. A much lower sea-level has been estimated based on planktic $\delta^{18}\text{O}$ from the Mediterranean Sea, documenting -15 m to +10 m for MIS 100–96 [Rohling *et al.*, 2014].

To reveal a better understanding of sea-level/ice-volume and deep-sea temperature evolution across prominent glacial-interglacial (G-IG) cycles of iNHG, we present new high-resolution (~430–1630 yr) benthic foraminiferal $\delta^{18}\text{O}$ and Mg/Ca records from Ocean Drilling Program Site 849 in the Eastern Equatorial Pacific (EEP) and Integrated Ocean Drilling Program Site U1313 in the North Atlantic for MIS G1–95 (~2.65–2.4 Ma). The most salient features of our study are as follows:

1. Deep-sea temperatures in the EEP were on average ~4°C colder than in the North Atlantic across the interval of study. Large G-IG amplitudes in the North Atlantic (~3.5°C) compared to rather small-scale G-IG fluctuations in the EEP (<2°C) dictate a diminished Pacific-to-Atlantic bottom-water temperature (BWT) gradient during glacials relative to interglacials. This indicates changing deep-water masses that alternately influence the sea floor on G-IG timescales in the North Atlantic (northern versus southern sourced waters), while the deep east Pacific was only bathed by southern sourced waters.

2. Our new sea-level estimates from the EEP and the North Atlantic indicate the same overall trend and encircle the global sea-level model of Bintanja and Van de Wal [2008] during the interval of study (Fig. 1). Sea-level lowstand estimates (in m below present) from Site 849 are more modest (~25–35 m) than those from Site U1313 (~110–130 m) for G-IG cycles MIS 100–96, while sea-level highstand estimates are consistent. Both sites indicate that iNHG is associated with a drop in sea-level, thus an increase in global ice volume, during both glacial and interglacial intervals. Because a similar pattern is not documented in our BWT records, this suggests that deep-ocean cooling might not have played an important role for iNHG.

3. The G-IG variability in sea level from MIS 100–96 determined for the North Atlantic resembles the

asymmetric “sawtooth” pattern of late Pleistocene G-IG cycles [Bintanja and Van de Wal, 2008; Sosdian and Rosenthal, 2009], with a gradual sea-level drop into glacial periods followed by an abrupt sea-level rise (1.1–1.3 m/century) during the termination. Moreover, our high-resolution (~430 yr) sea-level record for MIS 100 at Site U1313 demonstrates that the final ~10 kyr of this glacial are characterized by an additional drop in sea level before it rose rapidly during the following termination. Hence, the overall internal structure of MIS 100 appears to be strikingly similar to late Pleistocene glacials.

4. Our new sea-level records from the EEP and the North Atlantic also reveal important information about the contribution of major Northern and Southern Hemisphere ice sheets to global sea-level evolution. A sea-level rise of ~50–100 m into interglacials as evidenced from our records for MIS 100–96 implies complete melting of Greenland and the West Antarctic Ice Sheets and at least a partial retreat of the “stable” East Antarctic Ice Sheet, hinting at its future vulnerability under a warmer-than-present climate, thereby supporting previously published proxy records [Cook *et al.*, 2013] and model data [DeConto and Pollard, 2016].

References:

- Bintanja, R. & R. Van de Wal (2008), North American ice-sheet dynamics and the onset of 100,000-year glacial cycles, *Nature*, 454(7206), 869–872.
- Cook, C.P., *et al.* (2013), Dynamic behaviour of the East Antarctic ice sheet during Pliocene warmth, *Nature Geoscience*, 6(9), 765–769.
- DeConto, R.M. & D. Pollard (2016), Contribution of Antarctica to past and future sea-level rise, *Nature*, 531(7596), 591–597.
- Dwyer, G.S., *et al.* (1995), North Atlantic deepwater temperature change during late Pliocene and late Quaternary climatic cycles, *Science*, 270, 1347–1351.
- Lisiecki, L.E. & M.E. Raymo (2005), A Pliocene-Pleistocene stack of 57 globally distributed benthic $\delta^{18}\text{O}$ records, *Paleoceanography*, 20, PA1003, doi:10.1029/2004PA001071.
- Naish, T. (1997), Constraints on the amplitude of late Pliocene eustatic sea-level fluctuations: new evidence from the New Zealand shallow-marine sediment record, *Geology*, 25(12), 1139–1142.
- Rohling, E.J., *et al.* (2009), Antarctic temperature and global sea level closely coupled over the past five glacial cycles, *Nature Geoscience*, 2(7), 500–504.
- Rohling, E.J., *et al.* (2014), Sea-level and deep-sea-temperature variability over the past 5.3 million years, *Nature*, 508(7497), 477–482.
- Siddall, M., *et al.* (2003), Sea-level fluctuations during the last glacial cycle, *Nature*, 423, 853–858.
- Sosdian, S. & Y. Rosenthal (2009), Deep-sea temperature and ice volume changes across the Pliocene-Pleistocene climate transitions, *Science*, 325, 306–310.

IODP

Variation in the flow path of the Kuroshio Current and its impact on NW Pacific paleoclimate evolution

A.-S. JONAS¹, L. SCHWARK^{1,2}, T. BAUERSACHS¹¹ Christian-Albrechts-Universität, Institut für Geowissenschaften, Abteilung für Organische Geochemie, Ludewig-Meyn-Str. 10, 24118 Kiel² WA-OIGC, Department of Chemistry, Curtin University, 6845 Bentley Campus, Perth, Australia

The subtropical warm and saline Kuroshio Current (KC) is one of the two major western boundary currents of the NW Pacific Ocean and plays a significant role in the meridional transport of heat and moisture from the Western Pacific Warm Pool (WPWP) to northern mid-latitudes. At present, the KC and the subpolar cold and less saline Oyashio Current (OC) converge at ~36°N off central Japan where they are deflected eastward and form the KC/OC interfrontal zone. This interfrontal zone shows a mixed signal in terms of temperature and salinity and is place of intense mesoscale eddy formation (Shimizu et al., 2001) and upwelling of NPIW (North Pacific Intermediate Water) (Yasuda, 2003). Latitudinal fluctuations and variations in the relative strengths of the two western boundary currents and their interfrontal zone exert an important control on the climate evolution of the NW Pacific and adjacent continental areas. Hence, the investigation of past changes in the KC and OC is crucial for understanding the climate evolution of the NW Pacific and East Asia. Although the most recent history (~40 kyr), including millennial changes and latitudinal movements of the two currents, is well documented (e.g. Chinzei et al., 1987; Harada et al., 2004; Oba et al., 2006; Yasudomi et al., 2014), information on the long-term variation of the KC and OC and their impact on regional and global climate over geological time scales is still sparse.

In the past, the KC and OC and their interfrontal mixing zone were displaced north- or southward in response to global climate change (e.g. Chinzei et al., 1987;

Harada et al., 2004; Oba et al., 2006; Yasudomi et al., 2014), thereby exerting a significant control on the regional climate evolution of the NW Pacific and the East Asian region. Some paleoceanographic studies demonstrated that the axis of the KC was displaced southward during the last glacial period (e.g. Chinzei et al., 1987; Gallagher et al., 2015, and references therein), resulting in the southward migration of colder OC waters. Changes in the current velocity of the KC and its volume transport of warm water masses from the WPWP to the north lead to short-term fluctuations in the meander path of the KC southeast of Japan (Kawabe, 1995; Sawada and Handa, 1998). The short meander following strictly the coastline of Japan has been shown to form when both volume transport and current velocity of the KC are high (Yasuda et al., 1985), whereas a reduced velocity and volume transport foster the formation of its large meander. During the presence of the large meander, warm KC waters are found further offshore, allowing for the establishment of a cold surface water mass off central Japan (Sawada and Handa, 1998), which results in a drop in sea surface temperature (SST) in this area. Our study aims at (i) reconstructing long-term trends in water temperature evolution from late Miocene times to present related to global climate change and associated changes in meridional heat transport from the WPWP to northern mid-latitudes via the KC, (ii) studying changes in the meander path of the KC SE off Japan and (iii) determining the impact of variations in both ocean currents on the climate evolution of the NW Pacific and East Asia.

For this, we analyzed deep-sea sediments obtained from IODP Sites C0011 in the Nankai Trough area and U1437 in the Izu Bonin rear arc. The former was drilled during IODP Expedition 333 (“NanTroSEIZE Stage 2: Subduction inputs and heat flow”) and is located in a water depth of 4050 m beneath the short meander path of the KC. Site U1437 was obtained during IODP Expedition 350 (“Izu-Bonin-Mariana rear-arc: The missing half of the subduction factory”) and lies beneath the Kuroshio large meander at 2117 mbsl. Based on shipboard and postcruise dating via bio- and magnetostratigraphy, both sites cover a time interval from late Miocene times to present. 260 samples from Site C0011 spanning the last 8.2 Myr and 115 samples from Site U1437 covering the last 3 Myr so far have been analyzed for their bulk geochemical

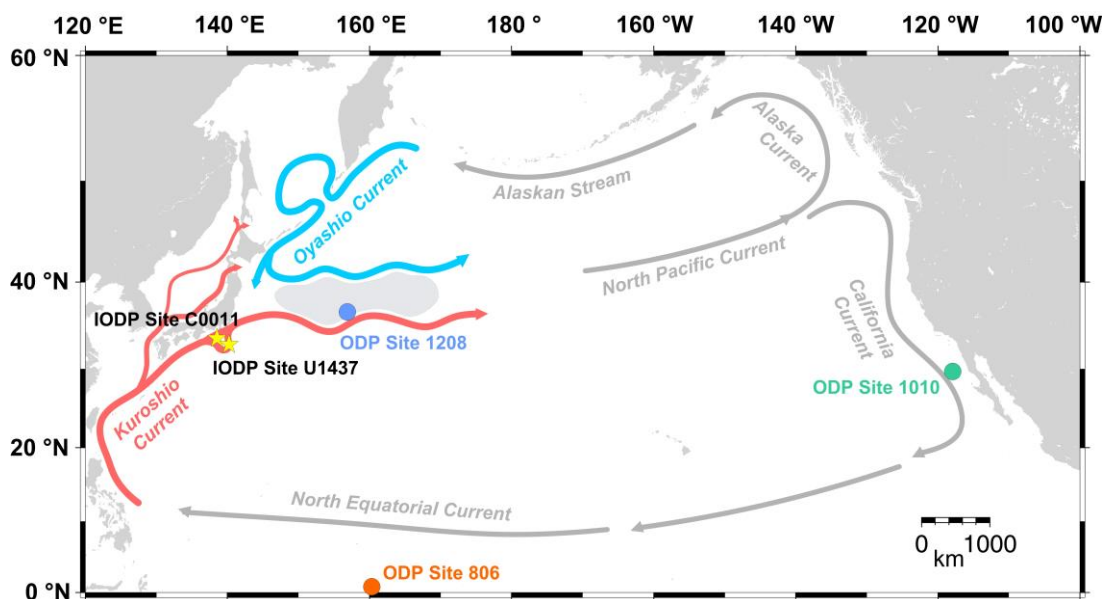


Figure 1: Map of the North Pacific showing the flow paths of the two major western boundary currents, the Kuroshio Current (red) and Oyashio Current (blue) and their interfrontal zone (shaded area) and other major currents of the NW Pacific. The yellow stars mark IODP Sites C0011 and U1437, which were drilled during IODP Expeditions 333 and 350. Core locations of other ODP Sites cited in Fig. 2 are marked by dots.

inventory and biomarker distributions, including the lipid paleothermometers U^{K}_{37} , LDI and TEX^{H}_{86} . The U^{K}_{37} (unsaturated ketone index) is based on the sedimentary distribution of alkenones, which are synthesized by haptophyte algae dwelling in the photic zone (Marlowe et al., 1984). The long chain diols used for the LDI (long chain diol index) calculation are found in eustigmatophyte algae (Volkman et al., 1992), which, like haptophyte algae, live in the photic zone. Therefore, the two lipid paleothermometers are considered to reflect SSTs. In contrast, the TEX^{H}_{86} , which is based on glycerol dialkyl glycerol tetraethers of marine Thaumarchaeota (Schouten et al., 2002), has previously been suggested to reflect subsurface temperatures corresponding to the depth of the thermocline (e.g., Lopes dos Santos et al., 2010; Yamamoto et al., 2012; Jonas et al., *in review*) instead of SST. Offsets between the proxies, among other factors, may result from different habitat depths and production seasons. Site U1437 water temperature records are currently being extended to late Miocene times and the temporal resolution will be increased for the last 1 Myr.

The late Miocene to present water temperature evolution at Site C0011 showed an unidirectional cooling trend with temperatures decreasing by up to 4 °C in U^{K}_{37} - and LDI-SSTs as well as TEX^{H}_{86} -based water temperatures (from a Miocene to mid-Pliocene average of 27 °C in U^{K}_{37} , 23.8 °C in LDI and 25 °C in TEX^{H}_{86} to a Pleistocene average of 23.5 °C in U^{K}_{37} , 23 °C in LDI and 21.7 °C in TEX^{H}_{86} reconstructions). While temperatures were on a

relatively stable level during the late Miocene up to the mid-Pliocene based on all three lipid paleothermometers, they declined significantly after 3.5 Myr and reached minimum values during the most recent 150 kyr, which is likely associated with the onset of northern hemisphere glaciation and the establishment of northern polar ice caps during the late Pliocene. This observation is also reflected in the global $\delta^{18}O$ -stack of benthic foraminifera (Lisiecki and Raymo, 2005) and is similar to those made at sites from the WPWP (Zhang et al., 2014), the interfrontal zone and the subtropical NE Pacific (LaRiviere et al., 2012) (Fig. 2). High temperatures during the late Miocene were attributed to a deep tropical thermocline associated with an open Central American Seaway and expanded tropical warm surface water masses (LaRiviere et al., 2012), resulting in lower meridional temperature gradients during the Miocene than at present. Indeed, late Miocene meridional SST gradients between Site C0011 and WPWP Site 806 (Zhang et al., 2014) were lower (~2 °C) than at present (~4 °C).

The increased decline both in U^{K}_{37} -SSTs and TEX^{H}_{86} -based water temperatures starting in the mid-Pliocene was also observed at Site U1437, where temperatures declined by up to 3 °C since ~3 Myr. Overall, U^{K}_{37} - and TEX^{H}_{86} -based temperatures at Site U1437 exceed those at Site C0011, except for some intervals during the past 200 kyr. This identifies the KC large meander as the dominant meander path configuration throughout the last 3 Myr. At both sites, U^{K}_{37} -SSTs are higher than TEX^{H}_{86} -temperatures

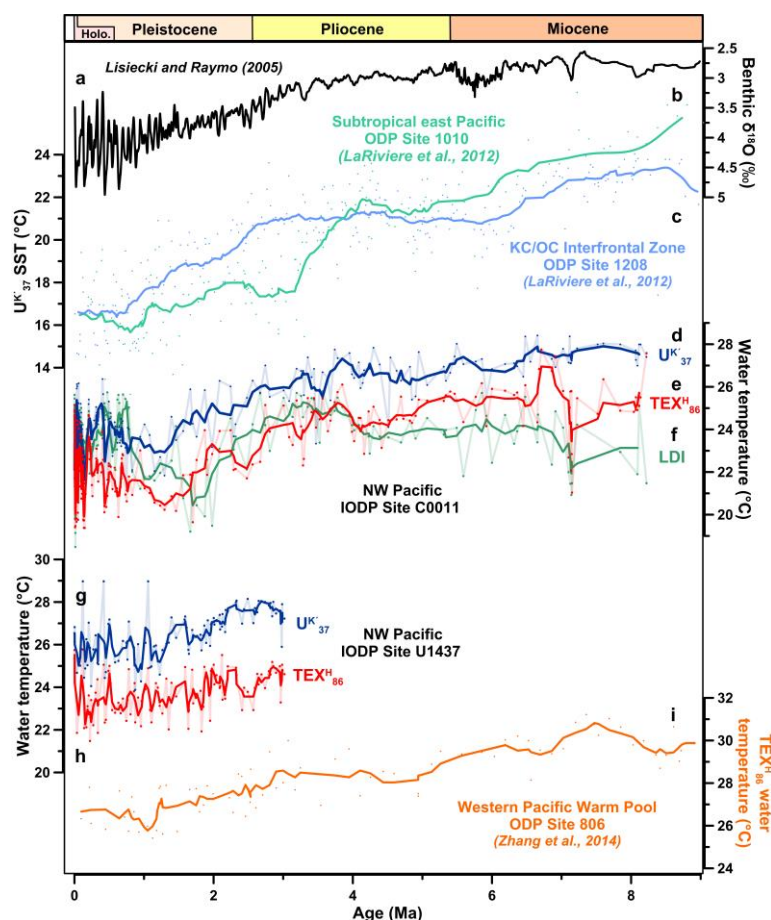


Figure 1: a) Global reference curve of stacked benthic foraminifera $\delta^{18}O$ (Lisiecki and Raymo, 2005) in comparison with Site C0011 sea surface (d: U^{K}_{37} , 5-point average; f: LDI, 5-point average) and thermocline (e: TEX^{H}_{86} , 5-point average) temperature records and Site U1437 sea surface (g: U^{K}_{37}) and thermocline (h: TEX^{H}_{86}) temperature records and water temperature records from b) the KC/OC interfrontal zone (ODP Site 1208 on Shatsky Rise, in 25-point average) and the subtropical east Pacific (c: ODP Site 1010, 15-point average) (both by LaRiviere et al., 2012) and i) the WPWP (ODP Site 806, 5-point average; Zhang et al., 2014).

over the whole record and temperature offsets between the two proxies average 1.8 °C at Site C0011 and 2.7 °C at Site U1437 over the last 3 Myr. Larger offsets at Site U1437 suggest a deeper thermocline, likely associated with the presence of the KC large meander, which brings warm surface water masses to the study site, whereas a colder surface water mass established over Site C0011. Site U1437 thermocline and SST records show a very similar pattern and nicely reflect the glacial-interglacial see-saw pattern of the mid- to late Pleistocene within the last 1 Ma.

Detailed studies of the water temperature evolution at Site C0011 over the past ~145 kyr based on the lipid paleothermometers UK³⁷, LDI and TEX^H₈₆ (Jonas et al., *in review*) showed that during cold phases (marine isotope (MIS) stages 2, 4 and 6) offsets between the various lipid paleothermometers were reduced. This was attributed to a more similar habitat depth and production season of the source organisms associated with a reduced warm surface water mass transport of the KC and a corresponding shoaling of the thermocline. During warm MIS 1, 3 and 5, on the contrary, larger offsets between the lipid paleothermometers indicate a stronger KC and a concurrent deepening of the thermocline. In addition, overall higher Holocene than Eemian water temperatures at Site C0011 indicate a stronger KC and the formation of its short meander south of Japan, whereas a less strong KC during the Eemian likely favored the formation of the large meander.

In addition to water temperature reconstructions, we investigated the relative distribution of long-chain *n*-alkyl lipids to obtain information on changes of the continental vegetation pattern on the East Asian continent associated with changes in paleoclimate. Schwark et al. (2002) demonstrated that deciduous pioneer vegetation has a predominance in *n*C₂₇-alkanes, while the *n*C₃₁ homologue occurs in grasses and herbs as well as in cold-climate preferring evergreen conifer species. The relative distribution of long chain *n*-alkanes at Site C0011 showed an increase in *n*C₃₁-alkane abundances on the expense of *n*C₂₇ during phases of low water temperatures, which was interpreted as an expansion of grasses and conifer species of colder climates on the continental areas surrounding the NW Pacific. These cold phases were also reflected in increased abundances of nonacosane-10-ol, a specific biomarker for the cold-temperature preferring conifer species *Picea* (Jetter et al., 2006) that is common in boreal forests and taiga vegetation. This was attributed to be a result of a southward migration of the OC and the atmospheric polar front. Hence, our SST records of the from Sites C0011 and U1437 area, in combination with terrestrial biomarker records from Site C0011 show that variations in the migration patterns and relative strengths of the KC and OC were closely coupled to the paleoclimate evolution of the East Asian continent.

References:

- Chinzei, K. et al. (1987). Postglacial environmental change of the Pacific Ocean off the coasts of central Japan. *Mar. Micropaleontol.* 11, 273-291.
- Gallagher, S. J. et al. (2015). The Pliocene to recent history of the Kuroshio and Tsushima Currents: a multi-proxy approach. *Prog. Earth Planet. Sci.* 2:17.
- Jonas, A.-S., L. Schwark, and T. Bauersachs. Late Quaternary water temperature variations of the Northwest Pacific based on the lipid paleothermometers TEX^H₈₆, UK³⁷ and LDI. *In review*, Deep-Sea Research Part I.
- Harada, N., N. Ahagin, M. Uchida, and M. Murayama (2004). Northward and southward migrations of frontal zones during the past 40 kyr in the Kuroshio-Oyashio transition area. *Geochem. Geophys. Geosyst.* 5, Q09004.
- Jetter, R., L. Kunst, and A. L. Samuels (2006). *Biology of the plant cuticle*. Annual plant reviews 23. Blackwell Publishing, Oxford.

- Kawabe, M. (1995). Variations of Current Path, Velocity, and Volume Transport of the Kuroshio in Relation with the Large Meander. *Journal of Physical Oceanography* 25, 3103-3117.
- LaRiviere, J. P. et al. (2012). Late Miocene decoupling of oceanic warmth and atmospheric carbon dioxide forcing. *Nature* 486, 97-100.
- Lisiecki, L. E., and M. E. A. Raymo (2005). Pliocene-Pleistocene stack of 57 globally distributed benthic delta δ¹⁸O records. *Paleoceanography* 20, PA1003.
- Lopes dos Santos, R. A. et al. (2010). Glacial-interglacial variability in Atlantic meridional overturning circulation and thermocline adjustments in the tropical North Atlantic. *Earth Planet. Sci. Lett.* 300, 407-414.
- Marlowe, I. T., S. C. Brassell, G. Eglinton, and J. C. Green J. C. (1984). Long-chain unsaturated ketones and esters in living algae and marine sediments. *Org. Geochem.* 6, 135-141.
- Sawada, K., and N. Handa (1998). Variability of the path of the Kuroshio ocean current over the past 25,000 years. *Nature* 392, 592-595.
- Oba, T. et al. (2006). Paleooceanographic change off central Japan since the last 144,000 years based on high-resolution oxygen and carbon isotope records. *Global Planet. Change* 53, 5-20.
- Schouten, S., E. C. Hopmans, E. Schefuß, and J. S. Sinninghe Damsté (2002). Distributional variations in marine crenarchaeotal membrane lipids: A new tool for reconstructing ancient sea water temperatures?. *Earth Planet. Sci. Lett.* 204, 265-274.
- Schwark, L., K. Zink, and J. Lechterbeck (2002). Reconstruction of postglacial to early Holocene vegetation history in terrestrial Central Europe via cuticular lipid biomarkers and pollen records from lake sediments. *Geology* 30, 463-466.
- Shimizu, Y., I. Yasuda, and S.-I. Ito (2001). Distribution and circulation of the coastal Oyashio-Intrusion. *J. Phys. Oceanogr.* 31, 1561-1578.
- Yamamoto, M. et al., (2012). Glycerol dialkyl glycerol tetraethers and TEX₈₆ index in sinking particles in the western North Pacific. *Org. Geochem.* 53, 52-62.
- Volkman, J. K., S. M. Barrett, G. A. Dunstan, and S. W. Jeffrey (1992). C₃₀-C₃₂ alkyl diols and unsaturated alcohols in microalgae of the class Eustigmatophyceae. *Org. Geochem.* 18, 131-138.
- Yasuda, I., J. H. Yoon, and N. Sugihara (1985). Dynamics of the Kuroshio large meander-Barotropic model. *J. Oceanogr. Soc. Jpn.* 41, 259-273.
- Yasuda, I. (2003). Hydrographic Structure and Variability in the Kuroshio-Oyashio Transition Area. *J. Oceanogr.* 59, 389-402.
- Yasudomi Y., I. Motoyama, T. Oba, T., and R. Anma (2014). Environmental fluctuations in the northwestern Pacific Ocean during the last interglacial period: evidence from radiolarian assemblages. *Mar. Micropaleontol.* 108, 1-12.
- Zhang, Y. G., M. Pagani, and Z. Liu (2014). A 12-Million-Year Temperature History of the Tropical Pacific Ocean. *Science* 344, 84-87.

IODP

Plio/Pleistocene SW Indian Ocean paleoceanography and stratigraphy using magnetic data (PLIOmag)

J. JUST¹ AND THE EXPEDITION 361 SCIENTISTS

¹ Institute of Geology and Mineralogy and Collaborative Research Center 806, *Our Way to Europe*, University of Cologne, Germany

The Mozambique Strait and western region of the Indian Ocean are key areas for global thermohaline circulation, because they are the main sectors where water from the North Atlantic and Southern Ocean are dispersed into the Indian Ocean. At different locations deep water mixes with overlying water masses and contribute to the warm surface water return flow into the Atlantic Ocean via the Agulhas leakage. In addition to the paleoceanographic significance, sea-surface temperatures (SST) in the western Indian Ocean sector have a strong effect on South African precipitation. This present day mode on South African climate influence has approximately been existing since about 1.5 Ma, while additional processes had affected the climatic development in South Africa during the Pliocene. Tectonic processes, i.e., modifications of ocean gateways in the Atlantic and Indian Ocean as well as the uplift in the East African rift, had modulated sea-surface conditions in the SW Indian Ocean and monsoonal flow into East Africa, respectively.

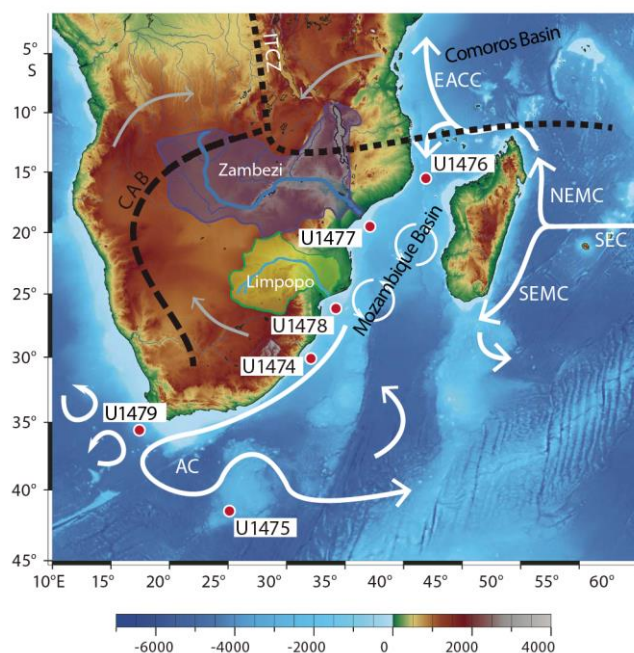


Figure 1: Map of SAFARI Sites, black-labelled sites will be investigated within this project. White arrows correspond to Agulhas Current (AC), East African Coastal Current (EAAC), South Equatorial Current (SEC) and North- and South East Madagascar Currents (NEMC, SEMC). Gray arrows: Main pathways of moisture. Black dashed line Intertropical Convergence Zone (ITCZ) and Congo Air Boundary (CAB). Modified after Hall et al. (2016).

In the course of IODP Expedition 361 – *South African Climates (SAFARI)* and ancillary project *Agulhas LGM Density Profile*, six sites were drilled in the SW Indian Ocean sector (Fig. 1). Major aims of the expeditions were to investigate 1) the sensitivity of the Agulhas leakage to changing climates of the Plio/Pleistocene 2) the dynamics of water exchange at the Indian-Atlantic gateway 3) the impact of the Agulhas leakage on the AMOC 4) Plio/Pleistocene evolution of South Africa climates. 5) changes in glacial deep ocean properties during the Last Glacial Maximum.

In the here proposed project, state-of-the-art paleomagnetic data will be acquired and combined with sedimentological and geochemical data to investigate the following paleoceanographic and paleomagnetic objectives.

Objective 1: Pliocene SE Africa Climate. At Site U1476 long-term changes in the concentration of terrigenous material are suggested by magnetic susceptibility and Natural Gamma Radiation (NGR) data but also the composition of the magnetic mineral assemblage varied. While the concentration of lithogenic material is primarily a function of terrigenous sediment accumulation vs. marine carbonate production, the compositional (magnetic) parameters will reveal changes in terrestrial weathering intensities during the Pliocene.

Objective 2: Glacial-Interglacial modulations of Indian Ocean circulation and SE African climate. After the Mid-Pleistocene Transition magnetic susceptibility at Site U1476 varies in concert with the benthic isotope stack, indicating a strong relationship between magnetic mineral content, paleoceanographic conditions and/or paleoclimate. Glacials (interglacials) appear to be associated with low (high) magnetic susceptibilities. It will be tested whether low susceptibilities are associated with higher marine productivity or reduced advection of lithic material because

of a change in nutrient supply, fluvial discharge or current strength.

Objective 3: Drift body formation off the Limpopo River. Interesting trends in magnetic susceptibility at Site U1478 show a cyclic pattern of gradual increases and sudden drops which are not captured in the shipboard NGR, suggesting different environmental control on the two parameters. The magnetic susceptibility is not solely a function of terrigenous input, but can also be influenced by the grain size of particles, and the preservation of magnetic minerals. Additionally, in sedimentary sequences, under sulfidic sedimentary conditions, magnetite dissolves in favor of Fe-sulfides. The magnetic data will be used, to reconstruct the variability in the drift depositions, including current strength and shift of the depocenter.

Objective 4: Indian Ocean Paleomagnetism. Paleomagnetic data will be acquired on samples taken around polarity transitions from Site U1474, U1475 and U1476 to refine the shipboard magnetostratigraphy. In particular, shipboard data from Site U1474 are of extremely high quality. Post-cruise post-processing of the data revealed the potential of this Site to produce a record of the relative paleointensity of the Earth's Magnetic Field, unprecedented in stratigraphic range (up to 6 Ma) and resolution (~2 kyrs). This goal will be achieved by cross-calibration of state-of-the-art paleomagnetic measurements on discrete samples with the available high-resolution shipboard data.

Reference:

Hall, I.R., Hemming, S.R., LeVay, L.J., Scientists, t.E., 2016. Expedition 361 Preliminary Report: South African Climates (Agulhas LGM Density Profile).

IODP

Exploring microbial sulphate reduction under high temperature and pressure – Results of a pilot study on samples from IODP Exp. 370

J. KALLMEYER¹, F. SCHUBERT¹, TINA TREUDE², IODP EXP. 370 SCIENTIFIC PARTY

¹ German Centre for Geosciences GFZ, Section 5.3 Geomicrobiology, Telegrafenberg, 14473 Potsdam

² University of California at Los Angeles, Dept. of Earth, Planetary, and Space Sciences

Sulphate reduction is the quantitatively most important process in the anaerobic degradation of organic matter in the sea floor (Jørgensen, 1982). Due to cryptic sulphur cycling it can proceed even if sulphate concentrations are near or below our detection limits (Glombitza et al., 2016; Holmkvist et al., 2011). While the effects of elevated pressure and temperature on microbial sulphate reduction have been studied for decades (Jørgensen et al., 1992; Trudinger et al., 1985), almost all studies were carried out in hydrothermal systems like Guaymas Basin, whereas sedimentary non-hydrothermal did not receive much attention.

IODP Exp. 370 (Temperature Limit of the Deep Biosphere off Muroto) was specifically planned to explore the upper temperature limit of life in a sedimentary system, visiting a single drill site located ~125 km offshore Shikoku Island, in the protothrust zone of the accretionary prism at a water depth of 4765 m (Heuer et al., 2017).

Due to the high heat flow in the area the geothermal gradient is high enough (ca. 100°C km⁻¹) to sample the putative temperature-dependent biotic–abiotic transition zone at relatively shallow sediment depth but still sufficiently gradual for the establishment of distinct, thick depth horizons (>10 m) with suitable conditions for psychrophilic (optimal growth temperature range: <20°C), mesophilic (20–45°C), thermophilic (45–80°C) and hyperthermophilic (>80°C) microorganisms. This unique location allows exploring the putative biotic fringe at a relatively shallow depth, but with high resolution of the temperature gradient. Radiotracer measurements of microbial turnover was one of the key aspects of this expedition, and each parameter that can be measured by radiotracer (methanogenesis, anaerobic oxidation of methane, hydrogenase enzyme activity, sulphate reduction) will be measured by a different group that has specialized in this kind of analysis.

Due to several logistical limitations it was decided to carry out those experiments mostly on shore, only for methanogenesis and sulphate reduction a small subset of samples was incubated at their approximate in-situ temperature.

The sulphate reduction rate samples from the on-board incubations were being processed at GFZ Potsdam to guide subsequent incubation experiments. Unfortunately much less radioactivity was injected into each sample than planned. Although some samples did not show any activity above the detection limit some turnover could be detected. Together with previous data from ODP Leg 190, Site 1174, which was drilled in close proximity to Exp. 370, sulphate reduction could be detected down to over 1000 mbsf. Further experiments under different temperature and pressure conditions as well as with additions of electron donors (e.g. volatile fatty acids, methane, hydrogen) will

explore the upper temperature limit of this important biogeochemical process.

References:

- Glombitza, C., Adhikari, R.R., Riedinger, N., Gilhooly, W.P., Hinrichs, K.-U., Inagaki, F., 2016. Microbial Sulfate Reduction Potential in Coal-Bearing Sediments Down to ~2.5 km below the Seafloor off Shimokita Peninsula, Japan. *Frontiers in Microbiology* 7.
- Heuer, V.B., Inagaki, F., Morono, Y., Kubo, Y., Maeda, L., Scientists, E., 2017. Expedition 370 Preliminary Report: Temperature Limit of the Deep Biosphere off Muroto, International Ocean Discovery Program, Preliminary Reports. International Ocean Discovery Program.
- Holmkvist, L., Ferdelman, T.G., Jørgensen, B.B., 2011. A cryptic sulfur cycle driven by iron in the methane zone of marine sediment (Aarhus Bay, Denmark). *Geochimica Et Cosmochimica Acta* 75, 3581–3599.
- Jørgensen, B.B., 1982. Mineralization of organic matter in the sea bed—the role of sulphate reduction. *Nature* 296, 643–644.
- Jørgensen, B.B., Isaksen, M.F., Jannasch, H.W., 1992. Bacterial sulfate reduction above 100°C in deep-sea hydrothermal vent sediments. *Science* 258, 1756–1757.
- Trudinger, P.A., Chambers, L.A., Smith, J.W., 1985. Low-temperature sulphate reduction: biological versus abiological. *Canadian Journal of Earth Sciences* 22, 1910–1918.

IODP

Pliocene oceanic seaways and global climate

CYRUS KARAS^{1,2,3,4}, DIRK NÜRNBERG³, ANDRÉ BAHR⁵, JEROEN GROENEVELD⁶, JENS O. HERMLE^{1,2}, RALF TIEDEMANN⁷, PETER B. DEMENOCAL⁴

¹ Goethe-University Frankfurt, Altenhoferallee 1, 60438, Frankfurt am Main, Germany.

² Biodiversity and Climate Research Centre (BIK-F), Senckenberganlage 25, 60325 Frankfurt am Main, Germany.

³ GEOMAR Helmholtz Centre for Ocean Research Kiel, Wischhofstrasse 1-3, 24148 Kiel, Germany.

⁴ Lamont Doherty Earth Observatory, Palisades, NY 10964, USA.

⁵ Ruprecht-Karls-Universität Heidelberg, Im Neuenheimer Feld 234, 69120 Heidelberg, Germany.

⁶ Center for Marine Environmental Sciences (MARUM), Univ. Bremen, Klagenfurter Strasse, 28359 Bremen, Germany.

⁷ Alfred Wegener Institute for Polar and Marine Research, Am Alten Hafen 26, 27568 Bremerhaven, Germany.

Tectonically induced changes in oceanic seaways had profound effects on global and regional climate during the Late Neogene. The constriction of the Central American Seaway reached a critical threshold during the early Pliocene ~4.8–4 million years (Ma) ago. Model simulations indicate the strengthening of the Atlantic Meridional Overturning Circulation (AMOC) with a signature warming response in the Northern Hemisphere and cooling in the Southern Hemisphere. Subsequently, between ~4–3 Ma, the constriction of the Indonesian Seaway impacted regional climate and might have accelerated the Northern Hemisphere Glaciation. We here present Pliocene Atlantic interhemispheric sea surface temperature and salinity gradients (deduced from foraminiferal Mg/Ca and stable oxygen isotopes, $\delta^{18}\text{O}$) in combination with a recently published benthic stable carbon isotope ($\delta^{13}\text{C}$) record from the southernmost extent of North Atlantic Deep Water to reconstruct gateway-related changes in the AMOC mode (Fig. 1). After an early reduction of the AMOC at ~5.3 Ma, we show in agreement with model simulations of the impacts of Central American Seaway closure a strengthened AMOC with a global climate signature (Fig. 2). During ~3.8–3 Ma, we suggest a weakening of the AMOC in line with the global cooling trend, with possible contributions from the constriction of the Indonesian Seaway.

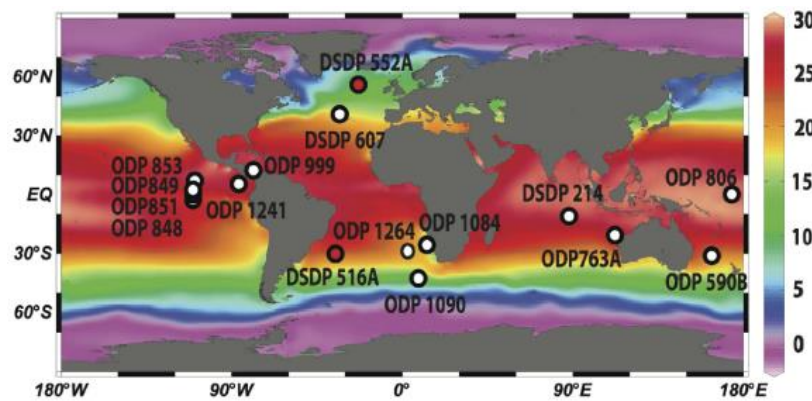


Figure 1: Modern annual sea surface temperature distribution at 30 m water depth. ODP/DSDP sites are indicated. Paleocceanographic proxy data were generated for South Atlantic DSDP Site 516A and North Atlantic Site 552A (red dots). Chart was created with Ocean Data View (<http://odv.awi.de>; version 4.5.1).

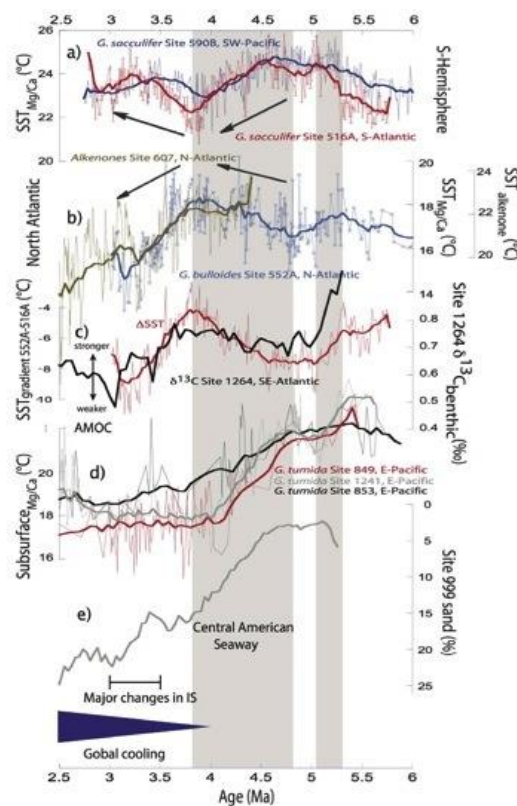


Figure 2: Pliocene paleoceanographic changes. (a) *G. sacculifer* SST_{Mg/Ca} records from Southern Hemisphere sites 516A (red line) and 590B (Karas et al., 2011; blue line). (b) *G. bulloides* SST_{Mg/Ca} record from Site 552A (blue line), and alkenone derived SST from Site 607 (Lawrence et al., 2010) from the North Atlantic (brown line). (c) Interhemispheric SST_{Mg/Ca} gradient between sites 552A and 516A (red; interpreted as deviation from 0) and benthic $\delta^{13}\text{C}$ record from Site 1264 (Bell et al., 2014; smoothed black line). (d) *G. tumida* subsurface Mg/Ca derived temperatures from Site 1241 (Steph et al. 2006; green line), and other sites 848 (blue line), 849 (red line), and 853 (black line) from Ford et al., 2012. (e) Sand percentages at Site 999 (Haug et al., 1998; smoothed line). Shaded areas indicate distinct changes in proxy records due to the tectonic constrictions of the CAS and the Mediterranean Seaway IS = Indonesian Seaway. Thick lines represent smoothed lines based on a Stineman function with +10% data range.

References:

- Bell, D. B., Jung, S. J. A., Kroon, D., Lourens, L. J. & Hodell, D. A. Local and regional trends in Plio-Pleistocene $\delta^{18}\text{O}$ records from benthic foraminifera. *Geochem., Geophys., Geosyst.* 15(8), 3304–3321 (2014).
- Ford, H. L., Ravelo, A. C. & Hovan, S. A deep Eastern Equatorial Pacific thermocline during the early Pliocene warm period. *Earth Planet. Sci. Lett.* 355–356, 152–161 (2012).
- Haug, G. H. & Tiedemann, R. Effect of the formation of the Isthmus of Panama on Atlantic ocean thermohaline circulation. *Nature* 393, 673–676 (1998).
- Karas, C., Nürnberg, D., Tiedemann, R. & Garbe-Schönberg, D. Pliocene climate change of the Southwest Pacific and the impact of ocean gateways. *Earth Planet. Sci. Lett.* 301, 117–124 (2011).
- Lawrence, K. T., Sosdian, S., White, H. E. & Rosenthal, Y. North Atlantic climate evolution through the Plio-Pleistocene climate transitions. *Earth Planet. Sci. Lett.* 300, 329–342 (2010).
- Steph, S., Tiedemann, R., Groeneveld, J., Sturm, A. & Nürnberg, D. Pliocene changes in tropical east Pacific upper ocean stratification: response to tropical gateways? In *Proc. ODP, Sci. Results*, 202, eds Tiedemann, R., Mix, A. C., Richter, C., Ruddiman, W. F. (College Station, TX) pp. 1–51 (2006).

IODP

Deep water circulation and productivity in the equatorial Indian Ocean (IODP Site U1443) through the Miocene Climatic Optimum

K.G.D. KOCHHANN¹, W. KUHN¹, A. HOLBOURN¹, N. ANDERSEN², S. SCHEIBLE¹

¹Institute of Geosciences, Christian-Albrechts-University, D-24118, Germany

²Leibniz Laboratory for Radiometric Dating and Stable Isotope Research, Christian-Albrechts-University, D-24118, Germany

International Ocean Discovery Program (IODP) Site U1443 (5°23.01'N/ 90°21.71'E, 2925 m water depth), drilled during Expedition 353 on the crest of the Ninetyeast Ridge at the southern end of the Bay of Bengal, provided the first complete middle Miocene carbonate-rich sedimentary archive in the Indian Ocean. High-resolution benthic stable oxygen ($\delta^{18}\text{O}$) and carbon ($\delta^{13}\text{C}$) isotope records, as well as X-ray fluorescence (XRF) scanner elemental records, track the abrupt onset and development of the Miocene Climatic Optimum (MCO) from ~16.9 to ~14.8 Ma followed by a transitional climatic phase (14.8 Ma to 13.8 Ma) and a two-stepped $\delta^{18}\text{O}$ increase at ~13.8 and ~13.1 Ma, reflecting global cooling and ice expansion over Antarctica. The U1443 $\delta^{13}\text{C}$ record closely matches records from the eastern equatorial Pacific Sites U1337 and U1338 with a ~250 kyr negative excursion at the onset of the MCO followed by the long-eccentricity paced "Monterey" $\delta^{13}\text{C}$ positive excursion between ~16.6 and 13.6 Ma (Holbourn et al., 2015), underscoring the global character of these deep-water isotope events. Increased XRF-derived log(Si/Ti) values suggest enhanced primary productivity and strengthening of the biological pump in the equatorial Indian Ocean during the "Monterey Excursion". Carbonate content at Site U1443, derived from calibrated XRF measurements, indicates episodic carbonate dissolution events correlated with low $\delta^{18}\text{O}$ and $\delta^{13}\text{C}$ during warm climate phases at eccentricity maxima. However, carbonate dissolution was less intense than at deeper sites in eastern equatorial Pacific Ocean (Kochhann et al., 2016). Comparison of deep water isotope records at Indian Ocean Site U1443 and eastern equatorial Pacific Expedition 320/321 sites reveals surprisingly small inter-basin $\delta^{18}\text{O}$ and $\delta^{13}\text{C}$ gradients between 17.8 and 12.8 Ma, indicating a common source for equatorial Pacific and Indian Ocean deep water masses during the late early and middle Miocene. Thus, these new results do not support a low latitude "Tethyan" origin for Indian Ocean deep water masses during the Miocene Climatic Optimum.

References:

- Holbourn, A., Kuhnt, W., Kochhann, K.G.D., Andersen, N., Meier, K.J.S., 2015. Global perturbation of the carbon cycle at the onset of the Miocene climatic optimum. *Geology* 43(2), 123-126, doi:10.1130/G36317.1.
- Kochhann, K.G.D., Holbourn, A., Kuhnt, W., Channell, J.E.T., Lyle, M., Shackford, J.K., Wilkens, R.H., Andersen, N., 2016. Eccentricity pacing of eastern equatorial Pacific carbonate dissolution cycles during the Miocene Climatic Optimum. *Paleoceanography* 31, 1176-1192, doi: 10.1002/2016PA002988.

ICDP

Report from the ICDP Oman Drilling Project: Phase 1 is in progress

J. KOEPKE¹, D. GARBE-SCHÖNBERG², S. MÜLLER², D. MOCK¹ AND THE OMAN DRILLING PROJECT SCIENCE TEAM

¹Institut für Mineralogie, Leibniz Universität Hannover (koepke@mineralogie.uni-hannover.de)

²Institut für Geowissenschaften, Universität Kiel

The Samail Ophiolite, in Oman and the United Arab Emirates, is the largest, best-exposed section of oceanic lithosphere in the World. The Oman Drilling Project is a comprehensive drilling program that will sample the whole ophiolite sequence, from crust through to upper mantle, in a series of diamond- and rotary-drilled boreholes. Data collection will include analysis of rock core, geophysical logging, fluid sampling, hydrological measurements and microbiological sampling. More than 40 scientists from a broad spectrum of disciplines will use these new datasets to address a diverse range of scientific questions relating to the formation, hydrothermal alteration and biotic and abiotic weathering of oceanic lithosphere. The overarching goal of scientific drilling in the Samail ophiolite is to understand the full spectrum of processes that create and modify oceanic crust and shallow mantle, involving mass and energy transfer between the mantle, the crust, the hydrosphere, the atmosphere and the biosphere over a range of temperatures from ~ 1350 to 20°C, depths from the surface to 10 or 20 km below the paleo-seafloor, and tectonic settings from spreading ridges to the deep ocean to surficial weathering to subduction zones. The Oman Drilling Project addresses long-standing unresolved questions regarding formation of oceanic lithosphere at mid-ocean ridges, hydrothermal alteration of the sea floor and subsequent mass transfer between the crust and the oceans and recycling of volatile elements in subduction zones. Furthermore, the science team will undertake frontier exploration of subsurface weathering processes that lead to natural uptake of CO₂ from surface waters and the atmosphere, and the nature of the subsurface biosphere in areas where these processes are occurring.

Due to problems with the signing of the contract from the Oman authorities, the starting of the active phase of the project was delayed about one year. The following Oman authorities are involved: Ministry of Regional Municipalities and Water Resources, Public Authority for Mining, Oman Water Society, Sultan Qaboos University and The German University for Technology. As outreach component students from SQU and GuTec will join the on-site science team for training and practice.

The active phase 1 started finally in December 2016. Wireline diamond coring takes place in the following sequence: Site GT2 (Wadi Gideah, mid-level gabbros), Site GT1 (Wadi Gideah, lower gabbros), Site GT3 (Wadi Abdah, dyke-gabbro transition), Site BT1 (Wadi Mansah, listvenites and basal thrust). Simultaneously to the diamond coring, rotary drilling will take place at Site BA1 (Active alteration) in early February. Coring is expected to last approximately four months, finishing in late March or early April 2017. The drilling contractor is a company active in Oman, Lalbuksh Voltas providing a drill rig which is able to drill boreholes of 600 meter depth maximum including

coring. Within phase 1 we plan to drill holes of 400 m depth. At the time of writing this abstract, Site GT2 was completed (400 m depth) and Site GT1 reached a depth of 250 m.

The basic core curation, initial description, scanning, piece labelling, data logging into the ICDP DIS system, and the packing into transport boxes for shipping was established by on site science teams of 3 to 6 persons who had to manage a core flow up to 33 meters core per day. The core conditions are excellent, with smooth cut surfaces enabling good conditions for macroscopic core description, and high recovery rates near 100%.

Detailed description of cores drilled in Phase 1 will take place over 60 days (two science parties, lasting 30 days each) in summer 2017. This is currently scheduled to take place on board the IODP drilling ship Chikyu, in Japan, in July and August 2017, during a non-IODP period. There, detailed core descriptions, instrumental scanning, measurements of physical properties, and individual sampling will be undertaken according to the "IODP standard" within small science groups related to igneous petrology, metamorphic petrology, structural geology, geochemistry, microbiology, paleomagnetism, and petrophysics. For each core, visual core descriptions (VCD) will be produced, and detailed thin section work will also be included. At the end of the survey on Chikyu, systematic and complete publication of basic observations from geophysical logging, water sampling, and core description will be undertaken in a standardized and accessible manner, analogous to the electronic, open-access Initial Reports volumes of the IODP. IODP Publications Services at Texas A&M University has offered to help us assemble and publish an Initial Report volume on Phase I of the Oman Crustal Drilling Campaign. This procedure guarantees the highest possible standard for core description and documentation, well-suited for designing further post-drilling research and for sample requests from interested scientists outside of the Oman Drilling Project science team.

Phase 2, the coring at sites BA1 (Active alteration) and MD1 (Crust-mantle boundary), as well as further rotary drilling, will take place during a second active phase, beginning October 2017. Detailed description of cores drilled in Phase 2 is planned to take place on board of the US drill ship JOIDES Resolution in summer 2018 during its non-IODP period.

IODP

MyDTW – Dynamic Time Warping program for stratigraphical time series

S. KOTOV¹, H. PAELIKE¹

¹MARUM, Bremen University, Bremen, Germany. E-mail: skotov@marum.de

One of the general tasks in many geological disciplines is matching of one time or space signal to another. It can be classical correlation between two cores or cross-sections in sedimentology or marine geology. For example, tuning a paleoclimatic signal to a target curve, driven by variations in the astronomical parameters, is a powerful technique to construct accurate time scales. However, these methods can

be rather time-consuming and can take ours of routine work even with the help of special semi-automatic software. Therefore, different approaches to automate the processes have been developed during last decades. Some of them are based on classical statistical cross-correlations such as the 'Correlator' after Olea [1]. Another ones use modern ideas of dynamic programming. A good example is as an algorithm developed by Lisiecki and Lisiecki [2] or dynamic time warping based algorithm after Pálíke [3].

We introduce here an algorithm and computer program, which are also stemmed from the Dynamic Time Warping algorithm class. Unlike the algorithm of Lisiecki and Lisiecki, MyDTW does not lean on a set of penalties to follow geological logics, but on a special internal structure and specific constrains. It differs also from [3] in basic ideas of implementation and constrains design. The algorithm is implemented as a computer program with a graphical user interface using Free Pascal and Lazarus IDE and available for Windows, Mac OS, and Linux. Examples with synthetic and real data are demonstrated. Program is available for free download at http://www.marum.de/Sergey_Kotov.html.

References:

- Olea, R.A. Expert systems for automated correlation and interpretation of wireline logs // *Math Geol* (1994) 26: 879. doi:10.1007/BF02083420
- Lisiecki L. and Lisiecki P. Application of dynamic programming to the correlation of paleoclimate records // *Paleoceanography* (2002), Volume 17, Issue 4, pp. 1-1, CiteID 1049, doi: 10.1029/2001PA000733
- Pálíke, H. Extending the astronomical calibration of the Geological Time

ICDP

Unraveling the trigger mechanisms for climate change in SE Europe during MIS 12-11 Based On A New High-resolution Pollen Record from Lake Ohrid

I. KOUSIS¹, A. KOUTSODENDRIS¹, M. KNIPPING², J. PROSS¹ AND THE SCOPSCO SCIENCE PARTY

¹Paleoenvironmental Dynamics Group, Institute of Earth Sciences, Heidelberg University, Heidelberg

²Institute of Botany, University of Hohenheim, Stuttgart

To better understand climate variability in SE Europe during extreme glacial and interglacial periods of the Quaternary, i.e., Marine Isotope Stages (MIS) 12 (~478–424 ka BP) and 11 (~424–368 ka BP), respectively, we here analyse new core material from Lake Ohrid (Albania/FYROM). We apply centennial-scale palynological analysis to the DEEP core, which was retrieved within the framework of an ICDP campaign in 2013, providing the first highly-resolved record for this interval in Europe. Our results show that MIS 12 is dominated by high non-arboreal pollen (NAP) percentages, suggesting a prevalence of cold and dry conditions. Notably, transient peaks in arboreal pollen (AP) percentages are also present, confirming the view that the Lake Ohrid area acted as a tree refugium during this extreme glacial (Sadori et al., 2016). These forest expansions coincide with Dansgaard-Oeschger-like warming events as documented in marine records from the North Atlantic (Naafs et al., 2014), suggesting a link between terrestrial ecosystem change and ocean circulation dynamics. On the contrary, MIS 11 is characterised by

predominantly high AP percentages, suggesting the persistent establishment of forests in the lake's catchment area. The major shifts in forest composition are concurrent with the transitions of the three MIS 11 substages in the marine realm. More specifically, MIS 11c (~424–398 ka BP) exhibits high pollen abundances of Mediterranean taxa (e.g., *Quercus ilex*-type, *Phillyrea*, *Pistacia*) that require mild, frost-free winters to grow; other thermophilous taxa such as *Abies*, *Carpinus*, *Fraxinus*, *Pterocarya*, *Quercus robur*- and *cerris*-types, *Tilia*, *Ulmus* and are also common. These observations define MIS 11c as the warmest and wettest interval of MIS 11 around Lake Ohrid. The subsequent MIS 11b (~398–372 ka BP) is marked by considerable millennial-scale variability as documented by abrupt shifts in AP percentages. In contrast to MIS 11c, it is also characterized by lower abundances of thermophilous taxa and higher percentages of *Picea*, which is an indicator of cool winters and pronounced seasonality. Finally, MIS 11a (~372–368 BP) is characterized by high NAP percentages indicating open landscapes. The increase of pioneer taxa pollen percentages (e.g., *Juniperus* and *Hippophaë*) at the expense of thermophilous taxa during MIS 11a marks the transition into the next glacial (MIS 10).

Based on the above, MIS 12 and 11 represent two climatically highly dynamic intervals of the Middle Pleistocene. Ongoing, pollen-based climate (i.e., temperature and precipitation) reconstructions will allow to quantitatively constrain the magnitude of climate change and seasonal variability. In addition, integration with emerging proxy data from Lake Ohrid and comparisons with pollen records from the Eastern Mediterranean region (e.g., Tenaghi Philippon; Pross et al., 2015) and the Iberian Margin (e.g., Tzedakis et al., 2009) will significantly refine the current understanding of regional climate variability in the greater Mediterranean region and thereby shed light onto climate gradients during MIS 12 and 11.

References:

- Naafs, B.D.A., Hefter, J., Stein, R., 2014. Dansgaard-Oeschger forcing of sea surface temperature variability in the mid-latitude North Atlantic between 500 and 400 ka (MIS 12). *Paleoceanography* 29, 1024-1030.
- Pross, J., Koutsodendris, A., Christanis, K., Fischer, T., Fletcher, W.J., Hardiman, M., Kalaitzidis, S., Knipping, M., Kotthoff, U., Milner, A.M., Müller, U.C., Schmiedl, G., Siavalas, G., Tzedakis, P.C., Wulf, S., 2015. The 1.35-Ma-long terrestrial climate archive of Tenaghi Philippon, northeastern Greece: Evolution, exploration and perspectives for future research. *Newsletters on Stratigraphy* 48, 253-276.
- Sadori, L., Koutsodendris, A., Panagiotopoulos, K., Masi, A., Bertini, A., Combourieu-Nebout, N., Francke, A., Kouli, K., Joannin, S., Mercuri, A.M., Peyron, O., Torri, P., Wagner, B., Zanchetta, G., Sinopoli, G., Donders, T.H., 2016. Pollen-based paleoenvironmental and paleoclimatic change at Lake Ohrid (south-eastern Europe) during the past 500 ka. *Biogeosciences* 13, 1423-1437.
- Tzedakis, P.C., Pälike, H., Roucoux, K.H., de Abreu, L., 2009. Atmospheric methane, southern European vegetation and low-mid latitude links on orbital and millennial timescales. *Earth and Planetary Science Letters* 277, 307-317.

ICDP

Seismic reconnaissance survey for the ICDP proposal 'Paleoclimate, Paleoenvironment, and Paleoecology of Neogene Central America: Bridging Continents and Oceans (NICA-BRIDGE)'

S. KRASTEL¹, S. KUTTEROLF², E. LEBAS¹, K. HAGEMANN¹, W. STRAUCH³

¹ Christian-Albrechts-Universität zu Kiel, Institut für Geowissenschaften

² GEOMAR Helmholtz-Zentrum für Ozeanforschung Kiel

³ Instituto Nicaraguense de Estudios Territoriales, Managua, Nicaragua

The two largest lakes in Central America, Lake Nicaragua and Lake Managua, are situated in the south-central part of Nicaragua. The location and the proposed long existence (at least Pliocene possibly Late Miocene) make these lakes promising targets for scientific drilling within the International Continental Drilling Program.

Drilling objectives of global relevance, assisted by the strategic lakes' location, include therefore 1) recovery and extension of a Neotropic paleo-climate record into the past, 2) investigation of marine-lacustrine interactions in the past (connections to the oceans), in the recent and the future (channel construction), 3) the history of long tectonic and sedimentary basin (lake) development, 4) arc evolution and related hazards due to the proximity to the volcanic arc, 5) deciphering their significance as an endemic hot spot over time, 6) investigation of an important paleozogeographic event, the great American biotic interchange, and 7) the ability to combine seismology, volcanology, paleoclimate, paleoecology, and paleoenvironment in one project.

Hence, in January 2015 and 2016, a group of international scientists submitted ICDP workshop proposals with the aim to develop a scientific drilling project focused on Lakes Nicaragua and Managua. The proposals were generally well received but noted a significant lack of seismic data, which makes site characterization impossible. Only very sparse seismic data have been collected in the past but failed to image the deeper subsurface due to technical problems during data acquisition and complicated depositional conditions (e.g., gas and tephtras). Hence, the workshop proposals were not accepted at the current stage.

In order to overcome this proposal, we will acquire reconnaissance seismic data of Lake Nicaragua in order to show that high-quality seismic pre-site survey data can be collected by means of modern equipment and considering the experience gained in the last decade at locations with volcanogenic lake sediments. A Micro or Mini GI-Gun will be used as source. The energy will be recorded by a 40 channel digital streamer. The survey is taking place from Mid February to Early March 2017. We will present very first results from this survey, which ends less than a week before the IODP/ICDP Colloquium.

ICDP

Integration of downhole logging and borehole seismic data to characterise mid-crustal deformation patterns in the Scandinavian Caledonides

F. KRAUB¹, P. HEDIN², B. ALMQVIST², H. SIMON³, S. PIERDOMINICI¹, R. GIESE¹, S. BUSKE³, C. JUHLIN², H. LORENZ²

¹ Section 6.4, Centre for Scientific Drilling, GFZ German Research Centre for Geosciences, Helmholtz Centre Potsdam

² Dept. of Earth Sciences, Uppsala University

³ Institute of Geophysics and Geoinformatics, TU Bergakademie Freiberg

The COSC drilling project (Collisional Orogeny in the Scandinavian Caledonides; <http://cosc.icdp-online.org/>) aims at a better understanding of deep orogenic processes in mountain belts (Gee et al., 2010). A prime example of a well preserved and deeply exhumed Palaeozoic orogenic belt is the Scandinavian Caledonides, formed by the collision of the Laurentia and Baltica continental plates. The tectonostratigraphy of the Caledonian foreland is centred around the Seve Nappe Complex (SNC), which is a during collisional orogeny highly metamorphosed and hot emplaced tectonic unit in the Middle Allochthon, i.e. metamorphism decreases both upwards and downwards (inverse gradient; Gee et al., 2013). The 2.5 km deep borehole COSC-1 was drilled into the Seve Nappe Complex (SNC) of the Middle Allochthon (Lorenz et al., 2015). The upper 2350 m of the borehole consists of alternating layers of highly deformed felsic and calc-silicate gneisses and amphibolites. At c. 2350 m, the borehole leaves the SNC and penetrates a meta-sedimentary unit of unknown tectonostratigraphic position. From about 1700 m to the final depth of 2500 m interfingering bands of mylonitic deformation increase in frequency and thickness successively, indicating a high strain zone of at least 800 m in thickness (Hedin et al., 2015).

Accompanying the drilling, several downhole logging campaigns and an extensive seismic survey were executed. The seismic survey comprised three parts: (i) a limited 3D-survey (Hedin et al., 2015), (ii) a high resolution zero-offset VSP (vertical seismic profile; Krauß et al., 2015) with 2-m-receiver spacing and (iii) a multi-azimuthal walkaway VSP (Simon et al., 2017) with sources and receivers both along three surface profiles and receivers at seven different depth levels of the borehole. For the latter two surveys three-component geophones were deployed in the borehole and at the surface.

The zero-offset VSP data have high signal-to-noise ratios with signal frequencies up to 150 Hz. Data processing allowed determination of P- and S-wave first arrival times for 1D velocity analysis. Furthermore, all reflection events were extracted to allow comparison with surface seismic results and to provide higher resolution data at the borehole location. Downhole logging surveys were conducted during and immediately after drilling. All logs sensitive to petrophysical parameters and available to total depth were used for cluster analysis to highlight common petrophysical features for different lithologies. The logs used include sonic (P-wave velocity), natural gamma, spectral gamma (elements K, U, Th) and magnetic susceptibility. A principal component analysis (PCA) has been performed to reduce the dimension of the data. A subsequent statistical test (Pham et al., 2005) suggested two clearly distinguishable clusters, but also provided evidence for separating the data set into four clusters. Thus,

cluster analysis was performed looking for two and four clusters using the k-means algorithm and the L²-norm. To improve the result of the k-means algorithm, the cluster analysis was performed 100 times for each k-value while the result with the minimum summed distances was used.

The outcomes of both cluster analyses match the alternating layering of felsic and mafic lithologies as determined in drill core. Especially mafic lithologies (meta-gabbro, amphibolites) are easily identified by low gamma values. However, first evaluation of the cluster analyses also suggests to differentiate this interpretation further at the beginning of the shear zone at c. 1700 m depth, because the petrophysical properties seem to change with the prolific occurrence of subhorizontal mylonitic bands. A first comparison of cluster analysis results and the 3D surface seismic shows good correlation of reflectors and changes of clusters. These results confirm that a combined utilization of borehole seismic and downhole logging data serve to elucidate basement structures in detail.

A future step will be a combination of cluster analysis results, surface and borehole seismic results to better characterise the SNC and its internal reflectors, as well as differences between the SNC outside and inside the shear zone.

References:

- Gee, D.G. et al. (2010). Collisional Orogeny in the Scandinavian Caledonides (COSC). *GFF*, 132(1), 29-44.
- Gee et al. (2013). Subduction along and within the Baltoscandian margin during closing of the Iapetus Ocean and Baltica-Laurentia collision. *Lithosphere*, 5(2), 169-178. doi: 10.1130/L220.1.
- Lorenz, H. et al (2015). COSC-1 – drilling of a subduction-related allochthon in the Palaeozoic Caledonide orogen of Scandinavia. *Sci. Drill.*, 19, 1-11. doi: 10.5194/sd-19-1-2015.
- Hedin, P. et al (2016). 3D reflection seismic imaging at the 2.5 km deep COSC-1 scientific borehole, central Scandinavian Caledonides. *Tectonophysics* 689, 40-55. doi: 10.1016/j.tecto.2015.12.013.
- Krauß et al. (2015). Zero-offset VSP in the COSC-1 borehole. *Geophys. Res. Abstr.* 17, EGU2015-3255.
- Simon et al. (2017). The derivation of an anisotropic velocity model from a combined surface and borehole seismic survey in crystalline environment at the COSC-1 borehole, central Sweden. *GJI*, under review.
- Pham et al. (2005). Selection of K in K-means clustering. *Proc. IMechE* 219 Part C: J. Mechanical Engineering Science, 103-119. doi: 10.1243/095440605X8298.

ICDP

Microbiological survey of mofette and mineral waters of the Cheb Basin, Czech Republic

P. KRAUZE¹, H. KÄMPF², F. HORN¹, D. WAGNER¹, M. ALAWI¹

¹ GFZ German Research Centre for Geosciences, Section 5.3 Geomicrobiology, Potsdam, Germany

² GFZ German Research Centre for Geosciences, Section 3.2 Organic Geochemistry, Potsdam, Germany

The Cheb Basin (NW Bohemia, Czech Republic) is a shallow neogene intracontinental basin that has formed since the Tertiary at the intersection of the E-NE trending Eger Rift and the N-S trending Regensburg-Leipzig-Rostock seismoactive zone (Bankwitz et al., 2003; Fischer et al., 2014). It is a non-volcanic region which features frequent earthquake swarms (Fischer et al., 2014) and large-scale diffuse degassing of mantle-derived carbon dioxide at the surface that occurs in the form of CO₂-rich mineral springs and wet and dry mofettes (Kämpf et al., 2013; Nickschick et al., 2015). These geodynamic

processes are most probably induced by an active magmatic process in the lithospheric mantle (Bräuer et al., 2009). Carbon isotope signatures up to -70‰ of methane, a minor component of the CO₂ dominated upstreaming gases, indicate an interaction between geological, geophysical and microbial driven processes in the deep subsurface (Bräuer et al., 2005). This observation leads to the question whether earthquakes can trigger microbiologically driven processes by delocalization of substrates and environmental changes. To get a better understanding of these geo-bio interactions and to determine to which extend the microbial communities are conditioned by CO₂ degassing, we analyzed the microbial community structure in detail. This work serves as a preliminary study for the ICDP deep drilling campaign “Drilling the Eger Rift: Magmatic fluids driving the earthquake swarms and the deep biosphere” and should give a first overview of microbial life facing strongly increased CO₂ concentrations. Therefore, waters from four mineral water springs and two wet mofettes located in the Cheb Basin were investigated. Besides geochemical analyses, high-throughput DNA sequencing of the 16S rRNA gene and quantitative PCR were conducted to get an extensive insight into the microbial communities of CO₂ influenced waters. All investigated waters were acidic (4.2 – 6.0), but differed greatly in terms of organic carbon contents and anion/cation concentrations. Chemolithotrophic, anaerobic/microaerophilic microorganisms shaped the microbial communities in these habitats. Especially organisms connected to sulfur (e. g. *Sulfuricurvum*, *Sulfurimonas*) and iron (e. g. *Gallionella*, *Sideroxydans*) cycling were highly abundant. Strictly anaerobic sulfate reducing bacteria and methanogenic archaea showed low abundances. The microbial community compositions varied according to geochemistry (e. g. pH, Fe concentration) and origin of the water, while bacterial abundances were mainly influenced by organic carbon contents. Remarkably, 99% of all observed taxa were shared between all investigated mofette and mineral waters. The core community could represent the adaptation of microbial communities to stable and long-term elevated CO₂ partial pressures in aquatic systems.

This work not only improves our understanding of geo-bio interactions and microbial life in such extreme habitats, but is also of interest regarding geotechnical applications (e. g. geothermal energy, drinking water reservoirs and regional spas) and their possible consequences for life in the subsurface.

References:

- Bankwitz, P., Schneider, G., Kämpf, H., Bankwitz, E., 2003. Structural characteristics of epicentral areas in Central Europe: study case Cheb Basin (Czech Republic). *Journal of Geodynamics* 35, 5–32.
- Bräuer, K., Kämpf, H., Faber, E., Koch, U., Nitzsche, H.-M., Strauch, G., 2005. Seismically triggered microbial methane production relating to the Vogtland-NW Bohemia earthquake swarm period 2000, Central Europe. *Geochemical Journal* 39, 441–450.
- Bräuer, K., Kämpf, H., Strauch, G., 2009. Earthquake swarms in non-volcanic regions: What fluids have to say. *Geophysical Research Letters* 36. doi:10.1029/2009GL039615
- Fischer, T., Horálek, J., Hrubcová, P., Vavryčuk, V., Bräuer, K., Kämpf, H., 2014. Intra-continental earthquake swarms in West-Bohemia and Vogtland: A review. *Tectonophysics* 611, 1–27. doi:10.1016/j.tecto.2013.11.001
- Kämpf, H., Bräuer, K., Schumann, J., Hahne, K., Strauch, G., 2013. CO₂ discharge in an active, non-volcanic continental rift area (Czech Republic): Characterisation ($\delta^{13}\text{C}$, $^3\text{He}/^4\text{He}$) and quantification of diffuse and vent CO₂ emissions. *Chemical Geology* 339, 71–83.
- Nickschick, T., Kämpf, H., Flechsig, C., Mrlina, J., Heinicke, J., 2015. CO₂ degassing in the Hartoušov mofette area, western Eger Rift, imaged by CO₂ mapping and geoelectrical and gravity surveys. *International Journal of Earth Sciences*. 104(8), 2107–2129

ICDP

Q Inversion employing double difference amplitude spectral ratio method: A case study of North West Bohemia

M. KRIEGEROWSKI¹, S. CESCA², T.DAHM^{1,2}, F. KRÜGER¹

¹ Universität Potsdam, Institut für Erd- und Umweltwissenschaften

² Helmholtz-Zentrum Potsdam Deutsches GeoForschungsZentrum GFZ

Physical parameters such as fluid content or brittleness of the subsoil are attributing to the attenuation of seismic waves. We develop an amplitude spectral ratio method which we apply to event couples within a compact seismic cluster. A differential t* operator serves as a measure of relative attenuation along pairs of two parallel ray path segments inside the source volume. T* is estimated based on the high frequency logarithmic spectral ratios applied to time windows around P and S phases of event couples which are selected based on a Fresnel volume criterion applied to select ray path segments. Besides selecting event couples this criterion also defines the frequency ranges which can be exploited and therefore ensures that the individual measure is representative for the inter-event rock properties.

This approach has similarities to double-difference relative location methods and allows a focused analysis of the properties inside the source region. It is expected that due to high ray path similarity outside the source volume effects along this ray path segment cancel out in the inversion.

We demonstrate the method using synthetic seismograms contaminated with recorded noise. This allows to simulate a realistic test scenario.

Furthermore, we extend the described approach which allows a determination of the absolute attenuation with a modification which aims at resolving spatial variations of attenuation inside the seismic cluster. In this case two differential t* values of up to four events form the data kernel elements of the inversion.

The key questions driving the development of the new method are how much the robustness against perturbations and unknowns in the velocity model and hypocenter locations changes in comparison to the standard spectral ratio method and if the resolution of the inversion can be improved. We address this question by applying resolution tests to the newly developed method as well as to a standard amplitude spectral ratio method.

The periodically active seismic swarm region beneath North West Bohemia provides us with a favorable test environment meeting the requirements of high event density in confined source regions. Therefore it serves as a case study for both synthetic tests as well as applications of the described method to real recordings. For both, noise is a limiting factor with significant influence on the stability of the inversion. Therefore a signal to noise ratio threshold of 5 in a frequency range of at least 30 Hz was used to exclude t* measurements from noisy phase recordings. A catalog of 5000 events recorded at 12 stations of the Western Bohemian seismological network (WEBNET) during a swarm period in October 2008 represent a large

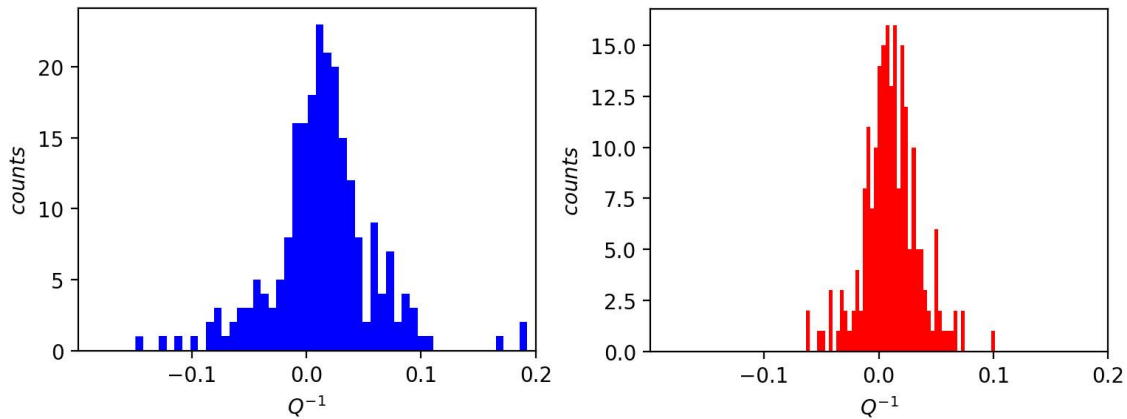


Figure 1: Distribution of Q_p (blue) and Q_s (red) based on 220 differential t^* measurements

potential to resolve attenuation. However, the Fresnel criterion, as well as the signal to noise limitation reduce the number of differential t^* candidates to few hundreds. Applying the double-difference amplitude spectral ratio method to these candidates yields an approximately normal distribution for Q , which is the inverse of the attenuation, with a maximum at 50 for P phases and 100 when applied to S phases (Figure 1).

Funded by ICDP project: HISS (CE 223/2-2)

IODP

Indian monsoon variability in a warmer world: Exploring the Miocene-Pliocene sediment archives of IODP Expedition 353 Sites U1447 and U1448 (Andaman Sea)

W. KUHN¹, A. HOLBOURN¹, J. JÖHNCK¹, N. ANDERSEN²

¹Institute of Geosciences, Christian-Albrechts-University, D-24118, Germany

²Leibniz Laboratory for Radiometric Dating and Stable Isotope Research, Christian-Albrechts-University, D-24118, Germany

The forcings and feedback processes that drive the short- and long-term variability of monsoonal circulation and precipitation patterns within the Earth's strongest monsoonal regime remain matters of intense debate. IODP Expedition 353 (iMonsoon) targeted the reconstruction of Indian monsoon precipitation through the Miocene to Pleistocene in its core geographic region of influence, the margins of the Bay of Bengal. Specifically two sites (U1447, 10°47.40'N/93°00.00'E, 1392 m water depth and U1448, 10°38.03'N/93°00.00'E, 1098 m water depth), drilled in the Andaman Sea, recovered extended upper Miocene to Pliocene successions, which provide an outstanding opportunity to assess the sensitivity of the Indian Monsoon to insolation forcing and to climate boundary conditions such as the extent of global ice volume and greenhouse gas concentrations on a warmer-than-today Earth. These new sediment archives will also allow to constrain the timing and boundary conditions under which monsoonal circulation initiated and will be crucial to test the hypothesis of a close linkage between the climatic evolution of South Asia and the tectonic development of the Himalayans, specifically the rising of the Tibetan Plateau. Based on a composite record from Sites U1447 and U1448, we are currently developing an orbitally-tuned benthic isotope stratigraphy over the interval 10 to 3 Ma as well as high-resolution monsoonal run-off records from XRF-scanning elemental data coupled with sea surface temperature/salinity reconstructions from paired stable isotopes and Mg/Ca. The records from the Andaman Sea will provide new insights into the linkages between Indian monsoonal circulation/rainfall and high-latitude climate change during intervals of warmer climate with widely differing mean-state background conditions: (1) during the Miocene Climate Optimum (16-14.5 Ma),

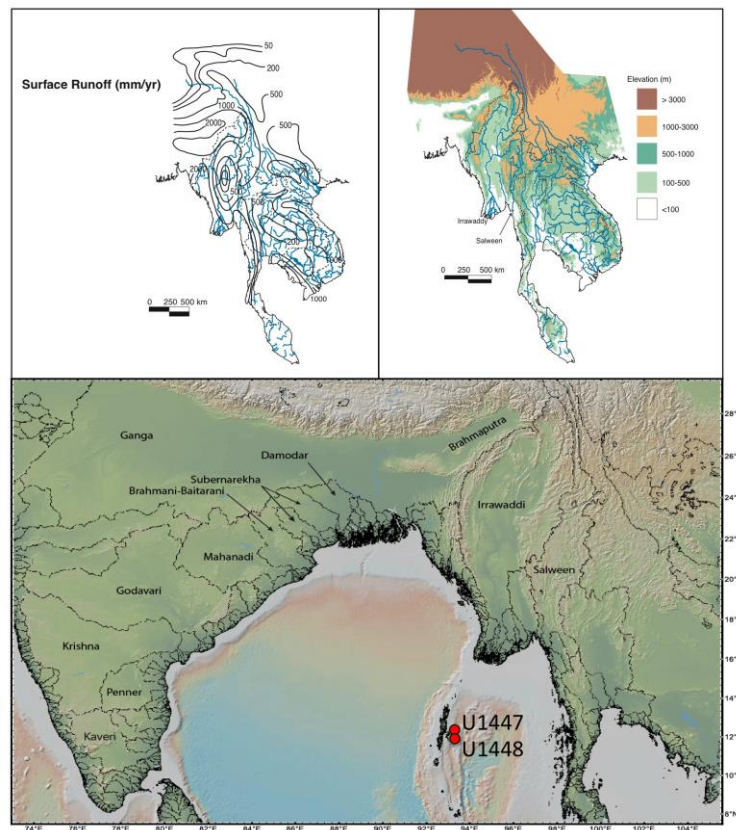


Figure 1: Location map of the new Andaman IODP sites in relation to the main drainage basins on the Asian continent. Today, sediment and freshwater runoff at Sites U1447 and U1448 mainly originate locally from the Andaman Islands and from the Irawaddi and Salween drainage basins on the Asian continent. During the late Miocene, when the uplift of the Andaman Islands was incomplete, the direct runoff from the continent was substantially higher. The extent, elevation and annual surface runoff from drainage basins are from Milliman and Farnsworth (2011).

when Antarctic ice sheets behaved in a highly dynamic manner and the main uplift and expansion phase of the Tibetan plateau had not yet taken place, (2) between 10 and 7 Ma, when Earth was unipolarly glaciated and the main uplift and expansion phase of the Tibetan plateau occurred, and (3) between 5 to 3 Ma when Northern Hemisphere glaciation was initiated.

References:

- Clemens, S.C., Kuhnt, W., LeVay, L.J., Anand, P., Ando, T., Bartol, M., Bolton, C.T., Ding, X., Gariboldi, K., Giosan, L., Hathorne, E.C., Huang, Y., Jaiswal, P., Kim, S., Kirkpatrick, J.B., Littler, K., Marino, G., Martinez, P., Naik, D., Peketi, A., Phillips, S.C., Robinson, M.M., Romero, O.E., Sagar, N., Taladay, K.B., Taylor, S.N., Thirumalai, K., Uramoto, G., Usui, Y., Wang, J., Yamamoto, M., and Zhou, L., 2016. Site U1447. In Clemens, S.C., Kuhnt, W., LeVay, L.J., and the Expedition 353 Scientists, *Indian Monsoon Rainfall*. Proceedings of the International Ocean Discovery Program, 353: College Station, TX (International Ocean Discovery Program). <http://dx.doi.org/10.14379/iodp.proc.353.107.2016>.
- Clemens, S.C., Kuhnt, W., LeVay, L.J., Anand, P., Ando, T., Bartol, M., Bolton, C.T., Ding, X., Gariboldi, K., Giosan, L., Hathorne, E.C., Huang, Y., Jaiswal, P., Kim, S., Kirkpatrick, J.B., Littler, K., Marino, G., Martinez, P., Naik, D., Peketi, A., Phillips, S.C., Robinson, M.M., Romero, O.E., Sagar, N., Taladay, K.B., Taylor, S.N., Thirumalai, K., Uramoto, G., Usui, Y., Wang, J., Yamamoto, M., and Zhou, L., 2016. Site U1448. In Clemens, S.C., Kuhnt, W., LeVay, L.J., and the Expedition 353 Scientists, *Indian Monsoon Rainfall*. Proceedings of the International Ocean Discovery Program, 353: College Station, TX (International Ocean Discovery Program). <http://dx.doi.org/10.14379/iodp.proc.353.108.2016>.
- Milliman, J.D., and Farnsworth, K.L., 2011. River discharge to the Coastal Ocean - a Global Synthesis. Cambridge University Press, 384 pp.

IODP

Traces of explosive eruptions in Cretaceous to Quaternary Indian Ocean sediments

S. KUTTEROLF¹, J.C. SCHINDLBECK¹

¹ GEOMAR, Helmholtz Center for Ocean Research, Kiel

During IODP Expeditions 353 and 362 sediments with intercalated tephra layers have been drilled and sampled that reach down to the Campanian. The drill sites are located ~800 km west of the volcanic front of the Sunda arc in the Indian Ocean. The objectives of the cruises were to determine the material properties causing the seismogenic slip (362) and to reconstruct and understand changes in Indian monsoon circulation (353). Our project aims to establish a marine tephrostratigraphic framework for the entire region, which will be supported by absolute age dating as well as by correlations to other ocean drill sites and if possible, to terrestrial eruptions. Therefore we will combine the tephra records of Expeditions 353 and 362 with marine tephra layers from previous ODP drillings from the whole Indian Ocean, and on the Ninetyeast Ridge in particular. We aim to constrain the temporal and spatial changes in eruption processes, magnitudes and frequencies of large volcanic eruptions from the Sunda arc, or so far unknown volcanic sources. Geochemical, petrological and volcanological approaches for tephra and sediment characterization will be used to quantitatively and qualitatively decrypt their provenance and the eruption succession. Especially the determination of the amount and character of volcanic matter that is incorporated in the

sediments is important to characterize the material and how it acts, when it is subducted at the seismogenic and tsunamogenic Sumatran convergent margin. Furthermore, we will learn more about the temporal evolution of different volcanic systems and establish long time series of explosive volcanism in this region. Within our record we will identify large, known, but also previously unknown, eruptions, which will enable us to study the respective recurrence rates from Pleistocene volcanic centres of the Sumatran arc and to elaborate on cyclicities in the tephra record. Finally, we will also study the Miocene to Pleistocene sediment record of the Nicobar Fan to detect potential episodes of enhanced volcanism or single events hidden in the background sedimentation.

IODP

IODP proposal DYNAPACC: Plio-Pleistocene Dynamics of the Pacific Antarctic Circumpolar Current

FRANK LAMY^{*1}, ROBERT ANDERSON², HELGE W. ARZ^{*3}, GIUSSEPPE CORTESE⁴, OLIVER ESPER^{*1}, KARSTEN GOHL⁺¹, IAN HALL⁵, C.D. HILLENBRAND⁶, CHRISTIAN HÜBSCHER⁷, CARINA LANGE^{*8}, LESTER LEMBKE-JENE^{*1}, ALFREDO MARTINEZ-GARCIA^{*9}, ULYSSES NINEMANN¹⁰, DIRK NÜRNBERG¹¹, KATHARINA PAHNKE^{*12}, ALINA POLONIA^{*13}, JOSEPH STONER¹⁴, RALF TIEDEMANN¹, GABI UENZELMANN-NEBEN¹, GISELA WINCKLER^{*2}

¹AWI, Bremerhaven, Germany

²Lamont-Doherty Earth Observatory, Columbia University, Palisades, NY, USA

³Leibniz Institute for Baltic Sea Research, Rostock-Warnemünde, Germany

⁴GNS Science, Lower Hutt, New Zealand

⁵School of Earth and Ocean Sciences, Cardiff University, Cardiff, CF10 3AT, UK

⁶British Antarctic Survey, Cambridge, UK

⁷University of Hamburg, Germany

⁸COPAS/IDEAL, University of Concepción, Concepción, Chile

⁹Max-Planck-Institut für Chemie, Mainz, Germany

¹⁰University of Bergen, Norway

¹¹GEOMAR Helmholtz-Zentrum für Ozeanforschung, Kiel, Germany

¹²ICBM, University of Oldenburg, Germany

¹³ISMAR/CNR - Institute of Marine Sciences, Bologna, Italy

¹⁴Oregon State University, Corvallis, USA.

The Antarctic Circumpolar Current (ACC) is the world's strongest zonal current system that connects all three major ocean basins of the global ocean, and therefore integrates and responds to global climate variability. Its flow is largely driven by strong westerly winds and constricted to its narrowest extent in the Drake Passage (DP). Transport of fresh and cold surface and intermediate water masses through the DP (cold-water route) strongly affect the Atlantic Meridional Overturning Circulation (MOC) together with the inflow of Indian Ocean water masses (warm-water route). Both oceanographic corridors are critical for the South Atlantic contribution to MOC changes.

In contrast to the Atlantic and Indian sectors of the ACC, and with the exception of drill cores from the Antarctic continental margin and off New Zealand, the Pacific sector of the ACC lacks information on its Cenozoic

paleoceanography from deep-sea drilling records. To advance our knowledge and understanding of Plio/Pleistocene atmosphere-ocean-cryosphere dynamics in the Pacific and their implications for regional and global climate and atmospheric CO₂, IODP proposal DYNAPACC proposes the recovery of 150 to 600 m long, high-resolution Plio/Pleistocene sediment sequences at: (1) Three primary sites located on a cross-frontal transect in the central Pacific between the modern Polar Front (Site CSP-3A) and the Subantarctic Zone (CSP-1A/2A). (2) Three primary and two alternate sites (CHI-1A to CHI-5A) at the Chilean Margin. (3) One site from the pelagic eastern South Pacific (ESP-1A) close to the entrance to the DP. The proposed sites represent a depth transect from ~1000 m at the Chilean margin (CHI-4A) to >5000 m in the Bellingshausen Sea (CSP-3A) and therefore allow to investigate Plio/Pleistocene changes in the vertical structure of the ACC – a key issue for understanding the role of the Southern Ocean in the global carbon cycle. All of the 9 proposed primary and alternate sites were surveyed with seismic lines in 2009/2010 and most recently in 2016. The proposed sites are located at latitudes and water depths where sediments will allow the application of a wide range of siliciclastic, carbonate, and opal-based proxies to address our objectives of reconstructing, with unprecedented stratigraphic detail, surface to deep ocean variations and their relation to atmosphere and cryosphere changes through stadial-to-interstadial, glacial-to-interglacial and warmer than present time intervals.

The overall goal of DYNAPACC is to improve our knowledge of Plio/Pleistocene atmosphere-ocean-ice-sheet dynamics of the ACC in the Pacific and their implications for regional and global climate and atmospheric CO₂ based on sediment records with unprecedented resolution. We test two major hypotheses:

(A) ACC dynamics and Drake Passage (DP) throughflow conditioned the global Meridional Overturning Circulation (MOC) and high-low climate linkages on orbital and sub-millennial time-scales since the Pliocene: - We will quantify the potential role of the DP throughflow (cold-water route) compared to the Agulhas leakage (warm-water route) in driving changes in global MOC on glacial-interglacial and millennial time-scales. - Changes in the ACC transport through the DP strongly affect the inter-basin water mass exchange in the Southern Ocean and the high-low latitude exchange within the Pacific Eastern Boundary Current system.

(B) Variations in the Pacific ACC determine the physical and biological characteristics of the oceanic carbon pump and atmospheric CO₂: - Atmosphere-ocean-cryosphere interactions and teleconnections between high and low latitudes provide the major link between Antarctica and the low-latitudes. These interactions are believed to control sea-ice cover, AIS dynamics, upper ocean stratification, biological nutrient utilization, and exposure rates of deep-water. - We will test to which extent processes found to be active in the Atlantic sector can be translated to the Pacific sector, thus allowing to construct a more global picture of the SO's role in nutrient distribution, biogenic export production and their impact on CO₂ variations.

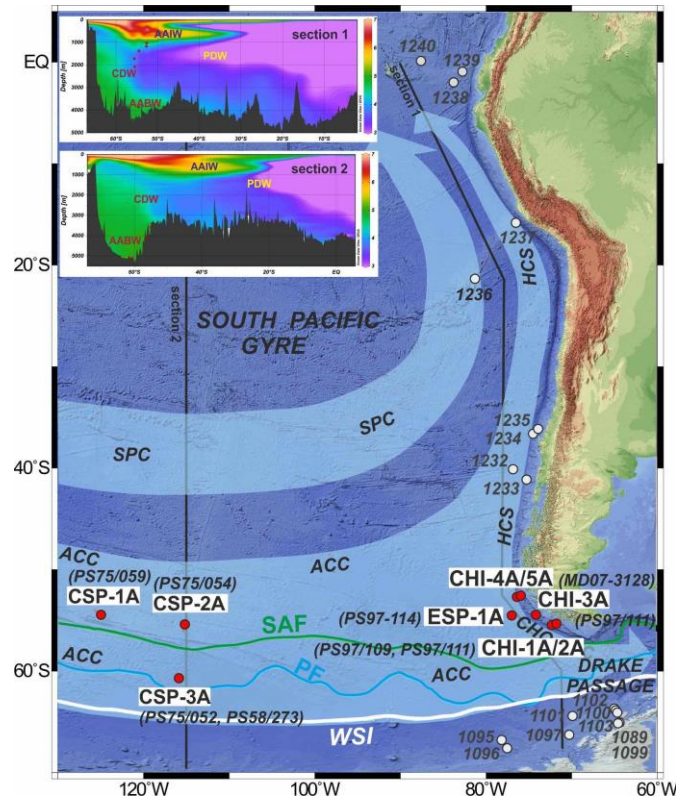


Figure 1: Map showing the location of the proposed drilling sites in the Pacific ACC (CSP, ESP, and CHI proposed sites with site survey cores; red dots) and of previously collected cores during various expeditions in the eastern Pacific referred to in text (white dots; ODP Leg 202 Sites 1232–1240; ODP Leg 178 Sites 1095–1102) in context of the modern oceanography. WSI=winter sea-ice; SAF=Subantarctic Front; dotted lines show inferred LGM positions; SPC= South Pacific Current; HCS= Humboldt Current System; HCH= Cape Horn Current. Small inset figures show vertical water mass structure along two transects in the central and eastern South Pacific (oxygen content; AABW=Antarctic Bottom Water; AAIW=Antarctic Intermediate Water; CDW=Circumpolar Deep Water; PDW=Pacific Deep Water).

The geographic locations and water depths of the proposed sites allow addressing: (i) To compare the dynamics of the ACC laterally between the CSP in vicinity of the East Pacific Rise (bathymetric constraints) and the ESP before entering DP. (ii) To investigate the vertical structure of the ACC. The proposed sites sample the major water masses of the ACC in the Pacific sector of the SO from Antarctic Intermediate Water (AAIW; Sites CHI-4A and 5A) across the Circumpolar Deep Water/Pacific Deep Water (CDW/PDW; Sites CSP-1A, 2A) and potentially down to Antarctic Bottom Water (AABW; Sites CSP-3A and ESP-1A) (at least for glacial times).

ICDP

Imaging the Alpine Fault: preliminary results from a detailed 3D-VSP experiment at the DFDP-2 drill site in Whataroa, New Zealand

V. LAY¹, S. BUSKE¹, J. TOWNEND², R. KELLETT³, M. SAVAGE², J. ECCLES⁴, D. SCHMITT⁵, A. CONSTANTINOU⁶, M. BERTRAM⁷, K. HALL⁷, D. LAWTON⁷, A. GORMAN⁸, AND DFDP WHATARO A 2016 SCIENCE TEAM

¹ Institute of Geophysics and Geoinformatics, TU Bergakademie Freiberg, 09596 Freiberg

² Victoria University Wellington, Wellington, New Zealand

³ GNS Science, Lower Hutt, New Zealand

⁴ University of Auckland, Auckland, New Zealand

⁵ University of Alberta, Edmonton, Canada

⁶ Schlumberger, London, United Kingdom

⁷ University of Calgary, Calgary, Canada

⁸ University of Otago, Dunedin, New Zealand

The plate-bounding Alpine Fault in New Zealand is an 850 km long transpressive continental fault zone that is late in its earthquake cycle. The Deep Fault Drilling Project (DFDP) aims to deliver insight into the geological structure of this fault zone and its evolution by drilling and sampling

the Alpine Fault at depth (Townend et al., 2009). Previously analysed 2D reflection seismic data image the main Alpine Fault reflector at a depth of 1.5-2.2 km with a dip of approximately 48° to the southeast below the DFDP-2 borehole (Lay et al., 2016). Additionally, there are indications of a more complex 3D fault structure with several fault branches which have not yet been clearly imaged in detail.

For that reason we acquired a 3D-VSP seismic data set at the DFDP-2 drill site in January 2016 (Townend et al., 2016). A zero-offset VSP and a walk-away VSP survey were conducted using a Vibroseis source. Within the borehole, a permanently installed “Distributed Acoustic Fibre Optic Cable” (down to 893 m) and a 3C Sercel slimwave tool (down to 400 m) were used to record the seismic wavefield. A first analysis of both borehole data sets shows a good correlation of both recording systems (Constantinou et al., 2016). Furthermore, the velocity features coincide with results obtained previously from borehole logging.

In addition, various receiver systems recorded the seismic wavefield at the surface: (i) an array of 160 three-component receivers, moved successively along the valley during the survey, (ii) two lines of 400 Aries vertical-component receivers parallel to source lines, (iii) five Reftek stations and (iv) a small-aperture far-offset vertical-component geophone array.

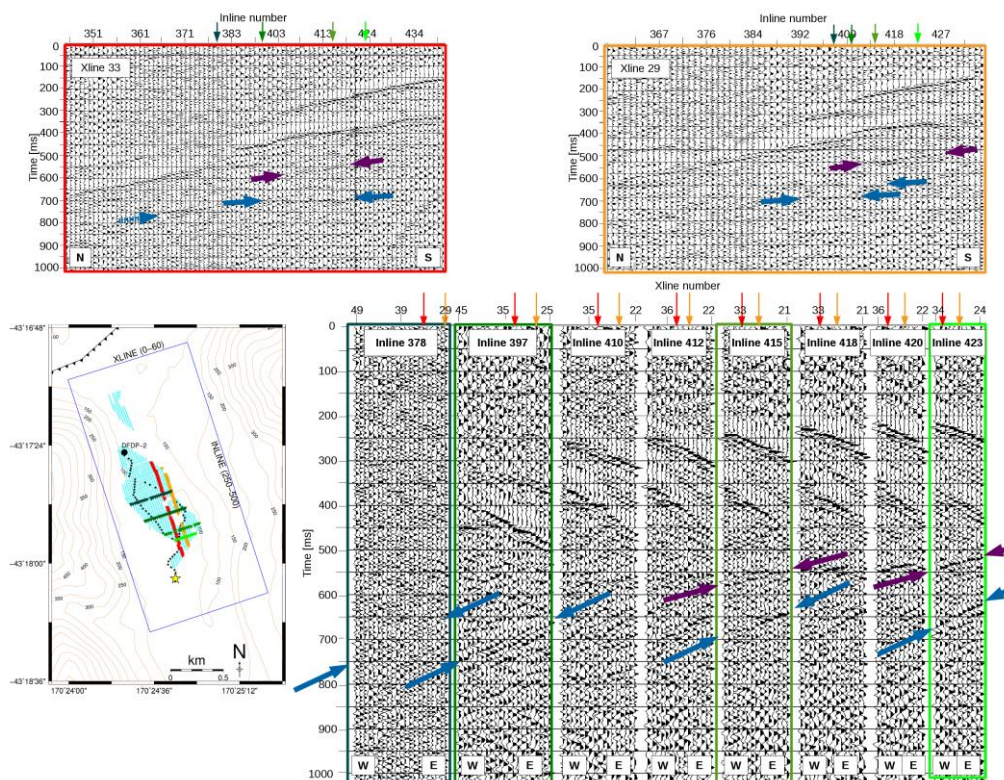


Figure 1: First results showing the 3D character of reflections identified on the dense 3C receiver array.

In the following, we will discuss the data set for the three-component receiver array in more detail. First, the receivers were widely distributed within the Whataroa valley during the multi-offset source lines. This data set is used to verify and improve the existing velocity model derived from a previously acquired 2D reflection line (Lay et al., 2016). First results of the detailed 3D tomographic velocity model building indicate the influence of the 3D valley structure but need to be investigated in more detail.

Second, a source loop with 71 different source locations was acquired with a total of 3502 sweeps. The 160 receivers were set up as an array with a spacing of 10 m perpendicular and 20 m parallel to the main strike of the Alpine Fault. The whole array was moved successively along the valley twelve times to record reflections from the main Alpine Fault zone over a broad depth range. Altogether, 1916 receiver locations were recorded for the 71 source locations. Thus, the detailed 3C array densely covers an area within Whataroa valley of approximately 1800 m inline along the river (i.e., perpendicular to the fault strike) and 600 m crossline perpendicular to the river (i.e., parallel to the fault strike).

First simple data processing results shows clear reflections on both inline and crossline profiles. Correlating single reflection events enables us to identify the origin of reflections recorded in the data and reveal their 3D character. Already preliminary interpretations from this array data set reveal strong evidence for reflections coming presumably from the steeply dipping valley flanks along the Whataroa river side, possibly from the valley flanks.

In Figure 1, data for the most southern source location (marked by a yellow star) is shown on two lines along the river (marked in red and orange) and at several perpendicular lines (marked in green). Identified reflections that coincide are marked by arrows (blue and violet). For the crosslines (marked in green) the first arrivals are

propagating from west to east, whereas the marked reflections are propagating in opposite direction from east to west. The latter are possibly side reflections originating from the steeply dipping valley flank on the eastern side. Further detailed analysis is ongoing and will help to understand the 3D subsurface structures causing these reflections.

The data will be further analysed using advanced seismic imaging methods to derive a 3D structural image of the valley and the Alpine fault zone at depth. Finally, the results will provide a detailed basis for a seismic site characterization at the DFDP-2 drill site. Since the existing borehole did not intersect the Alpine Fault at depth, detailed seismic images will be of crucial importance for further structural and geological investigations of the architecture of the Alpine Fault zone in this area.

References:

Constantinou, A., D. R. Schmitt R. Kofman, R. Kellett, J. Eccles, D. Lawton, M. Bertram, K. Hall, J. Townend, M. Savage, S. Buske, V. Lay and A. R. Gorman, (2016), Comparison of Fibre Optic Sensor and Borehole Seismometer VSP surveys in a Scientific Borehole - DFDP-2B, Alpine Fault, New Zealand, *SEG Technical Program Expanded Abstracts 2016*: pp. 5608-5612, doi: 10.1190/segam2016-13946302.1

Lay, V., S. Buske, A. Lukács, A. R. Gorman, S. Bannister, and D. R. Schmitt (2016), Advanced seismic imaging techniques characterize the Alpine Fault at Whataroa (New Zealand), *J.Geophys.Res.Solid Earth*, 121, doi:10.1002/2016JB013534

Townend, J., Sutherland, R., and V.G. Toy (2009), Deep Fault Drilling Project Alpine Fault, New Zealand, *Scientific Drilling*, 8, Sept 2009, 75-82, doi: 10.2204/iodp.sd.8.12.2009

Townend, J., J. Eccles, R. Kellett, S. Buske, A. Constantinou, D. Schmitt, M. Bertram, K. Hall, M. Savage, A. Gorman, R. Kofman, A. Benson, V. Lay, A. Gulley, A. McNab, D. Lindsay, C. Hopp, C. Mann, S. B. Bodenbunrg, F. Kleine, P. Lepine, H. Bowman, N. Broderick, L. Capova, D. Lawton; DFDP Seismic Project team, (2016), Whataroa 2016 Seismic Experiment Acquisition Report, *GNS Science Report 2016/36*, GNS Science, Lower Hutt, New Zealand

ICDP

Preliminary results of a seismic pre-site survey at Levinson-Lessing Lake, Northern Siberia

E. LEBAS¹, S. KRASTEL¹, B. WAGNER², R. GROMIG², F. FEDOROV³,
M. MELLES²

¹Institute of Geosciences, University of Kiel, Kiel, Germany

²Institute of Geology and Mineralogy, University of Cologne,
Cologne, Germany

³Arctic and Antarctic Research Institute, St. Petersburg, Russia

The German-Russian PLOT project (Paleolimnological Transect) aims at investigating the climatic and environmental changes in Northern Eurasia during the Late Quaternary, through analysis of sediment records within five lakes (Ladoga, Bolshoye Shuchye, Levinson-Lessing, Taymyr and Emanda). Together with Lake El'gygytgyn (already drilled), they form a 6000 km-long transect that will provide a comprehensive record of the Late Quaternary environmental history of Northern Eurasia. In

2013, a pilot study was carried out at Lake Ladoga, where seismic data and sediment cores have been collected. Analysis of the two datasets contributed to the reconstruction of the sedimentary and tectonic evolution of the lake. Last year, we undertook the third field campaign at Taymyr and Levinson-Lessing Lakes. Here, we present the preliminary results of the seismic survey carried out at Levinson-Lessing Lake only and discuss its potential of an ICDP proposal.

Levinson-Lessing Lake is situated on the northern Taymyr Peninsula in the southern part of the Byrranga Mountains. The lake basin is 15 km long and 1-2 km wide, with a maximum water depth of about 110 m in the central part. The lake catchment covers an area of about 515 km², while the lake itself only covers approximately 25 km². The geomorphological setting of Levinson-Lessing Lake reflects its tectonic origin, which was subsequently reshaped by glacial erosion (Niessen et al., 1999). During past Taymyr Expeditions, a sediment core (PG1228) and a network of seismic reflection data have been collected, respectively, in 1995 and 1996 (Bolshiyarov and

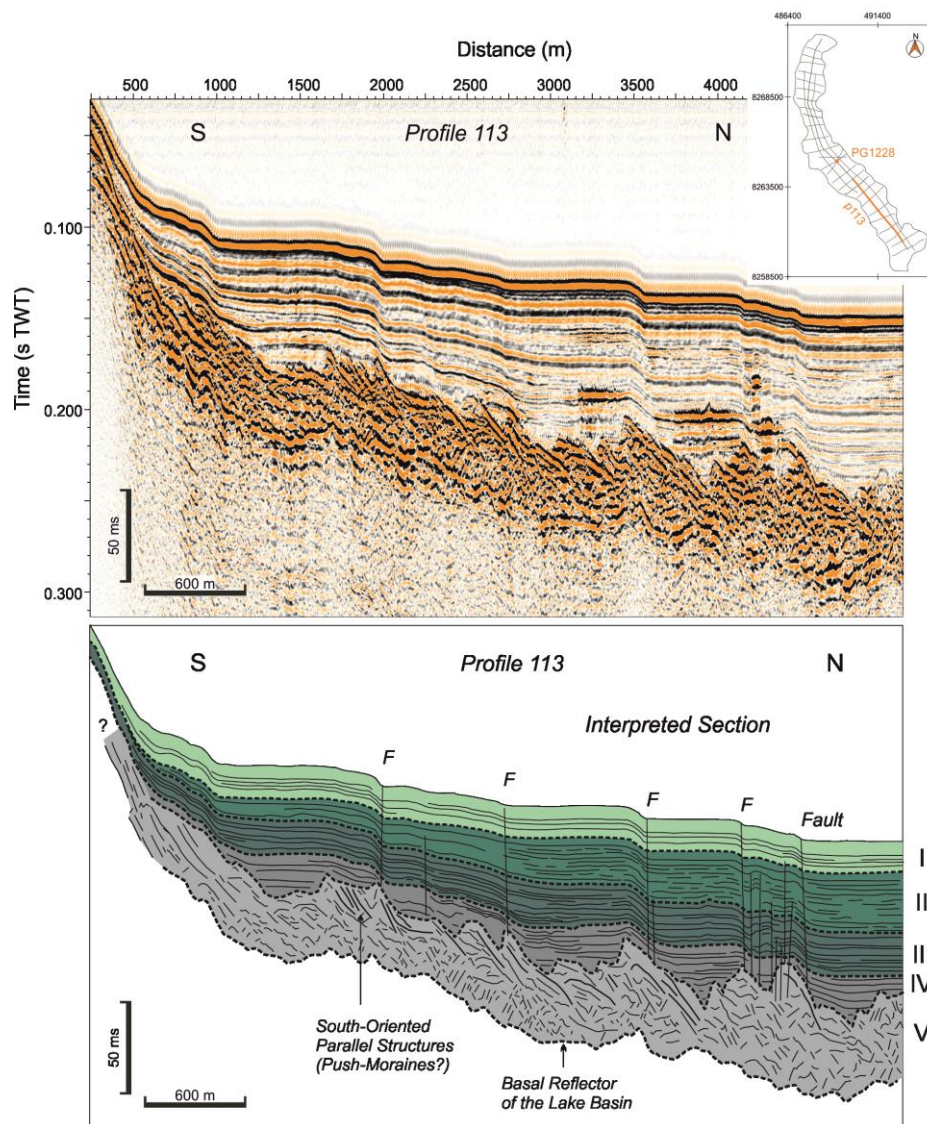


Figure 1: North-south longitudinal seismic profile crossing the southern part of the lake. The five units are represented on the seismic line, of which the four last ones are clearly dissected by faults (F). Note the south-oriented structures interpreted as being presumably push-moraines.

Hubberten, 1996; Melles et al., 1997). Four major seismic units have been identified, none of which have been overconsolidated by glacier ice (Niessen et al., 1999). Description of the sediment core PG1228 revealed a continuous sedimentary history of the lake since the late Middle Weichselian, excluding the occurrence of any major glaciation in the lake's catchment area during that period (Ebel et al., 1999). The authors concluded that the last major glaciation in the lake basin must have occurred earlier than the Mid-Weichselian, presumably during the Early Weichselian.

In summer 2016, we collected new high-resolution seismic reflection profiles using a mini-GI-gun (2*0.1 L) as a source and a 50 m-long streamer (32 channels). We also acquired echosounder data using an Innomar system, providing detailed imaging of the first tens of meters of sediments (up to >20 m). In total, ~70 km of seismic lines have been collected, three of which are north-south longitudinal profiles of 7 to 13 km and 26 are crosslines of 1 to 2 km. This configuration allowed us to capture the deepest sections of the lake, which was not possible with the seismic system used in 1996. The high-resolution of the seismic data allows us to investigate the sediment record of the lake in detail, up to its basement. Five major seismic units have been identified based on the data (Figure 1) and correspond, from top to bottom to: (1) *unit I*, which displays high-amplitude, well-bedded, continuous reflectors, showing a relatively constant thickness of ~0.017 s TWT (~13 m) within the entire lake; (2) *unit II*, which displays a higher frequency, medium- to high-amplitude, discontinuous reflectors, with a maximum thickness of ~0.04 s TWT (~30 m) in the central part of the lake; (3) *unit III*, which is characterized by low frequency, low- to medium-amplitude, bedded, continuous reflectors, of which the maximum thickness is also found in the central part of the lake with ~0.03 s TWT (~22 m); (4) *unit IV*, which also shows low- to medium-amplitude, bedded, continuous reflectors, with a maximum thickness of ~0.05 s TWT (~40 m); and (5) *unit V*, which displays high-amplitude, chaotic reflections of variable thickness, up to ~0.09 s TWT (>75 m). In total, >100 m of sediments document the sedimentary history of the lake. The seismic character of the unit V lead us to interpret the unit as tills/sand deposits, presumably moraine, as documented by the parallel, south-oriented structures identified in the southern part of the lake (Figure 1) that can be regarded as push-moraines formed during the advance or readvance of the ice sheet. Although we acknowledge that there are significant uncertainties involved in applying a single sedimentation rate across the entire lake, an initial indication of the relative age of the unit V can be given from the sediment core PG1228. As an age of ~30,000 ka has been proposed for the base of the core PG1228 (Ebel et al., 1999), a maximum age of ~130 ka can be inferred for the Unit V, suggesting a deposition during the Saalian. The sediment cores we will acquire this spring, in the frame of the fourth PLOT field campaign, will provide better age constraints for the Unit V (i.e. Saalian or Early Weichselian). Recent tectonic activity is also observed in the seismic data and confirmed by the Innomar data. Most of the identified faults are located in the central and southern part of the lake, whilst the northern part of the lake is mainly characterized by gas-bearing sediments.

Levinson-Lessing Lake has a potential for an ICDP drilling campaign, especially if a Saalian age is confirmed for the unit V by the new sediment cores. Such initiative would permit: (1) to identify the kinematics and deformation mechanisms related to the advance, potentially readvances and retreat of the ice-sheet on the lake basement, preexisting material and tills/sand; (2) to provide information on the dynamic of the ice sheet in the northern Taymyr Peninsula; (3) to obtain a continuous record containing information on climate changes in Northern Eurasia presumably since the Saalian; and (4) to unravel the tectonic history of the lake and estimate the rate of displacement of the faults identified in the lake.

References:

- Bolshiyarov and Hubberten (1996) Russian-German Cooperation: The Expedition TAYMYR 1995 and the Expedition KOLYMA 1995 of the ISSP Pushchino Group, Ber. Polarforsch. 211.
- Ebel et al. (1999) Laminated Sediments from Levinson-Lessing Lake, Northern Central Siberia – A 30,000 Year Record of Environmental History? Land Ocean System in the Siberian Arctic: Dynamics and History, (H Kassens, H A Bauch, I Dmitrenko, H Eicken, H-W Hubberten, M Melles, J Thiede, L A Timokhov, eds), Lecture notes in earth science, Springer, Berlin, pp. 425-435.
- Melles et al. (1997) Russian-German Cooperation: The Expedition TAYMYR / SEVERNAYA ZEMLYA 1996, Ber. Polarforsch. 237.
- Niessen et al. (1999) High-Resolution Seismic Stratigraphy of Lake Sediments on the Taymyr Peninsula, Central Siberia. Land Ocean System in the Siberian Arctic: Dynamics and History, (H Kassens, H A Bauch, I Dmitrenko, H Eicken, H-W Hubberten, M Melles, J Thiede, L A Timokhov, eds), Lecture notes in earth science, Springer, Berlin, pp. 437-456.

ICDP

Tephrostratigraphy of the DEEP site sediment record, Lake Ohrid (Albania, FYROM)

N. LEICHER¹, A. FRANCKE¹, B. WAGNER¹, J. JUST¹, G. ZANCHETTA², R. Sulpizio^{3,4}, B. GIACCIO⁵, S. NOMADE⁶

¹ University of Cologne, Institute for Geology and Mineralogy, Zulpicher Str. 49a, 50674 Cologne, Germany

² Dipartimento di Scienze della Terra, University of Pisa, Pisa, Italy

³ Dipartimento di Scienze della Terra e Geoambientali, University of Bari, Bari, Italy

⁴ Istituto per la Dinamica dei Processi Ambientali (IDPA) CNR, Milan, Italy

⁵ Istituto di Geologia Ambientale e Geoingegneria, CNR, Roma, Italy

⁶ Laboratoire des sciences du climat et de l'environnement, CEA/CNRS/UVSQ, Gif-Sur-Yvette, France

Lake Ohrid, located on the Balkan Peninsula, is one of the very few lakes in the world that provides a continuous and high-resolution record of the environmental history of at least the last 1.3 Ma. The sedimentary archive was drilled in spring 2013 within the scope of the International Continental Scientific Drilling Program (ICDP) and the Scientific Collaboration on Past Speciation Conditions in Lake Ohrid (SCOPSCO) project in order to investigate local and regional geological and paleoclimatic processes, as well as triggers of evolutionary patterns and endemic biodiversity. This abstract is part of the DFG-ICDP project "SCOPSCO - sedimentstratigraphy, tephrostratigraphy and chronostratigraphy" (WA 2109/13) and reports on the actual tephrostratigraphic progress.

The continuous composite profile (584 m) of the main drill site DEEP was logged (XRF, MSCL) and subsampled for biogeochemical (TIC, TOC, TN, TS) and

sedimentological (grain size) analyses. The lithology of the DEEP site indicates that the history of Lake Ohrid can roughly be separated into two parts, with the lower section between 584 and 450 m sediment depth being characterised by a sedimentary facies indicating shallow water conditions, which persisted likely before ca. 1.3 Ma. Together with geotectonic, seismic, and biological information, the data imply that the Ohrid basin formed by transtension during the Miocene, opened during the Pliocene and Pleistocene, and that the lake established between 1.9 and 1.3 Ma ago. Since then or in the upper 450 m sediment depth, biogeochemical and sedimentological proxy data indicate pelagic sedimentation which corresponds with global glacial/interglacial variability, with warm periods being characterized by high TIC and TOC concentrations and cold periods by negligible TIC and low TOC contents, respectively. More information about the sedimentology and paleoclimatology can be found in Francke et al. this issue.

To date, 56 tephra horizons have been identified in the upper 450 m of this sequence, focussing mainly on the macroscopic tephra layers (48). The number of cryptotephra horizons (8) is likely much higher, but detailed cryptotephra studies have not been conducted at the DEEP site so far. Major element analyses (SEM-EDS/WDS; see Leicher et al. 2016 for details) on juvenile glass fragments from all studeid tephra horizons suggest an volcanic origin exclusively from Italian volcanic provinces.

Despite the recent efforts (e.g. the investigations of mid-distal records from various Italian continental basins, such as Sulmona, Fucino, Acerno, Mercure, or Montalbano Jonico) the knowledge of the Early and Middle Pleistocene tephrostratigraphy is still relatively poor. Active volcanic centres during this time, covering one of the periods when the Italian Quaternary explosive volcanism was most active, include: the Cimini, Vulcini, Vico, Sabaitini, Colli Albani, Ernici-Roccamonfina, Pontine Islands, Vulture, and unknown-Campanian volcanoes. To date, there are only two other continuous records in the Mediterranean region besides the Lake Ohrid record, covering the entire Middle and parts of the Early Pleistocene. These two other archives are the Calabrian Ridge core KC01B (Lourens 2004; Insinga et al. 2014) and the peat record from Tenaghi Philippon, Greece (St. Seymour et al. 2004; Tzedakis et al. 2006; Pross et al. 2015). However, the published tephrostratigraphies of these records are limited to the late Middle Pleistocene (max. ca. 192 ka).

Sixteen tephra horizons have been identified within the DEEP site sequence between 450 and 248 mcd (ca. 1.3 - 0.64 Ma) and are the subject of on-going investigations aimed at identifying their specific volcanic sources and equivalent known tephra by using geochemical fingerprinting of glass fragments. Since the knowledge of tephrostratigraphy for this period is very restricted, only one tephra layer could be correlated with a dated eruption so far. This tephra, OH-DP-2669, is located 266.9 mcd and can be correlated with the Parmenide ash, found in a very similar climatostratigraphic position in the Sulmona basin and the Montalbano Jonico section and dated to 724 ± 1.6 ka (Giaccio et al., 2013) and 719.5 ± 12.6 ka (Ciaranfi et al., 2010), respectively, i.e., at the MIS17/18 boundary.

A combination of tephrostratigraphical with paleomagnetic information will improve the stratigraphic control of the older section of the DEEP Site. The Brunhes/Matuyama (B/M) boundary was identified at 283 m close to the two tephra layers OH-DP-2869 and OH-DP-2898. Geochemical fingerprinting will reveal, whether these tephra layers can be correlated to tephra layers found close to the B/M boundary e.g. in the Sulmona record.

Because of an diagenetic overprint of the paleomagnetic data of the DEEP site sequence, the top of the Jaramillo was not clearly pin-pointed, but occurs within 347-336 m. However, the base of the Jaramillo is recorded very sharply at 373 m. Further higher resolution paleomagnetic measurements are subject of ongoing work and will help to determine the precise position of the paleomagnetic boundaries and will also enable to reconstruct the dynamics of the Earth's Magnetic Field geometry and strength during polarity transitions. This multi-method dating approach will provide a robust chronology of the core, which is the backbone to fulfil the major aims of the SCOPSCO project and was successfully applied in the upper part of the succession. The tephrostratigraphic record covering the uppermost 247.8 mcd (MIS 1-15) of the DEEP site contains 13 well identified and correlated tephra layers of known and dated widespread eruptions (Leicher et al., 2016 and references therein). Existing $^{40}\text{Ar}/^{39}\text{Ar}$ ages of these eruptions were re-calculated by using the same flux standard (1.194 Ma for ACs, which corresponds to FCs at 28.02 Ma) in order to obtain a consistent set of ages. The chronological information of 11 of these well-identified tephras (1st order tie points) was complemented by tuning of biogeochemical proxy data to orbital parameters for a detailed age-depth model for the upper 247.8 m of the DEEP site sediments covering the time window between 637 ka and present day (Francke et al., 2016).

References:

- Ciaranfi, N., Lirer, F., Lirer, L., Lourens, L. J., Maiorano, P., Marino, M., Petrosino, P., Sprovieri, M., Stefanelli, S., Brilli, M., Girone, A., Joannin, S., Pelosi, N., and Vallefucio, M.: Integrated stratigraphy and astronomical tuning of Lower-Middle Pleistocene Montalbano Jonico section (Southern Italy), *Quaternary International*, 219, 109-120, 2010.
- Francke, A., Wagner, B., Just, J., Leicher, N., Gromig, R., Baumgarten, H., Vogel, H., Lacey, J. H., Sadori, L., Wonik, T., Leng, M. J., Zanchetta, G., Sulpizio, R., and Giaccio, B.: Sedimentological processes and environmental variability at Lake Ohrid (Macedonia, Albania) between 637 ka and the present, *Biogeosciences*, 13, 1179-1196, 2016.
- Giaccio, B., Castorina, F., Nomade, S., Scardia, G., Voltaggio, M., and Sagnotti, L.: Revised Chronology of the Sulmona Lacustrine Succession, Central Italy, *Journal of Quaternary Science*, 28, 545-551, 2013.
- Insinga, D. D., Tamburrino, S., Lirer, F., Vezzoli, L., Barra, M., De Lange, G. J., Tiepolo, M., Vallefucio, M., Mazzola, S., and Sprovieri, M.: Tephrochronology of the astronomically-tuned KC01B deep-sea core, Ionian Sea: insights into the explosive activity of the Central Mediterranean area during the last 200 ka, *Quaternary Science Reviews*, 85, 63-84, 2014.
- Leicher, N., Zanchetta, G., Sulpizio, R., Giaccio, B., Wagner, B., Nomade, S., Francke, A., and Del Carlo, P.: First tephrostratigraphic results of the DEEP site record from Lake Ohrid (Macedonia and Albania), *Biogeosciences*, 13, 2151-2178, 2016.
- Lourens, L. J.: Revised tuning of Ocean Drilling Program Site 964 and KC01B (Mediterranean) and implications for the $\delta^{18}\text{O}$, tephra, calcareous nannofossil, and geomagnetic reversal chronologies of the past 1.1 Myr, *Paleoceanography*, 19, PA3010, 2004.
- Pross, J., Christanis, K., Fischer, T., Fletcher, W. J., Hardiman, M., Kalaitzidis, S., Knipping, M., Kotthoff, U., Milner, A. M., and Muller, U. C.: The 1.35-Ma-long terrestrial climate archive of Tenaghi Philippon, northeastern Greece: Evolution, exploration, and perspectives for future research, *Newsletters on Stratigraphy*, 2015, 2015.
- St. Seymour, K., Christanis, K., Bouzinos, A., Papazisimou, S., Papatheodorou, G., Moran, E., and Denes, G.: Tephrostratigraphy and tephrochronology in the Philippi peat basin, Macedonia, Northern Hellas (Greece), *Quaternary International*, 121, 53-65, 2004.
- Tzedakis, P. C., Hooghiemstra, H., and Palike, H.: The last 1.35 million years at Tenaghi Philippon: revised chronostratigraphy and long-term vegetation trends, *Quaternary Science Reviews*, 25, 3416-3430, 2006.

DFG

Calibration of the coral Sr/Ca thermometer with in situ and satellite SST of open ocean and lagoonal settings in the tropical Indian Ocean – implications for fossil corals

M. LEUPOLD¹, M. PFEIFFER¹, D. GARBE-SCHÖNBERG²¹ RWTH Aachen University, Geological Institute, Wuellnerstr. 2, 52056 Aachen, Germany² Institute of Geosciences, Christian-Albrechts-University, Ludewig-Meyn-Str. 10, 24148 Kiel, Germany

Tropical corals can be used to reconstruct past changes of environmental parameters such as sea surface temperature (SST), rainfall and nutrient content by measuring Sr/Ca and $\delta^{18}\text{O}$ ratios (e.g. Gagan et al., 1998; Evans et al., 2000; Zinke et al., 2004; Pfeiffer et al., 2006), which has already been successfully applied to several fossil corals retrieved by IODP campaigns (e.g. Felis et al., 2012). To estimate past SST seasonality, a workable calibration of the coral Sr/Ca thermometer with temperature data sets is indispensable. However, for most studies local SST data was not available and larger-scale SST data sets were used. As there may be large differences in SST at different reef sites, it is important to calibrate coral data with SST recorded from the same site to estimate the spatial variability of SST within a reef setting.

Here, we calibrate two modern coral core tops drilled from living massive *Porites* corals from two different settings – open ocean and lagoonal setting – at Chagos, an archipelago in the tropical Indian Ocean. We use in-situ logger data and the now available high resolution satellite temperature products to evaluate the coral Sr/Ca thermometer. The in-situ logger temperature confirms the satellite data, and both settings reveal significant differences in seasonal amplitudes: Whereas the maximum amplitude of the satellite temperature for the period from 2006 to 2011 is 2.6°C in the lagoonal setting, the open ocean setting shows a temperature amplitude of 4.1°C for the same time period. Furthermore, there are repetitive phases of cooler temperatures recorded at the open ocean setting which are missing in the temperature data recorded in the lagoon. Two modern coral core tops drilled next to the temperature loggers were subsampled at a biweekly resolution for trace element analysis. Sr/Ca ratios of each coral powder sample were measured using an ICP-OES.

For each coral core, correlations of the Sr/Ca measurements with satellite data – we used the AVHRR product (Casey et al., 2010) – and in-situ logger data were carried out. The magnitude of the coral Sr/Ca variations at both sites reflects the local temperature variability. The correlation of the satellite data with the coral data from the open ocean setting is high and the slope of the calibration formula lies within the range of slopes of Sr/Ca vs. SST calibrations listed in Corregè (2006). In contrast, the small seasonal temperature amplitudes of the lagoonal setting prevent a high correlation of the coral temperature with both satellite and in-situ logger data. The Sr/Ca signal is relatively noisy. This shows that the reef setting has a tremendous effect on the temperature variability recorded by the coral Sr/Ca thermometer, and this should be taken into account when interpreting fossil corals. Our results suggest that the new very high resolution satellite

temperature products can be used to evaluate the reef-scale temperature variability and to evaluate the Sr/Ca measurements of fossil corals as an indicator for large-scale SST variability.

References:

- Casey, K.S., Brandon, T.B., Cornillon, P., & Evans, R. (2010): "The Past, Present and Future of the AVHRR Pathfinder SST Program", in *Oceanography from Space: Revisited*, eds. V. Barale, J.F.R. Gower, and L. Alberotanza, Springer. DOI: 10.1007/978-90-481-8681-5_16
- Corregè, T. (2006): Sea surface temperature and salinity reconstruction from coral geochemical tracers. *Palaeogeography, Palaeoclimatology, Palaeoecology*, 232(2), 408-428.
- Evans, M.N., Kaplan, A. & Cane, M.A. (2000): Intercomparison of coral oxygen isotope data and historical sea surface temperature (SST): Potential for coral-based SST field reconstructions. *Paleoceanography*, 15, 551-563.
- Felis, T., Merkel, U., Asami, R., Deschamps, P., Hathorne, E.C., Kölling, M., Bard, E., Caboich, G., Durand, N., Prange, M., Schulz, M., Cahyarini, S.Y. & Pfeiffer, M. (2012): Pronounced interannual variability in tropical South Pacific temperatures during Heinrich Stadial 1. *Nature communications*, 3, 965.
- Gagan, M.K., Ayliffe, L.K., Hopley, D., Cali, J.A., Mortimer, G.E., Chappell, J., McCulloch, M.T. & Head, M.J. (1998): Temperature and surface-ocean water balance of the mid-Holocene tropical western Pacific. *Science*, 279, 1014-1018.
- Pfeiffer, M., Timm, O., Dullo, W.-Chr. & Garbe-Schönberg, D. (2006): Paired Sr/Ca and $\delta^{18}\text{O}$ records from the Chagos Archipelago: late 20th century warming affects rainfall variability in the tropical Indian Ocean. *Geology*, 34, 1069-1072.
- Zinke, J., Dullo, W.-Chr., Heiss, G.A. & Eisenhauer, A. (2004): ENSO and Indian Ocean subtropical dipole variability is recorded in a coral record off southwest Madagascar for the period 1659 to 1995. *Earth Planet. Sci. Lett.*, 228, 177-194.

ICDP

Preliminary results of Multichannel Seismic Pre-site Surveys on Lake Prespa suggest a long sedimentary history

K. LINDHORST¹, S. KRASTEL¹, B. SCHRAMM², B. WAGNER³¹ Christian-Albrechts-Universität zu Kiel, Institut für Geowissenschaften, Abteilung Geophysik, Otto-Hahn-Platz 1, 24118 Kiel, Germany, klindhorst@geophysik.uni-kiel.de² Helmholtz-Zentrum für Ozeanforschung, Kiel, Germany³ Institute für Geologie und Mineralogie, Universität Köln, Germany

Lake Prespa is located on the Balkan Peninsula and is a transboundary lake shared by the Former Yugoslav Republic of Macedonia, Albania, and Greece. Lake Prespa is the sister lake of Lake Ohrid where a successful ICDP drilling campaign (SCOPSCO) took place in 2013 (Wagner et al., 2014). The lake is located 10 km to the east of Lake Ohrid at an altitude of 849 m above sea level. Lake Prespa has a surface area of 254 km², a catchment area of 1300 km², a maximum water depth of only 48 m (mean water depth 14 m), and a volume of 3.6 km³. It has no surface outlet but it loses water through evaporation (52%), irrigation (2%), and through karst aquifers (46%), which provide a direct connection to the 150 m lower Lake Ohrid. Both lakes have been formed tectonically in a late phase of the Alpine orogeny, which makes them unique sites to study the paleo-environmental history of the Mediterranean region. Lake Prespa is much shallower than Lake Ohrid and thus has probably been more vulnerable to lake fluctuations and even desiccation at various times in the past. Their differing geological histories might explain differences in extant faunas despite their hydrological connection via karst aquifers (Wilke et al., 2010).

Several acoustic pre-site surveys using a sediment echosounder were carried out since 2007 and image the upper 20 m of the lake subsurface in great detail (e.g. Wagner et al., 2012). A shallow plateau at a water depth of around 13 m forms the central part of Lake Prespa. The overall structure forms a contourite drift body. Trench-like depressions up to 12 km long (Anovska et al., 2008) can be found at the western and southwestern side with maximum water depth of 32 m. In general, a seismic survey on Lake Prespa is challenging for several reasons. First of all, the limited infrastructure around Lake Prespa, which makes it difficult to launch a reasonable-sized vessel in the lake and secondly seismic processing is difficult due to the shallow water depth and the occurrence of multiples. Only since 2015 a research vessel mainly for investigating the hydrobiology of Lake Prespa has been installed at the shoreline of Stenje. Attempts to collect (multichannel) seismic data on Lake Prespa were made for the first time in 2008, when a multichannel seismic system using a Mini-GI airgun as source and a short streamer were operated from small fishing boats. However, due to a failure of the recording unit no data were collected. A second seismic survey was carried out in 2013 after the successful drilling campaign at Lake Ohrid in spring. Several profiles of single channel seismic data were collected. This data showed that it is essential to use a multichannel device with a reasonable offset of at least 20 m in order to reduce multiple reflections on seismic lines caused by the shallow water depth of Lake Prespa. In September 2015 a third seismic campaign took place acquiring seismic profiles covering the northern part of Lake Prespa as well as some parts on the Albanian part of the lake. A Mini-GI-Gun (0.251) was towed 10.4m behind a catamaran. The data was received by two 12.5 m long segments of a Geometrics GeoEel Streamer that was towed about 9.5 m behind the boat. Two small diving compressors provided air with pressures of 100 to 120 bars and so a shot interval of 8 s could be achieved.

The interpretation of the seismic data suggests that Lake Prespa is a valuable archive for a long sediment record. Due to the shallow water depth of Lake Prespa we had to put some effort in minimizing multiple reflections in order to reveal sediment structures in a subsurface depth larger than 50 m. One attempt was made to use a Multiple suppression tool during the processing procedure of the seismic data. However, the short offset with a the streamer length of only 25 m impede to separate multiples based on their seismic velocity. We applied a Multiple attenuation tool (SRME - Surface Related Multiple Elimination) provided by VISTA Desktop Seismic data processing software. It predicts multiple reflections and subtracts them from the initial data set. Results show that we are able to suppress the upper most multiples reasonably, enabling us to interpret our seismic data in depth > 50 m. A second attempt to interpret deeper structures was made by predicting multiple reflections simply by multiplying the lake floor and the upper most reflections by two. By highlighting multiples on seismic cross section one can separate them from structures that are real within the subsurface. At the end we were able to identify some reflections that are assigned to sediments at about 300 to 350 m depth. This would imply that Lake Prespa also existed for a long time period and could provide a valuable archive for a continental sediment record.

References:

- Anovska, E., Jovcev, Z., Anovski, K., Stojmenovska, I., Milevski, J., Popov, V. and Anovski, T., 2008. Study on the relationship between the water level of the Prespa Lake and its volume. *Natura Montenegrina*, Podgorica, 7(3): 493-502.
- Wagner, B., Aufgebauer, A., Vogel, H., Zanchetta, G., Sulpizio, R. and Damaschke, M., 2012. Late Pleistocene and Holocene contourite drift in Lake Prespa (Albania/FYR of Macedonia/Greece). *Quaternary International*, 274: 112-121.
- Wagner, B., Wilke, T., Krastel, S., Zanchetta, G., Sulpizio, R., Reicherter, K., Leng, M., Grazhdani, A., Trajanovski, S., Francke, A., Lindhorst, K., Levkov, Z., Cvetkoska, A., Reed, J., Zhang, X., Lacey, J., Wonik, T., Baumgarten, H. and Vogel, H., 2014. The SCOPSCO drilling project recovers more than 1.2 million years of history from Lake Ohrid. *Scientific Drilling*, 17: 19-29.
- Wilke, T., Schultheiß, R., Albrecht, C., Bornmann, N., Trajanovski, S. and Kevrekidis, T., 2010. Native *Dreissena* freshwater mussels in the Balkans: in and out of ancient lakes. *Biogeosciences*, 7(10): 3051-3065.

IODP

The Atlantic Deep Circulation During the Past One Million Years

J. M. LINK^{1,2}, P. BLASER¹, J. LIPPOLD^{2,3}, M. GUTJAHR⁴, F. PÖPPELMEIER^{1,2}, A. H. OSBORNE⁴, E. BÖHM^{1,5}, M. FRANK⁴, O. FRIEDRICH², N. FRANK^{1,2}

¹ Institute of Environmental Physics, Heidelberg University, Germany

² Institute of Earth Sciences, Heidelberg University, Germany

³ Institute of Geological Sciences and Oeschger Center for Climate Change Research, University of Bern, Switzerland

⁴ GEOMAR, Helmholtz Centre for Ocean Research, Kiel, Germany

⁵ Laboratory for Climate and Environmental Sciences, Gif-sur-Yvette, France

The Atlantic Meridional Overturning Circulation (AMOC) is a key player in the global climate system due to its large contribution regarding matter and heat transport across the hemispheres. Neodymium isotopes stored in the authigenic fraction of deep Atlantic sediments have been proven valuable tools to reconstruct past circulation patterns. They trace the provenance of water masses, as the continental Nd isotopic composition, which is varying depending on the Sm/Nd ratio and the age of the crust, is imprinted into the ocean. Therefore different water masses can be distinguished (van de Flierdt et al., 2016).

In this project we investigate the process of water mass competition in the deep North Atlantic over the past one million years aiming at millennial resolution to reconstruct the long term evolution of deep water across numerous climate cycles. Moreover, we intend to retrieve the long term frequency of changes and possibly even discover yet unrecorded Dansgaard/Oeschger events from deep sea sediments. The latter seems possible as a previous study has revealed a strong link between deep water Nd isotope composition and D/O events during the past 150 ka (Böhm et al., 2015). The site of choice is the deep sea sediment core at ODP Leg 172 Site 1063 (33°41'N, 57°37'W, 4584m water depth), where measurements of authigenic Nd isotopes in Fe/Mn-leachates have successfully traced changes of deep water provenance related to millennial climate variability (Böhm et al., 2015). Moreover, our first results, using the improved leaching method of Blaser et al. (2016), have revealed a unique pattern across glacial terminations. So far, we have accomplished Nd records

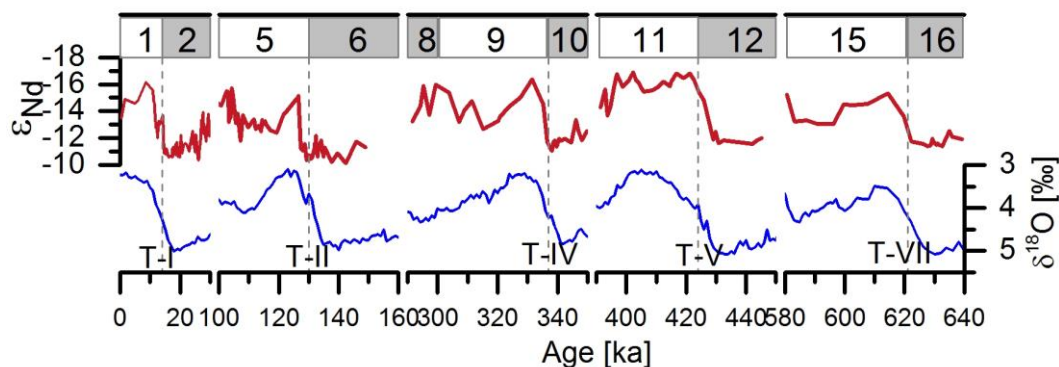


Figure 1: Evolution of the Nd isotopic composition at the Bermuda Rise for glacial terminations I, II (Roberts et al., 2010; Gutjahr & Lippold, 2011; Böhm et al., 2015), IV, V, and VII compared to the global benthic $\delta^{18}\text{O}$ stack of Lisiecki & Raymo (2005) (Note: truncated scale).

across termination I, II, IV, V, VII, and X, which demonstrate rather constant glacial values ranging between an ϵ_{Nd} value of -11 to -12, contrasting interglacial ϵ_{Nd} variability with values of -13 to -17 (see fig. 1). Hence, the previously observed glacial-interglacial water mass competition is a persistent feature at the Bermuda Rise at least for the past 640 kyr.

While most glacial terminations and their following interglacial reveal a similar pattern with a south-north shift in the provenance of water masses, T-V and MIS 11 stand out. Compared to the other interglacials, more unradiogenic ϵ_{Nd} are recorded during MIS 11, which also lasted for the entire interglacial for almost 30 kyr. This observation agrees with the ϵ_{Nd} retrieved from uncleaned planktic foraminifera. Such an extreme isotopic composition has previously been documented only during rapid climate warmings of the last glacial period (Böhm et al., 2015). Since the continents surrounding the Labrador Sea are an important source for unradiogenic Nd, the here traced low ϵ_{Nd} values are most likely indicative of a stronger influence of the Labrador Sea in the Bermuda Rise area during MIS 11, either through enhanced Nd input from weathering of the almost ice-free Greenland (Reyes et al., 2014) and / or intensification of Labrador Sea deep water formation. Overall, MIS 11 stands out as a super-interglacial in terms of North Atlantic deep circulation.

References:

- Blaser, P., Lippold, J., Gutjahr, M., Frank, N., Link, J. M., and Frank, M., 2016, Extracting foraminiferal seawater Nd isotope signatures from bulk deep sea sediment by chemical leaching: *Chemical Geology* 439, p. 189-204.
- Böhm, E., Lippold, J., Gutjahr, M., Frank, M., Blaser, P., Antz, B., Fohlmeister, J., Frank, N., Andersen, M. B., and Deininger, M., 2015, Strong and deep Atlantic meridional overturning circulation during the last glacial cycle: *Nature* 517, p. 73-76.
- Gutjahr, M., and Lippold, J., 2011, Early arrival of Southern Source Water in the deep North Atlantic prior to Heinrich event 2: *Paleoceanography* 26, PA2101.
- Lisiecki, L. E., and Raymo, M. E., 2005, A Pliocene-Pleistocene stack of 57 globally distributed benthic $\delta^{18}\text{O}$ records: *Paleoceanography* 20, PA1003.
- Reyes, A. V., Carlson, A. E., Beard, B. L., Hatfield, R. G., Stoner, J. S., Winsor, K., Welke, B., and Ullman, D. J., 2014, South Greenland ice-sheet collapse during Marine Isotope Stage 11: *Nature* 510, p. 525-528.
- Roberts, N. L., Piotrowski, A. M., McManus, J. F., and Keigwin, L. D., 2010, Synchronous deglacial overturning and water mass source changes: *Science* 327, p. 75-78.
- van de Flierdt, T., Griffiths, A. M., Lambelet, M., Little, S. H., Stichel, T., and Wilson, D. J., 2016, Neodymium in the oceans: a global database, a regional comparison and implications for palaeoceanographic research: *Philosophical Transactions of the Royal Society A: Mathematical, Physical and Engineering Sciences* 374.

IODP

Subduction initiation: petrological and experimental study of fore-arc basalts from the Izu-Bonin-Mariana island arc

S. A. LINSLER¹, R. R. ALMEEV¹, F. HOLTZ¹, R. E. BOTCHARNIKOV¹,
M. V. PORTNYAGIN²

¹Institute of Mineralogy, Leibniz Universität Hannover, Callinstr.
3, 30167 Hannover, Germany

²Helmholtz Centre for Ocean research (GEOMAR), Division of
the Ocean Floor, Wischofstr. 1-3, 24148 Kiel, Germany

The process of subduction is considered as one of the major manifestations of a dynamic Earth. However, little is known about how subduction starts and proceeds. According to one of the first conceptual model of Stern and Bloomer (1992), in the course of subduction initiation, the old and relatively dense oceanic lithosphere begins to sink into the asthenosphere. Lithosphere in the upper plate adjacent to the sinking lithosphere rapidly extends into the gap left as the dense lithosphere sinks. In this setting, mantle flows into the nascent mantle wedge and interacts with a small and variable contribution of fluids from the sinking plate. Melting induced by the fluid augments that resulting from decompression, leading to a higher degree of melting than at mid-ocean ridges. These MORB-like lavas with arc-signatures originating in this setting have been recently termed as *forearc basalts* (FABs, Reagan et al. 2010). Combination of rapid decompression melting with fluid enhanced lowering of the solidus leads to more extensive melting of the shallow asthenospheric wedge, creating refractory Mg-rich and Si-rich lavas such as *boninites* and high-Mg andesites and leaving an extremely refractory harzburgitic residue (Shervais, 2001). Thus, in the Stern-Bloomer model, the presence of boninites at the top of a FAB lava sequence is a major indicator of a subduction-initiation setting (Pearce, 2014). *The knowledge on the main changes in magma origin and magma evolution conditions at the transition from FAB to boninite is crucial to understand the general process of subduction initiation, the role of mantle reorganization and specifics of mantle melting regimes.* In 2014 IODP Expedition 352 successfully recovered 1.22 km of igneous basement of FABs and boninites at four drilling sites (Expedition 352 Scientists, 2015). The expected sequence of FABs

underlain by boninites was not however encountered. In contrast, dikes at the base of FABs (Sites U1440 and U1441) and boninite (Sites U1439 and U1442) sections provided rather an idea of most likely independent conduit systems for FABs and boninite magmas which were offset more horizontally than vertically (Expedition 352 Scientists, 2015).

Here we present our first results from the combined petrological and experimental investigations of the recovered fore-arc basalts. FABs are typically aphyric to sparsely phyrlic, plagioclase-pyroxene-phyric basalts and dolerites. Overall, the whole rock compositions of FAB lavas erupted at Sites U1440 and U1441 are relatively evolved, with most MgO concentrations within the range 5–8 wt%. The differentiation trends obtained from whole rock major element compositions (from basalt to andesite) indicate that all analyzed samples could be potentially derived from a similar parent magma composition. However, microprobe analyses of FABs glasses demonstrate that although they are principally in the range of whole rock compositions, they have slightly higher FeO and systematically lower Al₂O₃, Na₂O and K₂O contents. Results of our phase equilibria simulations conducted for some representative starting compositions indicate on possible variability of primitive FAB magmas which could follow similar but principally different liquid lines of descent in the course of magmatic differentiation. Most evolved glasses from UNIT 6 and intermediate Al₂O₃-enriched glasses from UNIT 13 cannot be produced by the process of fractional crystallization from the magmas parental to those from UNITS 2, 7, 8 and 14. Most primitive FAB magmas from UNIT 3 are too poorer in TiO₂ to be parental for the less evolved magmas from other groups. Our first calculations also demonstrate the generally low-pressure (most likely below 100-200 MPa) character of magma differentiation which proceeded most likely under nearly anhydrous conditions. The anhydrous MORB-like character of the FAB glasses is confirmed by the FTIR analyses of the dissolved H₂O, which ranges from 0.1 to 0.8 wt%. The UNIT13 basaltic glass strongly differs from other FABs showing anomalously high H₂O contents (~2wt%), high Al₂O₃ and low FeO. No fresh or altered olivine was found in FAB in the course of microscopic and microprobe study. Pheno- and subphenocrysts of plagioclase and clinopyroxene compositions are ranging from 86 to 60 in anorthite contents (in mol%) and from 0.86 to 0.53 in mg# number respectively. The interesting and intriguing feature of FABs is a close correspondence of glass compositions sampled at the top (UNIT 2), interior (Units 7 and 8) and bottom (Unit 14) of the site U1440, indicative of the steady state conditions in magma chamber(s).

The petrographic survey of the core samples and phase equilibria calculations allowed us to bracket the conditions of partial crystallization which can be attested in experiments. Two synthetic analogues of the FAB glasses 352-U1440B-12R-2W-67cm and 352-U1440B-24R-1W-13cm (with 8.5 and 7.5 wt% MgO respectively) have been experimentally investigated at 100 MPa under nominally dry conditions in internally heated pressure vessels. Two capsule configurations were used to model unhydrous (<0.1 wt% H₂O) and reduced (FMQ-1) conditions in Pt-lined graphite capsules and low H₂O (~0.6 wt% H₂O) and oxidized (FMQ+0.5) conditions in Fe-presaturated

Au₂₀Pd₈₀ capsules. Experiments at 1175, 1150 and 1125°C revealed the plagioclase and clinopyroxene onset crystallization under both unhydrous and low H₂O conditions with different degrees of crystallization which perfectly fits to the phenocrysts assemblage observed in natural FABs. The experimental liquid lines of descent are in a good agreement with those defined by natural glass compositions. This allows us to conclude that thermodynamic conditions utilized in our experiments (100 MPa; 1175-1125°C; FMQ-1<lgfO₂<FMQ+0.5) can be potentially considered as conditions of partial crystallization of the Units 7-8-14 and 13 FABs. However natural mineral compositions are not fully reproduced (less albitic plagioclase or more magnesian clinopyroxenes). This requires additional experimental tests *e.g.* at higher pressures.

References:

- Expedition 352 Scientists. (2015) IODP Prel. Rept. 352.
- Pearce, J.A. (2014) Immobile Element Fingerprinting of Ophiolites. *ELEMENTS* 10, 101-108.
- Reagan, M.K., et al. (2010) Fore-arc basalts and subduction initiation in the Izu-Bonin-Mariana system. *Geochemistry, Geophysics, Geosystems* 11, Q03X12.
- Shervais, J.W. (2001) Birth, death, and resurrection: The life cycle of suprasubduction zone ophiolites. *Geochem. Geophys. Geosyst.* 2.

ICDP

Microbial processes in the deep biosphere of the active CO₂-dominated fault zone in NW Bohemia

Q. LIU¹, H. KÄMPF², T. NICKSCHICK², P. KYSLIK⁵, P. BALDRIAN⁵,
R., BUSSERT⁴, B. PLESSEN³, D. WAGNER¹, M. ALAWI¹

GFZ German Research Centre for Geosciences, Helmholtz Centre Potsdam, ¹ Sect. 5.3 Geomicrobiology, ² Sect. 3.2 Organic Geochemistry, ³ Sect. 5.2 Climate Dynamics and Landscape Evolution, Telegrafenberg, 14469 Potsdam, mashal.alawi@gfz-potsdam.de

⁴ TU Berlin – Technical University Berlin, Germany

⁵ Institute of Microbiology of the Czech Academy of Sciences, Videnska 1083, 14220 Prague 4, Czech Republic

The Cheb Basin (W Eger Rift, NW Bohemia) is characterised by a network of diffuse degassing structures in mofette areas along an active fault zone (Kämpf et al., 2013). Further specific characteristics of this area are periodically occurring earthquake swarms and magmatic activities having strong impact on the changes in the composition and dynamics of the outflowing, mantle CO₂-dominated gases (Bräuer et al., 2005). From a biogeochemical and microbiological point of view these CO₂ seeps form an interesting and unique life habitat for microbial communities. The intense geogenic CO₂ fluxes provide a particular carbon and energy source forming the setting for a specific indigenous microbial community being well adapted to these specific environmental conditions.

We hypothesize that in active fault zones, due to an intensified substrate support, microbial processes are significantly accelerated compared to other continental Deep Biosphere ecosystems. Therefore active fault zones could be seen as „Hot Spots“ of microbial life in the deep subsurface. The main objective of the planned study is therefore to advance our understanding of the specific biogeo interactions between microbial communities and the seismic active environment in the Cheb Basin.

As a pilot study for the ICDP deep drilling campaign (Drilling the Eger Rift: Magmatic fluids driving the earthquake swarms and the deep biosphere) we conducted a first drilling campaign into a CO₂ degassing mofette structure from March to April 2016. A detailed microbiological, geochemical and mineralogical analysis of the obtained material is in preparation.

To gain first insight into the geochemical setting as well as into the microbial abundance and diversity a shallow drilling campaign (3 m deep) was performed in September 2015. These shallow cores are important for the project since the first meters of the subsequent 108.5 m deep drilling (in the direct proximity) could not be recovered. One drilling was located inside the CO₂ degassing area and the other, ca. 8 m away from the mofette, served as an undisturbed reference without CO₂ degassing. The locations were chosen based on the CO₂ degassing surveys from Nickschick et al., (2015). Total organic carbon and pore water geochemistry (anions/cations) varied significantly between both sides and indicate that the degradation of organic matter is strongly inhibited under elevated CO₂ concentrations. Bulk analyses of the soil organic matter reveal that TOC values in the reference core show a classical soil profile with decreasing values from shallow (0 – 4 cm, 11.1%) to deep (274 – 279 cm, 0.2%).

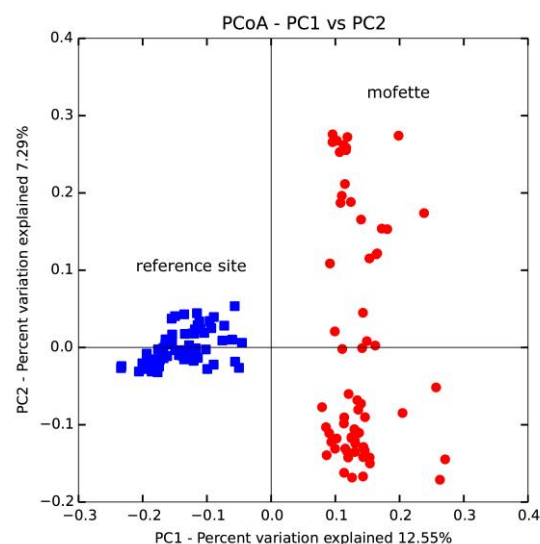


Figure 1: Principle component analysis (UNIFRAC) of the microbial communities at the mofette and reference site. Each dot represents one sampling depth (red, mofette; blue, reference site). The microbial communities of both sites significantly differ from each other.

In contrast in the mofette centre TOC values are higher and show a huge variety with no clear depth trend ranging from 1.8% to 20.1%. $\delta^{13}\text{C}$ values in the top layer (0 – 24 cm) of the reference soil are lower (-28.5‰) compared to the mofette samples (-26.6‰).

High-throughput DNA sequencing of 16S rRNA genes showed that the geogenic CO₂ strongly influences the community structure and abundances of specific microorganisms. Both communities, from the reference site and from the mofette, significantly differ from each other (Fig.1). The sequencing data and quantitative PCR analyses for 16S rRNA genes and functional genes (e.g. *mcrA* and *dsrB*) indicated that especially sulfate reducing bacteria and methanogens are more abundant in the CO₂ influenced soil. Activity test based on cultivation indicated that the microbial community in the CO₂ dominated area has a much higher methane production potential. In cultures incubated with soil from the mofette site methanogenesis started five weeks after the gas phase was changed from N₂/CO₂ to H₂/CO₂, a delay that was also observed during field measurements at the Wetztinger mineral spring (Bad Brambach, Germany) (Bräuer et al., 2005). This proved that hydrogen is one of the major limiting growth factor for methanogens in the Eger Rift sediments and the seismically triggered release of hydrogen has a high potential to influence methanogenic activity.

References:

- Bräuer, K., Kämpf, H., Faber, E., Koch, U., Nitzsche, H.-M., Strauch, G., 2005. Seismically triggered microbial methane production relating to the Vogtland-NW Bohemia earthquake swarm period 2000, Central Europe. *Geochemical Journal* 39, 441-450.
- Kämpf, H., Bräuer, K., Schumann, J., Hahne, K., Strauch, G., 2013. CO₂ discharge in an active, non-volcanic continental rift area (Czech Republic): Characterisation ($\delta^{13}\text{C}$, $^3\text{He}/^4\text{He}$) and quantification of diffuse and vent CO₂ emissions. *Chemical Geology* 339, 71-83.
- Nickschick, T., Kämpf, H., Flechsig, C., Mrlina, J., Heinicke, J., 2015. CO₂ degassing in the Hartoušov mofette area, western Eger Rift, imaged by CO₂ mapping and geoelectrical and gravity surveys. *International Journal of Earth Sciences* 104(8), 2107–2129

IODP

Climate change promotes the formation of cyanobacterial blooms in the Baltic Sea

N. LORBEER¹, L. SCHWARK^{1,2}, T. BAUERSACHS¹

¹ Christian-Albrechts-University, Institute of Geosciences, Department of Organic Geochemistry, Ludewig-Meyn-Straße 10, 24118 Kiel

² Curtin University, WA-OIGC, Department of Chemistry, G.P.O. Box U1987, 6845 Perth, Australia

The modern Baltic Sea is affected by the development of massive seasonal blooms of N_2 -fixing heterocystous cyanobacteria (Bianchi et al., 2000). The frequency and intensity of such blooms has increased considerably within the second half of the last century with significant consequences for the health of the Baltic Sea's aquatic ecosystem. For example, the spread of cyanobacterial blooms in connection with a slow overturning of Baltic Sea water masses through the Danish straits. This has promoted the spread of hypoxic conditions and resulted in a four times increase in the area affected by oxygen depletion with a total of 65,000 km² being a permanent dead zone (Zillen and Conley, 2010; Carstensen et al., 2014). In turn, this has resulted in a significant reduction of viable pelagic and benthic habitat, changes in aquatic community structures as well as alterations of major biogeochemical cycles. Although nutrient overenrichment by anthropogenic sources is considered to be the main driver for the development of massive cyanobacterial blooms in the contemporary Baltic Sea, there is evidence that periods of increased cyanobacterial activity have occurred repeatedly

during the last 7,000 years (Bianchi et al., 2000). In order to investigate the spread and the environmental factors that lead to cyanobacterial bloom formation in the Baltic Sea, we studied whole sediment profiles from three sites located in the Baltic Sea basin and spanning a SW/NE transect from the Kattegat to the central Baltic Proper.

In the Little Belt (Site M0059), the site closest to the North Sea, a 85 m long sediment core was taken. The first 47 mbsf consist of laminated, organic rich clays followed by a centimeter-scale silty sand unit. The sediments below are characterized by rhythmites of clayey silt and silty clay. The core of the Bornholm Basin (Site M0065) has a thickness of 46 m and consists of varved glacial clays and organic-rich mudstones showing a weak lamination. At the Landsort Deep (Site M0063), with 459 m the deepest morphological depression in the Baltic Sea, a 90 m-thick sediment sequence consisting of organic-rich mudstones with alternations of weakly and strongly laminated clays was collected. At all sites, a complete record of Baltic Sea history from the last glacial maximum to the present day was recovered including the Baltic Ice Lake (13,500-10,300 yrs. BP), the Yoldia Sea (10,300-9,500 yrs. BP), the Ancylus Lake (9,500-8,000 yrs. BP) and the Littorina Sea Phase (8,000-present day). The latter period is characterized by three distinct intervals of increased carbon burial and organic matter that represent the Holocene Thermal Maximum (HTM: 7,000-5,000 yrs. BP), the Medieval Climate Anomaly (MCA: 1,250-950 yrs. BP) and the Modern Hypoxic Period (MHP: 1950-present day).

The total organic carbon (TOC) content at the Bornholm Basin and the Landsort Deep is with an average value of < 0.7 wt% generally low in the glacial clays (13,500-8,000 yrs. BP). An exception is found a depth between 36.19 – 36.73 mbsf in the Bornholm Basin, at

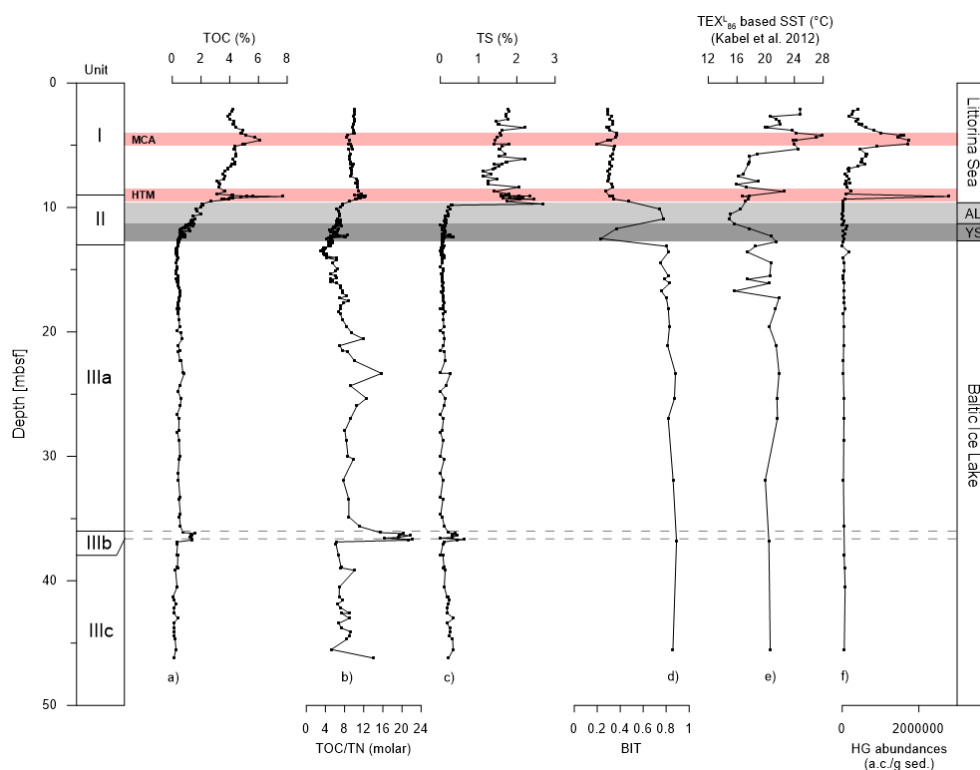


Figure 1: Downcore profiles of the Bornholm Basin showing (a) total organic carbon (TOC), (b) molar total organic carbon/ total nitrogen (TOC/TN ratios), (c) total sulphur (TS), (d) branched and isoprenoid tetraether index (BIT), (e) TEX_{86} -based sea surface temperatures (SSTs) based on the calibration by Kabel et al. 2012 and (f) heterocyst glycolipids (HG), a.c. = area counts. YS: Yoldia Sea (stage of the Baltic Sea history; 10,300-9,500 yrs. BP), AL: Ancylus Lake (stage of the Baltic Sea history; 9,500-8,000 yrs. BP), HTM: Holocene Thermal Maximum (7,000-5,000 yrs. BP), MCA: Medieval Climate Anomaly (1,250-950 yrs. BP)

which TOC values higher than 1.5 wt% occur. The overall low TOC content indicates an overall low primary productivity and/or oxygenated bottom waters in the early Baltic Sea, which is in agreement with low total sulphur (TS) values (< 0.2%). Low TOC/TN ratios ranging from 2.9-13.4 across sites indicate that the organic matter is primarily of aquatic origin with some admixture of terrestrial material. At the Landsort Deep and the Bornholm Basin major change in all bulk-geochemical characteristics are observed at a depth of 27 and 9 mbsf, respectively. Here, TOC values increase to an average of 3.3 wt% at the Landsort Deep and 4.3 wt% at the Bornholm Basin. Both sediment profiles show two distinct maxima exceeding values of 8 and 6 wt% TOC during the HTM and the MCA, respectively. In addition, sediments from the Landsort Deep show a third maximum in TOC at a depth interval from 0.03-0.42 mbsf representing the MHP. The improved preservation of organic matter under stagnant conditions during the Littorina Sea phase is in agreement with increasing TS values at the beginning of this phase (rise from 0.3 to 2.7 wt% in the Bornholm Basin and from 0.01 to 1.94 wt% in the Landsort Deep). Stable nitrogen isotope ($\delta^{15}\text{N}$) sediments deposited in the Baltic Ice Lake are on average 4.5 ‰ in agreement with values typically observed in nitrate-utilizing algae. During the following Yoldia Sea and Ancylus Lake stages, $\delta^{15}\text{N}$ values decrease to 3.5 ‰ and express their minimum with an average ~ 3 ‰ during the Littorina phase. Such a decline in $\delta^{15}\text{N}$ is considered to indicate an increased importance of cyanobacterial N_2 -fixation in the Holocene Baltic Sea as diazotrophic cyanobacteria show $\delta^{15}\text{N}$ values close to 0 ‰ (Goericke et al. 1994; Bauersachs et al., 2009a). Particular low $\delta^{15}\text{N}$ (< 2 ‰) are observed from sediments of the HTM, MCA and MHP indicating a repeated proliferation of cyanobacterial blooms in the Baltic Sea over the last 7,000 yrs BP.

The distribution of branched and isoprenoid glycerol dialkyl glycerol tetraethers (GDGTs) in sediments has previously been shown to vary with temperature (Schouten et al., 2002; Weijers et al., 2007). Using the $\text{TEX}_{86}^{\text{L}}$ lipid paleothermometer and a calibration specifically designed to reconstruct sea surface temperature (SST) changes in the Baltic Sea (Kabel et al., 2012), we investigated SST variations in the Baltic Sea since the last deglaciation. In the Bornholm Basin, SSTs were high with an average 21.2 °C during the Littorina Sea phase and two distinct maxima of 22.6 and 27.9 °C during the HTM and MCA, respectively. Both periods coincide with increased TOC accumulation rates, indicating higher primary productivity and more stagnant bottom waters in the Bornholm Basin. Similar temperature trends are also evident in the Landsort Deep although absolute temperatures somewhat vary between sites. During the HTM, SST are as high as 17 °C and thereafter slightly decrease to average values of 13 °C. With the start of the deposition of the TOC-rich sediments of the MCA SSTs increase to 17.1 °C at 5.52 mbsf. In accordance with trends observed in the Bornholm Basin, the warm intervals at the Landsort Deep correlate well with significantly higher TOC and TS values. The same temperature trends with two maxima of 20 °C at the beginning of the Littorina phase (corresponds to the HTM) and 26 °C during the MCA were also be apparent in the Little Belt region. A third temperature rise to 21.5 °C was noted for the MHP at the Little Belt and Landsort Deep. However, the application of the $\text{TEX}_{86}^{\text{L}}$ lipid paleothermometer in the Baltic Sea, is primarily restricted to sediments deposited during the Littorina Sea phase as strata deposited during the Ancylus Lake, the Yoldia Sea and the Baltic Ice Lake are characterized by elevated BIT

values varying between 0.37-0.89. BIT values higher than 0.3 are generally considered to indicate an increased influx of terrestrial organic matter, which may confound the reliable application of the $\text{TEX}_{86}^{\text{L}}$ lipid paleothermometer (see Schouten et al., 2013 and reference therein). While this indeed seems to be the case in the Bornholm Basin where $\text{TEX}_{86}^{\text{L}}$ -reconstructed SST are largely invariant and are higher than 20 °C in sediments deposited prior to the Littorina Sea phase, SST values show a gradual decline with depth in the Landsort Deep. This pattern is very similar to the one obtained via the determination of the long chain diol index (LDI), providing independent evidence that the SST in the Baltic Sea gradually increased from about 8 °C during the Baltic Ice Lake to about 18 °C at present.

Heterocyst glycolipids (HGs), specific biological markers for N_2 -fixing heterocystous cyanobacteria (Bauersachs et al., 2009b), substantially increased at the onset of the Littorina Sea phase. At the Bornholm Basin, HGs show trends parallel to the TOC content with two maxima of 1.7×10^6 a.c./g sediment and 2.7×10^6 a.c./g sediment in sediments deposited between 4.0-4.6 mbsf and 9.1 mbsf at the Bornholm Basin. Even higher values were measured at the Landsort Deep, where the values exceed to 7.0×10^8 a.c./g sediment during the HTM and MCA. On average HG values are 5.8×10^5 in sediments deposited in the Littorina phase and they decrease to 4×10^4 in the older record. Other biomarkers indicate for cyanobacterial activity are 6-methyl-, 7-methyl- and 8-methylheptadecane (Gelpi et al., 1970; Shiea et al., 1990). These components occur in higher concentrations during the HTM und MCA at the Landsort Deep as well as at the Bornholm Basin. Our results thus demonstrate a significant proliferation of cyanobacterial blooms in a larger area of the Baltic Sea coinciding with the establishment of a stratified water column, bottom water anoxia and increasing surface water temperatures. Hence, an increase in frequency and intensity of cyanobacterial blooms in the Baltic Sea is primarily controlled by climate variations and not necessarily by an anthropogenic loading of nutrients.

References:

- Bauersachs, T., Hopmans, E.C., Compaoré, J., Stal, L.J., Schouten, S., Sinninghe Damsté, J.S., (2009a): Rapid analysis of long-chain glycolipids in heterocystous cyanobacteria using high-performance liquid chromatography coupled to electrospray ionization tandem mass spectrometry. *Rapid Commun. Mass Spectrom.* 23, 1387–1394.
- Bauersachs, T., Compaoré, J., Hopmans, E.C., Stal, L.J., Schouten, S., Sinninghe Damsté, J.S. (2009b). Distribution of heterocyst glycolipids in cyanobacteria. *Phytochemistry* 70: 2034-2039.
- Bianchi, T. S., Engelhaupt, E., Westman, P., Andren, T., Rolff, C., & Elmgren, R. (2000): Cyanobacterial blooms in the Baltic Sea: natural or human-induced?. *Limnology and Oceanography*, 45(3), 716–726.
- Carstensen J., Conley D. J., Bonsdorff E., Gustafsson B. G., Hietanen S., Janas U., Jilbert T., Maximov A., Norkko A., Norkko J., Reed D. C., Slomp C. P., Timmermann K., Voss M. (2014): Hypoxia in the Baltic Sea: Biogeochemical Cycles, Benthic Fauna, and Management. Springer-Verlag, Volume 43, Issue 1, pp 26–36.
- Gelpi, E., Schneider, H., Mann, J., Oró, J. (1970): Hydrocarbons of geochemical significance in microscopic algae. *Phytochemistry*, Vol. 9, pp. 603-612.
- Goericke R.J., Montoya P. and Fry B. (1994): Physiology of isotopic fractionation in algae and cyanobacteria. In: Lajtha K. and Michener H. (eds), *Stable Isotopes in Ecology and Environmental Science*. Blackwell Scientific publications, New York.
- Kabel, K., Moros, M., Porsche, C., Neumann, T., Adolphi, F., Andersen, T.J., Siegel, H., Gerth, M., Leipe, T., Jansen, E., Sinninghe Damsté, J.S., (2012): Impact of climate change on the Baltic Sea ecosystem over the past 1,000 years. *Nature Climate Change* 2, 871-874.
- Schouten, S., Hopmans, E.C., Schefuss, E., Sinninghe Damsté, J.S., (2002): Distributional variations in marine crenarchaeotal membrane lipids: a new tool for reconstructing ancient sea water temperatures? *Earth and Planetary Science Letters* 204, pp. 265–274.

- Schouten, S., Hopmans, E. C., Sinninghe Damste, J. S., (2013): The organic geochemistry of glycerol dialkyl glycerol tetraether lipids: A review. *Organic Geochemistry* 54, pp. 19–61.
- Shiea, J., Brassell, S.C., Ward, D.M., (1990): Mid-chain branched mono- and dimethyl alkanes in hot spring cyanobacterial mats: a direct biogenic source for branched alkanes in ancient sediments? *Organic Geochemistry* 15, 223–231.
- Weijers, J.W.H., Schouten S., van den Donker, J. C., Hopmans E. C., Sinninghe Damste, J. S., (2007): Environmental controls on bacterial tetraether membrane lipid distribution in soils. *Geochimica et Cosmochimica Acta* 71, 703-713.
- Zillén, L., Conley, D.J., (2010): Hypoxia and cyanobacteria blooms - are they really natural features of the late Holocene history of the Baltic Sea? *Biogeosciences* 7, 2567-2580.

ICDP

Environmental history of the last 400,000 years in the northern Neotropical region based on Lake Petén Itzá sediments

L. MACARIO¹, S. COHUO¹, F. ANSELMETTI², D. SCHMID², L. PÉREZ³, S. KUTTEROLF⁴, J. CURTIS⁵, A. SCHWALB¹

¹ Institut für Geosysteme und Bioindikation, Technische Universität Braunschweig, Langer Kamp 19c, 38106 Braunschweig, Germany

² Institute of Geological Sciences and Oeschger Centre for Climate Change Research, University of Bern, Switzerland.

³ Instituto de Geología, Universidad Nacional Autónoma de México, Ciudad Universitaria, 04510 México, D.F. México

⁴ GEOMAR Helmholtz-Zentrum für Ozeanforschung, Kiel, Wischhofstr. 1-3, 24148 Kiel, Germany

⁵ Department of Geological Sciences and Land Use and Environmental Change Institute, University of Florida, Gainesville, FL.USA.

Tropical regions are important components of the Earth system, as they control the energy budget of the planet. How tropical regions react to long-term and abrupt climate changes, and what implications for the environment this may have, is one of the most uncharted ecological topics globally. Here, we evaluate the climatic and environmental history in the northern-most portion of the Neotropical region, based on sedimentary records from Lake Petén Itzá (Guatemala). We used cores PI-1 and PI-7 obtained during the Lake Petén Itzá Scientific Drilling Project (PISDP) in 2006. The main objectives of this study are: 1) the reconstruction of the environmental history of the northern Neotropical region during the last 400-85 ka BP; and 2) the quantitative estimation of the magnitude of climatic alterations, i.e. temperature and precipitation changes, during Marine Isotope Stages (MIS) 11 to 5.

Age model

Tephrochronology was used to constrain the age model. Los Chocoyos from Atitlán caldera and L-tephra from Amatitlán caldera dated ~84 ka BP and 191±11 ka BP, respectively, were used to establish the age model for core PI-1. The WFT tephra (158±3), the Atitlán old tephra (~306 ka BP), both from Atitlán caldera, and the Lower Ataco tephra (~400 ka BP) from Ataco, El Salvador, were used to constrain the age model for core PI-7 (Kutterolf et al., 2016).

Training set and transfer functions

We conducted a limnological survey across 76 lacustrine ecosystems of the northern Neotropical region in order to establish a well-fitted calibration data set for chemical and biological indicators. Bedrock type, elevation (temperature), precipitation-evaporation balance and the

influence of marine environments are the main controls of limnological properties of these aquatic ecosystems. Ostracodes were used for conducting transfer functions, because they display narrow ecological tolerances and high abundance in sedimentary sequences. Sixty-nine freshwater ostracodes were recognized and calibrated by determining species distribution and ecological niche optima and tolerances to species level.

Late Pleistocene climatic changes

Based on petrophysical (magnetic susceptibility), geochemical (Carbon/Nitrogen ratio, contents in calcite, organic and inorganic matter, biogenic silica and dolomite) and biological indicators (ostracodes), we inferred the following environments: From ~400 to 85 ka BP, the lake was an open system, contrary to the dynamics characterizing the most recent periods (85 to present) during which the lake was a closed basin. This change limits quantitative estimations of climate change. Qualitative estimations, however, suggest that the Neotropics followed from MIS 11 to MIS 5 the general thermal global trends as observed in Greenland ice cores. Precipitation regimes were highly variable as suggested by lake level high and low stands occurring invariably during glacial and interglacial cycles. A distinct draw down in lake level was detected during MIS 11 (400 ka BP), when inferred littoral conditions at site PI-7 suggest a lake level decrease of around 30m. MIS10 and MIS 6 were periods recognized as climatically unstable, because strong fluctuations in lake level and thus precipitation were detected. MIS 9 was characterized by rather high lake levels and highly dynamic lake waters. MIS 8 and MIS 5 were periods with rather moist climate at the beginning followed by progressively drier conditions. During the end of MIS 5 (85 ka BP), a layer characterized by gravel, coarse sand and terrestrial gastropods, suggests low lake level and arid conditions. During MIS 7, climate was rather moist during the beginning, and rather arid during the remainder of MIS 7. At around 200 ka BP, another period of desiccation of centennial scale was detected.

Intertropical teleconnections

Climate in the northern Neotropical region seems to have been dominated by Earth's orbital changes. Changes in temperature were apparently forced by precession-dominated insolation. Glacial temperatures suggested a maximum temperature decrease of 5°C (Hodell et al., 2008; Correa-Metrio et al., 2012a). These estimations are supported by the presence of tropical ostracode taxa during glacial periods. Precipitation was highly variable during Marine Isotope Stages. It is generally thought that the increase in insolation during interglacials increased convection and intensity of tropical convergence, and consequently led to an increase in precipitation rates over evaporation (Scholz et al., 2007). Our data, however, do not support an increase in precipitation coinciding exclusively with interglacials. Glacial periods show at least short phases of high lake levels and thus predominantly moist climate. Recent models have demonstrated that zonal and meridional gradients of atmospheric heating may control hydrological cycles in tropical regions (Clement et al., 2004). These regional alterations therefore seem to better explain the hydrological instability detected in the northern Neotropical region. Our work represents the first insight into the climatic history of the northern Neotropical region during the last ~400ka BP and contributes evidence to understand potential effects and consequences of global warming in the region.

Acknowledgements

The project was funded by grants from the U.S. National Science Foundation, the International Continental Scientific Drilling Program, the Swiss Federal Institute of Technology, the Swiss National Science Foundation, DFG-projects SCHW 671/16-1 and KU2685/3-1 as well as CONACYT scholarships 218639, 213456 to the first two authors.

References:

- Clement, A.C., A. Hall, A.J. Broccoli, 2004. The importance of precessional signals in the tropical climate. *Climate Dynamics* 22: 327–341.
- Correa-Metrio, A., M. Bush, K. Cabrera, S. Sully, M. Brenner, D. Hodell, Escobar J. & T. Guilderson, 2012a. Rapid climate change and non-analog vegetation in lowland Central America during the last 86,000 years. *Quaternary Science Reviews* 38: 63–75.
- Hodell, D., F. Anselmetti, D. Ariztegui, M. Brenner, J. Curtis, A. Gilli, D. Grzesik, T. Guilderson, A. Müller, M. Bush, A. Correa-Metrio, J. Escobar & S. Kutterolf, 2008. An 85-ka record of climate change in lowland Central America. *Quaternary Science Reviews* 27: 1152–1165.
- Kutterolf, S., J.C. Schindlbeck, F.S. Anselmetti, D. Ariztegui, M. Brenner, J. Curtis, D. Schmid, D.A. Hodell, A. Mueller, L. Pérez, W. Pérez, A. Schwalb, M. Frische & K.L. Wang, 2016. A 400-ka tephrochronological framework for Central America from Lake Petén Itzá (Guatemala) sediments. *Quaternary Science Reviews* 150: 200–220.
- Scholz, C.A., T.C. Johnson, A.S. Cohen, J.W. King, J.A. Peck, J.T. Overpeck, M.K. Talbot, E.T. Brown, L. Kalinidekafé, P.Y. O. Amoako, R.P. Lyons, T.M. Shanahan, I.S. Castaneda, C.W. Heil, S.L. Forman, L.R. McHargue, K. Beuning, J. Gomez & J. Pierson, 2007. East African megadroughts between 135 – 75 kyr ago and implications for early human history. *Proceedings of the National Academy of Sciences of the United States of America* 104: 16416–16421.

ICDP

A closer look at Lake Van's carbonates: Implications for lacustrine stable isotope analysis

JEREMY MCCORMACK¹, ADRIAN IMMENHAUSER¹, OLA KWIECIEN¹

¹ Sediment and Isotope Geology, Ruhr University Bochum, 44801 Bochum, Germany

Carbonate stable isotope ($\delta^{18}\text{O}$ and $\delta^{13}\text{C}$) analysis is a commonly applied and powerful proxy in lacustrine palaeoclimatology. In the absence of large quantities of detrital carbonates, the bulk carbonate is assumed to mainly represent inorganic carbonates precipitated in the epilimnion. However, in some cases, this approach turns out to be suboptimal; (1) bulk lacustrine records may be compromised by the presence of different inorganic carbonate minerals (calcite and/or aragonite), and (2) even in well-preserved, laminated sediments (e.g. varves), post-depositional processes could have affected the mineralogy or geochemistry of sedimentary carbonates. Therefore, the interpretation of bulk $\delta^{18}\text{O}$ and $\delta^{13}\text{C}$ signals based on false assumptions will be flawed. In case of terminal and alkaline Lake Van, the interpretation of the $\delta^{18}\text{O}$ and $\delta^{13}\text{C}$ signals of bulk carbonates, in comparison to other proxies including TOC (Stockhecke et al., 2014), arboreal pollen (Litt et al., 2014) and XRF-Ca/K ratio (Kwiecien et al., 2014), is far from straightforward when relying on traditional interpretative approaches. Consequently, using a multi-component approach we studied, individually and in detail, various components comprising Lake Van's bulk carbonates.

The material investigated here was recovered during the ICDP PALEOVAN project drilling campaign in 2010.

We focussed on the interval covering the last glacial/interglacial period. Inorganic ($< 63 \mu\text{m}$) and biogenic ($> 63 \mu\text{m}$) carbonates were isolated by wet-sieving and analysed by means of XRD, SEM and isotope mass spectrometry. High-resolution mineralogical analysis revealed variable amounts of aragonite and calcite as well as non-stoichiometric (calcian) dolomite. Isotopically aragonite is enriched in $\delta^{18}\text{O}$ and $\delta^{13}\text{C}$ in comparison to calcite, still the differences in aragonite-water and calcite-water fractionation factors are minor, and alone are insufficient in explaining changes observed in amplitude of the $\delta^{18}\text{O}$ and $\delta^{13}\text{C}$ signals. However, dolomite isotopic compositions differ significantly from the primary carbonates with typically enriched $\delta^{18}\text{O}$ and depleted $\delta^{13}\text{C}$ dolomite values.

High amounts (up to 90 % of total carbonate content) of dolomite can be found in the last glacial and interglacial period, but are missing in Holocene sediments. In contrast to the last interglacial, dolomites from the last glacial period appear in high concentrations almost exclusively within intercalations of finely-laminated, organic-rich material. The dolomite appears to be replacing the inorganic aragonite/calcite. The early diagenetic origin of these non-stoichiometric dolomites is supported by the pristine crystal morphology of interpenetrating rhombs with multiple distinctly defined edges, indicating slow crystallisation during multiple growth episodes. For Lake Van, our results suggest that the presence of diagenetic dolomite, together with the isotopic variability between calcite and aragonite masks the isotopic signature of the bulk carbonates. Set in a wider context, our findings, though preliminary, have implications for palaeolimnological analysis and call for caution when using bulk and/or inorganic carbonates as indicator of past hydrological changes.

References:

- Litt, T., Pickarski, N., Heumann, G., Stockhecke, M., Tzedakis, P. C. (2014). A 600,000 year long continental pollen record from Lake Van, eastern Anatolia (Turkey). *Quaternary Science Reviews*, 104, 30–41.
- Kwiecien, O., Stockhecke, M., Pickarski, N., Heumann, G., Litt, T., Sturm, M., Anselmetti, F. S., Kipfer, R., Haug, G. H. (2014). Dynamics of the last four glacial terminations recorded in Lake Van, Turkey. *Quaternary Science Reviews*, 104, 42–52.
- Stockhecke, M., Sturm, M., Brunner, I., Schmincke, H. U., Sumita, M., Kipfer, R., Cukur, D., Kwiecien, O., Anselmetti, F. S. (2014). Sedimentary evolution and environmental history of Lake Van (Turkey) over the past 600 000 years. *Sedimentology*, 61(6), 1830–1861.

ICDP

Lithology estimations from cluster analysis on borehole logging data, evaluated and extrapolated from core dataP. METHE¹, A. GOEPEL¹, N. KUKOWSKI¹¹Friedrich Schiller University Jena, Institute for Geosciences, Burgweg 11, 07749 Jena, Germany

To identify lithologies of subsurface rocks usually requires deep probing through coring, as only core samples allow to compile a lithological profile with high precision and spatial resolution. However, since coring is very expensive, geophysical borehole logs often are the only available data to obtain information on deep subsurface rock.

Different sedimentary rocks usually exert distinct specific physical properties, e.g. differ significantly with respect to properties as measured e.g. with gamma ray, density, caliper, P-wave velocity, or porosity logs. In order to derive information on lithology from a set of borehole logs, we tested several cluster analysis algorithms on such data (Ward hierarchical clustering, k-Means, Mean-Shift and DBSCAN). Our tests also included high-dimensional clustering with the DBSCAN algorithm applied on geophysical logs. In order to cluster alternating sequences with layers only a few cm thick, a high precision in log to log depth match is necessary. Whereas layers, which are thinner than the vertical resolution of the logging tool, cannot be resolved completely, i.e. the true value of a rock physical property is always underestimated, they can still be identified. Based on the analysis of prevailing lithology, which is known from coring sections, well-founded assumptions were made to characterise layers' lithology.

Our data set consists of borehole wireline logging data from the 1179 m deep drill hole EF-FB 1/12, which was drilled in summer 2013 during the INFLUINS (INtegrated FLUId dynamics IN Sedimentary basins) project in the centre of the Thuringian Basin (Central Germany) close to the city of Erfurt, and from which Triassic sedimentary rocks were recovered. To evaluate the outcome of our cluster analyses, we used independent data on physical rock properties (density, P-wave velocity, magnetic susceptibility) coming from laboratory MSCL (Multi Sensor Core Logger) measurements (533 m core in total) and from rock physical measurements on selected core samples.

Continuous borehole geophysical logging along the entire downhole length clearly resolves stratigraphic units from changes in lithology on the meter-scale, e.g. the Middle Dolomite (6 m thick) of the Middle Muschelkalk. Embedded layers of anhydrite and mudstone within the rock salt of the Salinarröt-formation in the Upper Buntsandstein were resolved in wireline and MSCL logging down to a thickness of about 20 cm. Furthermore, layers in the sub-dm scale can be still identified by wireline logging and resolved by MSCL measurements, if density and p-wave velocity show significant contrasts between different lithologies. For lithology classification, different physical properties from wireline and MSCL logs were compared by computational analyses, particularly the cluster analysis approaches mentioned above were applied. To do so, depth from log to log needs to be correlated

precisely to allow correlation of layers in the sub-dm scale. The certainty of cluster analysis algorithms for wireline logging data decreases in cases of gradual lithological changes, i.e. for the lack in contrast of physical properties between the lithologies. In contrast, MSCL is capable of resolving thin embedded layers, due to the usage of point measurement sensors. Here, minimum thickness of a resolved layer depends on the applied sampling interval.

ICDP

ICDP Oman Drilling Project: crystallographic preferred orientations in the lower crust - The Wadi Gideah transectD. MOCK¹, B. ILDEFONSE², J. KOEPKE¹, T. MÜLLER¹, D. GARBE-SCHÖNBERG³¹ Institut fuer Mineralogie, Leibniz Universität Hannover; dom.mock@web.de, koepke@mineralogie.uni-hannover.de, t.mueller@mineralogie.uni-hannover.de² Géosciences Montpellier, Université de Montpellier 2, benoit.ildefonse@umontpellier.fr³ Institut für Geowissenschaften, Universität Kiel, dgs@gpi.uni-kiel.de

The ICDP Oman Drilling Project (<http://www.omandrilling.ac.uk/>) is since mid December 2016 in the active phase, starting to drill the crustal profiles in the Wadi Gideah in the Wadi Tayin Massif of the Oman ophiolite. This is one of the most promising sites for a section through intact fast-spread paleo-oceanic crust. The aim is to drill 400 meter long sections from critical horizons of the lower crust: Site GT1 - lower gabbro; Site GT2 - transition between layered and foliated gabbros; Site GT3 - transition between gabbros and sheeted dikes. Within a previous project, we performed three field campaigns, where samples of the lower crust, mid-crust and the dike/gabbro transition of the Oman paleocrust were collected, in order to provide a reference frame for the individual crustal drillings within the Oman Drilling Project. Our current project within the SPP ICDP aims to provide constraints on the accretion and evolution of the Oman paleocrust with focus on depth logs with respect to (1) petrology, (2) major and trace element geochemistry on rocks and minerals, (3) crystallographic preferred orientations (CPO), (4) the evolution of hydrothermal alteration and (5) the sulfur cycle. More than 300 collected samples cover the whole oceanic crust from the mantle/crust boundary up to the dike/gabbro transition zone. This enabled us to establish a coherent and comprehensive reference data set. The obtained petrological and geochemical results provide evidence for an upward differentiation trend within a hydrous tholeiitic system, and for a change in the mode of differentiation process between the layered and the foliated gabbro. Here, we present our results on crystallographic preferred orientations obtained by EBSD.

The EBSD technique helps to quantify CPO of minerals in a rock, using the J-index of the Orientation Distribution Function (ODF J; e.g., Mainprice *et al.*, 2014) and the BA-index to quantify the shape of the crystal fabric (e.g., Satsukawa *et al.*, 2013; Mainprice *et al.*, 2014). The BA index was primarily calculated for plagioclase and is classified in three types: Axial-B fabric with a point

maximum in (010) and a girdle in [100] (BA-index ≈ 0); P-type fabric with point maxima in both (010) and [100] (BA-index ≈ 0.5); Axial-A fabric with a [100] point maximum and (010) girdle (BA-index ≈ 1 ; Satsukawa *et al.*, 2013).

Analyses in the Montpellier EBSD lab were done on 68 samples from the lower crustal section (layered gabbro, foliated gabbro and varitextured gabbro). Both J-index and BA-index were plotted versus depth, giving evidence for a significant change in CPO and the crystal fabric of plagioclase, in the transition zone between layered and foliated gabbro. Furthermore, a significant microstructural change in both J- and BA-index between foliated and layered gabbro is observed. This is consistent with the geochemical evidence for a change in formation/differentiation processes between the layered gabbros foliated gabbro sections. The scattering of BA indices of almost all analysed samples between 0.1 and 0.6 indicates a combination of Axial B- and Axial P-type which gives evidence for magmatic deformation (Satsukawa *et al.*, 2013). Combining EBSD and geochemical data supports the hypothesis of an hybrid model after Boudier *et al.* (1996) for crustal formation at fast-spreading mid-oceanic ridges, where both in-situ crystallization by sill intrusion as well as the transport of gabbroic mushes via a "gabbro glacier" play a role. The genesis of the upper foliated gabbro can be better explained by the gabbro glacier model (e. g., Henstock *et al.*, 1993), while in-situ crystallization according to the sheeted sill model (e. g., Keleman *et al.*, 1997) is plausible for sections below the upper foliated gabbro.

Another significant change of both J- and BA-index takes place within the layered gabbro at ~ 3200 meters above the crust mantle boundary (CMB): From the base of the crust, the BA-index progressively decreases up to 3200 m above CMB and suddenly increases above. The curve of the J-index shows a mirrored trend: it increases up to 3200 m and decreases above. These significant changes imply, that there is some kind of change in crystal growth in that crustal horizon and support the idea of the hybrid model with different crystallization processes in the upper foliated gabbro and the regions below, respectively.

References:

- Boudier, F., Nicolas, A., Ildefonse, B., 1996. Magma chambers in the Oman ophiolite: Fed from the top and the bottom. *Earth and Planetary Science Letters*, 144, 239-250.
- Henstock, T.J., Woods, A.W., White, R.S., 1993. The accretion of oceanic-crust by episodic sill intrusion. *Journal of Geophysical Research-Solid Earth*, 98, 4143-4161.
- Keleman, P.B., Koga, K., Shimizu, N., 1997. Geochemistry of gabbro sills in the crust-mantle transition zone of the Oman ophiolite: Implications for the origin of the oceanic lower crust. *Earth and Planetary Science Letters*, 146, 475-488.
- Mainprice, D., Bachmann, F., Hielscher, R., Schaeben, H., 2014. Descriptive tools for the analysis of texture projects with large datasets using MTEX: strength, symmetry and components. *Geological Society, London, Special Publications*, 409, SP409-8.
- Satsukawa, T., Ildefonse, B., Mainprice, D., Morales, L. F. G., Michibayashi, K., Barou, F., 2013. A database of plagioclase crystal preferred orientations (CPO) and microstructures-implications for CPO origin, strength, symmetry and seismic anisotropy in gabbroic rocks. *Solid Earth*, 4, 511-542.

IODP

Mid Pleistocene productivity events in the NE Pacific: multiple fertilization from aeolian dust, icebergs, and volcanic ash

J. MÜLLER¹, O. ROMERO², E. COWAN³, M. FORWICK⁴, E. MCCLYMONT⁵, H. ASAH⁶, C. MÁRZ⁷, C. MOY⁸, I. SUTO⁹, A. MIX¹⁰, J. STONER¹⁰

¹ Alfred Wegener Institute, Helmholtz Centre for Polar and Marine Research, Bremerhaven, Germany

² MARUM, Center for Marine Environmental Sciences, Bremen, Germany

³ Appalachian State University, Boone, USA

⁴ UiT The Arctic University of Norway in Tromsø, Norway

⁵ University of Durham, UK

⁶ KOPRI, Korea Polar Research Institute, Incheon, South Korea

⁷ University of Leeds, UK

⁸ University of Otago, New Zealand

⁹ University of Nagoya, Japan

¹⁰ Oregon State University, Corvallis, USA

IODP Expedition 341 succeeded in recovering a continuous sedimentary record of Miocene to Late Pleistocene climate history at drill Site U1417 in the Gulf of Alaska, NE Pacific. One of the major objectives of the DFG-funded PECA project was to understand the dynamics of productivity, nutrients, freshwater input to the ocean, and sea surface conditions in the study area and their role in the global carbon cycle. Sediments recovered from the distal (deep-water) Site U1417 provide an unrivalled opportunity to reconstruct North Pacific sea surface conditions during late Neogene large-scale (global) climate transitions. The shift from a 41 ka to a 100 ka world (i.e. the Mid Pleistocene Transition; MPT) - one of the most prominent intervals of global Quaternary climate change - is clearly identifiable in Site U1417 sediments (Jaeger *et al.*, 2014). Organic geochemical biomarker analyses performed within the PECA project aimed at the reconstruction of the sea surface conditions (e.g., sea surface temperature (SST), sea ice coverage, phytoplankton productivity) that characterised the subpolar NE Pacific during this critical time interval of climate change. Though shipboard microfossil and sedimentological data suggest the occurrence of sea ice in the study area at distinct time intervals, the identification of the sea ice biomarker IP25 - a highly branched isoprenoid (HBI) monoene (Belt *et al.*, 2007) - in U1417 sediments proved difficult. Possible explanations for the minimum abundance or lack of IP25 could be that i) the core site experienced only insignificant spring sea ice coverage during the deposition of the analysed sediments, ii) the sedimentary concentration of IP25 is too low to permit a proper identification of the molecule, or iii) the sea ice diatom species that produces this molecule is not prevalent in the study area. Due to the absence of IP25, no information on past sea ice changes at Site U1417 could be obtained and the focus of the research project was re-directed on a multi-proxy approach involving close cooperation with researchers from other disciplines. To fully exploit the environmental information archived in U1417 sediments, a sampling strategy has been pursued that permits direct correlation of different (independent) proxy data obtained from biomarker, micropalaeontological, sedimentological and geochemical (XRF) analyses. SST and the presence of polar waters were estimated from alkenone data, while changes in primary productivity were deduced from fluctuations in diatom

concentrations, biogenic silica content and Ba/Al values. The input of terrigenous organic matter was determined from the predominance of long-chain over short-chain n-alkanes (i.e. the terrigenous vs. aquatic ratio; TAR; Meyers, 1997). Coarse sand grains are interpreted to reflect deposition by iceberg rafting.

Mid Pleistocene SSTs in the Gulf of Alaska are in good agreement with SST reconstructions for the North Atlantic (ODP 983; McClymont et al, 2008) and the NW Pacific (ODP 882; Martínez-García et al., 2010). All three records reveal a significant cooling at about 1 Ma, which supports earlier hypotheses of an overall northern hemisphere ocean cooling as a prerequisite for the increase in continental ice volume (McClymont et al., 2008). While phytoplankton productivity seems rather independent from SST at Site U1417, it is strongly related to elevated TAR values depicting enhanced input of terrestrial leaf-wax lipids. The transport of these lipids is supposed to be effected by strong winds carrying dust from Alaskan loess deposits to the open ocean as well as by icebergs released from Alaskan tidewater glaciers. The latter is supported by the occasional coincidence of high IRD contents and TAR values. The close relationship between the TAR record, Ba/Al values and the abundance of diatoms, however, strengthens that together with the leaf-wax lipids also iron-bearing dust was exported leading to high productivity events at Site U1417 throughout the Mid Pleistocene. In addition to the airborne- and iceberg-related input of iron, volcanic ash seems to represent a third fertilization mechanism, as few (TAR independent) productivity peaks coincide with tephra layers preserved in U1417 sediments. The distinct "on-off" pattern in diatom productivity evolved with the onset of the MPT, which suggests that the Mid Pleistocene expansion of the Northwest Cordilleran Ice Sheet lead to an effective production of glacial iron-rich dust that was exported i) by strong northwesterly winds and ii) by icebergs. The observation that productivity peaks in the Gulf of Alaska are not confined to glacial or interglacial periods points to a rather local feedback between the export of iron-bearing dust and an immediately responding ocean surface. The identification of these hitherto unconsidered fertilization mechanisms that potentially fostered ocean productivity and hence the sequestration of atmospheric carbon into the deep ocean is a major outcome of the PECA project.

References:

- Belt, S. T., G. Massé, S. J. Rowland, M. Poulin, C. Michel and B. LeBlanc (2007). "A novel chemical fossil of palaeo sea ice: IP25." *Organic Geochemistry* 38(1): 16-27.
- Jaeger, J., S.P.S. Gulick, L. LeVay, H. Asahi, H. Bahlburg, C. Belanger, G.B.B. Berbel, L. Childress, E. Cowan, M.H. Davies, L. Drab, F. Dottori, M. Forwick, A. Fukumura, S. Ge, S. Gupta, A. Kioka, S. Konno, C. März, K. Matsuzaki, E. McClymont, A. Mix, C. Moy, J. Müller, A. Nakamura, T. Ojima, K. Ridgway, O. Romero, Slagle A., J. Stoner, G. St-Onge, I. Suto and L. Worthington (2014). "Southern Alaska margin: Interactions of tectonics, climate, and sedimentation." *Proceedings of the Integrated Ocean Drilling Program*, vol. 341.
- Martínez-García, A., A. Rosell-Melé, E. L. McClymont, R. Gersonde and G. H. Haug (2010). "Subpolar Link to the Emergence of the Modern Equatorial Pacific Cold Tongue." *Science* 328(5985): 1550-1553.
- McClymont, E. L., A. Rosell-Melé, G. H. Haug and J. M. Lloyd (2008). "Expansion of subarctic water masses in the North Atlantic and Pacific oceans and implications for mid-Pleistocene ice sheet growth." *Paleoceanography* 23(4): PA4214.
- Meyers, P. A. (1997). "Organic geochemical proxies of paleoceanographic, paleolimnologic, and paleoclimatic processes." *Organic Geochemistry* 27(5-6): 213-250.

ICDP

Hydrous lower oceanic crust: continuous activity of seawater-derived fluids at very high to medium temperatures – records from the Oman ophiolite (Wadi Gideah, Wadi Tayin massif)

S. MUELLER¹, J. KOEPKE², D. GARBE-SCHÖNBERG¹, F. TRAMM², K. HOERNLE³

¹ Kiel University, Germany (smueller@gpi.uni-kiel.de)

² Leibniz Universität Hannover, Germany

³ GEOMAR Helmholtz Centre for Ocean Research Kiel, Germany

The current project provides support for the ICDP Oman Drilling Project (<http://www.omandrilling.ac.uk/> and <https://twitter.com/OmanDrillProj>), which started its active phase in December 2016, with drilling of the crustal transects in the Wadi Gideah (Wadi Tayin Massif, Oman ophiolite). Within a previous project, we performed several field campaigns, in order to provide a reference frame for the individual crustal drillings within the Oman Drilling Project. Our current project within the SPP ICDP aims to provide constraints on the accretion and evolution of the Oman paleocrust with focus on depth logs with respect to (1) petrology, (2) major and trace element geochemistry on rocks and minerals, (3) crystallographic preferred orientations (CPO), (4) the evolution of hydrothermal alteration and (5) the sulfur cycle. More than 300 collected samples cover the whole oceanic crust from the mantle/crust boundary up to the dike/gabbro transition zone. Here we focus on deep hydrothermal circulation at elevated temperatures, which is recorded in the gabbros of our sample suite.

The formation of plutonic, fast-spread oceanic crust can be described by two conceptual endmember models. For the 'gabbro glacier' model (Nicolas et al., 1988), crystallization of primitive melts takes place within a small melt lens, sandwiched between the upper gabbros and the sheeted dikes (axial melt lens). From here, crystal mushes subside down along the flanks of the ridge axis forming the layered gabbros. In contrast, according to the 'sheeted sill' model (Kelemen et al., 1997), the lower crust is accreted in-situ by lateral sill intrusions, which needs efficient hydrothermal cooling and the presence of seawater-derived fluids within deep crustal regions.

In Wadi Gideah, dikelets of hornblende gabbro and magmatic amphibole veins are a common feature of the lower crustal section, implying presence of water during crystallization. They often occur in association with hydrothermal fault zones that are crosscutting coherent series of layered gabbros showing intense overprint under greenschist and sub-greenschist facies conditions as consequence of subsequent pervasive hydrothermal alteration. Here, we present major and trace element data mainly for different types of amphiboles from parageneses of such dikelets and veins. Temperature calculations of amphibole-plagioclase equilibrium (Blundy and Holland, 1990) and Titanium-in-amphibole (Ernst and Liu, 1998) suggest that water-rock interaction was initiated in a temperature regime (up to ~1000°C) above the solidus of wet gabbro, enabling hydrous partial melting within the host gabbro. The presence of characteristic microstructures

of anatectic events are visible in backscattered electron images. High chlorine contents of amphiboles formed at very high temperature (VHT) are explained by saline fluids or brines originating from seawater. Moreover, hydrothermal spinel associated with pargasite implying formation temperatures of about 700°C (Nozaka et al., 2016), and the formation of amphiboles formed at high and medium temperatures indicate a continuation of hydrothermal activity to lower temperatures. Greenschist and sub-greenschist facies overgrowth of the VHT veins points towards continuous fluid activity at even lower temperatures.

Our petrographic and geochemical results derived from different crustal depths (including gabbros from the Moho Transition Zone), document on-axis fluid flux initiated at very high temperatures. This, and the continuation of fluid flux for amphibolite and greenschist facies temperatures have the potential of significant contribution to the cooling of the lower oceanic crust.

References:

- Blundy, J.D., and Holland, T.J.B., 1990, *Contributions to Mineralogy and Petrology*, v. 104, no. 2, p. 208–224.
 Ernst, W.G., and Liu, J., 1998, *American Mineralogist*, v. 83, no. 9, p. 952–969.
 Kelemen, P.B., Koga, K., and Shimizu, N., 1997, *Earth and Planetary Science Letters*, v. 146, no. 3, p. 475–488.
 Nicolas, A., Reuber, I., and Benn, K., 1988, *Tectonophysics*, v. 151, no. 1, p. 87–105.
 Nozaka, T., Meyer, R., Wintsch, R.P., and Wathen, B., 2016, *Contributions to Mineralogy and Petrology*, v. 171, no. 53, p. 1–14.

ICDP

Earthquake swarms, Moffettes and mid Pleistocene volcanism – Electromagnetic imaging of the Eger Rift (W Bohemia)

GERARD MUÑOZ¹, UTE WECKMANN¹, JOSEF PEK², NASER MEQBEL¹, SVĚTLANA KOVÁČIKOVÁ², RADEK KLANICA²

¹ GFZ German Research Centre for Geosciences, Potsdam, Germany

² Institute of Geophysics of the Czech Academy of Sciences, Prague, Czech Republic

The Eger Rift (W Bohemia) is the easternmost termination of the European Cenozoic rift system (ECRS). Its western part is dominated by ongoing magmatic processes originated in the intra-continental lithospheric mantle including the occurrence of repeated earthquake swarms of $M_L < 4.5$ (Fischer et al., 2014). The intersection area between the Eger Rift and the Regensburg-Leipzig zone is called Cheb Basin and includes the main focal area, located close to Nový Kostel.

The increased geodynamic activity also implies neotectonic crustal movements, Quaternary volcanism and degassing of CO₂ from mineral springs and wet and dry mofettes. The high ³He/₄He ratio of the CO₂ dominated gases indicates a lithospheric mantle origin (Bräuer et al., 2014). At present, the Eger Rift is the only known intra-continental region of the ECRS where such deep seated, active lithospheric processes currently occur. However, its geodynamic nature and implications still are not fully understood.

In order to image the electrical conductivity on crustal scale two magnetotelluric (MT) experiments have been carried out in 2015 - 2016, with the aims of studying the behavior of rocks and fluids down to the source region of earthquake swarms, imaging fluid pathways and their interconnection. Two perpendicular profiles with 30 stations each with a site spacing of 2 km were measured in fall 2015. In addition a dense grid of 97 stations with a spacing of 500 x 500 m² and an extension of 10 x 5 km² was set up in winter 2016. The MT data were recorded in the frequency range 10 kHz – 0.001 Hz.

First inversion models show some enhanced conductivity regions. The most relevant is a good conductor beneath the earthquake swarm region extending from a depth of approx. 7 to 15 km. Near-surface high conductivity zones appear associated to the earthquake swarm region and to the Bublák and Hartoušov moffettes (Kämpf et al. 2013). While the former seems to be disconnected from the deep conductive anomaly by a low conductivity layer, the later shows a certain connection to the deep conductor through a moderate conductivity channel, indicating a possible fluid pathway. Another prominent conductive anomaly is a deep reaching conductive region found at the southern end of the profile, beneath the quaternary volcano Mýtina Maar and the Železná hůrka scoria cone (Flechsig et al. 2015).

References:

- Bräuer, K., H. Kämpf, and G. Strauch (2014). Seismically triggered anomalies in the isotope signatures of mantle-derived gases detected at degassing sites along two neighboring faults in NW Bohemia, central Europe. *J. Geophys. Res. Solid Earth*, 119, 5613–5632. doi:10.1002/2014JB011044.
 Fischer, T., Horálek, J., Hrubcová, P., Vavryčuk, V., Bräuer, K., and Kämpf, H. (2014). Intra-continental earthquake swarms in West-Bohemia and Vogtland: a review. *Tectonophysics*, 611, 1–27.
 Kämpf, H., Bräuer, K., Schumann, J., Hahne, K. & Strauch, G. (2013). CO₂ discharge in an active, non-volcanic continental rift area (Czech Republic): characterisation ($\delta^{13}C$, $^3He/4He$) and quantification of diffuse and vent CO₂ emissions. *Chem. Geol.*, 339, 71–83.
 Flechsig, C., Heinicke, J., Mrlina, J. et al. (2015). Integrated geophysical and geological methods to investigate the inner and outer structures of the Quaternary Mýtina maar (W-Bohemia, Czech Republic). *Int J Earth Sci (Geol Rundsch)* 104: 2087. doi:10.1007/s00531-014-1136-0

ICDP

First cryptotephra finding in sediment cores from the Dead Sea – Potential for further constraining the chronology of the ICDP Dead Sea palaeoclimate record

I. NEUGEBAUER^{1,2}, M. J. SCHWAB¹, S. WULF³, J. SERB¹, B. PLESSEN¹, R. TJALLINGII¹, O. APPELT⁴, M. STEIN⁵ AND A. BRAUER¹

¹ GFZ German Research Centre for Geosciences, Section 5.2 – Climate Dynamics and Landscape Evolution, Potsdam, Germany

² University of Geneva, Department of Earth Sciences, Geneva, Switzerland

³ Heidelberg University, Institute of Earth Sciences, Heidelberg, Germany

⁴ GFZ German Research Centre for Geosciences, Section 4.3 – Chemistry and Physics of Earth Materials, Potsdam, Germany

⁵ Geological Survey of Israel, Jerusalem, Israel

The ca. 450 m long Dead Sea Deep Drilling site 5017-1 is constrained by radiocarbon and U-Th dating and covers the last 220,000 years (Stein et al., 2011; Neugebauer et al., 2014; Torfstein et al., 2015). However, an independent

dating method is desirable as radiocarbon dating is limited to the last ~40,000 years and U-Th dating of authigenic carbonate requires a comprehensive correction procedure. Tephrochronology has been demonstrated a powerful tool for dating and synchronisation of palaeoclimate records for regional and global comparison. Due to a lack of visible tephra layers in the Dead Sea sediment record, apparent chronological links with the eastern Mediterranean tephrostratigraphical lattice are still absent.

We identified the first cryptotephra, *i.e.* macroscopically invisible volcanic ash, in the Holocene lacustrine sediment record of the Dead Sea, site DSEn. The major elemental chemistry of the rhyolitic glass shards proves this tephra identical to the distal 'S1 tephra' identified in the Yammoûneh palaeolake, Lebanon (Develle et al., 2009), in a marine sediment record from the SE Levantine basin (Hamann et al., 2010) and in the Sodmein Cave archaeological site in Egypt (Barton et al., 2015). The 'S1 tephra' was produced by the early Holocene 'Dikkartin' dome eruption of the Erciyes Dağ volcano in central Anatolia, Turkey, and has been dated in the marine record at 8830 ± 140 cal yr BP. We present a new age estimate of the 'S1 tephra' based on radiocarbon dating of terrestrial plant remains found in the DSEn core (Migowski et al., 2004), which reveals a modelled age of 8939 ± 83 cal yr BP and allows the estimation of an early Holocene marine reservoir age of ca. 320 years in the SE Levantine Sea. The timing of the volcanic eruption during the early Holocene humid period, which led to the formation of sapropel S1 in the Mediterranean Sea is crucial for the synchronisation of marine and terrestrial palaeoclimate records in the eastern Mediterranean region.

The detection of the Anatolian tephra in the marginal sediments of the Dead Sea encourages to systematically search for cryptotephtras in the ICDP deep-basin core 5017-1, which would allow to further constrain the chronology of the record. Thereby, the identification of the early Holocene S1 tephra indicates that potential tephra fingerprints might have spread towards the Dead Sea from other large eastern Mediterranean volcanic eruptions, such as the Campanian Ignimbrite (~40 ka) and the Ionian Sea tephtras X5 (~105 ka) and X6 (~109 ka). Furthermore, a systematic tephra search might allow identifying tephtras originating from the Arabian volcanic province including the Harrat Ash Shaam field of the southern Levant and northern Arabia, which so far has been only poorly studied.

References:

- Barton et al., 2015. The role of cryptotephra in refining the chronology of Late Pleistocene human evolution and cultural change in North Africa. *Quaternary Sci. Rev.* 118, 151-169.
- Develle et al., 2009. Early Holocene volcanic ash fallout in the Yammoûneh lacustrine basin (Lebanon): Tephrochronological implications for the Near East. *Journal of Volcanology and Geothermal Research* 186, 416-425.
- Hamann et al., 2010. First evidence of a distal early Holocene ash layer in Eastern Mediterranean deep-sea sediments derived from the Anatolian volcanic province. *Quaternary Res.* 73, 497-506.
- Migowski et al., 2004. Recurrence pattern of Holocene earthquakes along the Dead Sea transform revealed by varve-counting and radiocarbon dating of lacustrine sediments. *Earth Planet. Sc. Lett.* 222, 301-314.
- Neugebauer et al., 2014. Lithology of the long sediment record recovered by the ICDP Dead Sea Deep Drilling Project (DSDDP). *Quaternary Sci. Rev.* 102, 149-165.
- Stein et al., 2011. Dead Sea deep cores: A window into past climate and seismicity. *Eos, Transactions American Geophysical Union* 92, 453-454.
- Torfstein et al., 2015. Dead Sea drawdown and monsoonal impacts in the Levant during the last interglacial. *Earth Planet. Sc. Lett.* 412, 235-244.

IODP

Gulf Stream hydrography during the Late Pliocene/early Pleistocene: low versus high latitude forcing of the Atlantic Meridional Overturning Circulation

A. OSBORNE¹, M. FRANK¹, D. KROON², J. D. WRIGHT³, J. GROENEVELD⁴, M. GUTJAHR¹, L. REUNING⁵, R. TIEDEMANN⁶

¹ GEOMAR Helmholtz Centre for Ocean Research Kiel, Germany

² School of Geosciences, University of Edinburgh, UK

³ Department of Earth and Planetary Sciences, Rutgers University, USA

⁴ Center for Marine Environmental Sciences (MARUM) and Department of Geosciences, University of Bremen, Germany

⁵ Energy and Mineral Resources Group, Geological Institute, RWTH Aachen University, Germany

⁶ Alfred Wegner Institute for Polar and Marine Research, Bremerhaven, Germany

The majority of model experiments predicts that the strength of the Atlantic Meridional Overturning Circulation (AMOC) increased as the Central American Seaway (CAS) shoaled and terminated the supply of relatively fresh Pacific Water to the North Atlantic (see Zhang et al., 2012 for a review). This project uses samples from ODP Site 1000 in the central Caribbean and ODP Site 1006 in the Florida Strait to test the hypothesis that there was a direct link between CAS closure, warming and increased salinity of the Gulf Stream, and ultimately a strengthening of the AMOC. Our multi-proxy approach investigates surface- and upper-ocean water properties and intermediate depth water circulation. Two time slices during the final stages of CAS closure are investigated. The Late Pliocene glaciation during MIS M2 was an episode of transient CAS closure during an otherwise warm climate (De Schepper et al., 2013) and Marine Isotope Stages (MIS) 100 to 95 in the early Pleistocene were the first major glacial-interglacial cycles after the intensification of Northern Hemisphere Glaciation (Groeneveld et al., 2014), also leading to the first major incursions of glacial southern-sourced water in the deep North Atlantic (Lang et al., 2016).

The first objective of this project is to establish a Late Pliocene/early Pleistocene age model for Site 1006 and thus make this under-utilised Site fully accessible for future paleoceanographic research. During the first 16 months of this project 320 samples of the benthic foraminifera *Planulina ariminensis* have been picked and analysed for $\delta^{18}\text{O}$ and were combined with unpublished data from the same species (J. D. Wright). We used shipboard nannofossil biostratigraphy (Kroon et al., 2000) and the software *Analysieries* (Paillard et al., 1996) to correlate our expanded data set with the LR04 benthic $\delta^{18}\text{O}$ stack (Lisiecki and Raymo, 2005). Marine Isotope Stages 100 to 95 have been identified and further samples will be measured to confirm the core-depth of M2 (Figure 1).

The first 16 months of this project also saw the preparation and analysis of foraminifera samples from Site 1000 to produce a high-resolution record of intermediate depth seawater ϵ_{Nd} for MIS 100-95 (Figure 2). A similar record for M2 at Site 1000 is underway. Site 1000 benefits from a well established age model, based on $\delta^{18}\text{O}$ in the benthic foraminifera *Cibicides wuellerstorfi* (Steph et

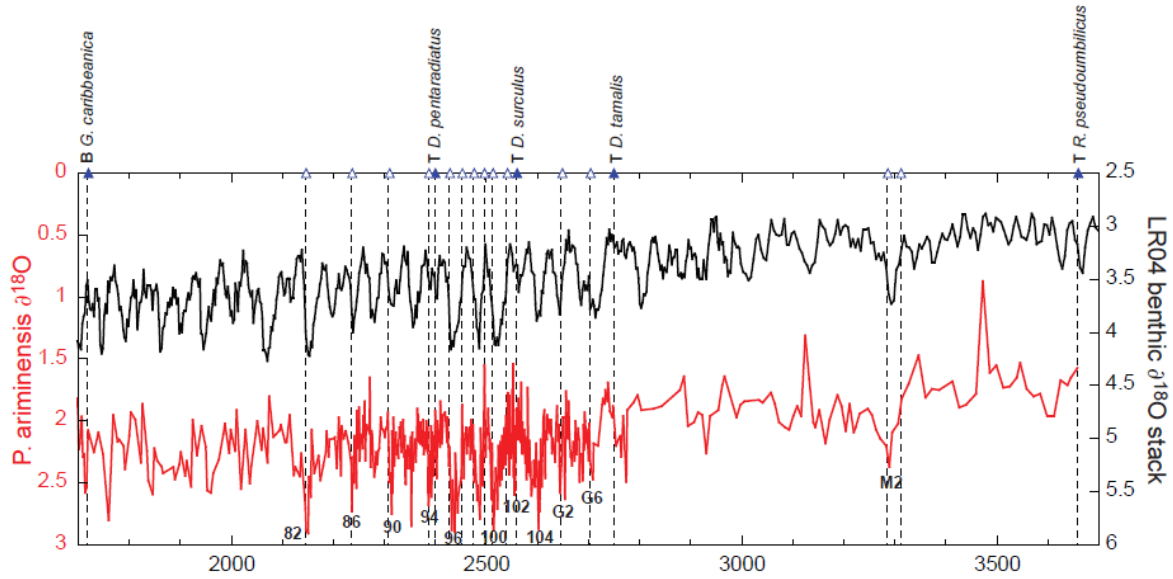


Figure 1: The Late Pliocene/early Pleistocene benthic $\delta^{18}\text{O}$ record for ODP Site 1006 of foraminiferal species *P. ariminensis* (red line), using data from this study and unpublished data from J. Wright. The record was correlated with the benthic $\delta^{18}\text{O}$ stack of Lisiecki and Raymo (2005) (black line) using the Analseries software (Paillard et al., 1996). Open triangles and vertical dashed lines show stratigraphic tie points with the LR04 record. Prominent isotope stages in the ODP Site 1006 record are labelled. Closed triangles and vertical dashed lines show tie points with nannofossil bioevents (Kroon et al., 2000).

al., 2006; 2010). There are also published records of shallow and deep planktonic foraminifera stable isotope compositions and Mg/Ca for Site 1000 (Groeneveld et al., 2008; Steph et al., 2006; 2010). Our new record of bottom water ϵ_{Nd} at Site 1000 adds an independent proxy of

intermediate water circulation in the Caribbean to the benthic $\delta^{13}\text{C}$ record of Steph et al. (2010) and is used to interpret the strength of the AMOC during M2 and MIS 100-95.

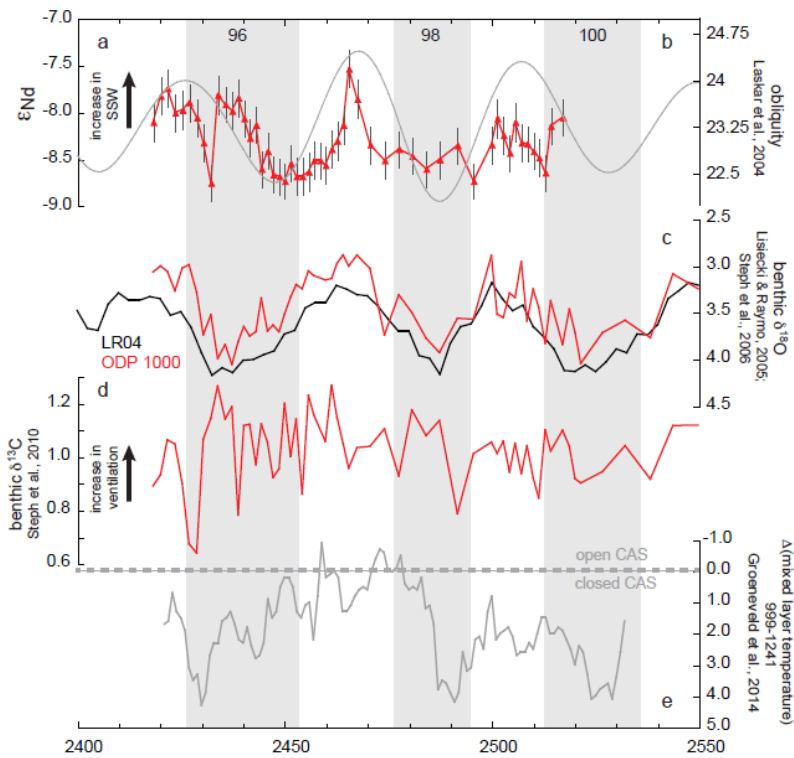


Figure 2: a) Foraminifera-based bottom water ϵ_{Nd} for ODP 1000 (red line and triangles), error bars indicate 2σ error, more radiogenic values are interpreted as a greater contribution from southern sourced waters (SSW); b) obliquity curve (Laskar et al., 2004); c) the LR04 benthic $\delta^{18}\text{O}$ stack (black line, Lisiecki and Raymo, 2005), ODP 1000 benthic $\delta^{18}\text{O}$ (red line, Steph et al., 2006), tuned for this time interval; d) ODP 1000 benthic $\delta^{13}\text{C}$ (Steph et al., 2010), higher $\delta^{13}\text{C}$ is interpreted as better ventilation (Kroopnick, 1985); e) difference in mixed layer temperature between the Caribbean and Pacific, horizontal dashed line shows the boundary between a fully open and a closed mixed layer connection across the Central American Seaway (CAS) (Groeneveld et al., 2014).

The Site 1000 ϵ_{Nd} record (Figure 2a) is taken to represent the balance between more radiogenic southern sourced waters and less radiogenic northern sourced waters in the intermediate depth tropical Atlantic (Osborne et al., 2014). Consequently, there are peaks in the supply of southern sourced waters during MIS 97 and in the mid-to-late part of MIS 96. There is ongoing debate as to whether a relative increase in the supply of southern sourced waters in the mid-depth tropical Atlantic was associated with a weakening (e.g. Pahnke et al., 2008) or a strengthening (e.g. Huang et al., 2014) of the AMOC. If the former is true, then the AMOC was weakest during MIS 97, when mixed layer temperature records also suggest that the CAS was open (Groeneveld et al., 2014), in line with model predictions (e.g. Zhang et al., 2012). However, an open CAS cannot explain the peak in ϵ_{Nd} during the mid-to-late part of MIS 96, when there was a large mixed layer temperature difference between the Caribbean and Pacific (Groeneveld et al., 2014). In fact, the Site 1000 benthic $\delta^{13}C$ record (Steph et al., 2010) indicates the exact opposite relationship between the shoaling of the CAS and strength of the AMOC. Higher $\delta^{13}C$ indicates better ventilation (Kroopnick, 1985), and Site 1000 was better ventilated when the CAS was open (Groeneveld et al., 2014). There are therefore at least two questions that remain to be answered: 1) How can the benthic $\delta^{13}C$ and ϵ_{Nd} records at Site 1000 be reconciled? 2) If the opening and closing of the CAS was not the driver for circulation change in the Atlantic, what alternative mechanism was responsible? The changes in the ϵ_{Nd} record resemble the obliquity curve (Laskar et al., 2004), with the most radiogenic values during times of highest obliquity. Does this indicate a high latitude control on circulation (Groeneveld et al., 2014)?

As well as addressing the questions highlighted above, the remaining 8 months of the project will be used as follows: 1) extension of the Site 1006 age model to include M2; 2) high-resolution bottom water ϵ_{Nd} at Site 1006 for MIS 100-95 and M2; 3) high resolution $\delta^{18}O$ in shallow and thermocline dwelling planktonic foraminifera *Globigerinoides sacculifer* and *Globorotalia medardii* at Site 1006 for MIS 100-95 and M2 to reconstruct upper ocean temperature and salinity. Now that the Site 1006 age model is established, the preparation and analyses of these samples can take place concurrently. A new collaboration with Lars Reuning (Aachen) will result in the production of a high resolution bottom water ϵ_{Nd} record for two precession cycles during the early Pliocene, to complement published *G. sacculifer* and *G. medardii* records for Site 1006 (Reuning et al., 2006). As for the main project, the purpose of this early Pliocene comparison is to establish whether warming in the Gulf Stream was directly linked to changes in the strength of the AMOC and, if so, the time scales on which such changes occurred.

References:

- De Schepper, S., J. Groeneveld, B. D. A. Naafs, C. Van Renterghem, J. Hennissen, M. J. Head, S. Louwye, and K. Fabian (2013), Northern Hemisphere Glaciation during the globally warm early Late Pliocene, *PLOS ONE*, 8(12), e81508.
- Groeneveld, J., E. C. Hathorne, S. Steinke, H. DeBey, A. Mackensen, and R. Tiedemann (2014), Glacial induced closure of the Panamanian Gateway during Marine Isotope Stages (MIS) 95-100 (similar to 2.5 Ma), *EPSL*, 404, 296-306.
- Groeneveld, J., D. Nurnberg, R. Tiedemann, G. J. Reichart, S. Steph, L. Reuning, D. Crudeli, and P. Mason (2008), Foraminiferal Mg/Ca

- increase in the Caribbean during the Pliocene: Western Atlantic Warm Pool formation, salinity influence, or diagenetic overprint?, *G-cubed*, 9.
- Huang, K.-F., D. W. Oppo, and W. B. Curry (2014), Decreased influence of Antarctic intermediate water in the tropical Atlantic during North Atlantic cold events, *EPSL*, 389, 200-208.
- Kroon, D., T. Williams, C. Pirmez, S. Spezzaferri, T. Sato, and J. D. Wright (2000), Coupled Early Pliocene-Middle Miocene bio-cyclostratigraphy of Site 1006 reveals orbitally induced cyclicity patterns of Great Bahama Bank carbonate production, *Proc. ODP, Scientific Results*, 166, 155-166.
- Kroopnick, P. M. (1985), The distribution of C-13 of sigma-CO2 in the world oceans, *Deep-Sea Research Part a-Oceanographic Research Papers*, 32(1), 57-84.
- Laskar, J., P. Robutel, F. Joutel, M. Gastineau, A. C. M. Correia, and B. Levrard (2004), A long-term numerical solution for the insolation quantities of the Earth, *Astronomy & Astrophysics*, 428(1), 261-285.
- Lang, D. C., I. Bailey, P. A. Wilson, T. B. Chalk, G. L. Foster, and M. Gutjahr (2016), Incursions of southern-sourced water into the deep North Atlantic during late Pliocene glacial intensification, *Nature Geoscience*, 9(5), 375.
- Lisiecki, L. E., and M. E. Raymo (2005), A Pliocene-Pleistocene stack of 57 globally distributed benthic delta O-18 records, *Paleoceanography*, 20(1).
- Osborne, A. H., D. R. Newkirk, J. Groeneveld, E. E. Martin, R. Tiedemann, and M. Frank (2014), The seawater neodymium and lead isotope record of the final stages of Central American Seaway closure, *Paleoceanography*, 29(7), 715-729.
- Pahnke, K., S. L. Goldstein, and S. R. Hemming (2008), Abrupt changes in Antarctic Intermediate Water circulation over the past 25,000 years, *Nature Geoscience*, 1(12), 870-874.
- Paillard, D., L. Labeyrie, and P. Yiou (1996), Macintosh program performs time-series analysis, *Eos Trans. Amer. Geophys. Union*, 77, 379.
- Reuning, L., J. J. G. Reijmer, C. Betzler, A. Timmermann, and S. Steph (2006), Sub-Milankovitch cycles in periplatform carbonates from the early Pliocene Great Bahama Bank, *Paleoceanography*, 21(1).
- Steph, S., R. Tiedemann, M. Prange, J. Groeneveld, D. Nurnberg, L. Reuning, M. Schulz, and G. H. Haug (2006), Changes in Caribbean surface hydrography during the Pliocene shoaling of the Central American Seaway, *Paleoceanography*, 21(4).
- Steph, S., R. Tiedemann, M. Prange, J. Groeneveld, M. Schulz, A. Timmermann, D. Nuernberg, C. Ruehleemann, C. Saukel, and G. H. Haug (2010), Early Pliocene increase in thermohaline overturning: A precondition for the development of the modern equatorial Pacific cold tongue, *Paleoceanography*, 25.
- Zhang, X., et al. (2012), Changes in equatorial Pacific thermocline depth in response to Panamanian seaway closure: Insights from a multi-model study, *EPSL*, 317, 76-84.

ICDP

First results from a Mediterranean biodiversity hotspot from palynological and biomarker analyses of Lake Ohrid sediments from the Early Pleistocene (> 1.2 Ma)

K. PANAGIOTOPOULOS¹, J. HOLTVOETH², R. D. PANCOST², B. WAGNER¹, M. MELLES¹

¹ Quaternary Geology Group, Institute for Geology and Mineralogy, University of Cologne, Germany

² Organic Geochemistry Unit, School of Chemistry, University of Bristol, UK

Mediterranean hotspots of plant diversity, such as the Ohrid region at present, are commonly associated with southern European glacial tree refugia. Existing paleobotanical evidence suggests that the SW Balkans have sheltered temperate tree populations over the last five eccentricity-controlled climatic cycles, i.e. 0.5 Ma (e.g. Sadori et al., 2016). Due to the scarcity of continuous terrestrial climate archives reaching beyond the Mid-Pleistocene transition (MPT), the Early Pleistocene (> 1.2 Ma) sediments from the 2013 ICDP drilling at Lake Ohrid (SCOPSCO Project) allow for unique insights into the climate and ecosystem dynamics during an obliquity-dominated world. This new ICDP project aims to use high-resolution pollen, charcoal and lipid biomarker analyses to study the development of plant biodiversity at a southern

refugium and to reconstruct the response of aquatic and terrestrial ecosystems to climate variability over the Early Pleistocene within the Ohrid Basin.

The first pollen results reveal a diverse palynoflora with several subtropical tree species growing in the study region 1.2 million years ago. More specifically, trees such as *Carya*, *Cedrus*, *Liquidambar*, *Pterocarya*, and *Tsuga* most likely formed significant constituents of the arboreal vegetation surrounding the lake. These findings confirm the hypothesis that the study area and consequently SW Balkans sustained considerable populations of subtropical tree species prior to the MPT. Moreover, the first biomarker analyses reveal rather subtle changes in the amount and distribution of lipid biomarkers during the Early Pleistocene. Nevertheless, shifts in chain-length distribution of leaf wax-derived *n*-alcohol between glacial and interglacial samples reflect changes in leaf-wax composition, and thus, point to changes in the dominant tree species. These findings appear to be consistent with pollen-inferred shifts in dominant tree species distribution. Lipid biomarkers and pollen indicate a rather forested landscape and a relatively stable soil pool in the Lake Ohrid catchment throughout the Early Pleistocene climatic cycles. Ohrid plant ecosystems show a relative high resilience to climate fluctuations during the Early Pleistocene, an interval characterized by climatic cycles of a shorter duration and lower amplitude variability in comparison to post MPT cycles.

Ongoing high-resolution pollen and biomarker analyses will contribute to the identification of the main drivers of terrestrial and aquatic ecosystem change in the Ohrid Basin since the formation of the lake, and the quantitative reconstruction and assessment of the nature and amplitude of climate variability during this interval in the Eastern Mediterranean region.

Reference:

Sadori, L., Koutsodendris, A., Panagiotopoulos, K., Masi, A., Bertini, A., Combourieu-Nebout, N., Francke, A., Kouli, K., Joannin, S., Mercuri, A. M., Peyron, O., Torri, P., Wagner, B., Zanchetta, G., Sinopoli, G., Donders, T. H. (2016): *Pollen-based paleoenvironmental and paleoclimatic change at Lake Ohrid (south-eastern Europe) during the past 500 ka*, Biogeosciences, 13, 1423-1437. DOI: [10.5194/bg-13-1423-2016](https://doi.org/10.5194/bg-13-1423-2016).

IODP

Indian Ocean circulation changes over the Middle Pleistocene Transition

B.F. PETRICK¹, G. AUER², D. DE VLEESCHOUWER³, B.A. CHRISTENSEN⁴, C. STOLFI⁴, L. REUNING⁵, A. MARTINEZ-GARCIA¹, G. HAUG¹, T. BUCKLEY⁵, S. J. GALLAGHER⁵, C. S. FULTHORPE⁶, K. BOGUS⁷, IODP 356 SHIPBOARD SCIENCE PARTY

¹Max-Planck-Institut für Chemie, Mainz

²Institute of Earth Sciences, University of Graz

³MARUM - Center for Marine Environmental Science

⁴School of Earth Sciences, University of Melbourne

⁵Geological Institute, RWTH Aachen University

⁶Institute for Geophysics, University of Texas at Austin

⁷Ocean Discovery Program, Texas A&M University

The Mid-Pleistocene Transition (MPT; ~1.4 – 0.4 Ma) represents a climatic shift towards climate cycles at a quasi-100-kyr frequency. High-resolution data covering the MPT from globally distributed archives, but there is only sparse evidence on changes in heat exchange between the Pacific and Indian Oceans, which represents a crucial part of the global thermohaline circulation. Deciphering the influence of this heat exchange via the Indonesian Throughflow (ITF) is an important step in understanding the causes of the MPT.

The Leeuwin Current off Western Australia is directly influenced by the ITF and can therefore be used to reconstruct ITF variability during the MPT. Today, the Leeuwin Current is the only southward flowing eastern boundary current in the southern hemisphere. The onset of the current is unknown but is proposed to have occurred ~1 Ma and was likely related to significant changes in ITF dynamics during the MPT.

We present the first continuous reconstruction of changes in the Leeuwin Current during the MPT using data from IODP Expedition 356 Site U1460. The site is located at 29°S in the path of the current. We reconstruct paleoenvironmental variability by combining XRF, organic geochemistry, ICP and XRD data with shipboard data, to reconstruct Leeuwin Current and ITF variability. High sedimentation rates (~30 cm/ka) at Site U1460 provide the opportunity for high-resolution reconstruction of the MPT.

Initial analyses show clear indications that upwelling off Western Australia intensified during the MPT, indicated by increased primary productivity related to increased nutrient levels, from 900-600 ka. This increase in upwelling indicates a reduction of the ITF, and thus implies that the heat transport from the Pacific to the Indian Ocean was reduced diminished during the MPT. Our results suggest, that reduced heat exchange via the ITF played a major role in forcing the climatic shift to the 100-kyr ice-house world of the Pleistocene.

IODP

The interaction of authigenic and detrital Nd in North Atlantic sediments

F. PÖPPELMEIER^{1,2}, P. BLASER¹, H. SCHULZ³, M. GUTJAHN⁴, J. LIPPOLD², N. FRANK¹

¹Institute of Environmental Physics, Heidelberg University

²Institute of Earth Sciences, Heidelberg University

³Department of Geosciences, Tübingen University

⁴GEOMAR Helmholtz Centre for Ocean Research Kiel

The neodymium isotopic composition (Nd IC) of seawater exhibits a quasi-conservative nature in the pelagic ocean and thus follows the flow path and admixtures of major water masses. Furthermore, it is thought to be independent of biological processes, making it an ideal complement to biogenic stable isotopes and other nutrient tracers [1]. Over the past decade authigenic Nd isotopes archived in marine sediments have become a commonly used method for the reconstruction of past ocean water mass provenance (e.g. [2,3]). In order to provide viable information, it is a necessary prerequisite that the extracted signal indeed reflects past bottom water compositions. Recent findings from the Pacific Ocean, however, showed that this assumption may not hold in general by suggesting that a local benthic Nd flux possibly modifies the pore water as well as the bottom water Nd isotopic composition [4]. Moreover, a recent study showed that the detrital material in sediments of the Gulf of Alaska slowly exchanges Nd with the archived authigenic fraction, thus altering it towards the associated detrital Nd isotope compositions over time [5]. This process can possibly limit the use of Nd isotopes as a paleo water mass tracer significantly.

Within the frame of the DFG project Neoglacial we aim to understand the Atlantic bottom water Nd isotope composition across termination I. To achieve this ambitious goal we have recently developed an improved leaching

method [6]. To test the integrity of authigenic Nd as a paleo water mass tracer, we here investigated the authigenic Nd across strong isotopic gradients recorded in marine sediment at a site of the ‘Dreizack’ seamount, located within the North-East Atlantic IRD belt. Due to a lack of pore water samples we were not able to directly study the sediment-pore water interaction. Instead we base our assessment on a detailed analysis of sediment data which provides the opportunity that we can investigate the outcome of mixing and exchange processes over the past using data from very different sedimentologic events. At this location two IRD layers associated with the Heinrich events 1 and 2 as well as an Icelandic ash turbidite provide extreme sedimentary conditions that are easily identified in the stratigraphy as well as in the geochemistry of the sediment. The exceptional Nd isotopic signatures associated with these events, thus allow us to resolve potential diffusive processes within the sediment during early diagenesis.

We generated a high resolution record of acid-reductively leachable Nd isotopic compositions as well as corresponding element concentrations. The deposition of ice rafted detrital carbonate and ash turbidites in the North-East Atlantic have indeed led to a certain extent to an exchange of Nd between authigenic and detrital phases. Although pore waters must have been the medium of exchange, we conclude that there was no significant flux of Nd through the sediment column or into overlying bottom waters. This is confirmed via analysis of neighboring sediment cores that were not exposed to these sedimentary events but recorded the same bottom water mass which indeed did not change its Nd isotopic composition. Thus, we propose that even though detrital Nd was released into pore waters under such extreme sedimentary conditions, the deep water Nd isotopic composition still appears to have been dominated by the advected deep water Nd isotope signal.

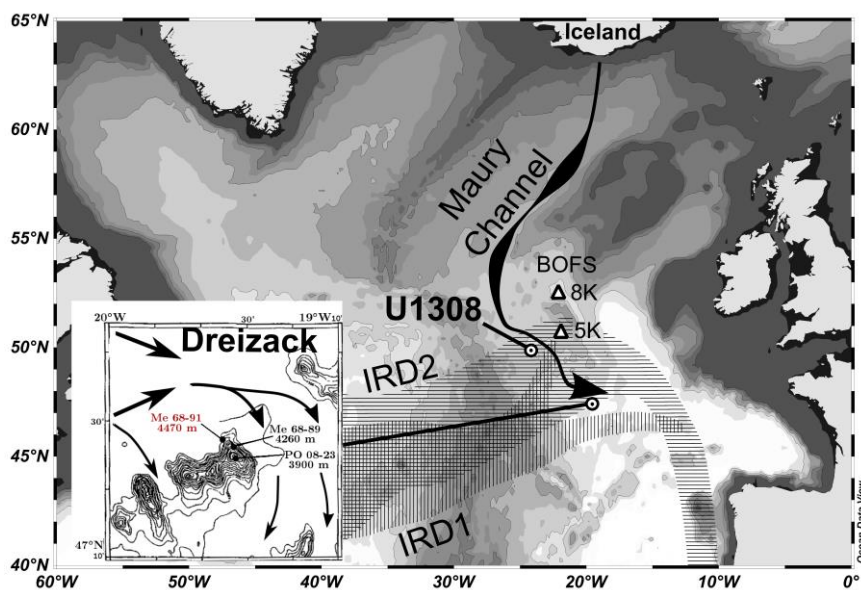


Figure 1: Bathymetric map of the core locations: Me68-91 (red) recorded all three sedimentary events described in the text. The other depicted cores are used for comparison. Shaded areas represent the IRD belts of H1 (vertical) and H2 (horizontal). Black arrows indicate the Maury Channel System which transports Icelandic ash turbidites.

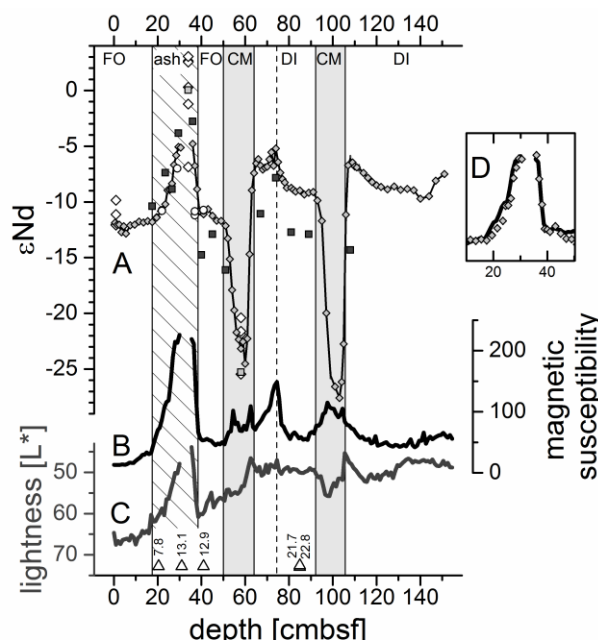


Figure 1: Records of Nd IC (A; in ϵ notation; deviation from CHUR standard $\times 10,000$), magnetic susceptibility (B) and lightness (C) of core Me68-91. Vertical shaded bars depict the sedimentary events of an Icelandic ash turbidite and IRD layers of H1 and H2 (FO: Foraminiferal Ooze; CM: Cemented Marl DI: Diamiction). Panel D shows a zoom of ϵ_{Nd} and magnetic susceptibility of the ash layer. Dark squares in the ϵ_{Nd} record show total digestions and white circles foraminiferal samples.

References:

- [1] Frank (2002), Reviews of Geophysics
- [2] Roberts et al. (2010), Science
- [3] Böhm et al. (2015), Nature
- [4] Abbott et al. (2015), Geology
- [5] Du et al. (2016), Geochimica et Cosmochimica Acta
- [6] Blaser et al. (2016), Chemical Geology

¹² Institute of Geological Sciences, University of Bern, Bern, 3012, Switzerland

¹³ Jackson School of Geosciences, The University of Texas at Austin, Austin, 78729, United States

ICDP

A proposal for a new ICDP task in Europe: The 'MICLIME' project

B. REICHENBACHER¹, P. GRUNERT², M. HARZHAUSER³, M. HINDERER⁴, K. HOLCOVÁ⁵, O. KEMPF⁶, M. KOVÁČ⁷, W. KRIJGSMAN⁸, O. MANDIĆ³, T. MATYS GRYGAR⁹, S. NEHYBA¹⁰, W. ORSI¹, W. PILLER², R.F. SACHSENHOFER¹¹, F. SCHLUNEGGER¹², G.R.SHARMAN¹³, D. STOCKLI¹³

¹ Department of Earth & Environmental Sciences, Ludwig-Maximilians Universität, 80333 Munich, Germany

² Institute of Earth Sciences, University of Graz, 8010 Graz, Austria

³ Geological-Paleontological Department, Natural History Museum Vienna, 1010 Vienna, Austria

⁴ Institut für Angewandte Geowissenschaften, Technische Universität Darmstadt, 64287 Darmstadt, Germany

⁵ Institute of Geology and Paleontology, Charles University, Prague 2, 128 43, Czech Republic

⁶ Swiss Geological Survey, Federal Office of Topography swisstopo, Wabern, Bern, 3084, Switzerland

⁷ Department of Geology and Paleontology, Comenius University, 84215 Bratislava, Slovakia

⁸ Paleomagnetic laboratory "Fort Hoofddijk", Utrecht University, 3584 CD Utrecht, The Netherlands

⁹ Institute of Inorganic Chemistry v.v.i., Academy of Sciences of the Czech Republic, 250 68, Czech Republic

¹⁰ Department of Geological Sciences, Masaryk University, Brno, 611 37, Czech Republic

¹¹ Department Applied Geosciences and Geophysics, Montanuniversität Leoben, 8700 Leoben, Austria

The Burdigalian interval (20.44–15.97 Ma, early Miocene) witnessed the transition of Earth's climate system into the most pronounced global warming phase of the entire Neogene, known as the 'Miocene Climate Optimum' (MCO). It thus represents an ideal time interval to study the impact of global climate change on ecosystems and environments in space and time. No section in the continental domain exists worldwide that exposes a complete Burdigalian succession, and few oceanic drilling sites have yet recovered the sediments of the Burdigalian stage. We are proposing a new ICDP drilling project dedicated to the **MI**ocene **CL**imate development in **EU**rope, i.e. the **MICLIME** project. It aims to construct a unique, complete, and c. 1400 m long stratigraphic record for the Burdigalian stage from two drilling sites in the continental setting of the North Alpine Foreland Basin. We consider this area to be unique because a thick, complete and undisturbed sedimentary archive with high accumulation rates (c. 45 cm/ka) is preserved there. We are not aware of any other area of the world where such an archive could be explored. The central aim of the proposed MICLIME project will be to investigate Burdigalian climate development based on the cores obtained from the two drillings. Scientific objectives include tests of long-standing and conflicting hypotheses for sediment formation, formulation/assessment of new hypotheses relating to the response of marine ecosystems to climate change in an ancient semi-closed sea, new insights into the interplay between climate, uplift and the driving forces acting at both crustal and subcrustal levels, as well as further evaluation of the 'paleome' hypothesis. New data acquired during the MICLIME project would ideally complement those derived from the SMS-AND 2A core obtained by the ANDRILL project in Antarctica and vice

versa. Comparison and combination of the SMS-AND 2A and MICLIME datasets will yield improved records of the pre-MCO period, provide new insights from sequence stratigraphy, permit evaluations of potential paleoclimatic teleconnections, and clarify low-resolution and/or questionable reconstructions of the European climate before the MCO. We are currently seeking funds to host a workshop in southern Germany, close to the envisaged drilling sites. The main aim of the workshop is to bring together a multidisciplinary team of PIs and collaboration partners, to strengthen the drilling proposal by carefully appraising the drill sites, to establish the final drilling strategy, and to refine the project's scientific goals.

IODP

Constraining the history of the Cenozoic marine silicon cycle with siliceous microplankton

J. RENAUDIE¹, G. FONTORBE², E.-L. DREWS^{1,3}, S. BÖHNE^{1,3}, D. LAZARUS¹

¹ Museum für Naturkunde, Leibniz-Institut für Evolutions- und Biodiversitätsforschung, Berlin.

² Department of Geology, Lund University, Sweden.

³ Rheinische Friedrich-Wilhelms-Universität, Bonn.

Marine planktonic diatoms play a unique role in the world's modern ocean as the main carbon exporter to the deep sea. They constitute the single largest component of the ocean biologic carbon pump. Many authors (e. g. Pollock, 1997; Falkowski et al., 2004) have speculated or modeled that the activity of diatoms as a carbon pump could have been strong enough to influence noticeably atmospheric pCO₂ on a geological timescale and thus affect the climate state. Additionally diatoms are also today the main silica exporter to the deep sea. Biogenic opal deposition is the only output in the marine silica cycle, while continental weathering is its main input: they should therefore balance on a geological timescale. All weathering proxies we have to date give us information about changing sources of weathering, but not so much about its intensity. Estimating global abundance of biogenic opal in sediments throughout the Cenozoic might therefore be the only way to evaluate changes in weathering intensity.

A preliminary study (Renaudie, 2016), based on an analysis of DSDP/ODP/IODP smear slide descriptions, has highlighted two main events in the Cenozoic history of diatoms and radiolarians. The first one near the Eocene-Oligocene boundary is a diatom diversity and abundance peak during which they took over radiolarians for control of the marine silicon cycle. The second one occurred during the Middle Miocene and witnessed a complete spatial reorganization of the biogenic opal deposition pattern as well as a sustained rise in diatom diversity and abundance. Both events are coeval with known shifts in atmospheric pCO₂ as well as shifts in strontium and osmium isotopes (indicative of changes in the silica weathering pattern).

The current study purpose is to constrain that preliminary study primarily with new timeseries of siliceous microfossils absolute abundances in 26 DSDP, ODP and IODP sites (ca. 650 samples) representing the

main biogeographic zones identified in Renaudie (2016), and spanning the last 55 Myr. The project aim at answering four main questions:

1) how stable was the marine silicon cycle during the Cenozoic, i. e. did continental weathering intensity change?

2) did diatoms bloom because the global climate cooled down; or did a bloom of diatom caused the atmospheric pCO₂ to drop, hence contributed to cool global climate?

3) what led the diatoms to outcompete the radiolarians for silica availability during the latest Eocene?

4) how did diatoms spread into the world oceans prior to the late Eocene and what does it say about Paleogene paleoceanography?

The sampling effort (currently on its way), together with solid, new age models made using the stratigraphic layer of the Neptune NSB database (Lazarus, 1994), will provide us with accurate, regional accumulation rates and thus, on one hand, determine the precise sequence of events during the two main phases of diatom expansion (and therefore document the relationship between diatoms and the carbon cycle on a geological timescale), but also, on the other hand, provide us with an estimate of the global accumulation rate of biogenic opal for the Cenozoic: since this quantity should mirror the amount of silica inputted in the marine cycle mostly through weathering (see Figure 1), it should provide us also with the first quantitative estimate of weathering intensity for the Cenozoic.

In parallel to the sampling effort, a database of measured biogenic silica accumulation rates in DSDP-ODP-IODP sediments (ca. 29k samples to date) has been gathered from the literature as a backbone to the siliceous microfossils timeseries (providing a way to translate siliceous microfossils accumulation rates into 'mass' accumulation rates) as well as a secondary line of evidence for the observed pattern. Preliminary statistical tests showed that the pattern observed in the preliminary study match the geochemical data reliably.

In order to investigate the early Cenozoic history of the marine silicon cycle (question 4), Paleocene diatom abundance were investigated (in addition to the main timeseries of siliceous microfossils) in various samples from the Micropaleontological Reference Center (MRC; Lazarus, 2006), from the Southern Ocean, and from the South and North Atlantic. Those samples show that diatoms were already locally abundant in open ocean sites, as early as the earliest Late Paleocene. Interestingly, while North Atlantic and Southern Ocean samples do not seem to show any noteworthy temporal patterns, South Atlantic samples seem to show an abundance peak at the Selandian/Thanetian boundary, seemingly concomitant with the Early Late Paleocene Event (ELPE; see e.g. Petrizzo, 2005).

Finally, in addition to these efforts in trying to quantify and constrain the history of the marine silicon cycle output, a new collaboration with Dr Fontorbe in Lund University aim at quantifying the main biological loop of this cycle (see Figure 1). Indeed, silicon isotopes ($\delta^{30}\text{Si}$) measured on sponge spicules, radiolarians and diatoms has been determined and used in a few studies so far to quantify the concentration of silicic acid in the water column (for

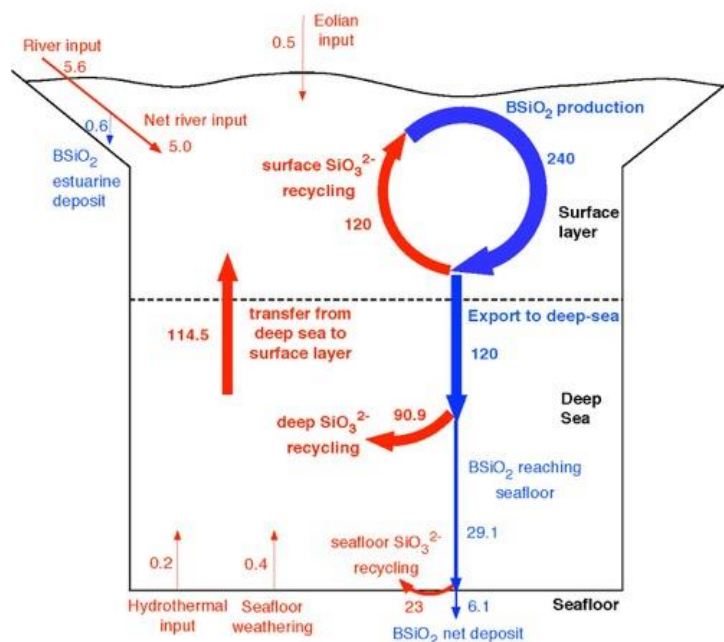


Figure 1: Modern Marine Silica Cycle. Redrawn after Tréguer et al. (1995). In blue, biogenic opal (here BSiO₂); in red, dissolved silicic acid (SiO₃²⁻). Values are given in Tmol/yr. The output of silicon from the marine system is the deposition of biogenic opal, while the input to the system is almost entirely from continental weathering (here river and eolian input).

sponges; Hendry & Robinson, 2012) and to quantify silicon usage, i. e. the amount of BSiO₂ produced and the amount of SiO₃²⁻ recycled (for diatoms and radiolarians; e. g. Egan et al. 2013, Fontorbe et al. 2016).

As this is a relatively new proxy, it still needs some testing, in particular for 'vital effect': indeed $\delta^{30}\text{Si}$ (radiolarians) is measured on bulk (i. e. undifferentiated) radiolarians. In the context of this study, we are testing the stability of this proxy by picking radiolarians from 12 common species from Late Eocene / Early Oligocene samples from equatorial Pacific sites 1217-1220: $\delta^{30}\text{Si}$ were measured on bulk radiolarians in these very samples in Fontorbe (2016). The selected species (*Podocyrtris chalara*, *P. goetheana*, *Thyrsoyrtris triacantha*, *T. rhizodon*, *T. lochites*, *Eusyringium fistuligerum*, *Calocyclus hispida*, *Dictyoprora mongolfieri*, *Dorcadospyrtris ombros*, *Periphaena decora* group, *Amphicraspedum prolixum* and *Lithocyclia ocellus*) should allow us to test a variety of influencing factors (phylogeny, endemicity or ecology): of particular interest, will be to test whether individual species record silicon isotopes differently depending on their living depth, as it would provide an invaluable tool to understand and reconstruct the past marine silicon cycle and more generally the past ocean chemistry.

All those efforts put together will help us constrain the Cenozoic history of the marine silicon cycle, and its relationship to the carbon cycle through diatoms, and thus, ultimately, provide strong numerical constraint on the input of that cycle: namely, chemical weathering.

References:

- Egan, K. E., Rickaby, R. E., Hendry, K. R., and Halliday, A. N. (2013). Opening the gateways for diatoms primes Earth for Antarctic glaciation. *Earth and Planetary Science Letters*, 375:34–43.
- Falkowski, P. G., Schofield, O., Katz, M. E., Van de Schootbrugge, B., and Knoll, A. H. (2004). Why is the land green and the ocean red? In

- Thierstein, H. and Young, J., editors, *Coccolithophores: from molecular processes to global impact*, pages 429–453. Springer.
- Fontorbe, G. (2016). *Marine silicon cycle through the Cenozoic*. PhD thesis, Lund University, Faculty of Science, Department of Geology.
- Fontorbe, G., Frings, P. J., Christina, L., Hendry, K. R., and Conley, D. J. (2016). A silicon depleted North Atlantic since the Palaeogene: Evidence from sponge and radiolarian silicon isotopes. *Earth and Planetary Science Letters*, 453:67–77.
- Hendry, K. R. and Robinson, L. F. (2012). The relationship between silicon isotope fractionation in sponges and silicic acid concentration: Modern and core-top studies of biogenic opal. *Geochimica et Cosmochimica Acta*, 81:1–12.
- Lazarus, D. (1994). Neptune: a marine micropaleontology database. *Mathematical Geology*, 26(7):817–832.
- Lazarus, D. (2006). The Micropaleontological Reference Center Network. *Scientific Drilling*, 3:46–49.
- Pettrizzo, M. R. (2005). An early late Paleocene event on Shatsky Rise, northwest Pacific Ocean (ODP Leg 198): evidence from planktonic foraminiferal assemblages. In Bralower, T. J., Premoli-Silva, L., and Malone, M. J., editors, *Proceedings of the Ocean Drilling Program, Scientific Results*, volume 198, pages 1–29. Ocean Drilling Program, College Station, TX.
- Pollock, D. E. (1997). The role of diatoms, dissolved silicate and antarctic glaciation in glacial/interglacial climatic change: a hypothesis. *Global and Planetary Change*, 14(3):113–125.
- Renaudie, J. (2016). Quantifying the Cenozoic marine diatom deposition history: links to the C and Si cycles. *Biogeosciences*, 13(21):6003–6014.
- Tréguer, P., Nelson, D. M., Van Bennekom, A. J., DeMaster, D. J., Leynaert, A., and Quéguiner, B. (1995). The silica balance in the world ocean: a reestimate. *Science*, 268(5209):375–379.

IODP

Sequence stratigraphy and palaeoenvironment of Miocene platform slope deposits from The Maldives

J. REOLID¹, C. BETZLER¹, G.P. EBERLI², T. LÜDMANN¹, C. ALVAREZ-ZARIKIAN³ AND IODP EXP. 359 SHIP-BOARD SCIENTISTS

¹ Institute of Geology, CEN, University of Hamburg, Bundesstrasse 55, Hamburg 20146, Germany.

² Department of Marine Geosciences, Rosenstiel School of Marine & Atmospheric Science, University of Miami, Miami FL 33149, USA

³ International Ocean Discovery Program, Texas A&M University, Discovery Drive, College Station TX 77845, USA.

The Inner Sea of The Maldives contains a carbonate edifice that bears a unique and mostly unread Indian Ocean archive of the evolving Cenozoic icehouse world. Two main episodes of carbonate platform development occurred during the Cenozoic. These episodes were interrupted by drowning events of the platform most likely related to the reconfiguration of the current system during the Oligocene/Miocene transition and in the Middle Miocene. This study presents the preliminary results of an analysis of a series of core sections, thin sections and well-log data from IODP Expedition 359 Sites U1466 and U1468. Data allow characterizing the palaeoenvironmental conditions of the platform slope deposits, as well as subtle changes of the slope depositional regime controlled by variations in the current regime and the intensity and frequency of the platform shedding. Here, we focus on the paleoichnological analysis of the sediments together with a classical facies and microfacies analysis. Twenty ichnofabrics were established based on the sediment texture, grain size, bioturbation index and the assemblage of ichnotaxa. The succession of ichnofabrics in a site starts with mud fabrics with scarce bioturbation that gradually change into coarser mud- to grain-supported fabrics that are completely bioturbated. This general trend responds to an evolution of the basin from restricted conditions during the early Miocene to a relatively more energetic environment in the Middle Miocene. Excursions within the general trend of ichnofabrics represent events of enhanced sediment export from the platform and periods of relatively low oxygenation, probably by decreasing circulation in the basin. The sediment export from the platform occurs as debris flows, sediment flows and slumping, and it is more significant and frequent in Site U1466. The ichnofabrics variability also depends on the proximity to the platform and the paleobathymetry, being sensibly higher in the most proximal Site U1466 than in the basinal Site U1468.

IODP

The rapid switch from inorganic tropical carbonates to bioclastic sedimentation across a drowning unconformity (North West Shelf of Australia)

L. REUNING¹, S. BACK¹, S.J. GALLAGHER², C.S. FULTHORPE³, A. RASTEGAR LARI⁴, T. HIMMLER⁵, H. IWATANI⁶, G. AUER⁷, K. BOGUS⁸ AND EXPEDITION 356 SCIENTISTS

¹ EMR-Group, Geological Institute, RWTH Aachen University, Germany

² School of Earth Sciences, University of Melbourne, Australia

³ Institute for Geophysics, University of Texas at Austin, USA

⁴ School of Applied Geology, Curtin University, Australia

⁵ Marine Geology, Geological Survey of Norway, Norway

⁶ School of Biological Sciences, The University of Hong Kong, China

⁷ Institute of Earth Sciences, University of Graz, Austria

⁸ International Ocean Discovery Program, Texas A&M University, USA

The North West Shelf of Australia (NWS) stretches between ~13° and 21°S and is situated at the transition between the tropical and sub-tropical realm. This distally steepened carbonate ramp equals in size the carbonate systems of the Bahamas or the Persian Gulf and forms an important template for the interpretation of ancient platform systems. During the Plio-Pleistocene a succession of regional-scale, flat-topped platforms developed on this larger scale carbonate ramp. Based on seismic geomorphological analysis it has been argued that the platform tops either represent flooding surfaces (Sanchez et al., 2016) or sequence boundaries (Goktas et al., 2016). In 2015, IODP Expedition 356 for the first time cored one of these platforms. The integration of seismic with core data shows that the flat-topped platform was dominated by inorganic tropical carbonates consisting nearly entirely of ooids and peloids deposited in shallow-waters during a sea-level highstand. During the following sea-level fall, the platform top was subaerially exposed and karstified. The sediments directly above this unconformity and infilling karstic cavities are completely different, indicating a major change in the carbonate system. They are virtually devoid of ooids and peloids and are composed of bioclasts such as bryozoan, foraminifers and echinoderms. Intra-skeletal pores filled by authigenic glauconite and the common occurrence of planktic foraminifers just cm above the karstic surface point to low sedimentation rates during the subsequent sea-level rise. The fact that anorganic sedimentation was terminated at the sequence boundary and was not able to reestablish after the renewed flooding likely is due to a major shift in environmental conditions.

References:

Goktas, P., J.A. Austin Jr., C.S. Fulthorpe, S.J. Gallagher (2016): Morphologies and depositional/erosional controls on evolution of Pliocene-Pleistocene carbonate platforms: Northern Carnarvon Basin, Northwest Shelf of Australia, *Continental Shelf Research*, Volume 124, Pages 63-82.

Sanchez, C. M., Craig S. Fulthorpe, Ronald J. Steel (2016): Influence of bathymetry and oceanic currents on the development of carbonate platforms: Northern Carnarvon Basin, Northwest Shelf of Australia, *Marine and Petroleum Geology*, Volume 77, November 2016, Pages 942-953

IODP

Sequence boundaries from time to depth: A seismic depth imaging workflow for groundwater modeling offshore New Jersey

M. RIEDEL¹, S. REICHE², K. ASSHOFF^{1,2}, S. BUSKE¹

¹Institute of Geophysics and Geoinformatics, Technische Universität Bergakademie Freiberg, Gustav-Zeuner-Straße 12, 09596 Freiberg, Germany

²Institute for Applied Geophysics and Geothermal Energy, E.ON Energy Research Center, RWTH Aachen University, Mathieustrasse 10, 52074 Aachen, Germany.

During IODP expedition 313 a transect of three holes was drilled into the New Jersey shelf. Pore water samples recovered at each of the drilling locations revealed rapid vertical alternations between fresh and saline groundwater (Mountain et al., 2010). The present study is part of a larger project aiming to understand the mechanisms behind fresh water emplacement offshore New Jersey based on numerical simulations. The basis for meaningful flow and transport simulations is a well-constrained hydrogeological model. An excellent seismic database is available across the New Jersey shelf but seismic profiles are only available in time. Reliable positioning of sequence boundaries in depth is needed as uncertain reflector depths may propagate significant uncertainty into the outcome of subsequent numerical simulations.

Here we present an enhanced seismic depth imaging workflow aiming to achieve reliable positioning of reflectors in depth. For this purpose, we apply a two-stage processing approach which consists of an initial standard time-domain processing part, followed by an advanced depth-imaging sequence. For the latter we mainly utilize an alternation of prestack depth migration and reflection tomography. We performed seismic depth imaging completely independent of velocity information available at the three boreholes. Instead we use these as an independent quality control for our estimated reflector depths. We find that from a total of 25 identified sequence boundary depths, 23 deviate less 10 m and 18 less than 5 m from those sequence boundary depths identified in IODP 313 cores and borehole logs (Millet et al., 2013). We conclude that we have developed a suitable processing workflow for seismic depth imaging offshore New Jersey with low and quantifiably uncertainty in reflector depths, forming a solid foundation for building a hydrogeological model and subsequent numerical simulations.

References:

- Miller, K.G., Mountain, G.S., Browning, J.V., Katz, M.E., Monteverde, D., Sugarman, P.J., Ando, H., Bassetti, M.A., Bjerrum, C.J., Hodgson, D., Hesselbo, S., Karakaya, S., Proust, J.-N., Rabineau, M., 2013. Testing sequence stratigraphic models by drilling Miocene foresets on the New Jersey shallow shelf. *Geosphere* 9, 1236-1256.
- Mountain, G.S., Proust, J.-N., McInroy, D., Cotterill, C., and the Expedition 313 Scientists, 2010. Proceedings of the Integrated Ocean Drilling Program. Volume 313: Tokyo (Integrated Ocean Drilling Program Management International, Inc.), doi:10.2204/iodp.proc.313.2010

IODP

Mechanisms of deformation during peak-ring formation of large impact structures in ferred from Expedition 364 drill core

U. RILLER¹, M. POELCHAU², A.S.P. RAE³, D. KRING⁴, R.A.F. GRIEVE⁵, J. LOFF⁶, J. MORGAN³, S. GULICK⁷ AND IODP EXPEDITION 364 SCIENCE PARTY

¹Institut für Geologie, Universität Hamburg, Bundesstrasse 55, 20146 Hamburg, Germany

²Universität Freiburg, Geologie, Albertstr. 23b, 79104 Freiburg, Germany

³Department of Earth Science and Engineering, Imperial College London, UK

⁴USRA-Lunar and Planetary Institute, 3600 Bay Area Blvd., Houston TX 77058 USA

⁵Earth Sciences Sector, Natural resources Canada, Ottawa, Ontario, Canada, K14 0E4

⁶Géosciences Montpellier, Université de Montpellier, France

⁷Institute for Geophysics, University of Texas, Austin, TX, USA

The floors of large impact structures (impact basins) are largely flat and contain one or more morphological rings. The formation of the innermost ring, the so-called peak ring, and the requisite causes of target rock weakening leading to overall flat crater floors are not well understood. Constraining these mechanisms is the prime structural geological objective of Expedition 364 "Drilling the K-Pg Impact Crater", using the Chicxulub impact structure, Mexico, as a terrestrial analogue for the formation of planetary impact basins.

A total of 829 meters of core was recovered from borehole M0077A drilled into the peak-ring of the crater. From bottom to top, the core is crudely composed of: (1) pervasively shocked granitoid target rock hosting meter- to decameter-thick impact melt rock and suevite dike-like bodies, (2) a 130 m thick impact melt rock and suevite unit overlying the target rocks, and (3) a 112 m thick section of post-impact pelagic carbonate rocks. Based on visual inspection of the drill core, we determined impact-induced deformation structures in target rock.

Target rocks are replete with impact-induced, mesoscopic planar deformation structures. In addition to microscopic planar structures formed by shock metamorphism, these include: (1) cataclastic deformation zones, (2) striated shear faults, (3) ductile shear band structures, and (4) open fractures. Structural overprinting criteria point to a relative age for these structures. Zones of cataclasite are consistently displaced or used by shear faults. Cataclasite bands in target rock fragments included in suevite are cut by the latter and a striated target rock fragment was found in impact melt rock. Suevite and impact melt were emplaced in zones of dilation, often localized by shear faults. Collectively, these observations suggest that cataclastic deformation was followed by shear faulting, followed in turn by emplacement of suevite and melt into dilation zones. This succession of deformation mechanisms is corroborated by the observation that suevite and impact melt bodies are devoid of cataclasite and shear faults. These lithological units were still viscous when they were deformed by ductile band structures consistently accomplishing horizontal extension. Thus, band structures formed after the shear faults. Open fractures hosting hydrothermal minerals occurred likely after crater formation. Based on the structural overprinting relationships, we attempt to relate the mesoscopic planar

structures to cratering stages known from impact mechanics.

IODP

Formation fluid pressure and temperature transients along the Nankai Trough Kumano Transect - SE Japan

A. RÖSNER¹, A. KOPF¹, D. SAFFER², S. TOCZKO³, EXPEDITION 365 SCIENTISTS

¹MARUM, University Bremen, 28359 Bremen, Germany

²Department of Geology Pennsylvania State University, USA

³JAMSTEC, Yokohama, Japan

The Nankai Trough Seismogenic Zone Experiment (NanTroSEIZE) is a multi-expedition Integrated Ocean Drilling Program (IODP) project along the Nankai Trough subduction zone with the purpose of better understanding subduction-zone earthquakes and seismogenic processes. Long-term pressure and temperature monitoring along the Kumano transect produced valuable data records which constrain potential fluid flow paths and help to identify regions of strain accumulation/release. Simultaneous pressure and temperature records are available for a mud volcano (MV4), IODP Site C0002 and IODP Site C0010.

Two recent expeditions, IODP Exp. 365 in April 2016 and Sonne Cruise 251 in October 2016, recovered an autonomous borehole observatory termed “GeniusPlug” and an earlier model observatory termed “SmartPlug”. The GeniusPlug was recovered from Site C0010, where it was installed within the mega splay fault zone at 407 mbsf. The SmartPlug observatory, initially also a borehole observatory, was recovered from a mud volcano in the Kumano Basin, where it was installed in the uppermost seafloor sediments. Both observatories were equipped with temperature loggers and two pressure sensors. One pressure sensor is used as hydrostatic reference, while the other measures formation pressure. The GeniusPlug record has a sampling period of 30 sec from November 2010 – April 2016, and the SmartPlug recorded data at 10 sec intervals from August 2012 – October 2015. Complementary formation pressure data at various depths are available via the C0002 long-term borehole monitoring system (LTBMS). These three observatories monitored temperature, formation and hydrostatic reference pressure over 45 km along dip from the megasplay fault zone into the deep Kumano Basin.

The data records are affected by sensor drifts, tidal loading and clock drifts. These artefacts were removed to analyze short-term and long-term pressure transients, which can be correlated with distant or regional earthquakes. Additionally, pressure transients were observed which correlate with a period of slow slip in the Kumano forearc basin. Moreover, periods of high-frequency energy are present in the dataset, as well as signals from tsunami passing by the observatory sites. The pressure transients are used for formation physical properties characterization and as a proxy for strain accumulation or release along the Kumano transect. The GeniusPlug temperature data shows cold fluid injections into the borehole. One of these injections can be correlated

with the M9 2011 Tohoku-Oki earthquake, whereas the rest is of unknown origin yet.

ICDP

Chew Bahir, the HSPDP drill site: half a million years of environmental history from southern Ethiopia

FRANK SCHAEBITZ¹ AND THE HSPDP- AND CRC806-TEAM

¹Institute of Geography Education, University of Cologne, 50931 Köln, Germany

The Chew Bahir drilling project (southern Ethiopia) is part of the Hominin Sites and Paleolakes Drilling Project (HSPDP). The deep drilling initiative was co-financed by ICDP-Germany, the Collaborative Research Center (CRC806) “Our Way to Europe” at Cologne University, Germany, as well as NERC (UK). The coring site, a sediment-filled deep tectonic basin in the Southern Ethiopian Rift, is close to the Lower Omo valley, well known for the Omo – Turkana key palaeoanthropological site of anatomically modern humans. Chew Bahir was cored in Nov-Dec 2014, when two overlapping cores (280 m and 270 m long) of mostly clayey silts, were collected, from the NW margin of the Chew Bahir basin. The record covers the last 550,000 years of environmental history, as first Ar/Ar ages on cryptotephra and OSL age determinations show. The composite record presented here was constructed by using MSCL, XRF and lithologic data, providing a potential archive of environmental history during the evolution and dispersal of anatomically modern humans. Initial sedimentological and geochemical results show that the Chew Bahir deposits respond sensitively to changes in moisture by sediment influx, provenance, transport and diagenetic processes, evident from mineralogy, elemental concentration and physical properties. The potassium record for example clearly traces dry-wet cycles on orbital to at least millennial timescales, as clearly evident for the youngest precession controlled cycle, the African Humid Period. Therefore, the Chew Bahir record will allow us to test different hypotheses concerning the influence of environmental change on the development and dispersal of *Homo sapiens* and his technological innovations such as Middle Stone Age tools.

ICDP

Decompression of Krafla magma: From immobile magma to explosive foaming?

B.SCHEU¹, F.CACERES¹, F.WADSWORTH¹, K.-U. HESS¹, D.B.

DINGWELL¹

¹Department für Geo- und Umweltwissenschaften, Ludwig-Maximilians Universität München, Theresienstrasse 41, 80333 München

Iceland’s rhyolites are associated with central volcanoes exhibiting calderas that are located along the rift system associated with the Mid-Atlantic plate boundary. In 1875, one of these predominantly basaltic volcanoes, Askja, released a devastating eruption of crystal-poor rhyolite after a period of basaltic rifting. To the north, in 1724, Krafla produced a small phreatic explosion with crystal-poor rhyolite pumice during a basaltic rifting event. Drilling in 2009 (IDDP-1) next to this crater encountered

similar melt-rich magma at 2100 m depth, a unique event in the drilling of active magmatic systems to date. Similar material was encountered by drilling to both the north and south, suggesting that unseen rhyolite magma underlies a substantial area of the caldera, much as must have been the case for Askja before 1875.

The finding of IDDP-1, that non-eruptively degassed rhyolite melt is present at about 2 km depth under Krafla Caldera, raised many questions, as: Is there true magma in IDDP-1, or only a melt ooze that entered the borehole from hypersolidus felsite? If the intrusion formed during the last eruption, why did it not erupt? Ultimately this finding and the questions arising from it triggered the work presented here, which is also intimately linked to the objectives of a new drilling project proposed to ICDP, the Krafla magma drilling (KMDDP).

Here we aim to constrain the response of rhyolitic magma in general, and Krafla magma in special to slow decompression (in shallow depths). This encompasses the questions if, when and how bubbles will nucleate and grow, the formation of permeable networks, and possibly magma fragmentation. The approach proposed is based on unique laboratory experiments, exploring possible scenarios as the rhyolitic magma responses to slow decompression under P-T conditions relevant to the Krafla system. Different silicate melts ('magma') are foreseen for these experiments as synthetic silicate melts with the major components of the rhyolite from IDDP-1 and natural and hydrated obsidian from the last rhyolitic eruption of Krafla (Hrafninnuhryggur – Obsidian Ridge). The samples should cover a range in water content from 0.13 – 1.8 wt%, the latter being the average volatile content of the magma tapped in IDDP-1 (Elders et al. 2011). The samples response to slow decompression will be mapped in the range of 800-920°C & 16-55 MPa, from 'nothing' to minor nucleation to explosive foaming and fragmentation, enabling us to constrain the 'eruptability' of Krafla magma. Firstly we characterise the bubble nucleation and foaming of surficial Hrafninnuhryggur obsidian with water contents typically in the range from 0.11 – 0.15 wt% (Tuffen and Castro, 2009) at varying temperatures with a highly sensitive optical dilatometer. Next we will analyse the effect of varying pressure drop scenarios at magmatic temperatures at these obsidian samples before moving to samples containing higher volatile contents.

The research proposed here is expected to provide answers critical for understanding how magmas are generated, evolve and interact in the shallow crust as well

as how they will react upon disturbance as for instance drilling

References:

- Elders WA, Friðleifsson GÓ, Zierenberg RA, Pope EC, Mortensen AK, Gudmundsson A, Lowenstern JB, Marks NE, Owens L, Bird DK, Reed M, Olsen NJ, Schiffman PA (2011) Origin of a rhyolite that intruded a geothermal well while drilling in a basaltic volcano, at Krafla, Iceland. *Geology* 39:231–234.
- Tuffen H, Castro JM (2009) The emplacement of an obsidian dyke through thin ice: Hrafninnuhryggur, Krafla Iceland. *Journal of Volcanology and Geothermal Research*, 185(4), 352-366.

IODP

Tephrostratigraphy, provenance and cyclicities – Findings from Expeditions 350 and 352

J.C. SCHINDLBECK¹, S. KUTTEROLF¹

¹GEOMAR Helmholtz Zentrum für Ozeanforschung Kiel, Wischhofstr. 1-3, 24148 Kiel

In the following we will summarize the results of the IBM Tephra project that is supported by the German Research Foundation since 2015. The work for this project is conducted in close collaboration with Susanne Straub (Lamont Doherty Earth Observatory), Marion Jegen (GEOMAR) and Alastair Robertson (University of Edinburgh) and several other cooperations.

In 2014 three closely related IODP Expeditions targeted the Izu-Bonin-Mariana arc (IBM). The IBM ranges from Izu Peninsula (Japan) to Guam (USA) over a distance of 2800 km. Volcanism is the result of the subduction of the Pacific plate beneath the Philippine plate. The investigated drill sites are influenced by highly explosive volcanism that originate from the Izu-Bonin arc as well as from the Japanese arcs.

Under the umbrella of the whole IBM project and the cross-cutting goals of IODP Expeditions 350 and 352 our own project focuses on the tephra layers from these highly explosive eruptions that were sampled during the cruises.

IODP Expedition 350 drilled two sites. Site U1436 was drilled in the IBM forearc as a geotechnical hole in preparation for the proposed deep drilling at Site IBM-4, whereas Site U1437 lies about 160 km WSW of Site U1436 in a basin between two Izu reararc seamount chains (Manji and Enpo chains). At Site U1436 a record of Late

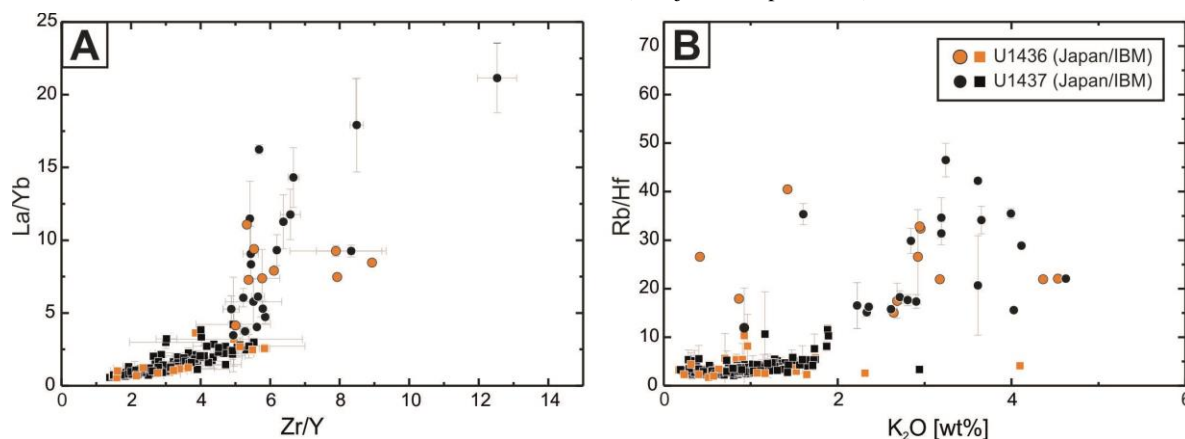


Figure 1: Glass shard major and trace element compositional variations of the 350 tephra layers to distinguish between Izu-Bonin and Japan origin. La/Yb versus Zr/Y and Rb/Hf versus K₂O. Typically higher Zr/Y, La/Yb and Rb/Hf ratios as well as high potassium contents indicate a tephra origin from the Japanese arcs.

Pleistocene forearc sedimentation has been recovered that is strongly influenced by explosive forearc volcanism (Tamura et al., 2015). In our studies we focus on the upper ~60 mbsf that are located on top of a hiatus and correspond to the upper ~0.95 Myr. At Site U1437 a coherent stratigraphy from 0 to 1806.50 mbsf was recovered in three holes (U1437B, D and E) with Miocene to Holocene sediments. The lithology is dominated by tuffaceous mud and mudstone with intercalated volcanoclastic layers. Our project focuses on the upper ~140 mbsf that correspond to the upper ~1.1 Myr. This sediment succession overlies the volcanoclastic apron and is characterized by tephra layers that are deposited within an undisturbed mud sequence.

IODP Expedition 352 recovered early Oligocene to recent sediments above Eocene igneous basement at four sites in the Izu-Bonin forearc. The sites were selected to investigate the forearc region since subduction initiation in the Eocene, with Sites U1439 and U1442 being cored into the upper trench slope and Sites U1440 and U1441 into the lower trench slope. In total 1.22 km of igneous basement and 0.46 km of overlying sediment (Expedition 352 Scientists, 2015) were recovered. The cored volcanic rocks provide diverse, stratigraphically controlled suites of forearc basalts, related to decompression melting as mantle rose to fill the space created by the initial sinking of the Pacific Plate, and boninite generated slightly later during earliest arc development. The igneous basement is overlain by late Eocene to Recent sediments. Three drill sites (Sites U1439-U1441) are located in small fault-controlled sediment basins up to several hundred meters thick, whereas one site (U1442) was positioned on thin sediments overlying a fault-controlled basement high.

In total, we geochemically analyzed ~500 tephra samples. Major elements were measured with an electron microprobe at the GEOMAR Helmholtz Centre for Ocean Research Kiel (~7000 single glass shard analyses) and trace elements were analyzed by Laser Ablation ICP-MS at the Academia Sinica in Taiwan (~1500 single glass shard analyses; cooperation with Kuo-Lung Wang).

Results Expedition 352 (ongoing work in cooperation with Susanne Straub (Lamont-Doherty Earth Observatory) and Marion Jegen (GEOMAR)):

We studied the marine tephra layers of Holes U1436A and U1437B in the Izu-Bonin fore- and rear-arc of the last ~1 Myr, regarding their provenance. For our provenance studies we applied major and trace element glass compositions and distinguished between Japanese and Izu-Bonin origin of the marine tephra layers (Figure 1). In total, we examined 304 tephra samples and identified 260 primary tephra layers. We established 23 correlations between the two sites. Furthermore we were able to correlate marine tephra layers to well-known and widely distributed highly explosive eruptions from the Japanese arc. We defined eleven correlations of marine tephra deposits to major Japanese eruptions from the 1.05 Ma Ss-Pnk Tephra to the 30 ka Aira-Tn Tephra, both from Kyushu Island.

The correlations to well-known eruptions from Japan support and improve the age models established on board and post-cruise, providing excellent time markers within the sediment sequence. Furthermore, we calculated minimum marine tephra volumes of all detected events. For some of the major Japanese eruptions these are the first volume estimations that also include the distal deposits.

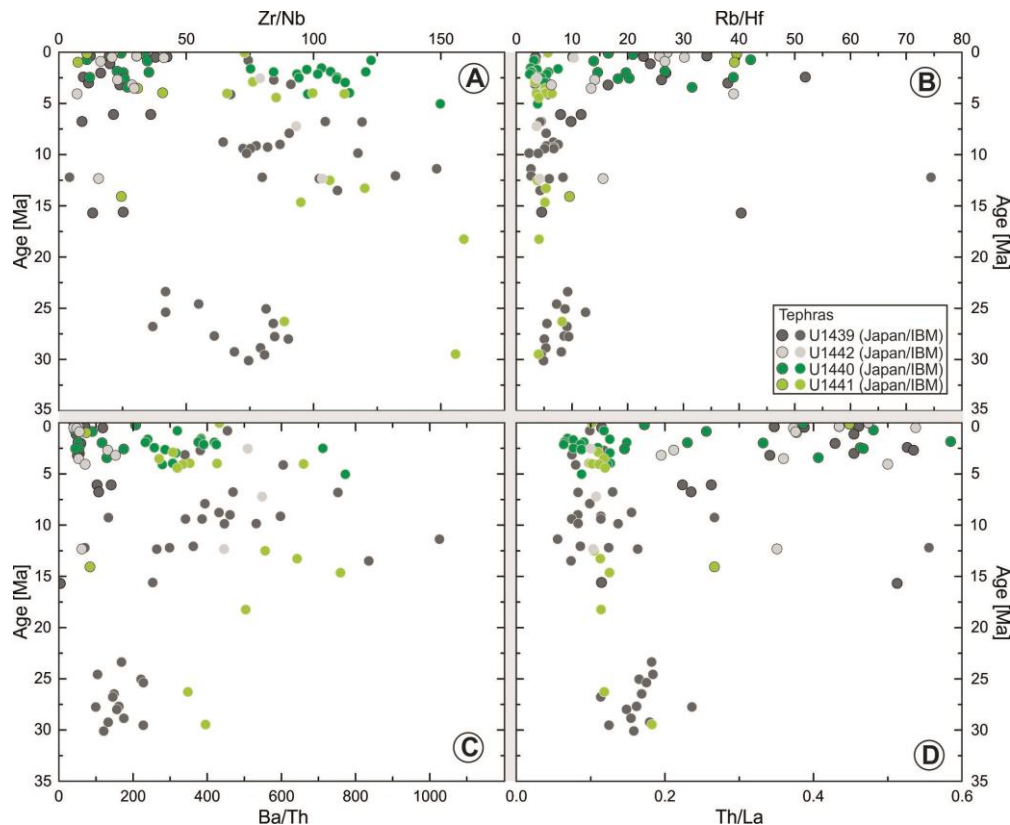


Figure 2: Age versus composition diagrams indicating compositional variations of the 352 tephra inventory with time for Zr/Nb, Rb/Hf, Ba/Th, and Th/La. Data represent averages of all glass analyses made for each individual tephra. Ages are constrained by biostratigraphy, correlations to well-dated Japanese on-land tephra, and paleomagnetic studies.

Beside the provenance study we studied the temporal distribution of the tephra layers in Hole U1437B (Schindlbeck et al., 2016 AGU Fall meeting) to contribute to the ongoing discussion whether volcanism influences the climate or vice versa. A major problem has been so far that other studies often lack records that go further back in time. During IODP Expedition 350 at Site U1437 an undisturbed sediment record with high sedimentation rates, a robust age model and abundant tephra layers representing single volcanic events has been drilled. Therefore it offers the unique opportunity to study the temporal variability of volcanic events over a long time period (~1.1 Myr) and the timing regarding glacial cycles. Strikingly, the distribution of ash layers in Hole U1437B seems to be synchronous with glacial cycles, with a distinct increase in eruption occurrences at the transitions of glacial/interglacial. This is confirmed by first results of a frequency analysis of the ash-time series that indicate a dominance of a 100 ka cycle.

Our results support the hypothesis that climatic changes induce volcanism. The physical link that is proposed for this linkage may be changes in crustal stress associated with the redistribution of ice shields and water masses during the global ice cycles.

Results Expedition 352 (ongoing work in cooperation with Alastair Robertson (University of Edinburgh)):

For Expedition 352 we established a first tephrostratigraphy. We observed the occurrence of at least three major episodes of highly explosive volcanism from Oligocene to Pleistocene (Figure 2). Provenance studies of the marine tephra, established by glass composition, allocated 56 marine tephra to an origin from the Japanese arc and 101 tephra can be assigned to four regions of origin along the Izu-Bonin arc. Twelve of the Japanese marine tephra layers can be further correlated to major widespread tephra layers from individual Japanese eruptions between 115 ka to 3.5 Ma from Kyushu, Central Japan (S- to Central Honshu) and North Japan (N-Honshu to Hokaido). The marine IBM tephra can be further allocated to four regions of origin along the arc. One, limited to the Oligocene and proximal situated between and Mokuyo and Kakiata Seamounts, close to the Bonin Ridge islands, two around Torishima, Sumisu, and Myojin Knoll reflecting volcanic front and back-arc region of the central Izu-Bonin arc and a fourth in the Northern Izu-Bonin arc area.

In summary, our results suggest an equivalent mixture of tephra sources from the (palaeo)Honshu and Izu-Bonin arc within the last ~5 Ma, an exclusively occurring tephra inventory from the Izu-Bonin arc from 15-5 Ma, and after a ~7 M.y. gap, a group of tephra between 30 to 22 Ma that show an overall Izu-Bonin signature, but also exhibit a slightly different geochemical signal than the Miocene to Pleistocene Izu-Bonin arc.

Beside the tephra provenance study we combined the results from biostratigraphy, sediment chemistry, tephra composition and chronology and magnetic properties along with observations from prior coring in a post-cruise study (Robertson et al., 2016 AGU Fall meeting). This study intend to constrain the overall regional geological development.

Volcanic activity in the area, as inferred from its influence on sediment composition, has varied between long periods of activity and quiescence. Combined whole-rock sediment chemistry and tephra compositions suggest that during the Oligocene to earliest Miocene (~30-22 Ma) tuffaceous input of predominantly dacitic composition was mainly derived from the intra-oceanic Izu-Bonin Arc. The

early Miocene interval (~22-15 Ma) lacks tuffaceous input, as supported by rock magnetic data. During this period, the forearc subsided beneath the carbonate compensation depth (CCD), as evidenced by radiolarian-bearing mud and metal-rich silty clay. This was followed by input of tephra with bimodal felsic and mafic compositions from the Izu-Bonin Arc from ~15 to 5 Ma. Middle Miocene to Quaternary time was characterized by increased carbonate preservation, coupled with abundant, predominantly felsic tephra input, which is chemically indicative of a Japan continental arc source (Honshu), with additional chemically distinctive input from the Izu-Bonin Arc. Extending back to 32 Ma, tephra layers can be correlated between the upper-slope sites, extrapolated to the less well-dated lower-slope sites, and further correlated with onland Japanese tephra. Overall, the new results provide an improved understanding of the regional tectonic evolution.

References:

- Tamura, Y., Busby, C.J., Blum, P., and the Expedition 350 Scientists, 2015. Proceedings of the International Ocean Discovery Program, Expedition 350: Izu-Bonin-Mariana Rear Arc: College Station, TX (International Ocean Discovery Program). <http://dx.doi.org/10.14379/iodp.proc.350.2015>
- Robertson, A.H.F., Kutterolf, S., Petronotis, K., Avery, A., Baxter, A., Schindlbeck, J.C., Wang, K.-L., & Acton, G.D. Geological Development of the Izu-Bonin Forearc Since the Eocene Based on Biostratigraphic, Rock Magnetic, and Sediment Provenance Observations from IODP Expedition 352 Drill Cores, V13C-2860, AGU Fall Meeting 2016, San Francisco.
- Schindlbeck, J.C., Straub, S.M., Jegen, M., Corry-Saavedra, K., Murayama, M., Woodhead, J.D., Kutterolf, S., Vautravers, M., Wang, K.-L., Volcanic cyclicities in the Pacific Northwest: insights from the marine tephra record from IODP Expedition 350, Izu Bonin Arc, V13C-2852, AGU Fall Meeting 2016, San Francisco.

ICDP

Fault core deformation mechanisms deduced from microstructures, mineralogy and geochemistry of the Alpine Fault, New Zealand

B. SCHUCK¹, C. JANSSEN¹, A. M. SCHLEICHER², V. G. TOY³, G. DRESEN^{1,4}

¹ Helmholtz-Zentrum Potsdam, GFZ, Section 4.2: Geomechanics and Rheology, Telegrafenberg 14473 Potsdam, Germany

² Helmholtz-Zentrum Potsdam, GFZ, Section 3.1: Inorganic and Isotope Geochemistry, Telegrafenberg 14473 Potsdam, Germany

³ Department of Geology, University of Otago, P.O. Box 56, Dunedin 9054, New Zealand

⁴ Institut für Erd- und Umweltwissenschaften, Universität Potsdam

The transpressive Alpine Fault is the main structure forming the Australian and the Pacific Plate boundary through New Zealand's South Island. It exposes rocks from 35 km depth with a long-term exhumation rate of 6 – 9 mm a⁻¹ (Little et al., 2005). The Alpine Fault is currently locked and it has been demonstrated that it is capable of generating large (i.e. $M_w > 8$) earthquakes with an assumed recurrence interval of 250 years (Nicol, 2016).

The Alpine Schist forms the hanging wall. Over a distance of about 1 km to the fault's principal slip zone (PSZ) it is progressively deformed into an ultramylonite. Fractured ultramylonites and cataclasites comprising the fault's damage zone outcrop within 50 m of the PSZ. The fault core is characterized by a 2 to 30 cm thick package of cataclasites and fault gouge (Toy et al., 2015). The footwall comprises Quaternary fluvio-glacial sediments, overlying

metasediments intruded by Paleozoic to Cretaceous granitoids.

The seismogenic zone and the underlying brittle-ductile transition are located at very shallow depths (likely < 8 km) due to the fast uplift rates. This provided motivation to drill the Alpine Fault to investigate seismogenic and brittle-ductile transition processes (Townend et al., 2009). In 2011, two shallow boreholes penetrated the Alpine Fault at 91 m and 128 m depth, respectively, during the first phase of the Deep Fault Drilling Project (DFDP-1) (Sutherland et al., 2012).

We are currently investigating outcrop samples and the DFDP-1 cores to describe and understand strain localization in the fault's PSZ. In this contribution we compare microstructural, mineralogical and geochemical analyses obtained from a transect across the fault core at the Waikukupa Slip location. At this exposure the PSZ is identified as a thin (<5 cm) and continuous band, which is formed by a complex structure consisting of several, clearly distinguishable layers ranging in size from < 1 to 2 cm. X-ray diffraction analysis indicates the mineralogy is mostly quartz, plagioclase, calcite, chlorite, illite and mica. Qualitatively, the mineralogical composition does not vary significantly from the hanging- to the footwall, but there are marked changes in the amount of individual mineral phases. High-resolution scanning and transmission electron microscopy demonstrates characteristic microstructural variations along the investigated transect. Grain sizes in the hanging-wall decrease towards the PSZ, within which pulverized rigid particles range down to 100 nm in size. The PSZ comprises distinct domains, each displaying different microstructures. These characteristically include fragments of mylonite as well as reworked gouge clasts (up to 1.5 and 0.5 cm, respectively) and chemically altered feldspars in a fine-grained matrix that includes newly grown phyllosilicates (mostly illite). Within distinct domains of the PSZ, calcite veins generated during multiple crack-seal events form a dense and anastomosing network with various cross-cutting relationships. These microstructures point to a variety of different deformation mechanisms such as grain scale fracturing, twinning, pressure solution and sealing.

The results presented imply that the PSZ served as pathway for large volumes of Ca-rich fluids circulating within the fault gouge. Additionally, fluid pulses resulted in the precipitation of several vein generations, which represent episodes of dilatant fracturing and sealing of the PSZ. This is notable, because the PSZ acts as an impermeable hydraulic seal in the current interseismic period (Menzies et al., 2016).

References:

- Little, T. A., Cox, S., Vry, J. K. & Batt, G. E. (2005): Variations in exhumation level and uplift rate along the oblique-slip Alpine Fault, central Southern Alps, New Zealand. – *Geological Society of America Bulletin* **117**: pp. 707 – 723.
- Menzies, C. D., Teagle, D., Niedermann, S., Cox, S. C., Craw, D., Zimmer, M., Cooper, M. J., Erzinger, J. (2016): The fluid budget of a continental plate boundary fault: Quantification from the Alpine Fault New Zealand. – *Earth and Planetary Science Letters* **445**: pp. 125 – 135.
- Nicol, A. (2016): Alpine Fault Paleoseismic Record and Seismic Hazard analysis. – *Proceedings of the Annual Conference of the Geoscience Society of New Zealand*, Nov 28 – Dec 1, 2016.
- Sutherland, R., Toy, V. G., Townend, J., Cox, S. C., Eccles, J. D., Faulkner, D. R., Prior, D. J., Norris, R. J., Mariani, E., Boulton, C., Carpenter, B. M., Menzies, C. D., Little, T. A., Hastings, M., De Pascale, G. P., Langridge, R. M., Scott, H. R., Reid Lindroos, Z., Fleming, B., Kopf, A. J. (2012): Drilling reveals fluid control on architecture and rupture of the Alpine fault, New Zealand. – *Geology* **40**: 1143 – 1146.
- Townend, J., Sutherland, R., and Toy, V. G. (2009): Deep Fault Drilling Project. – *Scientific Drilling* **8**: p. 75 – 82.
- Toy, V. G., Boulton, C., Sutherland, R., Townend, J., Norris, R. J., Little, T. A., Prior, D. J., Mariani, E., Faulkner, D. R., Menzies, C. D., Scott, H.,

Carpenter, B.M. (2015): Fault rock lithologies and architecture of the central Alpine Fault, New Zealand, revealed by DFDP-1 drilling. – *Lithosphere* **7**: pp. 155 – 173.

IODP

Structural characteristics of the impact melt rock and suevite of the Chicxulub Peak Ring – Initial results from IODP-ICDP Expedition 364

F. M. SCHULTE¹, U. RILLER¹, R.A.F. GRIEVE², D.A. KRING³, PH. CLAEYS⁴ AND IODP EXPEDITION 364 SCIENCE PARTY

¹ Institut für Geologie, Universität Hamburg, Bundesstraße 55, 20146 Hamburg, Germany

² Earth Sciences Sector, Natural Resources Canada, Ottawa, Ontario, Canada, K14 0E4

³ USRA-Lunar and Planetary Institute, 3600 Bay Area Blvd., Houston TX 77058, USA

⁴ Analytical-, Environmental- and Geo-Chemistry, Vrije Universiteit Brussel, B-1050 Brussels, Belgium

One of the prime objectives of IODP-ICDP Expedition 364 “Drilling the K-Pg impact crater” is to constrain peak-ring formation and associated processes at the 65.5 Ma Chicxulub impact structure, Mexico. A total of 829 meters of core were recovered from borehole M0077A. From bottom to top, the core is crudely composed of: (1) pervasively shocked granitoid target rock hosting meter to decameter-thick impact melt rock and suevite dike-like bodies, (2) a 130 m thick impact melt rock and suevite unit, and (3) a 112 m thick section of post-impact platform carbonate rocks. Units (1) and (2) make up rocks of the peak ring. Based on visual inspection and computer tomography analysis of drill core, we examined the structural characteristics of the impact melt rock and suevite unit to better understand its formation, emplacement and post-impact modification.

The lower portion of the impact melt rock and suevite unit (710 - 747 mbsf) is layered, whereas the upper portion of the unit (710 - 617 mbsf) is characterized by polymict, carbonate matrix-supported, sorted suevite. The lower portion can be further divided into four subunits. The basal subunit is 9 m thick, covers fragmented granitoid target rock, and consists of, at least, two pitch-black, silicate melt phases hosting few fragments, which are derived chiefly from gneissic basement rock. The glassy appearance and mottled texture of the melt phases points to quenching and (auto)-brecciation of solidifying melt. This subunit is overlain by a 16 m thick subunit characterized by, at least, two interlayered melt phases displaying convoluted, centimeter-scale folds. One melt phase consist of the pitch-black silicate phase. The other melt phase is bright green and possibly derived from carbonate rock, as evidenced by lenticular and drawn-out carbonate fragments spatially associated with this melt phase higher up in the core. The cusp-and-lobe geometry of the two melt phases suggests that the silicate phase was the more viscose one during folding and solidification of the melt phases. This contrast in mechanical competency between the two phases is exacerbated in the overlying 6 meter thick subunit. Although relics of the folded layers are evident, this subunit displays mostly angular to sub-rounded fragments of dark melt rock enveloped by the flow-textured, greenish melt phase. It appears that dark melt rock fragments formed from folded immiscible melt layers during cooling, whereby the silicate melt phase solidified prior to the green, possibly due to the lower solidus with respect to the

greenish one. The uppermost subunit is 5 meters thick and composed mostly of bright-green carbonate fragments set in a brown matrix, the composition of which remains to be determined.

The structural characteristics of the lower portion of the impact melt rock and suevite unit point to deformation of the melt rock during its solidification. By contrast, structural characteristics of the upper portion are best explained in terms of reworking by high-energy sedimentary processes.

ICDP

ICDP seismic pre-site survey on Lake Nam Co (Tibetan Plateau)

N. SCHULZE¹, V. SPIESS¹, G. DAUT², T. HABERZETTL², J. WANG³,
L. ZHU³

¹ University of Bremen, Department of Geosciences, MTU,
Klagenfurter Straße | 28359 Bremen | Germany

² Friedrich-Schiller-University Jena, Institute of Geography,
Physical Geography, Loebdergraben 32 | 07743 Jena |
Germany

³ Chinese Academy of Sciences, Institute of Tibetan Plateau
Research, 16 Lin Cui Road | Chaoyang District | Beijing
100101 | P.R. China

The influence of the Tibetan Plateau (TP) on the Indian monsoon system is of particular importance for the atmospheric circulation and consequently for the global hydrological and energy cycle (Liu & Yang, 2003). The TP feeds the major rivers of Asia, providing freshwater for the population (Lau *et al.*, 2010) as well as sediment for many megadeltas (Cruz *et al.*, 2007). Considering the economic and ecological importance of the TP, it is necessary to evaluate the reactions of its environment to past and future climate change scenarios.

Nam Co is located on the central TP at the intersection of westerly and monsoonal air masses and offers a high-resolution paleoclimate archive. Hitherto, sediments covering the past 24,000 years have been recovered in a 10.4 m long core, revealing environmental responses to climatic changes. Elevated lake terraces proof the existence of the lake for at least more than 115 kyr (Zhao *et al.*, 2003), potentially as part of an ancient large (mega-)lake on the TP (Zhu *et al.*, 2004). Long sedimentary records retrieved from one or several ICDP cores in Nam Co could provide the necessary material to study, amongst other goals, paleoclimatic variations and the associated environmental changes during glacial/interglacial cycles of the past.

After a pilot multichannel seismic survey in 2014, a more extended seismo-acoustic survey was realized in June 2016 in the frame of the ICDP project ‘*Seismic Pre-Site Survey for ICDP Drilling Locations at Lake Nam Co*’, to proof the existence of sufficiently thick sedimentary deposits with mostly undisturbed layers and continuous sedimentation, and to gain a detailed understanding of the sedimentation processes and the tectonic evolution in the lake area. In total, 89 deep penetration multichannel seismic (MCS) profiles (860 km total length) were recorded, allowing good coverage of the basin. Additionally, high-resolution data of the shallow sub-lake floor were acquired on each MCS track using a parametric sediment echosounder (SES 2000 light). Seismic profiles depict proof for at least several hundred meters of sediment infill with varying sediment thickness. In the eastern part of the lake a basement reflector appears at ~250 ms TWT (two-way travel time), whereas the western part allowed a signal penetration of >1 s TWT.

Seismic data from the center of the lake so far show no signs of erosion (truncations, erosional channels) or sediment relocation processes. This suggests that this

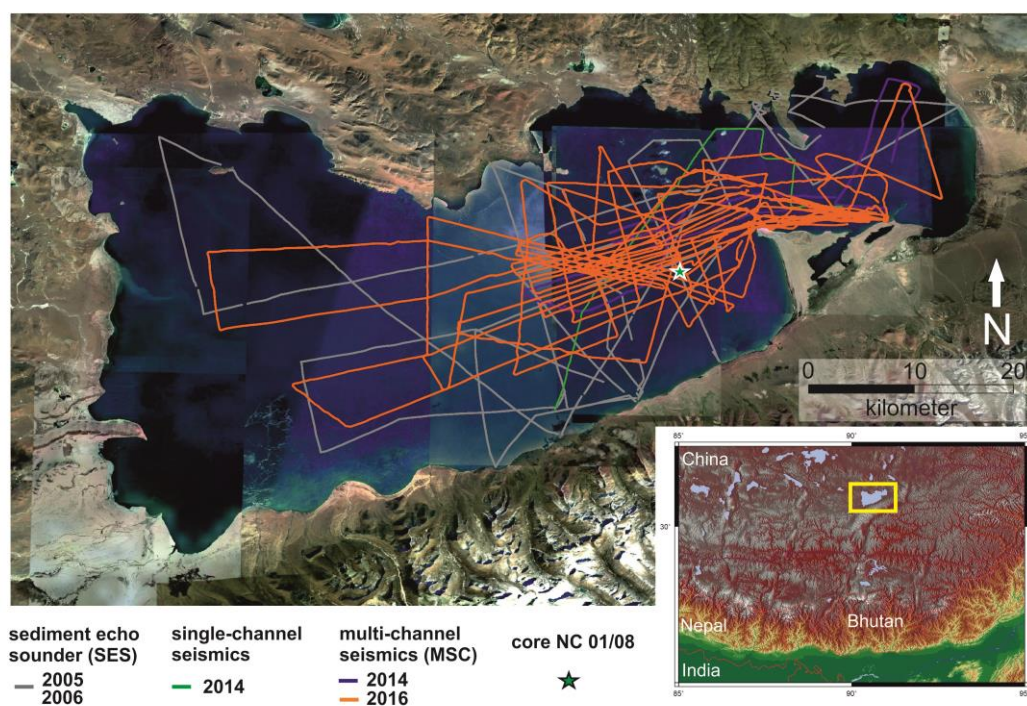


Figure 1: Overview map of the seismic and sediment echosounder surveys conducted in Lake Nam Co between 2005 and 2016. The location of Core NC01/08 is highlighted with a green star. The satellite image was retrieved from Google Earth 2016.

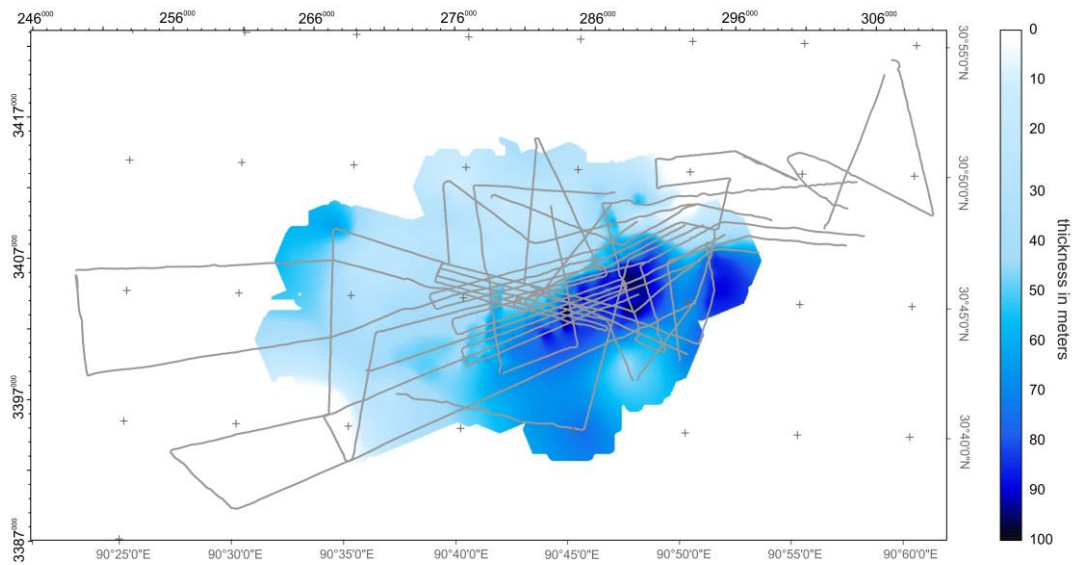


Figure 2: Thickness map of lacustrine sediments younger than Marine Isotope Stage 3 in Lake Nam Co. The thickest sediment packages are deposited in the center of the lake.

location has not experienced considerable additional deposition to the background sedimentation such as for example the deposition of major mass wasting events. These assumptions are in compliance with proxy studies, which indicate that continuous lacustrine deposition prevailed at Nam Co even during dry Marine Isotope Stage 2 (Daut *et al.*, 2010; Kasper *et al.*, 2015). Thus, a continuous sediment record is expected down to bedrock depth. In the new 2016 data set, it is possible to identify basement reflectors close to the northern and southern shore of the lake, which dip steeply towards the center. Hence, it seems possible that the sediment infill exceeds 1000 m in the central part of the lake.

In accordance with the age-depth model of reference Core NC 08/01, sediment accumulation rates (SAR) range between 2.4 and 0.1 mm a⁻¹ during the past 24 cal ka BP (Kasper *et al.*, 2015). Variations in sedimentation rate coincide with changes in lithology in the core and reflectivity changes in the seismic data. A preliminary seismic stratigraphy was derived accordingly, utilising reflection strength to differentiate high and low lake level stands and their transitions. During high lake levels fine-grained sediments are typically deposited with uniform thickness over large areas and can therefore be attributed to low amplitude reflectors. High amplitude seismic facies, however, indicate coarser material during lake level low stands. The seismic facies of the transition periods are defined in relation to low and high lake level facies by e.g., increasing reflectivity, thickness changes and also indications of erosion in the shallow lake sediments. Using this model, maximum ages of ~500 ka may be reached at 500 m, and 1 Ma at 1000 m sub-bottom depth.

Further careful analysis of the seismic lines will provide deeper insight into the sediment dispersal and accumulation patterns, the local tectonic regime, the possible range of lake level changes, and the nature of the sediments near a possible drilling location to develop evolutionary scenarios for Lake Nam Co. These results are

intended to support an ICDP drilling workshop in 2017, which had been proposed recently.

References:

- Cruz, R.V., Harasawa, H., Lal, M., Wu, S., Anokhin, Y., Punsalma, B., Honda, Y., Jafari, M., Li, C., Huu Ninh, N., 2007. Asia. Climate Change 2007: Impacts, Adaptation and Vulnerability. Contribution of Working Group II to the Fourth Assessment Report of the Intergovernmental Panel on Climate Change, Parry, M.L., Canziani, O.F., Palutikof, J.P., van der Linden, P.J., Hanson, C.E., Eds., Cambridge University Press, Cambridge, UK, 469-506.
- Daut, G., Mäusbacher R., Baade J., Gleixner G., Kroemer E., Mügler I., Wallner J., Wang J., Zhu L., 2010. Late Quaternary hydrological changes inferred from lake level fluctuations of Nam Co (Tibetan Plateau, China). *Quaternary International* 218(1-2), 86-93.
- Kasper, T., Haberzettl T., Wang J., Daut G., Doberschütz S, Zhu L., Mäusbacher R., 2015. Hydrological variations on the Central Tibetan Plateau since the LGM and their teleconnection to inter-regional and hemispheric climate variations. *Journal of Quaternary Science* 30(1), 70-78.
- Lau, W., Kim, M.-K., Kim, K.-M., Lee, W.-S., 2010. Enhanced surface warming and accelerated snow melt in the Himalayas and Tibetan Plateau induced by absorbing aerosols. *Environmental Research Letters* 5, 1-10.
- Liu, M., Yang, Y., 2003. Extensional collapse of the Tibetan Plateau: Results from three-dimensional modeling. *JGR*, 108, B082361.
- Zhao, X., Zhu, D., Yan, F., Wu, Z., Ma, Z., Mai, X., 2003. Climatic change and lake-level variation of Nam Co, Xizang since the last interglacial stage. *Quaternary Sciences* 23, 41-52
- Zhu, D.G., Meng, X.G., Zhao, X.T., Shao, Z.G., Xu, Z.F., Yang, C.B., Ma, Z.B., Wu, Z.G., Wu, Z.H., Wang J.P., 2004. Evolution of an Ancient Large Lake in the Southeast of the Northern Tibetan Plateau. *Acta Geologica Sinica - English Edition* 78(4), 982-992.

ICDP

The PALEX project –PALEohydrology and EXtreme Floods from the Dead Sea ICDP Core - First Years of Trilateral Dead Sea Research

M. J. SCHWAB¹, M. AHLBORN¹, R. TJALLINGII¹, B. PLESSEN¹, I. NEUGEBAUER^{1,2}, Y. ENZEL³, J. HASAN⁴, A. BRAUER¹ AND PALEX SCIENTIFIC TEAM

¹ GFZ German Research Centre for Geosciences, Section 5.2 – Climate Dynamics and Landscape Evolution, Potsdam, Germany

² Department of Earth Sciences, University of Geneva, Switzerland

³ The Hebrew University of Jerusalem (HUJ), Institute of Earth Sciences, Edmond Safra Campus, Givat Ram, Israel

⁴ Al Quds University, Department of Earth and Environmental Sciences, Abu-Dies, Jerusalem – Palestinian Authority

Extreme hydrometeorological events and especially floods are a major threat for humans. Therefore, it is an emerging challenge for science to investigate origin and mechanisms of floods in order to better anticipate their frequency and amplitudes as well as their impacts on regional environments. A very sensitive region in terms of both environmental conditions and the political situation is the Dead Sea area in the Near East. Ongoing global change is expected to even increase the environmental pressure and in particular hydrological processes in this part of the world. Therefore, this is an ideal and highly interesting region for Earth and environmental research.

The PALEX (‘Paleohydrology and Extreme Floods from the Dead Sea ICDP sediment core’) project addresses all aspects of extreme hydro-meteorological events in this region through a joint effort of scientist from Israel, Palestine and Germany. PALEX has been designed as a project within the DFG Trilateral program with the aim of fostering scientific cooperation in the Near East.

We apply a novel approach of combining the observation of recent flash floods using cutting-edge

technologies with advanced reconstructions of long flood time-series over several thousand years from the Dead Sea sediment record at high temporal resolution. In this respect, the long sediment cores obtained by the ICDP (‘International Continental Scientific Drilling Program’) drilling from the deep basin of the Dead Sea (DSDDP) provide a unique archive to reconstruct the natural hydro-climatic variability for the last 200 kyrs. In addition, the comprehensive process understanding of the meteorological origin of floods and their effects on erosion, sediment transport and deposition revealed by our combined meteorological and sedimentological monitoring allows an improved interpretation of this exceptional sediment record to utilize event-triggered sediments as proxies for past flooding. With this approach we aim at investigating the relation of changes in the occurrence and dynamics of floods to changing climatic boundary conditions and test the predicted increase of extreme floods in a warming climate.

Beyond the scientific goals, PALEX undertakes major efforts in capacity building and international networking in the Middle East to foster peaceful collaboration for solving common problems and development of human and technical resources. A crucial part of the project concept, therefore, is joint training of early stage researchers from Palestine, Israel and Germany. The PALEX personal mentoring concept will give young scientists the opportunity to work closely with senior scientists from all participating institutions and develop their research skills.



Figure 1: a) Location of flood monitoring stations in Al-Ghar/Arugot catchment including precipitation distribution; b, c, d) training on station installation in field and for AQU/HUJ partners by Yamma Company at HUJ; e) downstream flood sampling; f) clastic sediment sampling by Jawad Hasan and students (AQU); g) location for the upstream monitoring station (photos: PALEX members).

IODP

How did Pleistocene and Holocene sediments reach the sites of IODP Expedition 354 – an analysis of the surface channel pattern on the Bengal Fan

T. SCHWENK¹, V. SPIESS¹, F. BERGMANN¹

¹ Marine Technology/Environmental Research, Department of Geoscience, University of Bremen, Klagenfurter Str. 2-4, D-28359 Bremen, Germany

The Bengal Fan covers the floor of the whole Bay of Bengal from the continental margins of India and Bangladesh to the sediment-filled Sunda Trench off Myanmar and the Andaman Islands, and along the west side of the Ninetyeast Ridge. Its southern end is located at about 7°S. The length of at least 2800 km, a maximum width of 1430 km, the area of 3x10⁶ km² and the volume of 12.5x10⁶ km³ make the Bengal Fan the largest submarine fan in the world (Curry et al., 2003). The Bengal Fan is fed by the Ganges-Brahmaputra river system which drains approximately ¾ of the Himalayan mountain range and recently delivers more than 1 Gt/yr of terrigenous sediment. One third of these sediments is transported to the deep sea fan via a deeply incised shelf canyon by turbidity currents. This makes the Bengal Fan to the most complete recorder to study interactions among the growth of the Himalaya and Tibet, the development of the Asian monsoon, and processes affecting the carbon cycle and global climate. Because sedimentation in the Bengal Fan responds to both, climate and tectonic processes, its terrigenous sediment records the past evolution of both the Himalaya and regional climate.

Therefore IODP Expedition 354 was carried out in February/March 2015 to drill a seven-site, 320 km long transect along 8°N in the Bay of Bengal. In particular, three deep-penetration and four shallow holes were drilled to achieve a complete spatial overview of the turbiditic depositions in time and space. The recovered sediments have a full spectrum of grain sizes and document terrestrial changes of Himalayan erosion and weathering, as well as changes of source regions and impact on the global carbon cycle. Variations of terrestrial vegetation, sediment budgets and sediment transport will be addressed with the drilled sediments. Altogether, Expedition 354 provides a record of fan deposition since the late Oligocene, which is an extension by 10 My compared to former drillings (France-Lanord et al., 2016).

Channel-levee systems as main architectural elements of the Bengal Fan play a significant role in this source-to-sink system. Build-up by turbidity currents transporting terrigenous material, they represent high-resolution archives of the erosional history of the hinterland. However, to use these archives a detailed understanding of internal architecture and stacking pattern of channel-levee systems is necessary especially for interpreting the drilled sediments of IODP Expedition 354.

During four cruises with the German Research Vessel "Sonne" (1994, 1997 (2), and 2006) in the Bay of Bengal bathymetric swath-sounder and sediment echosounder PARASOUND were operated continuously. All together data are available from profiles of 23,000 km length crossing the fan in international waters. These multibeam

data were compiled to a single map imaging the surface channel-levee systems, which were drilled at four of the seven sites of IODP Expedition 354. Some of the profiles are long profiles running from west to east, i.e., perpendicular to the channels, but some profiles track distinct channels from north to south. Using the morphological character of the channels and their relative succession revealed from overlapping levee deposits visible in the sediment echosounder data, channels can be traced from profile to profile. Comparison with the map published by Curry et al. (2003) shows partly good agreement as shown for a few profiles by Schwenk&Spiess (2009), but especially multibeam profiles along channels reveal more avulsion points and more terminating channels on the middle fan. Such avulsions and terminations of pathways belonging to the active channel may explain times of non deposition on the levee of the active channel drilled at Site U1454 (see Poster by Bergmann et al.).

Before IODP Expedition 354, only two channel-levee systems have been dated, the active channel as active during the Holocene, and one eastern channel as has been active before 300,000 yrs bp (Weber et al., 2003). For most surface channels a succession could be estimated, and future correlation to new datings from IODP Expedition 354 may give the opportunity to link distinct surface channel-levee systems to time slices of quaternary Himalayan erosion. In general the results demonstrate that dispersal of the sediments onto the fan in time and space is complex and had to be considered during analysis of Expedition 354.

References:

- France-Lanord, C., Spiess, V., Klaus, A., Schwenk, T., and the Expedition Scientists, 2016. Bengal Fan. Proceedings of the International Ocean Discovery Program, 354: College Station, TX (International Ocean Discovery Program). <http://dx.doi.org/10.14379/iodp.proc.354.2016>
- Curry, J.R. et al., 2003, The Bengal Fan: morphology, geometry, stratigraphy, history and processes: Mar. and Petr. Geol., 19, 1191-1223
- Schwenk, T. & Spiess, V., 2009, Architecture and stratigraphy of the Bengal Fan as response to tectonic and climate revealed from high resolution seismic data. In Kneller, B., Martinsen, O.J., and McCaffrey, B., SEPM Spec. Pub. 92, 107-131
- Weber, M.E. et al., 2003, Bengal Fan sediment transport activity and response to climate forcing inferred from sediment physical properties: Sed. Geol., 155, 361-381

ICDP

Joint high-resolution seismic and large-scale geoelectrical surveys for characterization of the planned PIER-ICDP fluid monitoring site in the Eger Rift zone of NW-Bohemia

H. SIMON¹, S. BUSKE¹, C. FLECHSIG², T. GÜNTHER³, T. NICKSCHICK²

¹ Institute of Geophysics and Geoinformatics, TU Bergakademie Freiberg

² Institut für Geophysik und Geologie, Universität Leipzig

³ Leibniz-Institut für Angewandte Geophysik (LIAG), Hannover

The NW-Bohemia/Vogtland region is a intra-continental non-volcanic region and is characterized by outstanding geodynamic activities, which result in earthquake swarms and significant CO₂ emanations (e.g. Fischer et al., 2010; Heinicke et al., 2009; Horálek and Fischer, 2008; Bräuer et al., 2003; Weinlich et al., 1998; Kämpf et al., 1989). Because fluid flow and fluid-induced stress can trigger earthquake swarms, both natural

phenomena are probably related to each other. The epicentres of the earthquake swarms cluster at the northern edge of the Cheb Basin near the village Nový Kostel (Fischer and Michálek, 2008). Although the location of the cluster coincides with the major Mariánské-Lázně Fault Zone (MLFZ) the strike of the focal plane indicates another fault zone, the N-S trending Počátky-Plesná Zone (PPZ) (Bankwitz et al., 2003). Isotopic analysis of the CO₂-rich fluids revealed a significant portion of upper mantle derived components, hence a magmatic fluid source in the upper mantle was postulated (Weinlich et al., 1999).

Because of these phenomena, the Eger Rift area is a unique site for interdisciplinary drilling programs to study the fluid-earthquake interaction. The ICDP project PIER (Probing of Intra-continental magmatic activity: drilling the Eger Rift) will set up an observatory, consisting of five monitoring boreholes (Dahm et al., 2013).

In preparation for the drilling, the goal of the joint seismic and geoelectric surveys is the characterization of the projected fluid-monitoring drill site at the CO₂ degassing mofette field near Hartoušov. This will be achieved by an approximately 6 km long high-resolution seismic profile and a large scale geoelectric resistivity survey along the same line. The W-E trending profile will cross the proposed drill site at Hartoušov and the surface traces of MLFZ and PPZ.

The outcome of the seismic survey will be a high-resolution structural image of potential reflectors related to these fault zones. This will be achieved by the application of advanced pre-stack depth migration methods and a detailed P-wave velocity distribution of the area obtained from first arrival tomography. Furthermore, these images will provide crucial constraints on petrophysical parameters, especially on the suspected fluid pathways. On the geoelectric side the key aspects are to image the main resistivity characteristics of the fault zones and the possible fluid pathways of the degassing area and to establish a reference resistivity model for future monitoring. During interpretation of the seismic data, the geoelectrical resistivity model will provide important constraints, especially with respect to fluid pathways, and in a similar way the seismic image will constrain the geoelectrical inversion.

References:

- Bankwitz, P., G. Schneider, H. Kämpf, and E. Bankwitz (2003), Structural characteristics of epicentral areas in Central Europe: study case Cheb Basin (Czech Republic), *J Geodyn* 35(1-2), 5-32, doi: 10.1016/s0264-3707(02)00051-0.
- Bräuer, K., H. Kämpf, G. Strauch, and S. M. Weise (2003), Isotopic evidence (³He/⁴He, ¹³C, CO₂) of fluid-triggered intraplate seismicity, *J. Geophys. Res.*, 108(B2), 2070, doi:10.1029/2002JB002077.
- Dahm, T., Hrubcova, P., Fischer T., Horálek, J., Korn, M., Buske, S., and D. Wagner (2013), Eger Rift ICDP: An observatory for the study of non-volcanic, midcrustal earthquake swarms and accompanying phenomena, *Scientific drilling* 16, 93–99, DOI:10.5194/sd-16-93-2013.
- Fischer, T. and Michálek, J.(2008), Post 2000-swarm microearthquake activity in the principal focal zone of West Bohemia/ Vogtland: space-time distribution and waveform similarity analysis, *Stud. Geophys. Geod.*, 52, 493–511.
- Fischer, T., Horálek, J., Michálek, J. and A. Bouskova (2010), The 2008 West Bohemia earthquake swarm in the light of the WEBNET network, *J. Seismol.*, doi:10.1007/s10950-010-9189-4.
- Heinicke, J., Fischer, T., Gaupp, R., Götte, J., Koch, U., Konietzky, H., Stanek, K.-P. (2009) Hydrothermal alteration as a trigger mechanism for earthquake swarms: the Vogtland/NW Bohemia region as a case study, *Geophys. J. Int.*, doi: 10.1111/j.1365-246X.2009.04138.x.
- Horálek, J. and Fischer T. (2008) Role of crustal fluids in triggering the West Bohemia/Vogtland earthquake swarms: just what we know (a review), *Stud. Geophys. Geod.*, 52, 455-478.
- Kämpf, H., G. Strauch, P. Vogler, and W. Michler (1989), Hydrogeologic changes associated with the December 1985/January 1986 earthquake swarm activity in the Vogtland/NW Bohemia seismic area, *Z. Geol. Wiss.*, 17, 685–689.

Weinlich, F. H., J. Tesar, S. M. Weise, K. Bräuer, and H. Kämpf (1998), Gas flux distribution in mineral springs and tectonic structure in the western Eger Rift, *J. Czech. Geol. Soc.*, 43, 91–110.

Weinlich, F. H., K. Bräuer, H. Kämpf, G. Strauch, J. Tesar, and S. M. Weise (1999), An active subcontinental mantle volatile system in the western Eger Rift, central Europe: Gas flux, isotopic (He, C, and N) and compositional fingerprints, *Geochim. Cosmochim. Acta*, 63, 3653–3671.

ICDP

Seismic imaging in anisotropic crystalline environment at the COSC-1 borehole, central Sweden

H. SIMON¹, F. KRAUB², S. BUSKE¹, R. GIESE², P. HEDIN³, C. JUHLIN³

¹ Institute of Geophysics and Geoinformatics, TU Bergakademie Freiberg

² Centre for Scientific Drilling, Helmholtz Centre Potsdam GFZ German Research Centre for Geosciences

³ Department of Earth Sciences, Uppsala University

The Scandinavian Caledonides represent a well preserved deeply eroded inactive Palaeozoic orogen. Surface geology in combination with geophysical data provide control of the geometry of parts of the Caledonian structure, including the lowermost allochthon, the underlying autochthon and the shallow W-dipping décollement surface that separates the two. This surface is closely associated with a thin layer of Cambrian black shales. The structure of the basement underneath the décollement is highly reflective and apparently dominated by mafic sheets intruded into either late Paleoproterozoic granites or Mesoproterozoic volcanic rocks and sandstones. The ICDP project COSC (Collisional Orogeny in the Scandinavian Caledonides) focuses on the Caledonide Orogen in order to better understand orogenic processes from the past and in recent active mountain belts (Gee et al., 2010). Therefore, the structure and physical conditions of the orogen units, in particular the Seve Nappe Complex (SNC, “hot” allochthon), Lower Allochthons and the underlying basement will be investigated with two approximately 2.5 km deep fully cored scientific boreholes in central Sweden.

The COSC-1 borehole was successfully drilled to 2.5 km depth in 2014 (Lorenz et al., 2015) near the town of Åre (ICDP drill site 5054-1-A). Thus, a continuous geological section through the Lower Seve Nappe and the underlying mylonite zone was obtained. This unit, mainly consisting of gneisses, has been ductilely deformed and transported during the collisional orogeny that formed the Scandinavian Caledonides. In order to allow the extrapolation of results from core analysis and downhole logging to the structures around the borehole, several surface and borehole based seismic experiments were conducted right after drilling completed. These included: 1) a high-resolution zero-offset Vertical Seismic Profile (VSP) (Krauß et al., 2015), 2) a spatially limited 3D seismic survey (Hedin et al., 2016) and 3) a multi-azimuthal walkaway VSP in combination with three up to 10 km long surface profiles centred around the borehole (Simon et al., 2016).

In a first step the data from the walkaway VSP and the long offset lines were used to derive a detailed P-wave velocity model around the COSC-1 borehole (Simon et al., 2016). The first arrival times observed in the borehole and surface data were inverted separately for each line, using a tomographic approach (Zhang and Toksöz, 1998). This obtained isotropic velocity models for different azimuths

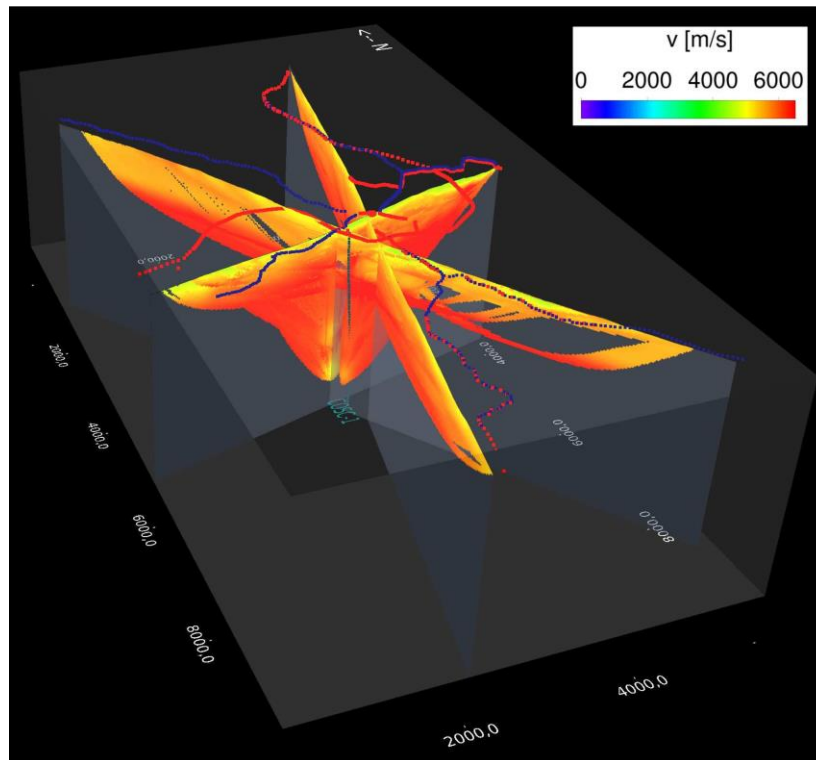


Figure 1: 3D view of the results from first-arrival seismic tomography using first-arrival traveltimes recorded in the borehole together with those recorded along the surface lines, showing the good agreement between the three independently inverted models. Parts with no ray coverage are masked. The positions of the surface source and receiver positions are marked in red and blue, respectively

around the borehole COSC-1 (see Fig. 1). Clear differences in vertical and horizontal velocities, observed by comparing velocities from the tomography results (mainly horizontally traveling rays) with a 1D velocity function calculated from zero-offset VSP first arrivals (mainly vertically traveling rays), made it necessary to also account for anisotropy. The resulting anisotropic VTI (transversely isotropic with vertical axis of symmetry) model consists of the 1D vertical P-wave velocity function from zero-offset VSP and homogeneous Thomsen parameters of $\delta = 0.3$ and $\epsilon = 0.03$. The latter were derived from lab measurements

(Wenning et al., 2016) and the seismic walkaway VSP data. This anisotropic model explains first arrivals for both surface and borehole data very well and provides the basis for the subsequent application of seismic imaging approaches, i.e. anisotropic Kirchhoff-based pre-stack depth migration. The resulting images were compared to the corresponding migration results based on an isotropic velocity model. Both images are dominated by strong and clear reflections, however, they appear more continuous and better focused in the anisotropic result (see Fig. 2). Most of the dominant reflections originate below the

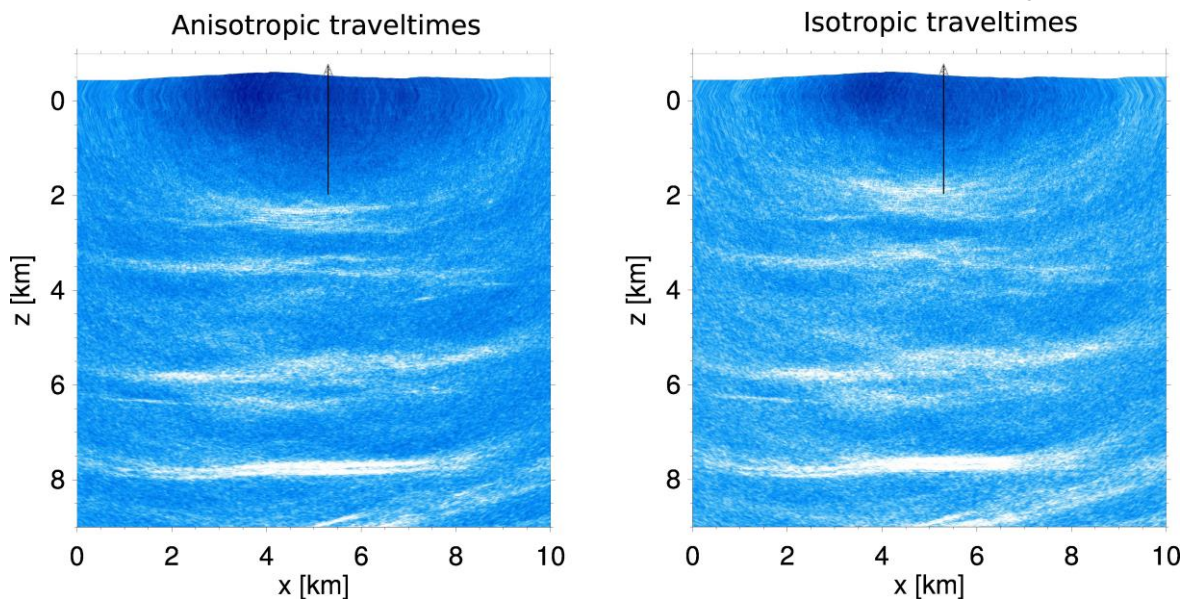


Figure 2: Kirchhoff pre-stack depth migration result from profile 3 (N-S), using anisotropic (left) and isotropic (right) traveltimes. The clear reflections appear more continuous and better focused in the anisotropic version.

borehole and therefore they are probably situated within the Precambrian basement. They might represent dolerite intrusions or faults of Caledonian or pre-Caledonian age. The definitive origin remains enigmatic and can only be clarified by the proposed borehole COSC-2.

References:

- Gee, D. G., Juhlin, C., Pascal, C., & Robinson, P. (2010). Collisional Orogeny in the Scandinavian Caledonides (COSC). *GFF*, 132(1), 29–44.
- Hedin, P., Almqvist, B., Berthet, T., Juhlin, C., Buske, S., Simon, H., Giese, R., Krauß, F., Rosberg, J. E., Alm, P. G. (2016). 3D reflection seismic imaging at the 2.5 km deep COSC-1 scientific borehole, central Scandinavian Caledonides. *Tectonophysics*, 689, 40-55.
- Krauß, F., Simon, H., Giese, R., Buske, S., Hedin, P., Juhlin, C., Lorenz, H. (2015). Zero-Offset VSP in the COSC-1 borehole. *Geophysical Research Abstracts*, 17, EGU2015-3255.
- Lorenz, H., Rosberg, J.-E., Juhlin, C., Bjelm, L., Almqvist, B. S. G., Berthet, T., Conze, R., Gee, D. G., Klonowska, I., Pedersen, K., Roberts, N. M. W., Tsang, C.-F. (2015). COSC-1 – drilling of a subduction-related allochthon in the Palaeozoic Caledonide orogen of Scandinavia. *Scientific Drilling*, 19, 1–11.
- Simon, H., Buske, S., Krauß, F., Giese, R., Hedin, P., Juhlin, C. (2016). The derivation of an anisotropic velocity model from a combined surface and borehole seismic survey in crystalline environment at the COSC-1 borehole, central Sweden. *Geophysical Journal International*, under review.
- Wenning, Q., Almqvist, B. S. G., Hedin, P., Zappone, A. (2016). Seismic anisotropy in mid to lower orogenic crust: Insights from laboratory measurements of Vp and Vs in drill core from central Scandinavian Caledonides. *Tectonophysics*, in press.
- Zhang, J., and Toksöz, M. (1998). Nonlinear refraction traveltimes tomography. *Geophysics*, 63(5), 1762-1737.

IODP

Structure and buildup of the Middle Bengal Fan at 8°N from multichannel seismic surveys and the IODP Expedition 354 drilling transect

V. SPIESS¹, F. BERGMANN¹, T. SCHWENK¹, H. LANTZSCH¹, C.

FRANCE-LANORD² AND IODP EXPEDITION 354 SCIENTIFIC PARTY

¹ Department of Geosciences, University of Bremen, Klagenfurter Strasse 2-4, D-28359 Bremen, Germany

² Centre de Recherches Pétrographiques et Géochimiques, CNRS Université de Lorraine, BP 20, 54501 Vandoeuvre les Nancy, France

IODP Expedition 354 to the Bengal Fan drilled a 320 km long E-W transect at 8°N with 7 drill sites, fully covering the uppermost 150-200 meters of fan deposits at a spacing of ~50 km, originating from Himalayan mountain ranges and the Ganges-Brahmaputra river system. A major goal of this transect approach was to ensure a continuous record of turbiditic material delivered over the last appx. 1 million year, considering frequent longitudinal depocenter shifts of the active channel.

By extensively utilizing the new half-APC coring technique, high quality and high recovery cores could be retrieved representing a wide range of grain sizes from hemipelagic deposits through clay rich turbidites to coarse silt and sandy units. Up to medium sand grain sizes were retrieved within the basal units of levees, which correspond to high-reflectivity units in high-resolution multichannel seismic profiles. Finely laminated sections with mm to cm-thick turbidites represents levee formations.

At Site U1453 for example, core logging and downhole logging data confirm the representative sampling based on a very good match of several physical property data sets. An expanded section was cored at Site U1454, where the

presumably currently active channel (see abstract Bergmann et al.) has built a levee, which likely represents major sediment supply within the last 45 kyr. A spatial grid of seismic and echosounder data in the vicinity of the active channel reveals a high spatial variability in sedimentation rates and distinct depocenter shifts in response to changes in channel geometry. Site U1452 has provided a full record a levee growth including interlevee sedimentation, sandy basal units characterized by a lobe formation, and a pronounced fining upward trend following the phase of channel erosion and levee buildup.

From all sites, detailed comparisons of physical and sedimentological shipboard results with seismic data will be presented. Expedition 354 has provided a unique sample and data set to better understand fan deposition and channel-levee growth including silt and sand grain sizes. It will also provide valuable constraints on the volume, nature and composition of suspension flows contributing to fan growth in the Middle Bengal Fan.

ICDP

Long term tectonic and paleoclimatic history of Lake Issyk-Kul, Kyrgyzstan - preliminary results from an ICDP-related deep seismic pre-site survey campaign

SPIEB, V.¹, REUSCH, A.¹, OBERHÄNSLI, H.², GEBHARDT, C.³,
ABDRAKHMATOV, K.⁴

¹ University of Bremen, Faculty of Geosciences, Klagenfurter Straße, 28359 Bremen, Germany

² Naturhistorisches Museum, Berlin, Germany

³ Alfred-Wegener Institut für Polar- und Meeresforschung, 27568 Bremerhaven, Germany

⁴ Institute of Seismology, NAS KR, Bishkek, Kyrgyzstan

Lake Issyk-Kul in Kyrgyzstan became a potential target for ICDP drilling through a group of scientists who applied for and organized an ICDP workshop in 2011 in Baet/Kyrgyzstan (Oberhänsli and Molnar, 2012). Lake Issyk-Kul, located in the Kyrgyz Republic, is one of the deepest and largest lakes in the world. It occupies a deep basin within the Tien Shan mountain range in Central Asia, which is presently one of the Earth's tectonically most active intra-continental mountain belts. Up to 3500 m of terrestrial sediments have been deposited in the basin, including glacial, fluvio-glacial, fluvial and lacustrine formations (Fortuna, 1993), of which the oldest are believed to date back to Oligocene – Miocene times (Abdrakhmatov et al., 1993; Chedia, 1986).

Lake sediments can act as important “recorders” of the regional processes active during and after their deposition. Lake Issyk-Kul's sediments likely comprise a promising record of tectonic events and past climate changes in the region, potentially ranging back to Miocene times. This sedimentary record is the base of a planned investigation of the International Continental Drilling Program (ICDP), with the aim to investigate the past climate conditions and the tectonic history of the region. In order to address these scientific objectives, ideal drilling sites are searched, with the aim to drill through a potentially complete, undisturbed sediment section representing the maximum amount of time. In 1997 and 2001, single-channel seismic sparker data were acquired by the Renard Centre of Marine Geology in Gent (RCMG) (DeBatist et al., 2002; Gebhardt

et al., 2016). In order to gain a better understanding of the deeper lake basin, a multichannel airgun seismic survey was organized in 2013, jointly funded by the Museum für Naturkunde Berlin, the University of Bremen, the AWI Bremerhaven, Centre of Seismology, Bishkek, Research Group Marine Technology/Environmental Research, Geosciences, Bremen and the ICDP coordination in May 2013. With these multichannel seismic data, it is possible to investigate the lake history further back in time, including reconstruction of the tectonic evolution, paleoseismic activity as well as climatic indications such as water level fluctuations.

First experiments of processing and interpreting of the multichannel seismic data were carried out as part of smaller projects at the University of Bremen, but further thorough and partially sophisticated processing (multiple/noise suppression) and interpretation work is needed to identify deeper sediment packages and potentially the basal reflector of the deep lake basin.

It is intended to revitalize the Issyk-Kul ICDP drilling proposal by giving it a different focus on paleoclimate and high-resolution sediment studies, involving the universities of Köln and Potsdam.

References:

- Abdrakhmatov, K. E., Turdukulov, A. T., and Khristov, E. B., 1993, Detailed seismic zoning of the Issyk-Kul basin.: Ilim Publications. Frunze.
- De Batist, M., Y. Imbo, P. Vermeesch, J. Klerkx, S. Giralt, D. Delvaux, V. Lignier, C. Beck, I. Kalugin, and K. E. Abdrakhmatov (2002), Bathymetry and Sedimentary Environments of Lake Issyk-Kul, Kyrgyz Republic (Central Asia): A Large, High-Altitude, Tectonic Lake, in Lake Issyk-Kul: Its Natural Environment, edited by J. Klerkx and B. Imanackunov, pp. 101-123, Springer Netherlands.
- Chedia, O. K., 1986, Morphology and neotectonics of the Tien Shan: Ilim Publications. Frunze, p. 313.
- Fortuna, A. B., 1993, Detailed seismic profiling of the Issyk-Kul depression.: Ilim Publications.
- Gebhardt, C.A., Naudts, L., De Mol, L., Klerkx, J., Abdrakhmatov, A., Sobel, E.R., De Batist, M., 2016, An extended history of high-amplitude lake-level changes in tectonically active Lake Issyk-Kul (Kyrgyzstan), as revealed by high-resolution seismic reflection data, *Climat of the past*, discussion, doi:10.5194/cp-2016-3
- Oberhänsli, H., and Molnar, P., 2012, Climate Evolution in Central Asia during the Past Few Million Years: A Case Study from Issyk Kul: *Sci. Drill.*, v. 13, p. 51-57.

ICDP & IODP

Report about a Magellan+ Workshop in February 2017: Structure and Evolution of Magmatic and Hydrothermal Volcanic Systems in offshore collapse/resurgent calderas - Development of an IODP Drilling Proposal at Campi Flegrei linking to active ICDP Drilling Initiatives

V. SPIESS¹, M. SACCHI², G. DE NATALE³, L. STEINMANN¹

¹ University of Bremen, Dept. of Geosciences & MARUM, Germany

² IAMC, CNR, Napoli, Italy

³ INGV - Osservatorio Vesuviano, Napoli, Italy

The workshop aims on collapse-resurgent calderas, with a focus on developing a Campi Flegrei caldera IODP drilling proposal, connecting to an active ICDP drilling campaign. The workshop shall 1) provide a global perspective on the potential/challenges of caldera drilling, 2) discuss drilling in a coastal offshore continental margin

setting, 3) discuss new site survey data, 4) develop and refine drilling objectives with respect to marine and volcanoclastic stratigraphy, reconstruction of caldera evolution, and study of the interaction of magmatism and hydrothermal activity in marine settings. Deep biosphere, hazard potential and integrating boreholes into monitoring networks are complimentary objectives.

Following themes shall be presented by participants and discussed in subgroups and plenum:

- **Caldera Volcanism and Formation:** Caldera-related magmatism and eruption, pyroclastic flows, ignimbrites, fissure vs central volcano eruption, linkage between magmatic and hydrothermal systems
- **Hydrothermal systems:** Comparison between water-saturated and terrestrial settings, pathways and flow pattern of hydrothermal circulation, structural constraints, origin of uplift (hydrothermal vs magmatic), control of small and large scale faulting on hydrothermal venting, unrest and volcanism
- **Chronology of catastrophic eruptions:** Onset, type and frequency of volcanism in Campi Flegrei region, reconstruction from sedimentary archives, caldera fill, long term sedimentary archive from a distal site
- **Depositional Setting:** Caldera fill, interaction with sea level change, terrestrial sediment fluxes, volcanic control on sediment transport pathways and accommodation space, distribution and pyroclastics and atmospheric control, characteristics of volcanoclastic deposits in a marine setting, diagenetic overprint by hydrothermalism
- **Monitoring:** Integration of boreholes into INGV-OV long-term observational network (earthquakes, tremor, micro-seismicity, temperature, pressure), lessons learned from IODP
- **Links to land drilling** State of knowledge (cores, borehole data) and progress report from ICDP and other land drilling
- **Technical Implementation (ESO):** Constraints from MSP operational viewpoint, water depth, technology, costs

Since 2006, two new multichannel seismic data sets, complemented by cores and acoustic survey data for the shallow subsurface and for hydrothermal venting, had been acquired, and the basis for planning a drilling campaign has significantly improved. In 2008, a high frequency (up to 300 Hz) seismic grid had been acquired at a spacing of 150 meters, and recently in January 2016, a low frequency (50 Hz) grid on 25-50 m line spacing was surveyed in the Gulf of Pozzuoli. While processing of the new data set is still to come, preliminary results will be available for the workshop to have an in-depth discussion on site selection and required drilling technologies.

The outcome of the workshop should be a pre- or full drilling proposal depending on the state of discussions. The drilling proposal shall integrate these topics, into a general view based on the analysis of collapse – resurgent calderas that develop over continental margins. Coastal offshore settings in fact provide a unique opportunity to reconstruct the chronostratigraphy and kinematic evolution of individual structures and components and understand the interaction between magmatic and hydrothermal processes

that characterizes the hinge zone between marine and continental areas.

IODP

Early Cretaceous climate and Arctic variability in the Kiel Climate Model

S. STEINIG¹, S. FLÖGEL¹, W. PARK¹, M. LATIF^{1,2}, W. DUMMANN³, P. HOFMANN³, T. WAGNER⁴, J.O. HERRLE⁵

¹ GEOMAR Helmholtz Centre for Ocean Research Kiel, Wischhofstr. 1-3, D-24148 Kiel, Germany

² Kiel University, Christian-Albrechts-Platz 4, D-24118 Kiel, Germany

³ Institute of Geology and Mineralogy, University of Cologne, Zùlpicher Str. 49a, D-50674 Cologne, Germany

⁴ Sir Charles Lyell Centre, School of Energy, Geoscience, Infrastructure and Society, Heriot-Watt University, Edinburgh, EH14 4AS, UK

⁵ Institute of Geosciences, Goethe-University Frankfurt, Altenh6ferallee 1, D-60438 Frankfurt am Main, Germany

Paleoceanographic data indicate large scale perturbations of the Aptian-Albian global climate system associated with severe changes of the marine carbon cycle (Jenkyns, 2010). At the same time, the ongoing break-up of Gondwana and the related opening of the South Atlantic and Southern Ocean led to the emergence of young ocean basins, characterised by vast shelf areas and limited circulation. Several studies relate these evolving basins and their restricted environments to periods of increased black shale formation and carbon burial (Trabucho-Alexandre et al., 2012) with a particular importance of the developing South Atlantic (McAnena et al., 2013).

Within this project, we target the question whether increased carbon burial in the early Cretaceous South Atlantic influenced or even triggered global climate perturbations. Further, we test the hypothesis if the development and destruction of regional marine carbon sinks is strongly controlled by the opening of the Georgia Basin/Falkland Plateau and the Walvis Ridge Gateway. For this purpose we tightly combine new geochemical proxy data from several DSDP sites (see abstract of Dumann et al.) with a joint physical and biogeochemical modelling approach to detect regional changes in carbon sequestration and assess their influence on the global carbon cycle.

Most of the Early Cretaceous (Aptian/Albian) time period was characterized by a warm and humid greenhouse

climate. The elevated pCO₂ concentrations and other vastly different boundary conditions (e.g. changes in the land-sea distribution, vegetation and land ice cover) still represent a fundamental challenge for global atmosphere-ocean general circulation models (AOGCMs) for correctly simulating the dynamics of past greenhouse intervals. Insufficient knowledge of the required boundary conditions, in combination with limited computational power led to inconsistent results in the simulation of the Early Cretaceous climate and its variability. Due to these persistent problems we aimed in the first phase of the project for a thorough investigation of the simulated Early Cretaceous climatic mean state. This will enable us to identify any changes to the regional oceanographic environment induced by the opening of several key gateways in future sensitivity experiments.

We employ the Kiel Climate Model (Park et al., 2009), a coupled atmosphere-ocean-sea ice general circulation model, under Early Aptian (120 Ma) boundary conditions. Land topography and ocean bathymetry are based on reconstructions from Mùller et al. (2008) and Blakey (2008). Due to the lack of robust and global information about river distribution the surface freshwater routing strictly follows the model topography (Hagemann and Dùmenil, 1998). We apply a zonal mean, climatic zone dependent surface vegetation with no continental ice and glaciers (Ando et al., 2009). The solar constant is reduced by 1% and the chosen pCO₂ value of 1200 ppm is within the large range of reconstructions (Bice et al., 2006). Initial temperatures and salinities for the ocean are derived from a present day simulation with a gradual increase of pCO₂ up to the Aptian value. We integrated the physical model until a steady state equilibrium was reached and present the main climatic features and differences to a pre-industrial reference simulation.

Due to the large contrast between the applied initial conditions and the Early Cretaceous boundary conditions the adjustments in the global density stratification took nearly 10,000 model years (i.e. about 10 months of computation time). This was in part caused by a strong vertical salinity gradient (Fig. 1b) induced by large surface freshwater fluxes in the early model years. The resulting sluggish overturning circulation only slowly redistributed higher saline waters from deeper levels to the surface, increasing vertical density gradients (Fig. 1c). The gradual build-up of a global meridional overturning circulation and the associated large scale salinity advection culminated into a shift of deep convection locations from the North Pacific

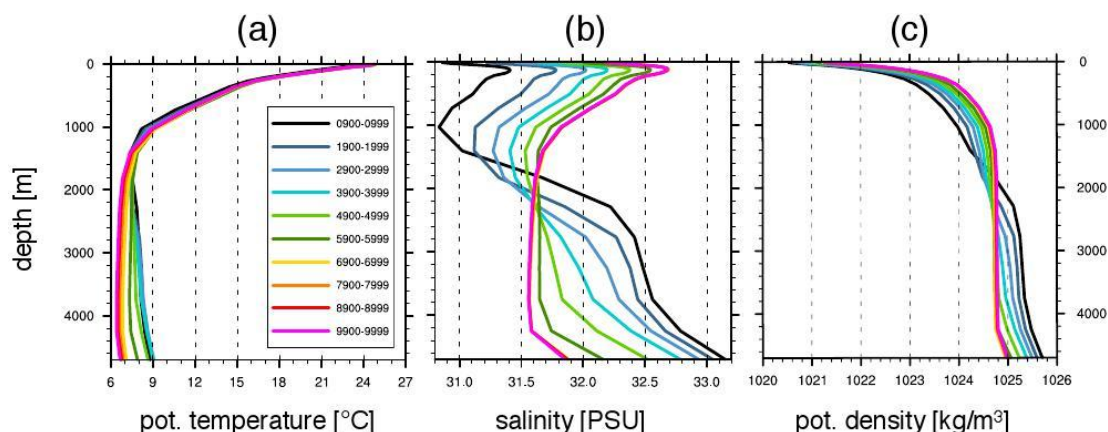


Figure 1: Annual mean profiles averaged over the global ocean showing (a) potential temperature, (b) salinity and (c) potential density. Color coding represents increasing model integration times. Values are shown for each 1,000 model years averaged over the respective last 100 years.

to the previously freshwater dominated Arctic Ocean after about 6,000 model years. The resulting increase in high-latitude oceanic heat advection lead to significant warming of the Arctic region of up to 4°C. The fact that this regime shift only occurred at integration times longer than commonly used for similar studies will be of particular interest for the paleo modelling community.

Steady state global mean surface air temperatures are elevated by nearly 10°C compared to pre-industrial and reach 23.5°C (Fig. 2). The surface warming is mainly radiatively driven by the higher atmospheric pCO₂ levels (~70% of the warming) and surface albedo changes (~30% of the warming) (Fig. 2b). Weaker tropical deep convection reduces low-latitude cloud cover compared to the present day and leads to a net cloud-induced small warming in the tropics. The absence of polar ice caps prevents high-latitude atmospheric subsidence resulting in thicker, low-level clouds that reflect incoming shortwave radiation and consequently cool the surface. These cloud radiative feedbacks contribute to maintain low and mid-latitude meridional temperature gradients similar to today. High latitude surface warming is attributable to significantly decreased Antarctic elevation levels and surface albedo reductions caused by the ice-free polar regions.

The simulated Arctic surface climate shows pronounced variability on multi-decadal and multi-centennial time scales with highest power around 80 and 200 years respectively. Surface temperatures and salinities drop over the course of 20-30 years by up to 3°C and 1.5 PSU and are strongest near the deep convection sites in the northernmost part of the Arctic Ocean. They are associated

with periods of a drastic reduction in wintertime mixed layer depth. We speculate that this variability in deep convection is caused by oscillations in the salt advection from the North Pacific and Tethys. This northward salt transport is necessary to produce dense surface waters in the Arctic Ocean because the basin is highly influenced by large freshwater inputs from the surrounding land masses. This internal variability only set in towards the end of the integration once the deep water formation in the Arctic Ocean was fully established. Even though frequency and magnitude of the variability and its feedback on the northward heat transport are most likely sensitive to the used model and land-sea mask, we argue that this behaviour conceptually illustrates the need for a long model spin-up especially of restricted, high-latitude basins.

References:

- Ando, A., B. T. Huber, K. G. MacLeod, T. Ohta, and B.-K. Khim, 2009, Blake Nose stable isotopic evidence against the mid-Cenomanian glaciations hypothesis, *Geology*, v. 37, pp. 451-454, doi:10.1130/G25580A.1.
- Bice, K. L., D. Birgel, P. A. Meyers, K. A. Dahl, K.-U. Hinrichs, and R. D. Norris, 2006, A multiple proxy and model study of Cretaceous upper ocean temperatures and atmospheric CO₂ concentrations, *Paleoceanography*, v. 21, no. 2, PA2002, doi: 10.1029/2005PA001203.
- Blakey, R.C., 2008, Gondwana paleogeography from assembly to breakup - A 500 m.y. odyssey, in: C.R. Fielding, T.D. Frank and J.L. Isbell (Eds.), *Resolving the late Paleozoic ice age in time and space*. Geological Society of America Special Paper, v. 441, p. 1-28.
- Hagemann, S., and L. Dümenil, 1998, A parameterization of the lateral waterflow for the global scale, *Climate Dynamics*, v. 14, pp. 17-31.
- Heinemann, M., Jungclaus, J. H., & Marotzke, J., 2009, Warm Paleocene/Eocene climate as simulated in ECHAM5/MPI-OM. *Climate of the Past Discussions*, 5(1987), 785-802. <http://doi.org/10.5194/cpd-5-1297-2009>

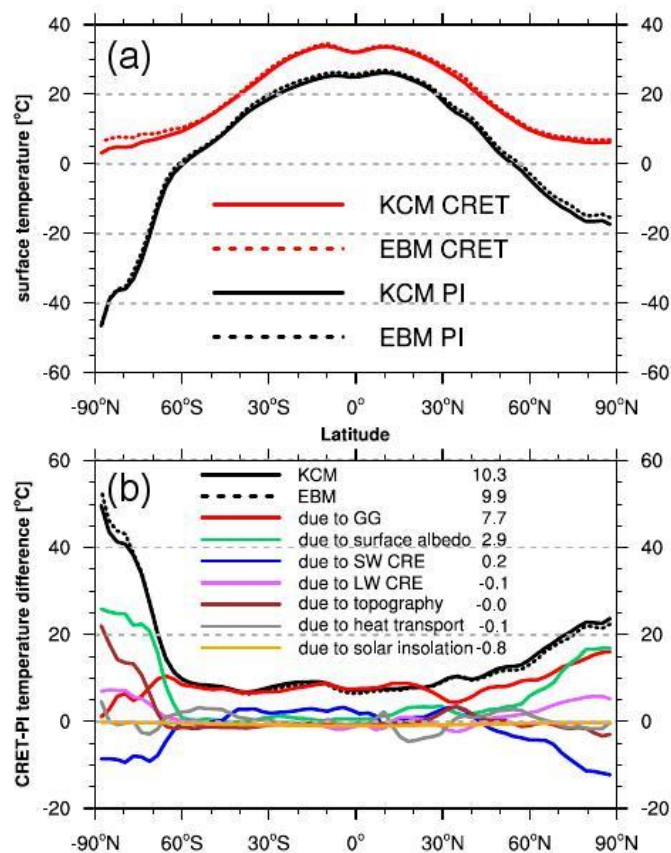


Figure 2: Results of the 1D-Energy Balance Model flux analysis following the procedure of Heinemann et al. (2009). Values are averaged over the last 1,000 model years for the pre-industrial (PI) and Early Cretaceous (CRET) simulation and are zonally averaged. Other abbreviations are used for greenhouse gases (GG) and shortwave and longwave cloud radiative effects (SW/LW CRE).

- Jenkyns, H. C., 2010. Geochemistry of oceanic anoxic events, *Geochem. Geophys. Geosyst.*, 11, Q03004
- McAnena, A., Flögel, S., Hofmann, P., Herrle, J., Griesand, A., Pross, J., Talbot, H., Rethemeyer, J., Wallmann, K. and Wagner, T., 2013. Atlantic cooling associated with a marine biotic crisis during the mid-Cretaceous period, *Nature Geoscience*, Vol. 6(7), pp. 558-561
- Müller, R.D., M. Sdrolias, C. Gaina, B. Steinberger, C. Heine, 2008, Long-Term Sea-Level Fluctuations Driven by Ocean Basin Dynamics, *Science*, 319, pp. 1357-1362, doi:10.1126/science.115154
- Park, W., N. Keenlyside, M. Latif, A. Ströh, R. Redler, E. Roeckner, and G. Madec, 2009, Tropical Pacific Climate and Its Response to Global Warming in the Kiel Climate Model, *J. Climate*, 22, 71-92, doi:10.1175/2008JCLI2261.1.
- Trabucho-Alexandre, J., Hay, W. and De Boer, P., 2012, Phanerozoic environments of black shale deposition and the Wilson Cycle, *Solid Earth*, Vol. 3(1), pp. 29-42

ICDP

Shallow structures of the marine Campi Flegrei Caldera and the volcanoclastic and sedimentary deposits in the Bay of Naples

L. STEINMANN¹, V. SPIESS¹

¹ Department of Geosciences, University of Bremen, Klagenfurter Strasse 2-4, D-28359 Bremen, Germany

The formation of large collapse calderas is associated with highly destructive explosive volcanic eruptions, which have the potential to trigger a global catastrophe in the same order of magnitude as a giant meteorite impact. Understanding caldera-forming eruption mechanisms and dynamics is of paramount importance in order to reliably assess volcanic hazards and risks of future eruptions.

The now finished DFG-ICDP Project "*Shallow structures of the marine Campi Flegrei Caldera and the volcanoclastic and sedimentary deposits in the Bay of Naples*" aimed at contributing to the overall knowledge of caldera volcanism by examining (1) the interplay between tectonism and volcanic activity, (2) the caldera architecture and collapse mechanisms, and (3) post-caldera volcano-tectonic processes at the most active caldera on Earth, the Campi Flegrei caldera located in southern Italy. Due to its history of large-scale explosive eruptions, its ongoing episodes of unrest, and its high population density with nearly 2.5 million people living in the close vicinity, the Campi Flegrei caldera represents one of the world's maximum volcanic risk areas. As a future eruption could have significant impact on regional as well as global scale, comprehending its genesis and evolution is a matter of global relevance.

The project was based on high-resolution multichannel reflection seismic data acquired in the offshore sector of the Campi Flegrei caldera and the greater vicinity of the Gulf of Naples. As part of it, the first semi-3D multichannel seismic investigation of a large collapse caldera is presented, providing novel insights on the shallow structures of the Campi Flegrei caldera.

For the first time, high-resolution multichannel seismic data show evidence for the existence of a nested-caldera system formed during two collapses associated with the Campanian Ignimbrite (CI) eruption at 39 ka and the more recent Neapolitan Yellow Tuff (NYT) eruption at 15 ka. An arc-shaped inner caldera ring-fault separating the caldera margin from the subsided caldera depression could clearly be imaged and spatially mapped. At the Eastern and Western caldera margin, this fault was already activated during the CI eruption. However, at the southern section of

the caldera margin, it seems to be associated with only the NYT collapse, while the CI fracture zone is assumed to lie further south and at greater depth. The NYT caldera probably formed during an asymmetrical, piecemeal-like collapse with a maximum subsidence of ~75 m in the offshore portion. The vertical displacement related to the CI caldera collapse may be significantly larger.

In the post-caldera phase, the NYT caldera depression acted as significant accommodation space and was rapidly filled with an on average 61-m thick sequence of marine and reworked volcanoclastic sediments deposited between 15 and 8.6 ka. Since 8.6 ka, the accommodation space was limited as a result of resurgence-related uplift in the caldera centre. Furthermore, the 3D aspect of the seismic dataset allows for the assessment of post-caldera eruption volumes. Specifically, the erupted volumes of the Nisida Bank, Nisida Island and Capo Miseno post-caldera eruptions are estimated to be at least 0.14 km³, 0.10 km³ and 0.08 km³, respectively. These values are significantly higher than previous estimates because the deposits in the offshore portion have previously not been considered.

Moreover, the effect of hydrothermalism on the offshore sector of the Campi Flegrei caldera is investigated in order to contribute to the understanding of the hypothesised shallow (<2 km) hydrothermal system, which is supposedly strongly linked to the recent unrest episodes. The findings from the current thesis reveal that the fractured caldera margin acts as pathway for the ascent of hydrothermal gases/fluids potentially originating from the hypothesised shallow hydrothermal system.

The multichannel seismic data from the Gulf of Naples are analysed in order to examine the interaction between fault activity, volcanism and sedimentary deposition with respect to the regional tectonic setting. Two tectonically active phases leading to the subsidence of the Gulf of Naples half-graben basin are recognized (1) between 1.0 and 0.4 Ma and (2) between 0.14 to 0.02 Ma. Time periods between 0.4 and 0.14 Ma and from 0.02 Ma onwards seem to have been tectonically stable. The onset of increased subsidence at 0.14 Ma was approximately coeval with the initiation of severe volcanic activity in the Campi Flegrei Volcanic Zone (CVZ) and at the adjacent Somma-Vesuvius. Hence, a close linkage between tectonism and volcanism is suggested, probably related to the reactivation of major NE-SW and NW-SE-trending normal faults. Therefore, it can be hypothesized that the large-scale CI eruption at 39 ka was triggered by regional tectonism. In contrast, the NYT eruption at 15 ka occurred during a phase of tectonic stability, which may either indicate that the tectonic control on eruptions played only a minor role from 0.02 Ma onwards, or that the presented seismic data were not able to resolve subsidence during that relatively short time interval.

The main outcomes are presented in three novel and comprehensive evolutionary models addressing (1) a 3D reconstruction of the tectono-sedimentary variability in the Gulf of Naples half-graben with respect to volcanism during the past one million years, (2) the conceptual formation of the Campi Flegrei nested-caldera complex, and (3) the 3D post-caldera evolution of the Campi Flegrei caldera. In summary, the findings represent a significant advancement towards understanding the genesis and evolution of the Campi Flegrei caldera as well as the tectonic formation of the Gulf of Naples half-graben basin

and its influence on volcanism. The suitability of multichannel reflection seismic data to investigate (partly) submerged collapse calderas was underlined and may also be applicable to other calderas.

ICDP

Interface driven Fe transfer from volcanic rocks of ICDP site Hawaii to ocean surface waters

M. STRANGHOENER¹, H. BEHRENS¹, S. DULTZ², A. SCHIPPERS³

¹ Institute of Mineralogy, Leibniz Universität Hannover, Callinstr. 3, D-30167, Hannover, Germany

² Institute of Soil Science, Leibniz Universität Hannover, Herrenhäuser Str. 2, D-30419, Hannover, Germany

³ Federal Institute for Geosciences and Natural Resources, Stilleweg 2, D-30655, Hannover, Germany

Fe is a limiting micronutrient regulating phytoplankton growth in surface ocean waters and, hence, may cause changes in atmospheric CO₂ and hereby potentially affecting climate. Volcanic rocks (containing 2-8 % Fe) are thermodynamically unstable under aqueous conditions resulting in large elemental release rates. Even if the impact of total soluble Fe from volcanic islands to surface ocean is relatively small compared to other sources (e.g. hydrothermalism; volcanic ash deposits) strong local effects are clearly shown (Brown et al. 2005). The release of Fe at the solid liquid interface from fresh to altered volcanic rocks as well as the control of Fe solubility are still not completely understood. In the ICDP drilling project HSDP2 a 3.1 km deep hole was drilled into the Mauna Kea Volcano on Hawai'i. A total of 83 rock samples covering the whole depth were achieved from the American Museum of Natural History (New York). The samples represent a unique record for different weak to strongly altered volcanic rocks comprising ashes, lavas and pillow basalts.

The DFG project was started in August 2016 and, thus, only preliminary results could be obtained so far. The set of natural samples was extended by basaltic glasses synthesized in the laboratory with the same base composition but varying Fe²⁺/Fe_{tot} (0.33 to 0.87). The redox state of the natural basaltic rocks and the synthetic glasses is analyzed by a colorimetric wet chemistry method modified by Schüssler et al. (2008). To characterize strength of bonding of Fe a four-step sequential extraction method (water, citrate-bicarbonate, oxalate, dithionite-citrate-bicarbonate) modified after Göttelein & Stanjek (1996) was used. Dissolved Fe, Al, Mn and Si was quantified by ICP OES. The results indicate increasing contents of water soluble Fe with progressing rock alteration. Furthermore, amorphous and weakly crystalline bound Fe dominate with increasing depth. A combination with the specific surface area measured by N₂ gas adsorption and Fe²⁺/Fe_{tot} determinations (both in progress) allows partitioning of rock samples in different solubility classes.

Microbiological experiments have been started to investigate the influence of microorganisms on Fe mobilisation. Two different microorganisms (*Mariprofundus ferrooxydans*; *Burkholderia fungorum*) were chosen for colonization experiments on synthetic

basaltic glasses with varying Fe²⁺/Fe_{tot}. Furthermore, incubation experiments will be performed on natural basaltic rocks from the HSDP2 drilling core to identify and quantify different biotic (microorganisms) and abiotic factors for Fe solubilization.

To investigate leached layer formation and the accumulation of Fe at surface position generating positive charges and having a beneficial effect for the sorption of negatively charged microorganisms (Kim et al. 2008) measurements of the zeta potential ζ are planned describing charge properties of the outermost surface. The data will be used to get detailed insights on reactions in glasses upon Fe²⁺ oxidation and leaching conditions.

The results of our research will be combined with findings from other groups working on rock alteration and element release to improve our understanding of interdependencies of mineralogical composition, solution composition, biochemical factors and alteration rates on release of soluble Fe.

References:

- Brown et al. 2005, *Geochemistry Geophysics Geosystems*, Vol.6, 10.
 Schüssler et al. 2008, *American Mineralogist*, Vol. 93, 1493-1504.
 Göttelein & Stanjek 1996, *European Journal of Soil Science*, Vol.47, 627-636.
 Kim et al. 2008, *Colloids and Surfaces B: Biointerfaces*, Vol.63, 236-242.

ICDP

Isotopic chemical weathering behaviour of Pb derived from a high-Alpine Holocene lake-sediment record

F. SÜFKE^{1,2}, M. GUTJAHR¹, A. GILLI³, F. ANSELMETTI⁴, L. GLUR⁵, A. EISENHÄUER¹

¹ GEOMAR Helmholtz-Zentrum für Ozeanforschung Kiel, Wischhofstr. 1-3, 24148 Kiel, Germany

² now at: Institute of Earth Sciences, Heidelberg University, Im Neuenheimer Feld 234, Heidelberg, Germany

³ Geological Institute, ETH Zürich, Zürich, Switzerland

⁴ Institute of Geological Sciences and Oeschger Centre for Climate Change Research, University of Bern

⁵ Eawag, Swiss Federal Institute of Aquatic Science and Technology, Dübendorf, Switzerland

Several studies assessing the chemical weathering systematics of Pb isotopes provided evidence for the incongruent release of Pb from source rocks during early stages of chemical weathering, resulting in runoff compositions more radiogenic (higher) than the bulk source-rock composition [e.g. 1]. Deep NW Atlantic seawater Pb isotope records covering the last glacial-interglacial transition further support these findings. Clear excursions towards highly radiogenic Pb isotopic input in the deep NW Atlantic seen during the early Holocene, hence after the large-scale retreat of the Laurentide Ice Sheet in North America, are interpreted to be controlled by preferential release of radiogenic Pb from U- and Th-rich mineral phases (e.g. apatite and allanite) during early stages of chemical weathering that are less resistant to chemical dissolution than other rock-forming mineral phases [2-4]. To date, however, no terrestrial Pb isotope record exists that could corroborate the evidence from deep marine sites for efficient late deglacial weathering and washout of radiogenic Pb. We present a high-resolution adsorbed Pb isotope record from a sediment core retrieved

from Alpine Lake Grimsel (1908 m.a.s.l.) in Switzerland, consisting of 117 Pb compositions over the past 10 kyr, which cover the period right after the final glacier retreat in the central Swiss Alps. With a homogeneous granitic bedrock and a small catchment (~2.5 km²), this high-Alpine study area is ideally located for incipient and prolonged chemical weathering studies. The method used to extract the adsorbed lake Pb isotope signal is identical to established marine approaches targeting the authigenic Fe-Mn oxyhydroxides fraction within the lake sediments [5, 6]. The Pb isotope compositions are further accompanied by various elemental ratios derived from the same samples that equally trace climatic boundary conditions in the Grimsel Lake area as well as lake water redox conditions. The Pb isotopic composition recorded in Lake Grimsel shows strong variations during the first 500 yrs of sedimentation but is remarkably constant throughout the majority of the Holocene afterwards until ~2.5 ka BP, despite variable sediment composition and -age, and isotopically relatively close to the signature of the granitic source rock. In contrast, adsorbed Th and U concentrations (given in concentrations of ng/g of sediment) are indeed significantly elevated during the earliest part of the record, while other adsorbed metals such as Al and Ti display highest adsorbed concentrations during the mid-Holocene. These findings fit established mineral weathering sequences with accessory minerals first followed by aluminosilicates such as feldspar and biotite during continuous weathering. Elements such as Nd display fairly constant normalised concentrations throughout the record. Hence, while our Pb isotopic record appears remarkably insensitive towards climatic perturbations during the Holocene, the various elemental records display a striking sensitivity towards the overall climate evolution of the Holocene. The Misox-Event at 8.2 ka BP, which was the strongest climate event within the Holocene, cannot be clearly identified in our records while smaller climate events have stronger effects. Finally, due to the high resolution of our record, the anthropogenic mining activity of the last 2200 yrs can be traced in our Pb isotopic record. Both the rise and fall of the Roman Empire as well as the onset of the industrial revolution are clearly resolvable.

References:

- [1] Harlavan, Y., Y. Erel, and J.D. Blum, Systematic changes in lead isotopic composition with soil age in glacial granitic terrains. *Geochimica et Cosmochimica Acta*, 1998. 62 (1): p. 33-46.
- [2] Gutjahr, M., M. Frank, A.N. Halliday, and L.D. Keigwin, Retreat of the Laurentide ice sheet tracked by the isotopic composition of Pb in western North Atlantic seawater during termination 1. *Earth and Planetary Science Letters*, 2009. 286: p. 546-555.
- [3] Kurzweil, F., M. Gutjahr, D. Vance, and L. Keigwin, Authigenic Pb isotopes from the Laurentian Fan: Changes in chemical weathering and patterns of North American freshwater runoff during the last deglaciation. *Earth and Planetary Science Letters*, 2010. 299 (3-4): p. 458-465.
- [4] Crockett, K.C., D. Vance, G.L. Foster, D.A. Richards, and M. Tranter, Continental weathering fluxes during the last glacial/interglacial cycle: insights from the marine sedimentary Pb isotope record at Orphan Knoll, NW Atlantic. *Quaternary Science Reviews*, 2012. 38: p. 89-99.
- [5] Gutjahr, M., M. Frank, C.H. Stirling, V. Klemm, T. van de Flierdt, and A.N. Halliday, Reliable extraction of a deepwater trace metal isotope signal from Fe-Mn oxyhydroxide coatings of marine sediments. *Chemical Geology*, 2007. 242 (3-4): p. 351-370.
- [6] Blaser, P., J. Lippold, M. Gutjahr, N. Frank, J.M. Link, and M. Frank, Extracting foraminiferal seawater Nd isotope signatures from bulk deep sea sediment by chemical leaching. *Chemical Geology*, 2016. 439: p. 189-204.

IODP

Seismic interpretation of Miocene sequences and facies distribution model, New Jersey shelf

A. THOMAS¹, S. REICHE¹, M. RIEDEL², S. BUSKE²

¹Institute for Applied Geophysics and Geothermal Energy, E.ON Energy Research Center, RWTH Aachen University, Mathieustrasse 10, 52074 Aachen, Germany.

²Institute of Geophysics and Geoinformatics, Technische Universität Bergakademie Freiberg, Gustav-Zeuner-Straße 12, 09596 Freiberg, Germany

The existence of offshore fresh groundwater has been observed in several regions around the world. The New Jersey passive margin represents one of the best documented occurrences of this phenomenon, with the first discovery of fresh groundwater dating back to the U.S Geological Survey Atlantic Margin Coring Project, 1976. Subsequent drilling during IODP Expedition legs 150, 174A and 313 revealed fresh water reservoirs that occur down to 400 m below the sea floor. This study is part of a project ultimately aiming to understand the mechanisms responsible for fresh groundwater emplacement offshore New Jersey based on numerical simulations. A detailed hydrogeological model, which accounts for the highly heterogeneous shelf environment, forms the basis for numerical simulations. In this study, we use newly re-processed, depth-migrated seismic data tied to IODP 313 wells to present a detailed seismostratigraphic interpretation along a 2D line extending from the New Jersey coast to the shelf break. We use the existing interpretation of Oligocene and Miocene sequences across the IODP drill sites as a starting point and extend this interpretation further towards the New Jersey slope.

The improved seismic data quality allowed for greater confidence in delineating sequence boundaries based on identification of onlap and offlap terminations as well as of erosional truncations. Therefore, an updated interpretation of the Expedition 313 area is presented in this study, where 32 horizons were interpreted that delineate 9 sequences and 27 parasequences from the Oligocene - Miocene boundary to the top of the Miocene section. The known ages of the sequence boundaries represented in the seismic data are compared with Cenozoic global eustasy curves to make an analysis of the systems tracts further basinward of the Expedition 313 area. The interpretation is cross-referenced with the expected sedimentary environment during marine transgression and regression cycles. Based on the seismostratigraphic interpretation, we derive a facies model, showing the grain size distribution within individual sequences and parasequences. This facies model will form the basis for assigning petrophysical properties to each model location and is thus of prime importance for subsequent numerical simulations.

ICDP

DNA-Metabarcoding of phyto- and zooplankton in East African lake sediments as proxies for past environmental perturbation

R. TIEDEMANN¹, J. KRÜGER¹, K. HAVENSTEIN¹, M.H. TRAUTH², K. HENNEBERGER³, S. HARTMANN³, M. HOFREITER³

¹ Unit of Evolutionary Biology/Systematic Zoology, Institute for Biochemistry and Biology, University of Potsdam

² Institute of Earth and Environmental Science, University of Potsdam

³ Unit of Evolutionary Adaptive Genomics, Institute for Biochemistry and Biology, University of Potsdam

Lake-sediment cores provide natural archives of past environmental changes, traditionally analyzed with sedimentological, geochemical and paleontological methods. More recently, samples from sediment cores have also been subjected to molecular DNA analysis, targeting either the living community of soil microbes or remnants of organisms that inhabited the lake, its surroundings and/or its surface sediment in the past. Our project evaluates the possibility for DNA metabarcoding in the up to 280 m long sediment cores from the Chew Bahir basin, southern Ethiopian Rift, which cover the last 550,000 years, combining state-of-the-art techniques of environmental genomics and ancient DNA analysis.

Our analyses revealed that DNA quantity and quality – even in the upper part of the core – did not allow for direct PCR amplification of taxon-specific barcoding genes. Instead, we applied a shotgun-sequencing approach on the entirety of DNA. This approach was successful for 10 samples from different strata present in the upper 10 meters of the cores, with a maximum age of about 20,000 years. Based on the results of BLAST searches, we used the MEGAN software to assign our sequence reads to taxonomic lineages that are represented in GenBank. Of the sequences that could be assigned to a lineage, the majority were shown to originate from prokaryote microbes, but several eukaryote taxa were also identified, among them taxa currently used as proxies in paleolimnological studies. This presentation will report this first encouraging results and outline our further analytical approach by designing taxon-specific baits for hybridization-capture-based metabarcoding on taxa which are informative for past environmental/climatic conditions.

IODP

Microbial nitrogen cycling potential in deep sediments of the Baltic Sea

S. TURNER¹, A. SCHIPPERS¹

¹ Geomicrobiology, Federal Institute for Geosciences and Natural Resources (BGR), Hannover

Nitrogen (N) availability is a key component in determining the dispersal of microorganisms in earth's ecosystems. The deep marine biosphere harbors remarkable numbers of microorganisms. However, little is known about the microbial N cycling potential as well as the abundances of N cycling microorganisms in deep marine sediments. Thus, we investigated potential activities of N-

hydrolyzing exoenzymes and the phosphatase as a general activity marker via HPLC and we quantified abundances of N functional genes via qPCR in deep sediments of the Baltic Sea (IODP Expedition 347). Preliminary results show that the phosphatase activity decreased in the upper part of the Little Belt sediment (hole E, till ~ 22 mbsf). Despite an improved extraction protocol for the fluorogenic substrates, activities of N-acetylglucosaminidase, alanine-aminopeptidase and phenylalanine-aminopeptidase were close to or below the detection limit for most samples. Genes for nitrate reduction (*narG*) were detected in almost all sediment depths. Surprisingly, we also detected genes for ammonia-oxidizing archaea (till ~ 6 mbsf) and bacteria (till ~ 8 mbsf). In addition, genes for chitin-degrading microorganisms (*chiA*) were detected in several depths along the sediment profile. Further analysis will reveal the occurrence and abundance of N₂ fixing and denitrifying microorganisms. Although the N cycling activities and abundances are rather low, our results suggest that microorganisms in deep sediments possess the potential of several N cycling pathways. Therefore, further research is necessary to improve the methods and to evaluate the importance of N cycling processes in situ.

ICDP

Imaging fluid channels within the NW Bohemia/Vogtland region using ambient seismic noise and MFP Analysis

J. UMLAUFT¹, H. FLORES ESTRELLA¹, M. KORN¹

¹ Institute of Geophysics and Geology, University of Leipzig, Talstraße 35, 04103 Leipzig

Presently ongoing geodynamic processes within the intracontinental lithospheric mantle give rise to different natural phenomena in the NW Bohemia/Vogtland region, among others: earthquake swarms, mineral springs and degassing zones of mantle-derived fluids (mofettes). Their interaction mechanisms and relations are not yet fully understood, therefore they are intensively studied using geophysical, geological and biological approaches.

The PIER-ICDP project focuses on the investigation of near-surface channels that conduct mantle-originating fluids as well as CO₂. It is aimed to detect and image the fluid channel structure as well as to characterize the degassing activity in terms of temporal and spatial fluctuations.

The Hartoušov Mofette Field and the Soos National Natural Reserve Area within the Cheb Basin (NW Bohemia/Vogtland region) are key sites to study fluid flow as they are characterized by strong surface degassing of CO₂. On these fields, we applied the noise source localization method Matched Field Processing (MFP) considering the fluid flow as seismic noise source. Within multiple campaigns, we measured ambient seismic noise in continuous mode during the night to avoid cultural noise generated by human activity. We used aperture arrays of different size (1 ha – 1 km²) and different amount of stations (30 - 130 units).

We compared the surface position of the MFP output with punctual CO₂ flux measurements performed by Nickschick et al. (2015) and observed a strong relation

between high CO₂ flux values and the position of the MFP maxima. Additionally, we observed surface indicators for CO₂ degassing on the same positions of the MFP predicted noise sources: wet and dry mofettes accompanied by bog cotton, bug traps and brown to yellow coloured grass.

Within the 3D MFP output, the source maxima can be followed into the subsoil to image the fluid channel structure (several 10th of a meter). We analyzed the influence of the array size on the vertical and horizontal MFP resolution as well as the temporal and spatial variability of the flow activity.

Preliminary results

Under the recent DFG grant KO 1068/17-1 seismic noise measurements and the implementation of the Matched Field Processing (MFP) analysis (Vandemeulenbrouck et al. 2010; Cross et al. 2011) have been performed on two mofette fields within the Cheb Basin (Czech Republic, NW Bohemia, Dolní Částkov and South Hartoušov). Mofettes are little sinks, which can be wet (filled with ground/ precipitation water) or dry and which are characterized by constant degassing of mantle-derived fluids as well as of CO₂. It is assumed that the CO₂ flow acts as a permanent seismic noise source that can be recorded by dense small seismic arrays (30 stations, about 1 ha extent). The MFP method, which serves as a noise source localization tool, outputs a 3D probability distribution of noise source positions within and beneath the array and hence, detects the positions of mofettes and images their corresponding feeding channels into the depth.

In the Dolní Částkov mofette field a 17 m deep borehole exists which acts as an “artificial” mofette as it conducts fluids from the depth up to the surface. It was aimed to relocate the position of the borehole and thereby to confirm the methods suitability for the detection of fluid channels. Three noise measurement campaigns were undertaken within four months. We stayed with almost the same array configuration using 30 vertical 4.5 Hz geophones connected to Reftek Texan recorders, which we distributed randomly within an area of approximately 60 x 60 m². The MFP output shows a distinct maximum at the position of the borehole at the surface as well as underlying depth maxima down to 20 m. Therefore, we could successfully validate the MFP method for the localization of flowing fluids.

On the South Hartoušov meadow, which is a natural mofette field, several surface signals, e.g. bug traps, brown grass and bog cotton, indicate the existence of CO₂ degassing. Using an aperture array of 30 vertical geophones (4.5 Hz) and Reftek Texan recorders (60 x 70 m² surface coverage) on this meadow, we could identify two areas with a maximum MFP output. Within the field it could be observed, that there are dry mofettes at these two areas as well. The maxima are well defined at the surface. Within depths of about 20 m, they extend more horizontally. This observation leads to the assumption that the fluid flows more diffusive within the subsoil, leading into one main channel up to the surface.

In general, the MFP analysis is a useful tool to locate persistent seismic noise sources that correspond to CO₂

degassing spots at the surface. Furthermore, the method seems capable of delineating the pathway of fluids into larger depth, if there is a distinct fluid channel beneath the mofette. Within the NW Bohemia/Vogtland region it gives the option to constrain the locations of potential drillholes that could be directed to directly drill into the fluid channels. Since these drillholes are destined for the use of borehole seismometers and long-term seismological observations, this would help to further investigate the assumed relation between the occurrence of earthquake swarms and the CO₂ degassing processes/ fluid flow within the Cheb Basin (Dahm & Fischer 2016: Drilling the Eger Rift).

IODP

Prydz Bay sediment drifts: Archives of modifications in East Antarctic climatic and oceanographic conditions

G. UENZELMANN-NEBEN¹

¹ Alfred-Wegener-Institut Helmholtz-Zentrum für Polar- und Meeresforschung, Am Alten Hafen 26, 27568 Bremerhaven, gabriele.uenzelmann-neben@awi.de

The detailed onset of the Antarctic glaciation during the Eocene/Oligocene and the later ice sheet dynamic in response to warm phases during the Miocene and Pliocene is still under discussion. Attempts to solve the open questions by scientific drilling have been limited by the fact that early Oligocene to early Miocene sediments, which bear witness to the onset of glaciation and early dynamics of the ice sheet, have been eroded from the continental shelf or are buried below thick Neogene sequences and could thus not be sampled during ODP Legs 119 and 188. Several hypotheses place the onset of bottom water formation as the result of down welling due to strong cooling into the Miocene, the late Oligocene, or the late Eocene, which shows the range of uncertainty in dating this event. The dynamical response, e.g., of the Lambert Glacier-Amery Ice Shelf drainage system to climate variability is recorded in the sediments of Prydz Bay and the adjacent slope and rise of the Cooperation Sea. Thus a study of sedimentary features and structures and the prevailing sediment transport patterns can help to understand the development of this system and its sensitivity to climate change.

The analysis of seismic reflection data allows to reconstruct sediment input and sediment transport patterns. This represents an important tool, even if an indirect one, to infer past changes in climate and oceanography in the absence of direct information from drilled geological samples. A large dataset of high-quality seismic lines has been acquired along the Prydz Bay margin, is available via the SCAR seismic data library system and will be analysed with respect to documents of down-slope, i.e., the result of material input via advancing the ice sheet, and along-slope, i.e., features resulting from the shaping of bottom and deep water, to infer past changes in climate and oceanography in combination with results from ODP Leg 119 and 188. This way we also intend to close the gap, which could not be sampled by drilling (the early Oligocene to early Miocene).

IODP

Dissolution and recrystallisation in planktonic foraminifera

J. VOIGT¹*, E. C. HATHORNE², J. FIETZKE² AND H. PÄLIKE¹

¹ MARUM – Center for Marine Environmental Sciences, Leobener Str. 8, 28359 Bremen, Germany (*correspondence: jvoigt@marum.de)

² GEOMAR Helmholtz Centre for Ocean Research Kiel, Wischhofstr. 1-3, 24148 Kiel, Germany

The calcite tests of foraminifera, which are used to reconstruct oceanic and climatic conditions in the past, can be altered after deposition by diagenetic processes replacing the original biogenic calcite by secondary calcite. This recrystallisation process is still poorly understood. Therefore, it is important to quantify changes in the elemental and isotopic composition of foraminiferal tests to reliably apply and interpret the obtained geochemical proxy data, and to provide further insights into the diagenetic process.

We studied two dissolution events in recrystallised Miocene sediment sections from IODP Expedition 320/321 by using laser ablation ICP-MS derived element/Ca ratio depth profiles through the test wall of the planktonic foraminifera *Dentoglobigerina venezuelana*: a) The peak warmth events of the middle Miocene climatic optimum (15.6 Ma) and b) of the time interval corresponding to a specific seismic reflector (the “Lavender” seismic reflector, 16.9 Ma, Mayer *et al.* 1985). These events are characterised by a massive decrease in CaCO₃ content (up to 73% carbonate loss, Keegan Wilson 2014; Kochhann *et al.* 2016), interpreted as an abrupt shoaling of the lysocline (Lyle 2003; Pälike *et al.* 2012), and marked declines in benthic foraminiferal stable isotopes ($\delta^{18}\text{O}$, $\delta^{13}\text{C}$) (Mayer *et al.* 1986; Holbourn *et al.* 2015; Kochhann *et al.* 2016). The triggers for the dissolution events are still not fully known, however, the events were associated with short, intense warming pulses coupled with C-cycle perturbations (Holbourn *et al.* 2015; Kochhann *et al.* 2016).

Decreases in Mg/Ca ratios of foraminiferal tests suggest dissolution (Sadekov *et al.* 2010), whereas recrystallisation tends to increase the Mg/Ca (Sexton *et al.* 2006). Preliminary results of tests from the peak warmth event at 15.6 Ma indicate no change in Mg/Ca, however, Sr/Ca decreases through the test wall. This points to recrystallisation, given that less Sr is incorporated into secondary calcite and primary/modern Sr/Ca ratios are homogenous through the test wall. Based on these Sr/Ca data, tests from Site U1336 are more recrystallised than tests from Sites U1337 and U1338. SEM images of wall cross sections at 15.6Ma are similar for all measured tests of the Sites U1336-U1338 and thus different preservation states during initial recrystallisation cannot be distinguished in SEM images. These results are compared to tests from older sediment sections (> 20 Ma) of Site U1336, where different Sr parameters (Sr²⁺, Sr/Ca, ⁸⁷Sr/⁸⁶Sr) suggest that bulk carbonates are extensively recrystallised at this site (Voigt *et al.* 2015). Nevertheless, laser ablation results obtained from tests from recrystallised sediments indicate that much of the original geochemical Mg/Ca signal is still preserved.

References:

- Holbourn A., Kuhnt W., Kochhann K.G.D., Andersen N., and Meier K.J.S. (2015) Global perturbation of the carbon cycle at the onset of the Miocene Climatic Optimum. *Geology* **43**, 123-126
- Keegan Wilson J. (2014) Early Miocene carbonate dissolution in the eastern equatorial Pacific. Ph.D. thesis, Texas A&M University
- Kochhann *et al.* (2016) Kochhann K.G.D., Holbourn A., Kuhnt W., Channell J.E.T., Lyle M., Shackford J. K., Wilkens R.H., and Andersen N. (2016) Eccentricity pacing of eastern equatorial Pacific carbonate dissolution cycles during the Miocene Climatic Optimum. *Paleoceanography* **31**, doi:10.1002/2016PA002988
- Lyle M. (2003) Neogene carbonate burial in the Pacific Ocean. *Paleoceanography* **18**, 1059, doi:10.1029/2002PA000777
- Mayer L.A., Shipley T.H., Theyer F., Wilkens R.H., and Winterer E.L. (1985) Seismic modeling and paleoceanography at deep sea drilling project Site 574. In: *Init. Repts. DSDP 85* (eds. L. Mayer, F. Theyer, *et al.*). Deep Sea Drilling Project, pp. 947-970
- Mayer L.A., Shipley T.H., and Winterer E.L. (1986) Equatorial Pacific seismic reflectors as indicators of global oceanographic events. *Science* **233**, 761-764
- Pälike H., *et al.* (2012) A Cenozoic record of the equatorial Pacific carbonate compensation depth. *Nature* **488**, 609-614
- Sadekov A.Y., Eggins S.M., Klinkhammer G.P., and Rosenthal Y. (2010) Effects of seafloor and laboratory dissolution on the Mg/Ca composition of *Globigerinoides sacculifer* and *Orbulina universa* tests – A laser ablation ICPMS microanalysis perspective. *Earth and Planetary Science Letters* **292**, 312-324
- Sexton P.F., Wilson P.A., and Pearson P.N. (2006) Microstructural and geochemical perspectives on planktic foraminiferal preservation: "Glassy" versus "Frosty". *Geochemistry, Geophysics, Geosystems* **7**, Q12P19, doi:10.1029/2006GC001291
- Voigt J., Hathorne E.C., Frank M., Vollstaedt H., and Eisenhauer A. (2015) Variability of carbonate diagenesis in equatorial Pacific sediments deduced from radiogenic and stable Sr isotopes. *Geochimica et Cosmochimica Acta* **148**, 360-377

ICDP

Isotopic record of diagenetic siderites from Lake Towuti's ferruginous sequence, Indonesia.

A. VUILLEMIN¹, J. KALLMEYER¹, H. KEMNITZ¹, R. WIRTH¹, A. LUECKE², C. MAYR³, J. A. SCHUESSLER¹, C. HENNY⁴, S. A. CROWE⁵, J. M. RUSSELL⁶, S. BIJAKSANA⁷, H. VOGEL⁸ AND THE ICDP TOWUTI DRILLING PROJECT SCIENCE TEAM

¹GFZ German Research Centre for Geosciences, Helmholtz Centre Potsdam, Sect. 5.3. Geomicrobiology, Sect. 4.1. Lithosphere Dynamics, Sect. 4.3. Chemistry & Physics of Earth Materials, Sect. 3.3. Earth Surface Geochemistry, Telegrafenberg, 14473 Potsdam, Germany

²Research Center Juelich, Institute of Bio- & Geosciences 3: Agrosphere, Wilhelm-Johnen-Straße, 52428 Juelich, Germany

³Institute of Geography, University of Erlangen-Nürnberg, Glückstrasse 5, 91054 Erlangen, Germany

⁴Research Center for Limnology, Indonesian Institute of Sciences (LIPI), Cibinong-Bogor, Indonesia

⁵Department of Microbiology and Immunology, Department of Earth, Ocean, and Atmospheric Sciences, University of British Columbia, Vancouver, Canada

⁶Department of Earth, Environmental, and Planetary Sciences, Brown University, 324 Brook St., 13 Providence, RI, 02912, USA

⁷Faculty of Mining and Petroleum Engineering, Institut Teknologi Bandung, Jalan Ganesa 10, 15 Bandung, 50132, Indonesia

⁸Institute of Geological Science, University of Bern, Baltzerstrasse 1+3, CH-3012, Bern, 17 Switzerland

Authigenic minerals formed biotically and abiotically in the water column and sediment have the potential to record paleoclimate and diagenesis. Here we present a study from Lake Towuti, a deep tectonic basin in Sulawesi, Indonesia. Its geographic position makes it a prime location to record paleoclimatic changes in the tropical Western Pacific warm pool in its sedimentary sequence (Russell et al., 2016). Ultramafic rocks and lateritic soils eroded from the catchment supply Lake Towuti with little sulfate but considerable amounts of iron oxyhydroxides/oxides (Vuillemin et al., 2016), which trap all available phosphate, leading to extreme phosphate limitation and thereby restraining primary productivity. In the hypolimnion however, bottom water anoxia allows for microbially mediated iron reduction and liberation of phosphorus. The extreme scarcity of sulfate and nitrate/nitrite make Lake Towuti's bottom water a modern analogue for the Archaean Ocean (Crowe et al., 2014). Development of specific microbial metabolisms during early diagenesis makes it an ideal site to study mineral formation under ferruginous conditions.

In May to July 2015, the Towuti Drilling Project led by the International Continental Drilling Program (ICDP) recovered a total >1000 m of sediment core from three drilling sites (Russell et al., 2016), including a 114 m long core (TDP-1A) drilled with a contamination tracer dedicated to geomicrobiological studies (Friese et al., 2017).

Siderites (i.e. FeCO₃) were recovered from 50 distinct layers of core TDP-1A and investigated to infer mineral formation and recording of microbial processes. SEM and TEM imaging showed that siderites grow from micritic phases into mosaic monocrystals, developing into aggregates with increasing burial depth. Green rust (i.e. Fe₆[OH]₁₂·[CO₃·2H₂O]) and magnetites (i.e. Fe₃O₄) were observed interlaced within siderites, suggesting successive diagenetic phases related to iron reduction. Elemental mapping revealed Mn/Fe zonations reflecting diagenetic

evolution of pore water chemistry. Intervals with persistent light δ¹³C and δ⁵⁶Fe compositions are interpreted to reflect long periods of bottom water anoxia with little siderite formation. The concomitance of vivianites (i.e. Fe₂[PO₄]₂·8H₂O) argues for accumulation of dissolved iron and potentially methane in the anoxic bottom water. We observe contrasting siderite-rich intervals that lack vivianite, which point toward bottom water oxygenation with increased burial of amorphous Fe³⁺. After burial, this amorphous Fe³⁺ is reduced and reacts with the pore water DIC to form siderite with heavy δ¹³C but light δ⁵⁶Fe compositions. We therefore consider siderite isotopic compositions to reflect intricate processes of redox fluctuations and diagenesis.

References:

- Crowe S.A., Paris G., Katsev S., Jones C.A., Kim S.T., Zerkle A.L., Nomosatryo S., Fowle D.A., Adkins J.F., Sessions A.L., Farquhar J., and Canfield D.E. (2014). Sulfate was a trace constituent of Archaean seawater. *Science* 346, 735–739. doi: 10.1126/science.1258966
- Friese A., Kallmeyer J., Kite J.A., Martinez I.M., Bijaksana S., Wagner D., the ICDP Lake Chalco Drilling Science Team, and the ICDP Towuti Drilling Science Team (2017). A simple and inexpensive technique for assessing contamination during drilling operations. *Limnology and Oceanography: Methods* in press. doi: 10.1002/lom3.10159.
- Russell J.M., Bijaksana S., Vogel H., Melles M., Kallmeyer J., Ariztegui D., Crowe S., Fajar S., Hafidz A., Haffner D., Hasberg A., Ivory S., Kelly C., King J., Kirana K., Morlock M., Noren A., O'Grady R., Ordóñez L., Stevenson J., von Rintelen T., Vuillemin A., Watkinson I., Wattrus N., Wicaksono S., Wonik T., Bauer K., Deino A., Friese A., Henny C., Imran, Marwoto R., Ngkoimani L.O., Nomosatryo S., Safiuddin L.O., Simister R., and Tamuntuan G. (2016). The Towuti Drilling Project: Paleoenvironments, biological evolution, and geomicrobiology of a tropical Pacific lake. *Scientific Drilling* 21, 29-40. doi: 10.5194/sd-21-29-2016.
- Vuillemin A., Friese A., Alawi M., Henny C., Nomosatryo S., Wagner D., Crowe S.A., and Kallmeyer J., 2016. Geomicrobiological features of ferruginous sediments from Lake Towuti, Indonesia. *Frontiers in Microbiology* 7, 1007. doi: 10.3389/fmicb.2016.01007.

ICDP

Petrogenesis of Snake River Plain basalts from the Kimama core and an experimental study on the link with associated rhyolites

M. WANG¹, O. NAMUR¹, R. ALMEEV¹, B. CHARLIER², D. A. NEAVE¹, F. HOLTZ¹

¹Institute of Mineralogy, Leibniz University of Hannover, Germany

²Department of Geology, University of Liege, Belgium

The Snake River Plain-Yellowstone (SRPY) province is among the most voluminous expressions of magmatic activity at the Earth's surface and also represents one of the best examples of bimodal basalt-rhyolite volcanism (Bonnichsen et al., 2008; Ellis et al., 2013). Drilling by the ICDP HOTSPOT project at Kimama was performed between September 2010 and January 2011 and reached a final depth of 1912 m. The Kimama drill hole is dominated by basalt, with thin intercalations of sediment in the upper 200 m and lower 300 m. Detailed lithologic and geophysical logging have documented ~557 basalt flows, comprising at least 30 flow groups (13 to 170 m thick) representing distinct time periods, and magma batches, with the oldest lavas being dated at ~6 Ma (Bradshaw et al., 2012; Champion and Duncan, 2012; Potter et al., 2012). In this study, we conducted a detailed petrological study of the rocks from the Kimama drill core that we combined with crystallization experiments. The aims are to understand the mechanisms of basaltic differentiation in the crust, the magma storage conditions and the petrological link between basalts and rhyolites.

Hundred and ninety core samples were studied carefully for petrography. Out of them, 105 samples were measured for major and trace elements analyses and 25 representative samples were chosen for detailed microprobe analyses. Kimama rocks range from highly-phyric to crystal-poor lavas with less than 10% of phenocrysts. The typical mineral assemblage contains

olivine (some with Cr-spinel inclusions) and plagioclase. Clinopyroxene is abundant in the groundmass along with plagioclase, olivine, magnetite, ilmenite and apatite. Harker diagrams and stratigraphic chemical trends demonstrate that fractionation is evident across different flow groups, with a progression from more primitive basalts at depth to evolved basalts in the upper section. The major and trace element variations are consistent with the fractionation of the observed mineral assemblage (Ol + Plg ± Cpx). The most evolved Fe-Ti-rich basalts with 17-19 wt% total Fe₂O₃ and 3.2-4.8 wt% TiO₂ occur in two stratigraphic intervals (1045-1047 m and 1731-1797 m). These rocks have a very fine-grained groundmass with abundant Fe-Ti oxide minerals.

Core and rim compositions of the plagioclase phenocrysts were obtained for 115 crystals. Core compositions of plagioclase phenocrysts can be classified into four groups by calcium contents, i.e., ~An₈₀, ~An₇₅, ~An₆₅, and ~An₅₅. Pyroxenes are represented by augite and pigeonite. Analyses of 290 crystals show that clinopyroxene compositions vary from Mg# 82 to Mg# 32, with a prominent peak at ~Mg# 70. Olivine compositions vary from Fo₈₂ to Fo₃₂. Detailed microprobe profiles (with intervals of ~4-6 μm) of major (Si, Fe, Mg, Mn) and minor (Ca, Ni) elements were measured in a total of 100 olivine crystals. Based on the range of Fo values and the shape of zoning patterns observed we distinguished four types of olivine zoning. Olivine crystals are characterized by zoning patterns ranging from 'normal' (decreasing Fo towards the rim) to 'reverse' (lower Fo core with higher rim), or more complex zoning, with reversely zoned interiors and normally zoned rims. Diffusion modeling is in progress to obtain time-scale information on magma storage conditions. To increase the accuracy and precision with which timescales can be retrieved, we determined crystallographic axis orientations by electron backscatter diffraction (EBSD, Prior et al., 1999). This allows us to correct the strongly anisotropic diffusion of Fe and Mg in olivine (Dohmen and Chakraborty, 2007).

Representative compositions were used as starting compositions for high-temperature experiments in order to

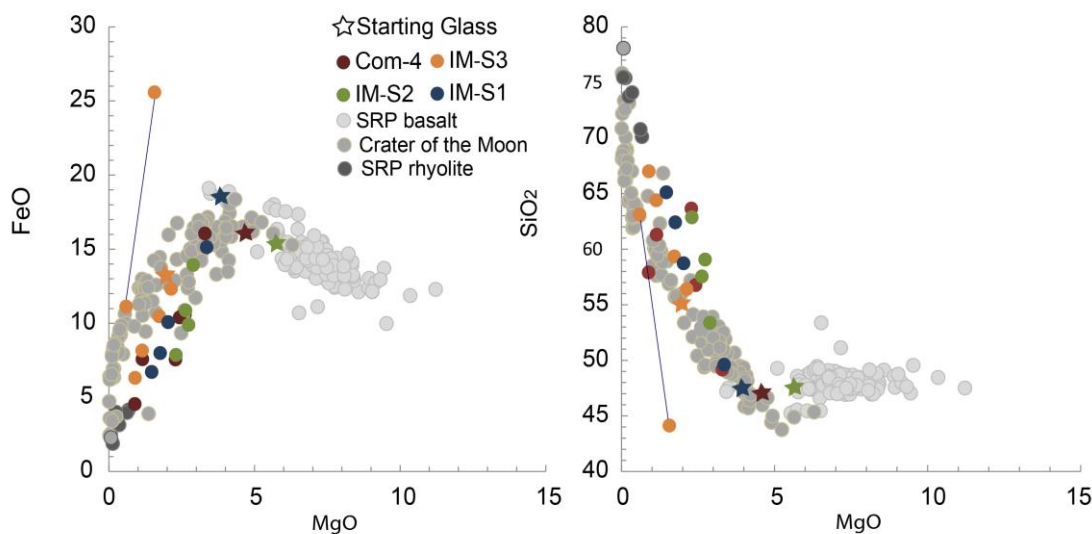


Figure 1: Starting compositions (stars) and selected residual liquid compositions produced in crystallization experiments plotted along with natural bulk compositions of basalts and rhyolites from the Kimama drill core and rocks from Snake River Plain (rhyolites) and Craters of the Moon (Leeman, 1976). The tie line joining the two orange circles join immiscible liquids obtained at 1040°C (600 MPa) for IM-S3.

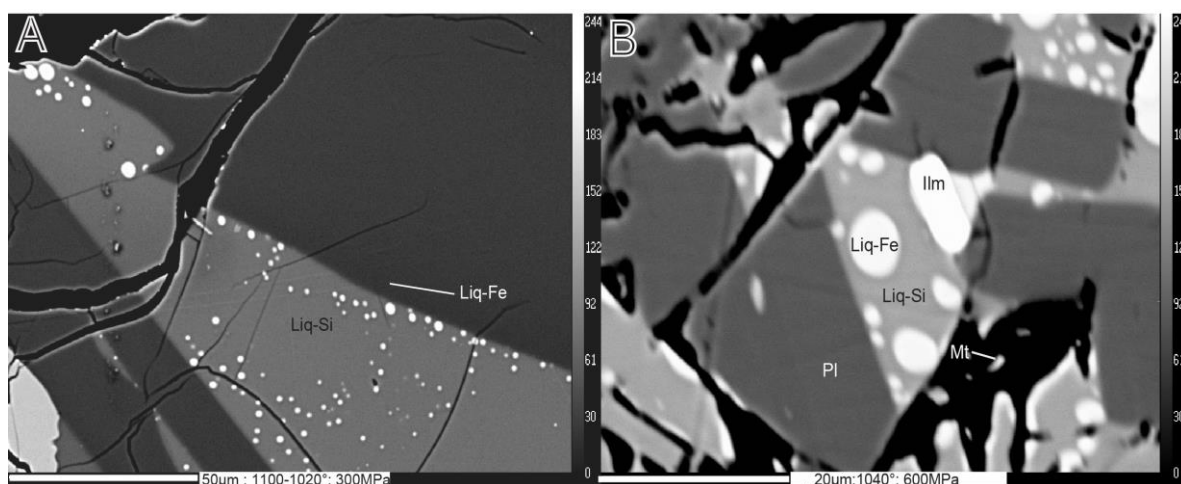


Figure 2: Immiscible textures in experiments performed on evolved ferrobasalts from the Kimama core. (A) Experiment performed at 300 MPa with continuous cooling (1.2 °C/hour) from 1100 to 1020 °C, composition IM-S3. (B) Experiment performed at 1040°C and 600 MPa; composition IM-S3.

understand the petrological link between basalts and rhyolites. So far, 32 individual experiments have been conducted using four selected evolved ferrobasic compositions as starting materials. Three compositions represent the most evolved basaltic lavas from the Kimama core. The last composition IM-S3 with 55 wt% SiO₂ represents ferrobasic from the Crater of the Moon (Leeman et al., 1976). All starting materials are synthetic glass analogues matching natural compositions and prepared using high purity reagent grade oxides, silicates and carbonates. The crystallization experiments were conducted at 300 and 600 MPa under nominally dry conditions (the water content of the melt is estimated to be less than 0.4 wt% H₂O; Husen et al., 2016), in ~20°C steps between 1080°C and 1020°C. Run durations ranged from 96 to 168 hours. All experiments have been conducted at intrinsic redox conditions corresponding to ca. FMQ buffer at nominally dry conditions. One slow-cooling experiment was also conducted from 1100 to 1020 °C, with a cooling rate of 1.2 °C/hour (at 300 MPa; Fig. 2). Our experimental results constrain the liquid line of descent of the ferrobasic (Fig.1). We obtained measurable glass pools up to the level of 82% of crystallization. The solid phase of the samples was always represented by Cpx + Pl ± Mt ± Ilm ± Ap mineral assemblage. Olivine was not observed in our experimental products, indicating that it was not stable at such high crystallization degrees. Experimental residual liquids contained up to 67 wt% SiO₂, thus generally approaching, but not yet fully representing natural rhyolite compositions (>72% SiO₂).

For one composition (IM-S3), immiscibility between a silica-rich melt and silica-poor melt has been observed (Fig. 2). It should be noted that the formation of immiscible Si-rich and Fe-rich liquids have been experimentally demonstrated at high pressure (600 MPa) for the first time: a Fe-rich liquid with 44.13 wt% SiO₂ and 25.58 wt% FeO formed globules in a Si-rich liquid with 63.13 wt% SiO₂ and 11.12 wt% FeO. The crystallization experiments are pertinent to test the potential development of silicate liquid immiscibility along basalt to rhyolite differentiation in Snake River Plain. Particularly, the range of alkali (Na₂O+K₂O) and P₂O₅ contents of the selected compositions is a critical parameter for the development of a two-liquid field (e.g. Charlier and Grove, 2012). The liquidus of these compositions is close to the highest temperature (1000-1020°C) for the onset of immiscibility.

It is also remarkable that the Si-rich immiscible liquid both at 600 MPa and 300MPa also approaches natural SRPY rhyolite compositions, providing new evidences for the potential importance of liquid immiscibility in magma genesis of rhyolites from the SRPY and other bimodal volcanic provinces.

The reliable analysis of experimental liquids under higher degrees of crystallization is not possible and is a challenging experimental problem. The use of the thermal cycling method (Erdmann and Koepke, 2016) in our experiments did help to produce relatively large melt pools. However, it is not yet sufficient to simulate and characterize the liquid phase after more than 80% of crystallization, which is required to produce SiO₂-rich compositions similar to those of natural SRP rhyolites. To achieve the goal, we synthesized new starting compositions based on the microprobe data of the glass compositions obtained from previous experiments at higher temperature. At this stage of the study, four new compositions have been synthesized (SiO₂ contents in the range 51 to 58 wt% SiO₂). The experiments with these compositions are ongoing and still require microprobe characterization of the melt and mineral phases. In the next months, our efforts will also focus on the determination of the binodal surface for the development of immiscibility. The step-wise approach (with new starting compositions), which simulates fractional crystallization, is a favourable process to constrain the binodal surface (Charlier and Grove, 2012). Investigating two pressures is also important because iron and titanium enrichments (more important at lower pressure) lead preferentially to the development of immiscibility.

References:

- Bradshaw, R.W., Christiansen, E.H., Dorais, M.J., Shervais, J.W., Potter, K.E., 2012. Source and crystallization characteristics of basalts in the Kimama core: Project Hotspot Snake River Scientific Drilling Project, Idaho. *Eos Trans. AGU*: V13B-2840
- Bonnichsen, B., Leeman, W., Honjo, N., McIntosh, W., Godchaux, M., 2008. Miocene silicic volcanism in southwestern Idaho: geochronology, geochemistry, and evolution of the central Snake River Plain. *Bulletin of Volcanology* 70(3): 315-342
- Champion, D., Duncan, R.A., 2012. Paleomagnetic and ⁴⁰Ar/³⁹Ar studies on tholeiitic basalt samples from "HOTSPOT" corehole taken at Kimama, Idaho, central Snake River Plain. *Eos Trans. AGU*: V13B-2842.
- Charlier, B., Grove, T., 2012. Experiments on liquid immiscibility along tholeiitic liquid lines of descent. *Contrib. Miner. Petrol.* 164(1): 27-44.
- Dohmen, R. and Chakraborty, S., 2007. Fe-Mg diffusion in olivine II: point defect chemistry, change of diffusion mechanisms and a model for

- calculation of diffusion coefficients in natural olivine. *Physics and Chemistry of Minerals*, 34(6): 409-430.
- Ellis, B.S., Wolff, J.A., Borougs, S., Mark, D.F., Starkel, W.A., Bonnicksen, B., 2013. Rhyolitic volcanism of the central Snake River Plain: a review. *Bulletin of Volcanology* 75(8): 1-19.
- Erdmann, M., J. Koepke., 2016. "Experimental temperature cycling as a powerful tool to enlarge melt pools and crystals at magma storage conditions." *American Mineralogist* 101(4): 960-969.
- Leeman, W.P., Vitaliano, C.J., Prinz, M., 1976. Evolved lavas from Snake-River Plain - Craters of Moon-National-Monument, Idaho. *Contributions to Mineralogy and Petrology*. 56(1): 35-60.
- Husen, A., Almeev RR, Holtz, F., 2016. "The effect of H₂O and pressure on multiple saturation and liquid lines of descent in basalt from the Shatsky Rise." *Journal of Petrology* 57(2): 1-35.
- Prior, D.J., 1999. Problems in determining the misorientation axes, for small angular misorientations, using electron backscatter diffraction in the SEM. *Journal of Microscopy*, 195(3): 217-225.
- Potter, K.E., Shervais, J.W., Champion, D., Duncan, R.A., Christiansen, E.H., 2012. Project Hotspot: temporal compositional variation in basalts of the Kimama core and implications for magma source evolution, Snake River scientific drilling project, Idaho. *Eos Trans. AGU*: V13B-2839.

IODP

Chronology of the Lower Bengal Fan (IODP Expedition 354) for the Late Quaternary – paleoclimate implications

M.E. WEBER¹, P.S. DEKENS², B.T. REILLY³, H. LANTZSCH⁴, P.A. SELKIN⁵, S.K. DAS⁶, T. WILLIAMS⁷, Y. MARTOS MARTIN⁸, R.R. ADHIKARI⁹, B.R. GYAWALI¹⁰, G. JIA¹¹, L.R. FOX¹², J. GE¹³, M.C. MANOJ¹⁴, J.F. SAVIAN¹⁵, L. MEYNADIER¹⁶, R.R. ADHIKARI⁴, V. SPIESS⁴, C. FRANCE-LANORD¹⁷, AND IODP EXPEDITION 354

SCIENTISTS

- ¹ University of Bonn, Bonn, Germany
² San Francisco State University, San Francisco, USA
³ Oregon State University, Corvallis, USA
⁴ University of Bremen, Bremen, Germany
⁵ University of Washington, Tacoma, USA
⁶ Presidency University, Kolkata, India
⁷ IODP Texas A&M University, College Station, USA
⁸ British Antarctic Survey, Cambridge, UK
⁹ Shimane University, Matsue, Japan
¹⁰ Tohoku University, Sendai, Japan
¹¹ Chinese Academy of Sciences, Guangzhou, China
¹² Natural History Museum, London, UK
¹³ Chinese Academy of Sciences, Beijing, China
¹⁴ Birbal Sahni Institute of Palaeobotany, Lucknow, India
¹⁵ Universidade Federal do Rio Grande do Sul, Alegre, Brazil
¹⁶ Université Paris, Paris, France
¹⁷ Centre National de la Recherche Scientifique, Vandoeuvre les Nancy Cedex, France

IODP Expedition 354 set out in February to March 2015 to drill seven sites along an east west oriented core transect of 320 km length at 8°N in the Bengal Fan (France-Lanord et al., 2015). The sites were recovered to reconstruct the Himalayan uplift since the Oligocene and to decipher the turbiditic depositional mechanisms on the lower Bengal Fan. The Bengal Fan accumulated the material from the erosional uplift of the Himalayan after the collision of India and Asia. The fan system, fed by turbidites coming from the Ganges and Brahmaputra river systems, contains the most complete flux signal since the continental collision. The majority of sediment supplied by the Ganges-Brahmaputra river system bypasses the shelf via the "Swath of No Ground", which connects to the only currently active channel-levee system. The new core transect of IODP Expedition 354 crosses the active channel on the lower Bengal Fan. Six sites are located on the eastern side, one on the western side. Seismic imaging shows a complex pattern of levees and deeply incised

channels, indicative of vertical aggradation and lateral migration.

Deposits along the core transect also show comprehensive internal facies variability with complex intercalation of turbiditic and hemipelagic deposits, documenting the complicated internal fan architecture and reflecting changes in the depositional system through time and with respect to uplift history, levee and channel development, and sea-level changes. Hemipelagic sequences represent a several meter thick top layer of Late Quaternary age. Here, deposits are either rich in biogenic opal/clay or in carbonate. We studied a number of physical, optical, geochemical, grain-size, and stable isotopic properties of this top layer in order to estimate sedimentary properties, and to assess the development of the region during the last glacial cycle. For this purpose, we sampled Site U1452C-1H continuously for the uppermost 480 cm in 2-cm increments.

Preliminary results indicate that the upper hemipelagic layer consists mostly of nannofossil or foraminifera bearing calcareous clays, and clays. Siltier sections are intercalated within the clays, and transitions are often difficult to discern. The lower boundary is usually shown by a sharp boundary with a coarser-grained, silty to sandy deposits in 6 – 18 m depth. The upper Toba Ash (74 ka) is a distinct time marker in most physical property data sets. It is documented for all sites in 2 – 6 m sediment depth except for U1454, which is from a levee immediately east of currently active channel and does possess a hemipelagic top of reduced thickness. This is presumably a site of very high sedimentation documenting currently active turbidite activity. Sediment lightness L* clearly distinguishes the facies variability and provides, alongside with existing biomagnetostratigraphic data, chronostratigraphic constraints for correlation. Accordingly, we identified the position of the Last Glacial Maximum (LGM) within the uppermost m of the sites and the three substages of Marine Isotopic Stage (MIS) 5. Also, MIS 6.3, 6.5, 7.1 occur at most sites. These observations imply that the uppermost sediment unit indicates hemipelagic sedimentation (i.e., relative fan inactivity, at least in this part of the lower fan) persisted at least during the last 200 ka. Extrapolating ages towards the lower, sandy boundary would indicate that hemipelagic sedimentation prevailed for ~300 ka. However, this is ambiguous because the facies transitions vary and future research has to show whether or not this lower transition is synchronous across the core transect.

For Site U1452C-1H, we sampled the uppermost 480 cm continuously in 2-cm increments. Here records of wet-bulk density as well as color reflectance b* (the red-green component) and L* (the lightness) show a dominant precession cyclicity. Hence, we are able to provide an insolation-tuned chronology for the last 200 ka (MIS1–7). The records agree well with δ¹⁸O records retrieved from Chinese caves. An independent age model is derived from records of relative paleointensity (RPI), including the assessment of the Laschamp Event (~40 ka), and on RPI tuning to global templates. We compare both chronologies and evaluate their chronological and paleoclimatic implications. Grain-size measurements show in-phase variability with monsoonal strength. In addition, color endmember modeling reveals strong correlation of three color components to monsoonal variability.

IODP

Transport, Removal and Accumulation of sediments Numerically Simulated for Paleo-Oceans and Reconstructed from cores of The Eirik Drift (TRANSPORTED)

T. WEBER¹, J. SAYNISCH¹, G. UENZELMANN-NEBEN², M. THOMAS^{1,3}

¹ GFZ German Research Centre for Geosciences, Telegrafenberg, 14473 Potsdam, Germany

² Alfred-Wegener-Institut Helmholtz-Zentrum für Polar- und Meeresforschung · Am Handelshafen 12, 27570 Bremerhaven, Germany

³ Freie Universität Berlin, Carl-Heinrich-Becker Weg 6-10, 12165 Berlin, Germany

The Western Boundary Undercurrent (WBUC) is a crucial component of the global ocean conveyor belt and is driven by Deep Water Formation (DWF) in the Greenland,

Labrador, Norwegian and Iceland Seas. Its path and strength are affected by changing climate conditions and tectonic events (Uenzelmann-Neben et al. (2016)) which are recorded in the sediments of Eirik Drift, south of Greenland. Seismic profiles (e.g., Müller-Michaels and Uenzelmann-Neben (2014, 2015)) and ODP Leg Site 646 and IODP Expedition 303 Sites U1305-U1307 drill cores (Expedition 303 Scientists (2006), Shipboard Scientific Party (1987)) give information about sedimentation rate and grain sizes since the late Miocene and the Pliocene. Both the late Miocene and Pliocene climates are similar to possible future anthropogenically modified climates (Salzmann et al. (2009)) and therefore have attracted numerous numerical and proxy-based studies. In this study we will link modifications in sedimentation rates and grain sizes recorded in the cores from Sites 646 and U1305-1307 to climatic and tectonically forced alterations of flowpaths and velocities of the WBUC.

We will simulate ocean dynamics with the Regional

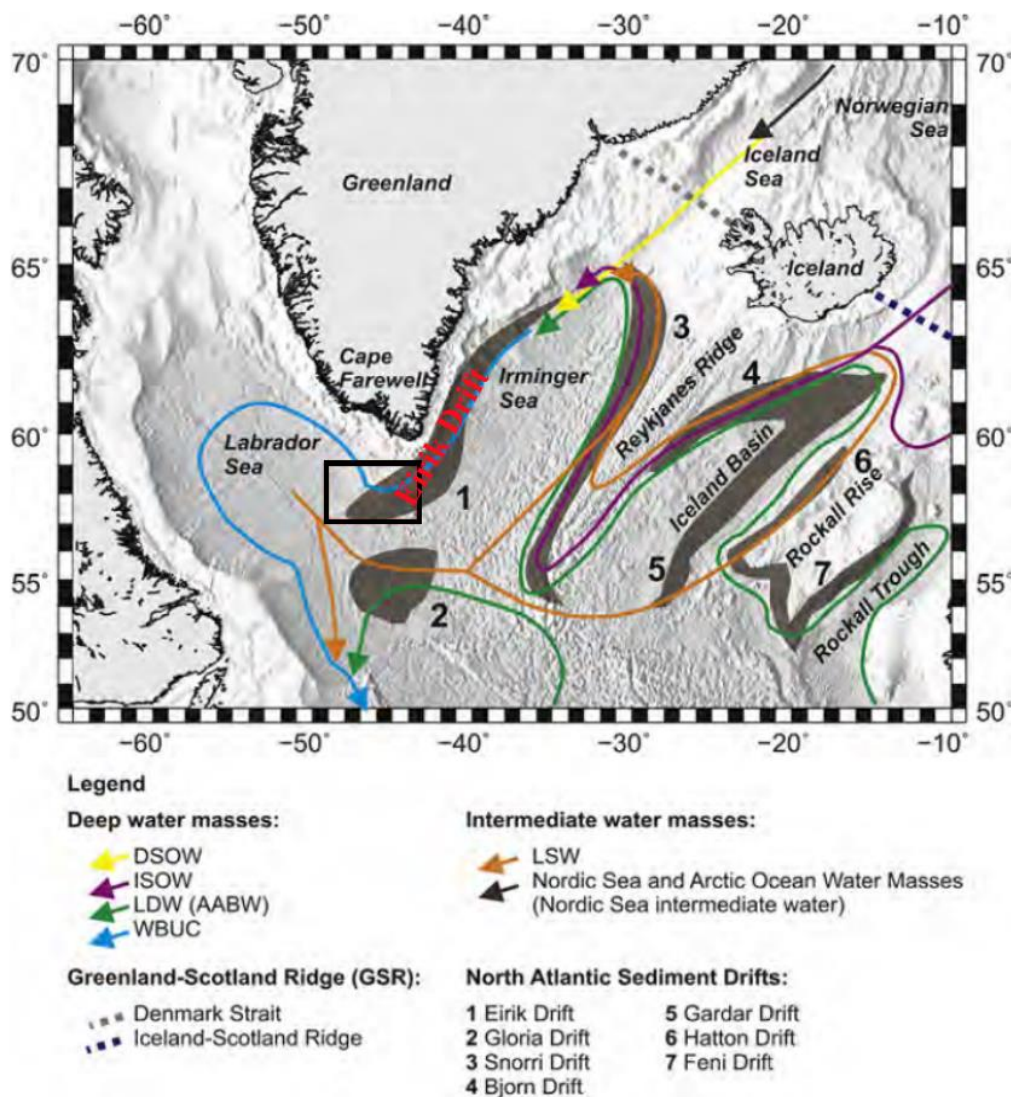


Figure 1: Satellite bathymetry map (Smith and Sandwell (1997)) including basins, ridges, sediment drifts and prevailing deep-current system of the North Atlantic Ocean (modified from Müller-Michaelis et al.(2013); sediment drifts after Faugères et al. (1999)). The present Western Boundary Undercurrent (WBUC) at Eirik Drift transports Denmark Strait Overflow Water (DSOW), Iceland–Scotland Overflow Water (ISOW), Lower Deep Water (LDW; also: modified Antarctic Bottom Water (AABW)) and Labrador Sea Water (LSW) (modified from Schmitz (1996)). [Modified after Müller-Michaels and Uenzelmann-Neben (2014), Figure 1].

Ocean Modeling System (ROMS, Shchepetkin and McWilliams (2005)) in the North Atlantic. The regionalization enables us to run several simulations at unusually high resolution and resolve the WBUC in time and space. The simulated region will encompass the North Atlantic, Labrador Sea, Norwegian Sea, Iceland Sea and Greenland Sea, thereby including all areas of deep water formation of importance for Eirik Drift. ROMS is a modern and highly modular ocean model code that uses terrain following sigma coordinates. The resulting higher resolution of oceanic bottom layers and the state of the art sediment and sea ice modules make ROMS a suitable choice for the proposed sensitivity simulations (cf., Li (2012)). As a result, quantitative comparisons between simulated and measured (i.e., reconstructed) sediment transports of the WBUC will be possible for the first time. Derived physical causalities will link variations in sedimentation rate, sediment transports and grain sizes to climate or tectonic changes. Furthermore, the origin of the sediments and the transporting water masses can be determined.

References:

- Expedition 303 Scientists, 2006, Expedition 303 summary, in Channell, J. E. T., Kanamatsu, T., et al. eds., Proc. IODP, Volume 303/306: College Station, Integrated Ocean Drilling Program Management International, p. 30.
- Li, X., 2012. Numerical Simulation of Sediment Transport at the Agulhas Drift on the South African Gateway in relation to its Geodynamic Development. (PhD thesis, University of Bremen).
- Müller-Michaelis, A., and Uenzelmann-Neben, G., 2014, Development of the Western Boundary Undercurrent at Eirik Drift related to changing climate since the early Miocene: Deep Sea Research Part I: Oceanographic Research Papers, v. 93, p. 21-34.
- Müller-Michaelis, A. & Uenzelmann-Neben, G., 2015. Using seismic reflection data to reveal high-resolution structure and pathway of the upper Western Boundary Undercurrent core at Eirik Drift. *Mar. Geophys. Res.* 36, 343–353.
- Salzmann, U., Haywood, A. M. & Lunt, D. J., 2009. The past is a guide to the future? Comparing Middle Pliocene vegetation with predicted biome distributions for the twenty-first century. *Philos. Trans. A. Math. Phys. Eng. Sci.* 367, 189–204.
- Shchepetkin, A. F., McWilliams, J. C., 2005. The regional oceanic modeling system (ROMS): a split-explicit, free-surface, topography-following-coordinate oceanic model. *Ocean Model.* 9(4), 347–404.
- Shipboard Scientific Party, 1987a, Site 646, in Srivastava, S. P., Arthur, M., Clement, B., and et al., eds., *Init. Repts.*, Volume 105: College Station, Ocean Drilling Program, p. 419-674.
- Uenzelmann-Neben, G., Weber, T., Thomas, M., and Gruetzner, J., 2016, in press, Transition from the Cretaceous ocean to Cenozoic circulation in the western South Atlantic - a twofold reconstruction: *Tectonophysics*, doi: 10.1016/j.tecto.2016.05.036.

IODP

Astronomical Calibration of the Ypresian Geomagnetic Polarity Time Scale: Implications for Seafloor Spreading Rates and the Chaotic Behaviour of the Solar System?

T. WESTERHOLD¹, U. RÖHL¹, T. FREDERICH², C. AGNINI³, I. RAFFI⁴, R. H. WILKENS⁵, J. C. ZACHOS⁶

¹MARUM – Center for Marine Environmental Sciences, University of Bremen, Leobener Straße, 28359 Bremen, Germany

²Faculty 5 Geosciences, University of Bremen, 28359 Bremen, Germany

³Dipartimento di Geoscienze, Università degli Studi di Padova, via G. Gradenigo 6, 35131 Padova, Italy

⁴Dipartimento di Ingegneria e Geologia (InGeo) – CeRSGeo, Università degli Studi “G. d’Annunzio” Chieti-Pescara, via dei Vestini 31, 66013 Chieti-Pescara, Italy

⁵Institute of Geophysics and Planetology, University of Hawaii, Honolulu, HI 96822, USA

⁶Department of Earth and Planetary Sciences, University of California Santa Cruz, 1156 High Street, Santa Cruz, CA 95064, USA

The Ypresian Stage from 56.0-47.8 Ma is representing the first ~8 million years of the Eocene Epoch characterized by the warmest deep sea temperatures of the Cenozoic era, multiple transient global warming events and major faunal as well as floral turnovers. Climatic records from the Ypresian greenhouse are of special interest because they provide a unique opportunity to decipher Earth’s climate system behaviour under those pCO₂ concentrations likely to be reached in the near future. For the detailed reconstruction of the Eocene greenhouse climate system a complete and precise stratigraphic framework is required to determine rates of climatic processes and timing of events.

To complement existing high resolution records spanning portions of the Ypresian Stage, we have generated high-resolution X-ray fluorescence (XRF) iron intensity, bulk stable isotope, calcareous nannofossil, and magnetostratigraphic records on core material from ODP Sites 1258 (Leg 207, Demerara Rise), 1262, 1263, 1265 and 1267 (Leg 208, Walvis Ridge) recovered in the Equatorial and South Atlantic Ocean. By combining new data with published records a new 405-kyr eccentricity cyclostratigraphic framework was established also revealing a 300-400 kyr long condensed interval for Magnetochron C22n in the Leg 208 succession.

Because the amplitudes of the XRF data are dominated by eccentricity they assist to identify the most reliable orbital solution suitable for astronomical tuning of the Ypresian. Our new records show best fit with the La2010b numerical solution for eccentricity, which was used as a target curve for compiling the Ypresian Astronomical Time Scale (YATS). The consistent positions of the very long eccentricity minima in the geological data and the La2010b solution suggest that the macroscopic feature displaying the chaotic diffusion of the planetary orbits, the transition from libration to circulation in the combination of angles in the precession motion of the orbits of Earth and Mars, occurred ~52 Ma ago. This is the first geological evidence for the chaotic behaviour of the solar system.

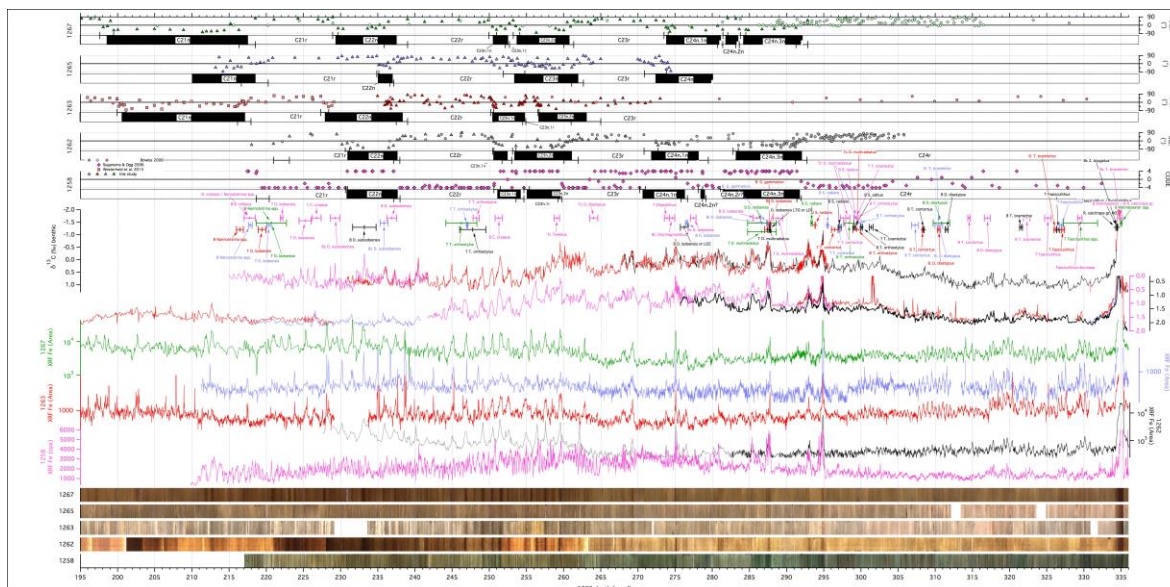


Figure 1: Overview of bio- and magnetostratigraphic data, XRF core scanning Fe intensity data and core images from ODP Sites 1258, 1262, 1263, 1265, and 1267 from 195-336 revised meters composite depth of Site 1263. Upper five panels show the inclination data from characteristic remanent magnetization investigations (new and incl. data from previous studies). The positions of calcareous nannofossil events including the depth error are plotted for all sites as well as the compiled benthic and bulk $\delta^{13}\text{C}$ data and XRF core scanning Fe intensities. Purple – 1258, Black and Grey – 1262; Red – 1263; Blue – 1265, Green – 1267.

Additionally, the new astrochronology and revised magnetostratigraphy provide robust ages and durations for Chrons C21n to C24n (47-54 Ma) revealing a major change in spreading rates in the interval from 51.0 - 52.5 Ma. Interestingly, this major change in spreading rates is synchronous with a global reorganization of the plate-mantle system and the chaotic diffusion of the planetary orbits. Therefore, we hypothesize that changes in the gravitational interaction of the sun and the planets may have affected the dynamic mantle flow of the Earth triggering plate motion reorganisations ~52 Ma ago. The newly provided YATS also includes new absolute ages for bio- and magnetostratigraphic events/reversals and early Eocene hyperthermal events. Our new biomagnetostratigraphically calibrated stable isotope compilation will likely act as a reference for a variety of paleoclimate studies covering the Ypresian, which is of high interest because of the waning warming but progressively cooling phase of the Earth's climate system clearly defining its role as a key interval.

ICDP

Integration of geological and biological histories: Unraveling drivers of diversification in ancient Lake Ohrid

T. WILKE¹, B. WAGNER², C. ALBRECHT¹, A. FRANCKE², T. HAUFFE¹, E. JOVANOVSKA¹, B. STELBINK¹ AND THE SCOPSCO SCIENCE TEAM

¹ Department of Animal Ecology and Systematics, Justus Liebig University Giessen, Giessen, Germany

² Institute of Geology and Mineralogy, University of Cologne, Cologne, Germany

What determines species diversity? This is one of top 25 questions facing science over the next 25 years, raised in the 125th anniversary issue of the journal *Science* (Pennisi, 2005). According to the author, answering this question requires a major interdisciplinary effort, comprising, among others, paleontological investigations, field work, genetic analyses, and state-of-the art statistics. The task is rather urgent because inferring the drivers of diversification (i.e., speciation minus extinction) might have important consequences for understanding the increase in extinction events – the biodiversity crisis – seen in recent years and for developing respective mitigation strategies (Pennisi, 2005).

Two central questions are currently being discussed. i) Do abiotic characteristics, such as climatic or environmental changes over time, drive diversification processes, and ii) can biotic interactions (e.g., species competition) lead to a saturation of species numbers in natural systems (i.e., are diversification rates diversity-dependent; Rabosky & Glor, 2010)? Both questions are controversially discussed as some investigations support these ideas, while others strongly reject them. In fact, recent studies pointed out a general lack of suitable data and methodological problems that may bias respective investigations (e.g., Marshall & Quental, 2016).

Studying drivers of diversification, indeed, is not trivial because the requirements for the study systems are complex:

- the systems and their biota should be relatively old, supporting consecutive speciation and extinction events,
- they should be relatively isolated, minimizing a potential bias introduced due to immigrating species,
- they should be characterized by a high number of endemic species across higher taxa, enabling statistically sound analyses, and
- detailed and continuous geological and biological records should be available, enabling an integration of these datasets over an extended period of time.

Unfortunately, such study systems remain scarce. A suitable candidate system would be Lake Ohrid in the Balkan Peninsula – the oldest lake in Europe. It is located at 693.5 m above sea level, has a maximum length of 30.4 km, a maximum width of 14.7 km, a surface area of 358 km², and a tub-shaped bathymetry with a maximum water depth of 293 m (Lindhorst et al., 2015). With > 300 endemic species described (Föller et al., 2015), 117 of which belonging to the diatoms (Levkov & Williams, 2012), it is one of the most biodiverse lakes in the world.

These unique characteristics of Lake Ohrid provided the main motivation for initiating an international deep drilling research project, which aims at integrating geological and biological histories over hundreds of thousands or even millions of years. In fact, the interdisciplinary ‘Scientific Collaboration on Past Speciation Conditions in Lake Ohrid’ (SCOPSCO) represents one of the very first ICDP campaigns, which has been driven by biological questions, that is, to evaluate the influence of major geological events on the generation of the extraordinary degree of endemic biodiversity in Lake Ohrid (Wagner et al., 2014).

Based on preliminary sedimentological, seismic and biological pre-site surveys, four sites were cored in spring 2013, using the Deep Lake Drilling System (DLDS) provided by DOSECC (Wagner et al., 2014). At the main site (DEEP) in the central part of the Lake Ohrid basin, six parallel holes were drilled, reaching a maximum depth of ~569 m blf. Subsampling and analyses are ongoing, but first detailed data for the upper 247.8 m of the sediment succession of the DEEP site, including the respective age model, were recently published in a special issue of *Biogeosciences* ("Integrated perspectives on biological and geological dynamics in ancient Lake Ohrid", eds. Wagner, B., Wilke, T., Cremer-Wagner, F., & Middelburg, J.).

Using preliminary environmental data (Francke et al., 2016; Wagner, unpublished data) and data of fossil diatoms (Jovanovska, unpublished data), we performed statistical analyses to link environmental proxies to diversification rates in diatoms over time. Our specific goals were to:

- i) test the influence of environmental parameters, such as TN, TOC, and TIC, on diversification rates in endemic diatoms, and
- ii) test whether diversification rates are diversity-dependent, i.e., whether they slow down over time.

For doing so we generated two sets of model data. The first set, referring to specific goal i), consisted of models that either assumed that diatom diversification is driven by specific environmental parameters or constant, and the second set, referring to specific goal ii), consisted of models that either assumed diversity-dependent or constant species rates.

Model comparison through Bayes Factor analyses strongly supported a relationship between total number of endemic species and speciation rate over rate constancy. Accordingly, the speciation rate decreases over time, suggesting that the ecosystem becomes saturated with species.

As for the impact of environmental parameters, model comparisons also showed a relationship between speciation rate and some, but not all, environmental parameters tested. The TOC dataset, for example, indicated that the speciation rate decreases with increasing TOC content.

These preliminary findings suggest that diversification rates in Lake Ohrid are both driven by abiotic changes over time and biotic interaction leading to a saturation of species numbers, though the latter affect is superior.

The SCOPSCO deep drilling campaign is therefore the very first interdisciplinary study that was able to infer the relative contribution of abiotic (i.e., environmental parameters) and biotic (i.e., species saturation) characteristics in driving diversification rates in highly isolated ecosystems over an extended period of time.

In the coming months we aim to: i) assess changes in the relative contribution of extrinsic and intrinsic factors over time, and ii) complement our paleontological analyses with analyses of time-dated phylogenies generated for several extant groups of endemic invertebrates in Lake Ohrid.

We think that this project may therefore provide important answers to one of the top 25 questions facing science over the next years – What determines species diversity?

References:

- Föller, K., Stelbrink, B., Hauße, T., Albrecht, C., Wilke, T., 2015. Constant diversification rates of endemic gastropods in ancient Lake Ohrid: ecosystem resilience likely buffers environmental fluctuations. *Biogeosciences* 12, 7209–7222.
- Francke, A., Wagner, B., Just, J., Leicher, N., Gromig, R., Baumgarten, H., Vogel, H., Lacey, J.H., Sadori, L., Wonik, T., Leng, M.J., Zanchetta, G., Sulpizio, R., Giaccio, B., 2016. Sedimentological processes and environmental variability at Lake Ohrid (Macedonia, Albania) between 640 ka and modern days. *Biogeosciences* 13, 1179–1196.
- Levkov, Z., Williams, D.M. 2012. Checklist of diatoms (Bacillariophyta) from Lake Ohrid and Lake Prespa (Macedonia), and their watersheds. *Phytotaxa* 45, 1–76.
- Lindhorst, K., Krastel, S., Reicherter, K., Stipp, M., Wagner, B., Schwenk, T. 2015. Sedimentary and tectonic evolution of Lake Ohrid (Macedonia/Albania). *Basin Research* 27, 84–101.
- Marshall, C.R., Quental, T.B., 2016. The uncertain role of diversity dependence in species diversification and the need to incorporate time-varying carrying capacities. *Philosophical Transactions B* 371, 20150217.
- Pennisi, E., 2005. What Determines Species Diversity? *Science* 309 (5731), 90.
- Rabosky, D.L., Glor, R.E., 2010. Equilibrium speciation dynamics in a model adaptive radiation of island lizards. *Proceedings of the National Academy of Sciences of the U.S.A.* 51, 22178–22183.
- Wagner, B., Wilke, T., Krastel, S., Zanchetta, G., Sulpizio, R., Reicherter, K., Leng, M.J., Grazhdani, A., Trajanovski, T., Francke, A., Lindhorst, K., Levkov, Z., Cvetkoska, A., Reed, J., Zhang, X., Lacey, J., Wonik, T., Baumgarten, H., Vogel, H., 2014. The SCOPSCO drilling project recovers more than 1.2 million history from Lake Ohrid. *Scientific Drilling* 17, 19–29.

IODP

Code for Ocean Drilling Data (CODD) - A New Tool for Integrating Complex Data Streams and Advancing Astronomical Tuning

R. H. WILKENS¹, T. WESTERHOLD², A. J. DRURY², M. LYLE³, T. GORGAS⁴, J. TIAN⁵

¹School of Ocean and Earth Science and Technology (SOEST), University of Hawai'i at Manoa, USA

²MARUM - Center for Marine Environmental Sciences, University of Bremen, Germany

³College of Earth, Ocean, and Atmospheric Sciences, Oregon State University, USA

⁴Zentrum für Wissenschaftliches Bohren, Deutsches GeoForschungsZentrum GFZ, Potsdam, Germany

⁵State Key Laboratory of Marine Geology, Tongji University, China

The proliferation and diversity of the data collected both during and after ocean drilling cruises can at times be somewhat overwhelming for the individual scientist. Data are now easily available through online databases maintained by the ocean drilling infrastructure (e.g. LIMS, JANUS), by national efforts (e.g. NGDC) or community efforts (e.g. PANGAEA). However, a unified and consistent system for integrating disparate data streams such as micropaleontology, physical properties, core images, geochemistry, and borehole logging has not been widely available. Here we describe an open source macro system that we have developed over several years to work with ocean drilling data and images (CODD - Code for Ocean Drilling Data). CODD takes advantage of the versatile graphical user interface and analytical functions contained in the IGORTM graphing and analysis program commercially available from Wavemetrics, Inc.

One of the great advantages of a modern analysis program paired with fast processors is the ability to use images as data. Rather than a static picture of a core or section, images may be scaled and plotted along with traditional data versus depth or age. Core images may be squeezed, stretched, subsampled, concatenated and spliced, allowing for great versatility. Ever since IODP Leg 200, core section images have been captured by line scanners as discrete files which are easily loaded into analysis programs with little or no preparation. For cruises prior to Leg 200 access to core images is limited to digitized photos of multiple sections in core boxes. CODD includes a module for cutting core section images from core table photos, correcting them for uneven lighting, scaling them to mbsf (meters below seafloor) and combining them into a single core image through a series of simple steps. In practice it takes between 1 and 2 minutes to go from loading a core table photo to producing a scaled merged core image. The visualization and impact of the core image is very much different from the core table photo and of much greater value during data analysis. The use of scaled merged core images has proven to be particularly effective in creating site splices or for the checking of existing splices.

The heart of the CODD data structure is the coring matrix - a 3 layered array in which the top layer contains the original depth to the top of each section (mbsf or csf) sorted by core (rows) and sections (columns). The middle layer contains the length of the sections and the third layer

the composite depth (mcd or ccsf). Sample depths are calculated by referencing the proper layer and coordinate by core and section and then adding the sample interval. The reverse process of returning the core, section, and interval designation of a given sample depth is accommodated by comparing it to the section top depth plus the section length to find where the sample originated.

The newly developed CODD software was used to check data splices of ODP Leg 154 sites (Ceara Rise - western equatorial Atlantic) and better align out-of-splice data with in-splice data. The splices of ODP Sites 925, 926, 927, 928 and 929 were reviewed. Most changes were minor although several are significant enough to affect age models based on orbital tuning. We revised the astronomically tuned age model for the Ceara Rise by tuning darker, more clay rich layers to Northern Hemisphere insolation minima. Then we assembled a regional composite benthic stable isotope record from published data. This new Ceara Rise stack provides an original regional reference section for the equatorial Atlantic covering the last 5 million years with an independent age model that can be compared to the non-linear ice volume models of the global oxygen isotope stack of Lisiecki and Raymo (LR04). Comparison shows that the benthic $\delta^{18}O$ composite is consistent with the LR04 stack from 0 - 4 Ma except for a short interval between 1.80 and 1.90 Ma, where LR04 exhibits 2 maxima but where Ceara Rise contains only 1. The interval between 4.0 and 4.5 Ma in the Ceara Rise compilation is decidedly different from LR04, reflecting both the low amplitude of the signal over this interval and the limited amount of data available for the LR04 stack. Our results suggest that precession cycles have been misinterpreted as obliquity in the LR04 stack at 4.2 Ma. Further study of data contributing to LR04 will lead to a clarification of the misfits we have found as well as establishing other regional isotope offsets from a global stack.

The CODD software package can play a role in the construction of a new generation of the benthic isotope stack and surely will be very helpful in extending the stack into the Miocene. CODD software is not limited to IODP data and images. It can be also used for assembling and integrating data and images for other drilling initiatives like ICDP. CODD was already successfully applied in the Bighorn Basin Drilling Project (BBCP), the El Kef Coring Program, and customized for MARUM University Bremen coring projects.

IODP

Effect of sampling techniques on Ca concentrations and isotope ratios of marine porewaters

A. WITTKÉ¹, N. GUSSONE¹, C. MÄRZ², B.M.A. TEICHERT³

¹ Institut für Mineralogie, Westfälische-Wilhelms-Universität Münster, Germany

² School of Earth and Environment, University of Leeds, United Kingdom

³ Institut für Geologie und Paläontologie, Westfälische-Wilhelms-Universität Münster, Germany

Changes in marine porewater chemical composition are important indicators of early diagenetic processes and fluid fluxes. Fluctuations in the concentration of Ca are of special interest, as this element is involved in diagenetic reactions such as carbonate dissolution, precipitation and dolomitization. Thus, it is part of the CO₂ cycle and directly linked to climate changes. In the past decade, the Ca isotope system has been applied as proxy for diagenetic reactions such as CaCO₃ dissolution (Fantle and DePaolo, 2007), CaCO₃ precipitation (Teichert et al., 2005), ion exchange (Teichert et al., 2009; Ockert et al., 2013) and recrystallization (e.g. Fantle and DePaolo, 2007; Turchyn and DePaolo, 2011). To extract the porewater from a sediment core, the so-called whole round (WR) method has been used for decades. The WR method has some limitations: It is usually applied at relatively low depth resolution because it disturbs the sediment record (Dickens et al., 2007), and the pressure exerted in the hydraulic press to extract the pore fluid (250-300 MPa) destroys microbial cells and was suggested to cause carbonate contamination (Schrum et al., 2012) since the pressure is much higher than any water pressure in the deep ocean (Miller et al., 2014). A more recent method to retrieve porewater is the so-called Rhizon sampling technique, first applied to marine sediment cores by Seeberg-Elverfeldt et al. (2005) and Dickens et al. (2007). A Rhizon sampler is a thin porous stick (diameter of 2.4 mm) which is introduced into the intact sediment core. Applying a gentle vacuum, the porewater is sucked out of the sediment without major disturbance of the sediment record. In addition, achieving a higher sampling resolution is more feasible using the Rhizon sampling techniques. There are only a few comparative studies, especially for isotope ratios, but initial results indicate possible differences between both sampling

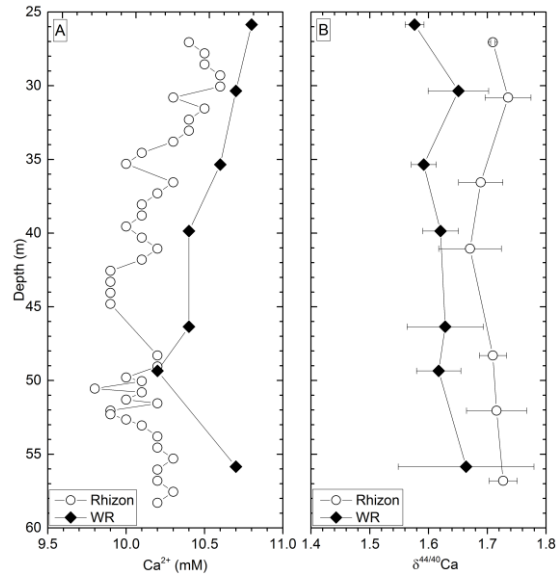


Figure 1: Comparison of Ca²⁺ concentration [A] (Pälike et al., 2010) and $\delta^{44/40}\text{Ca}$ ratio [B] in porewaters retrieved by Rhizon (white circle) and whole round sampling technique (black square) of IODP core U1332. [A]: The Ca²⁺ concentration has an offset of around 0.5 mM between both sampling methods, showing a similar offset identified for concentration of Ba²⁺, Li⁺ and Mg²⁺ (Pälike et al., 2010). [B]: $\delta^{44/40}\text{Ca}$ ratio of Rhizon and whole round sampling showing the same overall pattern with slightly higher $\delta^{44/40}\text{Ca}$ values for Rhizon samples than WR samples.

techniques, e.g. for alkalinity, Cl⁻ concentration, oxygen and hydrogen isotope ratios and dissolved inorganic carbon (DIC) (Schrum et al., 2012, Miller et al., 2014).

In this study, we systematically compare Rhizon and WR sampling techniques in terms of their effect on stable calcium isotope ratios in extracted porewaters. The WR and Rhizon sampling methods have been applied during IODP Exp. 320/321 at Site U1332 at the parallel Holes A and C (Pälike et al., 2010). The parallel sediment cores were selected for Ca isotope analyses because they show a difference in the porewater concentrations of Ba²⁺, Ca²⁺, Li⁺ and Mg²⁺ (Pälike et al., 2010) (Fig. 1). The mechanism responsible for this offset is not yet understood, but could be related to either different sampled reservoirs, such as dissolved and adsorbed species, or dissolution-precipitation reactions during sampling. Such processes could affect not only concentrations of dissolved species, but also result in

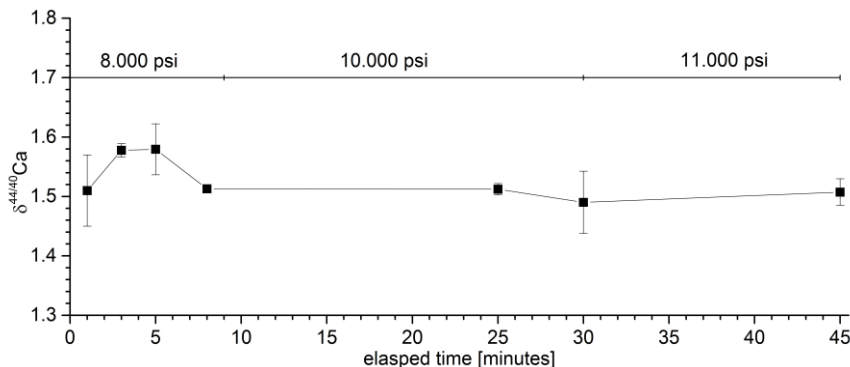


Figure 1: $\delta^{44/40}\text{Ca}$ as a function of elapsed time during WR porewater pressing with increasing pressure. The values show no significant variation within measurement uncertainties.

different stable Ca isotope ratios according to Ockert et al. (2013) who found that free dissolved Ca^{2+} and Ca^{2+} absorbed to clay minerals have different Ca isotope ratios. During sampling with the WR sampling technique, absorbed Ca^{2+} could be released from the clay mineral surfaces, while during Rhizon sampling carbonate precipitation could occur due to CO_2 degassing initiated by pressure reduction, both leading to a change in Ca isotope ratios. Our results demonstrate that the WR and Rhizon sampling methods result in a systematic offset in $\delta^{44/40}\text{Ca}$ of 0.05–0.13 ‰, but most sample pairs overlap within uncertainties (Fig. 1) Furthermore, we test on a sediment core from Hole U1417C (IODP Exp. 341) if the Ca isotope composition of porewater sampled by the WR method could be affected by time and pressure of the hydraulic press during sampling (with increasing pressure over a duration of ~1 hour). The WR press test shows that neither time nor exerted pressure leads to a change in the $\delta^{44/40}\text{Ca}$ ratio (Fig 2).

References:

- Dickens, G.R., Koelling, M., Smith, D.C., Schnieders, L., 2007. Rhizon Sampling of Pore Waters on Scientific Drilling Expeditions: An Example from the IODP Expedition 302, Arctic Coring Expedition (ACEX), in: Backman, J., Moran, K., McIntroy, D., Mayer, L. (Eds.), Proceedings of the IODP, 302, vol. 302. Integrated Ocean Drilling Program, pp. 22–25.
- Fantle, M.S., DePaolo, D.J., 2007. Ca isotopes in carbonate sediment and pore fluid from ODP Site 807A: The $\text{Ca}^{2+}(\text{aq})$ -calcite equilibrium fractionation factor and calcite recrystallization rates in Pleistocene sediments (71), 2524–2546.
- Miller, M.D., Adkins, J.F., Hodell, D.A., 2014. Rhizon sampler alteration of deep ocean sediment interstitial water samples, as indicated by chloride concentration and oxygen and hydrogen isotopes. *Geochem. Geophys. Geosyst.* 15 (6), 2401–2413.
- Ockert, C., Gussone, N., Kaufhold, S., Teichert, B., 2013. Isotope fractionation during Ca exchange on clay minerals in a marine environment. *Geochimica et Cosmochimica Acta* 112, 374–388.
- Pälike, H., Lyle, M., Nishi, H., Raffi, I., Gamage, K., Klaus, A. (Eds.), 2010. Proceedings of the IODP, 320/321. Integrated Ocean Drilling Program.
- Schrum, H.N., Murray, R.W., Gribsholt, B., 2012. Comparison of Rhizon Sampling and Whole Round Squeezing for Marine Sediment Porewater. *Scientific Drilling* (13, April 2012).
- Seeberg-Elverfeldt, J., Schlüter, M., Feseker, T., Kölling, M., 2005. Rhizon sampling of porewaters near the sediment-water interface of aquatic systems. *Limnol. Oceanogr. Methods* 3 (8), 361–371.
- Teichert, B., Torres, M.E., Bohrmann, G., Eisenhauer, A., 2005. Fluid sources, fluid pathways and diagenetic reactions across an accretionary prism revealed by Sr and B geochemistry. *Earth and Planetary Science Letters* 239 (1–2), 106–121.
- Teichert, B.M., Gussone, N., Torres, M.E., 2009. Controls on calcium isotope fractionation in sedimentary porewaters. *Earth and Planetary Science Letters* 279 (3–4), 373–382.
- Turchyn, A.V., DePaolo, D.J., 2011. Calcium isotope evidence for suppression of carbonate dissolution in carbonate-bearing organic-rich sediments. *Geochimica et Cosmochimica Acta* 75 (22), 7081–7098

ICDP

Subfossil Cladocera assemblages in Lake Petén Itzá (Guatemala) sediments

MARTA WOJEWÓDKA¹, EDYTA ZAWISZA¹, KRYSZYNA SZEROCZYŃSKA¹, SERGIO COHUO², LAURA MACARIO-GONZALEZ², LISETH PEREZ³, STEFFEN KUTTEROLF⁴, ANTIJE SCHWALB²

¹ Institute of Geological Sciences, Polish Academy of Sciences, Twarda 51/55, PL00818 Warsaw, Poland, e-mail:

m.wojed@twarda.pan.pl

² Institut für Geosysteme und Bioindikation, Technische Universität Braunschweig, Langer Kamp 19c, 38106 Braunschweig, Germany

³ Instituto de Geología, Universidad Nacional Autónoma de México (UNAM), Ciudad Universitaria, 04510, Ciudad de México, México

⁴ GEOMAR Helmholtz-Zentrum für Oceanforschung, Kiel, Germany

Lake Petén Itzá is located in the Petén District, northern Guatemala and is one of the largest (~100 km²) and deepest (~160 m) in the lowlands of Central America. Petén Itzá contains a continuous sediment sequence that accumulated over the last 400,000 years. Sediment cores (PI-1, PI-2, PI-3, PI-4, PI-6, PI-7 and PI-9) from Petén Itzá were collected within the International Continental Scientific Drilling Program in 2006. Cores were taken in water depths ranging from 30 to 150 m, using the Global Lakes Drilling (GLAD 800) platform. The main aim was to obtain high-resolution records to infer climate and environmental changes based on multiproxies. Here we present the results of subfossil Cladocera remain analysis carried out for core PI-2, collected from 54 m water depth. Sediments are represented mainly by gypsum and clay units. Dating of the PI-2 core provided an age of 53 ka.

Results of our investigation suggest limited existence of Cladocera in Lake Petén Itzá. Waterfleas were present only in Holocene sediments. Absence of cladoceran remains in Pleistocene sediments indicates unfavorable environmental conditions because these crustaceans do not tolerate high mineralization or salinity and/or bad preservation. In sediments deposited during the Holocene, we found ten species belonging to two families: Bosminidae and Chydoridae. The predominant species were planktonic species such as *Eubosmina* (*Bosmina*) (*E.*) *longispina*, *Bosmina* (*E.*) *corregoni* and *Bosmina longirostris*. We identified the following littoral species: *Alona ossiani*, *Alona quadrangularis* type, *Anthalona verrucosa*, *Leydigia louisiana*, *Leydigia striata*, *Ovalona glabra* and *Pleuroxus* sp. This study was funded by the Polish Ministry of Science (Grant NCN 2014/13/B/ST10/02534), Grant SCHW 671/16-1 and KU2685/3-1.

ICDP

The Cladocera community of Central America - ecology and distribution

MARTA WOJEWÓDKA¹, EDYTA ZAWISZA¹, KRYSZYNA SZEROCZYŃSKA¹, SERGIO COHUO², LAURA MACARIO-GONZALEZ², LISETH PEREZ³, ANTJE SCHWALB²

¹ Institute of Geological Sciences, Polish Academy of Sciences, Twarda 51/55, PL00818 Warsaw, Poland, e-mail: m.wojed@twarda.pan.pl

² Institut für Geosysteme und Bioindikation, Technische Universität Braunschweig, Langer Kamp 19c, 38106 Braunschweig, Germany

³ Instituto de Geología, Universidad Nacional Autónoma de México (UNAM), Ciudad Universitaria, 04510, Ciudad de México, México

The knowledge about Cladocera, their requirements and distribution in Central America before our study was still limited. Here we present results of a study on the distribution and ecology of waterfleas from Central America based on analysis of their subfossil remains in modern surface sediments. Surface sediments from 29 lakes from Guatemala, El Salvador and Honduras, representing a broad spectrum of environmental conditions, were collected using an Ekman grab in 2013. The lakes are situated between 3 and almost 3000 m asl. In total, 34 species were found, belonging to 3 families (Bosminidae, Daphnidae, Chydoridae). Within recognized species both planktonic and littoral forms were present. Planktonic families (Bosminidae and Daphnidae) showed highest abundance of specimens, while Chydoridae were the most species-rich family. For taxa typical of tropical zones we found: *Anthalona verrucosa*, *Euralona orientalis* and *Coranatella monacantha*. Daphnidae were present in mountain lakes whereas Bosminidae occurred in broad spectrum of abiotic conditions. Bosminidae species also existed in lakes which are characterized by a high-level of water mineralization (>900 $\mu\text{S cm}^{-1}$). The most frequent species was Chydorus cf. sphaericus, found in 20 lakes. Ubiquitous presence of this species reflects its tolerance to a wide spectrum of environmental conditions. Based on cluster analysis, 6 groups of Cladocera, with high correlation between species within a group (≥ 0.8), were discriminated. Each group demonstrated a distinct requirement for habitat conditions. For detecting correlations with environmental variables and lake characteristics, the canonical correspondence analysis (CCA) was used. Results of the statistical analysis showed that the most important factor influencing Cladocera communities was altitude. The second most valid driver was water electrical conductivity. The project was funded by the National Science Centre, Poland, contract no. 2014/13/B/ST10/02534.

IODP

Massive contribution of bacterial endospores to the marine deep biosphere – a global view (Project SPP 527/35 HI 616/17-1)

L. WÖRMER¹, T. HOSHINO², B. VIEHWEGER¹, Y. MORONO², F. INAGAKI², K.-U. HINRICHS¹

¹ MARUM & Department of Geosciences, University of Bremen, 28359 Bremen, Germany.

² Kochi Institute for Core Sample Research, Japan Agency for Marine-Earth Science and Technology (JAMSTEC), Nankoku, Kochi 783-8502, Japan.

Since the initial discovery of living microorganisms in marine sediment cores retrieved during the 1980s, scientific drilling has evidenced the abundance of Earth's deep microbial biosphere in terrestrial and marine realms (Parkes et al. 1994). However, it remains to be explained how these communities deal with progressive burial and the associated gradual energy starvation, i.e. how they achieve long-term survival on geological time scales.

Bacterial endospores are specialized, metabolically inactive, dormant cells that are structurally differentiated from vegetative cells and present specific resistance and persistence strategies. Sporulation is triggered by a variety of stimuli, the main one being prolonged starvation. At the same time, endospores have the ability to monitor their habitat to resume active growth when the conditions become favourable. Endospore formation is exclusive to the phylum Firmicutes and widespread among its different physiological groups. As Firmicutes are considered important members of the seafloor biosphere, and the harsh conditions in this ecosystem seem prone to the implementation of microbial actions leading to increased resistance, endospores may constitute a critical long-term survival strategy. Unfortunately, due to a lack of reliable analytical methods, endospores have been poorly accounted for in previous surveys of the seafloor microbiota. But with the implementation of HPLC-based protocols for the detection of the diagnostic biomarker dipicolinic acid (DPA) (Fichtel et al., 2007b), accurate and reliable quantification of intact bacterial endospores has become available.

Our project started in late 2015 at MARUM (University of Bremen). Its main goal is to tackle the abundance and ecological relevance of endospores in the marine subsurface. This project is based on two main hypotheses: The first one is that endospores are major, so far insufficiently accounted for, contributors to the deep biosphere. Testing this hypothesis includes determining the abundance of endospores in this realm, evaluating to which extent these endospores are included in previous estimates of the microbial deep biosphere and refining the DPA-based endospore quantification. The second hypothesis is that endospore formation is an effective survival strategy and permits the colonization of deep habitats. To validate this hypothesis, information from incubation experiments investigating the viability of endospores and endospore data from discrete sedimentary layers that positively or negatively affect microbial activity are of relevance. To allow a better understanding of changes in abundance and diversity along these interfaces, DPA-based quantification is being combined with molecular methods that specifically

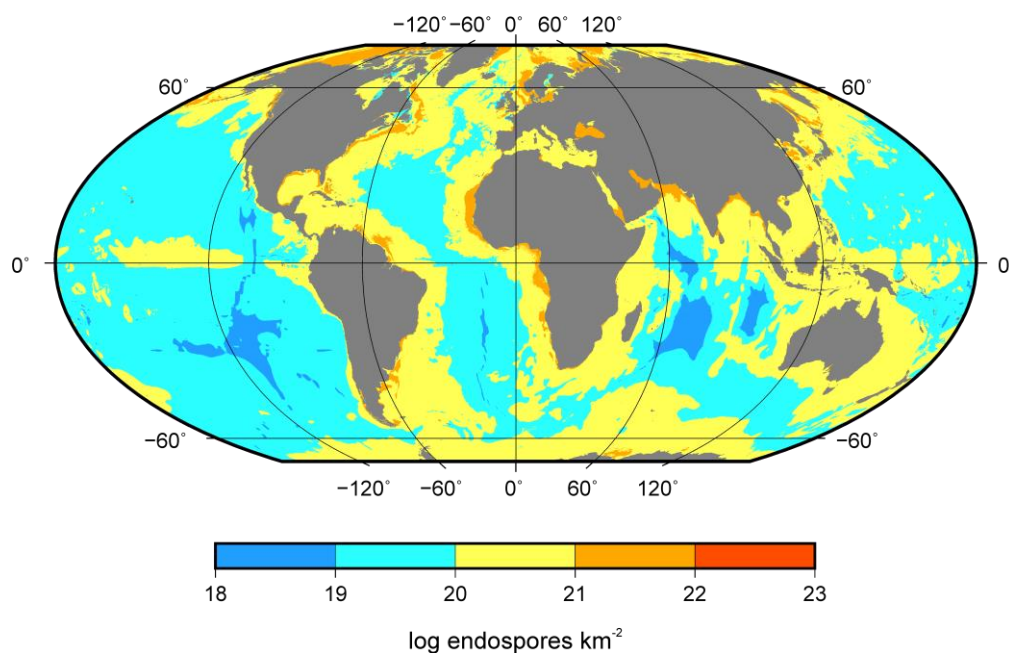


Figure 1: Estimated global distribution of endospores integrated over sediment depth and expressed per km².

target endospores and endospore forming Firmicutes. The understanding of the response of these communities particularly to shifts in the temperature regime will strongly benefit from the participation in cruise IODP 370, and the availability of dedicated samples.

Though work on this second hypothesis has intensified recently, most progress has so far been achieved in the assessment of the first hypothesis. Our main goal was to provide a robust estimation of the amount of endospores populating the marine subseafloor. Therefore, more than 300 sediment samples from ODP and IODP expeditions, as well as from German, Japanese and US-American cruises were evaluated. The selected samples provided a wide range of depths and depositional settings and represented a good geographical coverage. Besides bacterial endospore abundance (DPA-based), vegetative cell numbers and total organic carbon content were analyzed. DPA was extracted from sediments by autoclaving and quantified by recording the fluorescence of the DPA-Tb complex following a protocol based on (Fichtel et al. 2007b). Endospore numbers were calculated from DPA concentration by applying a DPA cell quota of 2.24×10^{-16} mol per endospore (Fichtel et al. 2007a). Cell numbers were obtained either by flow cytometry or digital PCR using microfluidics.

Following the typical trend observed in marine sediments, the number of vegetative cells in our study sites decreased with depth. Endospore abundance on the other hand remained relatively constant in a range between roughly 10^5 and 10^6 units per g. Only some surface samples from the brackish Baltic and Black Sea, and from the Rhone Delta, all heavily influenced by freshwater input, showed higher concentrations. This translates to a gradual enrichment of endospores against vegetative cells over depth, which even exceeds the prospects of Lomstein et al. (2012), who stated that endospores could be as abundant as vegetative cells in deep sediments. While accounting for ~0.1% of the vegetative cells in surface sediments, already at 100 m depth, endospores are typically more abundant

than their vegetative counterparts. In deeply buried sediments metabolically quiescent cells thus clearly outnumber vegetative cells, and the potential presence of spore-like resistance forms not associated with the Firmicutes could even tip the balance further towards dormancy.

In order to try to provide a global estimate of endospore abundance in the marine subsurface, we followed an approach based on the estimation of vegetative cells by Kallmeyer et al. (2012). Accordingly, decrease of endospores over depth at individual sites was adjusted to a power curve, which can be described by the variables cell concentration at 1 m depth and rate of decrease. These two variables were then correlated to environmental parameters. Making use of the available global grids of these parameters, abundance of bacterial endospores in the habitable marine subseafloor could be modelled (Fig. 1). Thereby we provide evidence for a formidable community of endospores populating the marine biosphere. The high abundance and wide distribution of endospores in the deep biosphere is consistent with the fact that Firmicutes often dominate isolation attempts from the subseafloor (e.g. Batzke et al. 2007; Fichtel et al. 2012).

Once the abundance of endospores has been evidenced, the question of their ecological relevance in the marine subsurface remains. By definition, endospores may be seen as a seed bank, their genomic and functional diversity remaining potentially available for germination and colonization of new habitats. But this view, in the case of sedimentary systems, also implies two fundamental questions: (i) to what degree do endospores in the deep biosphere retain viability? and (ii) Is the large endospore pool dynamic or stagnant, i.e. are endospores deposited once and then remain unaltered or is the endospore stock replenished by awakening and new sporulation, thereby subjecting the community to a selection process?

References:

- Batzke, A., Engelen, B., Sass, H., Cypionka, H., 2007. Phylogenetic and physiological diversity of cultured deep-biosphere bacteria from equatorial Pacific Ocean and Peru Margin sediments. *Geomicrobiology Journal* 24, 261-273.
- Fichtel, J., Koester, J., Rullkoetter, J., Sass, H., 2007a. Spore dipicolinic acid contents used for estimating the number of endospores in sediments. *Fems Microbiology Ecology* 61, 522-532.
- Fichtel, J., Koester, J., Scholz-Boettcher, B., Sass, H., Rullkoetter, J., 2007b. A highly sensitive HPLC method for determination of nanomolar concentrations of dipicolinic acid, a characteristic constituent of bacterial endospores. *Journal of Microbiological Methods* 70, 319-327.
- Fichtel, K., Mathes, F., Konneke, M., Cypionka, H., Engelen, B., 2012. Isolation of sulfate-reducing bacteria from sediments above the deep-sea seafloor aquifer. *Frontiers in Microbiology* 3.
- Kallmeyer, J., Pockalny, R., Adhikari, R.R., Smith, D.C., D'Hondt, S., 2012. Global distribution of microbial abundance and biomass in seafloor sediment. *Proceedings of the National Academy of Sciences of the United States of America* 109, 16213-16216.
- Lomstein, B.A., Langerhuus, A.T., D'Hondt, S., Jorgensen, B.B., Spivack, A.J., 2012. Endospore abundance, microbial growth and necromass turnover in deep sub-seafloor sediment. *Nature* 484, 101-104.
- Parkes, R.J., Cragg, B.A., Bale, S.J., Getliff, J.M., Goodman, K., Rochelle, P.A., Fry, J.C., Weightman, A.J., Harvey, S.M., 1994. Deep Bacterial Biosphere in Pacific-Ocean Sediments. *Nature* 371, 410-413.

ICDP

Chemistry, mineralogy and hydrothermal alteration of the Mt Unzen conduit (Shimabara/Japan)

T.I. YILMAZ¹, H.A. GILG², E. JANOTS³, K. MAYER¹, K.-U. HESS¹, S. NAKADA⁴, D.B. DINGWELL¹

¹ Department of Earth and Environmental Sciences, Ludwig-Maximilians-Universität München (LMU), Theresienstr. 41/III, 80333 Munich, Germany

² Lehrstuhl für Ingenieurgeologie, Technische Universität München (TUM), Arcisstr. 21, 80333 Munich, Germany

³ Institute des Sciences de la Terre (ISTerre), Université Grenoble Alpes, France

⁴ Earthquake Research Institute (ERI), University of Tokyo, 1-1-1 Yayoi, Bunkyo, 113-0032, Japan

Investigations were carried out on hydrothermally altered coherent dacitic dykes samples from (USDP-4) drill core at Mt Unzen stratovolcano (Shimabara/Japan). Optical hot-cathodoluminescence, XRF, XRD, EMPA, C-O-isotope and SEM analysis led to insights concerning chemistry, mineralogy, and intensity of alteration as well as the origin of carbonate-precipitating fluids. Additionally a textural characterization of the occurring replacement features in the magma conduit zone was performed. The occurrence of the main secondary phases such as chlorite, pyrite, carbonates, and R1 (Reichweite parameter) illite-smectite indicate a weak to moderate propylitic to phyllic hydrothermal alteration. The dacitic samples of the dykes show different hydrothermal alteration features: (i) carbonate pseudomorphs after hornblende as well as core and zonal textures due to replacement of plagioclase by R1 illite-smectite as well as kaolinite group minerals, (ii) colloform banded fracture fillings and fillings in dissolution vugs, and (iii) chlorite, kaolinite group minerals as well as R1 illite-smectite in the groundmass. Late chlorite veins crosscut precipitates of R1 illite-smectite as well as kaolinite group minerals. Carbonates in fractures and in pseudomorphs after hornblende comprise iron-rich dolomite solid solutions ("ankerite") and calcite. These carbonates show different luminescence (bright orange, reddish orange, weak orange and no luminescence) controlled by Mn/Fe ratios in which Mn acts as an activating element and Fe as a quenching element. Isotopic

values of $\delta^{13}\text{C}_{\text{VPDB}}$ range from -4.52 to -6.17 ($\pm 0.6\text{‰}$) and $\delta^{18}\text{O}_{\text{VSMOW}}$ values from 6.05 to 10.18 ($\pm 0.5\text{‰}$) indicate a hydrothermal-magmatic origin for the carbonate formation. The chlorite-carbonate-pyrite index (CCPI) and the Ishikawa alteration index (AI), applied to the investigated samples show significant differences (CCPI=52.7–57.8; AI=36.1–40.6) indicating their different degree of alteration.

According to Nakada et al., 2005, the C13 to C16 dykes represent the feeder dyke from the latest eruption (1991–1995) whereas C8 represents an earlier dyke feeder dyke from an older eruption. Weakest conduit alteration, which was obtained in samples C16-1-5 and C13-2-5, correlates with the alteration degree of the pristine dome rocks. Highest CCPI value was determined for sample C14-1-5 and the highest AI value was determined for sample C15-2-6. The degrees of alteration do not indicate highest alteration of the samples C8-1-2 and C8-2-1 from the older dykes.

Reference:

- Nakada, S., Uto, K., Sakuma, S., Eichelberger, J.C., Shimizu, H., 2005: Scientific Results of Conduit Drilling in the Unzen Scientific Drilling Project (USDP). *Scientific Drilling*, 1, 18–22.

IODP

Origin of the primitive layered gabbros from Hess Deep (EPR; IODP Expedition 345): Insights from mineral trace elements and MORB-peridotite interaction experiments

C. ZHANG¹, J. KOEPKE¹, R. MEYER², O. NAMUR¹, S. FEIG³

¹ Institut für Mineralogie, Leibniz Universität Hannover, 30167 Hannover, Germany

² Sektion 3.3: Oberflächennahe Geochemie, Geoforschungszentrum (GFZ) Potsdam, Germany

³ Central Science Laboratory, University of Tasmania, Australia

The coherent cores of layered gabbros drilled by IODP (International Ocean Discovery Program) Expedition 345 at Site 1415 at the Hess Deep Rift validates the use of Penrose model based on ophiolites for interpreting the structure of fast-spreading oceanic crust. Olivine gabbros and troctolites are dominant in lithology. In the olivine gabbros, both prismatic and interstitial clinopyroxene and orthopyroxene are ubiquitous phases. The occurrence of orthopyroxene as an abundant phase in these deep-level cumulate rocks is unexpected from experiments on the liquid line of descent of MORB. The new discovery of the high abundance of orthopyroxene in the primitive layered gabbros may have important implications for MORB evolution and crustal formation in the lower oceanic crust. The current model (Coogan et al. 2002) invokes interaction between MORB melt and mantle rocks and subsequent crystallization of modified MORB melt in an isolated environment. In the ongoing project, we performed (and will perform more) major and trace elemental analyses of phases from the natural drilled rock, as well as experimental simulations (i.e. melt-lherzolite interaction experiments), aiming to shed light on the origin of the primitive layered gabbros, particularly on formation of the mysterious orthopyroxene.

The Mg#s of coexisting ortho- and clinopyroxenes from the primitive layered gabbroic rocks vary within a

narrow range between 82-90 (clinopyroxene) and 80-86 (orthopyroxene), and the observed correlation between the Mg#s of orthopyroxene and clinopyroxene implies a common evolution by co-crystallization/fractionation. The clinopyroxene and orthopyroxene occur as both prismatic and interstitial (seams around other minerals), whereas Mg#s do not show difference between these two textural types. For clinopyroxene, LA-ICP-MS analytical data show that the interstitial crystals contain significantly lower Cr but higher Y concentrations (and other incompatible elements) than that of the prismatic ones, indicating an origin of crystallization from highly evolved melts (similar to that for the shallow-level gabbros drilled from Site 894). For orthopyroxene, however, the prismatic and interstitial ones have overlapping concentrations of Cr and incompatible elements, which are contrasting to the orthopyroxene in the shallow-level gabbros from Site 894. This observation conflicts with the idea that interstitial orthopyroxene crystallized from highly evolved melts, and thus we propose that the high-Cr interstitial orthopyroxene crystallized from a special "primary melt" which has been buffered by lherzolite via melt-rock interaction.

To simulate melt-lherzolite interaction experiments, we mixed the starting primitive MORB glass with a natural lherzolite and placed this mixture embedded by the primitive MORB glass. The experiments were designed to start from a high (reaction) temperature (T_1) and to finish at a low (crystallization) temperature (T_2), in between with slow cooling rate, similar to the approach of Saper and Liang (2014). In some previous simple crystallization experiment using the primitive MORB glass as starting material, strong Fe loss (occurrence of Fe metal sphere together with experimental products) was observed. Later, we used an improved capsule design in the melt-lherzolite interaction experiments, which yielded experimental products without Fe loss. Up to now, we performed two melt-lherzolite interaction experiments with $T_1=1300^\circ\text{C}$ and $T_2=1200^\circ\text{C}$, and we found that almost all lherzolite components have been reacted out (except for some cores of olivine), and no orthopyroxene formed. We can conclude from these experiments that $T_1=1300^\circ\text{C}$ (close to liquidus of MORB) is too high for melt-lherzolite reaction. Therefore, we plan to perform more such interaction experiments (and simultaneously crystallization experiments from pure MORB melt for comparison) starting from lower temperatures (such as 1250°C and even lower). In addition, we will also perform fractional crystallization experiments, in comparison with equilibrium crystallization experiments, to better understand the potential evolution of MORB melts in the lower oceanic crust.

References:

- Coogan LA, Gillis KM, MacLeod CJ, Thompson GM, Hékinian R (2002) Petrology and geochemistry of the lower ocean crust formed at the East Pacific Rise and exposed at Hess Deep: A synthesis and new results. *Geochemistry, Geophysics, Geosystems* 3(11):8604
- Saper L, Liang Y (2014) Formation of plagioclase-bearing peridotite and plagioclase-bearing wehrlite and gabbro suite through reactive crystallization: an experimental study. *Contrib Mineral Petrol* 167(3):1-16